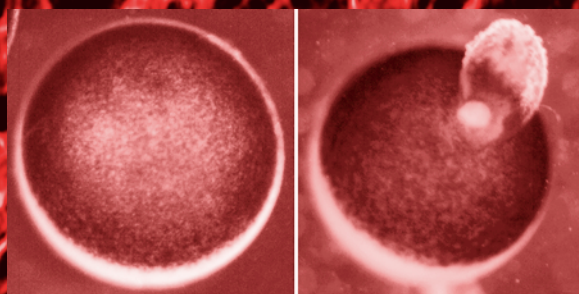


Xenopus Protocols

*Cell Biology and
Signal Transduction*

Edited by

X. Johné Liu



***Xenopus* Protocols**

METHODS IN MOLECULAR BIOLOGY™

John M. Walker, SERIES EDITOR

323. **Arabidopsis Protocols**, *Second Edition*, edited by Julio Salinas and Jose J. Sanchez-Serrano, 2006
322. **Xenopus Protocols: Cell Biology and Signal Transduction**, edited by X. Johné Liu, 2006
321. **Microfluidic Techniques: Reviews and Protocols**, edited by Shelley D. Minteer, 2006
320. **Cytochrome P450 Protocols**, *Second Edition*, edited by Ian R. Phillips and Elizabeth A. Shephard, 2006
319. **Cell Imaging Techniques, Methods and Protocols**, edited by Douglas J. Taatjes and Brooke T. Mossman, 2006
318. **Plant Cell Culture Protocols**, *Second Edition*, edited by Victor M. Loyola-Vargas and Felipe Vázquez-Flota, 2005
317. **Differential Display Methods and Protocols**, *Second Edition*, edited by Peng Liang, Jonathan Meade, and Arthur B. Pardee, 2005
316. **Bioinformatics and Drug Discovery**, edited by Richard S. Larson, 2005
315. **Mast Cells: Methods and Protocols**, edited by Guha Krishnaswamy and David S. Chi, 2005
314. **DNA Repair Protocols: Mammalian Systems**, *Second Edition*, edited by Daryl S. Henderson, 2005
313. **Yeast Protocols: Second Edition**, edited by Wei Xiao, 2005
312. **Calcium Signaling Protocols**, *Second Edition*, edited by David G. Lambert, 2005
311. **Pharmacogenomics: Methods and Applications**, edited by Federico Innocenti, 2005
310. **Chemical Genomics: Reviews and Protocols**, edited by Edward D. Zanders, 2005
309. **RNA Silencing: Methods and Protocols**, edited by Gordon Carmichael, 2005
308. **Therapeutic Proteins: Methods and Protocols**, edited by C. Mark Smales and David C. James, 2005
307. **Phosphodiesterase Methods and Protocols**, edited by Claire Lugnier, 2005
306. **Receptor Binding Techniques**, *Second Edition*, edited by Anthony P. Davenport, 2005
305. **Protein–Ligand Interactions: Methods and Applications**, edited by G. Ulrich Nienhaus, 2005
304. **Human Retrovirus Protocols: Virology and Molecular Biology**, edited by Tuofu Zhu, 2005
303. **NanoBiotechnology Protocols**, edited by Sandra J. Rosenthal and David W. Wright, 2005
302. **Handbook of ELISPOT: Methods and Protocols**, edited by Alexander E. Kalyuzhny, 2005
301. **Ubiquitin–Proteasome Protocols**, edited by Cam Patterson and Douglas M. Cyr, 2005
300. **Protein Nanotechnology: Protocols, Instrumentation, and Applications**, edited by Tuan Vo-Dinh, 2005
299. **Amyloid Proteins: Methods and Protocols**, edited by Einar M. Sigurdsson, 2005
298. **Peptide Synthesis and Application**, edited by John Howl, 2005
297. **Forensic DNA Typing Protocols**, edited by Angel Carracedo, 2005
296. **Cell Cycle Control: Mechanisms and Protocols**, edited by Tim Humphrey and Gavin Brooks, 2005
295. **Immunochemical Protocols**, *Third Edition*, edited by Robert Burns, 2005
294. **Cell Migration: Developmental Methods and Protocols**, edited by Jun-Lin Guan, 2005
293. **Laser Capture Microdissection: Methods and Protocols**, edited by Graeme I. Murray and Stephanie Curran, 2005
292. **DNA Viruses: Methods and Protocols**, edited by Paul M. Lieberman, 2005
291. **Molecular Toxicology Protocols**, edited by Phouthone Keohavong and Stephen G. Grant, 2005
290. **Basic Cell Culture Protocols**, *Third Edition*, edited by Cheryl D. Helgason and Cindy L. Miller, 2005
289. **Epidermal Cells, Methods and Applications**, edited by Kursad Turksen, 2005
288. **Oligonucleotide Synthesis, Methods and Applications**, edited by Piet Herdewijn, 2005
287. **Epigenetics Protocols**, edited by Trygve O. Tollefsbol, 2004
286. **Transgenic Plants: Methods and Protocols**, edited by Leandro Peña, 2004
285. **Cell Cycle Control and Dysregulation Protocols: Cyclins, Cyclin-Dependent Kinases, and Other Factors**, edited by Antonio Giordano and Gaetano Romano, 2004
284. **Signal Transduction Protocols**, *Second Edition*, edited by Robert C. Dickson and Michael D. Mendenhall, 2004
283. **Biconjugation Protocols**, edited by Christof M. Niemeyer, 2004
282. **Apoptosis Methods and Protocols**, edited by Hugh J. M. Brady, 2004
281. **Checkpoint Controls and Cancer, Volume 2: Activation and Regulation Protocols**, edited by Axel H. Schönthal, 2004
280. **Checkpoint Controls and Cancer, Volume 1: Reviews and Model Systems**, edited by Axel H. Schönthal, 2004
279. **Nitric Oxide Protocols**, *Second Edition*, edited by Aviv Hassid, 2004
278. **Protein NMR Techniques**, *Second Edition*, edited by A. Kristina Downing, 2004
277. **Trinucleotide Repeat Protocols**, edited by Yoshinori Kohwi, 2004
276. **Capillary Electrophoresis of Proteins and Peptides**, edited by Mark A. Strege and Avinash L. Lagu, 2004

METHODS IN MOLECULAR BIOLOGY™

Xenopus Protocols

Cell Biology and Signal Transduction

Edited by

X. Johné Liu

*Ottawa Health Research Institute
Ottawa Hospital
Ottawa, Ontario, Canada*


HUMANA PRESS  TOTOWA, NEW JERSEY

© 2006 Humana Press Inc.
999 Riverview Drive, Suite 208
Totowa, New Jersey 07512

www.humanapress.com

All rights reserved. No part of this book may be reproduced, stored in a retrieval system, or transmitted in any form or by any means, electronic, mechanical, photocopying, microfilming, recording, or otherwise without written permission from the Publisher. Methods in Molecular Biology™ is a trademark of The Humana Press Inc.

All papers, comments, opinions, conclusions, or recommendations are those of the author(s), and do not necessarily reflect the views of the publisher.

This publication is printed on acid-free paper. 
ANSI Z39.48-1984 (American Standards Institute) Permanence of Paper for Printed Library Materials.

Cover design by Patricia F. Cleary

Cover illustration: ENUCLEATION AND HEALING (*foreground*): an intact oocyte (*left*) and the extrusion of the nucleus (*right*; see complete illustration and caption on p. 38, Chap. 3). Confocal optical section of *Xenopus* oocyte (*background*; see complete figure and caption on p. 81, Chap. 6).

For additional copies, pricing for bulk purchases, and/or information about other Humana titles, contact Humana at the above address or at any of the following numbers: Tel.: 973-256-1699; Fax: 973-256-8341; E-mail: orders@humanapress.com; or visit our Website: www.humanapress.com

Photocopy Authorization Policy:

Authorization to photocopy items for internal or personal use, or the internal or personal use of specific clients, is granted by Humana Press Inc., provided that the base fee of US \$30.00 per copy is paid directly to the Copyright Clearance Center at 222 Rosewood Drive, Danvers, MA 01923. For those organizations that have been granted a photocopy license from the CCC, a separate system of payment has been arranged and is acceptable to Humana Press Inc. The fee code for users of the Transactional Reporting Service is: [1-58829-362-9/06 \$30.00].

Printed in the United States of America. 10 9 8 7 6 5 4 3 2 1

eISBN 1-59745-000-6

ISSN 1064-3745

Library of Congress Cataloging-in-Publication Data

Xenopus protocols : cell biology and signal transduction / edited by X. Johné Liu.

p. cm. -- (Methods in molecular biology ; 322)

Includes bibliographical references (p.).

ISBN 1-58829-362-9 (alk. paper)

1. Xenopus laevis--Eggs--Laboratory manuals. 2. Xenopus laevis--cytology--Laboratory manuals. 3. Cellular signal transduction --Laboratory manuals. I. Liu, X. Johné. II. Methods in molecular biology (Clifton, N.J.) ; v. 322.

QL668.E265X46 2005

571.6078--dc22

2005054573

Preface

Fully grown (stage VI) *Xenopus laevis* oocytes are very large cells, each measuring more than 1 mm in diameter, with an enormous nucleus (also called germinal vesicles) of 300 μm across. These cells are very rich in RNA, each containing up to 4.3 μg total RNA including about 40 ng poly(A)-containing RNA (mRNA), and up to 4 μg of ribosome RNA. The protein content of each oocyte is equally impressive, totaling more than 500 μg . When data are available, the quantities of specific proteins are staggering. For example, each oocyte contains an estimated 50 to 70 ng (1.25–1.75 μM) of the catalytic subunit of protein kinase A (*I*). Several thousand stage VI oocytes can be readily obtained from a single female (costing about US \$25). These oocytes are also physiologically synchronous (arrested at the diplotene stage of the first meiotic prophase) and will remain so for a considerable duration of time (routinely up to a week) when simply placed in an isotonic saline solution with appropriate antibiotics. The lack of requirement for external nutrients or other factors also means easier and better control for experimental manipulations.

Oocytes are best known for their extremely high capacity of protein synthesis—200–400 ng proteins per day per oocyte. Therefore, it is not surprising, but remarkable nonetheless, that one can measure chick brain GABA receptor activities in oocytes injected with total chick brain mRNA, as pioneered by Ricardo Miledi (*see* Chapter 24 for another innovative technique by Professor Miledi). Equally impressive, but less well known, is the assembly of infectious virus particles in frog oocytes via co-injection of genomic viral nucleic acids and capsid mRNAs (*see* Chapter 26). Frog oocytes are perhaps the only commonly used experimental model in which single cell enzymology is not only possible, but routine. For the vast majority of modern day molecular biologists who are most familiar with Western blotting, imagine that you can routinely perform anti-MAP kinase immunoblotting (developed within seconds of the addition of ECL reagents) with as little as one-tenth of a single cell! Because of this unique advantage, Ferrell's group was able to demonstrate the ultrasensitive, positive feedback-regulated, all-and-none MAP activation in single cells (*2*).

For all its advantages, a “frog oocyte facility” is easily and inexpensively assembled. For a low-budget setup, all you need are a dissecting microscope with an external fiberoptic light source (\$3000), a microinjector (\$1500–3000) and a pipet puller (\$1000). Even more important, you do not need extensive training or practice to acquire the necessary techniques, including mRNA injection, because the oocytes are so large. I was never formally trained in a “frog lab.”

Xenopus Protocols: Cell Biology and Signal Transduction is not intended to duplicate or replace the comprehensive frog book edited by Brian K. Kay and H. Benjamin Peng (*3*). Rather, it is intended to complement the Kay/Peng book by focusing on the versatility of frog oocytes and egg extracts in cell biology and signal transduction. As such, no information is included for the even more popular uses of

X. laevis as a developmental model for studying vertebrate embryogenesis. Readers interested in embryogenesis are also referred to a more recent book (4).

Readers will find that different laboratories use slightly different protocols for the same purposes (isolation of oocytes by collagenase treatment and preparation of egg extracts, just to name a couple). I have decided to allow these repetitions as it is impossible to choose one over another. In addition, some modifications may be inherent to the specific biological processes that are being investigated.

I have for many years felt that this wonderful experimental system is underutilized. I hope that *Xenopus Protocols: Cell Biology and Signal Transduction* will serve to increase awareness among the scientific community of the many possibilities that this system can offer. I am particularly intrigued by the possibility that *Xenopus* oocytes will serve prominently as a cell-based model to study functional genomics and proteomics in the postgenomic era.

X. Johné Liu

References

1. Schmitt, A. and Nebreda, A. R. (2002) Inhibition of *Xenopus* oocyte meiotic maturation by catalytically inactive protein kinase A. *Proc. Natl. Acad. Sci. USA* **99**:4361–4366.
2. Ferrell, J. E., Jr., Machleder, E. M. (1998) The biochemical basis of an all-or-none cell fate switch in *Xenopus* oocytes. *Science* **280**:895–898.
3. Kay, B. K. and Peng, H. B. (1991) *Xenopus laevis: Practical Uses in Cell and Molecular Biology*, Academic Press.
4. Sive, H. L., Grainger, R. M., and Harland, R. M., eds. (2000) *Early Development of Xenopus laevis: A Laboratory Manual*, Cold Spring Harbor Laboratory Press, Cold Spring Harbor, NY.

ACKNOWLEDGMENT

First and foremost, I would like to thank Ms. Terri van Gulik for administrative assistance, without which I would not have undertaken this project. Dr. Reiner Peters was instrumental in organizing the chapters on nucleocytoplasmic transport studies (Chapters 17–21) and recruiting authors. Dr. Catherine Morris also provided advice. I would also like to take this opportunity to thank the many colleagues who have helped in my own career transformation to the studies using *Xenopus* oocytes as a model system: Drs. Yoshio Masui, David Gard, Chris Kroll, Hazel Sive, Robert Grainger, and James Maller. Work in my laboratories has been supported by funding from the Canadian Institutes of Health Research, National Cancer Institute of Canada, Natural Sciences and Engineering Research Council of Canada, and the Ontario provincial government (in the form of a Premier's Research Excellence Award).

Contents

Preface	v
Contributors	xi
1 Resources for Genetic and Genomic Studies of <i>Xenopus</i> Steven L. Klein, Daniela S. Gerhard, Lukas Wagner, Paul Richardson, Lynn M. Schriml, Amy K. Sater, Wesley C. Warren, and John D. McPherson	1
2 The Physiology of the <i>Xenopus laevis</i> Ovary Melissa A. Rasar and Stephen R. Hammes	17
3 Oocyte Isolation and Enucleation X. Shawn Liu and X. Johné Liu	31
4 <i>Xenopus tropicalis</i> Oocytes: More Than Just a Beautiful Genome Jean-François L. Bodart and Nicholas S. Duesbery	43
5 Oocyte Expression With Injection of Purified T7 RNA Polymerase Xavier Altafaj, Nathalie Joux, Michel Ronjat, and Michel De Waard	55
6 Visualization of the Cytoskeleton in <i>Xenopus</i> Oocytes and Eggs by Confocal Immunofluorescence Microscopy Bret E. Becker and David L. Gard	69
7 Multiphoton Laser Scanning Microscopy as a Tool for <i>Xenopus</i> Oocyte Research Angela M. Prouty, Jun Wu, Da-Ting Lin, Patricia Camacho, and James D. Lechleiter	87
8 Imaging Ca ²⁺ Signals in <i>Xenopus</i> Oocytes Sheila L. Dargan, Angelo Demuro, and Ian Parker	103
9 Chromosomal DNA Replication in a Soluble Cell-Free System Derived From <i>Xenopus</i> Eggs Antonin V. Tutter and Johannes C. Walter	121
10 Chromatin Assembly of DNA Templates Microinjected Into <i>Xenopus</i> Oocytes Danièle Roche, Geneviève Almouzni, and Jean-Pierre Quivy	139
11 Pre-mRNA Splicing in the Nuclei of <i>Xenopus</i> Oocytes Kyong Hwa Moon, Xinliang Zhao, and Yi-Tao Yu	149

12	Chromatin Immunoprecipitation for Studying Transcriptional Regulation in <i>Xenopus</i> Oocytes and Tadpoles David Stewart, Akihiro Tomita, Yun-Bo Shi, and Jiemin Wong	165
13	Cytoplasmic mRNA Polyadenylation and Translation Assays María Piqué, José Manuel López, and Raúl Méndez	183
14	<i>Xenopus</i> Egg Extracts: A Model System to Study Proprotein Convertases Kathleen I. J. Shennan	199
15	Analysis of Molecular Chaperones Using a <i>Xenopus</i> Oocyte Protein Refolding Assay John J. Heikkilä, Angelo Kaldis, and Rashid Abdulle	213
16	Ubiquitin-Mediated Protein Degradation in <i>Xenopus</i> Egg Extracts Anna Castro, Suzanne Vigneron, Cyril Bernis, Jean-Claude Labbé, and Thierry Lorca	223
17	Introduction to Nucleocytoplasmic Transport: Molecules and Mechanisms Reiner Peters	235
18	Use of <i>Xenopus laevis</i> Oocyte Nuclei and Nuclear Envelopes in Nucleocytoplasmic Transport Studies Reiner Peters	259
19	Nuclear Pore Complex Structure and Plasticity Revealed by Electron and Atomic Force Microscopy Bohumil Maco, Birthe Fahrenkrog, Ning-Ping Huang, and Ueli Aebi	273
20	In Vitro Study of Nuclear Assembly and Nuclear Import Using <i>Xenopus</i> Egg Extracts Rene C. Chan and Douglass J. Forbes	289
21	Use of Intact <i>Xenopus</i> Oocytes in Nucleocytoplasmic Transport Studies Nelly Panté	301
22	Studying the Mechanosensitivity of Voltage-Gated Channels Using Oocyte Patches Catherine E. Morris, Peter F. Juranka, Wei Lin, Terence J. Morris, and Ulrike Laitko	315
23	Oocytes as an Expression System for Studying Receptor/Channel Targets of Drugs and Pesticides Steven David Buckingham, Luanda Pym, and David Barry Sattelle	331

24	Microtransplantation of Neurotransmitter Receptors From Cells to <i>Xenopus</i> Oocyte Membranes: <i>New Procedure for Ion Channel Studies</i> Ricardo Miledi, Eleonora Palma, and Fabrizio Eusebi	347
25	Reconstitution of Golgi Disassembly by Mitotic <i>Xenopus</i> Egg Extracts in Semi-Intact MDCK Cells Fumi Kano, Katsuya Takenaka, and Masayuki Murata	357
26	Exploring RNA Virus Replication in <i>Xenopus</i> Oocytes Andrea V. Gamarnik and Raul Andino	367
27	Study of Apoptosis in Vitro Using the <i>Xenopus</i> Egg Extract Reconstitution System Paula Deming and Sally Kornbluth	379
28	Studying Fertilization in Cell-Free Extracts: <i>Focusing</i> <i>on Membrane/Lipid Raft Functions and Proteomics</i> Ken-ichi Sato, Ken-ichi Yoshino, Alexander A. Tokmakov, Tetsushi Iwasaki, Kazuyoshi Yonezawa, and Yasuo Fukami	395
29	Localized Sampling, Electrophoresis, and Biosensor Analysis of <i>Xenopus laevis</i> Cytoplasm for Subcellular Biochemical Assays Christopher E. Sims, Veronica Luzzi, and Nancy L. Allbritton	413
30	Monitoring Protein Kinase A Activities Using Expressed Substrate in Live Cells Jing Wang and X. John� Liu	425
31	Using <i>Xenopus</i> Oocyte Extracts to Study Signal Transduction Richard F. Crane and Joan V. Ruderman	435
32	Oocyte Extracts for the Study of Meiotic M–M Transition Keita Ohsumi, Tomomi M. Yamamoto, and Mari Iwabuchi	445
33	Methods for Studying Spindle Assembly and Chromosome Condensation in <i>Xenopus</i> Egg Extracts Thomas J. Maresca and Rebecca Heald	459
Index	475

Contributors

- RASHID ABDULLE • *Department of Biology, University of Waterloo, Waterloo, Ontario, Canada*
- UELI AEBI • *M. E. Müller Institute for Structural Biology, Biozentrum, University of Basel, Basel, Switzerland*
- NANCY L. ALLBRITTON • *Department of Physiology and Biophysics, University of California Irvine, Irvine, CA*
- GENEVIÈVE ALMOUZZI • *Research Section, Institut Curie, UMR218 du Centre National de la Recherche Scientifique (CNRS), Paris, France*
- XAVIER ALTAFAJ • *Canaux Calciques, Fonctions et Pathologies, CEA, Département Réponse et Dynamique Cellulaire, Inserm U607, Grenoble, France*
- RAUL ANDINO • *Department of Microbiology and Immunology, University of California, San Francisco, San Francisco, CA*
- BRET E. BECKER • *Department of Biology, University of Utah, East Salt Lake City, UT*
- CYRIL BERNIS • *Centre de Recherche de Biochimie Macromoléculaire, CNRS FRE 2593, Montpellier, France*
- JEAN-FRANÇOIS L. BODART • *Laboratoire de Biologie du Développement, UPRES EA3, Université des sciences et technologies de Lille, Lille, France*
- STEVEN DAVID BUCKINGHAM • *MRC Functional Genetics Unit, Department of Human Anatomy and Genetics, University of Oxford, Oxford, UK*
- PATRICIA CAMACHO • *Department of Physiology, University of Texas Health Science Center at San Antonio, San Antonio, TX*
- ANNA CASTRO • *Centre de Recherche de Biochimie Macromoléculaire, CNRS FRE 2593, Montpellier, France*
- RENE C. CHAN • *Section of Cell and Developmental Biology, Division of Biological Sciences, University of California, San Diego, San Diego, CA*
- RICHARD F. CRANE • *Department of Cell Biology, Harvard Medical School, Boston, MA*
- SHEILA L. DARGAN • *Department of Neurobiology and Behavior, McGaugh Hall, University of California Irvine, Irvine, CA*
- PAULA DEMING • *Department of Pharmacology and Cancer Biology, Duke University, Durham, NC*
- ANGELO DEMURO • *Department of Neurobiology and Behavior, McGaugh Hall, University of California Irvine, Irvine, CA*
- MICHEL DE WAARD • *Canaux Calciques, Fonctions et Pathologies, CEA, Département Réponse et Dynamique Cellulaire, Inserm U607, Grenoble, France*
- NICHOLAS S. DUESBERY • *Laboratory of Developmental Cell Biology, Van Andel Research Institute, Grand Rapids, MI*

- FABRIZIO EUSEBI • *Istituto Pasteur–Fondazione Cenci Bolognetti, Dipartimento di Fisiologia Umana e Farmacologia, Centro di Eccellenza Biologia e Medicina Molecolare, Università di Roma La Sapienza, Roma, Italia*
- BIRTHE FAHRENKROG • *M. E. Müller Institute for Structural Biology, Biozentrum, University of Basel, Basel, Switzerland*
- DOUGLASS J. FORBES • *Section of Cell and Developmental Biology, Division of Biological Sciences, University of California, San Diego, San Diego, CA*
- YASUO FUKAMI • *Research Center for Environmental Genomics, Kobe University, Kobe, Japan*
- ANDREA V. GAMARNIK • *Fundacion Instituto Leloir, Buenos Aires, Argentina*
- DAVID L. GARD • *Department of Biology, University of Utah, Salt Lake City, UT*
- DANIELA S. GERHARD • *Office of Cancer Genomics, National Cancer Institute, Bethesda, MD*
- STEPHEN R. HAMMES • *Division of Endocrinology and Metabolism, Department of Internal Medicine ; Department of Pharmacology, University of Texas Southwestern Medical Center at Dallas, Dallas, TX*
- REBECCA HEALD • *Department of Molecular and Cell Biology, University of California Berkeley, Berkeley, CA*
- JOHN J. HEIKKILA • *Department of Biology, University of Waterloo, Waterloo, Ontario, Canada*
- NING-PING HUANG • *M. E. Müller Institute for Structural Biology, Biozentrum, University of Basel, Basel, Switzerland*
- MARI IWABUCHI • *Laboratory of Cell and Developmental Biology, Graduate School of Bioscience and Biotechnology, Tokyo Institute of Technology, Yokohama, Japan*
- TETSUSHI IWASAKI • *Research Center for Environmental Genomics, Kobe University, Kobe, Japan*
- NATHALIE JOUX • *Canaux Calciques, Fonctions et Pathologies, CEA, Département Réponse et Dynamique Cellulaire, Inserm U607, Grenoble, France*
- PETER F. JURANKA • *Department of Medicine, University of Ottawa; Neuroscience, Ottawa Health Research Institute, Ottawa Hospital, Ottawa, Ontario, Canada*
- ANGELO KALDIS • *Department of Biology, University of Waterloo, Waterloo, Ontario, Canada*
- FUMI KANO • *Department of Life Sciences, Graduate School of Arts and Sciences, The University of Tokyo, Tokyo, Japan*
- STEVEN L. KLEIN • *Developmental Biology, Genetics, and Teratology Branch, National Institute of Child Health and Human Development, Rockville, MD*
- SALLY KORNBLOTH • *Department of Pharmacology and Cancer Biology, Duke University, Durham, NC*
- JEAN-CLAUDE LABBÉ • *Centre de Recherche de Biochimie Macromoléculaire, CNRS FRE 2593, Montpellier, France*
- ULRIKE LAITKO • *Department of Medicine, University of Ottawa; Neuroscience, Ottawa Health Research Institute, Ottawa Hospital, Ottawa, Ontario, Canada*
- JAMES D. LECHLEITER • *Department of Cellular and Structural Biology, University of Texas Health Science Center at San Antonio, San Antonio, TX*

- DA-TING LIN • *Department of Neuroscience, Johns Hopkins University School of Medicine, Baltimore, MD*
- WEI LIN • *Department of Medicine, University of Ottawa; Neuroscience, Ottawa Health Research Institute, Ottawa Hospital, Ottawa, Ontario, Canada*
- X. JOHNÉ LIU • *Department of Biochemistry, Microbiology, and Immunology, University of Ottawa; Ottawa Health Research Institute, Ottawa Hospital, Ottawa, Ontario, Canada*
- X. SHAWN LIU • *Department of Biochemistry, Microbiology and Immunology, University of Ottawa; Ottawa Health Research Institute, Ontario, Canada*
- JOSÉ MANUEL LÓPEZ • *Program of Gene Expression, Centre de Regulació Genòmica (CRG), Barcelona, Spain*
- THIERRY LORCA • *Centre de Recherche de Biochimie Macromoléculaire, CNRS FRE 2593, Montpellier, France*
- VERONICA LUZZI • *Department of Physiology and Biophysics, University of California Irvine, Irvine, CA*
- BOHUMIL MACO • *M. E. Müller Institute for Structural Biology, Biozentrum, University of Basel, Basel, Switzerland*
- THOMAS J. MARESCA • *Department of Molecular and Cell Biology, University of California Berkeley, Berkeley, CA*
- JOHN D. MCPHERSON • *Genome Sequencing Center, Baylor University School of Medicine, Houston, TX*
- RAÚL MÉNDEZ • *Program of Gene Expression, Centre de Regulació Genòmica (CRG), Barcelona, Spain*
- RICARDO MILEDI • *Instituto de Neurobiología, Campus UNAM-Juriquilla, API Querétaro, México; Laboratory of Cellular and Molecular Neurobiology, Department of Neurobiology and Behavior, University of California Irvine, Irvine, CA*
- KYONG HWA MOON • *Department of Biochemistry and Biophysics, University of Rochester Medical Center, Rochester, NY*
- CATHERINE E. MORRIS • *Department of Medicine, University of Ottawa; Neuroscience, Ottawa Health Research Institute, Ottawa Hospital, Ottawa, Ontario, Canada*
- TERENCE J. MORRIS • *Department of Medicine, University of Ottawa; Neuroscience, Ottawa Health Research, Institute Ottawa Hospital, Ottawa, Ontario, Canada*
- MASAYUKI MURATA • *Department of Life Sciences, Graduate School of Arts and Sciences, The University of Tokyo, Tokyo, Japan*
- KEITA OHSUMI • *Laboratory of Cell and Developmental Biology, Graduate School of Bioscience and Biotechnology, Tokyo Institute of Technology, Yokohama, Japan*
- ELEANORA PALMA • *Instituto Pasteur, Fondazione Cenci Bologhetti, Dipartimento de Fisiologia Umana e Farmacologia, Università di Roma La Sapienza, Roma, Italia*
- NELLY PANTÉ • *Department of Zoology, University of British Columbia, Vancouver, British Columbia, Canada*
- IAN PARKER • *Department of Neurobiology and Behavior, University of California Irvine, Irvine, CA*

- REINER PETERS • *Institute of Medical Physics and Biophysics and Center for Nanotechnology (CeNTech), University of Münster, Münster, Germany*
- MARIA PIQUÉ • *Centre de Regulació Genòmica (CRG), Program of Gene Expression, Barcelona, Spain*
- ANGELA M. PROUTY • *Department of Cellular and Structural Biology, University of Texas Health Science Center at San Antonio, San Antonio, TX*
- LUANDA PYM • *MRC Functional Genetics Unit, Department of Human Anatomy and Genetics, University of Oxford, Oxford, UK*
- JEAN-PIERRE QUIVY • *Research Section, Institut Curie, UMR218 du Centre National de la Recherche Scientifique (CNRS), Paris, France*
- MELISSA A. RASAR • *Department of Internal Medicine, Division of Endocrinology and Metabolism; Department of Pharmacology, University of Texas Southwestern Medical Center at Dallas, Dallas, TX*
- PAUL RICHARDSON • *Functional Genomics, Department of Energy Joint Genome Institute, Walnut Creek, CA*
- DANIÈLE ROCHE • *Research Section, Institut Curie, UMR218 du Centre National de la Recherche Scientifique (CNRS), Paris, France*
- MICHEL RONJAT • *Département Réponse et Dynamique Cellulaire, Inserm U607, Canaux Calciques, Fonctions et Pathologies, CEA, Grenoble, France*
- JOAN V. RUDERMAN • *Department of Cell Biology, Harvard Medical School, Boston, MA*
- AMY K. SATER • *Department of Biology and Biochemistry, University of Houston, Houston, TX*
- KEN-ICHI SATO • *Research Center for Environmental Genomics, Kobe University, Kobe, Japan.*
- DAVID BARRY SATTELLE • *MRC Functional Genetics Unit, Department of Human Anatomy and Genetics, University of Oxford, Oxford, UK*
- LYNN M. SCHRIML • *National Center for Biotechnology Information, National Library of Medicine, Bethesda, MD*
- KATHLEEN I. J. SHENNAN • *Institute of Medical Sciences, School of Medical Sciences, College of Life Sciences and Medicine, University of Aberdeen, Aberdeen, UK*
- YUN-BO SHI • *Section on Molecular Morphogenesis, Laboratory of Gene Regulation and Development, National Institute of Child Health and Human Disease, National Institutes of Health, Bethesda, MD*
- CHRISTOPHER E. SIMS • *Department of Physiology and Biophysics, University of California Irvine, Irvine, CA*
- DAVID STEWART • *Department of Molecular and Cellular Biology, Baylor College of Medicine, Houston, TX*
- KATSUYA TAKENAKA • *Department of Radiation Genetics, Graduate School of Medicine, Kyoto University, Kyoto, Japan*
- ALEXANDER A. TOKMAKOV • *Genome Sciences Center, RIKEN Yokohama Institute, Yokohama, Japan*

- AKIHIRO TOMITA • *Section on Molecular Morphogenesis, Laboratory of Gene Regulation and Development, National Institute of Child Health and Human Disease, National Institutes of Health, Bethesda, MD*
- ANTONIN V. TUTTER • *Novartis Institutes for Biomedical Research, Cambridge, MA*
- SUZANNE VIGNERON • *Centre de Recherche de Biochimie Macromoléculaire, CNRS FRE 2593, Montpellier, France*
- LUKAS WAGNER • *National Center for Biotechnology Information, National Library of Medicine, Bethesda, MD*
- JOHANNES C. WALTER • *Biological Chemistry and Molecular Pharmacology, Harvard Medical School, Boston, MA*
- JING WANG • *Department of Biochemistry, Microbiology, and Immunology, University of Ottawa; Ottawa Health Research Institute, Ottawa, Ontario, Canada*
- WESLEY C. WARREN • *Genome Sequencing Center, Washington University School of Medicine, St. Louis, MO*
- JIEMIN WONG • *Department of Molecular and Cellular Biology, Baylor College of Medicine, Houston, TX*
- JUN WU • *Department of Cellular and Structural Biology, University of Texas Health Science Center at San Antonio, San Antonio, TX*
- TOMOMI M. YAMAMOTO • *Laboratory of Cell and Developmental Biology, Graduate School of Bioscience and Biotechnology, Tokyo Institute of Technology, Yokohama, Japan*
- KAZUYOSHI YONEZAWA • *Biosignal Research Center, Kobe University, Kobe; CREST, Japan Science and Technology Agency, Kawaguchi, Japan*
- KEN-ICHI YOSHINO • *Biosignal Research Center, Kobe University, Kobe; CREST, Japan Science and Technology Agency, Kawaguchi, Japan*
- YI-TAO YU • *Department of Biochemistry and Biophysics, University of Rochester Medical Center, Rochester, NY*
- XINLIANG ZHAO • *Department of Biochemistry and Biophysics, University of Rochester Medical Center, Rochester, NY*

Resources for Genetic and Genomic Studies of *Xenopus*

Steven L. Klein, Daniela S. Gerhard, Lukas Wagner,
Paul Richardson, Lynn M. Schriml, Amy K. Sater,
Wesley C. Warren, and John D. McPherson

Summary

The National Institutes of Health *Xenopus* Initiative is a concerted effort to interact with the *Xenopus* research community to identify the community's needs; to devise strategies to meet those needs; and to support, oversee, and coordinate the resulting projects. This chapter provides a brief description of several genetic and genomic resources generated by this initiative and explains how to access them. The resources described in this chapter are (1) complementary deoxyribonucleic acid (cDNA) libraries and expressed sequence tag (EST) sequences; (2) UniGene clusters; (3) full-insert cDNA sequences; (4) a genetic map; (5) genomic libraries; (6) a physical map; (7) genome sequence; (8) microarrays; (9) mutagenesis and phenotyping; and (10) bioinformatics. The descriptions presented here were based on data that were available at the time of manuscript submission. Because these are ongoing projects, they are constantly generating new data and analyses. The Web sites cited in each subheading present current data and analyses.

Key Words: BAC libraries; bioinformatics; cDNA; EST; genome sequencing; linkage map; microarrays; mutagenesis; phenotyping; physical map; UniGene; *Xenopus laevis*; *Xenopus tropicalis*.

1. Introduction

Xenopus is a major model for many areas of cell and developmental biology. The value of *Xenopus* as a model organism engendered numerous dialogues between the US National Institutes of Health (NIH) and the *Xenopus* research community to identify resources that would benefit *Xenopus* research. Those discussions led to a group of recommendations that resulted in the NIH *Xenopus* Initiative. The process that led to the recommendations, a complete list of the recommendations, and the activities of the NIH *Xenopus* Initiative have been reviewed ([1](#)) and are not recounted here. Instead, this chapter provides a brief description of several genetic and genomic resources that are being generated by this initiative and explains how to access those

resources. The descriptions presented here were based on data available at the time of manuscript submission. Because these are ongoing projects, they are constantly generating new data and analyses. The Web sites cited in each subheading present current data and analyses.

The *Xenopus* resources described in this chapter are (1) complementary deoxyribonucleic acid (cDNA) libraries and expressed sequence tag (EST) sequences; (2) UniGene clusters; (3) full-insert cDNA sequences; (4) a genetic map; (5) genomic libraries; (6) a physical map; (7) genome sequence; (8) microarrays; (9) mutagenesis and phenotyping; and (10) bioinformatics. These resources are generated by numerous research groups throughout the world. However, this review emphasizes the projects that are part of the NIH *Xenopus* Initiative (<http://www.nih.gov/science/models/Xenopus/>). A major strength of the NIH projects is that their resources are available to the worldwide community without restriction. That is, their sequence data are deposited in publicly available databases, their clones are available from distributors, and their mutant stains are available from individual laboratories. This chapter explains how to access these resources.

The NIH *Xenopus* Initiative is a concerted effort to interact with the *Xenopus* research community to identify the community's needs; to identify strategies to meet those needs; and to support, oversee, and coordinate the resulting projects. This initiative is supported and overseen by representatives of 10 NIH institutes and centers, who form the Trans-NIH *Xenopus* Working Group. Many of the activities are being performed by large national projects.

For example, the cDNA libraries, EST sequencing, UniGene clusters, and full-insert sequencing are part of the National Cancer Institute's Cancer Genome Anatomy Project (CGAP) and Mammalian Gene Collection (MGC; *see ref. 2*). These activities have been, and are being performed by many groups, including Lawrence Livermore National Laboratory, Washington University Genome Sequencing Center, Canada's Michael Smith Genome Sciences Center, the NIH Intramural Sequencing Center, and NIH's National Center for Biotechnology Information (NCBI). The genomic libraries and physical map are being made as part of the NIH Bacterial Artificial Chromosome (BAC) Resource Network and the NIH Genome Sequencing Consortium. In addition, the *X. tropicalis* genome is being sequenced by the US Department of Energy's Joint Genome Institute (JGI). These associations show that *Xenopus* is acknowledged as an important component of NIH's goal to determine the basis of human health and disease.

Unlike other models that have been selected for genetic and genomic resource development, we are developing resources for two *Xenopus* species at the same time: *X. laevis* and *X. tropicalis*. The community recommended generating tools for both species for several reasons. First, although most of the community currently uses *X. laevis*, a significant and growing proportion is beginning to use *X. tropicalis*. Second, the species' close similarity means that some of the resources for each can be useful for research on both species. These similarities include a high degree of developmental similarity as well as a high degree of cross reactivity of antibodies and cDNA probes.

Third, *X. tropicalis* offers the significant advantage that it should be amenable to genetic manipulation. This opportunity stems from the facts that it has a shorter generation time than *X. laevis* and that its genome is diploid (whereas *X. laevis* is pseudotetraploid). This means that *X. tropicalis* can be used to generate lines of mutant and transgenic *Xenopus*. These lines would enable genetic analyses to be included with the other types of analyses at which *Xenopus* already excels.

Fourth, *X. tropicalis* offers several advantages for cell biology research that are not related to their genetics. For example, many of its oocytes' properties may make it more amenable for studies of cellular properties, including the mechanistic details of meiosis (see ref. 3).

Fifth, the development of genomic resources represents an investment in future genetic research with *Xenopus*. Finally, sequence information from *Xenopus* will help to annotate the genomes of other animals because of its position in the phylogenetic tree and because of its superior ability to study gene function.

2. Resources

2.1. cDNA Libraries and EST Sequences

The NIH *Xenopus* Initiative includes cDNA libraries that are part of the IMAGE (Integrated Molecular Analysis of Genomes and Their Expression) Consortium gene collection. The collection currently contains 52 *X. laevis* libraries and 12 *X. tropicalis* libraries (Table 1). Details of each library can be found at the IMAGE Web site (<http://image.llnl.gov/>) and at NCBI's UniGene library browsers (<http://www.ncbi.nlm.nih.gov/UniGene/lbrowse2.cgi?TAXID=8355> and <http://www.ncbi.nlm.nih.gov/UniGene/lbrowse2.cgi?TAXID=8364> for *X. laevis* and *X. tropicalis*, respectively). The IMAGE cDNA clones are available to the research community, as explained at <http://image.llnl.gov/image/html/idistributors.shtml>.

Library quality was determined by sequencing the ends of several thousand clones from each library to estimate average insert length and transcript diversity. Libraries with inserts that averaged over 1 kb and had sufficient diversity were used to sequence many ESTs (see Table 2 in Subheading 2.3.). IMAGE libraries were used to generate sequence for over 325,000 ESTs (about 250,000 for *X. laevis* and about 75,000 for *X. tropicalis* as of November 2004).

These ESTs form the nucleus of NCBI's *Xenopus* database of ESTs (dbEST), which contained about 450,000 *X. laevis* ESTs and about 425,000 *X. tropicalis* ESTs in November 2004 (see current data at http://www.ncbi.nlm.nih.gov/dbEST/dbEST_summary.html). The other ESTs in dbEST were, and are being, sequenced by a variety of projects throughout the world, with major contributions from the UK's Sanger Center (http://www.sanger.ac.uk/Projects/X_tropicalis/) and from Japan's National Institute of Basic Biology (<http://Xenopus.nibb.ac.jp/>). The combined number of *Xenopus* ESTs in dbEST, about 875,000, is more than that of any other animal, with the exception of the human and the mouse. *Xenopus* EST traces are available at NCBI's Trace Archive (www.ncbi.nlm.nih.gov/Traces/trace.cgi?cmd=fstat&f=full_stat&m=stat&s=full_stat).

Table 1
IMAGE Consortium's *Xenopus* Library Official Names^a

Xenopus laevis IMAGE cDNA libraries

Oocyte

NICHD_XGC_OO1
Wellcome/CRC pRN3 oocyte
X. laevis oocytes, stages 5–6 mixed
Xenopus laevis oocyte [normalized]

Egg

RIKEN *Xenopus* egg
Soares NXEG [normalized]
Wellcome/CRC pcDNAI egg
Wellcome/CRC pSK egg
X. laevis unfertilized egg

Whole embryo

OW stage 6
NICHD_XGC_Emb1 [stage 10]
Kirschner embryo st.10–14
Wellcome/CRC pSK st.10.5
Wellcome/CRC pcDNAI st.10.5
Wellcome/CRC pRN3 st.10.5
X. laevis gastrula, stages 10.5–11.5
OW stage 11
Wellcome/CRC pcDNAI st.12
Xenla_13
Wellcome/CRC pRN3 st.13–17
NICHD_XGC_Emb2 [stages 17/18]
Harland stage 19-23
Wellcome/CRC pCS2+ st.19–26
Wellcome/CRC pRN3 st.19–26
Xenopus laevis tadpole stage 24
NICHD_XGC_Emb3 [stages 24/25]
Wellcome/CRC pcDNAI st.24–26
Wellcome/CRC pRN3 st.24–26
NICHD_XGC_Emb4 [stages 31/32]
NICHD_XGC_Tad 1 [stages 53]
NICHD_XGC Tad 2 [stages 62]

Adult tissues

Harland ovary NICHD_XGC_Ov1 [ovary]
NICHD_XGC_Brn1 [brain]
NICHD_XGC_Eye1 [eye]

Xenopus laevis IMAGE cDNA libraries

NICHD_XGC_He1 [heart]
NICHD_XGC_Kid1 [kidney]
NICHD_XGC_Li1 [liver]
NICHD_XGC_Lu1 [lung]
NICHD_XGC_Sp1 [spleen]
NICHD_XGC_Te1 [testis]
NICHD_XGC_Te2 [testis]
NICHD_XGC_Te2N [normalized testis]

Hyperdorsalized embryos

Xenla_13LiCl [stage 13, LiCl treated]
Cho Li-treated gastrula

Embryo regions

Wellcome/CRC pSK animal cap
Wellcome/CRC pRN3 dorsal lip
Blumberg_Cho *Xenopus laevis* organizer
Wellcome/CRC pRN3 head (st.30)
Wellcome/CRC pRN3 tail (st.30)

Subtracted libraries

Wellcome/CRC pRN3 st.13–17 egg/an cap [egg library minus stages 13–17 An. Cap]
Wellcome/CRC pRN3 st.19–26 egg/an cap [egg library minus stages 19–26 An. Cap]

Xenopus tropicalis IMAGE cDNA libraries

Egg

Wellcome/CRC pCS107 tropicalis egg

Whole embryo

Wellcome/CRC pCS107 tropicalis st.10–12
NICHD_XGC_Emb5 [stages 10–13]
NICHD_XGC_Emb6 [stages 14–19]
NICHD_XGC_Emb7 [stages 20–27]
NICHD_XGC_Emb8 [stages 40–45]
XtSt10-30 [normalized]

Adult tissues

NIH_XGC_tropInt [intestine]
NIH_XGC_tropKid [kidney]
NIH_XGC_tropSkeMus [skeletal muscle]

Whole adult

NICHD_XGC_Swb1
NICHD_XGC_Swb1N [normalized]

^aAvailable in November 2004, listed by embryonic stage and tissue type. Each library's name indicates its provider and source. Libraries designated "NICHD_XGC_xxx" were constructed by the XGC project from tissue provided by *Xenopus* laboratories. Additional details are shown in the brackets. A complete description of each library is at http://image.llnl.gov/image/html/Xenopuslib_info.shtml.

Table 2
Analysis of *Xenopus* cDNA Libraries for Full-Insert Sequencing^a

<i>X. laevis</i>						
Seqs	%Divers	%CDS-OK	InLen	AlnLen	%FLDivers	Library
5863	49.8	0.685	1394.6	660.0	34.1	NICHD_XGC_Te2N
2518	66.4	0.494	1665.0	408.9	32.8	<i>Xenopus laevis</i> oocyte nonnormalized
11,720	46.4	0.701	1829.5	599.9	32.5	NICHD_XGC_Ov1
2407	41.1	0.790	1329.1	544.9	32.5	NICHD_XGC_Te1
3231	56.3	0.522	1873.4	380.9	29.4	NICHD_XGC_Emb3
6016	44.2	0.609	1816.1	416.9	26.9	NICHD_XGC_Lu1
3072	55.2	0.482	1503.6	423.0	26.6	<i>Xenopus laevis</i> unfertilized egg cDNA library
3932	39.6	0.665	1866.3	434.6	26.3	NICHD_XGC_Li1
15,786	35.5	0.670	1791.2	553.2	23.8	NICHD_XGC_Sp1
9662	35.9	0.631	1765.8	665.7	22.7	NICHD_XGC_Kid1
9641	31.1	0.719	1659.6	595.5	22.4	Wellcome CRC pSK egg
3579	56.4	0.384	1190.9	376.0	21.7	<i>Xenopus laevis</i> gastrula nonnormalized
12,318	34.7	0.608	1594.8	598.4	21.1	NICHD_XGC_Eye1
12,230	27.9	0.735	1307.2	669.8	21.0	NICHD_XGC_Te2
22,248	29.9	0.682	1943.0	632.4	20.4	NICHD_XGC_Emb4
14,703	29.1	0.680	2235.5	669.2	19.8	NICHD_XGC_OO1
4496	34.4	0.565	1555.8	451.3	19.4	NICHD_XGC_He1
15,779	32.3	0.588	1962.7	648.0	19.0	NICHD_XGC_Emb1
11,005	33.2	0.570	1529.6	612.0	18.9	NICHD_XGC_Brn1

10,474	35.0	0.468	1390.0	589.7	16.4	NICHD_XGC_Tad1
8672	28.7	0.569	1717.4	597.5	16.3	NICHD_XGC_Emb2
13,898	28.6	0.463	1142.6	571.9	13.2	NICHD_XGC_Tad2
3960	57.6	0.143	1351.6	336.0	8.24	Blumberg_Cho dorsal blastopore lip

X. tropicalis

4203	31.3	1.000	560.2	528.9	31.3	NICHD_XGC_Swb1
9248	36.1	0.857	1220.3	625.0	30.9	NICHD_XGC_Emb7
6367	38.2	0.696	632.6	519.0	26.6	NICHD_XGC_Swb1N
10,139	32.3	0.700	1500.1	619.0	22.6	NICHD_XGC_Emb6
9864	28.8	0.643	1580.9	410.0	18.5	XtSt10-30
10981	31.9	0.514	1519.5	568.0	16.4	NICHD_XGC_Emb5

^acDNA libraries used for full-insert sequencing listed in order of the proportion of distinct sequences with full-length inserts (%FLDivers, column 6). Data are from November 2004. The fraction of the total sequences that have complete coding sequences (CDS) is indicated by column 3 (%CDS-OK), which is the ratio of known-gene-complete ESTs/known-gene-complete ESTs plus known-gene-incomplete ESTs. The number of distinct full-length clones expected per 100 ESTs (%FL Divers, column 6) is the proportion of clones with complete CDSs (%CDS-OK) times the library's diversity (%Divers). For libraries that have more than 40% complete CDSs, the proportion of distinct sequences with full inserts indicates the probability that sequenced inserts will be unique. Seqs, number of EST sequences; %Divers, percentage diversity: $100 \times \text{Genes/Clone}$; %CDS-OK, fraction of 5' ESTs that have complete coding sequences by comparison with reference sequences; InLen, mean predicted insert length of clones that match reference sequences; AlnLen, observed alignment length of clones that match reference sequences; %FLDivers, the proportion of full-length diverse clones within the library; EST, expressed sequence tag.

2.2. UniGene Clusters

Computational methods have been developed that predict transcriptional units from EST sequences. NCBI's UniGene project used an experimental algorithm to group hundreds of thousands of *Xenopus* dbEST sequences into a set of about 20,000 gene-oriented clusters (see <http://www.ncbi.nlm.nih.gov/entrez/query.fcgi?db=unigene>). The analyses included *Xenopus* messenger RNAs (mRNAs) and draft or high-throughput cDNA (HTC) sequences (HTC) available from GenBank. UniGene predicted that ~360,000 of the *X. laevis* sequences available in September 2004 represented about 24,000 gene-oriented clusters, and that approx 350,000 of the available *X. tropicalis* sequences represented about 15,000 gene-oriented clusters (**Table 3**). The current distribution of *X. laevis* and *X. tropicalis* UniGene clusters may be accessed at <http://www.ncbi.nlm.nih.gov/UniGene/UGOrg.cgi?TAXID=8355> and <http://www.ncbi.nlm.nih.gov/UniGene/UGOrg.cgi?TAXID=8364>, respectively. These clusters are very useful for discovering new genes and for determining gene function. They play a critical role in identifying cDNA clones for full-insert sequencing (see **Subheading 2.3.**) and in selecting oligonucleotides for microarrays (see **Subheading 2.8.**).

In general, the number of clusters predicted by the UniGene algorithm is greater than the actual number of protein-coding genes. This is because of the presence of transcribed sequences that do not encode proteins. For example, the number of human clusters assembled by the UniGene method (about 50,000) is larger than the predicted number of human protein-coding genes (about 23,000). Thus, only a proportion of the *Xenopus* UniGene clusters will be genes with distinct protein products.

The extent to which UniGene overestimates the number of genes depends on the proportion of clusters containing only one sequence, which may not be independent transcripts. About 15% of the *Xenopus* UniGene clusters contained only one sequence (vs 20% for the human UniGene). In fact, only about half of the annotated human protein-coding genes (human genome build 34.3) have a *Xenopus* homologue within this set of sequences. Thus, this project has only identified a proportion of *Xenopus* protein-coding genes so far. It will progressively identify more genes as it continues analyzing sequences that become available. The clusters that have the highest probability of being protein-coding genes are those with the larger cluster sizes.

2.3. Full-Insert cDNA Sequences

The NIH *Xenopus* Gene Collection (XGC) project is identifying and sequencing representative clones with predicted complete coding sequences (CDSs) of a finite number of *X. laevis* and *X. tropicalis* genes (see **ref. 2** for additional details). The proportion of clones with complete CDSs within each library was determined by aligning the 5' ESTs corresponding to known *Xenopus* genes with the sequence of the full-length clone. The libraries with a high proportion of complete CDS clones were selected for additional 5' sequencing. Twenty-one of the *X. laevis* libraries and six of the *X. tropicalis* libraries had a full-length fraction over 40% (**Table 2**, %CDS-OK).

A clone is selected for full-insert sequencing if its 5' sequence meets either of two criteria: (1) a BLAST search against well-characterized, complete *Xenopus* mRNA finds a starting methionine and an alignment of at least 95% identity over at least

Table 3
***Xenopus* UniGene Statistics, November 2004^a**

	<i>X. laevis</i>	<i>X. tropicalis</i>
A. Sequences included		
mRNA	10,451	5243
HTC	278	60
EST, 3' reads	130,639	124,813
EST, 5' reads	222,515	220,567
EST, other/unknown	86	543
Total sequences included	363,969	351,226
B. Number of clusters		
Containing at least one mRNA	8378	3777
Containing at least one HTC	270	60
Containing at least one EST	23,641	15,070
Containing both mRNAs and ESTs	7934	3710
Total clusters	24,087	15,137
C. Number of times portions of each predicted gene has been sequenced		
1	3968	2191
2	3293	1979
3-4	3885	2080
5-8	3836	2369
9-16	3739	2252
17-32	2861	1969
33-64	1592	1266
65-128	621	614
129-256	195	247
257-512	73	122
513-1024	20	39
1025-2048	3	10
2049-4096	1	2
4097-8192	—	1

^a**“Subheading A.** shows the total number of sequences included in the analysis and the number of sequences that are full-length or characterized mRNAs, “draft” or HTCs, or ESTs. **Subheading B.** shows the number of unique genes (total clusters) predicted to exist within these sequences and the number of clusters that contain mRNAs, HTCs, or ESTs. **Subheading C.** shows the number of times portions of predicted genes are represented in the total number of sequences. For example, portions of EF1alpha (the 1’s) have been sequenced thousands of times (= large cluster size), whereas thousand of other genes have had only one portion sequenced. Statistics from *X. laevis* UniGene Build 59. EST sequences are from dbEST, and genes are from GenBank; both values are as of September 11, 2004. Statistics from *X. tropicalis* UniGene Build 20. EST sequences are from dbEST, and genes are from GenBank; both values are as of September 11, 2004.

100 nucleotides or (2) a translating BLAST search against proteins from organisms with genomes that have been sequenced finds both a starting methionine and an alignment of the sequences with an e-value of at most 10^{-6} , except for the region at the protein's N-terminus. This region is excepted because many distant homologues do not have well-conserved N-termini and a clone may be a candidate for full length sequencing if the length of non-alignment is the same in the *Xenopus* cDNA and the orthologous protein(s).

As of November 2004, about 7000 *X. laevis* genes from 17 XGC libraries and about 2000 *X. tropicalis* genes from 7 XGC libraries have completely sequenced representative clones (<http://xgc.nci.nih.gov/>). All clones generated by the XGC are publicly available to the biomedical research community through the IMAGE Consortium distributors (<http://xgc.nci.nih.gov/Info/Buy>). The project aims to generate a total of about 16,000 clones with complete CDSs divided between the two *Xenopus* species within the next few years. Clones that are currently scheduled for full-insert sequencing are listed at <http://xgc.nci.nih.gov/Genes/PL?ORG=X1> and <http://xgc.nci.nih.gov/Genes/PL?ORG=Str> for *X. laevis* and *X. tropicalis*, respectively.

2.4. Genetic Map

A genetic map is under construction by the Houston Tropicalis Project, a collaboration between the University of Houston and the Human Genome Sequencing Center at Baylor College of Medicine. The project will generate a linkage map of 5000 simple sequence length polymorphisms (SSLPs, also known as microsatellites) by early 2007. SSLPs are identified by bioinformatic analysis of the *X. tropicalis* genome sequence to identify tri- and tetranucleotide simple sequence repeats (SSRs) of $n = 10$ or greater [e.g., (CAT) n or (CAGT) n , $n \geq 10$]. These sequences are then amplified by polymerase chain reaction of DNA from the parental strains to determine whether there are differences in the length of the repeat, which are revealed by differences in the size of the amplified fragment.

Initial studies indicate that approx 70% of trinucleotide SSRs over 30 bp are polymorphic, and thus they may be usable as SSLPs for mapping. Trinucleotide and tetranucleotide SSRs are estimated to occur at a frequency of 1/20 to 30 kb in vertebrate genomes (based on **ref. 4**), so the *X. tropicalis* genome is likely to include 40,000 to 80,000 SSRs. These estimates indicate that it will be possible to identify many more SSLPs than are needed for this initial mapping project.

These SSLPs will be amplified on the DNA from approx 500 F2 individuals produced from a single original cross of a Nigerian F7 male and an Ivory Coast F5 female. Given the number of F2 individuals represented in the mapping panel, the map will be based on 1000 informative meioses, yielding a theoretical limit of resolution of 0.1 cM. Genotyping is based on an analysis of amplified fragment sizes. Linkage analysis (frequencies of cosegregation between pairs of markers) will be used to identify linkage groups, establish marker order within a linkage group, and estimate intermarker distance. Linkage analyses will be performed by MAPMAKER or similar programs, which also allow assembly of the final map.

To aid in mapping mutations, the map, markers, and primer sequences will be incorporated in NCBI's UniSTS database (www.ncbi.nlm.nih.gov/entrez/query.fcgi?db=

unists) as they become available. An initial database of primer sequences and 900 markers representing about 100 scaffolds was posted in November 2004 at <http://tropmap.biology.uh.edu/>; additional markers will be incorporated as they are identified. Marker and map location information submitted to UniSTS will be used to connect marker and Entrez Gene records, allowing mapping data to be associated with XGC clones as part of the ongoing Entrez Gene-MGC collaboration. Genetic and physical maps will be available when completed at NCBI's Map Viewer (www.ncbi.nlm.nih.gov/mapview/) with connections to UniGene, Entrez Gene, and UniSTS. Links to UniSTS and Map Viewer are also available through NCBI's *Xenopus* Genome Resources site (www.ncbi.nlm.nih.gov/genome/guide/frog/).

2.5. Genomic Libraries

The *Xenopus* Initiative includes the generation and distribution of BAC libraries. Currently, there are two *X. tropicalis* BAC libraries. Library ISB-1 was made by the Institute for Systems Biology (ISB) from the DNA of a Nigerian female frog. It has an average insert size of 75 kb and 6.8× coverage. Library CHORI-216 was made by the Children's Hospital of Oakland Research Institute (CHORI) from the DNA of a seventh-generation inbred Nigerian male frog (stock 248 F7A2, R. Grainger, University of Virginia). It has an average insert size of 175 kb and coverage of about 11×. Clones from these libraries are available from CHORI's BAC Resource (<http://bacpac.chori.org/home.htm>). In addition, an *X. laevis* BAC library is currently under construction.

BAC clones were selected for sequencing based on community requests for BACs containing genes of high interest as well as syntenic regions targeted by the ENCODE (Encyclopedia of DNA Elements) Project for cross-species comparison (<http://www.genome.gov/Pages/Research/ENCODE/>). For example, JGI has selected and draft sequenced 419 BACs and deposited these in GenBank. These BACs are now being finished, and 55 of these have been deposited as final sequence. The JGI intends to finish and annotate all of the BACs and incorporate these sequences into their final genome assembly. The sequencing status and downloads of these BAC sequences are available at http://genome.jgi-psf.org/sfo/Xenopus_tropicalis.html.

2.6. Physical Map

Clone-based physical maps enable the integration of different types of genome data into more detailed clone maps that serve as the starting points for sequencing several genomes, including human (5) and mouse (6). In addition, comparison of whole genome sequence assemblies to BAC end sequences (BESs) within fingerprint contigs provides independent verification of the accurate representation of the genome. The Washington University Genome Sequencing Center will provide a whole genome BAC-based physical map as well as a minimum tiling path of the *X. tropicalis* genome. These will compliment the JGI's genome sequencing project (see **Subheading 2.7.**) and will enable numerous functional genomics experiments, such as comparative genome hybridization of *Xenopus* genome aberrations.

To develop a comprehensive physical map of *X. tropicalis*, fingerprint and BES production are conducted in parallel to maximize map construction efficiency as

described in **ref. 6**. A total of 268,000 fingerprint attempts will be made from the ISB-1 and CHORI-216 BAC libraries. On completion of these fingerprint attempts, the physical genome coverage in BAC clones should be 15 \times . The estimated number of BAC end sequences to be completed from these libraries is 193,000. As of November 2004 about 150,000 BESs had been deposited in NCBI's trace archive files (<http://www.ncbi.nlm.nih.gov/Traces>).

At later stages of map construction, these BESs will be used for alignment to the *X. tropicalis* and other species' genome assemblies. This strategy follows closely efforts employed in the successful completion of the mouse physical map (6). Sequence contig alignments to BES within fingerprint contigs will be used to further guide fingerprint contig merges for improved clone distribution, with the goal being larger, more contiguous contigs.

When complete, the data of the BAC fingerprint map will be made available to the public for download as a finger print Contig database (<http://genome.wustl.edu>). As the whole genome sequence assembly efforts progress toward a predetermined 8 \times coverage, efforts in collaboration with JGI will be made to integrate the fingerprint map and sequence assemblies and post this information on the appropriate Web site.

2.7. *Xenopus tropicalis* Genome Sequence

The JGI is sequencing the genome of *X. tropicalis* with the goal of producing a high-quality draft assembly. The DNA used for construction of whole genome shotgun libraries was isolated from two inbred individuals from the Nigerian strain of *X. tropicalis* (F6 and F7). The strategy involves end sequencing of approx 4 \times sequence coverage of a 3-kb insert plasmid library, approx 4 \times sequence coverage of an 8-kb insert plasmid library, and paired end sequences representing about 15 \times clone coverage of approx 35-kb insert fosmids. Additional end sequence generated at JGI will be combined with BAC end sequence and mapping information produced at the Washington University Genome Sequencing Center to produce a final assembly. The complete mitochondrial genome has also been assembled and annotated (<http://genome.jgi-psf.org/xenopus0/X.tropicalisMtGenome.gb>).

Four preliminary assemblies have been produced to date using JAZZ, the JGI genome assembler. The most recent assembly (version 4) used paired end sequencing reads at a coverage of 7.65 \times . The version 4 assembly is available for BLAST analysis and downloading at <http://genome.jgi-psf.org/Xentr3/Xentr3.home.html>. After trimming reads for vector and quality, 22.5 million reads assembled into 19,759 scaffolds totaling 1.51 Gb of genomic sequence, in agreement with previous estimates of the genome size. Approximately half of the genome is contained in 272 scaffolds, all at least 1.56 Mb long. This assembly and preliminary automated annotation are displayed through the JGI genome browser.

A preliminary set of 33,749 gene models was created using the JGI annotation pipeline and is composed of known *X. tropicalis* genes mapped onto the genomic sequence, homology-based, and *ab initio* gene models. Additional support for the predicted gene models was provided from available ESTs and cDNAs from *X. tropicalis* and *X. laevis*.

This assembly will be the basis for comprehensive annotation and analysis. The larger research community will assist with the manual examination of the automated annotation. A publication on the global analysis of the genome will be submitted soon.

2.8. Microarrays

Microarrays are important tools for gene discovery and for investigating gene function. Several groups are developing *Xenopus* microarrays. For example, the Affymetrix company has made an *X. laevis* oligonucleotide microarray that represents over 14,400 transcripts. The transcripts were selected by a group of *Xenopus* experts and bioinformatics experts from NCBI's UniGene project (process described at http://www.xenbase.org/genomics/microarrays/Xenbase_affy_upd_v5.html).

The chip includes about 10,400 EST-based gene clusters and about 3500 genes that were well characterized at design time (June 2003). Each transcript is represented by 25mer oligonucleotide probes in a set of 16 pairs. Each probe pair consists of a perfect match oligonucleotide and a mismatch oligonucleotide. A complete list of the transcripts and the sequence of each probe is available at www.affymetrix.com.

The initial lot of about 90 chips was distributed among nine *Xenopus* labs, including the labs of those who helped design the chip. Preliminary examinations showed that the chips have a good dynamic range and a high degree of reproducibility. The chips are sold by Affymetrix (www.affymetrix.com). Data from this chip are included in NCBI's Gene Expression Omnibus (<http://www.ncbi.nlm.nih.gov/geo/query/acc.cgi?acc=GPL1318>).

2.9. Mutagenesis and Phenotyping

One of the benefits of *X. tropicalis* is that its diploid genome and shorter generation time should make it amenable to genetic analyses. The addition of genetics to *Xenopus*' other advantages could benefit many types of studies. Several projects have begun to examine the potential of *X. tropicalis* as a genetic model. They are devising and optimizing strategies for mutation induction using a variety of mutagenesis strategies, including chemical mutagenesis, insertional mutagenesis, and γ -ray mutagenesis. They are also devising strategies to screen for altered phenotypes at different stages of development and in different organ systems.

So far, these projects have identified many mutagenized animals with interesting phenotypes. They can be divided into animals with alterations in specific organ systems and developmental events, including the cardiovascular system, the digestive system, the ear, and the eye and in axial patterning. For examples, see the Stemple/Zimmerman project at <http://www.sanger.ac.uk/Teams/Team31/phenotypes.shtml>. These putative mutants are back-crossed and sib-crossed to determine whether their phenotypic alterations are in fact heritable. So far, several of the interesting phenotypes have been determined to result from heritable mutations.

One of the goals of these projects is to serve as a community resource by disseminating the mutagenesis protocols and screening strategies that they devise and by making their mutant and transgenic strains available to the community. Each project has a Web site that describes their goals, strategies, and protocols and provides a description

of the putative mutants and of the mutant strains. They also explain how investigators can obtain mutant strains. Links to their Web sites may be found at the NIH *Xenopus* Initiative's Web site, <http://www.nih.gov/science/models/Xenopus/resources/I.html>.

2.10. Bioinformatics

Bioinformatics has become an essential research tool for sequencing projects. The NIH *Xenopus* Initiative has developed three types of databases that are useful for obtaining *Xenopus* sequence information: (1) databases that collect and distribute *Xenopus*-specific information; (2) databases that contain sequence information from many organisms, including *Xenopus*; and (3) databases of individual *Xenopus* projects. These databases are updated regularly and should be consulted for the current data.

2.10.1. *Xenopus* Genomic Databases

2.10.1.1. XENOPUS GENOME RESOURCES

NCBI's *Xenopus* Genome Resources Web site <http://www.ncbi.nlm.nih.gov/genome/guide/frog/index.html> provides links to NCBI resources, databases, and analytical tools and to many *Xenopus* community Web sites. This genome-specific guide page is intended as a gateway to the current set of informatics tools and databases available at NCBI and will continue to be updated with new resources pertinent to the *Xenopus* community. For example, this page will provide a link to NCBI's *Xenopus*-specific BLAST site when it is available. Until that time, users can restrict a query to *Xenopus* sequences by selecting *Xenopus laevis* or *Xenopus tropicalis* from the All organisms pull-down menu on the page where BLAST queries are submitted.

2.10.1.2. XENOPUS GENE COLLECTION

NCI's *Xenopus* Gene Collection Web site <http://xgc.nci.nih.gov/> lists the sequences of the genes with completely determined CDSs and the libraries from which they were taken. It also lists the clones that are scheduled for sequencing and enables BLAST analyses.

2.10.1.3. XENOPUS UNIGENE

NCBI's UniGene Web sites (<http://www.ncbi.nlm.nih.gov/UniGene/UGOrg.cgi?TAXID=8355> for *X. laevis* and <http://www.ncbi.nlm.nih.gov/UniGene/UGOrg.cgi?TAXID=8364> for *X. tropicalis*) contain the current statistics for the *Xenopus* UniGene clusters. The numerals in the Number of Clusters column of the histogram link to the sequences that they represent.

2.10.2. Databases That Include *Xenopus* Sequence Data

2.10.2.1. NCBI ENTREZ

Global searches of *Xenopus* data can be conducted at NCBI's Entrez cross-database search page (GQuery) <http://www.ncbi.nlm.nih.gov/gquery/gquery.fcgi>. This page allows all Entrez databases to be searched simultaneously by a single query and provides direct links to each database. The sequence databases included in Entrez are Nucleotide, Protein, Genome, Structure, and SNPs (Single Nucleotide Polymor-

phisms). Other Entrez databases include Taxonomy, Gene, HomoloGene, UniGene, CDD (Conserved Protein Domain Database), 3D Domains, UniSTS (Sequence Tagged Sites), PopSet (Population Set), Cancer Chromosomes, and GEO (Gene Expression Omnibus) Datasets. GQuery searches also identify related data in PubMed, PubMed Central, NCBI's Books, OMIM (Online Mendelian Inheritance in Man), and NCBI's Site Search. Navigation between NCBI resources is simplified by connections maintained between NCBI resources, which are displayed in the drop-down Links menu at the top of each Entrez database page.

2.10.2.2. NCBI TRACE ARCHIVE

NCBI's Trace Archive <http://www.ncbi.nlm.nih.gov/Traces/trace.cgi?#> contains raw DNA sequence reads generated from large-scale sequencing projects, including *X. laevis* EST traces and *X. tropicalis* EST, WGS (Whole Genome Shotgun), and CLONEEND traces. The Trace Archive can be queried by center name, the type of trace, or the organism at http://www.ncbi.nlm.nih.gov/Traces/trace.cgi?cmd=fstat&f=full_stat&m=stat&s=full_stat.

2.10.2.3. NCBI REFERENCE SEQUENCES

NCBI's Reference Sequence (RefSeq) project (<http://www.ncbi.nlm.nih.gov/RefSeq/index.html>) provides a nonredundant reference set of DNA, transcript (full-length representative mRNAs), and protein sequences. To facilitate annotation of the assembled genome, about 2000 RefSeqs representing full-length mRNAs and their encoded proteins from the *X. tropicalis* genome have been produced and included in the Entrez Gene database.

Xenopus tropicalis and *X. laevis* Entrez Gene records were created by coordinated efforts of the Entrez Gene, UniGene, and the XGC groups to identify gene-specific sequence clusters and name them according to community standards. NCBI staff encourages feedback regarding Entrez Gene, RefSeq, and OMIM through the on-line form (www.ncbi.nlm.nih.gov/RefSeq/update.cgi) and by submission of GeneRIFs (Reference into Function; www.ncbi.nlm.nih.gov/projects/GeneRIF/GeneRIFhelp.html) to submit PubMed IDs and associated functional information. Suggestions may also be sent to the NCBI Help Desk (info@ncbi.nlm.nih.gov). Current RefSeq statistics for *X. tropicalis* are found at www.ncbi.nlm.nih.gov/LocusLink/RSstatistics.html.

Xenopus tropicalis RefSeq accessions (mRNA, protein) are included in NCBI's Entrez Gene pages (<http://www.ncbi.nlm.nih.gov/entrez/query.fcgi?db=gene>) and can be downloaded from the RefSeq ftp site (ftp://ncbi.nlm.nih.gov/refseq/release/vertebrate_other/).

2.10.3. Databases of Individual Xenopus Projects

Current data from the *Xenopus* BAC End Sequencing and Finger Print Mapping projects at Washington University Genome Sequencing Center can be accessed at <http://genome.wustl.edu/projects/Xenopus/index.php>.

The Web site of JGI's *Xenopus* Genome Sequencing project can be accessed at <http://genome.jgi-psf.org/Xentr3/Xentr3.home.html>. It includes BLAST search capabilities and sequence information about JGI's BAC sequencing project.

The progress of the *X. tropicalis* Genetic Map can be examined at <http://tropmap.biology.uh.edu/>.

Acknowledgments

We would like to acknowledge Sandra W. Clifton and the Washington University EST Sequencing Group and the National Institutes of Health Intramural Sequencing Center EST Sequencing Group for EST sequencing, and the Trans-NIH *Xenopus* Working Group for their interest and support (members at <http://www.nih.gov/science/models/xenopus/contacts/index.html>).

References

1. Klein, S. L., Strausberg, R. L., Wagner, L., Pontius, J., Clifton, S. W., and Richardson, P. (2002) Genetic and genomic tools for *Xenopus* research: the NIH *Xenopus* initiative. *Dev. Dyn.* **225**, 384–391.
2. Gerhard, D. S., Wagner, L., Feingold, E. A., et al. (2004) The status, quality and expansion of the NIH full-length cDNA project (MGC). *Genome Res.* **14**, 2121–2127.
3. Stanford, J. S., Lieberman, S. L., Wong, V. L., and Ruderman, J. D. (2003) Regulation of the G2/M transition in oocytes of *Xenopus tropicalis*. *Dev. Biol.* **260**, 438–448.
4. Toth, G., Gaspari, Z., and Jurka J. (2000) Microsatellites in different eukaryotic genomes: survey and analysis. *Genome Res.* **10**, 967–981.
5. McPherson, J. D., Marra, M., Hillier, L., et al. (2001) A physical map of the human genome. *Nature* **409**, 934–941.
6. Gregory, S. G., Sekhon, M., Schein, J., et al. (2002) A physical map of the mouse genome. *Nature* **418**, 743–750.

The Physiology of the *Xenopus laevis* Ovary

Melissa A. Rasar and Stephen R. Hammes

Summary

Xenopus laevis has been used for many decades to study oocyte development and maturation. The *Xenopus* oocytes' large size, relative abundance, and clearly defined progression of physical characteristics from oogonia to eggs make them ideal for studying oogenesis. In addition, the ability of steroids to trigger *Xenopus* oocyte maturation in vitro has resulted in their extensive use for the study of the complexities of meiosis. Interestingly, steroid-induced maturation of *Xenopus* oocytes occurs completely independent of transcription; thus, this process serves as one of the few biologically relevant models of nongenomic steroid-mediated signaling. Finally, *Xenopus* oocytes appear to play a critical role in ovarian steroidogenesis, suggesting that the *Xenopus* ovary may serve as a novel system for studying steroidogenesis. Evidence indicates that many of the features defining *Xenopus laevis* oogenesis and maturation might also be occurring in mammals, further emphasizing the strength and relevance of *Xenopus laevis* as a model for ovarian development and function.

Key Words: Maturation; oocyte; ovary; steroidogenesis; vitellogenesis; *Xenopus*.

1. Anatomy of the Ovary

The ovaries are considered the largest organs in the adult female frog, filling a large portion of the abdominal cavity and contributing to nearly 15% of the total frog weight during breeding (1). The two ovaries resemble large transparent sacks subdivided into multiple lobes (~24 lobes per ovary), each containing hundreds of oocytes at all stages of development (Fig. 1). Unlike in mammals, the relatively large frog oocytes make up the majority of the ovarian volume. Furthermore, these oocytes contribute to important ovarian physiologic processes, such as steroidogenesis. The large size and easy accessibility of amphibian oocytes also make them useful tools for studying meiosis; thus, *Xenopus* oocytes have long served as an important model for examining the cell cycle.

Although they rest in the abdominal cavity, the ovaries are actually fixed to the retroperitoneum. They are attached to the kidneys and are surrounded by an epithelium

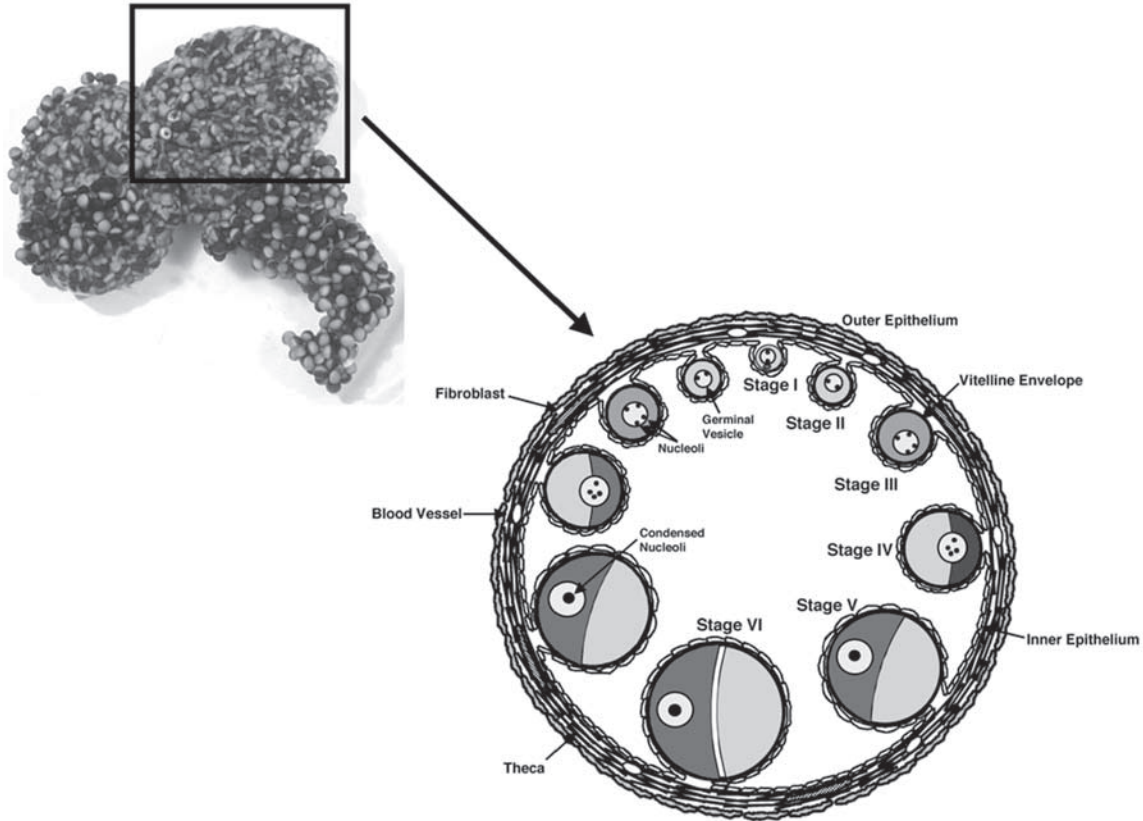


Fig. 1. Photograph and schematic representation of the *Xenopus* ovary and oogenesis. An individual ovary consists of approx 24 lobes (upper left). Every lobe is made up of hundreds of follicles, each of which contains an individual oocyte at any stage of development (schematic on the right). *See* text for details.

of ciliated cells derived from embryonic primordial medullary tissue that is continuous with the visceral peritoneum (2). This epithelium is made up of a single layer of flat cells covering an inner thecal layer. The thecal layer consists of extracellular matrix surrounding blood vessels and fibroblasts and covers another layer of cells that constitute the inner epithelium.

At the start of oogenesis, oocytes are located within the thecal layer. As they grow, they push the inner epithelium centrally to form bulges that represent individual follicles. The individual oocytes are surrounded by a layer of flattened cells that keep them isolated from the thecal layer, with each oocyte and associated cells representing an independent follicle.

During follicular development, the surrounding layer of follicle cells becomes separated from the oocytes by an acellular layer of mucopolysaccharide material called the vitelline membrane or zona radiata. Although the origin of this membrane is not certain, some evidence suggests that it might be secreted by the follicle cells themselves during secondary follicle growth (3).

As the follicles continue to grow, the follicle cells extend small projections that cross this vitelline membrane to contact the oocyte surface and form gap junctions. These gap junctions are felt to play important roles in the communication between oocytes and surrounding follicle cells and may be involved in essential processes such as yolk accumulation and the regulation of meiosis (4). A schematic representation of ovarian and oocyte anatomy is depicted in Fig. 1.

2. Anatomy of the Developed Oocyte

Oocytes that are in their final stage of development (stage VI) have completed oogenesis and are competent for ovulation and subsequent fertilization (3,5). These oocytes are approx 1.3 mm in diameter, with a volume of approx 1 μ L. They have a well-defined brown animal pole (containing the majority of the nucleus) and a weakly pigmented vegetal hemisphere (containing the majority of the yolk platelets). Between the two hemispheres is a thin, unpigmented ring called the equatorial band or belt.

The nucleus, or germinal vesicle, of a stage VI oocyte is quite large relative to a somatic cell nucleus ($\sim 10^5$ times the size), and holds multiple extranucleoli containing large amounts of ribosomal ribonucleic acid (RNA). The DNA within the nucleus has replicated and is arrested in the diplotene stage of prophase I. The germinal vesicle is surrounded by a nuclear envelope containing large pores, which are likely important for the transport of molecules such as messenger RNA (mRNA) between the cytoplasm and the nucleus (6).

The cytoplasm of the oocyte is also unique in developed oocytes, with 80% of the cytoplasmic proteins being yolk proteins stored in the yolk platelets (7). These consist of lipoproteins and glycoproteins that will serve as nutritive stores for the developing embryo. The process of yolk protein accumulation is known as *vitellogenesis* and is described in **Subheading 4**. The cytoplasm also contains a rich store of maternal mRNAs and ribosomes.

Although protein synthesis is very robust during oocyte development, only 2% of ribosomes are active, and only 20% of mRNAs are actively translated (8,9).

The remaining ribosomes are stored for later function. Inactive mRNAs are stored in ribonuclear protein (RNP) complexes, and specific transcripts may be compartmentalized within the oocyte. Furthermore, these dormant mRNAs may be incompletely polyadenylated, thus rendering them inactive until the resumption of meiosis, when the polyadenylation pattern of mRNA is dramatically altered (10,11).

One last important feature of the developed oocyte is its cortex. The cortex consists of a cytokeratin shell extending a few micrometers from the membrane toward the cytoplasm and appears to play an important role in maintaining the structural integrity of the oocyte (3). The melanin-containing pigmented granules are present in this region and are more concentrated around the animal pole of the oocyte. In addition, the microvilli from surrounding follicle cells extend through the cortex, allowing communication between the oocyte and surrounding cells. Finally, the cortex is surrounded by the plasma membrane, which directly contacts the vitelline envelope of the follicle.

3. Oogenesis

Oogenesis refers to the transformation of oogonia to oocytes. Oogenesis begins in the embryo approx 3 wk after fertilization, when the embryonic gonads start to become sexually differentiated. During this time, the primordial germ cells begin to multiply to form primary oogonia. This growth is still quite slow and asynchronous. By 4 wk, the oogonia have begun to couple together, resulting in the formation of secondary oogonia. During this time, meiosis begins. Meiosis continues to the diplotene stage of prophase I, at which point the oocyte is arrested until just prior to ovulation. During this protracted diplotene stage, the oocytes grow considerably, increasing their volume by well over 10,000-fold.

Amphibian oogenesis is persistent in the adult ovary, with oogonia constantly differentiating into oocytes. This process is not synchronized; thus, individual lobes will contain oocytes in many stages of oogenesis. Interestingly, although this asynchronous and persistent development of oocytes from oogonia in adults was at one time considered specific only to lower vertebrates, evidence suggests that oogenesis may also be occurring persistently in the ovaries of female mice (12).

Generally, a cycle of oogenesis is considered complete when an ovary has a large population of banded stage VI oocytes, at which point the animal is ready to ovulate. Studies have shown that approx 5 to 7 wk are needed to repopulate the ovary with stage VI oocytes after human chorionic gonadotropin (hCG)-stimulated ovulation, suggesting that this amount of time is needed for oocytes to progress to ovulatory competence (13,14).

The criteria for staging *Xenopus* oogenesis are based on a scale developed by James Dumont (5) that allows identification of stages by morphologic appearance of unfixed oocytes. Given that oogenesis is a continuous process, no precise boundaries can be defined between stages; however, the features described here provide a basis for identifying the approximate stage of development and therefore predicting the physiologic processes occurring in a given oocyte. The salient features of each stage of oocyte development are reviewed in Table 1 and are pictured in Fig. 1.

Table 1
Features of Oocytes at Stages I to VI of Development

	Stage					
	I	II	III	IV	V	VI
Size (µm)	50–300	300–450	450–600	600–1000	1000–1200	1200–1300
Features	Transparent	White	Pigmentation begins Light brown (early), dark brown-black (late)	Pigment polarizes: animal-vegetal hemispheres develop	Distinct hemispheres; pigment fades to brown	Formation of unpigmented equatorial band
Approximate percentage of stages II–VI population	NA	45%	15%	15%	10%	15%
Vitellogenesis ^a	—	—	+	+++	Decreasing	—

NA, not applicable.

^aVitellogenesis: stages I and II are considered previtellogenic; stage VI is considered postvitellogenic.

3.1. Stage I

Stage I oocytes are previtellogenic and range from 50 to 300 μm in diameter. A distinguishing feature of these oocytes is the transparent cytoplasm with an easily identified germinal vesicle that fills much of the cell. Large, irregular nucleoli are evident at the periphery of the nucleus by late stage I, and the nuclear envelope maintains a smooth outline. A densely packed collection of mitochondria that appears as a small, yellowish body, referred to as the mitochondrial mass or Balbiani body, can be visualized next to the nucleus. The cytoplasm usually appears diffusely granular, containing large amounts of RNA, ribosomes, and endoplasmic reticulum. In early stage I, follicle cells are tightly juxtaposed to the oocyte membrane; however, during late stage I, these follicle cells lift from the surface of the oocyte, and the microvilli begin to develop (15).

3.2. Stage II

Stage II oocytes are also previtellogenic and account for 45% of the total oocyte population in stages II to IV. Stage II oocytes range in diameter from 300 to 450 μm . At this point in development, oocytes acquire a characteristic opaque white color that obscures the mitochondrial mass and nucleus. Several changes begin to take place in the wall of the ovary and in the follicle cells during this stage:

1. Both the outer membrane and follicle cells grow in size, making these cell layers appear thicker.
2. Basement membranes develop on the basal (thecal) side of each cell layer.
3. The theca accumulates more collagen.
4. An expansive microvilli network that emanates from the apical side of the follicle cells and arches over the oocytes and the acellular vitelline envelope develops at the follicle cell-oocyte junction (1).
5. A periodic acid-Schiff (PAS)-positive granular layer develops along the periphery of the cytoplasm that contains cortical granules, mitochondria, small yolk platelets, lipid, and premelanosomes.
6. The nuclear envelope becomes progressively more irregular, and the nuclei acquire more irregularly shaped nucleoli along the periphery.

3.3. Stage III

Stage III oocytes range from 450 to 600 μm in diameter and account for 15% of the population in stages II to VI. Two important processes are initiated during stage III: acquisition of pigmentation and active uptake of yolk (vitellogenesis; see **Subheading 4**). Pigmentation is initially evident by the tan or light brown appearance of oocytes, caused by melanin produced from the melanosomes lying beneath the cortical layer of the oocyte. During this stage, oocytes continue to darken uniformly, with no distinction between animal and vegetal poles, until the entire oocyte appears dark brown or black. Other morphologic changes during stage III include development of visible blood vessels along the surface of the oocyte, increased height of the follicle cells, increased numbers and sizes of microvilli, and continued development of the vitelline envelope (16).

Finally, nuclear changes also occur. First, formerly peripheral nucleoli become vacuolated and relocate to the center of the nucleus. Second, to allow for efficient transcription of genes to service the 10^5 - to 10^6 -fold higher volume of cytoplasm compared to somatic cells, the chromosomes relax into a lampbrush configuration. The presence of this conformation coincides with peak RNA synthesis, which begins in late stage II and lasts until very late stage III (17,18). In fact, stage III oocytes have their full complement of poly(A) mRNAs, but only a small fraction is translated (19).

3.4. Stage IV

Stage IV oocytes range in size from 600 to 1000 μm in diameter and account for approx 15% of the stage II to VI oocyte population. Differentiation of the animal and vegetal hemispheres becomes evident during stage IV. Determination of this axis is not dependent on where the follicle is attached to the ovarian wall. Instead, the axis of polarity seems to be established early in the oogonium based on a line that passes from the nucleus to the centrosome in these very early germ cells (20). Subsequent events, such as fragmentation of the mitochondrial mass during stage II development, accumulation of yolk platelets, and asymmetric thinning of the cortex, fall along this axis (21).

Other features typical of stage IV development are increased numbers of blood vessels in the theca and the continued growth of follicle cells. Channels begin to develop between adjacent follicle cells. Cortical granules become more uniform beneath the oocyte membrane, and the majority of melanosomes are now restricted to the animal pole. The cortex of the vegetal pole begins to thin, perhaps because of stretching, and the animal pole remains thick (22). The nuclear envelope remains convoluted, albeit less so than in the earlier stages, and the lampbrush chromosomes retract along with the nucleoli.

Vitellogenesis is most rapid during stage IV oogenesis. The yolk platelet density gradient from the animal to the vegetal axis becomes pronounced, and the nucleus seems to be displaced to the animal pole. The density gradient appears to develop because younger, smaller yolk platelets are imported via micropinocytosis at the animal pole and transported to the vegetal pole along intermediate filament-rich radii. During transit to the vegetal half of the oocyte, these small yolk platelets fuse to form older, larger, and more densely packed platelets (21).

3.5. Stage V

Stage V oocytes range in size from 1000 to 1200 μm and account for 10% of the oocyte population in stages II to VI. At this point in oogenesis, the border between the animal and vegetal hemispheres becomes more distinct, and the pigmentation of the animal hemisphere begins to fade from the dark brown of stage IV oocytes to a more brown or beige color. Blood vessels are still prominent, the vitelline envelope has reached maximal thickness, and follicle cells appear to flatten. At this point, vitellogenesis starts declining, although the yolk gradient continues to displace the nucleus toward the animal pole. At this point, the nuclear envelope polarizes such that the vegetal half of the nucleus becomes more irregular than the animal half, and the nucleoli and chromosomes condense to form a centrally located mass.

3.6. Stage VI

Stage VI oocytes mark the end of oocyte development and, because of the cessation of vitellogenesis, are considered postvitellogenic. As mentioned, by this stage oocytes have a banded appearance as a result of an unpigmented equatorial 200- μm band separating the heavily brown-pigmented animal pole from the pale yellow vegetal pole. The follicle cells continue to appear flattened, and the nuclei shrink in size. The vitelline envelope develops two distinct layers, and the number and length of microvilli extending from the oocyte surface are markedly reduced. A few nucleoli persist in the nucleus and tend to be localized near the highly convoluted vegetal half of the nuclear envelope (23), which is the side that breaks down first during initiation of meiosis (maturation).

At this stage, the oocyte has accumulated enough resources to support development of the embryo through the swimming tadpole stage. The inherent polarity that was established in the oogonia and that later became visually evident as the animal and vegetal poles during oocyte development is maintained during maturation and fertilization and ultimately becomes important for the appropriate formation of embryonic structures.

4. Vitellogenesis

Vitellogenesis refers to the formation of the oocyte yolk. *Xenopus* oocytes contain large quantities of yolk in the cytoplasm in the form of yolk platelets (7,24). In stage VI oocytes, these yolk platelets encompass nearly 80% of the total oocyte protein and appear as thousands of small cytoplasmic droplets when sectioned oocytes are viewed under the microscope. Yolk platelets are asymmetrically distributed in the cytoplasm. The animal hemisphere contains the lowest yolk content with the smallest yolk platelets, and the vegetal region contains the highest yolk content with the largest yolk platelets.

The yolk platelets consist of a combination of lipo-, glyco-, and phosphoproteins that are packed together in a crystalline fashion. They contain primarily two types of yolk: protein yolk, which contains phosphoproteins that are often attached to lipid molecules, comprises approx 45% of the oocyte's dry weight (25); fatty yolk, which consists of neutral lipids with varying amounts of phospholipids, makes up approx 25% of the oocyte mass. Most of the yolk content is synthesized outside the ovary and transported into oocytes during the secondary phase of oocyte growth.

For example, one of the major components of the yolk is the phosphoprotein vitellogenin, which appears in the bloodstream of female frogs during breeding season. Vitellogenin is synthesized in the liver, where its production is stimulated by estradiol but not other ovarian steroids such as androgens or progesterone (26). Although exogenous administration of estradiol increases vitellogenin production by the liver, vitellogenin uptake by the oocytes remains low; thus, serum vitellogenin levels increase dramatically. In contrast, injection of exogenous gonadotropins into female frogs leads to liver vitellogenesis as well as rapid uptake of vitellogenin by the oocytes, resulting in relatively low serum vitellogenin levels.

The presumption is that gonadotropins stimulate vitellogenesis in the liver via ovarian estradiol production; vitellogenin uptake by oocytes is promoted through a separate, estradiol-independent, mechanism (27,28). Vitellogenin uptake begins when oocytes reach stage III of their growth and, although its mechanism is not completely understood, may involve pinocytotic and endocytotic events as well as communication between the follicle cells and oocytes via the gap junctions (29).

5. Steroidogenesis

Sex steroids appear to be secreted primarily by the ovaries of female frogs (30,31). During breeding season, serum estradiol levels increase, which stimulates vitellogenin production by the liver. The direct effects of estradiol on amphibian ovarian follicle development are still not well understood. Sex steroid production reaches a maximum during ovulation, when gonadotropins secreted from the pituitary stimulate both estrogen and androgen production; however, the exact amounts of the various ovarian steroids made in the ovaries during natural ovulation is not well documented. In contrast, both serum and ovarian steroid levels in female frogs injected with exogenous gonadotropins have been measured (32).

Injection of hCG promotes a rapid increase in ovarian sex steroid production that peaks after approx 8 h, which roughly coincides with ovulation. Exogenous hCG promotes moderate increases in estradiol production and dramatic increases in testosterone and androstenedione production. Although hCG stimulates ovarian progesterone production as well, its levels in the serum and ovaries relative to testosterone and estradiol remain quite low. This contrasts with gonadotropin-stimulated steroidogenesis in mammalian ovaries, where progesterone production exceeds that of androgens and estrogens.

Several studies have been directed toward characterizing the steroidogenic pathway in the *Xenopus* ovary. Together, these studies explain the high androgen, moderate estradiol, and low progesterone levels described. The classical ovarian steroidogenic pathway is depicted in Fig. 2 (33).

After synthesis of the steroid pregnenolone from cholesterol, sex steroid production relies on four important enzymes. First, the cytochrome p450 enzyme CYP17 converts pregnenolone and progesterone to dehydroepiandrosterone (DHEA) and androstenedione, respectively. Second, the steroid dehydrogenase 3 β HSD converts Δ 5 steroids (such as pregnenolone and DHEA) to Δ 4 steroids (progesterone and androstenedione, respectively). Third, 17 β -hydroxysteroid dehydrogenase (17 β HSD) metabolizes androstenedione to testosterone. Finally, the aromatase enzyme CYP19 converts androstenedione and testosterone to estrone and estradiol, respectively.

Several studies have demonstrated the presence of both 3 β HSD and 17 β HSD activities in *Xenopus* ovaries, localizing these enzymes primarily to follicle cells (34,35). In contrast, *Xenopus* CYP17 appears to be exclusively expressed in the oocytes themselves (32,35). Interestingly, pregnenolone is a very poor substrate for 3 β HSD-mediated conversion to progesterone but is an excellent substrate for *Xenopus* CYP17. Thus, pregnenolone is preferentially converted to DHEA, which in turn is a good substrate for 3 β HSD-mediated conversion to androstenedione. This selective

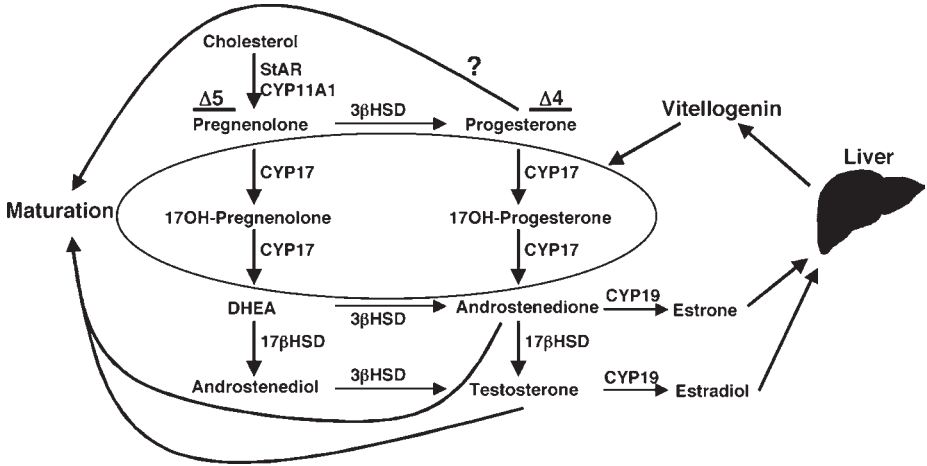


Fig. 2. Diagram of *Xenopus* ovarian steroidogenesis. CYP17 is expressed exclusively in the oocyte, which is represented by an oval shape in the center of the figure. All other steroidogenic enzymes are present in the surrounding follicle cells. Sex steroid production is therefore dependent on the germ cells, or oocytes. Estrogen and estrone enter the circulation to promote vitellogenesis in the liver. Vitellogenin then returns to the ovary and is taken up by oocytes. Androstenedione and testosterone are produced in large amounts prior to ovulation and may promote oocyte maturation. Although progesterone is also capable of promoting maturation, its production prior to ovulation is quite low; thus, the physiologic role of progesterone in regulating oocyte maturation is uncertain.

metabolism of pregnenolone via the $\Delta 5$ pathway likely explains why little progesterone is produced by the *Xenopus* ovary. Ovarian CYP19 activity, which seems to be primarily in follicle cells, is also relatively low, even in the presence of gonadotropins, thus explaining the reduced estradiol levels relative to testosterone (34).

The exclusivity of steroidogenic enzyme activities to specific cells within the ovary implies that *Xenopus* sex steroid production depends on both follicle cells and germ cells. This suggests an unusual positive-feedback model by which germ cells, or oocytes, are controlling their own growth and development by regulating synthesis of the steroids (estrogens) that promote vitellogenesis in the liver.

6. Oocyte Maturation and Ovulation

Just prior to ovulation, the microvilli between follicle cells and oocytes retract from the vitelline membrane so that the oocytes start to detach from the membrane (3). At the same time, chromosomal condensation begins, with spindle formation and loss of nuclear membrane definition (germinal vesicle breakdown). These features are part of oocyte maturation, which is defined as the resumption of meiosis beyond prophase I to metaphase II. Oocyte maturation is regulated by both pituitary and ovarian hormones.

In the 1930s, Rugh first demonstrated a role for pituitary factors in triggering amphibian ovulation by inducing the ovulation process with pituitary extracts (36). Shortly afterward, a role for ovarian factors in moderating ovulation was shown to be important through experiments in which ovulation in female frogs was triggered using ovarian tissue that had first been exposed to pituitary extract (37,38).

In the 1960s, progesterone was proposed to be the ovulation-inducing factor produced in the ovaries because submicromolar concentrations of progesterone promoted maturation in vitro (39). Since that time, nearly all of the seminal work studying meiosis in *Xenopus* oocytes has used progesterone as the trigger for maturation. However, many other steroids are equally or more capable of promoting oocyte maturation in vitro, including the androgens testosterone and androstenedione (32,39,40). Furthermore, as mentioned, gonadotropins stimulate very little ovarian progesterone production relative to these two androgens in vivo.

These observations suggest that androgens, rather than progesterone, may be the primary physiologic mediators of *Xenopus* oocytes in vivo. In addition, the CYP17 expressed in isolated oocytes rapidly converts progesterone to androstenedione; thus, in vitro “progesterone-induced maturation” likely involves androgen as well as progesterone actions (32). These observations suggest that, similar to the positive-feedback loop involving oocyte-dependent estrogen synthesis and oocyte growth via vitellogenesis, oocyte-mediated androgen production might also play a positive role in oocyte development by promoting maturation.

Investigation of the signaling mechanisms regulating steroid-induced oocyte maturation has been a subject of considerable interest for many decades (41). In contrast to most steroid-mediated signals, maturation appears to be transcription independent or nongenomic. Some nongenomic signals triggered by steroids during maturation include changes in intracellular cyclic adenosine monophosphate, promotion of the mitogen-activated protein kinase cascade, and activation of cyclin-dependent kinase 1. Many of these signals appear to involve steroid-induced changes in mRNA translation.

Interestingly, as mentioned, although transcription is very active during late oogenesis, only 20% of mRNA is translated (3). During maturation, a shift in the complement of translated mRNAs occurs, most likely because of changes in mRNA polyadenylation. One example is the MOS protein, a potent regulator of meiosis; its translation is increased by the addition of steroids (10,11,41). Studies suggest that these steroid-induced signals might in part involve classical steroid receptors that are signaling in a nongenomic fashion outside the nucleus. Other studies propose a “release of inhibition” model by which constitutive G protein-mediated signaling might be holding oocytes in meiotic arrest, and steroids might promote maturation by overcoming these inhibitory signals (42,43). More work is needed to confirm the validity of these models; however, studies in mammalian systems have shown that similar mechanisms may be present (44,45), emphasizing the usefulness of *Xenopus* oocytes as a general model for meiosis as well as for ovulation and oocyte development.

Acknowledgments

We thank Johné Liu for comments regarding this chapter. S. R. H. is funded by the National Institutes of Health (DK59913) and the Welch Foundation (I-1506). M. A. R. is funded in part by the Medical Scientist Training Program at the University of Texas Southwestern Medical Center.

References

- Lofts, B. (1974) Reproduction, in *Physiology of the Amphibia* (Loft, B., ed.), Academic Press, London, pp. 107–218.
- Franchi, L. L. (1962) The structure of the ovary—vertebrates, in *The Ovary* (Zuckerman, S., ed.), Academic Press, New York, pp. 121–142.
- Hausen, P. (1991) *The Early Development of Xenopus laevis: An Atlas of the Histology*, Springer-Verlag, Berlin.
- Browne, C. L., Wiley, H. S., and Dumont, J. N. (1979) Oocyte-follicle cell gap junctions in *Xenopus laevis* and the effects of gonadotropin on their permeability. *Science* **203**, 182–183.
- Dumont, J. N. (1972) Oogenesis in *Xenopus laevis* (Daudin). I. Stages of oocyte development in laboratory maintained animals. *J. Morphol.* **136**, 153–179.
- Scheer, U. (1973) Nuclear pore flow rate of ribosomal RNA and chain growth rate of its precursor during oogenesis of *Xenopus laevis*. *Dev. Biol.* **30**, 13–28.
- Follett, B. K. and Redshaw, M. R. (1974) The physiology of the vitellogenesis, in *Physiology of the Amphibia* (Lofts, B., ed.), Academic Press, London, pp. 219–308.
- Taylor, M. A. and Smith, L. D. (1985) Quantitative changes in protein synthesis during oogenesis in *Xenopus laevis*. *Dev. Biol.* **110**, 230–237.
- Dolecki, G. J. and Smith, L. D. (1979) Poly(A)⁺ RNA metabolism during oogenesis in *Xenopus laevis*. *Dev. Biol.* **69**, 217–236.
- de Moor, C. H. and Richter, J. D. (1997) The Mos pathway regulates cytoplasmic polyadenylation in *Xenopus* oocytes. *Mol. Cell Biol.* **17**, 6419–6426.
- Mendez, R., Hake, L. E., Andresson, T., Littlepage, L. E., Ruderman, J. V., and Richter, J. D. (2000) Phosphorylation of CPE binding factor by Eg2 regulates translation of c-mos mRNA. *Nature* **404**, 302–307.
- Johnson, J., Canning, J., Kaneko, T., Pru, J. K., and Tilly, J. L. (2004) Germline stem cells and follicular renewal in the postnatal mammalian ovary. *Nature* **428**, 145–150.
- Keem, K., Smith, L. D., Wallace, R. A., and Wolf, D. (1979) Growth rate of oocytes in laboratory maintained *Xenopus laevis*. *Gamete Res.* **2**, 125–135.
- Smith, C. L. (1955) Reproduction in female amphibia. *Mem. Soc. Endocrinol.* **4**, 39–56.
- Dumont, J. N. and Brummett, A. R. (1978) Oogenesis in *Xenopus laevis* (Daudin). V. Relationships between developing oocytes and their investing follicular tissues. *J. Morphol.* **155**, 73–98.
- Kemp, N. E. (1958) Electron microscopy of growing oocytes of *Rana pipiens*. *J. Biophys. Biochem. Cytol.* **2**, 281–292.
- Alfert, M. (1954) Comparison and structure of giant chromosomes. *Internal Rev. Cytol.* **3**, 131–175.
- Hill, R. S. and Macgregor, H. C. (1980) The development of lampbrush chromosome-type transcription in the early diplotene oocytes of *Xenopus laevis*: an electron-microscope analysis. *J. Cell Sci.* **44**, 87–101.
- Davidson, E. H. (1986) *Gene Activity in Early Development*, 3rd ed., Academic Press, New York.

20. Tourte, M., Mignotte, F., and Mounolou, J. C. (1981) Organization and replication activity of the mitochondrial mass of oogonia and previtellogenic oocytes in *Xenopus laevis*. *Dev. Growth Differ.* **23**, 9–21.
21. Danilchik, M. V. and Gerhart, J. C. (1987) Differentiation of the animal-vegetal axis in *Xenopus laevis* oocytes. I. Polarized intracellular translocation of platelets establishes the yolk gradient. *Dev. Biol.* **122**, 101–112.
22. Wylie, C. C., Brown, D., Godsave, S. F., Quarmby, J., and Heasman, J. (1985) The cytoskeleton of *Xenopus* oocytes and its role in development. *J. Embryol. Exp. Morphol.* **89 Suppl**, 1–15.
23. Coggins, L. W. (1973) An ultrastructural and radioautographic study of early oogenesis in the toad *Xenopus laevis*. *J. Cell Sci.* **12**, 71–93.
24. Follett, B. K., Nicholls, T. J., and Redshaw, M. R. (1968) The vitellogenic response in the South African clawed toad (*Xenopus laevis* Daudin). *J. Cell Physiol.* **72**, Suppl 1, 91+.
25. Barth, L. G. and Barth, L. J. (1951) The relation of adenosine triphosphate to yolk utilization in the frog's egg. *J. Exp. Zool.* **116**, 99–122.
26. Redshaw, M. R., Follett, B. K., and Nicholls, T. J. (1969) Comparative effects of the oestrogens and other steroid hormones on serum lipids and proteins in *Xenopus laevis* Daudin. *J. Endocrinol.* **43**, 47–53.
27. Wallace, R. A., Jared, D. W., and Nelson, B. L. (1970) Protein incorporation by isolated amphibian oocytes. I. Preliminary studies. *J. Exp. Zool.* **175**, 259–269.
28. Wallace, R. A., Nickol, J. M., Ho, T., and Jared, D. W. (1972) Studies on amphibian yolk. X. The relative roles of autosynthetic and heterosynthetic processes during yolk protein assembly by isolated oocytes. *Dev. Biol.* **29**, 255–272.
29. Wiley, H. S. and Dumont, J. N. (1978) Stimulation of vitellogenin uptake in stage IV *Xenopus* oocytes by treatment with chorionic gonadotropin in vitro. *Biol. Reprod.* **18**, 762–771.
30. Dodd, J. M. (1960) Gonadal and gonadotrophic hormones in lower vertebrates, in *Marshall's Physiology of Reproduction* (Parkes, A. S., ed.), Longmans Green, London, pp. 417–582.
31. Barr, W. A. (1968) Patterns of ovarian activity, in *Perspective in Endocrinology: Hormones in the Lives of Lower Vertebrates* (Jorgensen, E. J. W. Ba. C. B., ed.), Academic Press, New York, pp. 164–238.
32. Lutz, L. B., Cole, L. M., Gupta, M. K., Kwist, K. W., Auchus, R. J., and Hammes, S. R. (2001) Evidence that androgens are the primary steroids produced by *Xenopus laevis* ovaries and may signal through the classical androgen receptor to promote oocyte maturation. *Proc. Natl. Acad. Sci. U. S. A.* **98**, 13,728–13,733.
33. Ozon, R. (1967) [In vitro synthesis of steroid hormones in the testicle and ovary of the urodele amphibian *Pleurodeles waltlii* Michah]. *Gen. Comp. Endocrinol.* **8**, 214–227.
34. Redshaw, M. R. and Nicholls, T. J. (1971) Oestrogen biosynthesis by ovarian tissue of the South African clawed toad, *Xenopus laevis* Daudin. *Gen. Comp. Endocrinol.* **16**, 85–96.
35. Yang, W. H., Lutz, L. B., and Hammes, S. R. (2003) *Xenopus laevis* ovarian CYP17 is a highly potent enzyme expressed exclusively in oocytes. Evidence that oocytes play a critical role in *Xenopus* ovarian androgen production. *J. Biol. Chem.* **278**, 9552–9559.
36. Rugh, R. (1935) Ovulation in the frog. I. Pituitary relations in induced ovulation. *J. Exp. Zool.* **71**, 149–162.
37. Heilbrunn, L. V., Daugherty, K., and Wilbur, K. M. (1939) Initiation of maturation in the frog egg. *Physiol. Zool.* **12**, 97–100.
38. Ryan, F. J. and Grant, R. (1940) The stimulus for maturation and for ovulation of the frog's egg. *Physiol. Zool.* **13**, 383–390.

39. Smith, L. D., Ecker, R. E., and Subtelny, S. (1968) In vitro induction of physiological maturation in *Rana pipiens* oocytes removed from their ovarian follicles. *Dev. Biol.* **17**, 627–643.
40. Le Goascogne, C., Sananes, N., Gouezou, M., and Baulieu, E. E. (1985) Testosterone-induced meiotic maturation of *Xenopus laevis* oocytes: evidence for an early effect in the synergistic action of insulin. *Dev. Biol.* **109**, 9–14.
41. Maller, J. L. and Krebs, E. G. (1980) Regulation of oocyte maturation. *Curr. Top. Cell Regul.* **16**, 271–311.
42. Lutz, L. B., Kim, B., Jahani, D., and Hammes, S. R. (2000) G protein $\beta\gamma$ subunits inhibit nongenomic progesterone-induced signaling and maturation in *Xenopus laevis* oocytes. Evidence for a release of inhibition mechanism for cell cycle progression. *J. Biol. Chem.* **275**, 41,512–41,520.
43. Sheng, Y., Tiberi, M., Booth, R. A., Ma, C., and Liu, X. J. (2001) Regulation of *Xenopus* oocyte meiosis arrest by G protein $\beta\gamma$ subunits. *Curr. Biol.* **11**, 405–416.
44. Gill, A., Jamnongjit, M., and Hammes, S. R. (2004) Androgens promote maturation and signaling in mouse oocytes independent of transcription: a release of inhibition model for mammalian oocyte meiosis. *Mol. Endocrinol.* **18**, 97–104.
45. Conti, M., Andersen, C. B., Richard, F., et al. (2002) Role of cyclic nucleotide signaling in oocyte maturation. *Mol. Cell Endocrinol.* **187**, 153–139.

Oocyte Isolation and Enucleation

X. Shawn Liu and X. Johné Liu

Summary

Xenopus laevis oocytes are popular cells in experimental biology. Fully grown oocytes are large (~1.3-mm diameter) with an enormous nucleus (~300- μ m diameter). Oocytes are generally isolated by either manual dissection (manual defolliculation) or enzymatic (mainly with collagenase preparations) digestion of the extracellular connective tissues. In this chapter, we describe both procedures, which are routinely used in our laboratory. However, manual defolliculation does not actually remove the innermost layer of follicle cells, which are anchored to the vitelline membrane. To remove these follicle cells, further mechanical or enzymatic treatment is required. On the other hand, many have experienced nonspecific effects with collagenase-treated oocytes, including spontaneous oocyte maturation and reduced oocyte health. We discuss possible explanations and solutions to these problems. Finally, we also describe procedures we employ routinely to isolate oocyte nuclei and enucleated oocytes.

Key Words: Collagenase; defolliculation; enucleated oocytes; nucleus; spontaneous oocyte maturation; sandpaper.

1. Introduction

Fully grown *Xenopus laevis* oocytes are enclosed in follicle envelopes before ovulation and maturation. Electron microscopy study of follicles in *Rana pipiens*, which has a follicle structure that is presumably similar to its *Xenopus* counterpart, revealed that there are four tissue/cell layers outside the oocyte: the surface epithelium, the thecal or connective tissue layer, the follicle cell layer, and the vitelline membrane. Both the follicle cells and the oocyte are anchored to the vitelline membrane by numerous processes (macrovilli and microvilli, respectively) extending from their cell bodies (**I**).

Oocytes are freed from their follicle envelopes by either enzymatic defolliculation (treating the ovarian tissue in medium containing crude collagenase preparations) or manual defolliculation (dissecting them manually using watchmaker's forceps). In this chapter we describe the defolliculation protocols in our laboratory, and we discuss the problems associated with enzymatic defolliculation (detrimental effects on oocyte

health) and manual defolliculation (inability to remove the follicle cell layer). For some experiments, it is also desirable or necessary to remove the vitelline membrane. Refer to Chapter 8 for a protocol.

The large size of the fully grown amphibian oocytes makes it possible to manually isolate various subcellular components of a single cell. One of the most remarkable is the manual removal of the oocyte nucleus (enucleation) to yield a more or less intact oocyte without the nucleus (an enucleated oocyte). After piercing on the animal pole and the extrusion of the nucleus, a classic actomyosin “contractile ring” assembles around the edge of the wound and then directs the contraction and healing process (2), and most enucleated oocytes can achieve complete healing if the wound size is small and the oocytes go through proper treatment after enucleation. A classic application of this technique is the discovery of the transcription-independent action of progesterone in *Rana* oocytes (3). In this chapter, we describe the enucleation protocols in our laboratory.

2. Materials

1. Frogs: oocyte-positive *X. laevis* females are purchased from NASCO (Fort Atkinson, WI) and maintained according to local animal care guidelines. A number of Web resources describe husbandry of these animals in great detail (*see* www.xenbase.org for details and links).
2. Surgical instruments: Straight blunt specimen forceps and curved operating scissors for ovarian tissue separation; fine (no. 5) Dumont forceps for manual defolliculation and enucleation.
3. 0.5 U/ μ L Pregnant mare serum gonadotropin (PMSG) solution, dissolved in autoclaved double-distilled water and stored at -20°C .
4. OR2 medium: 82.50 mM NaCl, 2.5 mM KCl, 1 mM CaCl_2 , 1 mM MgCl_2 , 1 mM Na_2HPO_4 , 5 mM *N*-2-hydroxyethylpiperazine-*N'*-2-ethanesulfonic acid (HEPES), pH 7.8. We typically make large quantities of calcium-free OR2 (OR2 minus CaCl_2), autoclave, and store at room temperature. CaCl_2 is added from 1 M stock. We also supplement OR2 with antibiotic (100 $\mu\text{g}/\text{mL}$ gentamicin) and sometimes polyvinyl alcohol (PVA; 1 mg/mL) to prevent oocytes from sticking to the bottom of the Petri dishes.
5. Defolliculation medium: collagenase A (Roche, stored at 4°C) is dissolved in calcium-free OR2 to the concentration of 1.5 mg/mL and is supplemented with 1 mg/mL soybean trypsin inhibitor.
6. Healing medium: 90 mM potassium phosphate, pH 7.2, 10 mM NaCl, 1 mM MgSO_4 ; store at room temperature.
7. Gall's medium: 83 mM KCl, 17 mM NaCl, 1 mM MgCl_2 , 10 mM Tris-HCl, pH 7.2; store at room temperature.
8. Nucleus medium: 100 mM NaAc, pH 5.2, 5 mM ethylenediaminetetraacetic acid (EDTA); store at 4°C .
9. PBS lysis buffer: 10 mM sodium phosphate, pH 7.5, 150 mM NaCl, 1% Triton X-100; store at 4°C ; prior to use, supplement with 10 $\mu\text{g}/\text{mL}$ leupeptin (added fresh from 1 mg/mL frozen stock in water) and 1 mM phenylmethylsulfonate (from 200 mM frozen stock in dimethylsulfoxide).
10. Sandpaper: 0.05- μm sandpaper (Fiberlap, Tucson, AZ).

3. Methods

3.1. Ovarian Tissue Isolation

1. Frogs are injected in the dorsal lymph sac with PMSG (50 IU/frog) 3 to 10 d before oocyte retrieval (see **Note 1**).
2. At 30 min before the ovarian tissue isolation, the frog is placed in a plastic tank filled with icy water. The anesthetized frog is then decapitated with a guillotine, and an incision is made in the skin and body wall in the posterior ventral side of the animal, parallel to the dorsal-ventral midline. The ovary with multiple lobes is teased out with blunt-end forceps, snipped off using scissors, and placed in a Petri dish containing calcium-free OR2 medium.

3.2. Defolliculation by Collagenase Treatment

There are two obvious advantages in isolating oocytes by collagenase treatment. The first one is to obtain a large quantity of oocytes without stressing your eyes and hands. The second one is that the oocytes obtained in such a fashion are truly defolliculated (similar to that shown in **Figs. 2C,D**).

There are drawbacks as well. Collagenase treatment adversely affects the metabolic rate of oocytes. The most noticeable is the marked depression in endogenous protein synthesis (4). A common remedy for this is to include a recovery period, usually overnight incubation, before oocytes are used for further experiments. However, such oocytes remain less robust than manually defolliculated oocytes. For example, although it is not uncommon to observe a germinal vesicle breakdown (GVBD) response within 2 to 3 h of the addition of progesterone to manually defolliculated oocytes, it typically takes twice as long to observe it for collagenase-treated oocytes. Also, it is our experience that collagenase-treated oocytes do not always respond to insulin to undergo GVBD. On the other hand, manually defolliculated oocytes almost always respond to insulin (1 μ M) to undergo GVBD.

The other significant drawback is that collagenase treatment sometimes causes spontaneous GVBD. We discovered that some batches of Sigma type I collagenase cause spontaneous GVBD, but others do not. We have also been using Roche's collagenase A for a period of time without experiencing any spontaneous GVBD. Therefore, some caution should be exercised in choosing collagenase for defolliculation. In addition to some batches of collagenase, we have also found that other proteases, Blendzyme (a mixture of highly purified collagenase and dispase; Roche), trypsin, and proteinase K can also induce spontaneous GVBD. Most likely, some proteases destroy an oocyte surface protein (e.g., a G protein-coupled receptor) that is critical for maintaining G2 arrest (5,6).

1. Isolated ovarian tissue is minced into small pieces (each contains 20–30 stage VI oocytes) using Dumont forceps, washed once with calcium-free OR2 medium, and then transferred to a 100 \times 15 mm culture dish containing 14 mL defolliculation medium.
2. The dish is incubated at 20°C on a platform shaker for 2 to 3 h, until at least half of the oocytes are free from the follicular tissue. Defolliculated oocytes of various stages, together with residual tissue fragments and cell debris, are then transferred to a 50-mL Falcon tube. Fill the tube with calcium-free OR2 medium.
3. Invert the Falcon tube several times. In doing so, the larger oocytes tend to settle more quickly than the small oocytes and residual tissue fragments, and these impurities can be partially removed by simply decanting the solution. Another purpose of this step is to wash out the residual collagenase. This precleaning step is repeated four times.

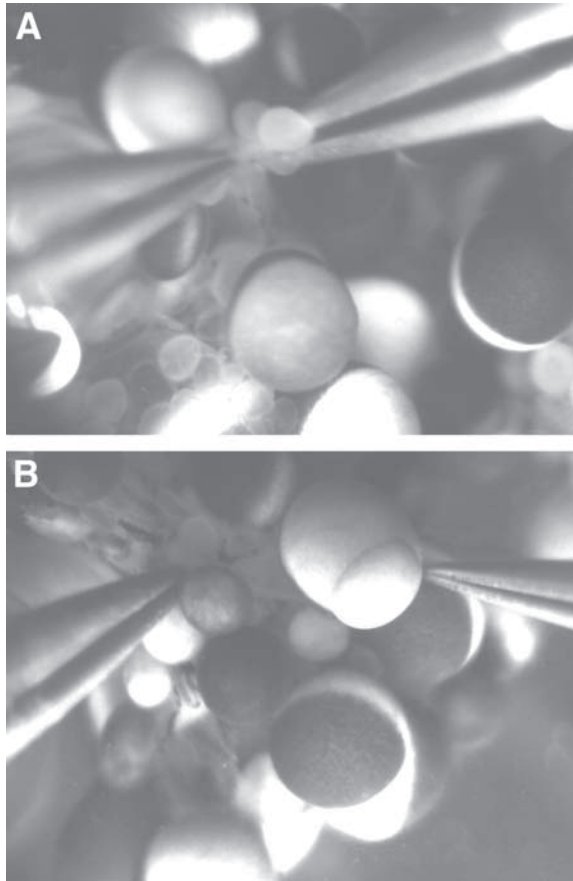


Fig. 1. Manual defolliculation. (A) Grab the “stalk” of the target follicle with two pairs of sharp watchman’s forceps. (B) Tease apart the follicle slowly so that the oocyte can “squeeze” out.

4. The remaining oocyte preparation is transferred to a 100 × 15 mm culture dish containing approx 14 mL calcium-free OR2, and the dish is gently shaken for 3 h with four changes of medium (two changes for the first hour and one change per hour for the next 2 h).
5. Oocytes are sorted under a dissecting microscope. Clean stage VI oocytes (*see* Chapter 2 for oocyte staging) are grouped and transferred to a Petri dish containing full-strength OR2 medium supplemented with gentamicin and stored overnight in an 18°C incubator. On the second day healthy oocytes (those that remain evenly pigmented in the animal hemisphere) are selected for further experiments.

3.3. Manual Defolliculation With Sandpaper Stripping

It is customary in our lab for a new recruit to spend the first 2 to 3 wk to learn and practice manual defolliculation. We follow the description provided in Smith et al. (7). Place a piece of ovarian tissue containing 50 to 100 oocytes in a 6-cm dish filled with Ca²⁺-free OR2. Under a dissecting microscope, place two pairs of sharp forceps

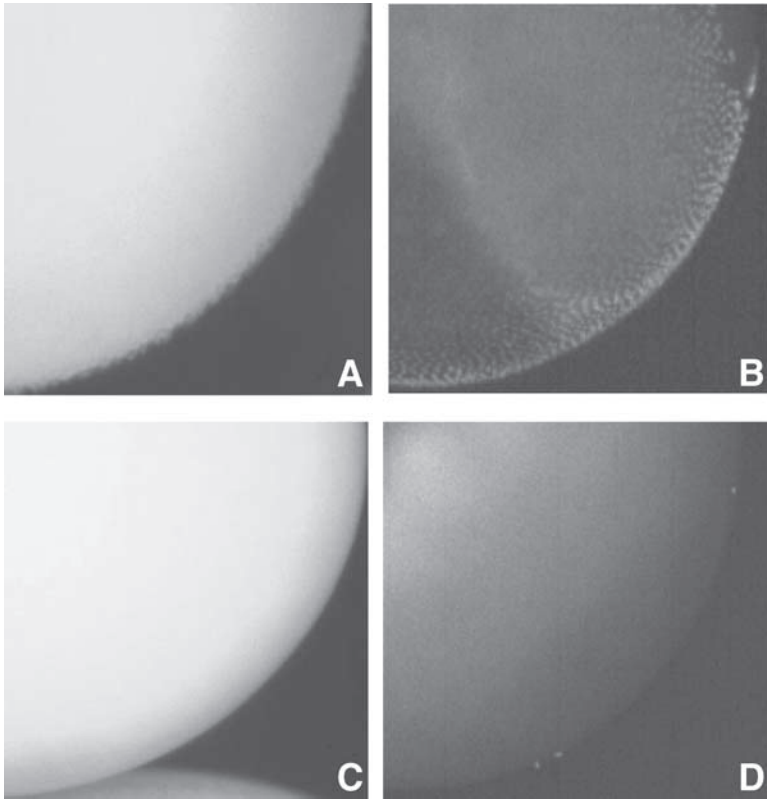


Fig. 2. Manually defolliculated oocytes before and after sandpaper stripping. (A) The surface of a manually defolliculated oocyte appears rough under a dissecting scope and (B) exhibits a full layer of follicle cells as their nuclei are revealed by the fluorescence DNA dye Sytox Green. In contrast, the surface of sandpaper-stripped oocytes (C) appears smooth and (D) exhibits no Sytox Green staining.

at the base of the target follicle (where the follicle is attached to the ovarian tissue). Gently grab the stalk (Fig. 1A) and tease apart the follicle envelope such that the oocyte slowly “squeezes” out of the follicle envelope (Fig. 1B). The defolliculated oocytes should contain no blood vessel but still contain almost a whole layer of follicle cells (Fig. 2A,B). This procedure can be very frustrating in the first week, but eventually (after many weeks of practice) one should be able to isolate 100 to 300 oocytes per hour. To remove these follicle cells, one might carry out a brief incubation with collagenase (a protocol can be found in Chapter 8). Alternatively, the follicle cells can be stripped by gentle shaking on fine-grade sandpaper, as first described by Vilain et al. (8):

1. Manually defolliculated oocytes are placed in a Petri dish with the bottom that is coated with a circular piece of 0.05- μ m sandpaper. The level of calcium-free OR2 in the Petri

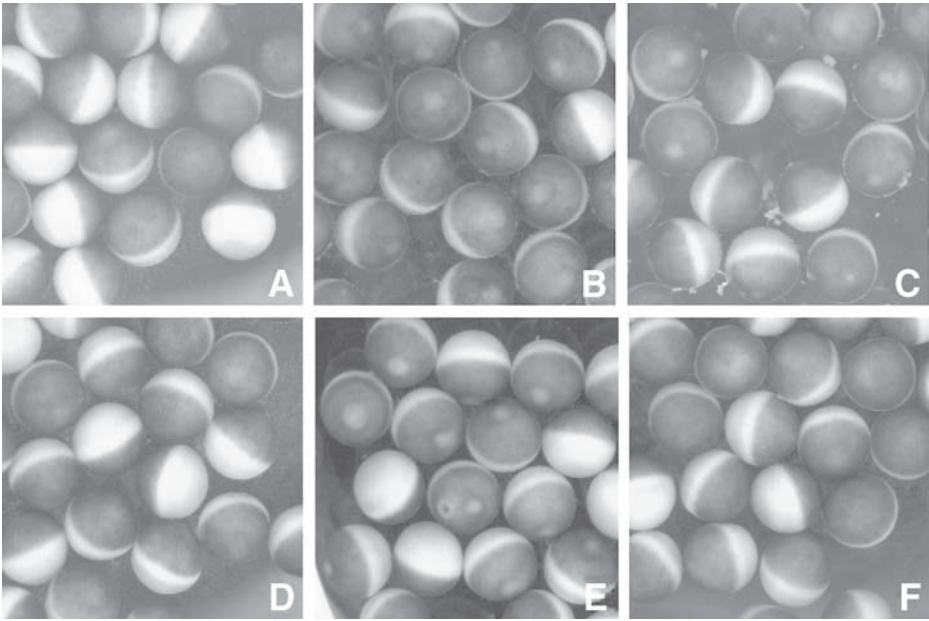


Fig. 3. Differential responses of manually defolliculated oocytes before and after sandpaper stripping. Both (A) manually defolliculated oocytes and (D) sandpaper-stripped oocytes remain indefinitely in germinal vesicle stage. Manually defolliculated oocytes respond to both (B) progesterone ($1 \mu\text{M}$) and (C) hCG (50 U/mL) to undergo GVBD; sandpaper-stripped oocytes only respond to progesterone (E) but not hCG (F).

dish is adjusted so that the surface of the medium can spread the oocytes into a single layer rolling on the sandpaper (rather than floating, when too much buffer is used) when the dish is shaken at a speed of 240 rpm on a platform shaker.

2. After 2 h, oocytes are examined under the dissecting microscope using the maximum magnification. A smooth and shiny oocyte surface indicates successful removal of follicle cells (Fig. 2C). If large patches of follicle cells are still attached to the oocyte surface, oocytes are incubated for an additional 1 to 2 h. In most cases, complete removal should be achieved after 4 h of stripping.
3. The presence of follicle cells can also be determined by fluorescence microscopy (Leica MZFLIII) following 30-min incubation with Hoechst dye ($10 \mu\text{g/mL}$) or with Sytox Green (Molecular Probes, Eugene, OR; used at $1000\times$ dilution) (Fig. 2B,D). Live follicle cells can be directly visualized by Hoechst dye, but methanol fixation (100% methanol for minimum of 1 h) is required for Sytox-Green staining.

Functionally, manually defolliculated oocytes respond to both progesterone and human chorionic gonadotropin (hCG) to undergo GVBD (Fig. 3). In contrast, sandpaper-stripped oocytes only respond to progesterone and not hCG to undergo GVBD (Fig. 3).

3.4. Enucleation for Functional Studies

Enucleation was originally developed in the 1960s (3,9,10). The healing solution (Steinberg's saline) used by Smith and Ecker for *Rana pipiens* did not result in high levels of healing with *Xenopus* oocytes. A *Xenopus* protocol was developed, and the resulting enucleated oocytes could support RNA synthesis by injected HeLa cell nuclei for at least 3 d (11). We successfully used the following protocol to generate apparently "healed" enucleated oocytes that reproducibly responded to progesterone, as measured by activation of mitogen-activated protein kinase and maturation promoting factor (not shown).

1. Defolliculated oocytes are transferred to a Petri dish containing half-strength OR2 medium (1/1 diluted with water) and incubated at room temperature for 30 min (see Note 2).
2. Two pairs of forceps with different tip conditions are used in the enucleation process. One pair with bent and blunt tips is used to hold the oocyte; another pair with straight and sharp tips is used to pick a small opening on the animal pole. Usually, the nucleus will immediately appear in the opening, and complete extrusion will take about 30 s. Sometimes, gentle squeezing with the blunt-end forceps is required to facilitate the extrusion of the nucleus (see Note 3).
3. When five enucleated oocytes have accumulated in the dish, they are immediately transferred to the healing solution to minimize the extrusion of cytoplasm. Enucleated oocytes are incubated in a Petri dish containing healing solution for 1.5 h. At the end of the healing process, the small piece of cytoplasm attached to the wound (if there is any) is gently dislodged using blunt-end forceps (see Note 4).
4. Oocytes are transferred to OR2 medium supplemented with gentamicin and PVA. At this stage, some oocytes have already achieved complete healing; others still have small openings. Oocytes are incubated for an additional 2 h and are then selected under the dissecting microscope. Most oocytes achieve complete healing at this time, as indicated by the complete closure of the wound (Fig. 4, panel G). Those that fail to completely close the wound at this time (Fig. 4, panel H) are discarded (see Note 5).

3.5. Enucleation for Western Blot Analysis

Although the aforementioned enucleation protocol is suitable for obtaining healed enucleated oocytes for functional studies, it is not recommended in studies in which the nucleus and enucleated oocyte are to be analyzed simultaneously. This is because the nucleus extruded into the half-strength OR2 will swell and become very fragile. The alternative enucleation method described in the following paragraph was originally developed by Gall et al. (12). The advantages of this protocol are as follows: (1) Gall's medium is designed to maintain the nuclear content as a gelatinous ball even after the removal of the nuclear envelope, so one can expect minimum loss of nuclear contents during the enucleation process; (2) the cytoplasm of the enucleated oocyte will remain very stiff in Gall's medium and will not be extruded, so minimum loss of cytoplasm can be achieved. It should be noted that neither the enucleated oocytes nor the nuclei isolated in this manner can be used for further functional assays.

1. Prepare two pairs of forceps with different tip conditions: One pair with bent and blunt tips is used to hold the oocyte; another pair with bent and sharp tips is used to snip a small opening on the animal pole.

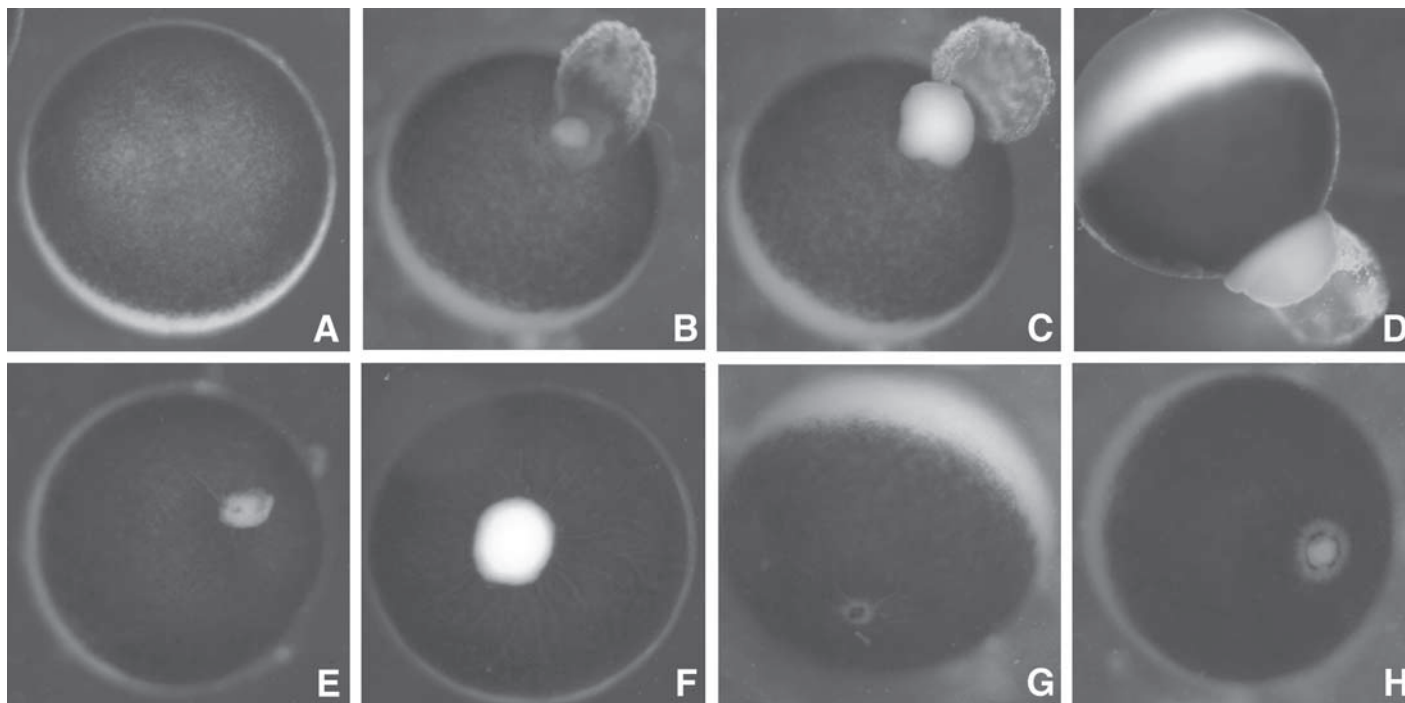


Fig. 4. Enucleation and healing: (A) A single oocyte after 30-min incubation in half-strength OR2 medium. (B) The extrusion of the nucleus. (C) The extrusion of cytoplasm after ejection of the nucleus. (D) Excessive loss of cytoplasm. (E) A well-healed oocyte after 1.5-h incubation in the healing medium, with a small piece of cytoplasm still attached. (F) A poorly healed oocyte with a big hole after 1.5-h incubation in the healing medium. (G) A well-healed oocyte after 2-h incubation in OR2 medium with gentamicin and PVA. (H) An oocyte that is not completely healed after 2-h incubation in OR2 medium with gentamicin and PVA; such oocytes were discarded.

2. Under a dissecting microscope, place a small group of oocytes (fewer than 10) in a Petri dish containing Gall's medium (plus Mg^{2+}). Use the sharp forceps to snip a small opening on the animal pole. Use both forceps to squeeze the nucleus out of the oocyte (see **Note 6**).
3. If the nuclei contain much cytoplasm, transfer them to another Petri dish containing Gall's medium and wash away the attached cytoplasmic fragments by blowing them gently using a P2 Pipetteman. Otherwise, transfer the nuclei to an Eppendorf tube containing 0.5 mL ice-cold nucleus medium. If the enucleated oocytes are also needed, transfer them to another tube (see **Note 7**).
4. Immediately centrifuge the tube containing nuclei at 400g in a refrigerated Eppendorf centrifuge (4°C) for 30 s, carefully aspirate the supernatant without disturbing the nuclei pellet, and then add 2X sodium dodecyl sulfate sample buffer.
5. Aspirate excess medium from the tube containing the enucleated oocytes, lyse the enucleated oocytes in ice-cold phosphate-buffered saline lysis buffer (10 nL per oocyte; lysis by passing the oocytes through a yellow pipette tip), centrifuge at 10,000g in a refrigerated Eppendorf centrifuge (4°C) for 5 min, and recover the supernatant and mix it with an equal volume of 2X sodium dodecyl sulfate sample buffer.

4. Notes

1. The purpose of the PMSG "priming" is to stimulate the growth of the ovarian tissue and hence increase the quantity of stage VI oocytes. Although the main purpose of this PMSG priming is to increase the population of stage VI oocytes, it also significantly shortens the time-course of GVBD. In oocytes from such stimulated females, GVBD is apparent within 2 h (for manually defolliculated oocytes) after steroid exposure, whereas GVBD in similar stage VI oocytes from unstimulated females may occur more than 6–8 h after exposure to progesterone (**13**).
2. In the original protocol, oocytes were incubated in half-strength oocyte incubation medium (equivalent of OR2 medium) for 5 min before an opening was made on the animal pole, and it usually took 10 to 20 min for the nucleus to be extruded. In our protocol, most nuclei will be extruded immediately, and the time during which an opened oocyte stays in half-strength OR2 is 1 to 2 min, which is much shorter. Another advantage of our protocol is that after 30-min incubation in half-strength OR2, the oocytes will be uniformly round and will automatically rotate (sometimes oocytes will slightly stick to the bottom of the plastic Petri dish, but this attachment can be easily disrupted by gently tapping the Petri dish) until the animal poles are uppermost, which is convenient for the later enucleation step. In contrast, in the original protocol, oocytes need to be adjusted individually to ensure that they stick to the bottom of the glass dish with animal poles uppermost.
3. Making the opening on the animal pole is the most critical step in the whole procedure. The first factor is the diameter: a minimum opening by the tip of a sharp watchmaker's forceps is sufficient for the nucleus to be extruded considering the osmotic pressure built up inside the oocyte and the plasticity of the nucleus, and an opening slightly larger will lead to substantial increase in the loss of cytoplasm. The second factor is the position of the opening: if the opening is made right at the animal pole, the nucleus will immediately emerge and prevent cytoplasm leakage by functioning as a temporary "seal." However, if the position is slightly away from the center, substantial loss of cytoplasm will occur before the nucleus appears underneath the opening. The correct way to make the opening is as follows: let the tip of the forceps touch the center of the animal pole, press down gently, and move the forceps backward immediately after breaking the plasma membrane.

The backward movement is necessary because otherwise it is very easy to break the nucleus, which pops out rapidly.

4. The precise role of the healing solution is not clear, but one apparent function is to prevent/minimize the exudation of cytoplasm from the wound (**II**). Oocytes will shrink in the healing medium, and the edge of the wound will contract and fold inward. Most enucleated oocytes will have some cytoplasm attached to the opening when placed in the healing solution. Because the removal of this piece of cytoplasm in the enucleation dish may enlarge the wound and lead to the exudation of more cytoplasm, the oocytes are transferred to the healing medium with the attached cytoplasm and left undisturbed until the end of incubation in healing solution. The whole piece can be easily detached from the oocyte by forceps before the oocytes are transferred into regular OR2 medium; at this time, the wounds underneath are healed.
5. When enucleated oocytes are incubated in the healing solution, they will not stick to the bottom of the Petri dish because there is always a layer of cytoplasm “coating” the bottom to prevent oocyte attachment. However, when healed enucleated oocytes are transferred to a new Petri dish containing OR2 medium, they will slightly stick to the bottom. This is problematic because attempts to dislodge them with a transfer pipet for further distribution into final assay wells may damage healed oocytes. To prevent this stickiness, PVA (1 mg/mL) is added to OR2 before the addition of the healed oocytes.
6. Oocyte cytoplasm is very rigid in Gall’s medium and will remain in the oocyte even after the opening is made. Because the oocyte will shrink in the medium and there is no osmotic pressure to facilitate the extrusion of the nucleus, the opening should be bigger than the one made in half-strength OR2 medium, and it takes some time (usually 1–2 min per oocyte) to slowly squeeze the nucleus out.
7. The nucleus medium will quickly precipitate the nuclear content (P. J. DiMario, personal communication). The nuclei will appear opaque once transferred to the nucleus medium and can be easily observed and counted.

References

1. Smith, L. D., Ecker, R. E., and Subtelny, S. (1968) In vitro induction of physiological maturation in *Rana pipiens* oocytes removed from their ovarian follicles. *Dev. Biol.* **17**, 627–643.
2. Mandato, C. A. and Bement, W. M. (2001) Contraction and polymerization cooperate to assemble and close actomyosin rings around *Xenopus* oocyte wounds. *J. Cell Biol.* **154**, 785–797.
3. Masui, Y. and Markert, C. L. (1971) Cytoplasmic control of nuclear behavior during meiotic maturation of frog oocytes. *J. Exp. Zool.* **177**, 129–145.
4. Wallace, R. A., Jared, D. W., Dumont, J. N., and Sega, M. W. (1973) Protein incorporation by isolated amphibian oocytes. 3. Optimum incubation conditions *J. Exp. Zool.* **184**, 321–333.
5. Gallo, C. J., Hand, A. R., Jones, T. L., and Jaffe, L. A. (1995) Stimulation of *Xenopus* oocyte maturation by inhibition of the G-protein alpha S subunit, a component of the plasma membrane and yolk platelet membranes. *J. Cell Biol.* **130**, 275–284.
6. Wang, J. and Liu, X. J. (2003) A G protein-coupled receptor kinase induces *Xenopus* oocyte maturation. *J. Biol. Chem.* **278**, 15,809–15,814.
7. Smith, L. D., Xu, W. L., and Varnold, R. L. (1991) Oogenesis and oocyte isolation. *Methods Cell Biol.* **36**, 45–60.

8. Vilain, J. P., Moreau, M., and Guerrier, P. (1980) Uncoupling of oocyte-follicle cells triggers reinitiation of meiosis in amphibian oocytes. *Dev. Growth Differ.* **22**, 687–691.
9. Dettlaff, T. A., Nikitina, L. A., and Stroeva, O. G. (1964) The role of the germinal vesicle in oocyte maturation in anurans as revealed by the removal and transplantation of nuclei. *J. Embryol. Exp. Morphol.* **12**, 851–873.
10. Smith, L. D. and Ecker, R. E. (1969) Role of the oocyte nucleus in physiological maturation in *Rana pipiens*. *Dev. Biol.* **19**, 281–309.
11. Ford, C. C. and Gurdon, J. B. (1977) A method for enucleating oocytes of *Xenopus laevis*. *J. Embryol. Exp. Morphol.* **37**, 203–209.
12. Gall, J. G., Murphy, C., Callan, H. G., and Wu, Z. (1991) Lampbrush chromosomes. *Methods Cell Biol.* **36**, 149–166.
13. Smith, L. D. (1989) The induction of oocyte maturation: transmembrane signaling events and regulation of the cell cycle *Development.* **107**, 685–699.

Xenopus tropicalis Oocytes

More Than Just a Beautiful Genome

Jean-François L. Bodart and Nicholas S. Duesbery

Summary

For more than 30 yr, *Xenopus laevis* has been the animal of choice for studying the biochemical regulation of the meiotic and early mitotic vertebrate cell cycles. Attracted by its diploid genome, several laboratories have begun using the similar, although evolutionarily distinct, frog *Xenopus tropicalis* for studies of vertebrate development. Comparisons between the two species indicate that their development is similar in most respects. Both frogs share many advantages, including their amenability to manipulation and their ability to produce large numbers of high-quality oocytes and eggs year round. In addition, *X. tropicalis* possesses several advantages that, when combined with its potential for genetic studies, makes it an attractive, complementary model for vertebrate developmental biology. In this chapter, we note some of these advantages and describe in detail techniques we have adapted for the study of meiosis in *X. tropicalis*.

Key Words: Amphibian; maturation; meiosis; oocyte; *Xenopus tropicalis*.

1. Introduction

Immature oocytes of vertebrates, arrested at prophase of meiosis I, resume the meiotic cell cycle in response to hormonal stimulation (1,2). The resumption of meiosis is followed by the dissolution of the nuclear envelope (germinal vesicle [GV] breakdown [GVBD]), diakinesis, first meiotic spindle formation, and separation of paired homologous chromosomes in the first meiotic division. Oocytes subsequently arrest at metaphase II as mature oocytes, or eggs, in anticipation of fertilization.

Studies of meiosis in the amphibian *Xenopus laevis* have contributed greatly to knowledge of the biochemical activities of key regulatory molecules involved in these processes. Meiotic cell cycle progression is regulated by the activity of a protein complex called maturation-promoting factor (MPF) (3). This complex is made up of two subunits: a catalytic Ser/Thr kinase subunit, p34^{cdc2}, and a regulatory subunit, cyclin B (4–7). The activation of p34^{cdc2} in meiosis requires not only its association with its

regulatory subunit but also the removal of inhibitory phosphates on residues Thr 14 and Tyr 15. Phosphorylation of these residues is regulated by the competing activities of Cdc25 phosphatase (8–10) and Myt1 kinase.

Hormonal stimulation of oocytes triggers increased protein synthesis and activation of the Mos/mitogen-activated protein kinase kinase/mitogen-activated protein kinase (MAPK)/p90 ribosomal S6-kinase pathway, leading to inhibition of Myt 1 (11,12), and at the same time activates polo-kinase 1 (Plx1) (13–15), which phosphorylates and activates Cdc25. Efforts are now directed toward understanding how the dynamic activities of these proteins drive changes in oocyte ultrastructure.

Some labs (16,17) have begun using *Xenopus tropicalis* as a complementary model for amphibian meiosis for several important reasons. First, while retaining the key experimental advantages of *X. laevis*—including rapid, synchronous cell division at early developmental stages, external development, large size, and ease of surgical manipulation of oocytes and embryos—*X. tropicalis* oocytes also mature at a faster rate and display external morphological markers that will allow researchers to distinguish different stages of meiotic cell cycle progression. In addition, *X. tropicalis* holds great potential as a genetic model of vertebrate development.

Despite the advantages of *X. laevis* as an animal model, its amenability to genetic approaches is limited as a consequence of its pseudotetraploidy (18), its relatively large genome (3.1×10^9 basepairs, $n = 18$), and its long generation time (1–2 yr). The use of *X. tropicalis* avoids these limits: it has a shorter generation time (0.5–1 yr; ref. 19) and a small (1.7×10^9 basepairs, $n = 10$), diploid genome (20). Significantly, the US Department of Energy has announced plans to sequence the *X. tropicalis* genome. For all these reasons, the importance of *X. tropicalis* as a model for vertebrate development in general is expected to increase significantly. In this chapter, we describe in detail techniques we have adapted for the study of meiosis in *X. tropicalis*.

2. Materials

Unless stated otherwise, all reagents may be purchased from Sigma Chemicals (St. Louis, MO; www.sigmaaldrich.com).

1. Frogs: *X. tropicalis* may be purchased from any of a number of commercial suppliers, including Xenopus One (Dexter, MI; www.xenopusone.com), NASCO (Fort Atkinson, WI; www.nascofa.com), or Xenopus Express (Plant City, FL; www.xenopus.com). A number of Web resources describe husbandry of these animals in great detail (see www.xenopusbase.org for details and links).
2. Masui's oocyte medium (21) (MOM): 85 mM NaCl, 0.8 mM KCl, 0.5 mM CaCl₂, 0.6 mM MgSO₄, 5.4 mM Tris-base, 4.0 mM sulfadiazine. For preparation of MOM, prepare 0.5 to 1 L each of stock A (1.7 M NaCl, 16 mM KCl) and stock B (10 mM CaCl₂, 12 mM MgSO₄). These may be stored at room temperature for several months. To prepare a working solution, mix 1.0 g sulfadiazine, 0.6 g Tris-base, and 800 mL deionized water in a 1 L Erlenmyer flask. Place on a heated stir plate and mix without boiling until the sulfadiazine goes into solution. (If the solution appears yellow after heating, then it has been overheated and should be discarded.) Cool to room temperature in a running cold water bath and add 50 mL each of stocks A and B. Bring the total volume to 1 L with deionized water and sterile filter to remove traces of undissolved sulfadiazine (which would otherwise act as nuclei for crystal formation).

3. Surgical instruments: fine (no. 55) Dumont forceps, 4-1/2-in. tissue forceps. Iris surgical scissors, 6-1/2-in. surgical scissors (useful for cutting vertebrae), needle holders, regular surgeon's needles (half circle, cutting edge no. 10), and 5-0 degradable surgical thread, all available from Fine Surgical Instruments, Inc. (Hempstead, NY; www.finesurgical.com).
4. Defolliculation medium: 2% (w/v) collagenase (type I or IV but not type II), 1 mg/mL soybean trypsin inhibitor, and 1 mg/mL bovine serum albumin (*see Note 1*).
5. Hormones: progesterone or androstenedione (4-androstene-3,17-dione); make a 10 mg/mL stock in ethanol and store at -20°C .
6. Oocyte fixative: 20% formalin (v/v), 60% ethanol, 10% acetic acid, 10% glycerol. This fixative should only be used in a well-ventilated area.
7. Smith's fixative (**22**): prepare stock solutions A (1% potassium dichromate) and B (20% formalin, 5% acetic acid) and mix 1/1 (v/v) just prior to use.
8. Nuclear Fast Red (Kernechtrot) solution: dissolve 5 g $\text{Al}_2(\text{SO}_4)_3$ hydrate in 100 mL warm distilled water. Add 0.1 g Nuclear Fast Red and heat with stirring until it is completely dissolved. Cool to room temperature, filter, and store at 4°C .
9. Picro-indigo carmine: add 0.25 g indigo carmine to 100 mL saturated picric acid. Mix at room temperature and store at 4°C .
10. Mounting medium: Entellan Mounting Medium (Merck, Darmstadt, Germany).
11. Phosphate buffered saline (PBS): 145 mM NaCl, 10 mM NaH_2PO_4 , 10 mM Na_2HPO_4 , pH 7.4.
12. Antibodies: monoclonal anti- α tubulin (Sigma, clone tub2.1), Oregon Green (Molecular Probes, Eugene, OR; www.probes.com) or fluorescein isothiocyanate conjugated goat anti-mouse.
13. Mounting medium for immunofluorescence: 80% glycerol, 20% PBS containing 1 $\mu\text{g}/\text{mL}$ Hoechst 33342.
14. Homogenization buffer: 60 mM β -glycerophosphate, 15 mM nitrophenyl phosphate, 2.5 mM 3-(*N*-morpholino)propanesulfonic acid (MOPS; pH 7.0), 15 mM ethylenediaminetetraacetic acid (EDTA), 15 mM MgCl_2 , 2 mM dithiothreitol, 0.1 mM NaF, 0.1 mM Na_3VO_4 , containing 1 tablet of Complete[®] EDTA-free protease inhibitor cocktail (Roche) per 50 mL (store at 4°C).
15. Sample buffer: 0.2 M Tris-HCl, pH 8.0, 20% glycerol (v/v), 10% β -mercaptoethanol, 6% sodium lauryl sulfate (w/v), 0.5% bromophenol blue.
16. Bead buffer (**23**): 50 mM Tris-HCl, pH 7.4, 250 mM NaCl, 5 mM EDTA, 50 mM EGTA, 0.2% Igepal CA-630, containing 1 tablet of Complete EDTA-free protease inhibitor cocktail per 50 mL. Store at 4°C .
17. Histone H1 kinase assay buffer: 60 mM β -glycerophosphate, 30 mM nitrophenyl phosphate, 2.5 mM MOPS, pH 7.0, 5 mM EGTA, 1 mM dithiothreitol, 0.1 mM Na_3VO_4 . Store at -20°C in 0.5-mL aliquots.
18. p13^{suc1}-Sepharose beads.
19. Histone H1: type IIIS, 1 mg/mL in histone H1 kinase assay buffer.
20. Adenosine triphosphate (ATP) solution: [$\gamma^{32}\text{P}$] ATP (90 μM , 4500 mCi/mmol; 10 $\mu\text{Ci}/\mu\text{L}$) (Amersham).

3. Methods

Ovarian oocytes are arrested at prophase of meiosis I and contain a prominent nucleus or GV. Oocytes resume meiosis (or mature) in response to hormonal stimulation (**1,2**). In *X. laevis*, the resumption of meiosis is followed 2 to 5 h later by the dissolution of the nuclear envelope (GVBD) and the outward appearance of a large

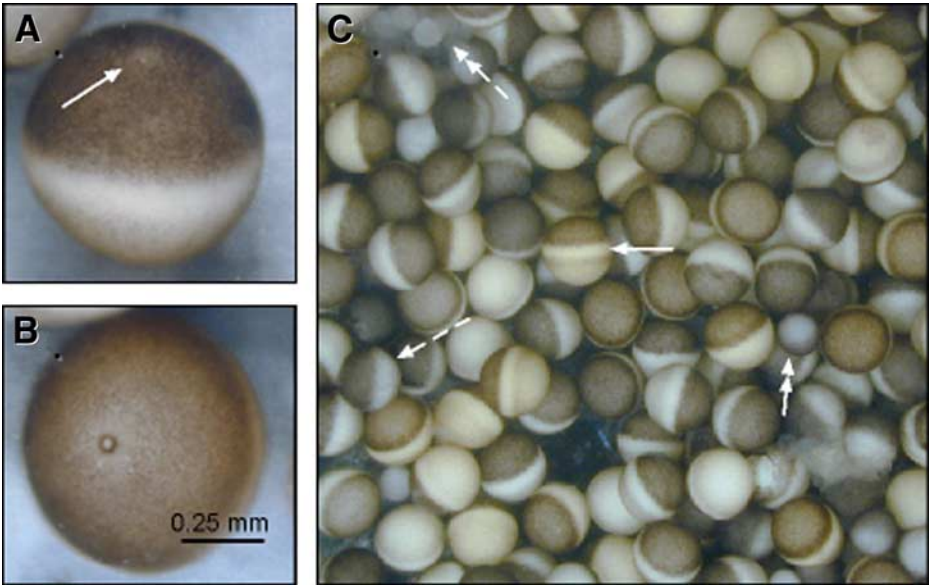


Fig. 1. The external morphology of *Xenopus tropicalis* oocytes. Treatment of stage VI oocytes with progesterone induces germinal vesicle breakdown and meiotic spindle formation. Where the first meiotic spindle contacts the cortex, (A) a small white spot appears, which subsequently alters appearance to (B) a dark ring as meiosis progresses beyond metaphase I. (C) Following collagenase defolliculation, stage VI oocytes (solid arrow) may be separated from immature oocytes (stage V, dashed arrow; stage IV, double arrowhead; stage III, dashed double arrowhead) using a Pasteur pipet.

(100- μ m) white spot. After completion of the first meiotic division and release of the first polar body, oocytes arrest at metaphase of the second meiotic division.

Similarly, maturation of *X. tropicalis* oocytes may be induced by continuous exposure of full-grown oocytes to MOM containing 10 μ g/mL of progesterone, androstenedione (4-androstene-3,17-dione), corticosterone (4-pregnene-11 β ,21-diol-3,20-dione), or Reichsten's substance (4-pregnene-17 α ,21-diol-3,20-dione). However, *X. tropicalis* oocytes mature much faster than *X. laevis*, with the majority of oocytes completing GVBD within 1 to 2 h of hormone treatment. In addition, rather than forming a large white spot, maturing *X. tropicalis* oocytes first form a small (10- μ m) spot (Fig. 1A), which is subsequently replaced by a larger dark ring (Fig. 1B). Significantly, the white spot and dark ring act as external markers of progression through the first meiotic division because their appearance correlates with first meiotic spindle formation and exit from metaphase I, respectively (17).

3.1. Oocyte Isolation

Ovaries may be surgically removed from anesthetized or euthanized frogs. Unlike mammals, amphibian ovaries are capable of regenerating. Therefore, we can mini-

mize the number of animals used in any study by performing multiple survival surgeries on a single animal, allowing at least 1–3 mo between operations on the same frog.

To comply with the National Research Council Institute of Laboratory Animal Resources' guidelines for the breeding, care, and management of amphibians, we recommend the following procedures be employed for the isolation of ovarian oocytes from *X. tropicalis*. All surgical instruments should be heat sterilized prior to use. We make up ahead of time sterile packs containing one pair of surgical scissors, two pairs of fine forceps (one having tissue grips), two cotton swabs, ten 6-in. lengths of precut surgical thread, two surgeon's needles, and one needle holder.

To minimize the risk of infection during surgery, clean a space on a workbench with ethanol, perform the operations (preferably) on disposable padding, and wear disposable medical gloves during surgery. Although frogs may be immobilized by a 20- to 30-min immersion in an ice water slurry, current guidelines require that this procedure now be performed with anesthetic agents. Frogs should be immersed in MOM containing tricaine methanesulfonate (MS-222) (2 g/L) for 20 to 30 min until they become nonresponsive to handling, that is, when they show no signs of voluntary movement and fail to return to a proper orientation after turned over (if this is to be a nonsurvival study; *see* **Note 2**).

Place the frog in a dorsal recumbant position. To keep the frog's skin moist during the surgery, cover it with a tissue that has been soaked in MOM containing MS-222. Make a cut through the tissue to expose the frog's abdomen. Then, make a 1-cm incision in the epidermis and peritoneal wall, parallel to the dorsal-ventral midline and in the lower abdominal quadrant. *Xenopus* ovaries are multilobed, resembling gloves with oocytes lining the inner surfaces of the fingers or lobes.

Depending on experimental requirements, tease two to three ovarian lobes from the body cavity with a forceps and a sterile cotton swab. Securely ligate the ovary using 5-0 degradable sutures, excise the externalized portion, and place it in MOM. Next, gently push the still-exposed portions of the ovary back into the body cavity using a sterile cotton swab that has been moistened with MOM. Separately seal the peritoneal wall and epidermis with two sutures (5-0 degradable) each. The slimy nature of the outer surface of the epidermis of *X. tropicalis* can make it difficult to push a needle through, so we usually pierce the epidermis from the inner surface of the skin.

Typically, this surgery may be expected to take 10 min to complete. Postoperative care should include incubating frogs in shallow water containing 10 µg/mL gentamicin until they have sufficiently recovered from anesthesia and housing them in a separate aquarium with daily monitoring for any signs of infection until the wound has healed.

3.2. Defolliculation of *Xenopus tropicalis* Oocytes

Ovarian oocytes are wrapped in several layers of follicle cells and theca, which protects them and provides them with nourishment during oogenesis. As with *X. laevis*, these layers may be removed by manually using forceps or enzymatically using a protease solution (24). However, the smaller size of *X. tropicalis* oocytes makes manual defolliculation a challenge (although not insurmountable) even to an accomplished

X. laevis defolliculator. In either case, first tease the ovarian fragments apart with fine forceps so that each lobe of the fragment is opened into a single sheet of oocytes.

For manual defolliculation, separate a small ovarian fragment containing 20 to 30 oocytes and transfer it to a separate Petri dish. Looking through a dissecting microscope, carefully grasp the ovarian tissue adjacent to an oocyte using fine forceps in both hands and gently tease the tissues apart to separate the oocyte. Patience and perseverance are required.

For enzymatic defolliculation, blot ovarian sheets on a paper tissue to remove excess liquid and transfer them to a 15-mL conical tube containing 2.5 mL defolliculation medium. Incubate at room temperature with gentle rocking. *Xenopus tropicalis* follicles are more sensitive to collagenase treatment than are those of *X. laevis* and should be monitored frequently in defolliculation medium. After approx 0.5 h, the ovarian tissues will begin to separate into individual oocytes that will still be surrounded by adhering thecal and follicle cells. Fill the tube containing the oocytes with 0.1 M KH_2PO_4 (pH 6.5), leaving a small space for air at the top of the tube. Cover the mouth of the tube with a piece of parafilm and invert the tube four or five times, allowing the trapped air bubble to pass through the descending mass of oocytes.

As you do this, you should notice that larger stage V and VI oocytes tend to settle quickly, and the smaller stage I to IV oocytes are in the topmost fraction. Using a Pasteur pipet, remove the KH_2PO_4 (along with smaller oocytes if desired). Repeat this wash four or five more times. You should notice that after two to three more washes the adherent thecal and follicle cells separate from the oocytes. These tissues also settle slowly and may be removed using a Pasteur pipet. When it appears that no more follicle cells are coming off the oocytes, rinse twice with MOM and using a transfer pipet remove the oocytes to a Petri dish containing MOM. Any remaining follicle cells stick to the surface of the Petri dish and can easily be excluded when sorting cells.

3.3. Induction of Oocyte Maturation

Immature oocytes may be induced to mature by treatment with 10 $\mu\text{g}/\text{mL}$ progesterone or other steroid hormones (ref. 17; see Note 3). Careful attention to experimental design can minimize subsequent difficulties in interpretation. First, determine how many oocytes you will need for a particular experiment. Plan to use at least 15 to 20 oocytes per time-point. Because these oocytes mature faster than *X. laevis* oocytes, you will need to take time-points more frequently; every 15 to 20 min should be sufficient. Carefully select the appropriate number of stage VI oocytes (Fig. 1C) and transfer them to a Petri dish containing fresh MOM. Stage VI oocytes are distinguished by their size (650–700 μm) and by the presence of an unpigmented equatorial band that separates the dark color animal hemisphere from the pale vegetal hemisphere.

3.4. Monitoring Progression Through Meiosis

Progression through meiosis may be determined by assaying cytological, morphological, and biochemical parameters. In the following subheadings, we describe in detail methods we have successfully applied for work with *X. tropicalis*.

3.4.1. Assaying GVBD in Fixed Oocytes

1. At 15- to 20-min intervals during each experiment, fix small groups of 15 to 20 oocytes by adding one volume of oocyte fixative directly to the culture dish or by transferring oocytes to a small Petri dish containing oocyte fixative diluted 50% with oocyte medium. After about 12 h, oocytes will have hardened to a point at which they may be dissected without losing their shape. Oocytes fixed under these conditions may be stored for weeks; preparations that have dried out may be rehydrated and examined months after fixation.
2. Using a dissecting microscope, examine each oocyte and record the presence or absence of a white spot or a dark ring.
3. Bisect each oocyte along the animal-vegetal axis with a sharp scalpel. Examine each oocyte and record the presence or absence of GV. The GV may be distinguished from the yolk cytoplasm by its pale color and consistency.

3.4.2. Expressing Results

The rate and extent of maturation vary between oocytes obtained from different females and under different environmental conditions. Moreover, it is not unusual to observe maturation in “unstimulated” oocytes, with the most likely source of error contamination by forceps that have come in contact with progesterone-containing medium. These difficulties may be overcome by including appropriate positive (hormone-treated) and negative (untreated) controls in every experiment and by expressing the timing of meiotic events in experimental treatments relative to that in oocytes treated with progesterone alone. For instance, timing is frequently expressed relative to the time at which control oocytes complete 50% GVBD (GVBD₅₀). If 50% of hormone-treated oocytes complete GVBD by 80 min and 50% of experimentally treated oocytes complete GVBD within 40 min, then the experimental group should be reported as having GVBD₅₀ equal to 0.5. A similar approach may be used to express the timing of white spot or dark ring formation.

3.4.3. Assaying Spindle Formation in *Xenopus tropicalis* Oocytes

Accurate determination of meiotic cell cycle progression requires assaying meiotic spindle formation. There are two basic methods to do this: histochemical staining or immunocytochemistry. The former is time consuming and requires practice to perfect the technique but offers superior resolution of subcortical and spindle structures.

3.4.3.1. HISTOCHEMICAL STAINING OF OOCYTES

1. Fix oocytes in Smith's fixative overnight at room temperature (keep in the dark).
2. Dehydrate oocytes in an ethanol series going from 70 to 95% in three washes of 10 min each. Then, wash twice (30 min) in absolute ethanol.
3. Wash twice (30 min each) with butanol. Oocytes may be stored for several days in either 70% ethanol or butanol.
4. Infiltrate oocytes with paraffin by incubating first in butanol/paraffin (1/1) at 60°C for 20 min and then in three changes of paraffin (30 min each).
5. Embed in paraffin blocks, mount, and trim. Cut in 7- μ m sections with a microtome. Coat slides with a 1/1 mixture of egg albumin/glycerol to promote adherence of sections. Allow section to adhere to slides at 38 to 40°C for at least 24 h. To obtain egg albumin, strain an egg white overnight at 4°C through a piece of cheesecloth fastened over the mouth of a 100-mL beaker with an elastic band.

6. Remove paraffin by incubating slides in methyl-cyclohexane baths (twice, 30 min each).
7. Rehydrate slides in an ethanol series going from 100 to 70% in three washes of 10 min each and finally rinsing with double-distilled water.
8. Incubate slides in Nuclear Red solution for 1 h.
9. Rinse with double-distilled water (five times for 1 min each).
10. Incubate slides in picro-indigo carmine for 30 s and rinse once with 0.3% acetic acid.
11. Dehydrate oocytes in an ethanol series going from 70 to 95% (three washes, 10 min each). Then, wash twice (10 min each) in absolute ethanol.
12. Incubate slides in methyl-cyclohexane (three washes, 10 min each).
13. Attach cover slips with mounting medium and allow slides to dry.

3.4.3.2. IMMUNOCHEMICAL STAINING OF SQUASHED OOCYTES (25)

1. Fix 15 to 20 oocytes in ice-cold methanol in a 1.5-mL Eppendorf tube for 2 h to overnight at -20°C .
2. Rehydrate oocytes in a methanol/PBS series going from 100 to 70% (three washes of 10 min each). Then, rinse five times with PBS.
3. Incubate oocytes in 100 to 200 μL PBS containing 0.1% Tween-20 and a 1/100 dilution of anti- α -tubulin antibody for 6 to 12 h at 4°C .
4. Rinse oocytes with PBS five times for 5 min each.
5. Incubate oocytes with 100 to 200 μL PBS containing 0.1% Tween-20 and a 1/100 dilution of secondary antibody conjugated to a fluorescent marker such as Oregon Green or fluorescein isothiocyanate for 6 to 12 h at 4°C .
6. Rinse oocytes with PBS five times for 5 min each.
7. Place oocytes in a 0.8-mm deep well of a depression slide. Carefully bisect each oocyte at the animal-vegetal equator using a sharp scalpel and place the animal half on a standard slide with the cut side facing downward. As many as 12 to 16 oocytes may be placed on a single slide. To make it easier to find the oocytes under the microscope, we usually arrange them in a grid pattern.
8. Remove excess PBS using a rolled-up paper tissue or a piece of filter paper and dry the slide in a gentle stream of air. Add four or five drops of mounting medium and, using moderate force, squash the oocytes beneath a cover slip.
9. Examine oocytes under an epifluorescent microscope. These preparations are stable for months if stored at 4°C .

3.4.4. Making Lysates for Immunoblotting

Because of their large size relative to somatic cells, it is easy to make cellular lysates of oocytes that can be used for immunoblotting. Methods developed for *X. laevis* (26) are readily applied to *X. tropicalis* after taking into account the differing size of oocytes between the two species.

1. At each time-point, transfer 10 to 20 oocytes to an Eppendorf tube containing 1 μL of homogenization buffer per oocyte.
2. Lyse the oocytes by passing them up and down repeatedly through a pipet tip. Sediment the yolk platelets by centrifugation for 10 min at $10,000g$ at 4°C .
3. Transfer the supernatant to a clean Eppendorf tube and add an equal volume of sample buffer. Heat samples in boiling water for 3 min before separating proteins by denaturing polyacrylamide electrophoresis. Typically, 10 μL sample is sufficient to allow detection of a protein such as MAPK by Western blotting.

3.4.5. Making Lysates for Histone H1 Kinase Assays

1. At each time-point, transfer 10 oocytes to an Eppendorf tube containing 100 μ L homogenation buffer.
2. Lyse the oocytes by passing them up and down repeatedly through a pipet tip. Sediment the yolk platelets by centrifugation for 10 min at 10,000g at 4°C.
3. Transfer 40 μ L supernatant to a clean Eppendorf tube. Add 10 μ L packed p13^{suc1}-sepharose beads (Sigma, St. Louis, MO) and 450 μ L bead buffer. Incubate on a rotator at 4°C for 1 h.
4. Briefly centrifuge at 10,000g in a bench-top centrifuge to pack the p13^{suc1}-sepharose beads. The supernatant may be discarded or saved for additional assays.
5. Gently resuspend the p13^{suc1}-sepharose beads in 50 μ L bead buffer, centrifuge, and discard supernatant. Repeat four times.
6. Add 15 μ L histone H1 kinase assay buffer, 5 μ L histone H1 and 5 μ L [γ ³²P] ATP and incubate for 10 min at 30°C.
7. Terminate reaction by placing the tubes on ice (or *see step 11*).
8. After a brief centrifugation to pack the beads, spot 10 μ L on each of three 1-cm² pieces of Whatman P81 phosphocellulose filter paper.
9. Wash the filter papers five times with 1% phosphoric acid.
10. After drying the filter papers on absorbent towels, transfer each to a separate scintillation vial containing 1 mL scintillation fluid and assay incorporated ³²P using a liquid scintillation counter.
11. Alternatively, histone H1 kinase assays may be terminated by addition of one volume of sample buffer. Samples may then be separated by denaturing polyacrylamide electrophoresis and histone H1 activity quantitated using a phosphorimager.

4. Notes

1. Commercial grades of collagenase are a heterogeneous mixture of proteases, so we include bovine serum albumin and soybean trypsin inhibitor in the defolliculation medium to reduce the actions of nonspecific proteases and minimize unintended damage to the oocyte. To prepare defolliculation medium, dissolve 1 g collagenase (Sigma, type I or IV but not type II), 50 mg soybean trypsin inhibitor, and 50 mg bovine serum albumin in 10 mL deionized water and freeze in 0.5-mL aliquots. Stock solutions stored at -20°C are stable for up to 1 yr. To make a working solution, thaw and dilute with 2.0 mL MOM.
2. If this is to be a nonsurvival surgery, cut the spine of an anesthetized frog just posterior to the skull and pith the frog by inserting one blade of a pair of 6 1/2-in. surgical scissors through the foramen magnum and crush the skull.
3. The optimal temperature for these experiments lies between 22 and 25°C. At lower temperatures (16–18°C), the formation of white spots and dark rings is delayed or prevented following GVBD, and at higher temperatures (28°C), we have observed that some batches of oocytes lyse or undergo spontaneous GVBD. Optimally, oocytes will be used on the day that they are isolated. However, if required, oocytes may be used up to 48 h after isolation if they are stored at 18°C between uses. Oocytes stored at room temperature show a progressive delay of approx 1 h additional in the time to GVBD per day of extended storage.

Acknowledgments

We thank David Nadziejka for technical editing of this manuscript and Jeanine Myles (supported by the Grand Rapids Area Pre-College Engineering Program) for technical assistance.

References

1. Masui, Y. (1967) Relative roles of the pituitary, follicle cells, and progesterone in the induction of oocyte maturation in *Rana pipiens*. *J. Exp. Zool.* **166**, 365–375.
2. Smith, L. D., Ecker, R. E., and Subtelney, S. (1968) In vitro induction of physiological maturation in *Rana pipiens* oocytes removed from ovarian follicles. *Dev. Biol.* **17**, 627–643.
3. Masui, Y. and Markert, C. L. (1971) Cytoplasmic control of nuclear behavior during meiotic maturation of frog oocytes. *J. Exp. Zool.* **177**, 129–145.
4. Dunphy, W. G., Brizuela, L., Beach, D., and Newport, J. (1988) The *Xenopus* cdc2 protein is a component of MPF, a cytoplasmic regulator of mitosis. *Cell* **54**, 423–431.
5. Gautier, J., Norbury, C., Lohka, M., Nurse, P., and Maller, J. (1988) Purified maturation-promoting factor contains the product of a *Xenopus* homolog of the fission yeast cell cycle control gene *cdc2⁺*. *Cell* **54**, 433–439.
6. Draetta, G., Luca, F., Westendorf, J., Brizuela, L., Ruderman, J., and Beach, D. (1989) Cdc2 protein kinase is complexed with both cyclin A and B: evidence for proteolytic inactivation of MPF. *Cell* **56**, 829–838.
7. Labbe, J. C., Capony, J. P., Caput, D., et al. (1989) MPF from starfish oocytes at first meiotic metaphase is a heterodimer containing one molecule of cdc2 and one molecule of cyclin B. *EMBO J.* **8**, 3053–3058.
8. Gautier, J., Solomon, M. J., Booher, R. N., Bazan, J. F., and Kirschner, M. W. (1991) cdc25 is a specific tyrosine phosphatase that directly activates p34^{cdc2}. *Cell* **67**, 197–211.
9. Kumagai, A. and Dunphy, W. G. (1991) The cdc25 protein controls tyrosine dephosphorylation of the cdc2 protein in a cell-free system. *Cell* **64**, 903–914.
10. Strausfeld, U., Labbe, J. C., Fesquet, D., et al. (1991) Dephosphorylation and activation of a p34cdc2/cyclin B complex in vitro by human CDC25 protein. *Nature* **351**, 242–245.
11. Palmer, A., Gavin, A.-C., and Nebreda, A. R. (1998) A link between MAP kinase and p34^{cdc2}/cyclin B during oocyte maturation: p90^{rsk} phosphorylates and inactivates the p34^{cdc2} inhibitory kinase Myt1. *EMBO J.* **17**, 5037–5047.
12. Gavin, A. C., Ni Ainle, A., Chierici, E., Jones, M., and Nebreda, A. R. (1999) A p90(rsk) mutant constitutively interacting with MAP kinase uncouples MAP kinase from p34(cdc2)/cyclin B activation in *Xenopus* oocytes. *Mol. Biol. Cell* **10**, 2971–2986.
13. Kumagai, A. and Dunphy, W. G. (1996) Purification and molecular cloning of Plx1, a Cdc25-regulatory kinase from *Xenopus* egg extracts. *Science* **273**, 1377–1380.
14. Qian, Y. W., Erikson, E., and Maller, J. L. (1999) Mitotic effects of a constitutively active mutant of the *Xenopus* polo-like kinase Plx1. *Mol. Cell. Biol.* **19**, 8625–8632.
15. Qian, Y. W., Erikson, E., Taieb, F. E., and Maller, J. L. (2001) The polo-like kinase Plx1 is required for activation of the phosphatase Cdc25C and cyclin B-Cdc2 in *Xenopus* oocytes. *Mol. Biol. Cell* **12**, 1791–1799.
16. Stanford, J. S., Lieberman, S. L., Wong, V. L., and Ruderman, J. V. (2003) Regulation of the G2/M transition in oocytes of *Xenopus tropicalis*. *Dev. Biol.* **260**, 438–448.
17. Bodart, J. F., Gutierrez, D. V., Nebreda, A. R., Buckner, B. D., Resau, J. R., and Duesbery, N. S. (2002) Characterization of MPF and MAPK activities during meiotic maturation of *Xenopus tropicalis* oocytes. *Dev. Biol.* **245**, 348–361.
18. Tinsley, R. C. and Kobel, H. R. (1996) *The Biology of Xenopus*. Symposia of the Zoological Society of London, 68, Clarendon Press, Oxford.
19. Hirsch, N., Zimmerman, L. B. and Grainger, R. M. (2002) *Xenopus*, the next generation: *X. tropicalis* genetics and genomics. *Dev. Dyn.* **225**, 422–433.

20. Tymowska, J. and Fischberg, M. (1982) A comparison of the karyotype, constitutive heterochromatin, and nucleolar organizer regions of the new tetraploid species *Xenopus epitropicalis* Fischberg and Picard with those of *Xenopus tropicalis* Gray (Anura, Pipidae). *Cytogenet. Cell Genet.* **34**, 149–157.
21. Zhang, S. C. and Masui, Y. (1992) Activation of *Xenopus laevis* eggs in the absence of intracellular Ca activity by the protein phosphorylation inhibitor, 6-dimethylaminopurine (6-DMAP). *J. Exp. Zool.* **262**, 317–329.
22. Smith, B. G. (1912) The embryology of *Cryptobranchus allegheniensis* including comparisons with some other vertebrates. *J. Morphol.* **23**, 61–153.
23. Azzi, L., Meijer, L., Ostvold, A. C., Lew, J., and Wang, J. H. (1994) Purification of a 15-kDa cdk4- and cdk5-binding protein. *J. Biol. Chem.* **269**, 13,279–13,288.
24. De Sousa, P. A. and Masui, Y. (1990) The effect of cytochalasin D on protein synthesis in *Xenopus laevis* oocytes. *Mol. Reprod. Dev.* **26**, 248–252.
25. Duesbery, N. S., Choi, T., Brown, K. D., et al. (1997) CENP-E is an essential kinetochore motor in maturing oocytes and is masked during Mos-dependent, cell cycle arrest at metaphase II. *Proc. Natl. Acad. Sci. USA* **94**, 9165–9170.
26. Shibuya, E. K., Boulton, T. G., Cobb, M. H., and Ruderman, J. V. (1992) Activation of p42 MAP kinase and the release of oocytes from cell cycle arrest. *EMBO J.* **11**, 3963–3975.

Oocyte Expression With Injection of Purified T7 RNA Polymerase

Xavier Altafaj, Nathalie Joux, Michel Ronjat, and Michel De Waard

Summary

The *Xenopus* oocyte is a widely used system for protein expression. Investigators have had the choice between two different techniques: injection into the cytoplasm of in vitro transcribed complementary RNA (cRNA) or injection into the nucleus of complementary DNA (cDNA). We report on a third expression technique that is based on the combined injection of cDNA and purified T7 RNA polymerase directly into the cytoplasm of oocytes.

Key Words: Exogenous protein; expression technique; injection; T7 RNA polymerase; *Xenopus* oocyte.

1. Introduction

The genomic era has generated an ever-increasing need for protein structure and functional analyses. The *Xenopus laevis* oocyte cell machinery is remarkably well adapted for exogenous protein expression. Through specific technical developments, the ever-increasing use of this expression system has allowed the implementation of many new applications. *Xenopus* oocytes have been used to study protein posttranslational modifications, channel ion fluxes with various biophysical approaches (1), changes in membrane capacitance (2), reconstituted transmitter release (3), channel gating currents, multiprotein subunit assembly (4), receptor pharmacology (5), sub-cellular metabolic activity (6), and so on. Their relatively large sizes (~1 mm) allow investigators to perform biochemical analyses on single cells. For many applications, it takes one cell or less to detect expressed proteins by Western blotting or a metabolic labeling approach. The ease with which an oocyte can be injected allows experiments that are difficult to achieve otherwise: injection of peptides (7) or recombinant proteins (8) and on-line recordings of the functional effects of nonpermeable metabolic analogs.

Original reports showed that exogenous membranes, containing exogenous channels and receptors, can be inserted into the plasma membrane of oocytes and characterized. Examples include the microtransplantation of secretion vesicles from

From: *Methods in Molecular Biology*, vol. 322: *Xenopus Protocols: Cell Biology and Signal Transduction*
Edited by: X. J. Liu © Humana Press Inc., Totowa, NJ

chromaffin cells and of membrane preparations from Alzheimer's brain (9) or Torpedo electroplaque membranes (10). Many of these applications have required methodological developments that are often specific for the oocyte system.

For biochemical or biophysical studies, receptors and channels expressed in the plasma membrane can be studied in isolation following plasma membrane isolation (11–14). Similarly, nuclear functions can be studied after isolation of individual oocyte nuclei (15,16); conversely, the function of oocytes can be studied after their nuclei have been removed (17). New electrophysiological recording techniques have been developed specifically for the oocyte system, such as the cut-open oocyte voltage clamp (18) or the transoocyte voltage clamp (19) techniques. Similarly, improved oocyte preparations have been proposed for patch-clamp experiments (20).

Along with these techniques, the great size of these cells has required the development of new extracellular (21) or intracellular (22) perfusion systems. Regarding structure–function analyses, unique *in vivo* incorporation of unnatural amino acids is possible into proteins expressed in *Xenopus* oocytes (23). Oocytes have also been used for expression cloning experiments (24). These are a few examples of the technological advances that have been made specifically for the oocyte system.

The use of the *Xenopus* oocyte system as an expression reporter was initially boosted with the discovery that exogenous hemoglobin messenger RNA (mRNA) is efficiently translated in frog oocytes (25). Two techniques have been widely used to induce the expression of proteins of exogenous origin: (1) complementary DNA (cDNA) injection in the nucleus (26) or (2) injection of complementary RNA (cRNA) into the cytoplasm (27).

Although nuclear injection is greatly facilitated by the relatively important size of the nucleus (up to a one-third of the total volume of the oocyte), it is still unreliable for two reasons. First, depending on each individual's dexterity for injecting into the nucleus, only a fraction of the oocytes will express the gene of interest (one-third, rarely more) (26). Second, the efficacy of transcription will heavily depend on the type of eukaryotic promoter used. With different promoters, if one seeks to coexpress at least two different genes, there is a nonnegligible risk that the expression level of each desired gene turns out to be very different. Injection of cRNA in the cytoplasm of oocytes appears more reliable as a method for expression because 100% of the cells express the gene of interest, and the expression level is easily controlled by defining the cRNA concentration and the injected volume.

The main drawback of the technique, however, is the time-consuming experimentation linked to cRNA production, storage, and manipulation. The aim of the present chapter is thus to present an alternative method that circumvents some of the drawbacks of both cytoplasmic cRNA and nuclear cDNA injections. This new technique takes advantage of the reliability of cytoplasmic injection without the requirement for an *in vitro* transcription step. The method relies on an autonomous cDNA transcription system, driven by the DNA-dependent T7 promoter of the bacteriophage T7 RNA polymerase (T7 RNAP). Thanks to the optimization in critical steps of T7-RNAP purification, this new procedure turns out to be less time consuming and is more cost-effective than the two classical expression techniques. Proper functional protein

expression has been assessed by different methodologies, such as metabolic labeling and electrophysiological recordings on different proteins forming K^+ , Na^+ , and Ca^{2+} channel subunits of different species (ref. 28; see Notes 1–5). We present here the protocols required for the use of this T7 RNAP expression technique.

2. Materials

2.1. T7 RNA Polymerase Purification

1. *Escherichia coli* strain BL21 (DE3) (Invitrogen).
2. pMR-T7 RNAP plasmid (29).
3. Luria Bertani (LB) medium: 10 g/L tryptone, 5 g/L yeast extract, and 10 g/L NaCl.
4. Ampicillin.
5. Isopropylthio- β -D-galactoside (IPTG) (Sigma, St. Louis, MO).
6. Tris-buffer saline (TBS): 150 mM NaCl, 25 mM Tris-HCl, pH 7.4.
7. Benzamide.
8. Phenylmethylsulfonyl fluoride (PMSF).
9. Triton X-100 (Sigma).
10. Resuspension buffer: 150 mM NaCl, 25 mM Tris-HCl, pH 7.4, with 0.1% Triton X-100, 1 mM benzamide, and 0.23 mM PMSF.
11. Sepharose beads coupled to iminodiacetic acid (Sigma).
12. Disposable Poly-Prep[®] chromatography columns (Bio-Rad, Hercules, CA).
13. Spectra/Por[®] membrane (Biovalley, Conches, France).
14. Activation buffer: 50 mM NiSO₄.
15. Loading buffer: 40 mM imidazole, 500 mM NaCl, 50 mM Tris-HCl, pH 7.9.
16. Elution buffer: 400 mM imidazole, 500 mM NaCl, 50 mM Tris-HCl, pH 7.9.
17. Coomassie blue staining solution (Bio-Rad).
18. Gel destaining solution: 50% ethanol, 10% acetic acid.
19. Bradford assay using commercial reagents (Bio-Rad).

2.2. In Vitro T7 RNAP Western Blot Detection and Transcriptional Activity

1. SDS-PAGE (sodium dodecyl sulfate-polyacrylamide gel electrophoresis) equipment.
2. Nitrocellulose membrane (Hybond[®] ECL, Amersham Biosciences, Bucks, UK).
3. Transfer buffer: 48 mM Tris-HCl, 39 mM glycine, 20% methanol, and 0.0375% SDS.
4. Luminescent reagent (Western Lightning[™] Chemiluminescence Reagent Plus; Perkin-Elmer, Boston, MA).
5. Monoclonal anti-T7 antibody (Novagen, Madison, WI).
6. Monoclonal anti-mouse immunoglobulin G antibody conjugated to peroxidase (Zymed, San Francisco, CA).
7. Blocking solution: 150 mM NaCl, 50 mM NaH₂PO₄, 5% milk, 0.05% Tween-20, pH 7.4.
8. Hyperfilm[™] ECL[™] (Amersham Biosciences).
9. Transcription buffer is from the mMessage mMachine[™] kit (Ambion, Cambridgeshire, UK).
10. Agarose electrophoresis grade (GIBCO BRL, Paisley, Scotland).

2.3. Xenopus oocyte Experiments

(Preparation, Maintenance, Injection, and Metabolic Labeling)

1. Mature *X. laevis* female frogs (CRBM, Montpellier, France).
2. Anesthetics: 3-aminobenzoic acid ethyl ester (Sigma).
3. Collagenase type IA (Sigma). Store at -20°C .

4. Ca²⁺-free Barth's medium: 88 mM NaCl, 1 mM KCl, 0.82 mM MgSO₄, 2.4 mM NaHCO₃, 15 mM *N*-2-hydroxyethylpiperazine-*N'*-2-ethanesulfonic acid (HEPES), pH 7.4 with NaOH. Filter sterilize and store at 4°C.
5. Barth's medium: 88 mM NaCl, 1 mM KCl, 0.33 mM Ca(NO₃)₂, 0.41 mM CaCl₂, 0.82 mM MgSO₄, 2.4 mM NaHCO₃, 15 mM HEPES, pH 7.4 with NaOH. Filter sterilize and store at 4°C.
6. Defined nutrient oocyte medium (DNOM). Filter sterilize and store at 4°C. Stable for 2 wk.
7. Falcon 24-well plates (Becton-Dickinson, Le pont de Claix, France).
8. Nanoliter injector (World Precision Instruments [WPI], Sarasota, Florida; www.wpiinc.com).
9. [³⁵S]-L-Methionine at 1175 Ci/mmol (Perkin-Elmer).
10. Glycerol (Sigma).
11. All four deoxyribonucleoside triphosphates (dNTPs) and Cap analog (Ambion).
12. Homogenization buffer: 1% Triton X-100, 50 mM Tris-HCl, pH 6.8.
13. Protease inhibitor cocktail CompleteTM (Boehringer-Mannheim, Mannheim, Germany).

3. Methods

The methods described here allow: (1) a single-step purification of large and pure amounts of recombinant T7 RNAP, (2) the coinjection into the cytoplasm of *Xenopus* oocytes of T7-driven plasmids and purified T7 RNAP, and (3) the characterization by biophysical and biochemical means of the expressed proteins.

3.1. Expression Plasmids

3.1.1. Expression Vector

The cDNA encoding for the full-length wild-type T7 RNAP has been previously cloned in the pMR-78 vector (29) and is presented in Fig. 1. The expression of the insert is under the control of the P_{tac} promoter, which is inducible by IPTG. This vector has a specific *bla* gene that confers ampicillin resistance for colony selection and growth. It is designed to express an N-terminal his-tagged T7 RNAP for purification with a Ni²⁺/iminodiacetic acid affinity column.

3.1.2. cDNA Constructs

The cDNAs used should contain a T7 promoter at the 5' end of the gene of interest. For protein production in oocytes, the cDNA should encode a Kozak's sequence for initiation of translation (30) and a stop codon. cRNA stability, and thus protein yield, can be greatly improved by the presence of a poly A tail sequence at the 3' end of the gene of interest (31).

3.2. Protein Induction

3.2.1. Escherichia coli Transformation and Plasmid Selection

Escherichia coli strain BL21(DE3)pLysS-competent cells were transformed with the pMR-T7 RNAP plasmid and plated on selective LB-agarose dishes containing 0.1 mg/mL ampicillin. A single colony was grown overnight at 37°C under agitation in 5 mL of LB supplemented with 0.1 mg/mL ampicillin. Half of this culture was used to extract the plasmid DNA and check its identity using restriction enzymes. The other half of the culture was used to inoculate a larger bacterial culture (40 mL LB with 0.1 mg/mL ampicillin), which was grown overnight at 37°C under agitation until reaching saturation.

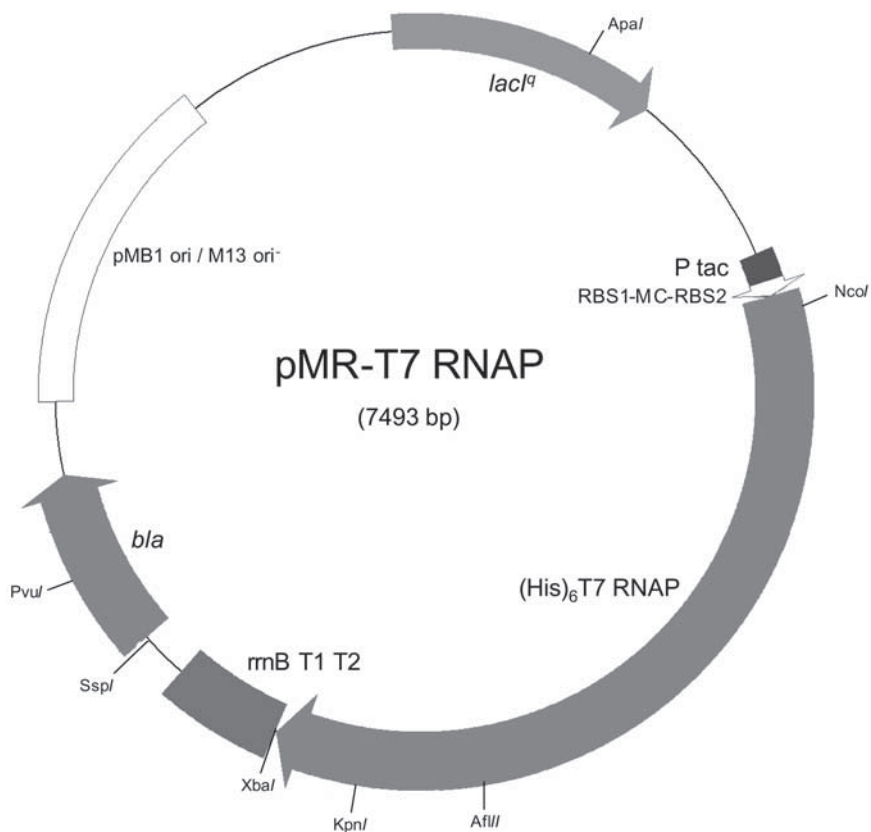


Fig. 1. Structure of pMR-T7 RNAP expression vector adapted from Arnaud and collaborators (29). Ptac, tac promoter; RBS1-MC-RBS2, minicistron flanked by two ribosome binding sites (RBSs); $(\text{His})_6$ T7-RNAP, T7-RNAP coding region tagged with polyhistidine motif; rrnB T1 T2, strong transcription terminators; bla, gene conferring ampicillin resistance; pMB ori/M13 ori-, plasmid origin of replication; lacIq, gene encoding for the lacI^q repressor.

3.2.2. Induction and Bacteria Harvesting

1. Dilute 40 mL of the overnight culture into 400 mL of standard LB medium supplemented with 0.1 mg/mL ampicillin.
2. Once the optical density of 600 nm (OD_{600}) reaches 0.6 (about 2–3 h later), induce protein synthesis by adding a final concentration of 1 mM IPTG to the culture medium for 4 h.
3. Harvest the bacteria by centrifuging at 4000g for 10 min at 4°C and resuspend the pellet in 10 mL resuspension buffer. Use conical 15-mL polypropylene Falcon tubes.

3.3. Protein Purification

3.3.1. Cell Disruption

1. Sonicate four times the resuspended pellet in bursts of 30 s at maximum power using a microtip probe. The Falcon tube should be immersed on ice. Special care should be taken to avoid heating the preparation.

2. Centrifuge the lysate at 14,000g for 15 min. Keep the supernatant, containing the soluble T7 RNAP fraction of interest, on ice for subsequent treatment.

3.3.2. Protein Purification

1. Add 5 mL suspended iminodiacetic acid-Sepharose beads to a disposable 10-mL polypropylene column with a final bed volume of 2.5 mL.
2. Wash the column with 3 bed volumes of water.
3. Charge the column with 5 bed volumes of activation buffer (50 mM NiSO₄).
4. Equilibrate the column with 3 bed volumes of loading buffer.
5. Load the supernatant bacterial preparation of T7 RNAP onto the column.
6. Wash the column with 20 mL loading buffer.
7. Elute the immobilized T7 RNAP by adding 15 mL elution buffer and collect 1-mL fractions.

3.3.3. Detection of T7 RNAP

(Coomassie Blue Staining and Western Blotting)

The quality of the purification procedure can be assessed by gel electrophoresis and immunoblotting as shown in **Fig. 2**. The purity and amount of T7 RNAP are analyzed as described next:

1. Load 3 μ L of each eluted fraction on a 5–15% gradient SDS-PAGE.
2. Stain the gel with Coomassie blue staining solution (Bio-Rad).
3. Destain the gel with destaining solution and check for a protein band with a molecular weight of 98 kDa, corresponding to purified T7 RNAP. Determine the most concentrated elution fractions and analyze them by Western blotting. In our experience, the two most concentrated fractions correspond to elution fractions 3 and 4.
4. For immunodetection, first transfer the proteins from the gel to a nitrocellulose membrane (Hybond ECL). Perform the transfer during 1 h 30 min at 400 mA in transfer buffer.
5. Block the membrane overnight at 4°C in blocking solution.
6. Incubate the membrane for 30 min at 37°C with an anti-T7 monoclonal antibody (from Novagen) previously diluted 5000-fold in the same blocking solution.
7. After four 10-min washing steps in TBS, incubate the membrane for 30 min with the secondary antibody conjugate (anti-mouse immunoglobulin G coupled to peroxidase from Zymed diluted 1/5000).
8. Wash the membrane again four times with TBS.
9. Reveal the peroxidase activity by a 1-min incubation of the membrane with the chemiluminescent reagent (Perkin-Elmer) and its exposure to a Hyperfilm ECL film (Amersham Biosciences). **Figure 2** shows a representative example of immunodetection of purified T7 RNAP.

3.3.4. Dialysis of Purest and Most Concentrated Fractions

1. According to a visual examination of SDS-PAGE analysis, pool together the purest and most concentrated elution fractions for dialysis and buffer exchange (up to 4–6 mL in volume).
2. Load the pooled eluted T7 RNAP fractions into a dialysis tube (Spectra/Por membrane, Biovalley) with a molecular weight cutoff of 10,000 Da.
3. Dialyze the fractions overnight at 4°C against 1 L TBS. Repeat the operation once for 2 h by replacing the external TBS solution.
4. Recover the dialyzed sample, which is ready for protein dosage.

3.3.5. Yield Analysis

Determine the protein concentration of the dialyzed T7 RNAP sample using a Bradford assay following manufacturer's instructions (Bio-Rad commercial reagents). Expect total T7 RNAP quantities to be in the range of 20–40 mg.

3.3.6. Aliquoting and Storage

Purified T7 RNAP is stable for 2 wk at 4°C and can be used as such without further aliquoting. For long-term storage, it is recommended to adjust the concentration of the sample to 10 mg/mL with TBS and by adding 40% glycerol. Small-volume aliquots of the sample (10–100 µL) should be produced and kept at –20°C.

3.4. Activity of Purified T7 RNAP

The activity of the purified T7 RNAP can be evaluated by an in vitro transcription assay.

1. To 40 µL of transcription buffer (mMessage mMachine kit, Ambion), add 100 ng of purified T7 RNAP and 2 µg of a linearized cDNA clone carrying a T7 promoter.
2. Carry out the reaction for 2 h at 37°C.
3. Check cRNA production after gel electrophoresis onto an agarose gel containing formaldehyde (32).

3.5. Oocyte Preparation, Maintenance, and Injection

3.5.1. Oocyte Preparation

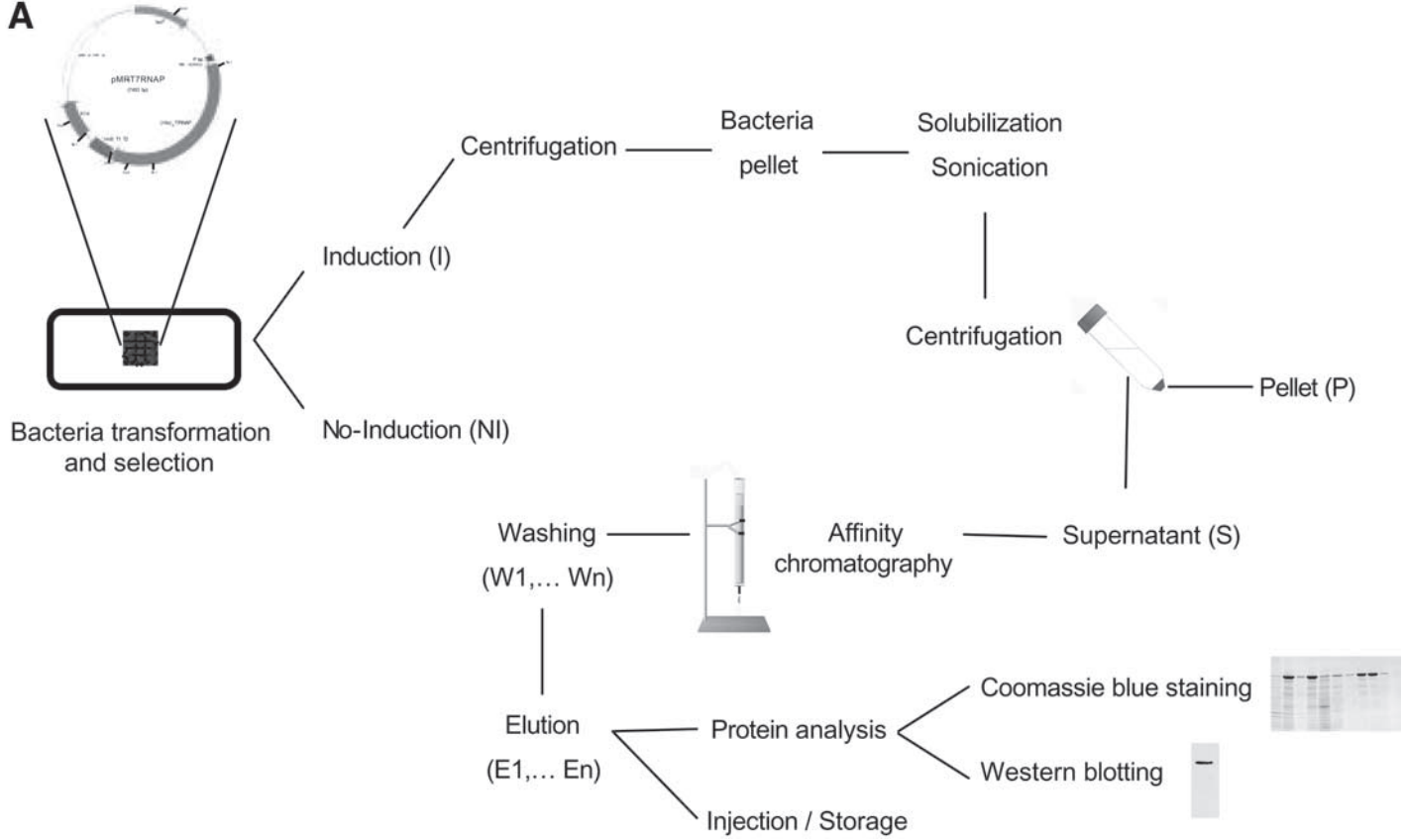
Stage V and VI oocytes are prepared according to the procedure described by De Waard and Campbell (33), which is further described next:

1. Maintain mature *X. laevis* female frogs under a cycle of 12 h light/12 h dark in water tanks at 16°C.
2. Choose a healthy frog, place it into a small and secure container, add water for partial body immersion, and add 0.03% (w/v) of 3-aminobenzoic acid ethyl ester to the water to anesthetize the animal. Partial body immersion is important to avoid drowning of the animal. Leave the frog under anesthetics until it does not react anymore to a leg pinch test.
3. Surgically remove some of the ovaries by making a small incision in the abdomen. Place the ovaries in Ca²⁺-free Barth's solution. The incision is sutured immediately thereafter, and the frog is left to recover in the secure tank after washing out the anesthetics. The animal will return to the water tank after full recovery from surgery and should not be reused for at least 2 mo after the operation.
4. Isolate individual oocytes by an enzymatic digestion of follicle membranes for 2 h with 2 mg/mL of collagenase IA (Sigma) in Ca²⁺-free Barth's solution. Select only stages V and VI oocytes and wash them several times with Ca²⁺-free Barth's solution to remove any remaining enzymatic activity.
5. Visually inspect with a microscope that all oocytes are correctly defolliculated. If not, manual defolliculation is required at this stage.
6. Wash all defolliculated oocytes again with regular Barth's solution.

3.5.2. Oocyte Maintenance

1. Stages V and VI oocytes can be kept for extremely long periods of time (>3 wk) if incubated in DNOM at a temperature range of 16–18°C before and after injection. The composition of DNOM was defined by Eppig and Dumont (34). It has been optimized for

A



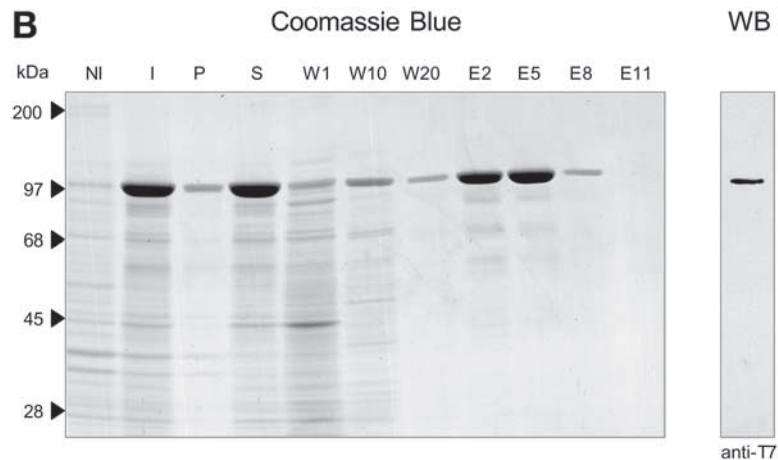


Fig. 2. Expression, purification, and analysis of T7 RNAP. (A) Schematic representation of the protocol used for pMR-T7 RNAP transformation, induction of the expression, purification, and analysis. (B) Left, Coomassie blue staining of a gradient 5 to 15% SDS-polyacrylamide gel illustrating the various steps for T7 RNAP expression in bacteria and purification. Lanes 1 and 2 correspond, respectively, to crude lysate *E. coli* BL21 cells transformed with pMR-T7 RNAP in the absence of induction (NI) or after induction (I); lanes 3 and 4 indicate pellet (P) and supernatant (S) after sonication and centrifugation of bacterial suspension; lanes 5 to 7 correspond, respectively, to the 1st, 10th, and 20th column wash (W1, W10, and W20, respectively); lanes 8 to 12 correspond to elution fractions 2, 5, 8, and 11 (E2, E5, E8, E11), respectively. Right, Western blot (WB) of the second elution fraction (1 μ g) with an anti-T7 RNAP monoclonal antibody.

oocyte survival and maintenance and basically contains amino acids, carbohydrates, salts, vitamins, antibiotics, amphotericin B, phenol red for pH control, and polyvinylpyrrolidone to avoid oocyte attachment to the plastic surface. We strongly recommend the use of DNOM instead of Barth's solution for oocyte maintenance as expression and survival rates were significantly improved.

2. Distribute 10 oocytes in each well of a Falcon 24-well plate and hermetically seal the plate with parafilm to avoid water evaporation and DNOM concentration.

3.5.3. Oocyte Injection

1. *Xenopus* oocytes can sustain up to 50-nL injection in the cytoplasm. For reliability results, we use a nanoliter injector of WPI based on the displacement of an oil/aqueous solution interface.
2. Mix the cDNA of interest with purified T7 RNAP and adjust the concentration with water. In our hands (28), maximal expression level is reached by injecting 5 ng of cDNA and 5 ng of T7 RNAP in each oocyte. If the assumptions are made that the average volume of an oocyte is about 1 μL and that each oocyte is injected with a total volume of 50 nL, then the injected solution should contain 100 ng/ μL of cDNA and 100 ng/ μL of T7 RNAP. These concentrations should represent the upper limits, although some adaptation may be required for each plasmid. With a single purification of T7 RNAP, more than 2000 oocytes can be injected. We successfully expressed various voltage-gated K^+ channels, a voltage-gated Na^+ channel, and a Ca^{2+} channel auxiliary subunit with this technique (28). With T7 RNAP aliquots stored at -20°C , oocytes will also contain 0.02% glycerol. This is not a problem as these cells can contain up to 0.05% glycerol without noticeable effect on protein expression (28).
3. After injection, maintain the oocytes 3 to 6 d at 18°C in DNOM before proceeding with other functional tests. It should be emphasized that cell survival is excellent with this technique. We routinely keep healthy oocytes for 2 to 3 wk after injection. The aim of this chapter is not to describe the functional tests used to reveal the expression of the protein of interest. However, we describe a rapid biochemical test to assess the presence of the protein that one wishes to express in oocytes.

3.6. Metabolic Labeling

The metabolic labeling procedure should be used to determine that protein synthesis is effective. It can also be used to optimize T7 RNAP and cDNA concentrations (see Notes 1 and 2).

1. Coinject 0.2 μCi of [^{35}S]-methionine per oocyte along with the mixture of cDNA and T7 RNAP.
2. After injection, maintain oocytes for 24 h in Barth's medium.
3. Resuspend 20 oocytes for each experimental condition in 1 mL of ice-cold buffer A (50 mM Tris-HCl, 1% Triton X-100, pH 6.8) supplemented with Complete, a protease inhibitor cocktail, and then mechanically homogenize the cells with a 1-mL potter (Bioblock).
4. Incubate the homogenate at 4°C for 30 min under agitation and centrifuge 20 min at 10,000g.
5. Collect the supernatant with a Pasteur pipet, making sure to avoid the lipid layer.
6. Analyze the proteins by SDS-PAGE and autoradiogram analysis.

4. Notes

1. For voltage-gated K^+ channel expression, the effective range of T7 RNAP concentration was between 1 and 100 ng/ μ L. Maximal protein expression is reached at 50 ng/ μ L. A similar concentration dependence was observed with two different plasmids (SP72 and pGEM3) encoding two different proteins (*Shaker* B channel and calcium channel β_3 -subunit), suggesting that it may be generalized. We recommend the use of 100 ng/ μ L T7 RNAP as a first assay of the technique, although some minor optimization may be required.
2. A cDNA dose–response curve has also been realized (28). Expression appeared around 20 ng/ μ L of cDNA, whereas it saturated at concentrations above 100 ng/ μ L. Here again, one should start with 100 ng/ μ L of cDNA, although higher concentrations of cDNA can be attempted. Here, we should emphasize that the quality of the cDNA is a critical factor for the success of this technique. A reliable index of cDNA quality is to achieve an in vitro coupled transcription/translation assay. If the protein is readily produced in vitro by this technique, then it should also be produced with the T7 RNAP procedure in oocytes. If the assay using coupled in vitro transcription/translation is not effective, two conclusions can be drawn: The cDNA construct is either defective, in which case it should be improved, or the cDNA is of poor quality, and a new plasmid preparation and purification is thus required. We have used standard commercial columns for plasmid preparation (Promega, Qiagen, etc.) without encountering any problems.
3. We have not noticed any significant difference in protein expression time with the cRNA injection technique. Our observations suggest that the additional transcription step required by cDNA injection, compared to direct cRNA injection, does not significantly slow protein expression in oocytes. The expression time in oocytes is generally short (1–2 d). For instance, we obtained a maximal expression level 2 d only after injection for a voltage-gated K^+ channel. What seems to delay expression level is the time required for cell trafficking. The appearance of multisubunit calcium channel complexes in the plasma membrane of oocytes can take 4 to 7 d and reflect the time required for translocation to the plasma membrane. These expression times will vary depending on the nature of the protein expressed.
4. We have successfully used this expression technique by also using commercial T3 and SP6 RNA polymerases along with the appropriate plasmids instead of purified T7 RNAP (28). The main drawback of commercial reagents is that their concentration is not provided by the manufacturer. However, using 10-fold diluted commercial T3 or SP6 RNAP (Ambion source) turned out to be fully functional. The use of commercial sources of RNA polymerases is thus perfectly valid for this expression technique if one does not want to perform the affinity purification of RNA polymerase. We can only recommend either to obtain the concentration value of the polymerase or to perform a dose–response curve to define the ideal dilution of the commercial reagent. Care should also be taken to assess the cell toxicity of high concentration of glycerol for those dilution values that are extremely low.
5. We have frequently observed that the level of protein translation is smaller with the T7 RNAP technique than with direct cytoplasmic RNA or nuclear cDNA injections. Also, very large proteins appeared more difficult to synthesize with this technique. It has been observed that DNA injected into the cytoplasm is less stable than DNA injected in the nucleus (35). One hypothesis is that the cytoplasm of oocytes may have an endonuclease activity that would be absent from, or ineffective in, their nuclei. This may well explain the observed limitations of our T7 RNAP technique, although it should be emphasized

that we did not observe any major differences in translation efficiency between circular and linear cDNA. A clear improvement in protein yield was observed if a mix of dNTPs and cap (3.22 mM 2'-deoxyadenosine 5'-triphosphate [dATP]; 3.22 mM 2'-deoxycytidine 5'-triphosphate [dCTP]; 3.22 mM 2'-deoxyuridine 5'-triphosphate [dUTP]; 0.64 mM 2'-deoxyguanosine 5'-triphosphate [dGTP]; and 2.58 mM Cap analog) is coinjected along with purified T7 RNAP and the plasmid of interest (28). This may well represent a technical solution for expression problems encountered with larger proteins. Finally, it should be emphasized that the cytoplasm is not the normal locus for DNA transcription, and one should expect the technique to be drastically improved if the mix of cDNA/T7 RNAP is further injected into the nucleus.

References

1. Dascal, N. (1987) The use of *Xenopus* oocytes for the study of ion channels. *CRC Crit. Rev. Biochem.* **22**, 317–387.
2. Schmitt, B. M., and Koepsell, H. (2002) An improved method for real-time monitoring of membrane capacitance in *Xenopus laevis* oocytes. *Biophys. J.* **82**, 1345–1357.
3. Scheuener, D., Logsdon, C. D., and Holz, R. W. (1992) Bovine chromaffin granule membranes undergo Ca^{2+} -regulated exocytosis in frog oocytes. *J. Cell Biol.* **116**, 359–365.
4. Jaunin, P., Horisberger, J. D., Richter, K., Good, P. J., Rossier, B.C., and Geering, K. (1992) Processing, intracellular transport, and functional expression of endogenous and exogenous α - β 3 Na,K-ATPase complexes in *Xenopus* oocytes. *J. Biol. Chem.* **267**, 577–585.
5. Buller, A. L. and White, M. M. (1992) Ligand-binding assays in *Xenopus* oocytes. *Methods Enzymol.* **207**, 368–375.
6. Lee, C. L., Linton, J., Soughayer, J. S., Sims, C. E., and Allbritton, N. L. (1999) Localized measurement of kinase activation in oocytes of *Xenopus laevis*. *Nature Biotech.* **17**, 759–762.
7. Zagotta, W. N., Hoshi, T., and Aldrich, R. W. (1990) Restoration of inactivation in mutants of *Shaker* potassium channels by a peptide derived from *ShB*. *Science* **250**, 568–571.
8. Geib, S., Sandoz, G., Mabrouk, K., et al. (1992) Use of a purified and functional recombinant calcium-channel β_4 subunit in surface-plasmon resonance studies. *Biochem. J.* **364**, 285–292.
9. Miledi, R., Duenas, Z., Martinez-Torres, A., Kawas, C. H., and Eusebi, F. (2004) Microtransplantation of functional receptors and channels from the Alzheimer's brain to frog oocytes. *Proc. Natl. Acad. Sci. USA* **101**, 1760–1763.
10. Marsal, J., Tigyi, G., and Miledi, R. (1995) Incorporation of acetylcholine receptors and Cl^- channels in *Xenopus* oocytes injected with *Torpedo* electroplaque membranes. *Proc. Natl. Acad. Sci. U. S. A.* **92**, 5224–5228.
11. Wall, D. A. and Patel, S. (1989) Isolation of plasma membrane complexes from *Xenopus* oocytes. *J. Membr. Biol.* **107**, 189–201.
12. Kamsteeg, E. J. and Deen, P. M. T. (2001) Detection of aquaporin-2 in the plasma membranes of oocytes: a novel isolation method with improved yield and purity. *Biochem. Biophys. Res. Comm.* **282**, 683–690.
13. Schillers, H., Danker, T., Schnittler, H. J., Lang, F., and Oberleithner, H. (2000) Plasma membrane plasticity of *Xenopus laevis* oocyte imaged with atomic force microscopy. *Cell. Physiol. Biochem.* **10**, 99–107.
14. Perez, G., Lagrutta, A., Adelman, J. P., and Toro, L. (1994) Reconstitution of expressed KCa channels from *Xenopus* oocytes to lipid bilayers. *Biophys. J.* **66**, 1022–1027.
15. Paine, P. L., Johnson, M. E., Lau, Y. T., Tluczek, L. J., and Miller, D. S. (1992) The oocyte nucleus isolated in oil retains in vivo structure and functions. *Biotechniques* **13**, 238–246.

16. Lehman, C. W. and Carroll, D. (1993) Isolation of large quantities of functional, cytoplasm-free *Xenopus laevis* oocyte nuclei. *Anal. Biochem.* **211**, 311–319.
17. Ford, C. C. and Gurdon, J. B. (1977) A method for enucleating oocytes of *Xenopus laevis*. *J. Embryol. Exp. Morphol.* **37**, 203–209.
18. Stefani, E. and Bezanilla, F. (1998) Cut-open oocyte voltage-clamp technique. *Methods Enzymol.* **293**, 300–318.
19. Cucu, D., Simaels, J., Jans, D., and Van Driessche, W. (2004) The transoocyte voltage clamp: a noninvasive technique for electrophysiological experiments with *Xenopus laevis* oocytes. *Pflügers Arch.* **447**, 934–942.
20. Choe, H. and Sackin, H. (1997) Improved preparation of *Xenopus* oocytes for patch-clamp recordings. *Pflügers Arch.* **433**, 648–652.
21. Hering, S. (1998) Small-volume and rapid extracellular solution exchange around *Xenopus* oocytes during voltage-clamp recordings. *Pflügers Arch.* **436**, 303–307.
22. Dascal, N., Chilcott, G., and Lester, H. A. (1991) Recording of voltage and Ca²⁺-dependent currents in *Xenopus* oocytes using an intracellular perfusion method. *J. Neurosci. Methods* **39**, 29–38.
23. Nowak, M. W., Gallivan, J. P., Silverman, S. K., Labarca, C. G., Dougherty, D. A., and Lester, H. A. (1998) In vivo incorporation of unnatural amino acids into ion channels in *Xenopus* oocyte expression system. *Methods Enzymol.* **293**, 504–529.
24. Frech, G. C. and Joho, R. H. (1992) Isolation of ion channel genes by expression cloning in *Xenopus* oocytes. *Methods Enzymol.* **207**, 592–604.
25. Gurdon, J. B., Lane, C. D., Woodland, H. R., and Marbaix, G. (1971) Use of frog eggs and oocytes for the study of messenger RNA and its translation in living cells. *Nature* **233**, 177–182.
26. Swick, A. G., Janicot, M., Cheneval-Kastelic, T., McLenithan, J. C., and Lane, D. (1992) Promoter-cDNA-directed heterologous protein expression in *Xenopus laevis* oocytes. *Proc. Natl. Acad. Sci. U. S. A.* **89**, 1812–1816.
27. Krieg, P. A. and Melton, D. A. (1984) Functional messenger RNAs are produced by SP6 in vitro transcription of cloned cDNAs. *Nucleic Acids Res.* **12**, 7057–7070.
28. Geib, S., Sandoz, G., Carlier, E., Cornet, V., Cheynet-Sauvion, V., and De Waard, M. (2001) A novel *Xenopus* oocyte expression system based on cytoplasmic coinjection of T7-driven plasmids and purified T7-RNA polymerase. *Receptors Channels* **7**, 331–343.
29. Arnaud, N., Cheynet, V., Oriol, G., Mandrand, B., and Mallet, F. (1997) Construction and expression of a modular gene encoding bacteriophage T7 RNA polymerase. *Gene* **199**, 149–156.
30. Kozak, M. (1986) Point mutations define a sequence flanking the AUG initiator codon that modulates translation by eukaryotic ribosomes. *Cell* **44**, 283–292.
31. Drummond, D. R., Armstrong, J., and Colman, A. (1985) The effect of capping and polyadenylation on the stability, movement and translation of synthetic messenger RNAs in *Xenopus* oocytes. *Nuc. Acids Res.* **13**, 7375–7394.
32. Lehrach, H., Diamond, D., Wozney, J. M., and Boedtker, H. (1977) RNA molecular weight determinations by gel electrophoresis under denaturing conditions, a critical reexamination. *Biochemistry* **16**, 4743–4751.
33. De Waard, M. and Campbell, K. P. (1995) Subunit regulation of the neuronal α_{1A} Ca²⁺ channel expressed in *Xenopus* oocytes. *J. Physiol.* **485**, 619–634.
34. Eppig, J. J. and Dumont, J. N. (1976) Defined nutrient medium for the in vitro maintenance of *Xenopus laevis* oocytes. *In Vitro* **12**, 418–427.
35. Wyllie, A. H., Laskey, R. A., Finch, J., and Gurdon, J. B. (1978) Selective DNA conservation and chromatin assembly after injection of SV40 DNA into *Xenopus* oocytes. *Dev. Biol.* **64**, 178–188.

Visualization of the Cytoskeleton in *Xenopus* Oocytes and Eggs by Confocal Immunofluorescence Microscopy

Bret E. Becker and David L. Gard

Summary

Xenopus oocytes and eggs are popular models for studying the developmental and cellular mechanisms of RNA localization, axis specification and establishment, and nuclear envelope assembly/disassembly. However, their large size and opacity hamper application of many techniques commonly used for studying cell structure and organization, including immunofluorescence and other techniques of fluorescence microscopy. In this chapter, we describe techniques and procedures that we have used to preserve, stain, and view the cytoskeleton in *Xenopus* oocytes and eggs by confocal immunofluorescence microscopy.

Key Words: Actin; antibodies; eggs; confocal microscopy; immunofluorescence; intermediate filaments; microtubules; oocytes; *Xenopus*.

1. Introduction

The ease of in vitro maturation and fertilization make *Xenopus* oocytes and eggs popular models for studying many developmental mechanisms, including axis specification, RNA localization, signal transduction, and oocyte maturation. Moreover, *Xenopus* oocytes and eggs have proven to be informative models for studying cellular mechanisms, including protein targeting and secretion, nuclear envelope dynamics, and the dynamics and organization of the cytoskeleton.

Unfortunately, the large size that makes oocytes and eggs amenable to experimental manipulations also hampers high-resolution microscopy of their cytoplasmic or cellular organization. Over the past 15 yr, we have adapted and developed techniques for examining the organization of the cytoskeleton of *Xenopus* oocytes and eggs using immunofluorescence and confocal laser scanning microscopy (1–14). In this chapter, we summarize our procedures for confocal immunofluorescence microscopy of *Xenopus* oocytes and eggs, including recent advances in fluorescent dyes useful for dual and triple labeling. For more thorough discussions of the techniques described in this chapter, see refs. 14–17.

2. Materials

1. Rotary mixer modified to handle microcentrifuge tubes (PELCO® R2; cat. no. 1050; Ted Pella, Inc.; *see Note 1*).
2. Orbital shaker or nutator.
3. No. 5 Watchmaker forceps (cat. no. 505; Ted Pella Inc.).
4. 1.7-mL Polypropylene microcentrifuge tubes.
5. Modified Barth's saline with HEPES (MBSH): 10 mM HEPES, pH 7.4, 88 mM NaCl, 1 mM KCl, 2.4 mM NaHCO₃, 0.82 mM MgSO₄, 0.33 mM Ca(NO₃)₂, 0.41 mM CaCl₂ (make as a 10X stock, autoclave).
6. Collagenase A (10 mg/mL in MBSH; cat. no. 1 088 785; Roche Diagnostics Inc.; *see Note 2*).
7. Vacuum aspirator with trap.
8. 15- and 50-mL Polypropylene conical tubes.
9. Pasteur pipets.
10. Formaldehyde (37% stock liquid).
11. Glutaraldehyde (50% stock, electron microscopy grade; cat. no. 18431; Ted Pella Inc).
12. Fix buffer: 80 mM K Pipes, pH 6.8, 1 mM MgCl₂, 5 mM ethylene glycol *bis*(2-aminoethyl ether)-*N,N,N',N'*-tetraacetic acid (EGTA), 0.2% Triton X-100.
13. FGT fix: 3.7% formaldehyde, 0.25% glutaraldehyde, 0.5 μM paclitaxel in fix buffer (make fresh daily).
14. FT fix: 3.7% formaldehyde, 0.5 μM paclitaxel in fix buffer (make fresh daily).
15. Low-FGT fix: 0.25 to 0.50% formaldehyde, 0.1% glutaraldehyde, 0.5 μM paclitaxel in fix buffer (make fresh daily).
16. 100% methanol.
17. H₂O₂ bleach (10% H₂O₂ in methanol): add 1 volume of 30% H₂O₂ to 2 volumes 100% methanol.
18. TBS: 10 mM Tris-HCl, pH 7.4, 155 mM NaCl (make as a 10X stock and add 0.65 g/L of NaN₃ to retard bacterial growth).
19. TBSN: TBS + 0.1% Nonidet P-40 (NP-40). Add 1% NP-40 to 10X TBS. The 10X TBSN will be cloudy, and detergent may partition from the aqueous phase during prolonged storage at room temperature. To make 1X stock, mix well and dilute 10-fold with distilled water. TBSN solutions last months at room temperature.
20. 100 mM NaBH₄ in TBS (make fresh).
21. Primary antibodies diluted in 1X TBSN + 2% bovine serum albumin (BSA) (*see Table 1*).
22. Fluorochrome-conjugated secondary antibodies diluted in 1X TBSN + 2% BSA (*see Tables 1 and 2*).
23. Liver acetone powder (Sigma cat. no. L-1380).
24. TO-PRO-3 or other chromatin dyes (*see Table 2*).
25. Glycerol mounting buffer: 10 mM Tris-HCl, pH 8.0, 50 mM NaN₃, or 25 to 50 mg/mL propyl gallate in 90% glycerol.
26. BA:BB clearing/mounting solution: 1/2 (v/v) benzyl alcohol/benzyl benzoate.
27. Standard microscope slides.
28. 0.5- to 0.6-mm Well slides (cat. no. 12-560B; Fisher Scientific).
29. 0.2- to 0.3-mm Steel spacers (stainless steel sheets of various thickness are available from Small Parts Inc.).
30. Double-sided 0.7- to 1.0-mm aluminum slides.
31. Nos. 1 and 2 cover slips (18 mm and 22 mm² slides).
32. Sally Hansen's Hard as Nails clear nail polish (*see Note 3*).
33. Confocal microscope.

Table 1
List of Primary Antibodies Used in Examining the Cytoskeleton in *Xenopus* Oocytes and Eggs

Antibody (host and type ^a)	Company/ cat. no.	Concentration ^b (mg/mL)	Working dilution	Comments
Microtubules				
YL1/2 (rm)	Accurate ^c , YSRT-MCAP77	1.0	1/100	Works well but has reduced penetration compared to DM1A (1)
DM1A (mm)	ICN ^d	NA ^e	1/100	No longer used ^f (8)
DM1A (mm)	Sigma, T-9026	3.3	1/100	No longer used ^f (4)
6-11B-1 (mm)	Sigma, T-6793	0.15–0.6	1/100	Recognizes acetylated tubulin (8)
Tub-1A2 (mm)	Sigma, T-9028	NA	1/100	Recognizes tyrosinated tubulin (12)
TUB 2.1 (mm)	Sigma, T-4026	NA	1/100	Does not work well for oocytes and eggs
Keratin filaments				
C11 (mm)	Sigma, C-2931	~6–10	1/200	Works very well (6)
IH5 (mm)	NA	NA	1/50	Provided by Dr. Michael Klymkowsky (6)
Actin microfilaments				
Antiactin (mm)	Sigma, A-5441	NA	1/100	Recognizes large pool of monomeric actin (5,15)
Others				
XMAP215 (rp)	NA	5	1/100	Requires methanol fixation only (1)
XMAP230 (rp)	NA	1–2	1/100	Best with low-FGT fixation only (2–4)
XMAP310 (rp)	NA	NA	1/100	Requires methanol fixation only (23)
NuMA (rp)	NA	NA	1/100	Requires methanol fixation only (1)
XKCM1 (rp)	NA	1	1/100	Requires methanol fixation only (1)
γ-tubulin (mm)	Sigma, GTU-88	~3	1/100	Stains spindle poles and centrosomes well
Secondary antibodies	Molecular Probes	2	1/100	See Table 2 for the different fluorochromes and their spectral properties

^amm, mouse monoclonal; rm, rat monoclonal; rp, rabbit polyclonal.

^bThe antibody concentration for ascites (most of the mouse monoclonals) can be different depending on lots; however, we use the same dilution as a starting point.

^cAccurate Chemical and Scientific Co. (Westbury, NY).

^dICN Biomedicals is now MP Biomedicals.

^eNA, not applicable.

^fOur initial studies used DM1A from ICN and Sigma with excellent results. However, beginning in 1997, we noted problems with penetration and staining of microtubules and have discontinued their use.

Table 2
Spectral Properties of Fluorochromes and Chromosome Dyes Used for *Xenopus* Oocytes and Eggs

Fluorochrome/dye	λ_{ex} (nm) ^a	λ_{em} (nm) ^a	Lasers ^b	Comments
Antibody-conjugated				
Fluorescein	494	518	Ar, Ar-Kr	Fades quickly, antifade required
Alexa 488	495	519	Ar, Ar-Kr	Photostable, bright
Oregon Green 488	496	524	Ar, Ar-Kr	Photostable, very bright
Alexa 546	556	573	HeNe543	Bright, photostable, good with Alexa 488 for multiple labeling
Tetramethylrhodamine	555	580	HeNe543	Bright but rarely used now
Alexa 568	578	603	HeNe543	Bright but not as good of a match for HeNe543 laser as Alexa546
Texas-Red	595	615	Ar-Kr	Photostable, poor excitation with Ar ion laser, but good with Ar-Kr laser
Chromosome dyes				
Propidium iodide	535	617	HeNe 543	20- to 30-fold brighter when bound to DNA; only good for methanol-fixed samples
Ethidium homodimer	528	617	Ar	40-fold brighter when bound to DNA; only good for methanol-fixed samples
BO-PRO-3	575	599	Ar-Kr	Good with Ar-Kr laser but not Ar ion laser; also works well with aldehyde-fixed samples
YO-PRO-1	491	509	Ar, Ar-Kr	Works good for double labeling; also works well with aldehyde-fixed samples
TO-PRO-3	642	661	HeNe 633, RD	Good for triple labeling; very bright; also works well with aldehyde-fixed samples

^aPeak excitation λ_{ex} and emission λ_{em} wavelengths for each fluorochrome and dye.

^bThe laser lines for each laser are argon laser (Ar, 458, 488, 514 nm); argon–krypton laser (Ar-Kr, 466, 567, 647 nm); and helium–neon lasers (HeNe, 543, 633 nm). The HeNe are single-line lasers. The red diode (RD) laser has a 637-nm line.

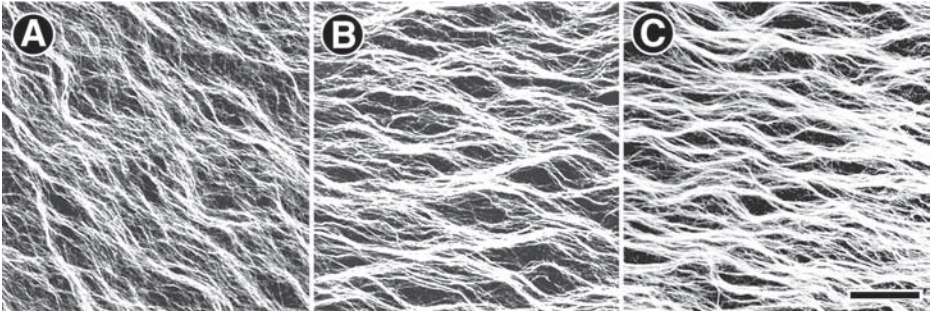


Fig. 1. A comparison of microtubule preservation in methanol and FGT-fixed *Xenopus* eggs. Fertilized *Xenopus* (0.7 NT) eggs were fixed in (A) 100% methanol, (B) low FGT, and (C) FGT as described in text. Eggs were hemisected, stained with rat anti- α -tubulin (YL1/2) and Alexa 546-conjugated antirat immunoglobulin G, and mounted to view microtubules in the vegetal cortex. Images were collected with a Zeiss LSM-510 (images shown are maximum brightness projections of five optical sections). Although visible, (A) cortical microtubules in methanol-fixed oocytes appeared fragmented. Better preservation of the cortical microtubule array was obtained with (B) low FGT and (C) FGT. Scale bar is 25 μ m.

3. Methods

3.1. Preservation of Cytoskeletal Filaments in *Xenopus* Oocytes and Eggs

Fixation of *Xenopus* oocytes and eggs for immunofluorescence microscopy requires a compromise between optimal preservation of cellular structures and preservation of antigenicity and antibody reactivity. Over the past 15 yr, we have tested more than three dozen fixation protocols for the ability to preserve cytoskeletal structure and antigenicity in *Xenopus* oocytes and eggs. We have developed four standard fixation procedures useful for microtubules, microtubule-associated proteins, intermediate filaments, and actin microfilaments. Not surprisingly, optimal fixation conditions for each of the cytoskeletal systems differ. Although these protocols serve as starting points for preserving the oocyte cytoskeleton, optimal fixation conditions for other structures or antibodies must be determined empirically.

3.1.1. Fixation of Microtubules With FGT, FT, and Low FGT

Fertilized eggs should be completely dejellied and washed in the suitable buffer prior to fixation. The layer of follicle cells surrounding large *Xenopus* oocytes hampers fixation and penetration of antibodies, resulting in unsatisfactory preservation and staining. Therefore, large oocytes (stages III–VI) should be completely freed of all follicular tissue prior to fixation (*see Note 2*). Manually removing follicle cells from smaller oocytes is not practical. However, we have successfully prepared stages I and II oocytes from ovary tissue dissociated with collagenase (8,12). Even smaller oocytes/oogonia can be fixed *en bloc* in ovary tissue dissected from juvenile frogs (12).

In our experience, microtubules are best preserved with a combination of formaldehyde (3.7%) and glutaraldehyde (0.25%) in a buffer containing a substoichiometric concentration (0.5 μ M) of the microtubule-stabilizing drug paclitaxel (FGT fix; *see Fig. 1*).

Formaldehyde-paclitaxel alone (FT fix) also adequately preserves most microtubule arrays in both oocytes and eggs. Lower concentrations of formaldehyde (0.25–0.50%) and glutaraldehyde (0.1%) for shorter periods (0.5–1 h, low-FGT fix) provide adequate fixation of microtubule structures and organization while preserving reactivity with antibodies against some microtubule-associated proteins (**Fig. 1**) (2–4). FGT-, low-FGT-, or FT-fixed oocytes and eggs are postfixed in 100% methanol overnight, and samples can be stored for months in methanol without any noticeable changes in preservation or staining.

Procedure:

1. Prepare the desired number of microcentrifuge tubes with approx 1.5 mL FGT, low FGT, or FT fix.
2. Taking care to minimize the volume of buffer transferred, carefully pipet as many as 15 oocytes or eggs to microcentrifuge tubes containing fix (small pieces of ovary tissue from juvenile frogs can be transferred with forceps).
3. Mix gently and lay tubes on their sides (to allow the oocytes or eggs to disperse and minimize clumping) for 4 to 6 h at room temperature (for FGT and FT fix) or 0.5 to 1.0 h (for low-FGT fix).
4. Carefully aspirate the fix from the samples (*see Note 4*).
5. Add 100% methanol.
6. Carefully aspirate and replace methanol. Incubate at room temperature overnight. Samples are stable in methanol for several months.

3.1.2. Methanol Fixation for Microtubules and Keratin Filaments

Preservation of interphase microtubules in *Xenopus* oocytes and eggs by 100% methanol, ethanol, acetone, or other combination of organic solvents is generally unsatisfactory (8). However, methanol fixation has proven useful for examining meiotic and mitotic spindles in oocytes and cortical microtubules in fertilized *Xenopus* eggs (*see Figs. 1 and 2*) (1,9,18).

The epitopes recognized by all the commercially available antibodies (*see Table 1*) against keratins that we have used are sensitive to aldehydes. Even brief fixation in formaldehyde rendered keratin antibodies unreactive. Similar results with vimentin antibodies were observed by Klymkowsky and colleagues (13,19,20). Although fixing in methanol has proven useful for some antibodies that are incompatible with aldehyde fixatives, overall preservation is poor, shrinkage artifacts are common, and methanol-fixed oocytes and eggs are quite fragile. For these reasons, fixation in methanol should be used only as a last resort.

For the procedure:

1. Prepare the desired number of 15-mL conical tubes and fill with 100% methanol.
2. Transfer up to 30 large oocytes or eggs (in a minimum volume of buffer) to each tube.
3. Rock briefly to mix and place tubes on their sides to prevent clumping and aid uniform fixation.
4. Fix oocytes overnight at room temperature.

3.2. Hemisecting *Xenopus* Oocytes and Eggs

The large size of *Xenopus* oocytes and eggs hampers the penetration of antibodies, particularly after fixation with aldehydes. To aid antibody penetration, we routinely

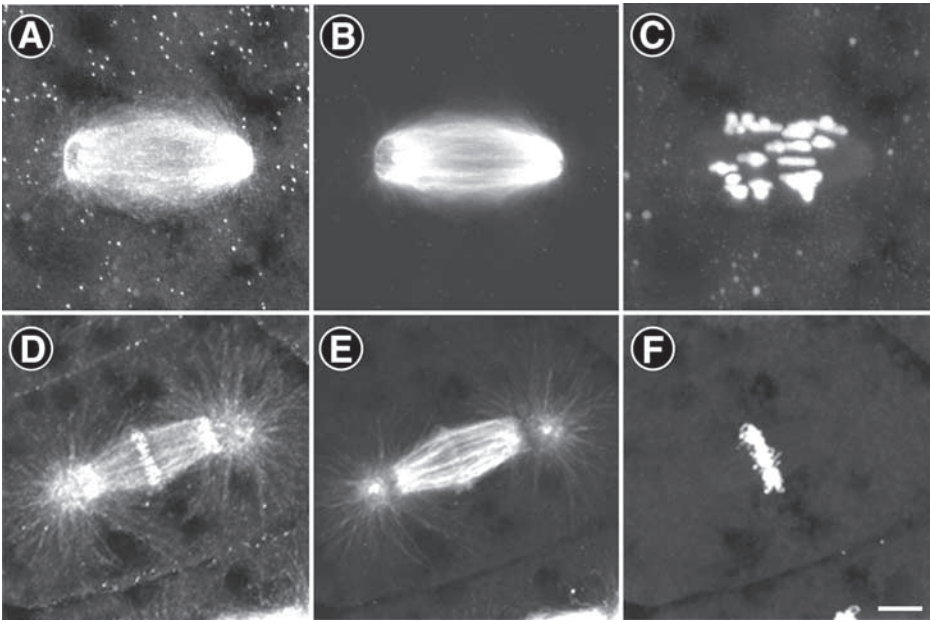


Fig. 2. Triple-fluorescence labeling of mitotic and meiotic spindles in *Xenopus* oocytes and embryos. Oocytes (A–C) and blastula-stage embryos (D–F) were fixed in methanol as described and stained with rabbit anti-XKCM1 and Alexa 488-conjugated goat antirabbit immunoglobulin G (A and D), rat anti- α -tubulin (YL1/2) and Alexa 546 goat antirat immunoglobulin G (B and E), and TO-PRO-3 (C and F). Three channel images were collected with a Zeiss LSM-510 and were merged in *Photoshop*. Scale bar is 10 μ m.

“hemisect” oocytes with a sharp scalpel prior to bleaching or staining. We cut oocytes and eggs either equatorially to observe the animal or vegetal cortex or laterally along the animal–vegetal axis. When properly mounted, hemisected oocytes and eggs also allow visualization of regions of interest deep within the oocytes or eggs that would otherwise be inaccessible with high numerical aperture objectives (*see Subheading 3.6*). In addition, hemisecting allows separate processing of the two oocyte or egg halves with different antibodies. In our experience, it is best to change the scalpel blade often to ensure as smooth a cut surface as possible. Although tedious, we have hemisected oocytes as small as approx 400 μ m in diameter. Smaller oocytes (<200 μ m) are processed whole, and antibodies generally diffuse throughout the cytoplasm, allowing optical sectioning of the complete cytoplasmic volume (6,8,12,14).

The procedure is as follows:

1. Rehydrate/wash samples with either TBS or TBSN.
2. Transfer oocytes to a Petri dish or glass agglutination slide with a large amount of buffer surrounding the oocytes to reduce movements caused by surface tension.
3. Hemisect oocytes or eggs either in the plane of the equator or along the animal–vegetal axis.

4. After cutting, return oocytes to microcentrifuge tubes filled with TBS or TBSN. If desired, transfer the halves (animal vs vegetal or right vs left) to different tubes for processing.

3.3. Bleaching of *Xenopus* Oocytes and Eggs

The cortical pigment of stages IV to VI *Xenopus* oocytes and eggs attenuates laser illumination and obscures fluorescence from the underlying cytoplasm. Pigmentation of fixed *Xenopus* oocytes and eggs can be reduced or eliminated by bleaching them with 10% H₂O₂ in methanol (1 part 30% H₂O₂/2 parts 100% methanol; see **Note 5** (21)). The animal and vegetal hemispheres of bleached *Xenopus* oocytes and eggs are almost indistinguishable. If desired, oocytes should be hemisected prior to bleaching. Peroxide bleach is very reactive with clothing and causes painful chemical “burns” on contact with skin. Gloves should be worn and care taken when using bleach.

Oocytes and eggs from albino frogs (supplied by most distributors of *Xenopus*) can be used when the antibodies/epitopes are incompatible with peroxide bleach or methanol. However, distinguishing the animal and vegetal axis of albino oocytes and eggs can be very difficult.

The procedure is as follows:

1. Carefully aspirate the TBSN or TBS.
2. Bleach samples by adding approx 1.5 mL of 10% H₂O₂ in methanol.
3. Incubate samples with the tubes on their sides for 12 to 48 h at room temperature under fluorescent illumination.
4. Carefully aspirate the bleaching solution and rinse samples three times (~1 h each) with TBSN (or TBS if NaBH₄ reduction is required).

3.4. Borohydride Reduction of Glutaraldehyde-Fixed Oocytes and Eggs

Xenopus oocytes and eggs that have been fixed with glutaraldehyde should be treated with sodium borohydride to reduce unreactive aldehydes and the autofluorescence of Schiff bases generated during fixation (22). Borohydride reduction is unnecessary for samples fixed in methanol or FT. We typically treat FGT-fixed oocytes with 50 mM NaBH₄ in TBS overnight at 4°C or 100 mM for 4 to 6 h at room temperature. Borohydride solutions are effervescent, and the buffers used should lack all detergents. In addition, tubes or vials should be left open and upright during this treatment to prevent pressure buildup that may result in the caps popping open, which can send the tubes flying.

For the procedure,

1. Rinse samples three times with TBS to remove bleach or detergent from previous steps.
2. Aspirate off the TBS.
3. Add approx 1 mL of 50 or 100 mM NaBH₄ in TBS.
4. Incubate either overnight at 4°C or 4 to 6 h at room temperature in uncapped tubes.
5. Add 1 to 2 drops of TBSN to break the surface tension of the bubbles formed from NaBH₄.
6. Tap tubes to help break the surface tension and allow the oocytes and eggs to sink to the bottom.
7. Carefully aspirate off the overlying NaBH₄ solution.
8. Wash samples in several changes of TBSN for 1 to 3 h at room temperature.

3.5. Processing of *Xenopus* Oocytes and Eggs for Immunofluorescence

The large size of *Xenopus* oocytes and eggs limits penetration of antibodies to approx 75 to 100 μm during an overnight incubation. Therefore, processing *Xenopus* oocytes and eggs for immunofluorescence requires that the incubation of antibodies be substantially increased compared to cultured cells or sections, with corresponding increase in the duration of intermediate washes. In our experience, antibody incubation times of 24 to 48 h and washes of 48 to 72 h are satisfactory for hemisected oocytes and eggs.

We have used a number of antibodies against cytoskeletal proteins with varying degrees of success (for a complete list, see **Table 1** and **ref. 15**). The appropriate fixation conditions and the working dilutions for each primary and secondary antibody must be determined empirically. We typically start with a 1/100 dilution of the stock provided in TBSN + 2% BSA (a final concentration of 10 to 50 $\mu\text{g}/\mu\text{L}$) and adjust the dilution to minimize background or increase brightness. NaN_3 can be added to 0.1% to retard bacterial growth during storage at 4°C (see **Note 6**). In our experience, we have found that preblocking *Xenopus* oocytes and eggs is not required. In some cases, we have reused diluted primary antibodies several times, observing that the background or nonspecific staining is reduced in subsequent uses.

The choice of a fluorescently conjugated secondary antibody must satisfy several criteria: The fluorochrome must match the excitation wavelengths available, and the fluorochrome must be sufficiently photostable to allow the collection of many optical sections, including frame averaging. Moreover, fluorochromes used for dual or triple labeling must be spectrally separable (either the absorption or emission spectra; see **Fig. 2** and **Note 6**).

Our early studies relied heavily on Texas Red-, tetramethylrhodamine-, and fluorescein-conjugated antibodies for both single- and multiple-labeling strategies (see **Table 2**). More recently, we have used Alexa-conjugated secondary antibodies available from Molecular Probes Inc. (Eugene, OR) with excellent results. The excitation and emission spectra of Alexa 488 and Alexa 546 are readily separable with filters available on most common confocal microscopes (consult the specifications of your confocal to determine which excitation/emission wavelengths are compatible), and the Alexa dyes exhibit excellent photostability.

Many dyes are available for counterstaining nuclei and chromosomes. Hoechst and 4',6-Diamidino-2-phenyl indole (DAPI), commonly used to stain nuclei and chromosomes for conventional fluorescence microscopy, are not compatible with laser lines in most confocal laser scanning microscopes (they can be used with instruments capable of multiphoton excitation). We have used propidium iodide, ethidium homodimer, YO-PRO-1, BO-PRO-3, and TO-PRO-3 with good results (see **Table 2**). Propidium iodide and ethidium homodimer work best on oocytes and eggs fixed with methanol. The cyanine dyes YO-PRO-1, BO-PRO-3, and TO-PRO-3 work well with aldehyde-fixed samples. The spectrum of TO-PRO-3 is readily separated from both Alexa 488 and Alexa 546, allowing triple-fluorescence labeling of two antibodies and chromosomes/nuclei (see **Fig. 2** and **ref. 1**).

The protocol outlined here is used for triple labeling with two antibodies and the far-red chromosome dye TO-PRO-3. For single- or double-labeling strategies, omit the appropriate steps. This protocol has been adapted from **refs. 1, 2, 11, and 15**:

1. Fix, hemisect, bleach, and reduce samples with NaBH_4 as desired in 1.7-mL microcentrifuge tubes (*see above*).
2. Wash samples with several changes of TBSN over 4 to 6 h.
3. Incubate samples with 100 to 200 μL of the first primary antibody (diluted in TBSN + 2% BSA) for 24 to 48 h at 4°C with gentle rotation using a rotary mixer (*see Note 7*).
4. Wash samples with TBSN at 4°C with gentle rotation for 48 to 72 h, changing the buffer every 8 to 12 h (*see Note 8*).
5. For dual fluorescence, incubate samples with 100 to 200 μL of the second primary antibody (diluted in TBSN + 2% BSA) for 24 to 48 h at 4°C with gentle rotation using a rotary mixer (*see Note 7*).
6. Wash samples as described in **step 4**.
7. Incubate samples with 100 to 200 μL fluorescent-conjugated secondary antibodies (diluted in TBSN + 2% BSA) at 4°C for 24 to 48 h with gentle rotation using the rotary mixer (*see Note 9 and Table 2*).
8. Wash samples as in **step 4**.
9. If staining for chromosomes with TO-PRO-3, wash samples in TBS for 1 to 2 h with three or four changes at room temperature.
10. Stain samples with approx 1 mL of 5 μM TO-PRO-3 in TBS for 30 to 60 min at room temperature with gentle rotation on a nutator or orbital shaker with samples lying flat (cover samples to keep dark after this step).
11. Wash samples two or three times overnight with TBS at 4°C with gentle rotation.

3.6. Clearing and Mounting *Xenopus* Oocytes and Eggs for Confocal Microscopy

The accumulation of yolk during oogenesis renders oocytes and eggs opaque and prevents visualization of structures no more than a few micrometers below the cell surface of uncleared oocytes and eggs. Fluorescence imaging of “intact” *Xenopus* oocytes and eggs was greatly facilitated by the discovery that a 1:2 mixture of benzyl alcohol and benzylbenzoate (BA:BB) closely matches the refractive index of yolk, thereby rendering *Xenopus* oocytes and eggs nearly transparent (Murray and Kirschner, as cited in **ref. 21**). In addition, the refractive index of BA:BB (~1.55) closely matches that of common immersion oils (~1.52) and glass cover slips, reducing the image-degrading effects of spherical aberration.

Although clearing with BA:BB dramatically improves imaging deep within *Xenopus* oocytes and eggs, the use of BA:BB is not without its drawbacks. First, because BA:BB is immiscible in aqueous solutions, samples must be completely dehydrated with methanol or ethanol prior to clearing (*see Subheading 3.7*. for staining of actin microfilaments). In addition, samples cleared in BA:BB tend to be brittle and can easily be damaged during mounting. BA:BB also dissolves many plastics, including polystyrene, cellulose acetate, and the plastics used for computer keyboards. Polyethylene and polypropylene tubes are resistant and should be used for all steps utilizing BA:BB. Finally, caution should be used when handling BA:BB because benzyl benzoate is an eye and skin irritant.

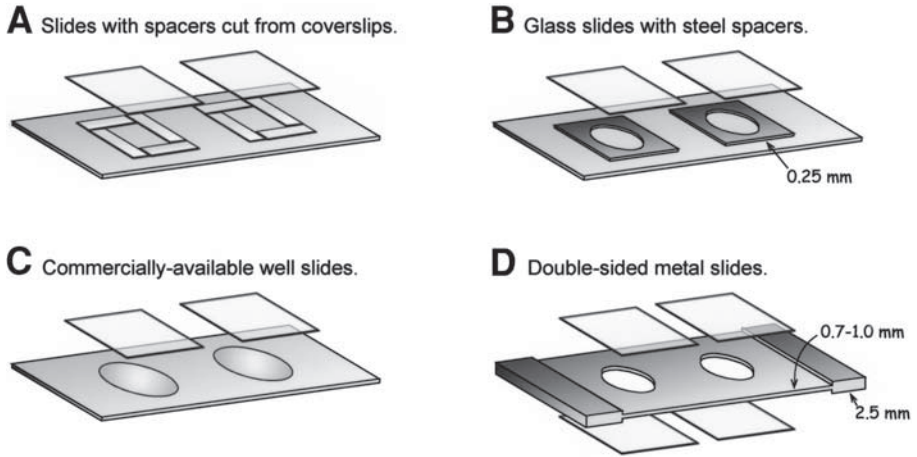


Fig. 3. Slides for mounting *Xenopus* oocytes and eggs for confocal microscopy. (A) Pieces of ovary from juvenile frogs and small (stage I) oocytes are mounted on slides with spacers cut from no. 1 or 2 cover slips. Spacers are “glued” to the slides with fingernail polish and allowed to dry thoroughly before mounting samples. (B) Larger stages I to II and hemisected stages III to IV oocytes are mounted in chambers formed by 0.25-mm steel spacers glued to glass slides with fingernail polish. (C) Hemisected stages V to VI oocytes and eggs are mounted in commercially available well slides (0.5- to 0.6-mm wells). (D) Intact oocytes and eggs are mounted in 1.0 to 1.2 mm thick slides machined from aluminum, with cover slips glued to both faces with fingernail polish. In all cases, cover slips are sealed to slides with liberal applications of fingernail polish and allowed to dry thoroughly before viewing. Reprinted from *Methods in Cell Biology*, Vol. 70, 2002, pp. 299–416, with permission from Elsevier.

Because of their size and physical properties, mounting oocytes for high-resolution microscopy poses challenges not faced with smaller cells or sections. *Xenopus* oocytes and eggs are not adherent to cover slips or slides. Therefore, the oocytes or eggs must be securely mounted or “wedged” between the cover slip and slide to prevent movement during image collection on the confocal microscope. In addition, the region of interest must be sufficiently close to the cover slip to allow image collection with high numerical aperture objectives, which typically have working distances less than 200 μm .

Small oocytes (<150 μm in diameter) or pieces of ovary tissue are mounted on standard slides in wells formed by spacers cut from no. 1 or 2 cover slips (Fig. 3A) and affixed to the slide with fingernail polish. Larger stages I to II oocytes and hemisected stages III to IV oocytes are mounted in glass slides to which stainless steel 0.25-mm spacers have been attached with fingernail polish (Fig. 3B). Hemisected stages V to VI oocytes and eggs are mounted in commercially available glass-well slides (0.5- to 0.6-mm wells; Fig. 3C), with the region of interest (cortex or cut surface) mounted up. Finally, whole oocytes and eggs are mounted in double-sided chambers fabricated from aluminum sheet (0.7–1.0 mm thick), with cover slips attached to both sides (Fig. 3D). These slides allow the imaging of both sides of uncut oocytes and eggs.

1. Dehydrate samples 1 to 2 h with three or four changes of 100% methanol (samples can be stored several months in methanol).
2. Remove the methanol and add approx 1.5 mL BA:BB to the oocytes or eggs. *Do not mix.*
3. Allow oocytes and eggs to sink slowly to the bottom of the tube (takes 5 to 15 min). Oocytes and eggs will clear and sink as they are infiltrated by BA:BB (*see Note 10*).
4. Carefully aspirate the BA:BB from the samples to be mounted.
5. Carefully resuspend the samples in a small volume of new BA:BB.
6. Transfer the samples to the appropriate slides in a drop of BA:BB.
7. Aspirate most of the BA:BB.
8. Orient the oocytes and eggs in the desired manner in the slides with forceps or scalpels, if necessary.
9. Fill the well with BA:BB.
10. Drop a no. 1 cover slip quickly on top of the well with gentle pressure.
11. Gently press down on the cover slip to seat it properly on top of the slide. Aspirate any excess BA:BB expelled from the well.
12. Seal the cover slip to the slide with a liberal application of fingernail polish.
13. Allow the slides to dry thoroughly overnight at room temperature or several hours in a fume hood prior to viewing on the confocal microscope.
14. Well-sealed slides are stable for several months in the dark at room temperature (stained with Alexa dyes and TO-PRO-3).

3.7. Fixation and Phalloidin Staining of Actin Microfilaments in *Xenopus* Oocytes and Eggs

The large pool of monomeric actin (G-actin) in *Xenopus* oocytes and eggs precludes the use of antiactin antibodies for staining F-actin. We have successfully used fluorescently conjugated phalloidin to stain F-actin in previtellogenic *Xenopus* oocytes and have had limited success staining F-actin in stage VI oocytes and eggs (5,7). In our experience, even brief treatments with organic solvents such as methanol abolish phalloidin staining of actin microfilaments in oocytes and eggs, prohibiting postfixation with methanol and bleaching with peroxide–methanol. Therefore, albino female frogs should be used to examine the actin cytoskeleton in postvitellogenic oocytes and eggs.

Moreover, dehydration of phalloidin-stained samples in methanol or other BA:BB-compatible solvents extracts any bound phalloidin, prohibiting use of BA:BB as a clearing agent. Although previtellogenic oocytes can easily be stained for F-actin, the absence of bleaching and clearing limits the visualization of phalloidin-stained F-actin to only approx 5 to 10 μm of the cell cortex of postvitellogenic oocytes (stages II–VI) or eggs. Hemisection can be used to examine structures deep within the cytoplasm. However, the inability to section optically below the region of knife damage hinders collection of high-quality images.

1. Fix 5 to 15 oocytes (*see Note 11*), dejellied eggs, or pieces of ovary tissue from juvenile frogs in 1.0 to 1.5% formaldehyde in fix buffer for 4 to 18 h at room temperature in 1.7-mL microcentrifuge tubes (place tubes on their side to increase exposure of samples to fix and avoid clumping).
2. Wash overnight with several changes of TBSN at room temperature with gentle rotation using an orbital shaker or nutator. If needed, the samples can be hemisected with a sharp scalpel (no. 15) as described above (*see Note 12*).

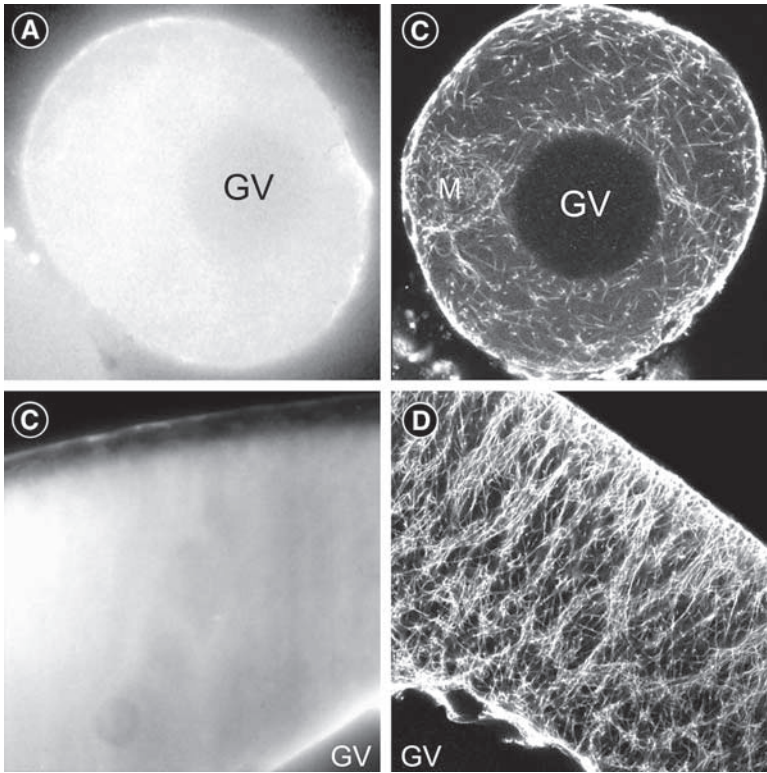


Fig. 4. Optical sectioning eliminates the out-of-focus fluorescence that hampers conventional fluorescence imaging of *Xenopus* oocytes. Conventional images (A and B) and confocal optical sections (C and D) of stage I (A and C) and stage VI (B and D) *Xenopus* oocytes fixed in FGT as described and stained with mouse anti- α -tubulin and rhodamine-conjugated antimouse immunoglobulin G. C and D are single optical sections collected with a Biorad MRC-600. Reprinted from *Methods in Cell Biology*, Vol. 70, 2002, pp. 279–416, with permission from Elsevier.

3. Replace last TBSN wash with fluorescently labeled phalloidin (2.4 units/mL in TBSN) and incubate for 6 to 18 h at room temperature (see **Note 13**).
4. Wash samples with TBSN with several changes for 24 to 48 h.
5. Mount pieces of ovaries (from juvenile frogs) and small stage I oocytes in glycerol-mounting buffer. For larger oocytes, mount in appropriate slides with TBSN, pH 8.0) containing NaN_3 or *n*-propyl gallate (25–50 mg/mL) to retard photobleaching, if necessary (see **Note 14**).

3.8. Confocal Immunofluorescence Microscopy of the Cytoskeleton in *Xenopus* Oocytes and Eggs

The “optical sectioning” afforded by confocal microscopy dramatically reduces the out-of-focus light that degrades the quality and sharpness of images collected from oocytes or other large samples (see **Fig. 4**). In addition, the collection of serial optical

sections and three-dimensional (3D) reconstructions has allowed unparallel views of the organization of the cytoskeleton of *Xenopus* oocytes and eggs in 3D space (6,14). The following discussion of confocal microscopy is based on our experience with Bio-Rad MRC600 and Zeiss LSM510 confocal laser scanning microscopes. However, aspects of this discussion should be useful with other commercially available confocal microscopes (see your instrument's instructional manual).

The apparent brightness of the image is a function of several parameters. First, the intrinsic brightness of the sample is affected by the quality of the primary antibody or stain, the choice of fluorochrome, and the abundance of the antigen or structure. In addition, the apparent brightness is dependent on the laser power used for illumination and the photomultiplier or detector gain. In practice, the last two parameters must be determined empirically to optimize image quality. In general, the lowest laser power possible should be used to reduce photobleaching. Reduced laser power may be offset by increasing the detector gain, which can result in increased image noise, resulting in images that appear grainy. Image noise can be reduced or eliminated by line or frame averaging, which in turn increases exposure of the sample to laser illumination, resulting in increased photobleaching or photodamage. Laser power, detection gain, and frame averaging should be set to optimize brightness while minimizing image noise, bleaching, and photodamage.

The apparent brightness can also be increased by increasing the thickness of the section collected (by increasing the pinhole size). This in effect increases the volume of the sample from which photons are collected and thus image brightness. However, the superposition of additional cytoplasmic structure and increased fluorescent signal from above and below the focal plane may affect image clarity.

Most commercially available confocal microscopes collect images with 8, 12, or 16 bits of information per pixel in each channel, corresponding to 256, 4096, or 65,536 gray levels per channel. We have found that 8-bit images, which include 256 gray levels per channel, are sufficient for most purposes and require only half the disk storage space required by 16-bit images. The increased number of gray levels provided by 12- or 16-bit images is useful when collecting images with extreme contrast (very bright and very faint details).

The black level and gain of the confocal detection should be adjusted to make maximum use of the full dynamic range of the instrument. This is accomplished by adjusting the black level (also known as baseline or amplifier offset, depending on the instrument) and gain such that the darkest pixels have an intensity value of 0, and the brightest pixels have a value of 255 (in an 8-bit image). This process is facilitated by using a false-color lookup table that maps extremes in intensity (0 and 255) to contrasting colors such as green/blue and red (see **Note 15**). Adjusting the black levels and gain so that the image includes both green/blue and red pixels ensures that the image utilizes the full range of gray levels available (see **Note 15**).

One of the major benefits or an advantage of confocal microscopes is the ability to project serial optical sections, resulting in images with extended depth of focus. Most software bundled with confocal microscopes includes tools for projection of optical sections and may include tools for simple 3D reconstructions. In our experi-

ence, to prevent discontinuities or “banding” in projected images or 3D reconstructions, the section interval or spacing must be matched to the section thickness. In practice, we have found that slight oversampling is required to prevent “gaps” or banding. Greater overlap (oversampling) is required to reduce banding in images collected with low-power objectives (10× and 20×) objectives. When collecting multi-channel images, pinholes for each channel should be adjusted to provide uniform section thickness.

Finally, the digital nature of confocal images facilitates postprocessing to optimize brightness, contrast, and other image parameters. Many software packages that allow viewing, processing, and printing of confocal images are available (see **Note 16**). In general, we limit postprocessing to minor adjustments of image brightness and contrast and to resizing. These processed images are saved as copies, and the original unprocessed images are archived. Proprietary image or data formats used by some confocal microscopes may require that the image be exported into one of the standard digital image file formats (TIFF or JPEG) before they can be opened into an image-processing application. For further discussion of postprocessing of confocal images, see **refs. 14 and 15**.

In conclusion, the advent and widespread availability of confocal microscopes and development of techniques for fluorescence imaging of *Xenopus* oocytes and eggs allows visualization of cellular organization heretofore impossible in these large cells. Although optimum processing conditions for each structure or antibody will vary and must be determined empirically, these protocols should prove to be useful starting points.

4. Notes

1. The rotary mixers designed for infiltration of embedding plastics and waxes can easily be modified for this purpose by attaching one or more microfuge tube racks with epoxy, silicon sealant, or other adhesives to the rotor plate.
2. Collagenase A is available from several vendors. However, we have found that collagenase from Roche Diagnostics Inc. gives consistent results at 10 mg/mL in MBSH without the variability noted with collagenase A from other sources. Treatment with collagenase A for 60 to 90 min removes most of the follicular tissue; however, the remaining layer of follicle cells must be manually removed with watchmaker’s forceps.
3. Fingernail polish must be compatible with BA:BB. In our experience, Sally Hansen’s Hard as Nails clear nail polish (with or without nylon) works well.
4. To minimize accidental aspiration of oocytes or eggs, we often use a micropipet tip to reduce the bore of the Pasteur pipet used on the aspirator. The micropipet tip will be held securely by the vacuum.
5. Bleaching seems to be enhanced by illumination from fluorescent lights or sunlight.
6. Commercially available antibodies are reconstituted (if needed), aliquoted, quickly frozen in liquid nitrogen, and stored at -80°C . Secondary antibodies are first preabsorbed with liver acetone powder for approx 2 to 4 h prior to aliquoting and freezing. To preabsorb the secondary antibodies,
 - a. Transfer dry liver acetone powder to a 1.7-mL microfuge tube, filling the tube about one-third full.
 - b. Fill the tube with TBSN and mix thoroughly by vortexing (use a spatula to break apart clumps of powder).

- c. Sediment acetone powder in microcentrifuge (3 min at full speed) and remove/discard supernatant.
 - d. Wash acetone powder several more times with TBSN until the supernatant is clear and colorless.
 - e. After the final wash, remove all TBSN, leaving wet liver acetone powder, and add reconstituted secondary antibody to the washed powder.
 - f. Mix thoroughly with a spatula and then incubate for several hours at 4°C.
 - g. Centrifuge for 10 min in microfuge to pellet acetone powder.
 - h. Carefully remove antibody solution.
 - i. Aliquot, rapid freeze in liquid nitrogen, and store secondary antibodies at -80°C.
7. Attention should be paid to the order of primary antibody addition because the first antibody may sterically hinder binding of the second antibody to its epitope. For example, we generally bind antibodies to microtubule-associated proteins (i.e., XMAP215, XMAP230, etc.) first to prevent masking by subsequent binding of tubulin antibodies.
 8. To minimize background, samples must be thoroughly washed free of any unbound primary antibodies before adding secondary antibodies. Wash efficiency is a factor of both the total time of washing and the number of changes.
 9. When feasible, we add secondary antibodies as a cocktail at the appropriate dilutions in TBSN + 2% BSA. Secondary antibodies need to be chosen carefully to avoid unintentional crossreaction. For example, primary antibodies against rat and mouse cannot be used together because the secondary antibodies will crossreact with both primary antibodies. Similarly, you should not use secondary antibodies generated in the same or closely related species (i.e., sheep and goat) as either of the primary antibodies.
 10. If oocytes or eggs retain a milky appearance after clearing, they may not have been completely dehydrated. Pass them through several changes of methanol to remove BA:BB and the remaining aqueous buffer and reclear with BA:BB.
 11. Collagenase digestion disrupts the organization of actin microfilaments in *Xenopus* oocytes. Therefore, oocytes must be manually isolated or dissected from ovaries of juvenile frogs.
 12. In the absence of methanol postfixation, the nucleoplasm is not well fixed with formaldehyde and may be lost from oocytes when they are hemisected.
 13. In our experience, fluorescently labeled phalloidin can also be added to the fix without any differences in F-actin staining.
 14. Despite fixation and permeabilization in buffers containing detergents, larger oocytes shrink appreciably in glycerol-based mounting solutions and must be mounted in aqueous solutions such as TBSN or TBS (antifade chemicals can be added).
 15. We have used several false-color lookup tables, including the "setcol" table for the Bio-Rad MRC600, which shows bright pixels as red and black pixels as green. The "range indicator" lookup table furnished with the Zeiss LSM510 shows bright pixels as red and black pixels as blue.
 16. We usually use Adobe *Photoshop* (<http://www.adobe.com>) for most of our postprocessing. Other free software packages useful for postprocessing of confocal images include NIH *Image* for McIntosh computers (<http://rsb.info.nih.gov/nih-image/Default.html>), Scion *Image* for personal computers (<http://www.scioncorp.com>), and the Java script *ImageJ* (<http://rsb.info.nih.gov/ij/>).

Acknowledgments

We would like to thank Ed King for all of his help with the confocal microscopes and Claire Walczak for providing the anti-XKCM1 antibodies used to generate the

images for **Fig. 2**. We also would like to thank present and past members of the lab for their contributions to the methods and protocols discussed. Work presented in this chapter was supported by National Science Foundation grants MCB-950651 and MCB-9904504 and equipment grant DBI-9977204 for the Zeiss 510 confocal microscope.

References

1. Becker, B. E., Romney, S. J., and Gard, D. L. (2003) XMAP215, XKCM1, NuMA, and cytoplasmic dynein are required for the assembly and organization of the transient microtubule array during the maturation of *Xenopus* oocytes. *Dev. Biol.* **261**, 488–505.
2. Cha, B. J., Error, B., and Gard, D. L. (1998) XMAP230 is required for the assembly and organization of acetylated microtubules and spindles in *Xenopus* oocytes and eggs. *J. Cell Sci.* **111**, 2315–2327.
3. Cha, B., Cassimeris, L., and Gard, D. L. (1999) XMAP230 is required for normal spindle assembly in vivo and in vitro. *J. Cell Sci.* **112**, 4337–4346.
4. Cha, B. J. and Gard, D. L. (1999) XMAP230 is required for the organization of cortical microtubules and patterning of the dorsoventral axis in fertilized *Xenopus* eggs. *Dev. Biol.* **205**, 275–286.
5. Roeder, A. D. and Gard, D. L. (1994) Confocal microscopy of F-actin distribution in *Xenopus* oocytes. *Zygote* **2**, 111–124.
6. Gard, D. L., Cha, B. J., and King, E. (1997) The organization and animal-vegetal asymmetry of cytokeratin filaments in stage VI *Xenopus* oocytes is dependent upon F-actin and microtubules. *Dev. Biol.* **184**, 95–114.
7. Gard, D. L., Cha, B. J., and Roeder, A. D. (1995) F-Actin is required for spindle anchoring and rotation in *Xenopus* oocytes: a re-examination of the effects of cytochalasin B on oocyte maturation. *Zygote* **3**, 17–26.
8. Gard, D. L. (1991) Organization, nucleation, and acetylation of microtubules in *Xenopus laevis* oocytes: a study by confocal immunofluorescence microscopy. *Dev. Biol.* **143**, 346–362.
9. Gard, D. L. (1992) Microtubule organization during maturation of *Xenopus* oocytes: assembly and rotation of the meiotic spindles. *Dev. Biol.* **151**, 516–530.
10. Gard, D. L. (1993) Ectopic spindle assembly during maturation of *Xenopus* oocytes: evidence for functional polarization of the oocyte cortex. *Dev. Biol.* **159**, 298–310.
11. Gard, D. L. (1994) γ -Tubulin is asymmetrically distributed in the cortex of *Xenopus* oocytes. *Dev. Biol.* **161**, 131–140.
12. Gard, D. L., Affleck, D., and Error, B. M. (1995) Microtubule organization, acetylation, and nucleation in *Xenopus laevis* oocytes: II. A developmental transition in microtubule organization during early diplotene. *Dev. Biol.* **168**, 189–201.
13. Gard, D. L. and Klymkowsky, M. W. (1998) Intermediate filament organization during oogenesis and early development in the clawed frog, *Xenopus laevis*. *Subcell. Biochem.* **31**, 35–70.
14. Gard, D. L. (1999) Confocal microscopy and 3-D reconstruction of the cytoskeleton of *Xenopus* oocytes. *Microsc. Res. Tech.* **44**, 388–414.
15. Gard, D. L. (2002) Confocal fluorescence microscopy of the cytoskeleton of amphibian oocytes and embryos. *Methods Cell Biol.* **70**, 379–416.
16. Gard, D. L. (1993) Confocal immunofluorescence microscopy of microtubules in amphibian oocytes and eggs. *Methods Cell Biol.* **38**, 241–264.
17. Robb, D. L. and Wylie, C. (1999) Confocal microscopy on *Xenopus laevis* oocytes and embryos. *Methods Mol. Biol.* **122**, 173–183.

18. Schroeder, M. M. and Gard, D. L. (1992) Organization and regulation of cortical microtubules during the first cell cycle of *Xenopus* eggs. *Development* **114**, 699–709.
19. Torpey, N. P., Heasman, J., and Wylie, C. C. (1992) Distinct distribution of vimentin and cytokeratin in *Xenopus* oocytes and early embryos. *J. Cell Sci.* **101**, 151–160.
20. Dent, J. A., Cary, R. B., Bachant, J. B., Domingo, A., and Klymkowsky, M. W. (1992) Host cell factors controlling vimentin organization in the *Xenopus* oocyte. *J. Cell Biol.* **119**, 855–866.
21. Dent, J. and Klymkowsky, M. W. (1989) Whole-mount analysis of cytoskeletal reorganization and function during oogenesis and early embryogenesis in *Xenopus*, in *The Cell Biology of Fertilization* (Schatten, H. and Schatten, G., eds.), Academic Press, New York, pp. 63–103.
22. Weber, K., Rathke, P. C., and Osborn, M. (1978) Cytoplasmic microtubular images in glutaraldehyde-fixed tissue culture cells by electron microscopy and by immunofluorescence microscopy. *Proc. Natl. Acad. Sci. U. S. A.* **75**, 1820–1824.
23. Andersen, S. S. and Karsenti, E. (1997) XMAP310: a *Xenopus* rescue-promoting factor localized to the mitotic spindle. *J. Cell Biol.* **139**, 975–983.

Multiphoton Laser Scanning Microscopy as a Tool for *Xenopus* Oocyte Research

Angela M. Prouty, Jun Wu, Da-Ting Lin,
Patricia Camacho, and James D. Lechleiter

Summary

Multiphoton laser scanning microscopy (MPLSM) has become an increasingly invaluable tool in fluorescent optical imaging. There are several distinct advantages to implementing MPLSM as a *Xenopus* oocyte research tool. MPLSM increases signal-to-noise ratio and therefore increases image quality because there is no out-of-focus fluorescence as would be created in conventional or confocal microscopy. All the light that is generated can be collected and used to generate an image because point detection of descanned fluorescence is not required. This is particularly useful when imaging deep into tissue sections, as is necessary for *Xenopus* oocytes, which are notoriously large (~1-mm diameter). Because multiphoton lasers use pulsed energy in the infrared wavelengths, the energy can also travel further into tissues with much less light scattering. Because there is no out-of-focus excitation, phototoxicity, photodamage, and photobleaching are significantly reduced, which is particularly important for long-term experiments that require the same region to be scanned repeatedly. Finally, multiple fluorophores can be simultaneously excited because of the broader absorption spectra of multiphoton dyes. In this chapter, we describe the advantages and disadvantages of using MPLSM to image *Xenopus* oocytes as compared to conventional and confocal microscopy. The practical application of imaging oocytes is demonstrated with specific examples.

1. Introduction

Xenopus oocytes are relatively difficult to image with conventional fluorescent techniques because of their large size (~1-mm diameter). Confocal microscopy overcomes some of the problems of large sample thickness by rejecting out-of-focus fluorescence (1–7). As discussed elsewhere in this volume (see Chapter 8), confocal microscopy relies on the principle of point excitation and point detection. Application of this technique to fluorescent imaging in oocytes has been very successful in providing images with higher contrast (8–10).

However, confocal microscopy also has its limitations. Because point excitation still excites out-of-focus fluorophores, preparations imaged with confocal microscopy are susceptible to phototoxicity and photodamage (3). This limitation is most pronounced when long-term recordings are performed in which accumulative damage may alter the physiology.

Deep tissue sectioning is also problematic in confocal microscopy because of issues with light scattering (3,10). Light scattering diminishes the intensity of light that can be delivered to the fluorophore in a deep imaging plane, as well as significantly reduces the amount of fluorescent light that can be collected at the point detector of the confocal microscope. Light scattering in deep tissue sections essentially enlarges the size of the diffraction-limited excitation spot as well as enlarges the size of the in-focus fluorescent spot at the point detector. This effectively increases the size of the minimal pinhole that captures the light, increasing the thickness of the optical section and lowering the image contrast.

Multiphoton laser scanning microscopy (MPLSM) provides an attractive alternative method for fluorescent optical imaging that overcomes many of the limitations just described. In this chapter, we provide a simple conceptual framework to understand the basic theory of MPLSM. We discuss how multiphoton excitation results in higher fluorescence sensitivity, less phototoxicity, and better image contrast compared to confocal microscopy. Finally, we present representative images collected in *Xenopus* oocytes using MPLSM. These data are discussed in terms of both advantages and disadvantages of using MPLSM for imaging fluorescence in *Xenopus* oocytes.

Figure 1 is a diagram comparing the basic components of conventional, confocal, and multiphoton microscopy. In conventional microscopy, excitation light is generally

Fig. 1. (*opposite page*) Schematic diagram comparing the basic components of conventional, confocal, and multiphoton fluorescence microscopy. (A) Conventional fluorescence microscopy implements the use of a xenon or halogen light source to illuminate the plane of focus uniformly, resulting in parallel excitation. Filters, placed in front of the light source and camera, provide selection of specific excitation and emission wavelengths, respectively. All light from the focal plane is reflected back through the objective lens and detected by the camera. (B) Confocal microscopes use a laser of discrete wavelengths to excite fluorophores in the sample. Lasers with multiple wavelength lines can be specifically selected for using an excitation filter. The laser is directed to a point in the focal plane, resulting in point excitation. Fluorescence emitted from the sample is reflected back through the objective lens, through a pinhole to a photomultiplier tube (PMT). Light, from fluorophores excited above and below the plane of focus, will be blocked by the barrier filter, resulting in point detection. (C) A pulsed laser is used as the excitation source in multiphoton microscopy, which concentrates the laser energy into brief pulses. To excite fluorophores, two or three photons, each with one-half to one-third the energy required for single photon excitation, must be absorbed simultaneously. The probability of this occurring is only significant at the plane of focus, which results in no out-of-focus excitation. Therefore, all the light that is produced can be collected by the PMT and used to generate an image. (D) A Jablonski plot describing the principle of one-photon vs two-photon excitation. Because the energy of photons decreases as wavelengths increase, two photons, each at 700 nm, would be needed to excite a fluorophore normally excited by a single photon at 350 nm. Em., emission; Ex., excitation.

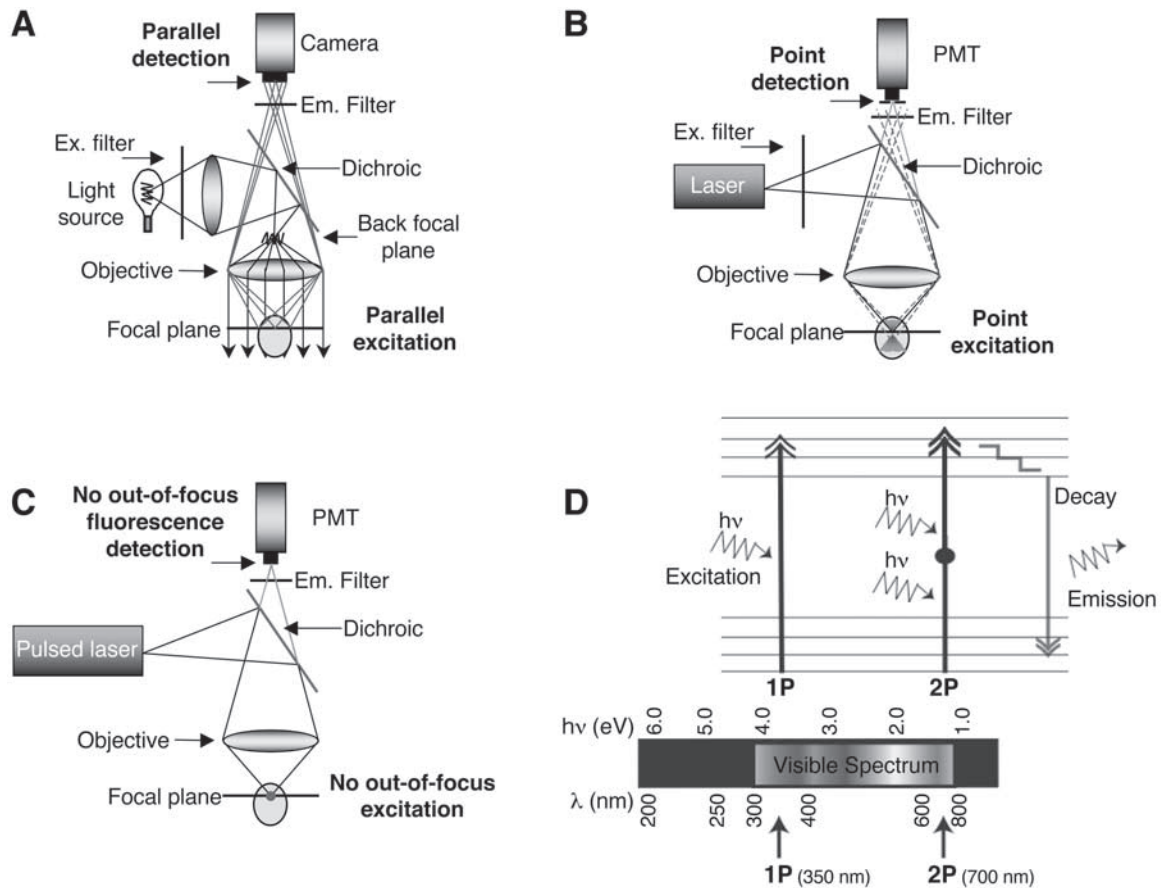


Fig. 1.

emitted from a mercury or xenon lamp source. The wavelength is established by placing an excitation filter in the light path. An image of the light source, depicted here as the filament in a lightbulb (**Fig. 1A**), is placed at the back aperture of the objective by a lens. From this focal plane, diverging light emitted from each point on the filament is collected by the objective lens and projected through the imaging plane as parallel rays.

A significant advantage of the conventional optical configuration is that the specimen is simultaneously flooded with parallel light that results in a very even illumination across the entire imaging plane. Fluorescent light that is emitted by the specimen is collected again by the objective lens, which in turn focuses an image onto a camera. A barrier filter is placed in front of the detector to reject any remaining excitation light. Another advantage of conventional fluorescence imaging is rapid image acquisition. The only limitation is the acquisition speed of the camera. However, conventional fluorescence microscopy results in excitation of fluorophores in the fields above and below the plane of focus. Light emitted as a result of this out-of-focus excitation results in blurring from out-of-focus fluorescence, which in turn significantly lowers image quality. Overall, conventional fluorescence microscopy should be limited to examination of relatively thin samples, such as a monolayer of cultured cells, or when rapid image acquisition is required.

Confocal microscopy provides a significant improvement in image quality when compared to conventional fluorescence microscopy. The essence of this imaging technique is point excitation and point detection (**Fig. 1B**). The light source for confocal microscopy is a laser that emits light at several discrete wavelengths. The specific wavelengths that are available to the user depend on the type of laser. Two to three lasers are frequently used with commercial confocal microscopes to provide excitation light at wavelengths including 405, 457, 488, 514, 543, 568, and 647 nm. Individual lines are selected with an excitation filter.

The ability to select a single wavelength for excitation is an important advantage of single-photon microscopy. Individual fluorophores can be specifically excited or photobleached. Once selected, the laser line is directed to the specimen with an appropriate dichroic mirror and focused onto the specimen as a diffraction-limited spot.

This type of illumination, point excitation, is quite distinct from the parallel illumination used for conventional fluorescence (cf. **Fig. 1A**). The excitation beam is generally scanned across the specimen with galvanometer mirrors or beam deflectors, which greatly slows image acquisition time. Fluorescence is collected by the objective and focused onto a detector, usually a photomultiplier. The advantage of this configuration is that a mechanical aperture, a pinhole, can be placed just in front of the detector. The pinhole permits only in-focus light to be measured. Out-of-focus fluorescence light that is emitted above or below the plane of focus is rejected because this light comes to a focus either beyond or in front of the detector, respectively. Consequently, out-of-focus fluorescence at the detector is diffuse and predominantly blocked by the pinhole aperture. The end result is a significant increase in signal-to-noise ratio that greatly increases the image quality when compared to conventional wide-field fluorescent microscopy.

The primary disadvantage of the confocal configuration is that out-of-focus fluorophores are still excited. This means that the preparation is still susceptible to out-of-focus photodamage, photobleaching, and phototoxicity. These problems are generally more pronounced in protocols that require multiple scans, such as when collecting a large stack of optical z-sections or when a single optical plane is imaged multiple times during a time series experiment.

MPLSM is a more recent advance in microscopy that has further improved the fluorescent image quality when compared to confocal microscopy (2,4,6,7,11,12). The underlying principle of MPLSM is that fluorophore excitation is accomplished by the simultaneous absorption of two or three photons, each with about one-half to one-third the energy required for single-photon excitation (Fig. 1C,D). Simultaneity is defined as the absorption of these lower-energy photons within approx 10^{-15} s. The probability that such an event transpires is very low for normal continuous power lasers. To increase the likelihood of multiphoton absorption, two tactics are employed. First, pulsed lasers are used as an excitation source. This concentrates the laser energy of photons into brief pulses of approx 150 fs. Ti-sapphire lasers are the most frequently used pulsed laser systems for MPLSM. The pulse repetition rate of these lasers is approx 80 MHz. The higher photon flux, combined with an objective that focuses the beam onto the specimen as a diffraction-limited spot, greatly increases the probability of simultaneous absorption. Once the fluorophore is excited, fluorescence is collected by the objective and focused onto a detector similar to the confocal configuration shown in Fig. 1B. A key difference between the two configurations is that a pinhole aperture is not required to exclude out-of-focus fluorescence at the detector. In fact, there is no out-of-focus fluorescence to reject because the probability of two- or three-photon absorption out of the plane of focus is essentially zero.

The benefits of this imaging configuration are severalfold. First, signal-to-noise ratio is increased because there is no out-of-focus blurring to lower the image quality. Second, fluorescence can be collected as close to the point of excitation as possible because point detection of the descanned fluorescence is not required. This greatly increases the efficiency of light collection and is especially important in thick specimen imaging, for which tissue scattering reduces the amount of light that reaches the point detector. Third, because pulsed lasers use a wavelength within the infrared range (~700–1000 nm), light scattering is much less of a problem as compared to excitation from visible wavelengths (~400–700 nm). Hence, preparations can be imaged at much deeper levels than can be practically reached by shorter-wavelength single photons. Fourth, the absence of out-of-focus fluorophore excitation limits photodamage, phototoxicity, and photobleaching to the imaging plane. Consequently, image acquisition of a large z-series or a long time series is much less damaging to the preparation. Finally, multiple fluorophores can be simultaneously excited by a single pulsed laser because two-photon absorption spectra tend to be much broader than single-photon absorption (13). However, this does limit the user's ability to select excitation of a discreet fluorophore, which can be seen as a major disadvantage.

Overall, there are many theoretical and practical benefits of using MPLSM for fluorescence measurements in comparison to either conventional or confocal microscopy. In the remainder of this chapter, we present some of our experiences in applying this technique to the *Xenopus* oocyte.

2. Materials

1. Albino *Xenopus laevis* oocytes.
2. Messenger ribonucleic acid (mRNA) of sarco-endoplasmic reticulum Ca^{2+} ATPase (SERCA) 2b, mitochondrially targeted green fluorescent protein (GFP), and calnexin–cyan fluorescent protein (CFP) made from deoxyribonucleic acid (DNA) construct using MEGAscript T7 (Ambion, Austin, TX).
3. IP_3 (inositol 1,4,5-triphosphate) (Sigma, St. Louis, MO).
4. TMRE (tetra-methyl-rhodamine ethyl ester) (Molecular Probes, Eugene, OR).
5. Oregon Green 488 BAPTA-2 (OG-2; Molecular Probes).

3. Methods

3.1. Pigmented vs Albino *Xenopus* Oocytes

Xenopus oocytes have proven to be an excellent cell model system based largely on their ease of manipulation. We have successfully used the preparation discussed here to study multiple processes in the $\text{IP}_3/\text{Ca}^{2+}$ signaling pathway. A mainstay in these studies was the use of confocal imaging to monitor changes in intracellular Ca^{2+} (8,9,14–22). More recently, we have begun to employ MPLSM in studying both Ca^{2+} signaling and mitochondrial physiology. As with conventional and confocal microscopy, oocytes are generally harvested from albino frogs. For MPLSM imaging, the absence of pigmented granules is particularly important because of problems with infrared absorption. Pigmented granules absorb so much infrared energy that local lesions are produced resulting in focal Ca^{2+} release events (Ian Parker, personal communication).

As with conventional imaging, defolliculated oocytes are generally injected with indicator dyes via microelectrodes (14). Oocytes readily heal their microelectrode puncture wounds when the injections are performed in saline solution with 1 mM extracellular Ca^{2+} . In addition to indicator dyes, second messengers (i.e., IP_3), and mRNA are also injected using the same technique with microelectrodes. To express exogenous protein in *Xenopus* oocytes, complementary DNA (cDNA) should first be subcloned into a *Xenopus* β -globin expression vector. Then, mRNA is synthesized from a T7 promoter using the MEGAscript T7 kit as instructed and is capped with m7G(5')ppp(5'') (Ambion). The mRNA is resuspended in di-ethyl-pyro-carbonate-treated water at a concentration of 1.5 to 2.0 $\mu\text{g}/\mu\text{L}$ in 3- μL aliquots and stored at -80°C (9,14,21,22).

Because of their relatively large mass, oocytes sink to the bottom of the recording chamber solution and slightly flatten against the cover slip. This creates an excellent uniform surface for imaging. A disadvantage of this arrangement is that the large oocyte-to-glass surface area creates a significant diffusional barrier. For example, application of an extracellular ligand to activate a plasma membrane receptor that

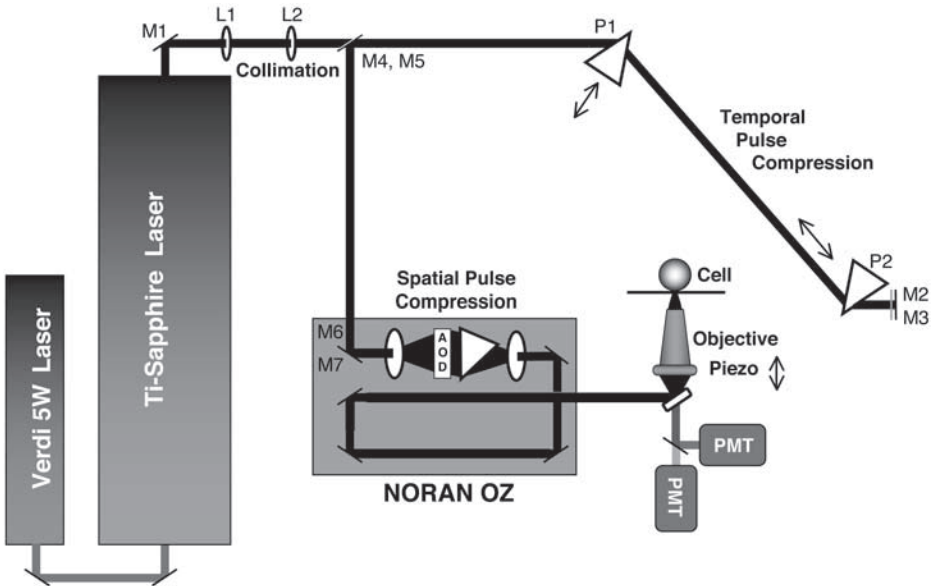


Fig. 2. A schematic diagram of the physical layout and optical components of the multiphoton-adapted NORAN OZ confocal microscope. A Verdi 5W laser is used to pump a MIRA 900-F Ti-sapphire laser to generate pulsed radiation (coherent lasers). Locations of steering mirrors (M), lenses (L), and prisms (P) are designated. Temporal pulse compression for temporal dispersion is added between prisms P1 and P2 as described in the text, and spatial compression is added within the NORAN OZ scan box. External photomultiplier tubes (PMTs) are used for nondescanned detection of fluorescence. The objective lens is mounted on a piezoelectric drive to permit rapid xz and xyz scanning.

generates IP_3 clearly results in an increase in Ca^{2+} that begins at the edge of the oocyte-to-glass contact region and propagates into the center.

3.2. Multiphoton Microscopes

A large number of in-house confocal microscopes have been adapted for multiphoton imaging because of the high cost of commercially available MPLSM. The primary component required for this adaptation is the incorporation of a laser source with pulsed radiation, such as that generated by a Ti-sapphire laser pumped with a solid-state laser. The experiments described in this chapter were acquired using an acoustic optical modulator adapted to the NORAN OZ confocal microscope for multiphoton imaging (Fig. 2) (23).

In brief, the infrared laser beam was introduced into the scan box by placing a 45° dichroic mirror in the beam path that reflects infrared wavelengths of light and transmitting short wavelengths of light less than 700 nm. Short-pass (<700 nm) barrier filters were also placed in front of the photodetectors. On confocal microscopes that use galvanometer-based mirrors to scan the beam across the specimen, these changes are

all that are required. However, for the NORAN OZ confocal microscope, two additional corrections had to be made.

The NORAN OZ confocal uses an acoustic optical deflector (AOD) to rapidly scan the excitation beam. This introduces both lateral and temporal spreading of the laser pulses, referred to as dispersion, because of the highly dispersive nature of the AOD. Laser pulses are composed of a collection of photons of variable wavelengths that are emitted from the laser within approx 150 fs. The wavelength range is typically ± 10 –20 nm. Temporal dispersion is caused by the fact that the shorter wavelengths of light have slower velocities within a medium, which causes the shorter wavelengths to lag when the pulse encounters a lens. Temporal dispersion is compensated for by directing the laser beam through two prisms, which in essence provide a greater path length for the longer wavelengths. This permits the shorter wavelengths of light initially to get ahead of the longer wavelength photons. By adjusting the distance between the two prisms, the amount of compensation can be adjusted to equal the amount of dispersion through the confocal microscope (23–25).

When an AOD is used for beam scanning, a second error is introduced. AODs alter the beam direction by changing their diffraction grating in response to sound waves. This results in the movement of the position of the first order of diffraction, which is used by the instrument as the excitation beam. This type of beam scanning is approx 1000 \times faster than galvanometer mirrors, but the amount of movement of the first-order diffraction beam is also dependent on the wavelength of light. The longer wavelengths of light within the laser pulse are deflected further, resulting in lateral beam spreading or spatial dispersion. Compensation for this dispersion is accomplished by placing a third prism in the beam path, which deflects shorter wavelengths to a greater extent. The precise degree of correction is determined by the apex angle of the correction prism and theoretically can be placed either before or after the AOD (23).

3.3. Examples of Imaging Oocytes Using MPLSM

3.3.1. IP_3 -Induced Ca^{2+} Wave Activity Visualized by OG-2

As described in the preceding subheading, one of the advantages of using a multiphoton-adapted, AOD-based confocal scanning microscope is speed of image acquisition. Our first example of the use of this imaging system in *Xenopus* oocytes is IP_3 -mediated Ca^{2+} wave activity (Fig. 3). Manually defolliculated oocytes were first injected with a 50-nL bolus (final ~ 300 nM) of IP_3 to stimulate Ca^{2+} release. To visualize Ca^{2+} movement, 12.5 μM of the Ca^{2+} -sensitive dye OG-2 was also injected 30 min prior to imaging. OG-2 was the preferred indicator dye for this experiment because the affinity of OG-2 for Ca^{2+} is lower than that of Oregon Green 488 BAPTA-1, and a higher concentration of OG-2 could be used (26). The oocyte was also overexpressing the SERCA isoform 2b, which significantly affects Ca^{2+} wave activity (9,22).

The clear advantage of using two-photon imaging for this experiment is that fluorescence is only emitted from the plane of focus. With a 60 \times 1.4-numerical aperture (NA) objective, the plane of focus is estimated to be less than 0.5 μm . This optical sectioning was used to image the spiral tip at several depths within the oocyte (Fig. 3). Because the same spiral rotation on different cycles is observed at each imaging plane,

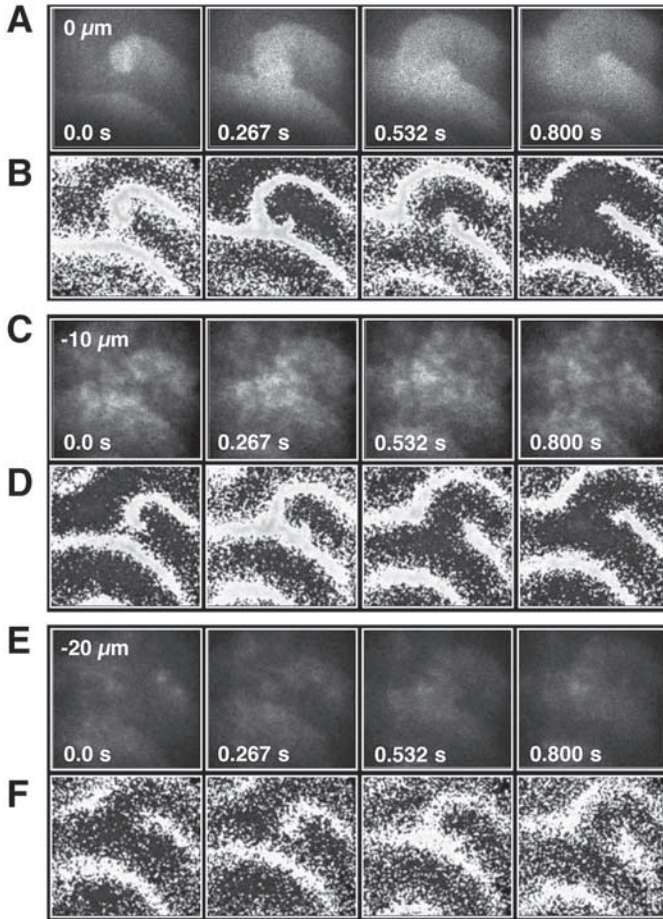


Fig. 3. IP_3 -mediated Ca^{2+} scroll wave visualized with the Ca^{2+} -sensitive dye Oregon Green 488 BAPTA-2 (OG-2) using the multiphoton-adapted NORAN OZ confocal microscope. A 50-nL bolus (final ~ 300 nM) of IP_3 is injected into an oocyte overexpressing the Ca^{2+} pump SERCA 2b. OG-2 is injected at a concentration of $12.5 \mu\text{M}$. **Panels A, C, and E** are raw intensity images for which excitation power and photodetector gain were not altered. **Panels B, D, and F** are difference images produced by subtracting sequential images. **Panels C, D and E, F** are images taken at increasing depths ($-10 \mu\text{m}$ and $-20 \mu\text{m}$, respectively) within the oocytes as compared to **panels A, B**, which is the designated starting point. Images within a panel are taken in a time series between 0.0 and 0.800 s.

this demonstrates that the spiral wave is actually a two-dimensional slice through a scroll wave of Ca^{2+} release. Scroll waves have been demonstrated in classical excitable media such as the Belousov-Zhabotinsky chemical reaction and aggregating slime mold (27–30). **Figure 3** also demonstrates that, as the laser penetrates deeper into the

sample, the light available to work with becomes significantly diminished. **Panels A, C, and E** in **Fig. 3** are raw intensity images for which the excitation power and photo-detector gain was not altered. **Panels B, D, and F** of **Fig. 3** are difference images produced by subtracting sequential images. The intensity of each difference image was increased to use the full 8-bit scale for optimal viewing of the wave pattern.

Generally, we have found that fluorescence emitted from the two-photon excitation at approx 810 nm of fluorescein-based Ca^{2+} indicator dyes, such as OG-2, is less intense than conventional excitation with single photons at 488 nm. This is attributed to several reasons. First, the optimal two-photon excitation wavelength would be better matched for fluorescein absorption at longer wavelengths. Increasing the wavelength of the excitation light is clearly one option to achieve greater fluorescence, but the peak power of the Ti-sapphire laser begins to diminish beyond approx 800 nm. Depending on the type of laser system, this generally is not a problem until the wavelength is adjusted well beyond 900 nm. Another inherent problem is that the probability of two-photon absorption of fluorescein-based dyes is relatively low (**13,31**). The simplest solution around this problem is to use Fura-2 as the Ca^{2+} -sensitive dye. Fura-2 in the Ca^{2+} free form readily absorbs light at 380 nm (**26**). This wavelength is ideally located for the peak power of the Ti-sapphire laser near 800 nm. It should be noted that it is not possible to use Fura-2 as a ratiometric dye with two-photon excitation, but the fluorescent output is much stronger than fluorescein-based dyes at 800 nm.

3.3.2. Imaging of Oocyte Mitochondria Using TMRE

In addition to Ca^{2+} imaging, we have had excellent success using MPLSM to study mitochondrial physiology. Our dye of choice to image mitochondria is the potential-sensitive dye TMRE. This dye distributes itself across charged membranes in an Nernstian fashion. Loew and coworkers have extensively characterized the use of this dye to estimate membrane potentials based on the fluorescent intensity of a compartment, which is directly proportional to the concentration of the dye (**32**). The primary limitation of estimating mitochondria membrane potentials with this dye is that the diameter of mitochondria is approx 250 nm, less than the diffraction limit of light. This means that the fluorescent intensity of the matrix mitochondria will not properly reflect the matrix concentration of the dye because the point spread function of the fluorescence is scattered out in the z direction (~ 500 nm) and slightly in the xy direction (**32**).

An example of oocyte mitochondria imaged with MPLSM is presented in **Fig. 4**. The oocytes were incubated in TMRE (200 nM) for 10 min prior to imaging at 800 nm using a $60\times$ 1.4-NA objective. The first observation common to all oocyte preparations is that manual defolliculation of the oocyte is not complete. This is evident by the bright TMRE fluorescence of these cells as well as their distinct cellular morphology (i.e., follicular cells) (**Fig. 4A,B**).

Oocyte mitochondria also have a recognizable spatial distribution that is apparent in the images of **Fig. 4B to D**. Near the surface of the oocyte, the mitochondria are diffusely distributed, similar to branches in a tree. As the user focuses into the oocytes, mitochondria, as well as other cytosolic organelles, are funneled into yolk-free corridors, similar to the lower branches and main trunks of trees. The presence of yolk-free

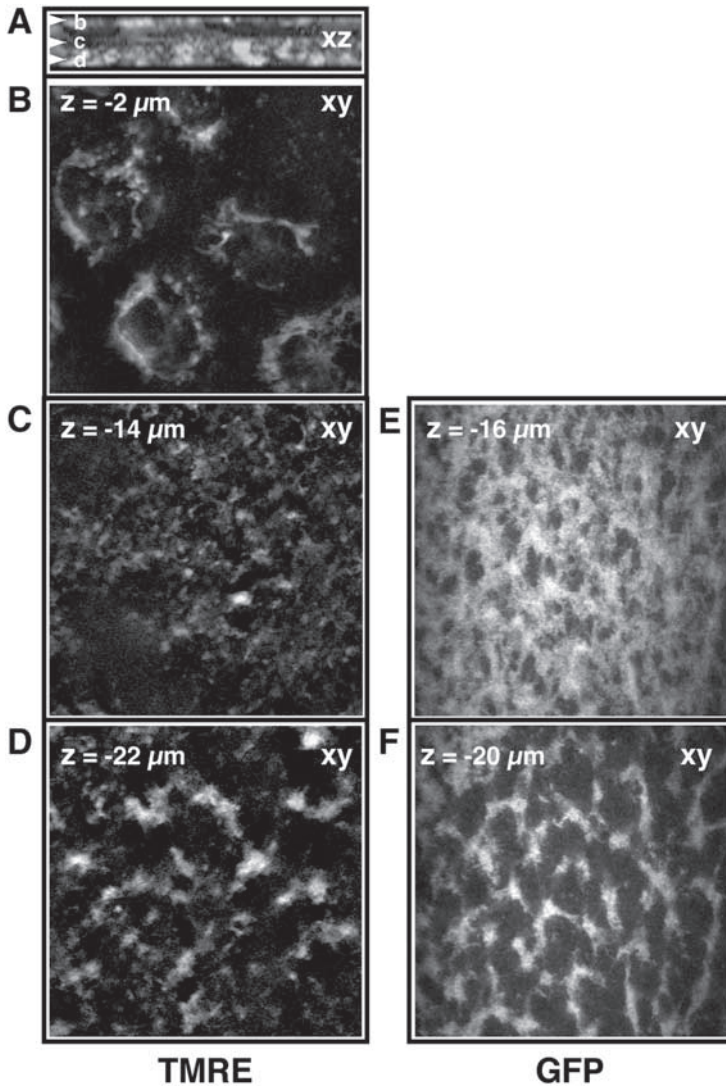


Fig. 4. Oocyte mitochondria imaged with MPLSM using TMRE as an indicator dye. Oocytes incubated in 200 nM TMRE for 10 min and imaged with MPLSM at 800 nm using a $60\times 1.4\text{-NA}$ objective are pictured in **panels A–D**. **Panel A** is representative of the image in the xz dimension, and the b–d arrows correspond to the lower **B** to **D** panels, which are images in the xy dimension. **Panel B** demonstrates nonspecific staining of follicular cells, indicating incomplete defolliculation. **Panel C** is an image of mitochondria near the surface of the oocytes; their distribution gives a diffuse appearance. **Panel D** is an image of mitochondria further within the cell, where they begin to demonstrate a more constricted appearance, being funneled into yolk-free corridors. **Panels E–F** are MPLSM images of mitochondrially targeted GFP to corroborate TMRE-specific staining of mitochondria. GFP is imaged with MPLSM at 810 nm . **Panel E** is an image near the surface, indicated by the diffuse fluorescence, and **panel F** is deeper within the oocyte, where the mitochondrial pattern becomes more defined.

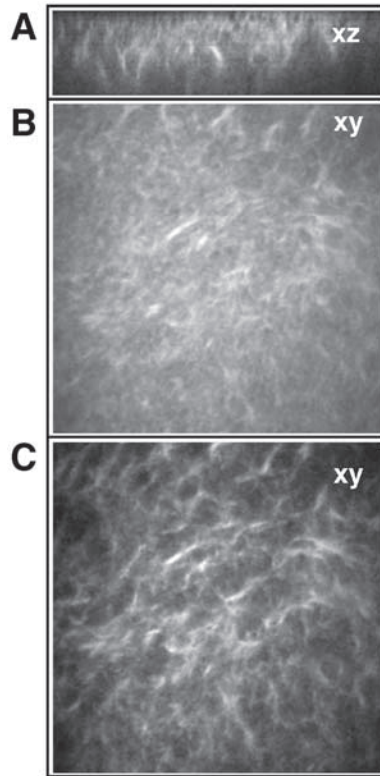


Fig. 5. Oocyte endoplasmic reticulum (ER) imaged with MPLSM visualizing CFP-labeled calnexin. Images were collected using a $60\times$ 1.4-NA objective at 800-nm excitation. **Panel A** is an image in the xz dimension representative of the xy images in **panels B** and **C**. The distribution pattern of ER, as demonstrated by the top 10 slices acquired (**panel B**), appears to be diffuse near the surface of the oocyte and becomes more constricted as they are funneled into the yolk-free corridors, as seen in the lower 10 slices (**panel C**).

corridors in oocytes was first reported from electron micrographs by Speksnijder et al. in 1993 (33).

Another oocyte imaging caveat is that the oocyte yolk has a tendency to non-specifically stain with TMRE. This is generally not a problem when imaging mitochondria with high potentials. However, potentials of mitochondria in oocytes are very low, less than -90 mV by our estimates (34).

For comparison, we have also included images of GFP-labeled mitochondria (Fig. 4E–F). A GFP construct with a mitochondrial targeting sequence was created, and mRNA was injected into the oocyte. After 2 to 3 d of expression, the oocyte was imaged with MPLSM at 810-nm excitation. The distribution pattern of mitochondria tagged with GFP was similar to that observed with the potential sensitive dye TMRE. GFP in the follicular cells was not observed because mRNA for GFP was not injected into these cells.

3.3.3. Oocyte Endoplasmic Reticulum Visualized With CFP-Tagged Calnexin

In the final example of MPLSM with *Xenopus* oocytes, we used CFP, a GFP mutant, to tag calnexin, a molecular chaperone protein that is targeted to the endoplasmic reticulum (ER). CFP is optimally excited by single photons from approx 430 to 460 nm. This absorption spectrum is ideal for two-photon excitation near peak power at 800 nm. The calnexin-CFP construct was allowed to express for 3 d in the oocyte before the oocyte was imaged with MPLSM using a 60× 1.4-NA objective at 800-nm excitation (Fig. 5). The distribution pattern of the ER is similar to mitochondria in that ER is more diffuse near the surface of the oocyte and becomes more constricted deeper into the yolk-free corridors of the oocyte.

4. Conclusions

MPLSM has proven to be a very useful technique for imaging *Xenopus* oocytes. The primary advantage is the ability to image deeper into tissue than with single-photon imaging. This is primarily because of reduced scattering of longer excitation wavelengths used in MPLSM. Because out-of-focus fluorescence does not occur with MPLSM, all fluorescent light can be collected with nondescanned detectors. This provides a higher signal-to-noise ratio, allowing for significantly improved image contrast deeper within regions of the oocytes. Significant reductions in phototoxicity and photobleaching are also major advantages of MPLSM.

The primary disadvantages of MPLSM in oocytes include the presence of autofluorescent yolk platelets as well as the lack of bright fluorescent dyes that have been optimized for MPLSM excitation. The mitochondrial dye TMRE is an exception to this rule. This dye is very bright and provides an excellent signal-to-noise ratio. We routinely use this dye as a standard to rapidly judge the performance of other dyes in the oocyte. Another caveat of MPLSM is that the absorption bandwidth for fluorophores is generally much broader for MPLSM than it is for single-photon absorption curves. This makes it much more difficult to excite a single fluorophore when two are present.

Overall, the advantages of MPLSM outweigh its disadvantages, and we would recommend that users strongly consider this imaging approach when studying physiology in oocytes.

Acknowledgments

This work was supported by a National Institutes of Health R01 award to J. D. Lechleiter (GM48451) and National Institutes of Aging P01 award to J. D. Lechleiter (AG19316).

References

1. Brakenhoff, G. J., van der Voort, H. T., van Spronsen, E. A., Linnemans, W. A., and Nanninga, N. (1985) Three-dimensional chromatin distribution in neuroblastoma nuclei shown by confocal scanning laser microscopy. *Nature* **317**, 748–749.
2. Denk, W. and Svoboda, K. (1997) Photon upmanship: why multiphoton imaging is more than a gimmick. *Neuron* **18**, 351–357.

3. Pawley, J. B. (1995) *Handbook of Biological Confocal Microscopy*, 2nd ed. (Pawley, J. B., ed.), Plenum Press, New York.
4. Piston, D. W. (1999) Imaging living cells and tissues by two-photon excitation microscopy. *Trends Cell Biol.* **9**, 66–69.
5. White, J. G., Amos, W. B., and Fordham, M. (1987) An evaluation of confocal vs conventional imaging of biological structures by fluorescence light microscopy. *J. Cell Biol.* **105**, 41–48.
6. Williams, R. M., Zipfel, W. R., and Webb, W. W. (2001) Multiphoton microscopy in biological research. *Curr. Opin. Chem. Biol.* **5**, 603–608.
7. Zipfel, W. R., Williams, R. M., and Webb, W. W. (2003) Nonlinear magic: multiphoton microscopy in the biosciences. *Nat. Biotechnol.* **21**, 1369–1377.
8. Camacho, P. and Lechleiter, J. D. (1995) Calreticulin inhibits repetitive intracellular Ca²⁺ waves. *Cell* **82**, 765–771.
9. John, L. M., Lechleiter, J. D., and Camacho, P. (1998) Differential modulation of SERCA2 isoforms by calreticulin. *J. Cell Biol.* **142**, 963–973.
10. Robb, D. L. and Wylie, C. (1999) Confocal microscopy on *Xenopus laevis* oocytes and embryos. *Methods Mol. Biol.* **122**, 173–183.
11. Denk, W., Strickler, J. H., and Webb, W. W. (1990) Two-photon laser scanning fluorescence microscopy. *Science* **248**, 73–76.
12. Piston, D. W. and Knobel, S. M. (1999) Quantitative imaging of metabolism by two-photon excitation microscopy. *Methods Enzymol.* **307**, 351–368.
13. Xu, C., Zipfel, W., Shear, J., Williams, R., and Webb, W. (1996) Multiphoton fluorescence excitation: new spectral windows for biological nonlinear microscopy. *Proc. Natl. Acad. Sci. USA* **93**, 10,763–10,768.
14. Camacho, P. and Lechleiter, J. D. (2000) *Xenopus* oocytes as a tool in calcium signaling research, in *Methods in Calcium Signaling Research* (Putney, J., ed.), CRC Press, Boca Raton, FL, pp. 157–181.
15. Camacho, P. and Lechleiter, J. D. (1995) Spiral calcium waves: implications for signaling, in *Calcium Waves, Gradients and Oscillations*, Vol. 188 (Symposium, C. F., ed.), Wiley, Chichester, UK, pp. 66–84.
16. Camacho, P. and Lechleiter, J. (1993) Increased frequency of calcium waves in *Xenopus laevis* oocytes that express a calcium-ATPase. *Science* **260**, 226–229.
17. Falcke, M., Hudson, J. L., Camacho, P., and Lechleiter, J. D. (1999) Impact of mitochondrial Ca²⁺ cycling on pattern formation and stability. *Biophys. J.* **77**, 37–44.
18. Falcke, M., Or-Guil, M., and Bar, M. (2000) Dispersion gap and localized spiral waves in a model for intracellular Ca²⁺ dynamics. *Phys. Rev. Lett.* **84**, 4753–4756.
19. John, L. M., Mosquera-Caro, M., Camacho, P., and Lechleiter, J. D. (2001) Control of IP(3)-mediated Ca(2+) puffs in *Xenopus laevis* oocytes by the Ca(2+)-binding protein parvalbumin. *J. Physiol.* **535**, 3–16.
20. John, L. M., Zhang, M., Camacho, P., and Lechleiter, J. D. (1998) Parvalbumin enhances activity of Ca²⁺ puffs/sparks while restricting Ca²⁺ wave propagation in *Xenopus* oocytes. *Biophys. J.* **74**, 238a.
21. Roderick, H. L., Llewellyn, D. H., Campbell, A. K., and Kendall, J. M. (1998) Role of calreticulin in regulating intracellular Ca²⁺ storage and capacitative Ca²⁺ entry in HeLa cells. *Cell Calcium* **24**, 253–262.
22. Roderick, H. L., Lechleiter, J. D., and Camacho, P. (2000) Cytosolic phosphorylation of calnexin controls intracellular Ca(2+) oscillations via an interaction with SERCA2b. *J. Cell Biol.* **149**, 1235–1248.

23. Lechleiter, J. D., Lin, D. T., and Sieneart, I. (2002) Multi-photon laser scanning microscopy using an acoustic optical deflector. *Biophys. J.* **83**, 2292–2299.
24. Fork, R., Martinez, O., and Gordon, J. (1984) Negative dispersion using pairs of prisms. *Optic Lett.* **9**, 150–152.
25. Soeller, C. and Cannell, M. B. (1996) Construction of a two-photon microscope and optimisation of illumination pulse duration. *Pflugers Arch.* **432**, 555–561.
26. Takahashi, A., Camacho, P., Lechleiter, J. D., and Herman, B. (1999) Measurement of intracellular calcium. *Physiol. Rev.* **79**, 1089–1125.
27. Allesie, M. A., Bonke, F. I. M., and Schopman, F. J. G. (1973) Circus movement in rabbit atrial muscle as a mechanism of tachycardia. *Circ. Res.* **33**, 54–62.
28. Devreotes, P. N., Potel, M. J., and Mackay, S. A. (1983) Quantitative analysis of cyclic AMP waves mediating aggregation in *Dictyostelium discoideum*. *Dev. Biol.* **96**, 405–415.
29. Winfree, A. T. (1972) Spiral waves of chemical activity. *Science* **175**, 634–636.
30. Zaikin, A. N. and Zhabotinsky, A. M. (1970) Concentration wave propagation in two-dimensional liquid-phase self-oscillating systems. *Nature* **225**, 535–537.
31. Xu, C., and W. Webb. (1996) Measurement of two-photon excitation cross sections of molecular fluorophores with data from 690 to 990 nm. *J. Opt. Soc. Am. B* **13**, 481–491.
32. Loew, L. M., Carrington, W., Tuft, R. A., and Fay, F. S. (1994) Physiological cytosolic Ca^{2+} transients evoke concurrent mitochondrial depolarizations. *Proc. Natl. Acad. Sci. USA* **91**, 12,579–12,583.
33. Speksnijder, J. E., Terasaki, M., Hage, W. J., Jaffe, L. F., and Sardet, C. (1993) Polarity and reorganization of the endoplasmic reticulum during fertilization and ooplasmic segregation in the ascidian egg. *J. Cell Biol.* **120**, 1337–1346.
34. Jouaville, L. S., Ichas, F., Holmuhamedov, E. L., Camacho, P., and Lechleiter, J. D. (1995) Synchronization of calcium waves by mitochondrial substrates in *Xenopus laevis* oocytes. *Nature* **377**, 438–441.

Imaging Ca²⁺ Signals in *Xenopus* Oocytes

Sheila L. Dargan, Angelo Demuro, and Ian Parker

Summary

Xenopus oocytes have become a favored preparation in which to study the spatiotemporal dynamics of intracellular Ca²⁺ signaling. Advantages of the oocyte as a model cell system include its large size, lack of intracellular Ca²⁺ release channels other than the type 1 inositol trisphosphate receptor, and ease of expression of foreign receptors and channels. We describe the use of high-resolution fluorescence imaging techniques to visualize Ca²⁺ signals in *Xenopus* oocytes at levels ranging from global Ca²⁺ waves to single-channel Ca²⁺ microdomains.

Key Words: Ca²⁺; caged IP₃; calcium; confocal; dye; flash photolysis; fluorescence; imaging; inositol; IP₃; linescan; microinjection; microscopy; receptor; signaling; TIR; video rate; *Xenopus* oocytes.

1. Introduction

Xenopus oocytes are a favored model cell system in which to image Ca²⁺ signals evoked by inositol 1,4,5-trisphosphate (IP₃) and possess distinct advantages over most other cell types. Intracellular Ca²⁺ liberation is mediated only by type 1 IP₃ receptors in the absence of ryanodine receptors (**1**), their large size greatly facilitates intracellular injections, and they are among the best-characterized cells for Ca²⁺ signaling (**2,3**). Moreover, the ability of *Xenopus* oocytes to express foreign receptors and ion channels (**4**), such as calcium channels, further enhances the versatility of this already-favorable model system.

The protocols described in this chapter are aimed at the beginner in the field, assuming no previous knowledge of the methods. We describe the use of confocal microscopy techniques, together with flash photolysis of caged IP₃, for imaging intracellular Ca²⁺ signals in *Xenopus* oocytes. We use “custom-built” confocal microscopes, but the methods are directly applicable to the use of commercial instruments. We also describe the use of total internal reflection fluorescence microscopy (TIRFM) for visualizing Ca²⁺ signals from individual voltage-gated channels.

2. Materials

2.1. Preparation and Microinjection of *Xenopus Oocytes*

1. Female *Xenopus laevis* frogs (Nasco, Fort Atkinson, WI; *see* **Notes 1–3**).
2. MS-222 (Sigma, St. Louis, MO). Store at -20°C in a desiccator. This is a possible carcinogen; wear gloves.
3. Frog guillotine.
4. Gentamicin solution, 50 mg/mL (Sigma). Store at 4°C ; toxic.
5. Modified Barth's solution (MBS): 88 mM NaCl, 1 mM KCl, 2.4 mM NaHCO_3 , 0.82 mM MgSO_4 , 0.33 mM $\text{Ca}(\text{NO}_3)_2$, 0.14 mM CaCl_2 , 5 mM *N*-2-hydroxyethylpiperazine-*N*-2-ethanesulfonic acid (HEPES), pH 7.4, containing 0.5 mg/mL gentamicin. Store at 17°C (*see* **Note 4**).
6. Two forceps (Dumont 5) (Fine Science Tools Inc., Foster City, CA).
7. Upright light stereo dissection microscope.
8. Regular Petri dishes and one lined with nylon netting (for oocyte injection).
9. Glass vials (~15-mL capacity).
10. Collagenase type 1 (Sigma). This is toxic.
11. Ringer's solution: 120 mM NaCl, 2 mM KCl, 1.8 mM CaCl_2 , 5 mM HEPES, pH 7.3. Store at 4°C (*see* **Note 4**).
12. Glass capillaries (7-in. Drummond 3-00-203-G/XL).
13. Horizontal pipet puller (Narishige, Tokyo, Japan).
14. Microinjector (Drummond Nanoject Drummond Scientific Co, Broomall, PA).

2.2. Imaging

2.2.1. Confocal Imaging

1. Caged IP_3 (Molecular Probes, Eugene, OR). Store at -20°C ; light sensitive (but *see* **Note 5**).
2. Ca^{2+} indicator dyes (Molecular Probes). Store at -20°C ; light sensitive.
3. Inverted confocal microscope with excitation laser (e.g., 488-nm argon ion laser).
4. 40 \times Oil objective (numerical aperture [NA] = 1.35) and low-viscosity immersion oil.
5. Oocyte recording chamber.
6. Glass cover slips (12-545C, 22 \times 40-1, Fisher Scientific, Pittsburgh, PA).
7. Image acquisition and processing software. We use custom routines in *Labview* (National Instruments, Austin, TX) for acquisition and IDL (Interactive Data Language: RSI Inc., Boulder, CO) for processing.

2.2.2. Total Internal Reflection Fluorescence Microscopy

1. Stripping solution: 200 mM K-aspartate, 20 mM KCl, 10 mM MgCl_2 , 10 mM EGTA (ethyleneglycol *bis*-(2-aminoethylether)-*N,N,N',N'*-tetraacetic acid), 10 mM HEPES, pH 7.4.
2. High- Ca^{2+} Ringer's solution: 110 mM NaCl, 6 mM CaCl_2 , 2 mM KCl, 5 mM HEPES, pH 7.4.
3. Calcium indicator dye (Fluo-4 dextran; Molecular Probes, Eugene, OR).
4. Complementary RNA (cRNA) encoding N-type Ca^{2+} channel $\alpha_{1\text{B-d}}$ and β_3 subunits (mixed 1/1 to a final concentration of 0.1–1 $\mu\text{g}/\mu\text{L}$ in diethylpyrocarbonate [DEPC] water).
5. Inverted microscope equipped for TIRFM, including TIRF (total internal reflection microscopy) objective lens (e.g., Olympus 60 \times oil immersion, NA 1.45), laser (e.g., 100-mW argon ion laser), low-light level, high-speed camera (e.g., Cascade; Roper Scientific, Tucson, AZ). *See* **Subheading 3.2.8.** for more details.

6. Low-fluorescence immersion oil for TIRFM (type DF; Cargill Laboratories, Cedar Grove, NJ).
7. Image acquisition and analysis package (e.g., *MetaMorph*, Universal Imaging Corp., West Chester, PA).

2.2.3. Two-Electrode Voltage Clamp

1. Two manual micromanipulators (e.g., model MM-3; Narishige USA, East Meadow, NY) mounted on the microscope stage.
2. Glass capillaries (e.g., 1.5 mm × 0.86 mm, 6 in., with filament; A-M Systems Inc., Carlsborg, WA).
3. 3M KCl solution for filling electrodes.
4. Chlorided silver wires (chloride silver wire by dipping in solution of household bleach for a few minutes) for electrodes and ground wire for recording chamber.
5. Voltage clamp (e.g., Geneclamp 500, Axon Instruments, Foster City, CA).
6. Recording and analysis software (e.g., *pClamp*, Axon Instruments; or *Strathclyde WinWCP*, available as a free download to academic users at <http://www.bio-logic.fr/electrophysiology/winwcpandwinedr.html>).

3. Methods

The methods described are aimed at the beginner in the field and outline the preparation and microinjection of *Xenopus* oocytes and techniques for imaging intracellular Ca²⁺ signals.

3.1. Preparation and Microinjection of *Xenopus* Oocytes

Because detailed protocols for preparing and microinjecting *Xenopus* oocytes are listed elsewhere in this book, we only give a brief summary covering the essential steps. The subheadings outline terminal and survival surgery; removal of epithelial layers, follicular cells, and the vitelline membrane; and oocyte microinjection.

3.1.1. Terminal and Survival Surgery

1. Place a female *X. laevis* frog (Fig. 1A) in a 0.17% solution of MS-222 (made up in water) until sufficiently anesthetized.
2. If all of the oocytes are to be used, terminal surgery is performed: the frog is anesthetized and decapitated prior to removal of ovaries.
3. If only a few lobes are required for experiments, survival surgery may be performed. Make a small incision (~5–10 mm long) into the abdominal cavity of a fully anesthetized frog and remove a few ovarian lobes (using presterilized instruments) and place them directly into MBS. Suture the incision, using separate stitches for the abdominal wall and skin. Allow the frog to recover in fresh water and monitor for a few hours before returning to the vivarium. Perform alternate surgeries on opposite sides of the frog, with intervals of longer than 1 mo between successive surgeries.

3.1.2. Removal of Epithelial Layers and Follicular Cells

1. Place individual ovarian lobes in MBS, cut them open, and view them under a stereomicroscope (Fig. 1B).
2. Carefully remove epithelial layers (5) from healthy (uniform pigmentation) stages V and VI oocytes (6) using two fine forceps (Dumont 5): one to hold the ovary membrane steady and the other to manually “peel” the epithelial layers from the oocyte. Repeat this procedure until enough oocytes have been obtained for experiments (typically 200 oocytes).

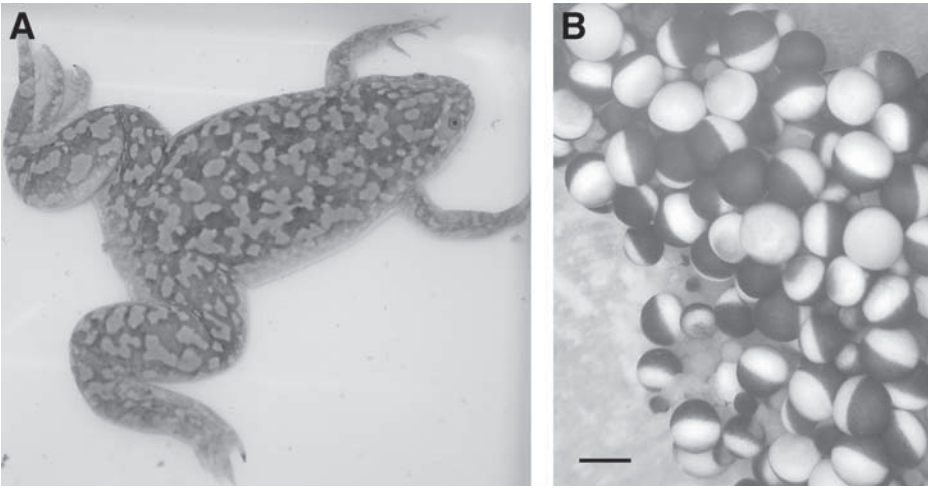


Fig. 1. (A) Female *Xenopus laevis* frog. (B) Ovarian lobe (cut open); scale bar = 1 mm. The pigmented (black) and unpigmented hemispheres, termed the animal and vegetal poles, respectively, can be seen.

3. Remove surrounding follicular cells, which are electrically coupled to the oocyte itself through gap junctions. Place oocytes (with the epithelial layers already removed) in approx 5 mL of 0.5 mg/mL collagenase type 1 (in Ringer's solution) with gentle agitation for approx 45 min. Wash repeatedly (about five washes) in MBS.
4. Store oocytes in MBS at 17°C until use. They can be stored in batches of approx 20 oocytes in individual vials filled with about 10 mL MBS. Rinse with fresh MBS twice daily and discard unhealthy oocytes. Alternatively, oocytes can be maintained individually in multiwell plates. Oocytes usually remain healthy for about 7 d. We do not remove the vitelline membrane for standard confocal imaging experiments, but this is stripped (as described in **Subheading 3.1.4.**) prior to TIRFM or patch-clamp recording.

3.1.3. Microinjection

1. After collagenase treatment, leave oocytes overnight in MBS at 17°C. Oocytes are easier to inject after overnight incubation because the membrane becomes firmer.
2. Pull a glass capillary (Drummond) (**Fig. 2A**) and examine under the microscope; using a fine pair of forceps, gently break off the end of the needle. For cytoplasmic injections, the needle width can be around 15 to 20 μm .
3. Backfill the needle with mineral oil, avoiding air bubbles, and assemble it onto the nanoinjector (**Fig. 2C**). Once the needle is mounted, press the "empty" button on the injector for a few seconds to dispel any air bubbles from the tip.
4. Prepare the solution to be injected. For calcium imaging and photolysis of caged IP_3 , this is an aqueous solution containing Ca^{2+} indicator dye (1.5 mM) together with caged IP_3 (0.25 mM) D-*myo*-inositol 1,4,5-trisphosphate, $\text{P}_{4(5)}\text{-(1-(2-nitrophenyl)ethyl) ester}$). For injection of cRNAs, thaw the selected cRNA preparation (e.g., 1/1 mixture of $\alpha_{1\text{B-d}}$ and β_3 cRNA N-type calcium channel clones) and spin at approx 9000g for 1 min to precipitate any salt crystals.

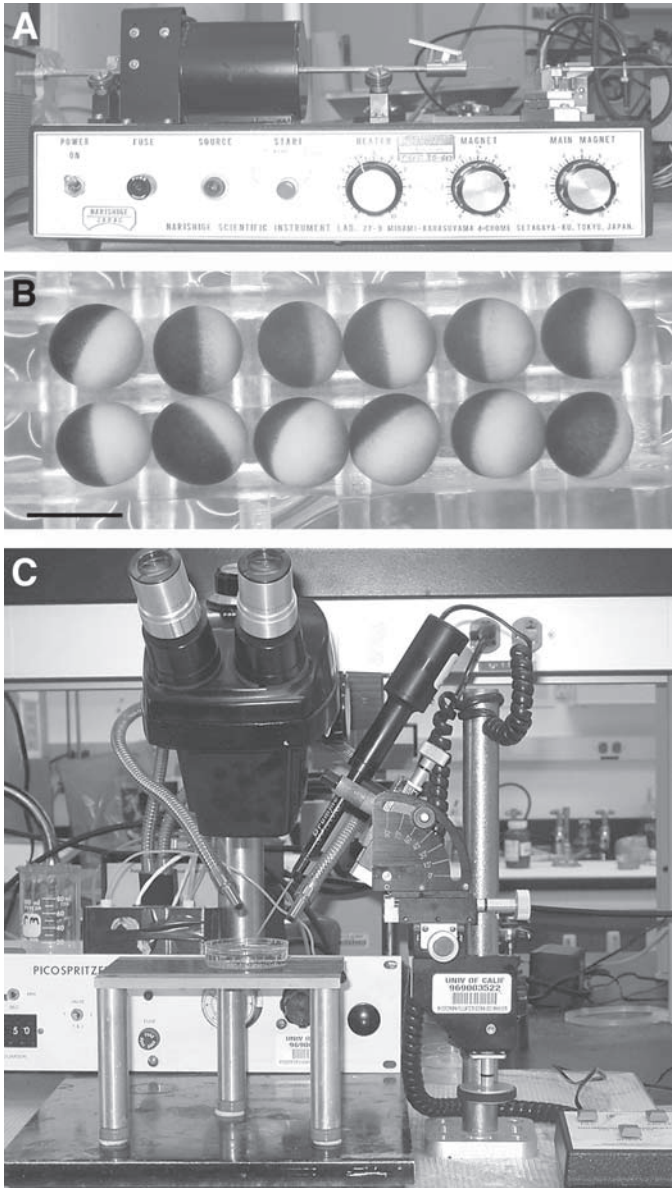


Fig. 2. Equipment for microinjection. **(A)** Pipet puller (Narishige, Tokyo, Japan); **(B)** oocytes aligned for microinjection; and **(C)** Drummond microinjector.

5. Pipet 1 to 2 μL of the injection solution onto a piece of fresh Parafilm positioned under the microscope. When injecting cRNA, wear clean gloves and use fresh pipet tips to avoid degradation by RNAases.
6. Using a stereomicroscope, focus on the drop under the microscope and position the micropipet over it; make sure you can see the micropipet enter the drop, then press the “fill” button on the Drummond nanoinjector. After the sample has been loaded, immediately position the tip of the micropipet in the injecting chamber containing MBS to avoid drying solution at the tip.
7. Transfer 10 to 30 oocytes into an injection chamber made by cementing a plastic net into the bottom of a Petri dish to obtain individual “wells” in the bottom of the Petri dish. In this situation, the oocytes can be steadily positioned in each mesh in any required orientation. Line the oocytes up with the equatorial band facing upward toward the injecting needle to avoid penetrating the nucleus (**Fig. 2B**).
8. Position the micropipet as vertically as possible with respect to the oocyte (angle $\sim 75^\circ$) and gently lower the pipet until the tip penetrates the oocyte. The oocyte will at first dimple and then “spring back” as the pipet penetrates the membrane.
9. Inject the required volume of solution (*see Note 7*).
10. After all oocytes have been injected, place them into a glass vial containing approx 5 mL MBS and store at 17°C for about 30 min (*see Note 5*) to allow for intracellular distribution of the dye and caged IP_3 prior to imaging Ca^{2+} responses.

3.1.4. Stripping the Vitelline Membrane for TIR Imaging

For TIRFM imaging, the plasma membrane of the oocyte must approach within less than 100 nm of a glass cover slip forming the base of the imaging chamber. It is therefore necessary to first remove the vitelline envelope, a connective tissue layer that remains even after collagenase treatment and removal of follicular cells.

1. After injecting collagenase-treated oocytes with calcium indicator dye, place a few oocytes in cooled hypertonic stripping solution at 10°C .
2. Wait for 10 to 20 min and then observe oocytes under a stereomicroscope using a fiberoptic illuminator with the light directed from the side. The oocyte should have shrunk, revealing the vitelline membrane as a surrounding translucent membrane. Grip the membrane using two pairs of fine forceps (Dumont 5), taking care not to pinch the oocyte, and gently tear open the membrane.
3. Use a dropper pipet to transfer the oocyte briefly to wash in a Petri dish filled with normal Ringer’s solution, then transfer again to the imaging chamber. Once the vitelline membrane is removed, oocytes are extremely fragile and quickly adhere to clean glass and plastic surfaces.

3.2. Imaging Techniques

We describe the basic principles of epifluorescence microscopy, video rate and linescan confocal laser scanning microscopy (CLSM), and TIRFM with respect to imaging intracellular Ca^{2+} signals in *Xenopus* oocytes.

3.2.1. Ca^{2+} Indicator Dyes

The most commonly used Ca^{2+} indicators are comprised of a chromophore conjugated to a Ca^{2+} chelator (BAPTA (1,2-bis(*o*-aminophenoxy)ethane-*N,N,N'*-*N'*-tetracetic acid))) backbone (**7,8**). Ratiometric Ca^{2+} indicators demonstrate a spectral

shift in either their excitation (e.g., Fura-2) or their emission (e.g., Indo-1) spectra on Ca²⁺ binding, whereas the nonratiometric dyes do not. The most obvious advantage of using ratiometric dyes is that they provide an intrinsic normalization, eliminating variations in factors such as probe loading, dye retention, photobleaching, and cell thickness. Moreover, measurements obtained using ratiometric dyes can be converted into absolute free [Ca²⁺]. However, ratio imaging is slow and complex and, because currently available ratiometric dyes (e.g., Fura-2 and Indo-1) are excited in the ultraviolet (UV) spectrum, they cannot readily be used for confocal imaging and cannot be used in conjunction with photolysis of caged compounds.

Nonratiometric indicator dyes (such as Oregon Green 488 BAPTA, Fluo-3, Fluo-4, Calcium Green, and Calcium Orange) are more popular for imaging Ca²⁺ signals in *Xenopus* oocytes for several reasons. These long-wavelength indicators generally demonstrate a large increase in fluorescence emission intensity on Ca²⁺ binding (except for Fura red, which shows a decrease) and are optimally excited at wavelengths compatible with those produced by laser illumination (e.g., the 488-nm line of the argon ion laser). The problems commonly associated with dye (am-ester) loading and retention in small cells (9) are obviated in oocytes because the free indicator dye can be directly injected into these “giant” cells. Because the most commonly used Ca²⁺ indicator dyes do not show a spectral shift on binding Ca²⁺, fluorescence signals are generally expressed as “pseudoratio” (F/F_0 or $\Delta F/F_0$) of the fluorescence F at each pixel relative to the mean resting fluorescence F_0 at that pixel prior to stimulation.

To select the most appropriate indicator dye for the application at hand, the parameters of the indicator (*in situ* binding affinity, dynamic range, rate of compartmentalization, and sensitivity to photo-damage) need to be taken into consideration (9). For example, small Ca²⁺ signals are best monitored using an indicator that binds Ca²⁺ with high affinity (e.g., Oregon Green 488 BAPTA-1, OG-1), whereas if the main goal is to track high-amplitude signals, then a low-affinity dye (e.g., Oregon Green BAPTA-5N) should be used to avoid saturation. Because the “apparent” binding affinities of indicator dyes *in situ* can vary significantly from those measured *in vitro* and affinities can even vary between different intracellular compartments, you may wish to calibrate the properties of your dye of choice in the oocyte (9). A relatively recent report demonstrating that the Ca²⁺ indicator dye OG-1 can evoke elementary Ca²⁺ signals in *Xenopus* oocytes (10) attributed this action to the mobility of the indicator. If dye mobility is important for your application, you may wish to use a “low-mobility” (dextran-conjugated) Ca²⁺ indicator dye (see **Note 6**), available from Molecular Probes.

3.2.2. Basic Principles of Ca²⁺ Imaging and Epifluorescence Microscopy

Epifluorescence microscopy involves the use of short-wavelength (e.g., blue) light to excite fluorophore molecules within a specimen (e.g., an oocyte). The light source is directed to the specimen through an objective lens. As fluorophore molecules absorb high-energy incident photons, provided by the light source, they rapidly (nanoseconds) emit photons of lower energy (longer wavelength; e.g., green light). Emitted fluorescence is imaged through the same objective lens. This is made possible by a filter “cube” (containing a dichroic mirror together with excitation and barrier filters)

that is positioned directly behind the objective to enable satisfactory separation of excitatory and emitted light. Because the objective lens also functions as the condenser in this arrangement, the NA is a very important consideration. Overall, the brightness of the fluorescence image increases as the fourth power of the NA. Attaining high numerical apertures requires use of immersion objectives. In principle, a water immersion objective should be optimal to avoid spherical aberration caused by refractive index mismatch, but in practice we achieve best results using a 40× oil immersion objective (NA 1.35).

3.2.3. Confocal Laser Scanning Microscopy

Confocal microscopy differs from regular wide-field epifluorescence in that the excitation light is focused as a diffraction-limited spot in the specimen, and emitted light is detected through a small aperture (pinhole) to reject out-of-focus fluorescence. This has the great advantage of providing a thin optical “slice” within a thick specimen but involves additional complexity as the confocal spot must be raster scanned, point by point, to build up an image. It is not possible to cover all of the principles of confocal microscopy in this short review; thus, we refer the reader to the *Handbook of Biological Confocal Microscopy* (11) for a more extensive description of the technique.

3.2.4. Commercial vs Homemade CLSMs

Commercial CLSMs, such as the Nikon (Melville, NY) RCM 8000, Noran Odyssey (Middleton, WI), and Bio-Rad (Hercules, CA) RTS2000, are expensive, generally surpassing the budget of individual investigators. Most research institutions therefore have shared optical imaging facilities, and a handful of researchers have even taken to building their own confocal instruments (e.g., 12–14). Many commercially available CLSMs (and associated software) were not designed with dynamic studies in mind, which can present many problems for users wishing to image fast events, such as Ca^{2+} transients, and can thus constrain the types of recordings that can be made. Moreover, the light paths in such instruments are generally complex, and adjusting the alignment can be difficult. To obviate such problems, in our laboratory we image intracellular Ca^{2+} signals using homemade CLSMs (Figs. 3.4; refs. 12–15).

3.2.5. Framescan vs Linescan Confocal Microscopy

Most commercial confocal microscopes can acquire full-frame images at rates of only one or a few frames per second. This is too slow to resolve dynamic changes in intracellular $[\text{Ca}^{2+}]$, which typically occur on a time-scale of tens of milliseconds. However, it is still possible to obtain good temporal resolution by imaging in linescan mode. Here, spatial information is traded for temporal information, and the laser spot is repeatedly scanned along a line to image a single spatial dimension with a time resolution as good as 1 or 2 ms per line (Fig. 3). As well as the improved temporal resolution, advantages of this technique are that the resulting data files are relatively compact, and that the spatiotemporal profile of Ca^{2+} signals is readily apparent from single images (Fig. 3C). Disadvantages include the limited spatial information, sampling from only a very small region of the oocyte, and uncertainty regarding whether the observed local Ca^{2+} signals originated directly on the scan line.

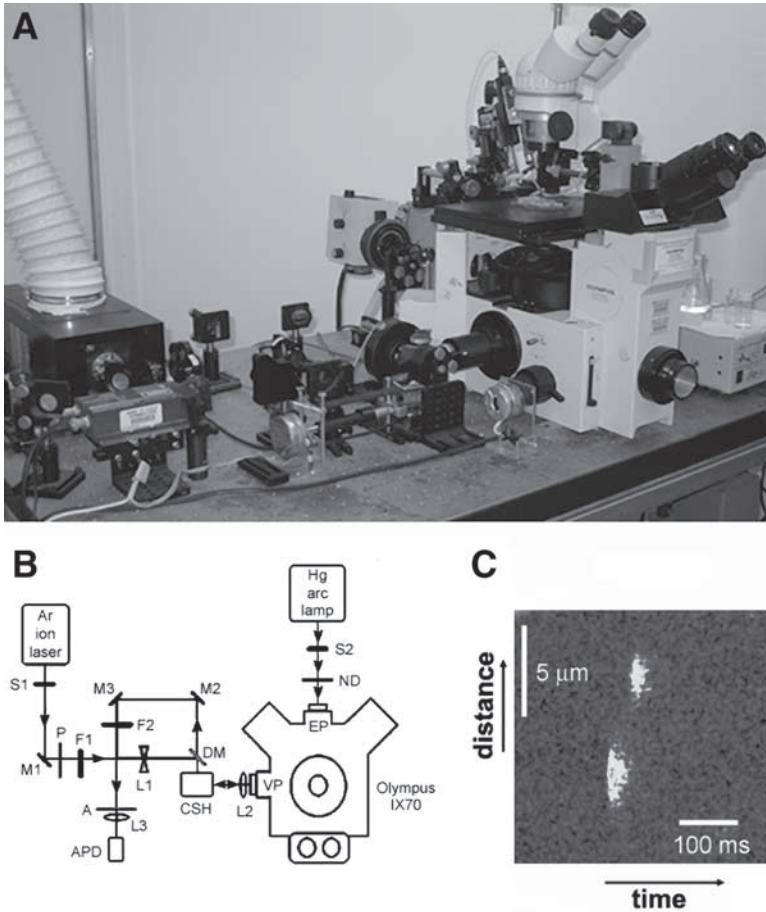


Fig. 3. Linescan CLSM. **(A)** Photograph; **(B)** schematic diagram of the optical layout of our homemade linescan CLSM. The CLSM is interfaced through the video port (VP) of an inverted microscope (Olympus IX70), and the photolysis system (light path of the mercury arc lamp) is interfaced through the epifluorescence port (EP). Electronic shutters (S1 and S2); mirrors (M1–M3) are fully reflecting front surface mirrors and DM is a dichroic mirror, $\lambda = 500$ nm); a rotating polarizer (P); filters (F1 is a 488 narrowband interference filter, and F2 is a barrier filter); lenses (L1 is a diverging lens with focal length of -10 cm, L2 is a scan lens made from a Zeiss 10 \times wide-field eyepiece, and L3 is a converging lens with a focal length of 5 cm); and a confocal aperture (A) were placed in the laser path as stated. The intensity of the UV photolysis light was attenuated using neutral density filter wheels (ND), and an avalanche photodiode module (APD) was used to detect photons. The scan mirror in the confocal scan head (CSH) is positioned 2 cm from the front surface of L2; the distance from L2 to A is 80 cm, from L2 to L1 is 70 cm, and from L3 to APD is 5 cm. **(C)** A representative image of IP₃-evoked Ca²⁺ puffs.

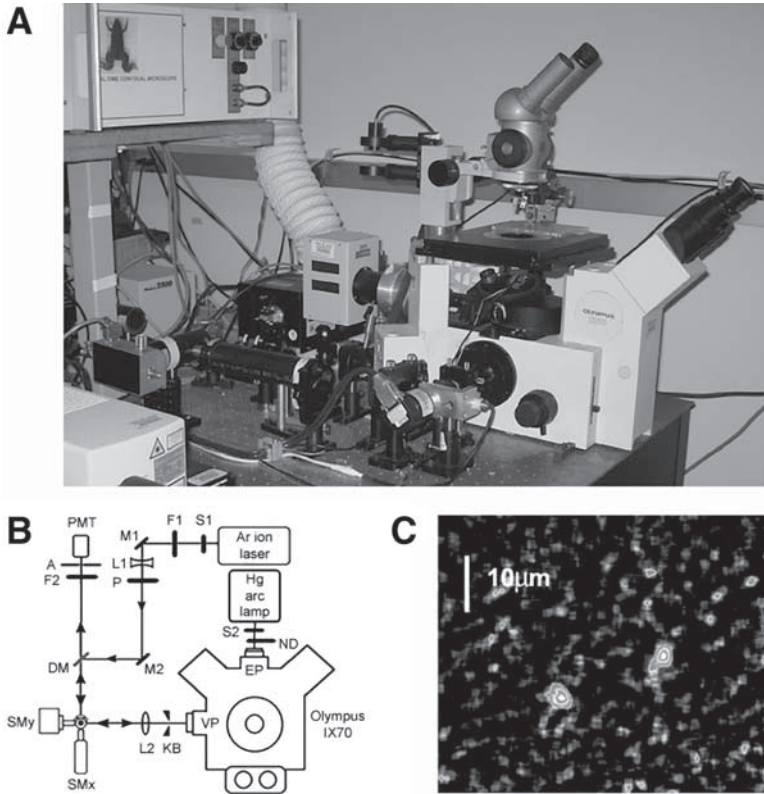


Fig. 4. (A) Homemade videorate CLSM. (B) Schematic of optical system. (C) A representative image of IP₃-evoked Ca²⁺ puffs. The optical components of the laser scanning system are interfaced through the video port (VP) of the Olympus IX70 microscope, and the UV light path generated by the mercury arc lamp is directed through the epifluorescence port (EP) at the rear of the microscope. Electronic shutters (S1 and S2); mirrors (M1–M4) are fully reflecting, broadband coated mirrors, and DM is a dichroic mirror, $\lambda = 500$ nm; lenses (L1 is a plano-concave lens [$f = -50$ cm], and L2 is a scan lens [$10\times$ Olympus eyepiece lens]); and a knife blade (KB) aperture are situated in the light path of the laser beam as illustrated. The scan head comprises two galvanometer-driven mirrors: a y-scan off-axis scan mirror (SM_y) and a resonant scanning mirror (SM_x).

A few confocal microscopes are available that permit full-frame imaging at video rate (30 frames per second) or even higher based on rapid scanning systems utilizing a resonant mirror, acousto-optic deflector, or spinning microlens array. These provide good two-dimensional spatial information and thus offer an intuitive view of intracellular Ca²⁺ signaling events (Fig. 4). However, the temporal resolution still does not approach that of linescan imaging, and the signal-to-noise ratio is not as good because of shot noise constraints arising from the brief dwell time at each pixel.

3.2.6. Setting Up an Inverted CLSM for Oocyte Imaging

Whichever technique you chose to use, the basic principles of setting up the microscope to obtain good images are the same.

1. Place a small drop of immersion oil on the 40× oil objective lens.
2. Using the coarse focus knob, lower the objective as far as possible.
3. Prepare the recording chamber: mount a clean, new cover slip in the recording chamber and secure the chamber to the stage of the inverted CLSM. Be aware that the cover slips tend to stick together. If two are inadvertently mounted, it will not be possible to focus on the oocyte because the working distance of oil immersion objectives is very short.
4. Using the coarse focus knob, raise the objective slowly until the oil makes contact with the cover slip of the recording chamber.
5. Fill the chamber with Ringer's solution and place an oocyte into the chamber.
6. Manipulate the position of the oocyte such that it is centered directly over the objective lens with the animal pole (dark side) facing down.
7. Focus in the layer of pigment granules in the animal hemisphere.
8. Open the laser shutter and focus the laser scan at the pigment granules of the oocyte (at a depth of ~5 μm into the animal hemisphere of the oocyte; this is where the Ca²⁺ release sites are most concentrated).
9. Acquire images (linescan or framescan) using software provided by the microscope manufacturer, third-party image acquisition software (e.g., *MetaMorph*, Universal Imaging, West Chester, PA), or custom-written software (we have written linescan acquisition and analysis routines using the IDL programming environment of Research Systems Inc., Boulder, CO).
10. The nanoinjector can be mounted on the microscope stage to make successive injections while imaging (*see Note 8*).

3.2.7. Flash Photolysis of Caged IP₃

Caged IP₃ (*see Note 5*) injected into oocytes cannot bind to IP₃ receptors and is therefore inactive. Irradiation with a short pulse of UV light (~360 nm) generates a concentration jump in IP₃, by releasing it from its caged precursor. This photo-released IP₃ can bind to, and open, IP₃ receptors (IP₃Rs) on the endoplasmic reticulum (ER), liberating Ca²⁺ from this intracellular store. Advantages of this technique for studying IP₃-mediated Ca²⁺ signaling include the facts that complexities resulting from upstream agonist activation of the phosphoinositide pathway are circumvented, and that precise control is achieved of the relative amount of IP₃ formed, its timing, and (by restricting where the UV light is focused on the oocyte) its spatial distribution.

A mercury arc lamp (50 or 100 W) provides a good source of UV light, and a regular microscope epifluorescence illuminator can be readily modified for flash photolysis by incorporating an electronic shutter (e.g., Uniblitz, Vincent Associates, Rochester, NY) and a filter cube with a dichroic mirror and excitation filter designed to reflect light less than 400 nm toward the objective lens (**Figs. 3B** and **4B**; also *see Note 9*).

1. Prefocus the UV light beam of a xenon or mercury arc lamp as a 200-μm spot surrounding the image scan line (**16**). This can be visualized using a test slide made by rubbing a yellow highlighter pen on the upper side (i.e., the side away from the objective lens) of a cover slip.

2. Mount the recording chamber and focus the microscope at the depth of the pigment granules in an oocyte as above. Photorelease IP₃ from its caged precursor by briefly opening the electronic shutter in the UV light path to deliver a very brief UV flash (in the order of milliseconds). This will result in a uniform release of IP₃ throughout the 200- μ m region.
3. The amount of photoreleased IP₃ can be controlled (in a linear manner) by varying the flash duration (by altering the open duration of the electronic shutter). Because each flash consumes only a negligible fraction of the caged IP₃ (16), it is possible to acquire numerous consistent responses from the same oocyte using repeated flashes. Neutral density filters can be inserted into the UV light path to evoke responses over an appropriate range of flash durations (we typically use 5–100 ms). Mechanical inertia in the shutter limits the shortest flashes to about 5 ms, whereas flashes longer than a few hundred milliseconds may outlast the Ca²⁺ response itself.
4. Intervals of longer than 90 s should be respected between recordings to allow IP₃Rs to recover from desensitization, and for cytosolic [Ca²⁺] to recover to basal levels.

3.2.8. Total Internal Reflection Fluorescence Microscopy

Although confocal imaging provides an optical slice within the oocyte and can thus localize Ca²⁺ signals in the axial (*z*) dimension much more effectively than wide-field epifluorescence microscopy, the axial resolution is nevertheless limited to about 700 nm. Evanescent wave imaging, or TIRFM, provides a way to obtain a much thinner section, which we have used to visualize Ca²⁺ signals arising from activation of individual voltage-operated Ca²⁺ channels expressed in the plasma membrane of oocytes (17).

The principle of this technique is that light undergoing total internal reflection at an interface from high to low refractive index (e.g., from glass to aqueous solution) penetrates a short distance into the low refractive index medium. This creates an evanescent wave that can be used to excite fluorescence confined within the thin plane (30–100 nm) immediately adjacent to the interface (18). Thus, if a cell containing a fluorescent Ca²⁺ indicator is made to adhere closely to a glass cover slip, fluorescence signals are recorded only from a region immediately adjacent to the cell membrane.

Advantages are that the TIRFM section is much thinner than can be achieved with confocal microscopy, and because no scanning is required, images can be acquired with regular or intensified charge-coupled device (CCD) cameras. The major disadvantage is that imaging is restricted to objects immediately adjacent to the interface, and unlike confocal microscopy, it is not possible to focus more deeply into the specimen.

Our homemade TIRFM system is based around an Olympus IX7I microscope (Fig. 5B,C). Similar systems are now commercially available from Olympus and other microscope manufacturers. An Olympus 60 \times TIRFM objective with high NA (NA = 1.45) allows the excitation light from an argon-ion laser to be directed through the extreme edge of the objective aperture for TIRF excitation or to be directed more centrally for conventional wide-field excitation. In this epi-illumination configuration, both the excitation and emission light paths travel through the same objective lens. Thus, it is possible to obtain TIRFM images from thick, opaque specimens (such as the *Xenopus* oocyte), and space above the specimen is freely accessible for positioning microelectrodes for electrophysiological recording. The emitted fluorescence is collected after passage

through barrier filters (>510 nm to block 488-nm laser excitation and > 650 nm to block infrared emission from the laser tube) and is imaged using a fast, cooled CCD camera.

The generation of cameras (such as the Roper Scientific Cascade) employing on-chip electron multiplication provide high sensitivity (quantum efficiency as good as 90%), low noise, and fast frame rates (500 fps or higher with subregion binning).

Procedures for TIRFM imaging of Ca²⁺ flux through individual N-type channels expressed in the oocyte membrane are described next.

1. Before beginning experiments, ensure that the microscope is properly adjusted for TIRF operation. Place a small drop of low-fluorescence immersion oil on the objective and raise this to contact a clean glass cover slip on the microscope stage. Pipet a small (~10 μ L) droplet of aqueous suspension of fluorescent microspheres (0.2 μ m diameter fluospheres, Molecular Probes Inc.) on the cover slip. Focus the microscope on beads that have adhered to the cover slip. Adjust the position of lens L3 (**Fig. 5C**) so that the laser light leaves the objective lens at an angle greater than the critical angle for total internal reflection. If adjusted correctly, stationary beads adhered to the cover glass will appear bright, whereas beads moving by Brownian motion deeper in the droplet will not be visible.
2. Load oocytes previously injected with cRNAs to express N-type Ca²⁺ channels with Fluo-4 dextran and strip the vitelline membrane.
3. Mount a fresh cover slip in the TIRFM imaging chamber (**Fig. 6**), place the chamber on the microscope, fill with Ringer's solution containing 6 mM [Ca²⁺], and introduce an oocyte with the animal hemisphere facing the objective. An elevated Ca²⁺ concentration is used to enhance Ca²⁺ flux through plasma membrane channels.
4. Penetrate the oocyte with two microelectrodes to allow voltage clamp control of the membrane potential. Clamp at a resting potential of -80 mV.
5. View the resting fluorescence of the indicator dye by TIRFM. Move the microscope stage (and attached micromanipulators) to find a region of the oocyte showing roughly uniform fluorescence throughout the imaging field (indicative of a "footprint" in which the membrane lies at about the same depth in the evanescent field).
6. Apply voltage clamp depolarizations (to about 0 mV for a few seconds). Look for the appearance of localized flashes of increased fluorescence ("sparklets") arising from Ca²⁺ flux through individual N-type channels (**Fig. 5D**). The distribution of channels in the oocyte is very "patchy," and it will probably be necessary to search throughout different regions of the oocyte.
7. Stream image TIRFM sequences to computer memory for subsequent analysis. In favorable cases, more than 100 separate channels can be captured in the image frame (80 \times 80 μ m). Process records by dividing each frame by an average image of resting fluorescence before stimulation, so that measurements reflect fractional increases in fluorescence ($\Delta F/F_0$), thus correcting for differences in fluorescence resulting from factors including uneven laser illumination and variation in distance of the membrane from the cover glass (**Fig. 5A**).
8. Measure fluorescence ratio signals from small (<1 μ m) regions of interest centered on sparklet sites to resolve the gating of individual channels (**Fig. 5E**).

4. Notes

1. Alternative suppliers of *X. laevis* frogs include *Xenopus* express (www.xenopus.com), *Xenopus* 1 (Dexter, MI; www.xenopusone.com), and Carolina Biological Supply (Burlington, NC; www.carolina.com).

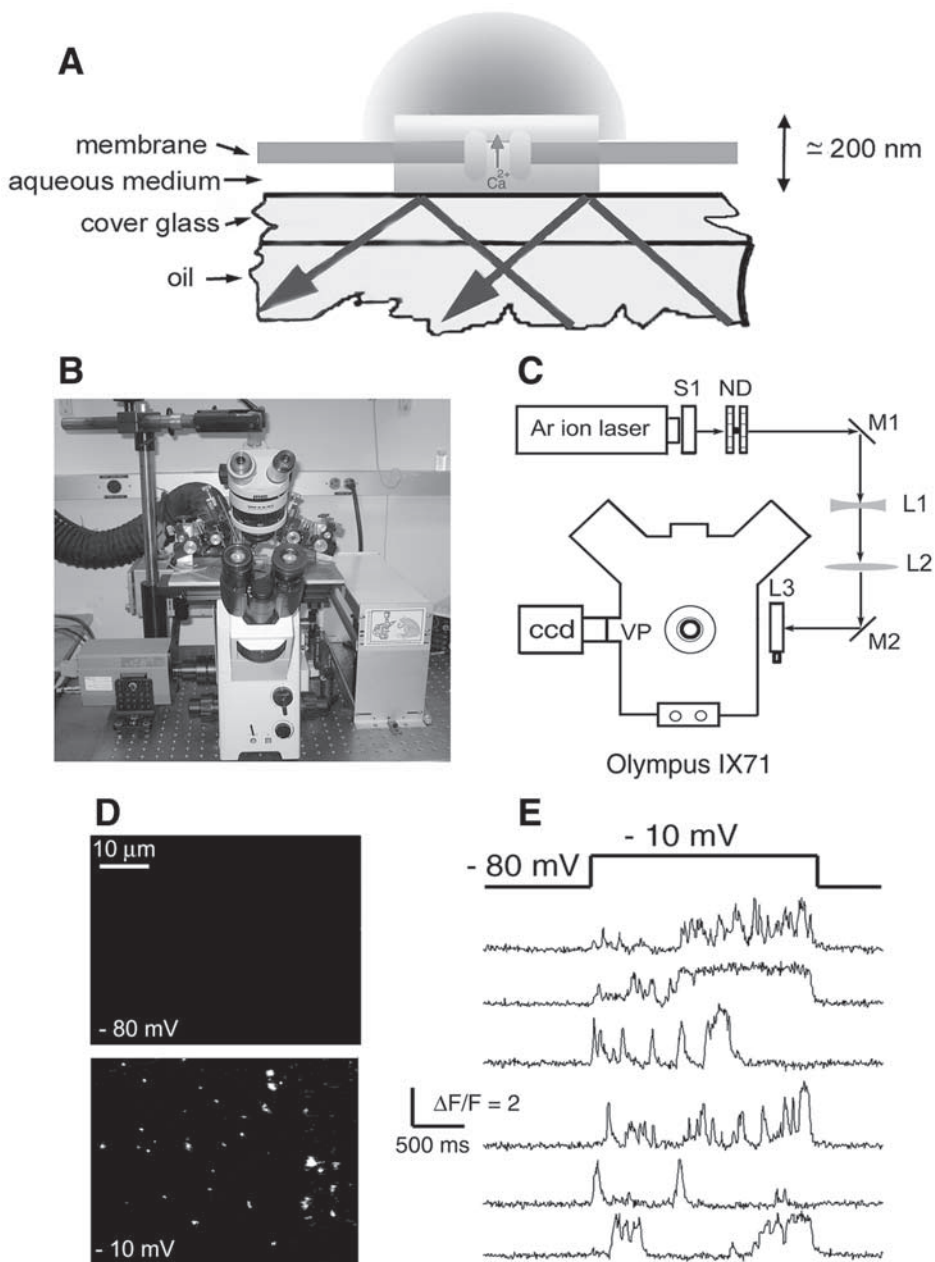


Fig. 5.

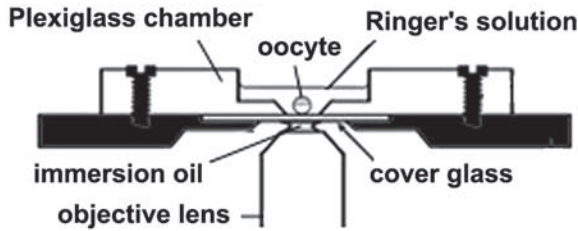


Fig. 6. Oocyte imaging chamber. The chamber is machined from two pieces of Plexiglas, which are held together to clamp a glass cover slip that forms the base of the recording chamber. A thin film of Vaseline applied to the upper section provides a watertight seal to retain Ringer's solution in the chamber. The chamber mounts onto the stage of an inverted microscope, and the oocyte is visualized through the cover glass by an oil immersion objective.

2. For experiments in which light absorption by pigment may lead to artifactually high thresholds in the animal hemisphere, oocytes from albino frogs may be preferable (19).
3. *Xenopus tropicalis* oocytes may be suitable for certain experiments: the spatiotemporal characteristics of Ca²⁺ signals have been shown to be similar those in *X. laevis* oocytes, and *X. tropicalis* oocytes may offer further practical advantages with respect to imaging depth, Ca²⁺ signal magnitude, and electrical properties (20).
4. Barth's (no gentamicin) and Ringer's solutions can be made up as 10X stocks (1 L), stored in the refrigerator, and diluted as needed. Gentamicin needs to be added to 1X Barth's dilutions, pH 7.4, then stored at 17°C. The 1X Ringer's, pH 7.3, can be stored at room temperature or in the refrigerator (but bring to room temperature prior to recording).
5. Caged IP₃ can also be purchased from Calbiochem (La Jolla, CA), but in our experience the caged IP₃ from Molecular Probes is preferable because it has lower contamination levels of active IP₃. Caged IP₃ is highly charged and thus does not permeate through cell membranes. Although by-products of photoreleasing IP₃ (H⁺ and nitroacetophenone) are toxic at high concentrations (1 mmol/L), this toxicity does not appear to be problematic in the oocyte (and other cells) because the concentrations of IP₃ required to evoke even maximal Ca²⁺ release are very small (16). We have not found it necessary to take any

Fig. 5. (previous page) Total internal reflection fluorescence microscope (TIRFM). (A) Principle of through-the-lens TIRFM. Laser light directed through the periphery of a high-NA objective lens (NA = 1.45) passes through the immersion oil and cover glass at a shallow angle and undergoes total internal reflection at the interface between the glass and the aqueous medium, resulting in an evanescent wave propagating about 200 nm into the aqueous phase. The surface membrane of a vitelline-stripped oocyte lies within the evanescent field, allowing the imaging of near-membrane fluorescence from a Ca²⁺ indicator dye (Fluo-4 dextran) previously loaded into the oocyte. (B, C) Photograph and schematic diagram of the TIRFM imaging system. (D) Fluorescence images (single video frames) showing Ca²⁺-dependent fluorescence at a negative holding potential and after depolarizing to -10 mV to cause openings of voltage-gated N-type Ca²⁺ channels in the oocyte membrane. Note the appearance of bright spots (sparklets) resulting from Ca²⁺ influx through individual channels. (E) Fluorescence traces monitored from small (1 μm²) regions of interest centered on sparklet sites show pulsatile changes reflecting stochastic channel gating.

- special precautions when handling caged IP₃ because standard room lights and even halogen fiber optics cause surprisingly little photolysis of the compound. Photolysis of caged IP₃ has advantages over injection of IP₃ in that homogeneous elevations in [IP₃] can be induced (by focusing a broad light spot), thus circumventing problems of diffusion delays.
6. If you choose to use a dextran-conjugated Ca²⁺ indicator dye, then the equilibration time (time between injection and confocal recording) must be extended to allow for the lower mobility inferred by its higher molecular weight (as a rough guide, we find that 2 h is usually sufficient for equilibration of dextran-conjugated Fluo-4, and compartmentalization does not occur until approx 5 h after injection).
 7. As a rough guide, the cytosolic volume of the oocyte is usually estimated as approx 1 μL; therefore, to obtain final intracellular concentrations of 48 μM dye and 8 μM caged IP₃ you would inject 32 nL of a solution comprised of 1.5 mM dye and 0.25 mM caged IP₃. To minimize the possibility of accidentally “pinching” the nucleus, try to inject as close to the equator as possible.
 8. When performing successive “experimental” injections (e.g., via an injector mounted on the confocal microscope) to obtain concentration–response relationships, we would recommend removing the pipet between successive injections to prevent any possible excess leakage of the experimental solution into the oocyte. When injecting large volumes (>50 nL) of solution, we usually perform multiple small-volume injections to try to minimize trauma to the oocyte.
 9. The filter cube introducing UV photolysis light into the microscope light path should be positioned close to the objective lens. The dichroic mirror reflects UV light, but transmits visible light, so that both the laser excitation and emitted fluorescence light pass through without attenuation to the confocal scanner. Depending on the microscope design, engineering changes may be required to add an extra port for UV photolysis to an existing confocal microscope.
 10. *The Axon Guide* (21) is a useful starting point for newcomers to the field of electrophysiology and includes a chapter entirely devoted to electrophysiological recordings from *Xenopus* oocytes.

Acknowledgments

We thank Diane Lipscombe, who provided the cDNA for N-type Ca²⁺ channels. This work was supported by grant GM80471 from the National Institutes of Health.

References

1. Parys, J. B., Sernett, S. W., DeLisle, S., Snyder, P. M., Welsh, M. J., and Campbell, K. P. (1992) Isolation, characterization, and localization of the inositol 1,4,5-trisphosphate receptor protein in *Xenopus laevis* oocytes. *J. Biol. Chem.* **267**, 18,776–18,782.
2. Lechleiter, J. D. and Clapham, D. E. (1992) Spiral waves and intracellular calcium signaling. *J. Physiol. Paris.* **86**, 123–128.
3. Parker, I., Choi, J., and Yao, Y. (1996) Elementary events of InsP₃-induced Ca²⁺ liberation in *Xenopus* oocytes: hot spots, puffs and blips. *Cell Calcium* **20**, 105–121.
4. Sumikawa, K., Parker, I., and Miledi, R. (1989) Expression of neurotransmitter receptors and voltage-activated channels from brain mRNA in *Xenopus* oocytes. *Methods Neurosci.* **1**, 30–44.
5. Dascal, N. (1987) The use of *Xenopus* oocytes for the study of ion channels. *CRC Crit. Rev. Biochem.* **22**, 317–387.

6. Dumont, J. N. (1972) Oogenesis in *Xenopus laevis*. Stages of oocyte development in laboratory maintained animals. *J. Morphol.* **136**, 153–164.
7. Tsein, R. Y. (1980) New calcium indicators and buffers with high selectivity against magnesium and photons: design, synthesis and properties of prototype structures. *Biochemistry* **19**, 2396–2404.
8. Tsein, R. Y. (1992) Intracellular signal transduction in four dimensions: from molecular design to physiology. *Am. J. Physiol.* **263**, C723–C728.
9. Thomas, D., Tovey, S. C., Collins, T. J., Bootman, M. D., Berridge, M. J., and Lipp, P. (2000) A comparison of the fluorescent Ca²⁺ indicator properties and their use in measuring elementary and global Ca²⁺ signals. *Cell Calcium* **28**, 213–223.
10. John, L. M., Mosquera-Caro, M., Camacho, P., and Lechleiter, J. D. (2001) Control of IP₃-mediated Ca²⁺ puffs in *Xenopus laevis* oocytes by the Ca²⁺-binding protein parvalbumin. *J. Physiol.* **535.1**, 3–16.
11. Pawley, J. B. (ed.) (1995) *Handbook of Biological Confocal Microscopy*, Plenum Press, New York.
12. Callamaras, N. and Parker, I. (1999) Construction of a confocal microscope for real-time x-y and x-z imaging. *Cell Calcium* **26**, 271–279.
13. Callamaras, N. and Parker, I. (1999) Construction of a line-scan confocal microscope for physiological recording. *Methods Enzymol.* **307**, 152–170.
14. Sanderson, M. and Parker, I. (2003) Video-rate confocal microscopy. *Methods Enzymol.* **360**, 447–479.
15. Parker, I., Callamaras, N., and Wier, W. G. (1997) A high-resolution, confocal laser-scanning microscope and flash photolysis system for physiological studies. *Cell Calcium* **21**, 441–452.
16. Callamaras, N. and Parker, I. (1998) Caged inositol 1,4,5-trisphosphate for studying release of Ca²⁺ from intracellular stores. *Methods Enzymol.* **291**, 380–403.
17. Demuro, A. and Parker, I. (2004) Imaging the activity and localization of single voltage-gated Ca²⁺ channels by total internal reflection fluorescence microscopy. *Biophys. J.* **86**, 3250–3259.
18. Axelrod, D. (2003) Total internal reflection microscopy in cell biology. *Methods Enzymol.* **361**, 1–33.
19. Girard, S. and Clapham, D. (1994) Calcium signaling in oocytes. *Methods Cell Biol.* **40**, 274–284.
20. Marchant, J. S. and Parker, I. (2001) *Xenopus tropicalis* oocytes as an advantageous model system for the study of intracellular Ca²⁺ signaling. *Br. J. Pharmacol.* **132**, 1396–1410.
21. Axon Instruments Inc. (1993) *The Axon Guide for Electrophysiological and Biophysics Laboratory Techniques*, Axon Instruments Inc., Foster City, CA.

Chromosomal DNA Replication in a Soluble Cell-Free System Derived From *Xenopus* Eggs

Antonin V. Tutter and Johannes C. Walter

Summary

Cytoplasmic egg extracts from the frog *Xenopus laevis* represent a powerful cell-free system to study eukaryotic chromosomal DNA replication. In the classical approach, sperm chromatin is added to unfractionated egg cytoplasm, leading to the assembly of transport-competent nuclei that undergo a single, complete round of DNA replication. The need for nuclei in this system has been circumvented. Sperm chromatin or plasmid DNA is first incubated with clarified egg cytoplasm to form chromatin-bound prereplication complexes. Subsequently, a highly concentrated nucleoplasmic extract is added that stimulates initiation from these prereplication complexes, and a single complete round of chromosomal DNA replication ensues. This review describes the preparation of the cytosolic and nucleoplasmic extracts, as well as their use in DNA replication, origin unwinding, and chromatin isolation assays.

Key Words: Cell-free system; DNA replication; geminin; MCM2-7; nucleoplasmic extract; ORC; origin unwinding; prereplication complex; *Xenopus laevis*.

1. Introduction

Cell-free extracts made from the eggs of the frog *Xenopus laevis* represent a powerful system to study the biochemical mechanisms underlying eukaryotic DNA replication. Addition of demembranated sperm chromatin to cytoplasmic extracts of unfertilized eggs leads to the formation of nuclei that undergo a single, complete round of semiconservative DNA replication per cell cycle (1–4). The use of these “nuclear assembly” extracts has led to many fundamental insights into the mechanism and regulation of eukaryotic DNA replication (5).

However, nuclear assembly extracts have several drawbacks. First, any manipulations that interfere with the delicate process of nuclear assembly indirectly affect DNA replication because of defects in nuclear transport, a frequent source of artifacts. Second, although nuclear assembly extracts support DNA replication of purified DNA molecules such as plasmids, the efficiency is very low (1,4). Third, the requirement

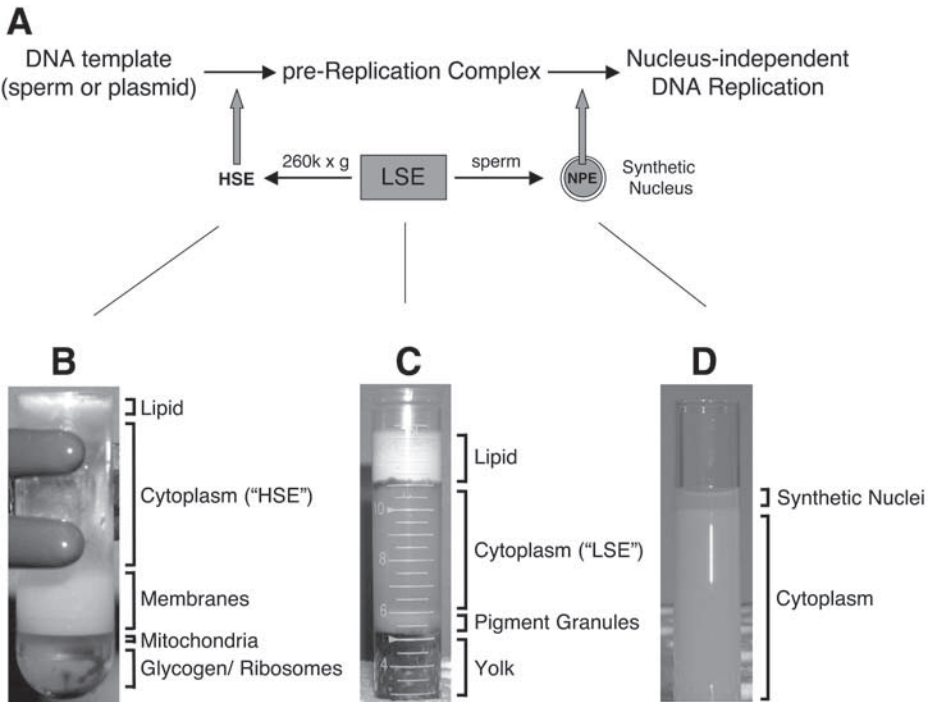


Fig. 1. DNA replication in nucleus-free extracts. (A) Schematic representation of the nucleus-free DNA replication assay. Sperm chromatin or plasmid DNA is incubated in HSE to promote the assembly of prereplication complexes (pre-RCs). Addition of NPE after pre-RC assembly converts the pre-RCs to active replication forks, and replication commences. NPE also contains inhibitors that prevent *de novo* pre-RC assembly and thus restricts replication to a single round. (B–D) Photos of various centrifugation fractions during the production of LSE, HSE, and NPE, respectively.

for a nuclear envelope to initiate DNA replication precludes biochemical fractionation of the factors required for these steps.

In this review, we describe a procedure for DNA replication in *Xenopus* egg extracts that circumvents the need for nuclear assembly (6). In this approach, DNA replication is carried out using two extracts, both of which are derived from low-speed extract (LSE) of egg cytoplasm (Fig. 1A). To make the first extract, LSE is centrifuged at high *g*-force to generate clarified egg cytosol or high-speed extract (HSE). To make the second extract, LSE is supplemented with sperm chromatin to assemble nuclei on a large scale. The nuclei are harvested and centrifuged at high *g*-force to separate the soluble nucleoplasmic extract (NPE) from the chromatin and nuclear envelopes.

To initiate DNA replication, DNA templates are first incubated with HSE to form the prereplication complex (pre-RC). This reaction does not require a specific DNA sequence and involves the sequential loading of the initiation factors ORC, Cdc6, Cdt1,

and MCM2-7. To initiate DNA replication from pre-RCs, two vol of NPE are added. NPE supplies high concentrations of Cdk2/cyclin E (7), Cdc7/Dbf4 (8), MCM10 (9), and possibly other factors. DNA replication initiates, and a single complete round of DNA replication takes place during which MCM2-7 is lost from chromatin (6). Additional rounds of DNA replication in the nucleus-free system are inhibited because NPE blocks the *de novo* loading of MCM2-7 (6) to high concentrations of the inhibitor geminin (ref. 10 and our unpublished results).

The nucleus-free system has several advantages over nuclear assembly extracts. First, the system can be used to resolve whether a particular protein is required for DNA replication directly rather than indirectly because of involvements in nuclear envelope assembly (11). Second, in this system, the nuclear environment can be extensively manipulated. For example, different DNA templates can be replicated simultaneously in the same biochemical environment, a feature that was used to demonstrate the existence of diffusible checkpoint signals (12). Third, the nucleus-free system supports efficient DNA replication of small plasmids, allowing structural analysis of key replication events such as origin unwinding (13). In addition, the effects of DNA sequence on DNA replication can be examined. Finally, the demonstration that DNA replication can take place in a completely soluble environment holds the promise that this process can eventually be reconstituted from purified components. Although the current preparation method for NPE is too cost and labor intensive to allow fractionation, NPE may ultimately be replaced with purified components.

In this review, we describe the protocols that are necessary to carry out DNA replication in the nucleus-free system. We first describe how to isolate *Xenopus* sperm chromatin (Subheading 3.1.). We then describe how to induce egg laying in female frogs (Subheading 3.2.) and the preparation of LSE (Subheading 3.3.), HSE (Subheading 3.4.), and NPE extracts (Subheading 3.5.). Finally, we present protocols for measuring DNA replication (Subheading 3.6.), origin unwinding (Subheading 3.7.), and chromatin loading in the nucleus-free system (Subheading 3.8.); we describe how to use immunodepletion to remove specific proteins from the system to assess their roles in DNA replication (Subheading 3.9.).

2. Materials

1. [α - 32 P]dATP (3000 Ci/mmol).
2. Aphidicolin (cat. no. A0781; Sigma): dissolve in dimethylsulfoxide (DMSO) to 5 mg/mL. Store 5- μ L one-use aliquots at -70°C .
3. Adenosine triphosphate (ATP; cat. no. A-7699 disodium salt; Sigma): dissolve in water and adjust to pH 7.0 with NaOH. Prepare as a 0.2 M stock and store 50- μ L and 1-mL aliquots at -20°C .
4. ATP regeneration mix: combine 10 μ L of 1 M phosphocreatine (PC), 5 μ L of 0.2 M ATP, and 0.5 μ L of 5 mg/mL creatine phosphokinase (CK). Prepare fresh and keep on ice before use.
5. Benzocaine (cat. no. E-1501; Sigma): prepare a 10% solution in ethanol at room temperature on the day of use.
6. Bovine serum albumin (BSA; cat. no A7906-100G; Sigma).
7. Buffer X: 10 mM HEPES, pH 7.4, 80 mM KCl, 15 mM NaCl, 5 mM MgCl_2 , 1 mM ethylenediaminetetraacetic acid (EDTA). Prepare as a 10X stock and filter sterilize.

8. Chloroquine phosphate (cat. no. C-6628; Sigma): dissolve in water to 40 mM final concentration. Prepare fresh on the day of use.
9. CK (35,000 U; cat. no. C-3755; Sigma): dissolve in 50 mM NaCl, 50% glycerol, 10 mM HEPES, pH 7.5. Prepare as a 5 mg/mL stock and store as 1-mL aliquots at -20°C for up to several months.
10. Cycloheximide (cat. no. 239763; Calbiochem): dissolve in water to 10 mg/mL. Prepare fresh at 4°C on the day of use.
11. Cysteine HCL (cat. no. CY115; Spectrum): prepare a 2.2% solution in room temperature water immediately before use and adjust to pH 7.7 with KOH.
12. Cytochalasin B (cat. no. 6762; Sigma): dissolve in DMSO to 5 mg/mL. Store 50- μL aliquots at -20°C .
13. 10X ELB (egg lysis buffer) salts: 25 mM MgCl_2 , 500 mM KCl, 100 mM HEPES. Adjust pH to 7.7 with KOH, filter sterilize, and store at 4°C .
14. ELB: 1 mM dithiothreitol (DTT), 50 $\mu\text{g}/\text{mL}$ cycloheximide, 0.25 M sucrose, 1X ELB salts. Prepare at room temperature on the day of use.
15. Ethanol.
16. Glycogen (cat. no. 901393; Roche).
17. hCG (human chorionic gonadotropin): 10,000 U (cat. no. CG010; Sigma).
18. Hoechst fix solution: 8 $\mu\text{g}/\text{mL}$ Hoechst, 7.4% formaldehyde, 200 mM sucrose, 10 mM HEPES, pH 7.6. Store at room temperature.
19. MMR (Marc's modified Ringer's): 100 mM NaCl, 2 mM KCl, 0.5 mM MgSO_4 , 2.5 mM CaCl_2 , 0.1 mM EDTA, 5 mM HEPES, pH 7.8. Prepare as a 10X stock and store at 4°C .
20. NaOAc: prepare a 3 M stock and adjust pH to 5.8. Autoclave and store at room temperature.
21. Hypodermic needles (21, 27 gage).
22. Nocodazole (cat. no. M1404; Sigma): dissolve in DMSO to 5-mg/mL and 0.5-mg/mL concentrations. Store 50- μL aliquots of each concentration at -20°C .
23. PC (cat. no. P-6502; Sigma; disodium salt, hydrate, synthetic): dissolve in 10 mM sodium phosphate, pH 7.0. Prepare as a 1 M stock and store 50- and 1-mL aliquots at -20°C .
24. Phenol:chloroform (1/1).
25. Pregnant mare serum gonadotropin (PMSG; 5000 U; cat. no. 367222; Calbiochem).
26. Protease inhibitor mix (Aprotinin; cat. no. 981532; Roche; Leupeptin; cat. no. 1034626; Roche): dissolve each part of the mix in water to 10 mg/mL (1000X stock). Freeze 25- μL aliquots in liquid N_2 and store at -70°C .
27. Proteinase K (cat. no. 3115879; Roche): prepare a 20-mg/mL stock in water. Store 50- μL aliquots at -80°C .
28. Replication stop solution: 8 mM EDTA, 0.13% phosphoric acid, 10% Ficoll, 5% sodium dodecyl sulfate (SDS), 0.2% bromophenol blue, 80 mM Tris-HCl, pH 8.0. Store at room temperature.
29. Ribonuclease A (cat. no. R-4875; Sigma): prepare a 2-mg/mL stock in water. Store 50- μL aliquots at -20°C .
30. SDS sample buffer (2X): 50 mM Tris-HCl, pH 6.8, 2% SDS, 100 mM DTT, 10% glycerol, 0.1% bromophenol blue. Store at room temperature for up to 1 wk.
31. Sybergold (cat. no. S-11494; Molecular Probes).
32. Syringes (1, 3, 5 mL).
33. 6X TBE loading dye: 50 mM Tris-HCl, pH 7.9, 50% glycerol, 30 mM EDTA, 0.25% bromophenol blue. Store at room temperature for up to 1 mo.
34. Triton X-100 (cat. no. BP151-100; Fisher).
35. Unwinding stop solution: 1% SDS, 20 mM EDTA. Store at room temperature for up to 1 wk.

36. *Xenopus laevis* females (cat. no. LM00531M; Nasco).

37. *Xenopus laevis* males (cat. no. LM00713M; Nasco).

3. Methods

The methods described next outline: (1) the preparation of demembrated sperm chromatin, (2) the induction of oocyte maturation and ovulation and the harvesting of eggs, (3) the preparation of interphase LSE, (4) the preparation of interphase HSE, (5) the preparation of NPE, (6) DNA replication in NPE, (7) DNA unwinding in NPE, (8) chromatin loading of replication factors in NPE, and (9) the immunodepletion of proteins from HSE or NPE.

3.1. Demembrated Sperm Chromatin

Demembrated sperm chromatin is the conventional template for DNA replication in *Xenopus* egg extracts and is a necessary reagent in the production of nucleoplasmic extract described in **Subheading 3.5**. The preparation of demembrated sperm chromatin is described in **Subheadings 3.1.1. to 3.1.4.** This includes: (1) euthanization of *Xenopus* male frogs, (2) surgical extraction of the testes, (3) extraction and purification of sperm from the testes, and (4) determination of sperm concentration. This procedure is designed to yield approx 10^9 sperm and requires four to six male frogs. All steps in **Subheadings 3.1.1. to 3.1.4.** are performed at room temperature unless otherwise noted.

3.1.1. Euthanization of *Xenopus* Males

Anesthetize one frog at a time by placing into 1 L 0.05% benzocaine (5 mL 10% benzocaine in 1 L water). After about 5 to 7 min, the frog should exhibit no movement and should not be able to right itself when turned over. The frog also should not exhibit a sucking reflex on insertion of a finger into its mouth. Remove the frog from the benzocaine solution and place on several paper towels. Euthanize by pithing.

3.1.2. Extraction of Testes

Open the peritoneal cavity by creating a midline incision through the abdominal wall. Move the organs of the intestinal tract to one side to reveal the testes. They are located in the midbody on either side of the midline. The testes appear grayish-white and almond shaped and are about 5 to 8 mm long. Remove them by cutting them with dissection scissors along the base. Blot excess blood away from the testes and place them in a Petri dish containing about 2 mL of 200 mM sucrose in buffer X. Repeat steps in **Subheadings 3.1.1. and 3.1.2.** for the remaining frogs.

3.1.3. Sperm Extraction and Purification

1. Mince the testes from all frogs in the Petri dish with a fresh single-edge razor blade. Use a repeated chopping motion until the tissue forms a viscous sludge.
2. Transfer the minced testes to a 15-mL screw-cap conical tube using a wide-bore disposable transfer pipet. Rinse the Petri dish with 1 to 2 mL 0.2 M sucrose in buffer X and combine with the testes in the 15-mL tube. Vortex vigorously for 1 min and pellet the larger tissue fragments by mild centrifugation for 10 s at 1000 rpm (170g) in a clinical centrifuge.

3. Transfer the supernatant to a new 15-mL tube. Add 2 to 3 mL 0.2 M sucrose in buffer X to the pellet, vortex vigorously for 1 min, and recentrifuge for 10 s at 1000 rpm (170g). Combine the supernatants and repeat the pellet extraction three or four times or until the supernatant is not cloudy.
4. Centrifuge the combined supernatants in a clinical centrifuge for 50 s at 1.5 rpm (380g) to pellet the larger tissue fragments. Transfer the supernatant to a new 15-mL tube. Add 5 mL of 0.2 M sucrose in buffer X to the pellet, vortex vigorously for 1 min, and recentrifuge for 50 s at 1500 rpm (380g). Combine the supernatants.
5. Transfer the combined supernatants into Falcon 2059 tubes and pellet the sperm by centrifugation for 10 min at 4°C in a Sorvall HB4 or HB6 swinging bucket rotor at 4000 rpm (2600g).
6. Prepare sucrose step gradients in four 2.5-mL Beckman ultracentrifuge tubes (cat. no. 347356). To each tube, add 0.25 mL 2.5 M sucrose in buffer X. Carefully overlay with 1.7 mL 2.3 M sucrose in buffer X.
7. Resuspend the sperm pellets thoroughly by pipeting up and down with 0.8 mL 2 M sucrose in buffer X.
8. Overlay each gradient with 0.2 to 0.25 mL resuspended sperm. Stir the interface between the sperm and the 2.3 M sucrose *extensively* with a flame-sealed Pasteur pipet tip. The interface should no longer be visible.
9. Centrifuge the gradients for 25 min at 33,000 rpm (93,300g) at 2°C in a Beckman Optima MAX-E ultracentrifuge using a TLS55 swinging bucket rotor.
10. The sperm pellets to the bottom of the gradient and is visible as a light gray pellet (*see Note 1*). Red blood cells from the testes sediment on top of the 2.3 M sucrose layer. Aspirate off the top half of the gradient containing the red blood cells. Transfer the remainder of the gradient, including the sperm pellet, to a new Falcon 2059 tube. Completely resuspend the sperm pellet with gentle pipeting with 0.5 mL 0.2 M sucrose in buffer X. Avoid contamination with the upper walls of the tube, which may contain residual red blood cells. Transfer the resuspended sperm to the Falcon 2059 tube that contains the lower half of the gradient.
11. Dilute the sperm to 12 mL with 0.2 M sucrose in buffer X and mix well. Pellet the sperm by centrifugation for 10 min at 5000 rpm (3000g) in the HB4 or HB6 swinging bucket rotor at 4°C.
12. Aspirate the supernatant and resuspend the sperm pellet in 0.8 mL 0.2 M sucrose in buffer X supplemented with 0.4% Triton X-100, 1X protease inhibitor mix, and 1 mM DTT. Incubate on a rotating wheel for 30 min at 4°C.
13. Prepare four sucrose cushions by placing 0.5 mL 0.5 M sucrose in buffer X supplemented with 3% BSA, 1 mM DTT, and 1X protease inhibitor mix in 1.5-mL microcentrifuge tubes. Overlay each cushion with 25% of the sperm prep. Centrifuge for 10 min at 2100 rpm (750g) in a clinical centrifuge at room temperature.
14. Aspirate the supernatant and resuspend each sperm pellet with 0.2 mL 0.2 M sucrose in buffer X supplemented with 3% BSA, 1X protease inhibitor mix, and 1 mM DTT. Avoid contaminating the pellet with residual Triton X-100 from the walls of the tube. Transfer the sperm to four new microcentrifuge tubes, dilute to 0.7 mL total with the same buffer, and recentrifuge for 5 min at 2100 rpm (750g) in a clinical centrifuge at room temperature. Repeat once.
15. Resuspend and combine the sperm pellets in a total of 2 mL 0.2 M sucrose in buffer X supplemented with 3% BSA, 1X protease inhibitor mix, and 1 mM DTT.

3.1.4. Determination of Sperm Concentration and Storage

1. Dilute 3 μL of the sperm prep from **Subheading 3.1.3.** into 267 μL water and 30 μL Hoechst fix solution (*see Note 2*).
2. Pipet 12 μL into a standard hemocytometer and count the sperm on a fluorescence microscope with a 10 \times nonoil objective lens. Use the DAPI channel to visualize the sperm and simultaneous low-level bright field illumination to visualize the grid lines on the hemocytometer. Count the sperm in 0.1- μL volume (usually 16 squares) and multiply by 10^3 to calculate the number of sperm per microliter.
3. Dilute the sperm preparation to 200,000/ μL with 0.2 M sucrose in buffer X supplemented with 3% BSA, 1X protease inhibitor mix, and 1 mM DTT. Freeze 90- μL aliquots in 1.5-mL microcentrifuge tubes in liquid N_2 . These aliquots will be used in the preparation of NPE, described in **Subheading 3.5.** Save 100 to 200 μL , dilute further to 100,000/ μL , and freeze as 5- μL aliquots (in 0.65-mL or similar tubes) in liquid N_2 . These aliquots will be used in the assays described in **Subheadings 3.6 to 3.8.** Frozen sperm are stable for up to several years.

3.2. Oocyte Maturation, Ovulation, and Collection

Unfertilized eggs from *Xenopus* females are the source of interphase extracts used in the study of DNA replication in vitro. The injection of *Xenopus* females with hormone and the collection of unfertilized eggs is described in **Subheadings 3.2.1 to 3.2.3.** This includes: (1) the priming of *Xenopus* females by injection of PMSG to induce ovulation, (2) the induction of egg laying by injection of hCG, and (3) the collection and dejellying of the eggs for subsequent extract preparation.

3.2.1. Priming *Xenopus* Females With PMSG to Induce Ovulation

Females are primed with 75 U of PMSG at least 2 but not more than 8 d before the secondary injection with hCG, described in **Subheading 3.2.2.** The number of frogs to be injected (6–15) depends on the extract to be prepared (*see Subheading 3.3.*).

1. Prepare a 2500-U/mL stock of PMSG by slowly injecting 2 mL sterile water into a vial of 5000 U of PMSG using a 3-mL syringe and a 21-gage needle. Also, insert a 27-gage needle to relieve pressure. Mix by gentle inversion. This preparation can be stored at 4°C for up to 2 wk.
2. Transfer an appropriate amount of PMSG from the vial to a sterile Falcon 2059 tube using a 1-mL syringe. Dilute 10-fold with sterile water to a final concentration of 250 U/mL.
3. Fill the necessary number of 3-mL syringes with the diluted PMSG and inject each female subcutaneously along the leg with 0.3 mL using a 27-gage needle. You can use the same needle for about five frogs.

3.2.2. Induction of Egg Laying With hCG

1. Prepare a 2000-U/mL stock of hCG by slowly injecting 4.8 mL sterile water into a vial of 10000 U of hCG using a 5-mL syringe and a 21-gage needle. Also, insert a 27-gage needle to relieve pressure. Mix by gentle inversion. This preparation can be stored at 4°C for up to 2 wk.
2. Fill the necessary number of 3-mL syringes with the hCG and inject each female as above with 0.3 mL using a 27-gage needle. Injection is performed 18 to 22 h before the eggs are needed.

3. Each injected frog is placed into a separate bucket containing 100 mM NaCl (it is critical that the water not contain chlorine).

3.2.3. Harvesting and Dejellinging the Eggs

Eggs are harvested 18 to 22 h after injection with HCG. Eggs from each frog are not combined until after they are dejellied and have been inspected under a dissection microscope.

1. Remove the frogs from the buckets and slowly decant all but about 100 mL of water from each bucket. Decant the remainder of the water and the eggs from each bucket into 250-mL beakers.
2. Decant as much of the water as possible from each beaker. Add 3 vol of 2.2% cysteine and mix every 30 s using a glass rod until the eggs are dejellied. Up to eight batches of eggs are dejellied at a time. Dejellinging should be complete within 6 to 8 min. Dejellied eggs form a much more highly compact layer at the bottom of the beaker than eggs with jelly coats. The jelly coats can be seen as clear halos floating above the eggs before they dissolve completely in the cysteine.
3. Decant the cysteine and quickly wash the eggs three times with about 50 mL of 0.5X MMR at room temperature. Decant as much of the MMR as possible between washes.
4. Quickly wash the eggs twice with ELB, decanting as much of the ELB as possible between washes. Before decanting the last wash, remove any debris with a Pasteur pipet. Inspect each batch of eggs under a dissection microscope. Discard batches of eggs if the majority of eggs do not contain a visible germinal vesicle, if the majority of eggs have lysed, or if the pigment appears extensively mottled in appearance (*see Note 3*).
5. Combine the eggs and wash them once more with ELB. Eggs are now ready to be crushed for the production of LSE, described in **Subheading 3.3**.

3.3. Low-Speed Interphase Extract

Described next are the steps involved in preparing an LSE from eggs that have been harvested and washed as described in the **Subheading 3.2.3**. Preparation of LSE is an intermediate step in the preparation of HSE (**Subheading 3.4.**) and NPE (**Subheading 3.5.**). For HSE, we first prepare LSE from the eggs of 6 frogs; for NPE, we prepare LSE from the eggs of 15 frogs.

1. Transfer the washed eggs to Falcon 2059 tubes. Allow the eggs to settle and aspirate the supernatant. Pack the eggs by gentle centrifugation at 1100 rpm (200g) in a clinical centrifuge for 1 min at room temperature. Aspirate as much supernatant as possible.
2. Add 0.5 μ L protease inhibitor mix and 0.5 μ L 5 mg/mL cytochalasin per milliliter of packed eggs on top of the packed eggs. Do not put the eggs on ice.
3. Crush the eggs by centrifugation for 20 min at 11,000 rpm (20,000g) in a Sorvall HB4 or HB6 rotor at 4°C. Precool the centrifuge to 4°C but keep the rotor and eggs at room temperature until the spin is begun to ensure optimal activation of the eggs. For all subsequent steps, keep the extract on ice.
4. Transfer the tubes to ice. For each tube, puncture the side with a 21-gage needle just above the mitochondrial layer, remove the needle, and insert a fresh needle attached to a 5-mL syringe in the same hole (**Fig. 1C**). Withdraw as much of the cytoplasm or LSE as possible until just before the pigment granules and lipid begin to enter the syringe. Typically, for a Falcon 2059 tube with 13 mL of packed eggs, we recover 4 to 5 mL of LSE. Combine the LSE fractions from each tube in a 50-mL tube on ice (*see Note 4*).

5. For each milliliter of LSE, add 5 μL 10 mg/mL cycloheximide, 1 μL 1000X protease inhibitor mix, 1 μL 5 mg/mL cytochalasin, and 1 μL 1 M DTT. Mix thoroughly by gentle inversion. The yield of LSE is typically 1 to 2 mL per injected frog.
6. Immediately follow the protocol for HSE (see **Subheading 3.4.**) or NPE (see **Subheading 3.5.**).

3.4. High-Speed Interphase Extract

This subheading describes how to prepare HSE using freshly prepared LSE (described in **Subheading 3.3.**). All steps are carried out on ice unless otherwise noted.

1. Transfer the freshly prepared LSE (prepared from the eggs of six frogs) from **Subheading 3.3.** into four 2.5-mL thin-walled ultracentrifuge tubes (cat. no. 347356; Beckman) and centrifuge for 90 min at 55,000 rpm [260,000g] in the TLS55 rotor at 2°C. As shown in **Fig. 1B**, the extract separates into a thin layer of lipids, clarified egg cytosol (the HSE), a membrane fraction, mitochondria, and glycogen.
2. Remove the lipid layer by aspiration with a very thin pipet (i.e., a gel-loading pipet tip).
3. Transfer the HSE from the top of the tube to a new ultracentrifuge tube using a cut-off P1000 pipet tip.
4. If the extract is contaminated with membranes or other debris, recentrifuge as in **step 1** for 30 min.
5. Remove the top lipid layer as in **step 2**, if necessary, and harvest the HSE as in **step 3**. Freeze the extract as one-use aliquots (50 μL) by submerging tubes in liquid N_2 . Store the extract at -70°C , at which it can be stable for up to several years.

3.5. Nucleoplasmic Extract

Subheadings 3.5.1. to 3.5.4. describe how to prepare an NPE extract using freshly prepared LSE described in **Subheading 3.3.** This includes (1) preparing the nuclear assembly reactions, (2) monitoring nuclear assembly and growth, (3) harvesting the nuclei, and (4) isolation of the nucleoplasm. All steps are carried out on ice unless otherwise noted.

3.5.1. Preparing the Nuclear Assembly Reactions

1. Note the final volume of the freshly prepared LSE (from the eggs of 15 frogs) from **Subheading 3.3.** and add 0.15 vol of ELB and 1/1500 vol of 5 mg/mL nocodazole. Mix gently yet thoroughly by inversion. Avoid introducing air bubbles.
2. Transfer the extract to new Falcon 2059 tubes and centrifuge for 20 min at 11,000 rpm (20,000g) in a Sorvall HB4 or HB6 rotor at 4°C.
3. Carefully and *completely* remove the residual lipids and brown material forming the top layer by aspiration with a P200 tip attached to a vacuum line. It is normal to lose about 0.5 mL of extract during this step.
4. Gently decant the extract into a 50-mL conical tube, taking care not to decant any of the dark granular material from the pellet. About 1 mL will have to be left behind per tube to avoid decanting any of the pellet material.
5. Per 1 mL of LSE, add 10 μL 0.2 M ATP, 20 μL 1 M PC, and 1 μL 5 mg/mL creatine kinase. Mix gently yet thoroughly by inversion.
6. Transfer the extract to 5-mL Falcon 2063 tubes and allow to warm to room temperature (22–23°C, about 5 min). Add at least 4 mL but not more than 4.7 mL to each tube.
7. To each tube, add 90 μL 200,000/ μL demembrated sperm (**Subheading 3.1.**). To thoroughly resuspend the sperm in the extract, first add 1 mL of extract from the 2063 tube to

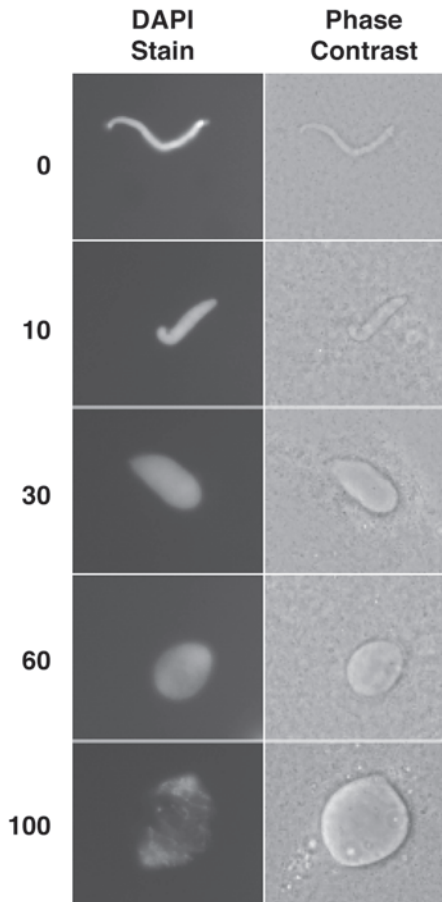


Fig. 2. Nuclear assembly in LSE. 1- μ L aliquots of a nuclear assembly reaction are taken at the indicated time-points (in minutes), fixed with Hoechst dye, and visualized at 40 \times magnification on a fluorescence microscope. As the nucleus matures, the DNA staining pattern changes from diffuse to punctate. The mature nucleus shown at the 100-min time-point is 30 μ m in diameter.

the tube with 90 μ L of sperm. Pipet the mixture 15 times with a P1000 pipet tip and transfer the mixture back to the Falcon 2063 tube. Cap the tube and invert 10 times to distribute the sperm evenly. Repeat for each tube of extract.

3.5.2. Monitoring Nuclear Assembly and Growth

1. Incubate the nuclear assembly reactions at room temperature (22–23°C), gently inverting the tubes approximately once every 10 min.
2. At 20-min intervals, monitor nuclear assembly by mixing 1 μ L of each assembly reaction with 1 μ L Hoechst fix solution on a microscope slide. Cover each sample with a cover slip and examine the nuclei using a 40 \times oil immersion objective in the DAPI channel (**Fig. 2**).

3. Allow nuclei to grow to an average diameter of 25 to 30 μm , which should take about 90 min.

3.5.3. Harvesting the Nuclei

1. Transfer the nuclear assembly reactions from the Falcon 2063 tubes to 13×100 mm disposable glass tubes (cat. no. 60825-924; VWR) on ice, combining the contents of two nuclear assembly reactions into each glass tube. Place the glass tubes inside Falcon 2059 tubes containing 3 mL cold water to create a jacket that prevents the glass from cracking. Adjust the level of water in each 2059 tube so that the meniscus is at the same height as the meniscus of the nuclear assembly reactions. Harvest the nuclei by centrifugation for 3 min at 11,000 rpm (20,000g) in a Sorvall HB4 or HB6 rotor at 4°C. A gray, viscous layer of nuclei about 2 to 4 mm thick will form at the top of the glass tubes (**Fig. 1D**). Transfer the tubes to ice (*see Note 5*).
2. Remove the entire layer of nuclei to a new 1.5-mL tube on ice, combining the nuclei from all the tubes. The nuclei layer is very viscous and is sometimes difficult to separate from the cytoplasmic layer beneath it. It is most effectively removed by using a P200 Pipetman and a cut-off P200 pipet tip, slowly rotating the tube as the layer is very slowly withdrawn from the perimeter of the tube. When no more nuclei can be harvested this way, continue withdrawing from a smaller radius around the center axis of the tube, working inward. Finally, there may come a point when nuclei remain but are inseparable from the underlying cytoplasm. In this case, transfer the uppermost approx 500 μL of the nuclear assembly reaction (which may appear as a viscous, darker brown fraction) to a 0.5-mL microcentrifuge tube and centrifuge at top speed for 2 min. Frequently, this results in a clear layer of nuclei that is easily harvested. Although the underlying cytoplasm is not inhibitory for DNA replication, contamination of the nuclei with this fraction should be minimized because it will dilute the nucleoplasm recovered from the nuclei.

3.5.4. Isolation of the Nucleoplasm

1. Transfer the pooled nuclei to 5×20 mm tubes (cat. no. 342630; Beckman) using a cut-off P200 pipet tip. Centrifuge the nuclei in a Beckman Optima MAX-E ultracentrifuge using a TLS55 swinging bucket rotor (Teflon adaptors [cat. no. 358614; Beckman] are required for the 5×20 mm tubes) for 30 min at 55,000 rpm (260,000g) at 2°C.
2. Remove the tubes to ice. Remove any lipids that may be visible on the top of the tubes by careful aspiration with a narrow-tip gel-loading pipet tip attached to a vacuum line. Care must be taken not to remove a significant volume of the clear nucleoplasm. Using a P200 pipet tip, carefully transfer the nucleoplasm to a new tube, avoiding contamination by the pellet of membranes and chromatin at the bottom of the tube.
3. Freeze the NPE in 20- μL aliquots in liquid N_2 and store at -70°C . Optimal yields of NPE are 30 to 40 μL per milliliter of nuclear assembly reaction. The NPE is stable for several years at -70°C , but it loses approx 50% activity for every freeze-thaw cycle.

3.6. DNA Replication in NPE

Sperm chromatin or plasmid DNA can be used as a template for efficient DNA replication when incubated sequentially in HSE and NPE (**Fig. 1A**). Incubation of the DNA template with HSE leads to pre-RC formation. Subsequent addition of NPE

stimulates replication initiation by providing high levels of several replication factors (see **Subheading 1.**), while also limiting DNA replication to a single round because of the presence of inhibitors that block the formation of pre-RCs (**6**). Complete DNA replication of a 3-kb plasmid usually takes 20 to 30 min, whereas replication of sperm chromatin takes 45 to 60 min.

1. Rapidly thaw 1 aliquot of HSE (50 μ L) and demembrated sperm (5 μ L; 100,000 sperm/ μ L), then transfer immediately to ice.
2. To 30 μ L HSE, add 1 μ L of ATP regeneration mix, 0.2 μ L of 0.5 mg/mL nocodazole, 0.1 to 0.5 μ L [³²P]dATP (3000 Ci/mmol), and either 3 μ L of 100,000 sperm/ μ L or 20 ng/ μ L final concentration of a purified, supercoiled plasmid DNA (3–12 kb). Mix thoroughly by repeated pipeting (10 times).
3. Immediately subdivide the reaction into smaller aliquots (usually 3–5 μ L), which will later be stopped at different time-points, and incubate for 30 min at 22 to 23°C to allow the assembly of pre-RCs (see **Note 2**).
4. After pre-RC assembly has been initiated, thaw an appropriate amount of NPE and supplement it with ATP regeneration mix (1/30 vol) and DTT to 20 mM final concentration. The NPE is incubated at room temperature for 10 min before 2 vol are added to each aliquot of HS/DNA template. Mixing is carried out by flicking the tube or by gentle pipeting (see **Notes 6** and **7**).
5. The reaction is transferred to room temperature (22–23°C) and immediately subdivided into several 2.5- μ L aliquots, each of which is stopped at different time-points. To stop the reactions, add 5 μ L replication stop buffer in 20- to 30-min intervals and vortex briefly to mix.
6. Once all reactions have been stopped, add 1 μ L 20 mg/mL proteinase K to each reaction and vortex briefly to mix. Incubate for 30 min at 37°C.
7. If sperm DNA is the template, vortex each reaction vigorously for 30 s to reduce the viscosity of the DNA. Then, load each reaction on a 0.8% agarose gel in 1X TBE. Electrophoresis is carried out at 25 V/cm, until the bromophenol dye migrates at least 2 cm. If the DNA template is plasmid, vortexing is not necessary, and electrophoresis is performed for 6 cm.
8. Cut the gel immediately above the dye front and discard the bottom part of the gel. Reduce the water content of the gel by placing, on both sides of the gel, a single sheet of Whatman paper and a stack of approx 10 paper towels (in the case of plasmid DNA, place a piece of diethylaminoethyl [DEAE] paper between the gel and the Whatman paper). Place a weight on top of the stack for approx 30 min. Remove the paper towels and Whatman paper (but not the DEAE paper) and place the gel on a fresh piece of Whatman paper, transfer to a preheated gel dryer (with the gel facing up), and cover with Saran Wrap. Dry at 80°C under vacuum.
9. The amount of input DNA replicated is calculated by determining the fraction of radioactive dATP that was consumed (**I**). To this end, spot 1 μ L of the final replication reaction on the filter paper supporting the dried gel and air dry. Expose the gel to a PhosphorImager. Comparing the amount of radioactivity in the replicated DNA with the amount of radioactivity in the replication reaction and assuming 50 μ M endogenous dATP concentrations for HSE and NPE, the picomoles of dATP consumed in the reaction can be calculated. An Excel spreadsheet that calculates replication efficiency is available on request.

3.7. Using DNA Structure to Monitor Replication Initiation Events: Origin Unwinding

An important advantage of the soluble DNA replication system is that it supports extremely efficient DNA replication of small circular plasmids, which have a structure that can be used to monitor different steps of DNA replication. For example, origin unwinding can be detected as a substantial increase in negative supercoiling of plasmid DNA (6). Although the assembly of nucleosomes onto plasmids in HSE causes the plasmids to become underwound and therefore negatively supercoiled on protein extraction (14), origin unwinding on addition of NPE leads to further underwinding of the template.

This underwinding is dramatically enhanced in the presence of aphidicolin, an inhibitor of replicative DNA polymerases. Aphidicolin appears to uncouple the activity of the helicase that unwinds the DNA from the replication fork, leading to extensive negative supercoiling. Because plasmid incubated in HSE is already underwound because of the presence of nucleosomes, the further increase in underwinding that results from initiation of DNA replication can only be detected when the extracted DNA is separated on a gel containing an appropriate concentration of chloroquine, an intercalating agent.

The structure of the plasmid can be used to observe other events in DNA replication. Most notably, when DNA replication is allowed to proceed in the absence of aphidicolin, several low-mobility forms of the plasmid are observed that persist after DNA replication has ceased. These likely represent catenated daughter molecules that are only later resolved, presumably by topoisomerase II. In this subheading, we describe the origin unwinding assay.

1. Follow **steps 1-4** in the DNA replication protocol in **Subheading 3.6.**, except that a 3- to 4-kb circular plasmid should be used as the DNA template at a concentration of 40 ng/ μ L in the HSE. Also, the NPE is supplemented with 50 μ g/mL aphidicolin.
2. Immediately before, and at different times after, NPE addition, aliquots containing 40 ng DNA (1 μ L before NPE addition, 3 μ L after NPE addition) are mixed with 100 μ L unwinding stop solution. A potent preparation of NPE will completely unwind all added plasmid within 10 min.
3. After all time-points are collected, add 2 μ L of 20 mg/mL proteinase K to each time-point and incubate for 30 min at 37°C.
4. Extract each sample with 100 μ L of 1/1 phenol/chloroform. Do not vortex the samples. Mix gently by repeated inversion. Centrifuge at top speed in a microcentrifuge for 1 min.
5. Remove 80 μ L of the aqueous layer to a new 1.5-mL tube. Precipitate the samples by adding 1 μ L 20 mg/mL glycogen, 9 μ L 3 M NaOAc, and 230 μ L 100% EtOH. Mix well by inversion.
6. Chill on ice for 15 min. Spin at top speed in a microcentrifuge for 15 min. Aspirate the supernatant and allow the pellet to air dry for at least 5 min at room temperature.
7. Resuspend the pellet in 20 μ L 1X TBE loading dye supplemented with 100 ng/mL ribonuclease A and incubate for at least 10 min at room temperature.
8. Load one-half of the sample on a freshly poured 0.8% TBE agarose gel supplemented with 1.8 μ M chloroquine. Also, add fresh chloroquine to the TBE running buffer to a final concentration of 1.8 μ M. Load 25 ng of a 1-kb DNA ladder as a marker.

9. Perform electrophoresis at 10 V/cm until the dye has migrated 9 to 10 cm. Stain the gel for 60 min in 100 mL Sybergold nucleic acid stain diluted 1/10,000 in water, keeping protected from light. Photograph using a yellow filter if available.

3.8. Chromatin Loading of Replication Factors in NPE

Most of the key events in DNA replication result in the loading or unloading of DNA replication proteins onto and off of chromatin. To monitor these events, chromatin that has been incubated in HSE or HSE followed by NPE can be isolated by centrifugation through a sucrose cushion and analyzed by immunoblotting. In HSE, ORC loading occurs within seconds, Cdc6 and Cdt1 loading occurs within 3 to 5 min, and maximal MCM2-7 loading requires 15 to 20 min. On NPE addition, Cdc7 and MCM10 load onto chromatin within 1 min, and Cdc45, RPA, and DNA polymerase- α load within 5 to 15 min. Some proteins, such as RPA, are sometimes isolated non-specifically during the chromatin isolation step after NPE addition. It is therefore important to include control reactions that lack sperm chromatin.

1. Repeat **steps 1 to 4** in the DNA replication protocol.
2. Transfer the reaction to room temperature and subdivide into several 6- μ L aliquots.
3. Prepare as many sucrose cushions as the number of aliquots. To do this, add 180 μ L 1X ELB salts containing 0.5 M sucrose to 5 \times 44 mm microfuge tubes (cat. no. 342867; Beckman) and place on ice.
4. At the desired time, supplement an aliquot with 60 μ L cold ELB containing 0.2% Triton X-100 (but lacking cycloheximide or DTT), mix by pipeting up and down three times, and place on ice. Carefully overlay the entire volume (~70 μ L) onto a sucrose cushion. Centrifuge for 25 s at 12,000 rpm (16,000g) in a Prima 18R horizontal centrifuge at 4°C.
5. Aspirate the supernatant with a narrow gel-loading tip, leaving behind about 3 μ L. Do not touch the bottom of the tube with the gel-loading tip.
6. Add 200 μ L cold ELB (lacking cycloheximide or DTT), but do not mix, and centrifuge as in **step 4**.
7. Aspirate the supernatant, this time leaving behind about 1 μ L. Again, do not touch the bottom of the tube with the gel-loading tip.
8. Add 12 μ L 1X SDS sample buffer, vortex gently, boil for 2 min, collect the condensate with brief centrifugation, vortex gently again, and load the entire sample onto SDS-PAGE (polyacrylamide gel electrophoresis).
9. Perform Western blotting using antibodies against factors of interest.

3.9. Immunodepletion From HSE or NPE

An important tool in the study of DNA replication in *Xenopus* egg extracts is the removal of specific proteins using immunodepletion so that their function in DNA replication can be assessed. This subheading describes immunodepletion of HSE and NPE using crude antisera or affinity-purified antibody. For some factors, a single round of immunodepletion is sufficient to remove the protein, whereas in many cases, two to three rounds are needed. The number of rounds required must be determined empirically. Because of the high concentration of replication factors present in NPE, sometimes greater than 99% of a protein must be removed to observe a defect in DNA

replication. Unlike HSE, NPE is very sensitive to dilution, and it can become inactivated over time. Therefore, it is important first to determine the minimum number of depletions required to remove the factor of interest effectively. Typically, NPE is not depleted for longer than a total of 8 h, although some extract preparations are robust enough to survive 16 h of immunodepletion.

The protocol described next is for depletion from 40 μ L HSE or NPE, but all vol in the protocol can be scaled up or down proportionally. The smallest volume of extract that can be practically depleted using this protocol is 20 μ L. It is important to perform a “mock” depletion using preimmune serum or an unrelated affinity-purified antibody. In addition, any defects in DNA replication should be reversible by adding back the depleted protein from a heterologous source.

1. Transfer 8 μ L packed bed volume of Protein A Sepharose Fast Flow beads (cat. no. 17-1279-01; Amersham) to a siliconized 0.65-mL microfuge tube (cat. no. 3206; Costar). This is the volume of beads required for a single round of depletion of 40 μ L of extract. If multiple rounds of immunodepletion are required, multiply 8 μ L of beads by the number of rounds to be performed (*see step 4*). Wash the beads three times with 10 vol of ELB (lacking cycloheximide and DTT). For each wash, centrifuge for 40 s at 5000 rpm (2800g) in a horizontal centrifuge at 4°C to pellet the beads. Aspirate the supernatant with a 27-gage needle attached to a vacuum source.
2. Add 3 vol of crude antiserum to the beads and mix well. If using affinity-purified antibody, add roughly 3 to 6 μ g of antibody in 3 to 5 vol of buffer. Incubate for 30 min at 4°C. Mix on a rotating wheel to prevent the beads from settling.
3. Wash the beads five times as in **step 1**. After the last wash, aspirate as much of the supernatant and void volume as possible by sticking the 27-gage needle directly into the settled Sepharose. The Sepharose will become opaque. If multiple rounds of immunodepletion will be performed, subdivide the antibody-coupled beads into multiple 8- μ L aliquots before the final aspiration. Keep on ice until use.
4. Rapidly thaw HSE or NPE and transfer to ice. Supplement HSE with nocodazole (3.3 μ g/mL final concentration; this obviates the need to add nocodazole during replication). Add 40 μ L extract to the tube containing 8 μ L of aspirated Sepharose and mix well. Incubate at 4°C on a rotating wheel. Care should be taken to ensure that the extract remains at the bottom of the tube, rather than coating the entire inside of the tube, because this will lead to loss and inactivation of extract. A single round of depletion is performed for 1 to 2 h. If the factor of interest is not completely depleted after a single round, transfer the supernatant from the first aliquot of Sepharose to a new aliquot of aspirated Sepharose (**step 1**) using the spin filter technique described in **Note 8** and incubate at 4°C for an additional 2 h. Repeat if necessary.
5. After the final round of incubation, collect the supernatant in a new tube using the spin filter technique.
6. NPE is frequently inactivated because of oxidation during the immunodepletion procedure. Therefore, after immunodepletion, NPE is supplemented with 20 mM DTT.
7. The degree to which the factor was immunodepleted should be assessed for every experiment. This is done by analyzing 1 μ L of immunodepleted extract alongside a dilution series of mock-depleted extract using Western blotting with antibodies against the factor of interest.

4. Notes

1. If the interface of the sperm and the 2.3 M sucrose layer are not thoroughly stirred prior to centrifugation, a significant amount of sperm may not sediment to the bottom. If after the first centrifugation you see a cloudy layer above the red blood cell layer, remix the cloudy layer and centrifuge for another 20 min.
2. Sperm settles quickly. Thoroughly resuspend sperm by pipeting 10 times before and about once every minute when aliquoting to maintain accurate concentration.
3. Healthy eggs have a uniformly light-to-dark-brown animal hemisphere with a germinal vesicle centered in the middle, appearing as a white spot. Batches of eggs in which the majority of eggs lack a germinal vesicle or with animal hemispheres that are extensively variegated or mottled in pigment should be discarded. It is normal for some eggs to lyse, resulting in an empty sphere, mostly white in appearance. Any batch of eggs in which more than 10% of the eggs have lysed should be discarded.
4. The first needle is used to poke a hole in the side of the tube. This needle cannot be used to withdraw the cytoplasm because it becomes clogged with the plug of polypropylene removed from the tube. Therefore, the second needle, attached to a syringe, is inserted in the hole to withdraw the cytoplasm. To minimize the amount of cytoplasm that flows out of the hole on removal of the first needle, seal the top of the tube with parafilm, which will prevent significant loss of cytoplasm by vacuum. Before withdrawing the cytoplasmic fraction from the crushed eggs, be sure to remove the parafilm or the vacuum created by the syringe will perturb the layers. Avoid withdrawing from the mitochondrial layer immediately above the cytoplasmic layer and from the pigment layer below. Keep the beveled side of the needle tip facing up and centered in the tube. Withdraw slowly to minimize the amount of turbulence generated while withdrawing. Continue withdrawing until the cytoplasmic layer is less than 2 mm thick.
5. If the nuclear layer is too thin to harvest, check the following: first, verify that the average nucleus really grew to the desired size. Second, double check the concentration of the sperm preparation used. Third, examine the nuclei that are in the layer using Hoechst dye. Extracts sometimes undergo apoptosis, which can cause complete, irreversible destruction of nuclei within minutes.
6. Although HSE has never been observed to support DNA replication of duplex DNA in our hands, a control in which the NPE is supplemented with 50 $\mu\text{g}/\text{mL}$ aphidicolin, an inhibitor of DNA polymerase- α can be included to verify that any DNA replication observed is caused by replicative DNA polymerases and not to repair synthesis.
7. Depending on the relative concentration of factors between preparations of NPE, NPE may not need to be used at full concentration to achieve efficient DNA replication. For each preparation of NPE, a titration experiment should be performed. Test NPE at 100, 80, and 60% concentrations (diluted with ELB) but always add 2 vol of NPE to 1 vol of HSE. Using NPE at less than 100% concentration effectively increases the usable size of a given preparation. Further, having a preparation of NPE that can support efficient replication even when diluted will facilitate extensive manipulation of the NPE. For example, if you are performing immunodepletion studies with NPE, the procedure (**Subheading 3.9.**) usually causes about 10 to 20% dilution of the NPE. Last, having a dilutable NPE preparation will also facilitate efficient replication if the NPE becomes diluted in experiments by addition of recombinant proteins when performing depletion/add-back studies.
8. To remove extract from a mixture with antibody beads with minimum volume loss, we use a homemade spin filter using a 0.65-mL microfuge tube, a P200 pipet tip, and a Nitex mesh membrane (cat. no. 03-20/14; Sefar). To fabricate the filter, cut the bottom 2 cm off

of a P200 pipet tip with a clean razor blade and discard the bottom portion. Cut the top portion precisely where the protruding ridge along the side ends (this is where the pipet tip is “seated” in the pipet tip box). You now have a top segment of the pipet tip with the ridges and the narrower tapered segment. Cut a 1.5×1.5 cm square of Nitex mesh. Direct the mesh square into the upper segment through the top by using the narrow end of the lower segment. The lower segment will fit snugly into the upper segment and, because of its tapered shape, will fit more tightly the farther in it is pushed. The snug fit between the two segments holds the mesh in place. The whole filter “assembly” can hold up to 100 μ L above the mesh membrane and fits inside a 0.65-mL microfuge tube. To recover extract from the Sepharose, pipet the mixture into the filter assembly and centrifuge for 40 s at 5000 rpm (2800g) in a Prima 18R horizontal centrifuge at 4°C. When another round of depletion follows, place the filter inside a new 0.65-mL tube containing a fresh aliquot of aspirated Sepharose. After the final round of depletion, place the filter assembly in a fresh empty tube. Using this approach, approx 5% of the starting volume of extract will be lost for every round of immunodepletion.

References

1. Blow, J. J. and Laskey, R. A. (1986) Initiation of DNA replication in nuclei and purified DNA by a cell-free extract of *Xenopus* eggs. *Cell* **47**, 577–587.
2. Lohka, M. J. and Masui, Y. (1983) Formation in vitro of sperm pronuclei and mitotic chromosomes induced by amphibian ooplasmic components. *Science* **220**, 719–721.
3. Munshi, R. and Leno, G. H. (1998) Replication of nuclei from cycling and quiescent mammalian cells in 6-DMAP-treated *Xenopus* egg extract. *Exp. Cell Res.* **240**, 321–332.
4. Newport, J. (1987) Nuclear reconstitution in vitro: stages of assembly around protein-free DNA. *Cell* **48**, 205–217.
5. Arias, E. E. and Walter, J. C. (2004) Initiation of DNA replication in *Xenopus* egg extracts. *Front. Biosci.* **9**, 3025–3049.
6. Walter, J., Sun, L., and Newport, J. (1998) Regulated chromosomal DNA replication in the absence of a nucleus. *Mol. Cell* **1**, 519–529.
7. Prokhorova, T. A., Mowrer, K., Gilbert, C. H., and Walter, J. C. (2003) DNA replication of mitotic chromatin in *Xenopus* egg extracts. *Proc. Natl. Acad. Sci. USA* **100**, 13,241–13,246.
8. Walter, J. C. (2000) Evidence for sequential action of cdc7 and cdk2 protein kinases during initiation of DNA replication in *Xenopus* egg extracts. *J. Biol. Chem.* **275**, 39,773–39,778.
9. Wohlschlegel, J. A., Dhar, S. K., Prokhorova, T. A., Dutta, A., and Walter, J. C. (2002) *Xenopus* mcm10 binds to origins of DNA replication after mcm2-7 and stimulates origin binding of cdc45. *Mol. Cell* **9**, 233–240.
10. Hodgson, B., Li, A., Tada, S., and Blow, J. J. (2002) Geminin becomes activated as an inhibitor of Cdt1/RLF-B following nuclear import. *Curr. Biol.* **12**, 678–683.
11. Lin, X. H., Walter, J., Scheidtmann, K., Ohst, K., Newport, J. and Walter, G. (1998) Protein phosphatase 2A is required for the initiation of chromosomal DNA replication. *Proc. Natl. Acad. Sci. USA* **95**, 14,693–14,698.
12. Stokes, M. P., Van Hatten, R., Lindsay, H. D., and Michael, W. M. (2002) DNA replication is required for the checkpoint response to damaged DNA in *Xenopus* egg extracts. *J. Cell Biol.* **158**, 863–872.
13. Walter, J. and Newport, J. (2000) Initiation of eukaryotic DNA replication: origin unwinding and sequential chromatin association of Cdc45, RPA, and DNA polymerase α . *Mol. Cell* **5**, 617–627.
14. Almouzni, G. and Wolffe, A. P. (1993) Nuclear assembly, structure, and function: the use of *Xenopus* in vitro systems. *Exp. Cell Res.* **205**, 1–15.

Chromatin Assembly of DNA Templates Microinjected Into *Xenopus* Oocytes

Danièle Roche, Geneviève Almouzni, and Jean-Pierre Quivy

Summary

The packaging of deoxyribonucleic acid (DNA) into chromatin within the eukaryotic nucleus can affect processes such as DNA replication, transcription, recombination, and repair. Therefore, studies aimed at understanding at the molecular level how these processes are operating have to take into account the chromatin context. We present a method to assemble DNA into chromatin by nuclear microinjection into *Xenopus* oocytes. This method allows in vivo chromatin formation in a nuclear environment. We provide the experimental procedures for oocyte preparation, DNA injection, and analysis of the assembled chromatin.

Key Words: Microinjection; oocytes; chromatin assembly; nucleosomes.

1. Introduction

In the nucleus of eukaryotic cells, DNA is packaged into chromatin, a nucleoprotein complex consisting of a basic repeating unit known as the nucleosome. A single nucleosome contains two turns of DNA wrapped around a core histone octamer comprised of the histones H2A, H2B, H3, and H4 (1). Nucleosomes represent the first level of compaction in chromatin, the dynamics of which will influence access to enzymes involved in DNA metabolism (2). In addition to these basic components, linker histones and a variety of nonhistone proteins are incorporated to achieve complete genome organization within a higher-order chromatin structure (3).

Thus, studies aimed at understanding mechanisms such as transcription, replication, repair, or recombination at the molecular level have to incorporate the nucleosomes and chromatin components. Although chromatin can be reconstituted using pure histones (4,5), the nucleosomal templates generated in this way do not necessarily possess some physiological characteristics of native chromatin, such as the spacing of the nucleosomes, the diversity of histone posttranslational modifications, or the presence of nonhistone-associated proteins.

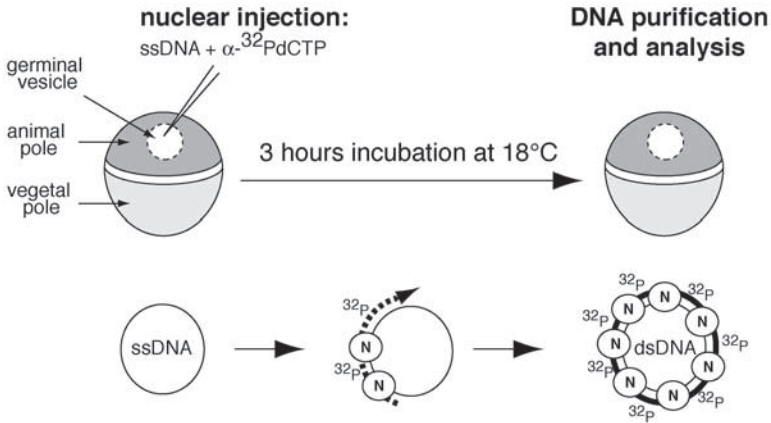


Fig. 1. Simplified scheme of the experimental strategy. *Above*: single-stranded circular DNA (ssDNA) molecules with α - ^{32}P -dCTP are injected into the nucleus (germinal vesicle, dashed circle) of a stage VI oocyte. The animal and vegetal poles are indicated. After 3 h at 18°C, the DNA is extracted and purified. *Below*: following its injection, the circular naked ssDNA undergoes a complementary strand synthesis (dashed arrow). During this synthesis, α - ^{32}P -dCTP is incorporated in the synthesized DNA (^{32}P), and nucleosomes (N in circles) are deposited concomitantly. After 3 h, the reaction is complete and yields a radioactively labeled double-stranded closed circular DNA molecule (dsDNA) on which nucleosomes are assembled (about 1 nucleosome for 185 bp).

Efficient chromatin assembly can be reproduced *in vitro* in crude extracts derived from *Xenopus* oocytes or eggs (6–9), *Drosophila* embryos (10–12), or human cells (13–16). However, these extracts are usually not simultaneously competent for transcription, repair, and replication. The injection of DNA templates in *Xenopus* oocytes as a “living test tube” (17) provides a convenient and highly efficient means to assemble *in vivo* the DNA into chromatin in a nuclear compartment (germinal vesicle) proficient for transcription and DNA synthesis and repair (18–23). Thus, the impact of the chromatin structure on these processes can be studied directly, provided that the DNA template contains adequate features such as sequence control elements, reporter genes, and so on. In this chapter, we describe this powerful approach for chromatin assembly and discuss potential applications.

The experimental strategy is summarized in Fig. 1. Following injection of a circular single-stranded DNA (ssDNA; M13 derivative) into the nucleus (germinal vesicle) of a stage VI oocyte, complementary-strand DNA synthesis occurs, leading to a closed circular double-stranded DNA (dsDNA) (21). Coupled to this process, nucleosomes are efficiently assembled onto the DNA template. If radioactive deoxycytidine-5'-triphosphate (α - ^{32}P) (α - ^{32}P -dCTP) is coinjected with DNA, it will be incorporated during synthesis, enabling the concomitant labeling of the DNA assembled into chromatin.

After 3 h, the efficiency of nucleosome assembly can be assessed by purification of injected DNA. Two assays can be performed: (1) a supercoiling assay and (2) a micro-

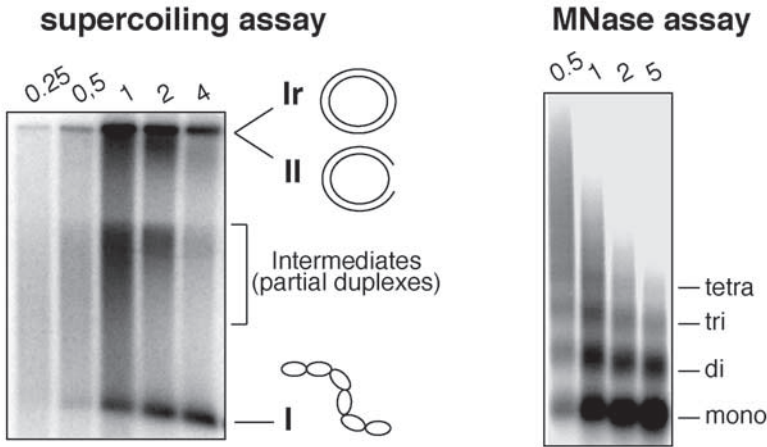


Fig. 2. Analysis of chromatin assembly. *Left*: Autoradiography of a supercoiling gel showing a time-course of chromatin assembly coupled to DNA synthesis. DNA was extracted and purified after 15 min, 30 min, 1 h, 2 h, and 4 h following injection. The positions of the supercoiled form (form I) and the nicked and closed relaxed forms (forms II and Ir, respectively) are indicated on the right. The intermediates reflecting partial duplexes for which complete complementary DNA synthesis is not achieved are indicated. *Right*: Autoradiography of the agarose gel showing the oligonucleosomal DNA fragments produced by micrococcal nuclease digestion at the end of an assembly reaction (3 h) in the oocyte. Time of digestion in minutes is indicated on the top, and the positions of the fragments corresponding to the mono-, di-, tri-, and tetranucleosome are indicated.

coccal nuclease assay (MNase assay), which are presented on [Fig. 2](#). The supercoiling assay makes use of the topological properties of closed circular DNA molecules. During nucleosome assembly, the progressive deposition of nucleosomes in the presence of topoisomerase activity leads to conformational changes easily detectable on closed circular DNA molecules. Indeed topoisomerase activity allows the absorption of the constraints generated during the process ([24](#)). After deproteinization, topoisomers with an increasing number of negative supercoils correlate with the number of nucleosomes assembled. Resolution and detection of topoisomers is achieved using gel electrophoresis. The accumulation of the supercoiled form (form I) provides a semiquantitative estimation concerning the extent of assembly that can be followed as a function of time (*see* [Fig. 2](#), left). The MNase assay for chromatin assembly makes use of MNase, which cleaves the most accessible regions in a chromatinized DNA. Cleavage occurs preferentially in the linker region between adjacent core nucleosomes, generating digestion products with sizes that are multiples of the basic nucleosomal unit. The corresponding DNA fragments, when analyzed by gel electrophoresis, give rise to a characteristic profile or nucleosomal ladder. The regularity of the pattern and the spacing between adjacent bands provides information on the quality of the final product obtained in the assembly reaction (*see* [Fig. 2](#), right).

Importantly, specific pathways are involved in chromatin formation and are coupled and not coupled to DNA synthesis (25–27). The method described here uses a DNA synthesis-coupled chromatin assembly pathway. If dsDNA is injected (instead of ssDNA), chromatin assembly also occurs on the DNA template, but it is not coupled to DNA synthesis and proceeds at a slower rate (21). The methods described here for the ssDNA (injection and analysis) can also be used for the injection of dsDNA. However, the detection of DNA has to be achieved by hybridization procedures, after electrophoresis, as no labeling of the injected DNA occurs in the oocyte, which is not competent to initiate replication on a double-stranded template (no incorporation of α -32P-dCTP).

Perturbations or alterations of specific pathways involved in the regulation of the DNA metabolism can easily be obtained in the oocytes by expression of ectopic proteins, injection of antibodies, drugs, and so on. Following DNA injection, the impact of such perturbations onto DNA metabolism (including transcriptional responses, protein–DNA interactions) can then be monitored in the context of chromatin. The combination of dedicated DNA sequences, functional assays, DNA–protein interactions assays with the approach described herein could thus be further adapted to study specific mechanisms at the level of chromatin.

2. Materials

2.1. Oocytes and Injection of SSDNA

1. Female *Xenopus*.
2. Surgical kit containing scissors, scalpel, and forceps.
3. OR2 medium: 5 mM HEPES, pH 7.8, 87 mM NaCl, 2.5 mM KCl, 1 mM MgCl₂, 1 mM Na₂HPO₄-2 H₂O, 0.05% polyvinyl pyrrolidone.
4. 1X Modified Barth's Saline (MBSH) buffer: 10 mM HEPES, pH 7.6, 88 mM NaCl, 1 mM KCl, 2.4 mM NaHCO₃, 0.82 mM MgSO₄, 0.41 mM CaCl₂, 0.33 mM Ca(NO₃)₂.
5. Collagenase (Sigma, St Louis, MO) solution in OR2 at 2 mg/mL stored at –20°C.
6. 10 mg/mL Gentamicin (Sigma, St Louis, MO), stored at 4°C.
7. M13 derivative ssDNA (see Note 1).
8. Injection buffer: 15 mM HEPES, pH 7.6, 88 mM NaCl.
9. α -32P-dCTP, 3000 Ci/mmol, 10 μ Ci/ μ L (MP Biochemicals, Asse-Relegen, Belgium).

2.2. Analysis by Supercoiling Assay

1. Oocyte homogenization solution: 10 mM HEPES, pH 7.5, 5% sucrose, 70 mM KCl, 1 mM dithiothreitol (DTT).
2. 2X Stop mix: 60 mM EDTA (ethylenediaminetetraacetic acid), 1% SDS (sodium dodecyl sulfate).
3. 20 mg/mL Proteinase K (Roche, Mannheim, Germany) stored in water at –20°C.
4. Ribonuclease A (Roche, Mannheim, Germany): 10 mg/mL in 0.01M sodium acetate, pH 5.2, heated 15 min at 100°C and completed with 0.1 vol of Tris-HCl, pH 7.4. Aliquot and store at –20°C.
5. Phenol/chloroform/isoamyl alcohol (25/24/1; Invitrogen, Paisley, UK).
6. Glycogen (Roche, Mannheim, Germany): 20 mg/mL.
7. 5M Ammonium acetate.
8. 100% Ethanol stored at –20°C.

9. 70% Ethanol stored at -20°C
10. TE, pH 8.0: 10 mM Tris-HCl, pH 8.0, 1 mM EDTA, pH 8.0.
11. 5X Loading buffer: 0.5% bromophenol blue, 5 mM EDTA, 50% glycerol.
12. Agarose (Ultrapure, Sigma, Saint Louis, MO).
13. 50X TAE stock solution buffer: 242 g Tris-base, 57.1 mL glacial acetic acid, and 100 mL 0.5 M EDTA, pH 8.0 dissolved in deionized water to a final volume of 1 L.
14. Intensifying screens for X-ray films.
15. Amersham Hyperfilm MP (Amersham Biosciences, Buckinghamshire, UK).

2.3. Analysis by Micrococcal Digestion Assay

1. Oocyte homogenization solution (*see Subheading 2.2., item 1*).
2. MNase (Roche, Mannheim, Germany) solution in water at 15 U/ μL .
3. 100 mM CaCl_2 solution.
4. **Items 2 to 6** as in **Subheading 2.2.**
5. 3 M Sodium acetate, pH 5.2.
6. 100% Ethanol stored at -20°C .
7. TE, pH 8.0: 10 mM Tris-HCl, pH 8.0, 1 mM EDTA, pH 8.0.
8. 5X MNase loading buffer: 0.3% Orange G (Sigma, Saint Louis, MO), 5 mM EDTA, 50% glycerol (*see Note 2*).
9. Agarose (Ultrapure, Sigma, Saint Louis, MO, USA).
10. 10X TBE stock solution buffer: 108 g Tris-base, 55 g boric acid, and 40 mL 0.5M EDTA, pH 8.0, dissolved in deionized water to a final volume of 1 L.
11. *See Subheading 2.2., items 14,15.*

3. Methods

3.1. Oocytes and Injection of Single-Stranded DNA

1. One adult female frog is anesthetized on ice (at least 30 min) and sacrificed.
2. Immediately perform a ventral cut 1 to 2 cm long with a razor blade, pull out the ovaries with pincets, and transfer into a glass Petri dish containing OR2 medium. Quickly rinse several times to eliminate blood. Using two pairs of forceps, tear apart and open up the ovary lobes and cut with scissors until pieces of ovaries homogeneous in size (about 1 cm^2) are obtained. Rinse again with OR2 to eliminate blood and lysed or broken oocytes. Transfer about 7.5 to 10 mL into a new 50-mL tube and add the same volume of collagenase solution. Incubate at room temperature to dissociate follicular cells for about 2 h on a rolling shaker. Check regularly to avoid overtreatment (*see Note 3*). Appearance of individual oocytes dissociated from follicles or follicular membranes indicates that the collagenase treatment is achieved. Rinse thoroughly with OR2 and eliminate by sedimentation the youngest stages (**ref. 28**; small and nonpigmented, which sediment the slowest) and all debris. Wash again two times with 1X MBSH (*see Note 4*). Oocytes can be stored for several days at 18°C in 1X MBSH complemented with 10 $\mu\text{g}/\text{mL}$ gentamicin (*see Note 5*).
3. Sort manually under a dissecting microscope healthy stage VI oocytes according to **ref. 28** (*see Note 6*).
4. Make 10 μL of a solution of the ssDNA to be injected at 100 ng/ μL in the injection buffer, including 3 μL of $\alpha\text{-}^{32}\text{P}\text{-dCTP}$ (*see Note 7*).
5. This solution is aspirated in a capillary containing mineral oil mounted on the injection system under the microscope (*see Note 8*).

6. Inject this radioactive DNA solution into the nucleus located one-third deep in the animal part of the oocyte (*see Note 9*); a volume of 20 to 30 nL corresponding to 2 to 3 ng of DNA is injected.
7. Following injection, transfer the oocytes at 18°C in fresh 1X MBSH medium and incubate for chosen times (usually 3 h for a complete assembly).

3.2. Analysis by Supercoiling Assay

1. Collect 10 healthy oocytes into an Eppendorf tube (*see Notes 6 and 10*).
2. Remove as much as possible the MBSH buffer and place on dry ice or liquid nitrogen to stop the reaction. This allows the oocytes to be kept for a short time before they are all processed for analysis when several conditions of injections, time-points, or treatments are performed.
3. Homogenize the oocytes by crushing them in 50 μ L of oocyte homogenization buffer with a Pipetman tip and then by pipeting up and down several times.
4. Add the same volume (50 μ L) of 2X stop mix, 3 μ L ribonuclease A; incubate 30 min at 37°C.
5. Add 3 μ L proteinase K and incubate for at least 2 h at 37°C.
6. Add 100 μ L phenol/chloroform/isoamyl alcohol and vortex 10 s minimum each tube. Centrifuge 10 min at 15,000g at room temperature, collect 100 μ L of a clear aqueous upper phase, and transfer into a clean tube. Be careful not to take material from the interphase. A second phenol/chloroform/isoamyl alcohol extraction can be performed if the upper phase is not clear.
7. Add 2 μ L of glycogen and precipitate DNA with 1 vol of ammonium acetate (100 μ L) and 2 vol (400 μ L) of cold 100% ethanol.
8. Centrifuge 30 to 45 min at 15,000g at 4°C to collect the DNA pellet, wash with 800 μ L of cold 70% ethanol, centrifuge 5 to 10 min at 15,000g at 4°C, and carefully remove the supernatant, dry the pellet in the Speed Vac, and resuspend in 10 μ L TE.
9. Add 2.5 μ L of 5X loading buffer, load on a 1% agarose gel in 1X TAE *without* ethidium bromide, and run at 1.5 V/cm until the dye migrates to the bottom of the gel (*see Notes 11–13*).
10. Expose the dried gel against an X-ray film for autoradiography to visualize the migration pattern of the radiolabeled DNA. Use two intensifying screens and leave at –80°C for at least 4 h. Exposition time may vary according to the efficiency of DNA synthesis and the number of oocytes used. PhosphorImaging system can also be used (Storm, Amersham Pharmacia Biotech, Uppsala, Sweden)

3.3. Analysis by Micrococcal Digestion Assay

1. Homogenize 20 to 30 healthy injected oocytes in 200 μ L of homogenization buffer (*see Subheading 3.2., item 2, and Notes 6 and 10*).
2. Adjust to 3 mM CaCl₂ with the 100 mM solution before addition of 60 units of MNase and digest at room temperature.
3. Remove 50- μ L aliquots at 0.5, 1, 2, and 5 min and immediately transfer to a tube containing 50 μ L of stop mix to stop the digestion.
4. Add 3 μ L of RNase A and incubate at 37°C for 30 min.
5. Proceed to DNA extraction as in **Subheading 3.2., steps 4 to 6**.
6. Precipitate the DNA by adding 2 μ L glycogen, 10 μ L 3M sodium acetate, 330 μ L 100% ethanol. Vortex and store at –80°C for 30 min.

7. Centrifuge 30 min at 15,000g at 4°C, wash the pellet with 800 μ L 70% ethanol. centrifuge 10 min at 15,000g at 4°C before removing the ethanol. Repeat twice. Dry the DNA pellet in the Speed Vac.
8. Resuspend in 10 μ L TE and add 2.5 μ L of 5X MNase loading buffer.
9. Load on a 1.3% agarose gel in 0.5X TBE buffer and run at 5 V/cm until the Orange G dye migrates through two-thirds of the gel (*see* **Notes 2** and **12**).
10. *See* **Subheading 3.2, step 10**.

4. Notes

1. The single-stranded M13 DNA should be of high quality and not contaminated by dsDNA. It is obtained after phage purification and further purification through a CsCl gradient (**29**).
2. If an ethidium bromide picture is required, it is important not to use a loading buffer containing bromophenol blue as this dye will migrate at about the same position as the mononucleosomal DNA and will interfere with the analysis of the migration pattern. Thus, as an alternative to bromophenol blue, Orange G is used.
3. The collagenase treatment is a critical step for successful injections. Overtreatment will result in very fragile oocytes that will not support storage and the injection injury. Undertreatment will result in oocytes difficult to pierce. Therefore, frequent monitoring of the oocytes during collagenase treatment is strongly advised. Different treatment times can be performed and the corresponding defolliculated oocytes stored. The best time treatment can be quickly determined at the time of injection.
4. The MBSH contains Ca^{2+} ions that inhibit the action of collagenase, therefore preventing overtreatment on storage.
5. Do not keep oocytes too concentrated. They should not be in contact with each other.
6. The quality of the oocyte is crucial. Avoid taking any oocyte that does not look healthy and that is not stage VI (**28**). Stage VI oocytes should have a white band separating the upper brown animal pole from the whitish lower vegetal pole (*see* scheme of the oocyte in **Fig. 1**). They should not be grayish or have white spots on the animal pole.
7. Follow safety rules concerning the handling of radioactivity. Plexiglas screens and protection devices should be implemented in the microinjection system. Check after use that the injector is free of contamination.
8. We use a nanoject injector (Drummond) mounted on a Leica micromanipulator, which we found most convenient for these types of injections. The volume of injection can be adjusted within a range of 4.6 to 73.6 nL. Capillaries used are first beveled (with the beveler model EG-40, Narishige) to ensure the best penetration into the oocyte as well as reproducible injection without clotting the tip of the capillary.
9. An increase in size of the oocyte is visualized by quick swelling, which is the sign of a successful nuclear injection. When removing the needle, only limited leakage of the cytoplasmic material should occur.
10. In these assays, the DNA is radioactive and may be subjected to radiolysis. Analysis should thus be performed rapidly to avoid degradation of DNA, which could lead to loss of detectable supercoiled forms or to smeary MNase digestion patterns.
11. Because intercalation of ethidium bromide modifies the topology of closed double-stranded molecules, its presence must be avoided during the electrophoresis to ensure good separation of the supercoiled form (form I) and the nicked and closed relaxed forms (forms II and Ir).
12. We use gels that are 20 cm long (model SGE, VWR International) to obtain good resolution of topoisomers and oligonucleosomal DNA fragments. If an ethidium bromide pic-

ture is required, soak the gel in a 1 $\mu\text{g}/\text{mL}$ ethidium bromide solution and rinse 30 min in water at room temperature. Visualize the DNA by placing the gel on an ultraviolet transilluminator. Note that, to be visible, at least 100 ng of DNA should have been loaded on the gel.

13. The absolute number of superhelical turns, corresponding to each assembled nucleosome, can be determined by visualization of the plasmid topoisomers on a two-dimensional (2D) agarose gel (30). Furthermore, closed circular relaxed (Ir) and nicked (II) forms of the plasmid can only be separated in a 2D gel. In some cases, it can be informative to determine the amount of nicked plasmids because these may correspond to plasmids assembled into chromatin in which there are nicks. The 2D gels are set up as classical 1D gels, but after migration in the first dimension, the gel is rotated by 90° , and chloroquine is added at 10 $\mu\text{g}/\text{mL}$ to the electrophoresis buffer. The gel is then left to equilibrate for 45 min in the dark. The second dimension electrophoresis is then run in the dark under the same conditions as for run. Under those conditions, the closed circular relaxed form (Ir), indicating that no nucleosomes are assembled, migrates faster than the nicked form (II). During the second run, it is important to recirculate the running buffer to maintain an even distribution of chloroquine.

Acknowledgments

This work was supported by la Ligue Nationale contre le Cancer (Equipe labellisée la Ligue); Euratom (FIGH-CT-1999-00010 and FIGH-CT-2002-00207); the Commissariat à l'Énergie Atomique (LRC 26); European Contracts RTN (HPRN-CT-2000-00078 and HPRN-CT-2002-00238); and Collaborative Programme between the Curie Institute and the Commissariat à l'Énergie Atomique (PIC Paramètres Epigénétiques).

References

1. Luger, K., Mäder, A. W., Richmond, R. K., Sargent, D. F., and Richmond, T. J. (1997) Crystal structure of the nucleosome core particle at 2.8 Ångstrom resolution. *Nature* **389**, 251–260.
2. Wolffe, A. P. (1997) *Chromatin: Structure and Function*, Academic Press, New York.
3. Vaquero, A., Loyola, A., and Reinberg, D. (2003) The constantly changing face of chromatin. Available at: <http://sageke.sciencemag.org/cgi/content/full/sageke;2003/14/re4>.
4. Carruthers, L. M., Tse, C., Walker, K. P., and Hansen, J. C. (1999) Assembly of defined nucleosomal arrays from pure components. *Methods Enzymol.* **304**, 19–35.
5. Clapier, C. R., Langst, G., Corona, D. F., Becker, P. B., and Nightingale, K. P. (2001) Critical role for the histone H4 N terminus in nucleosome remodeling by ISWI. *Mol. Cell. Biol.* **21**, 875–883.
6. Laskey, R. A., Mills, A. D., and Morris, N. R. (1977) Assembly of SV40 chromatin in a cell free system from *Xenopus* eggs. *Cell* **10**, 237–243.
7. Glikin, G. C., Ruberti, I., and Worcel, A. (1984) Chromatin assembly in *Xenopus* oocytes: in vitro studies. *Cell* **37**, 33–41.
8. Almouzni, G. and Méchali, M. (1988) Assembly of spaced chromatin involvement of ATP and DNA topoisomerase activity. *EMBO J.* **7**, 4355–4365.
9. Almouzni, G. and Méchali, M. (1988) Assembly of spaced chromatin promoted by DNA synthesis in extracts from *Xenopus* eggs. *EMBO J.* **7**, 665–672.
10. Nelson, T., Hsieh, T.-S., and Brutlag, D. (1979) Extracts of *Drosophila* embryos mediate chromatin assembly in vitro. *Proc. Natl. Acad. Sci. USA* **76**, 5510–5514.

11. Becker, P. B. and Wu, C. (1992) Cell-free system for assembly of transcriptionally repressed chromatin from *Drosophila* embryos. *Mol. Cell. Biol.* **12**, 2241–2249.
12. Kamakaka, R. T., Bulger, M., and Kadonaga, J. T. (1993) Potentiation of RNA polymerase II transcription by Gal4-VP16 during but not after DNA replication and chromatin assembly. *Genes Dev.* **7**, 1779–1795.
13. Stillman, B. (1986) Chromatin assembly during SV40 DNA replication in vitro. *Cell* **45**, 555–565.
14. Banerjee, S. and Cantor, C. R. (1990) Nucleosome assembly of simian virus 40 DNA in a mammalian cell extract. *Mol. Cell. Biol.* **10**, 2863–2873.
15. Gruss, C., Gutierrez, C., Burhnans, W. C., DePamphilis, M. L., Koller, T., and Sogo, J. M. (1990) Nucleosome assembly in mammalian cell extracts before and after DNA replication. *EMBO J.* **9**, 2911–2922.
16. Krude, T. and Knippers, R. (1991) Transfer of nucleosomes from parental to replicated chromatin. *Mol. Cell. Biol.* **11**, 6257–6267.
17. Brown, D. D. and Gurdon, J. B. (1977) High fidelity transcription of 5S DNA injected into *Xenopus* oocytes. *Proc. Natl. Acad. Sci. USA* **74**, 2064–2068.
18. McKnight, S. L. and Kingsbury, R. (1982) Transcriptional control signals of a eucaryotic protein coding gene. *Science* **217**, 316–325.
19. Wyllie, A., H., Laskey, R., A., Finch, J., and Gurdon, J., B. (1978) Selective DNA conservation and chromatin assembly after injection of SV40 into *Xenopus* oocytes. *Dev. Biol.* **64**, 178–188.
20. Ryoji, M. and Worcel, A. (1984) Chromatin assembly in *Xenopus* oocytes: in vivo studies. *Cell* **37**, 21–32.
21. Almouzni, G. and Wolffe, A. P. (1993) Replication-coupled chromatin assembly is required for the repression of basal transcription in vivo. *Genes Dev.* **7**, 2033–2047.
22. Gaillard, P.-H., Martini, E., Kaufman, P. D., Stillman, B., Moustacchi, E., and Almouzni, G. (1996) Chromatin assembly coupled to DNA repair: a new role for chromatin assembly factor I. *Cell* **86**, 887–896.
23. Belikov, S., Gelius B., Almouzni, G., and Wrangé, O. (2000) Hormone activation induces nucleosome positioning in vivo. *EMBO J.* **16**, 1023–1033.
24. Germond, J. E., Rouvière-Yaniv, J., Yaniv, M., and Brutlag, D. (1979) Nicking-closing enzyme assembles nucleosome-like structures in vitro. *Proc. Natl. Acad. Sci. USA* **76**, 3779–3783.
25. Ray-Gallet, D., Quivy J.-P., Scamps, C., Martini, E. M., Lipinski, M., and Almouzni, G. (2002) HIRA is critical for a nucleosome assembly pathway independent of DNA synthesis. *Mol. Cell* **9**, 1091–1100.
26. Ahmad, K. and Henikoff, S. (2002). The histone variant H3.3 marks active chromatin by replication-independent nucleosome assembly. *Mol. Cell* **9**, 1191–200.
27. Tagami, H., Ray-Gallet, D., Almouzni, G., and Nakatani, Y. (2004). Histone H3.1 and H3.3 complexes mediate nucleosome assembly pathways dependent or independent of DNA synthesis. *Cell* **116**, 51–61.
28. Dumont, J. N. (1972) Oogenesis in *Xenopus laevis* (Daudin). *J. Morphol.* **136**, 153–180.
29. Sambrook, J., Fritsch, E. F., and Maniatis, T. (1989). *Molecular Cloning—A Laboratory Manual*, Cold Spring Harbor Laboratory Press, Cold Spring Harbor, NY.
30. Peck, L. J. and Wang, J. C. (1985) Transcriptional block caused by a negative supercoiling induced structural change in an alternating CG sequence. *Cell* **40**, 129–137.

Pre-mRNA Splicing in the Nuclei of *Xenopus* Oocytes

Kyong Hwa Moon, Xinliang Zhao, and Yi-Tao Yu

Summary

Xenopus oocytes have been utilized in a number of laboratories as an experimental system to study a variety of biological processes. Here, we describe its application to functional studies of spliceosomal small nuclear RNAs (snRNAs) in pre-messenger RNA (pre-mRNA) splicing, a process that occurs extremely efficiently in *Xenopus* oocytes. A DNA oligonucleotide complementary to an snRNA of interest is injected into the oocyte cytoplasm. The oligonucleotide subsequently diffuses into the nucleus and hybridizes to the target snRNA, thereby triggering snRNA degradation via endogenous RNase H activity. By the time the endogenous snRNA is depleted, the DNA oligonucleotide itself is degraded by endogenous deoxyribonuclease (DNase) activity. In principle, this procedure enables one to quantitatively deplete any snRNA of choice. Subsequently, a rescuing snRNA that is constructed in vitro may be injected into the snRNA-depleted oocytes to restore the splicing function. After reconstitution, a radiolabeled splicing substrate is injected into the nuclei of the oocytes. These oocyte nuclei are then manually isolated and used to prepare both nuclear RNA for splicing assays and nuclear extract for spliceosome assembly assays. The ability of an injected rescuing snRNA to reconstitute splicing can therefore be tested. Because all types of rescuing snRNAs (e.g., mutant snRNAs, snRNAs with or without modified nucleotides) can be constructed readily, the results obtained from this procedure provide valuable information on the function of a particular snRNA of interest in pre-mRNA splicing.

Key Words: Depletion–reconstitution; microinjection; nuclear isolation; pre-mRNA splicing; spliceosome; U2 snRNA; *Xenopus* oocytes.

1. Introduction

Most eukaryotic protein-coding genes are interrupted by introns (1). Initially copied into pre-mRNAs, the introns must be removed before the mature mRNAs can be produced and transported to the cytoplasm, where they direct the translation of proteins (2). The removal of the introns, a process termed pre-mRNA splicing, occurs in a large multicomponent complex consisting of five small nuclear RNAs (snRNAs), including U1, U2, U4, U5, and U6, and a number of proteins (3,4).

From: *Methods in Molecular Biology*, vol. 322: *Xenopus Protocols: Cell Biology and Signal Transduction*
Edited by: X. J. Liu © Humana Press Inc., Totowa, NJ

For over two decades, several laboratories have developed a few different experimental systems to study pre-mRNA splicing (see, e.g., refs. 5–16). The most widely used are the yeast genetic system (5) and the cell-free in vitro system involving yeast cell extracts (6) or HeLa nuclear extracts (7–10). Several other systems, such as the *Xenopus* oocyte microinjection system (13,14,17), are largely underutilized. For several reasons, we believe that *Xenopus* oocytes provide an excellent experimental system for studying pre-mRNA splicing, and that its usage should be increased. First, pre-mRNA splicing occurs extremely efficiently in stage VI *Xenopus* oocytes (13,14,17), thus enhancing our ability to analyze this process. Second, because the oocytes are kept intact and alive during the entire course of splicing, this system closely recapitulates in vivo circumstances. Third, because *Xenopus* oocytes are large and contain a massive volume of cellular contents (18), including the spliceosomal components (19,20), they also constitute an excellent system for biochemical analysis. Finally, the spliceosomal snRNAs can be readily targeted for degradation by endogenous RNase H activity following microinjection with complementary deoxyribonucleic acid (DNA) oligonucleotides (14,17,21–23). Injecting rescuing snRNA into the depleted oocytes can then restore the function of degraded snRNA. These features offer an excellent opportunity to study, in great detail, the function of snRNAs in pre-mRNA splicing (13,14,17).

In this chapter, we describe how the *Xenopus* oocyte system can be utilized to study specifically the function of U2 snRNA in pre-mRNA splicing. This procedure involves several basic steps, including three injections, nuclear isolation, and splicing assay (Fig. 1). In the first injection, an antisense U2 DNA oligonucleotide is injected into the cytoplasm of *Xenopus* oocytes. The oligonucleotide subsequently diffuses into the nucleus and hybridizes with the endogenous U2 snRNA, thereby triggering the degradation of the U2 snRNA via endogenous RNase H activity. When the endogenous U2 snRNA is depleted, the DNA oligonucleotide is also degraded via endogenous deoxyribonuclease (DNase) activity. In the second injection, a rescuing U2 snRNA (wild-type U2 or modified U2) is injected into the cytoplasm of U2-depleted oocytes. Because the U2 transcript contains a 5' GpppG cap and an Sm-binding site, it is transported to the nucleus (24), where it restores U2 function (if the injected U2 is functional). In the last injection, a radiolabeled pre-mRNA, such as the standard adenovirus pre-mRNA, is injected directly into the nuclei of the reconstituted oocytes to monitor pre-mRNA splicing and the effectiveness of U2 rescue. One hour after nuclear injection, the oocyte nuclei are isolated, total nuclear RNA are extracted, and pre-mRNA splicing is assayed (a denaturing gel analysis). The nuclear extract can also be prepared from the oocyte nuclei for spliceosome assembly assays (a native gel analysis). The entire procedure, along with additional preparatory steps, is described in detail in this chapter.

2. Materials

2.1. Reagents

1. Ampicillin (VWR; store at -20°C).
2. Gentamicin sulfate (Sigma; store at 4°C)
3. Mineral oil (VWR).
4. Urea (VWR).

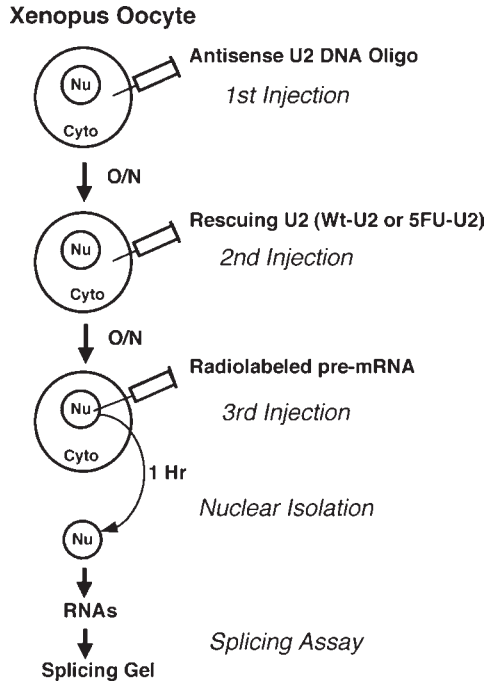


Fig. 1. The *Xenopus* oocyte microinjection system. The depletion–reconstitution procedure consists of three sequential microinjections followed by nuclear isolation and splicing gel analysis. In the first injection, 50.6 nL of an antisense U2 DNA oligonucleotide (3 $\mu\text{g}/\mu\text{L}$) complementary to the branch site recognition region of U2 snRNA are injected into the cytoplasm of *Xenopus* oocytes, which are then incubated at 18°C overnight. During the incubation, the oligonucleotide readily diffuses into the nucleus and base-pairs with the endogenous U2 snRNA. This base-pairing induces the endogenous RNase H activity that degrades the U2 strand of the RNA/DNA hybrid. Soon after the depletion of U2 snRNA, the DNA oligonucleotide is also degraded. In the second injection, 50.6 nL of the newly transcribed wild-type U2 snRNA or 5FU-substituted U2 snRNA (50 $\text{ng}/\mu\text{L}$) are injected into the cytoplasm of the U2-depleted oocytes. The oocytes are then incubated overnight to allow sufficient time for the completion of U2 reconstitution. Because the U2 snRNAs contain a 5' GpppG cap and an Sm-binding site, they are quickly assembled, 5' hypermethylated, and transported into the nucleus (24). In the third injection, 13.8 nL of radiolabeled pre-mRNA (500,000 cpm/ μL) are injected directly into the nuclei of the reconstituted oocytes. After 1 h, the nuclei are isolated, and total nuclear RNA is recovered and analyzed on a denaturing gel.

5. 40% Acrylamide:*bis* (19:1) (VWR).
6. GpppG (guanosine-5'-triphosphate-5'-guanosine), GTP (guanosine-5'-triphosphate), ATP (adenosine-5'-triphosphate), CTP (cytidine-5'-triphosphate), UTP (uridine-5'-triphosphate) (Amersham; store at -20°C).
7. 5-Fluorouridine 5' triphosphate (5FUTP; Sierra Bioresearch; store at -20°C).
8. [α - ^{32}P]GTP (guanosine-5'-[α - ^{32}P]-triphosphate) (NEN; store at -20°C).
9. T7 RNA polymerase (USB; store at -20°C).

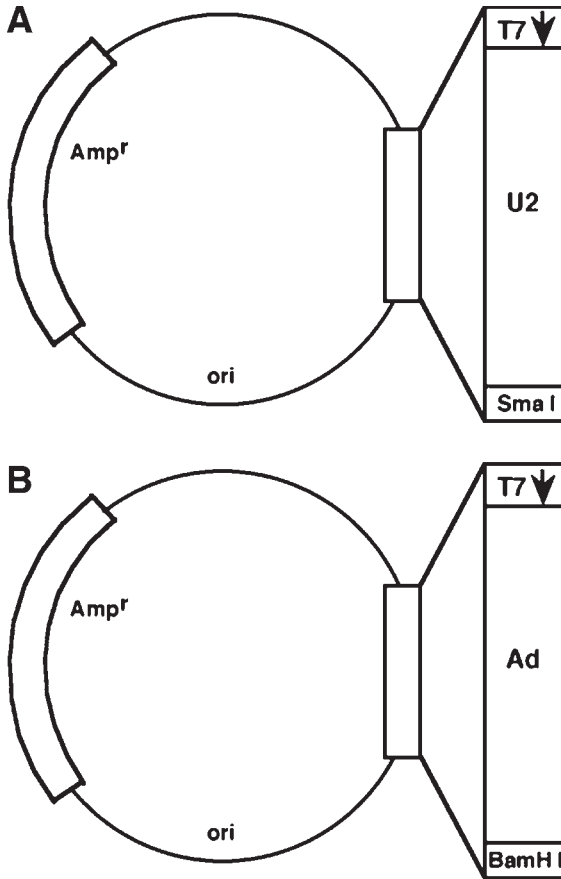


Fig. 2. The plasmids containing a *Xenopus* wild-type U2 gene (A) or a standard adenovirus pre-mRNA sequence (B) are shown.

10. pT7-U2 plasmid (Fig. 2).
11. pT7-Ad plasmid (Fig. 2).

2.2. Equipment

1. Nanoject II (cat. no. 3-000-204; Drummond Scientific Company).
2. Zoom stereo microscopy (Olympus SZ-STB1).
3. Small scissors.
4. Forceps (Dumont).
5. Suturing kit.
6. Scalpels (Bard-Parker no. 23).
7. Flaming/Brown Micropipette Puller (Sutter Instrument Co., model P-97).
8. 7-in. Drummond 100 replacement tubes (cat. no. 3-00-203-G/XL; Drummond Scientific Company).
9. Scintillation counter (cat. no. LS 6000SC; Beckman).

2.3. Solutions

1. 2X Benzocaine buffer: dissolve 0.3 g powdered benzocaine (cat. no. 1080-01; J. T. Baker) in 10 mL ethanol first and then add deionized water to 500 mL.
2. OR2 (oocyte Ringer's medium) buffer: 82.5 mM NaCl, 2 mM KCl, 1 mM MgCl₂, and 5 mM HEPES, pH 7.5. Sterilize using a 0.22- to 0.45- μ m filter.
3. Collagenase type I solution: dissolve collagenase (cat. no. 234153; Calbiochem) in OR2 buffer to bring the final concentration to 1 mg/mL (make fresh).
4. 10X Modified Barth's solution (MBS) Buffer: 0.8 M NaCl, 10 mM KCl, 8 mM MgSO₄, 24 mM NaHCO₃, and 10 mM HEPES, pH 7.4 (add 700 μ L 1M CaCl₂ into 100 mL 10X MBS buffer before use).
5. 5:1 Isolation buffer: 83.0 mM KCl, 17.0 mM NaCl, and 6.5 mM Na₂HPO₄, and 3.5 mM KH₂PO₄ (add 500 μ L of 1M MgCl₂ and 50 μ L of 1M dithiothreitol (DTT) into 50 mL 5:1 isolation buffer before use).
6. 10X T7 transcription buffer: 0.4M Tris-HCl, pH 7.5, 100 mM NaCl, 60 mM MgCl₂, and 20 mM spermidine.
7. G50 buffer: 20 mM Tris-HCl, pH 7.5, 300 mM NaAc, 2 mM EDTA (ethylenediamine-tetraacetic acid), and 0.3% sodium dodecyl sulfate (SDS).

3. Methods

3.1. Synthesis of *Xenopus* U2 snRNA and Adenovirus Pre-mRNA

Two types of RNA, including U2 snRNA (functional and nonfunctional) and radiolabeled pre-mRNA, are needed in the following procedure. To synthesize these RNAs, an Sma I-linearized pT7-U2 plasmid, containing a *Xenopus* U2 snRNA gene under the control of a T7 promoter, and a BamH I-linearized pT7-Ad plasmid, containing a standard adenovirus pre-mRNA sequence under the control of the T7 promoter, are used as templates for T7 transcription in vitro (**Fig. 2**).

3.1.1. T7 Transcription of U2 snRNA In Vitro

1. At room temperature, set up a 100- to 200- μ L transcription reaction containing 1.2 mM each of GpppG, ATP, CTP, and UTP (for functional wild-type U2) or 5FUTP for altered U2 snRNA with all uridines substituted with 5-fluorouridines (5FU), 0.3 mM GTP, 0.005 μ Ci/ μ L [α -³²P]GTP (*see Note 1*), 40 mM Tris-HCl, pH 7.5, 6 mM MgCl₂, 2 mM spermidine, 5 mM DTT, 0.1 μ g/ μ L of Sma I-linearized T7-U2 plasmid, and 4 U/ μ L T7 phage polymerase.
2. Remove 1 μ L of the reaction and determine the radioactivity (cpm) using a scintillation counter (*see Note 1*).
3. Incubate the rest of the reaction (99–199 μ L) at 37°C for 1 h.
4. Extract U2 snRNA transcript with PCA (Tris-HCl [pH 7.5]-buffered phenol:chloroform:isoamyl alcohol [50:49:1]) and precipitate it with ethanol.
5. Resolve the precipitated U2 snRNA sample on a 6% polyacrylamide-8M urea gel (**Fig. 3, lane 1**).
6. Identify U2 band using autoradiography.
7. Excise the trace-labeled U2 band and transfer the gel slice to a new 1.5-mL microfuge tube.
8. Add 450 μ L of G50 buffer and quickly freeze the sample in dry ice for 5 min.
9. Elute U2 snRNA at room temperature overnight.
10. Extract eluted U2 snRNA with PCA and precipitate it with ethanol (*see Note 2*).

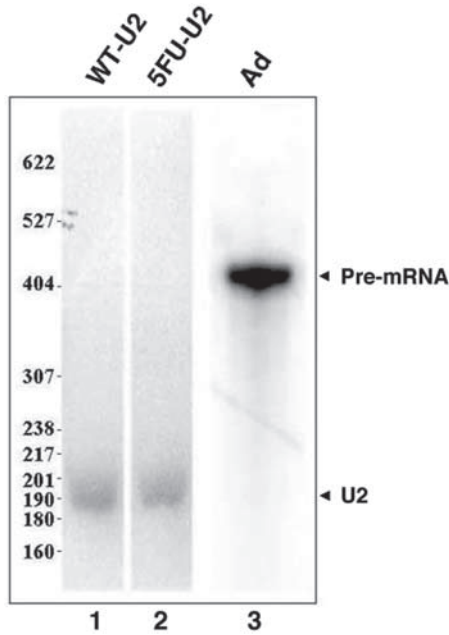


Fig. 3. In vitro transcription of U2 snRNA and adenovirus pre-mRNA. Trace-radiolabeled wild-type U2 snRNA (**lane 1**) and 5FU-sustituted U2 snRNA (**lane 2**), as well as radiolabeled standard adenovirus pre-mRNA (**lane 3**) are transcribed in vitro. After transcription, RNAs are resolved on a 6% polyacrylamide-8M urea gel and exposed to a PhosphorImager screen for 5 min for wild-type U2 snRNA and 5FU-U2 snRNA and 30 s for pre-mRNA. The wild-type U2 snRNA, 5FU-U2 snRNA, and pre-mRNA bands (indicated on the right) are identified and excised, and RNAs are recovered. The numbers on the left are size markers of MspI-digested pBR322 DNA.

11. Determine the radioactivity (cpm) using a scintillation counter and quantitate the amount of U2 snRNA transcript (*see Note 1*). Typically, the reaction produces about 3 to 6 μg of 5' capped wild-type U2 snRNA (**Fig. 3, lane 1**) or 5' capped 5FU-U2 snRNA (**Fig. 3, lane 2**). Both U2 snRNAs are made in parallel to test their ability to reconstitute pre-mRNA splicing.
12. Dissolve the U2 snRNA transcript in RNase-free water at 50 ng/ μL .

3.1.2. T7 Transcription of Adenovirus pre-mRNA In Vitro

1. At room temperature, set up a 10- to 25- μL transcription reaction containing 1.2 mM each of GpppG, ATP, CTP, UTP, 0.3 mM GTP, 2 $\mu\text{Ci}/\mu\text{L}$ [α - ^{32}P]GTP, 40 mM Tris-HCl, pH 7.5, 6 mM MgCl_2 , 2 mM spermidine, 5 mM DTT, 0.1 $\mu\text{g}/\mu\text{L}$ of BamH I-linearized T7-Ad plasmid, and 4 U/ μL T7 phage polymerase.
2. Carry out the reaction and gel purify the pre-mRNA according to the procedure described for U2 snRNA transcription in **Subheading 3.1.1**. Suspend the pre-mRNA in RNase-free water at 500,000 cpm/ μL (**Fig. 3, lane 3**).

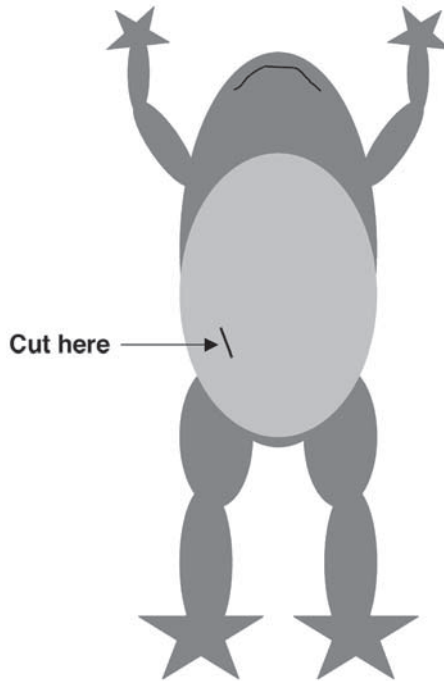


Fig. 4. The frog should be cut at the lower abdomen as indicated.

3.2. Preparation of Oocytes

3.2.1. Anesthesia of Frog

A female frog is anesthetized in a 2000-mL container containing a mixture of 200 mL 2X benzocaine buffer and 200 mL ice for about 10 to 15 min (see **Note 3**).

3.2.2. Dissection and Suturing

Place the frog on her back on an ice bed. Using a sterile scalpel, make an incision about 0.8 to 1.0 cm wide at the abdomen in two steps (see **Note 4**) (**Fig. 4**). First, using evenly distributed pressure, carefully incise the skin. Second, lift the skin off the muscle layer using a pair of forceps and make a small and precise incision through the muscle layer. Take out the ovarian lobes carefully, overestimating the number of oocytes needed, and place them in 1X MBS buffer. Suture the muscle layer first with a few stitches and then suture the skin. Monitor the frog closely for a day to ensure that she is healthy before returning her to the tank.

3.2.3. Separation/Isolation of Oocytes (see **Note 5**)

1. Place the oocytes in a Petri dish filled with 50 mL of OR2 buffer.
2. Cut the membrane of the ovarian lobes.
3. Swirl the dish slowly for 10 min, changing the buffer five times.

4. Change OR2 buffer to collagenase type I buffer.
5. Swirl gently for 20 min on a shaker (*see Note 6*).
6. Remove healthy individual oocytes to new OR2 buffer in a new Petri dish.
7. Swirl and change the buffer twice.
8. Change OR2 buffer to 1X MBS buffer containing gentamicin.
9. Keep the healthy oocytes at 18°C (*see Note 7*).

3.3. Microinjection

After U2 snRNA and pre-mRNA have been transcribed and healthy oocytes have been separated and kept at 18°C, the next crucial step is to carry out three sequential microinjections (**Fig. 1**). The microinjection protocols, including the preparatory steps of making the needles, are described next.

3.3.1. Preparation of Needles for Microinjection

To carry out successful microinjections, good needles are essential. The needles are made using a micropipet puller. We use 7-in. Drummond tubes with the following program to create a fine tip: heat = 310, pull = 65, velocity = 50, time = 150. The needles can be made in a large batch and stored. The tip of the needle is snapped off to create a blunt end. We suggest trying different pulling conditions to find the best one for each laboratory.

3.3.2. Microinjection Protocols

3.3.2.1. DAY 1: CYTOPLASMIC INJECTION OF AN ANTISENSE U2 DNA OLIGONUCLEOTIDE (**Fig. 6A**)

1. Press “empty” on the injector to near completion.
2. Fill the needle with mineral oil using a syringe.
3. Assemble the needle onto the injector (**Fig. 5**).
4. Set the volume to 50.6 nL and set speed to “fast speed” on a dip switch.
5. Pipet 2 μ L of an antisense U2 DNA oligonucleotide (3 μ g/ μ L) on a piece of stretched-out parafilm (for a control experiment, pipet 2 μ L of water instead) (*see Note 8*).
6. Adjust the microscope so that both the sample on the parafilm and the needle tip are in the field of view.
7. Lower the needle so that the tip is placed inside of the drop of the sample. Make sure the tip is not touching the parafilm.
8. Press “fill” to fill the needle with the sample (*see Note 9*).
9. Place a batch of 20 oocytes to be injected on a meshed Petri dish filled with 1X MBS buffer (*see Note 10*).
10. Place the needle above the buffer, press “inject,” and observe that a small drop of sample exits (*see Note 11*).
11. Using a pair of forceps, position the oocytes with their midlines (between animal hemisphere and vegetal hemisphere) directly toward the tip of the needle (**Fig. 6A**) (*see Note 12*).
12. Inject the sample into the cytoplasm at the midline, pause 1 s after the injection, and take out the needle slowly after the pause (*see Note 13*).
13. Inject the sample into the rest of the oocytes, repeating **step 10** after every five oocytes (*see Note 14*).
14. Incubate overnight (*see Note 15*).

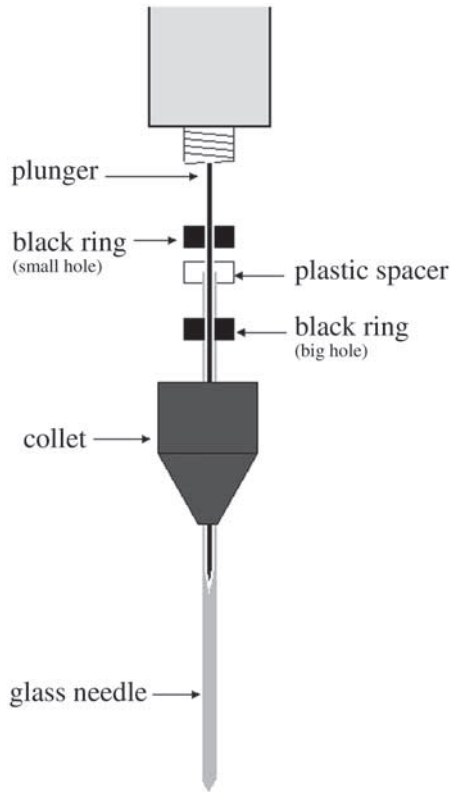


Fig. 5. The assembly of the needle onto the injector is shown.

3.3.2.2. DAY 2: CYTOPLASMIC INJECTION OF RESCUING U2 snRNA (FIG. 6A)

15. Follow **steps 1 to 4**.
16. Pipet 2 μL of rescuing U2 (50 ng/ μL , wild-type or 5FU-substituted U2) on a piece of stretched-out parafilm (for a control, pipet 2 μL of water instead).
17. Follow **steps 6 to 14** (*see Note 16*).

3.3.2.3. DAY 3: NUCLEAR INJECTION OF RADIOLABELED PRE-mRNA (FIG. 6B) (SEE NOTE 17)

18. Follow **steps 1 to 3**.
19. Set the volume to 13.8 nL and set speed to “fast speed” on a dip switch.
20. Pipet 1 μL of adenovirus pre-mRNA (500,000 cpm/ μL) on a piece of stretched-out parafilm.
21. Follow **steps 6 to 10**.
22. Using a pair of forceps, position the oocytes with the center of the animal hemisphere toward the tip of the needle.
23. Aim the tip at the center of the animal hemisphere (Fig. 6B) and carefully lower the needle so that the tip has entered the outer membrane and the nucleus but has not gone completely through the nucleus.

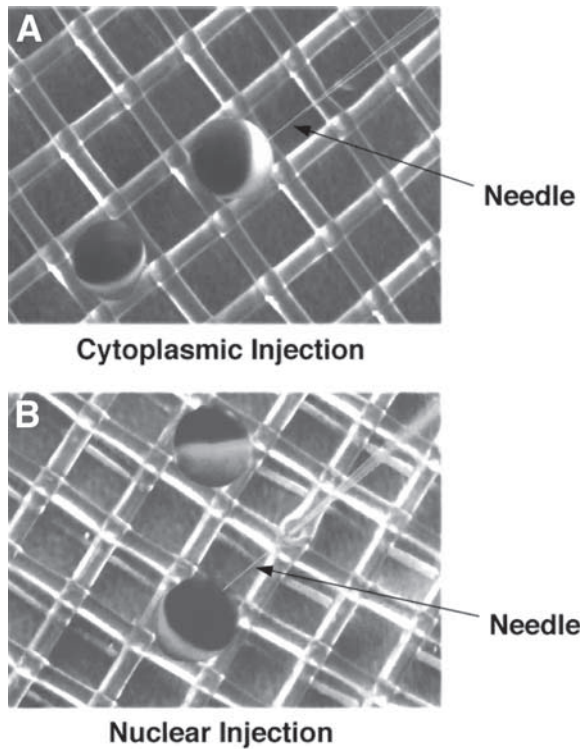


Fig. 6. The relative positions of the glass needle and the oocytes in (A) cytoplasmic injection and (B) nuclear injection are shown.

24. Press “inject,” pause 2 s, and take out the needle slowly after the pause.
25. Inject the rest of the oocytes, repeating **step 10** after every five oocytes.
26. Incubate for 1 h in 1X MBS buffer.
27. Proceed with nuclear isolation.

3.4. Nuclear Isolation

After the injections are finished, the next major step is nuclear isolation. This step is imperative to the assay, given the fact that cytoplasmic content would smear the gels, hindering us from analyzing the splicing pattern. Using nuclear isolation followed by RNA extraction, we can obtain a clean nuclear RNA sample that enables us to analyze splicing profile accurately. It should be noted that when doing nuclear isolations, oocytes are healthy, the buffer is pristine, and forceps are sharp and precise (see **Note 18**). Described next is the protocol for nuclear isolation.

3.4.1. Nuclear Isolation Protocol (Fig. 7A)

1. Transfer the oocytes from 1X MBS buffer to a new Petri dish containing 5:1 isolation buffer.
2. Gently hold the oocytes with a pair of forceps so that the animal hemisphere is on the top.

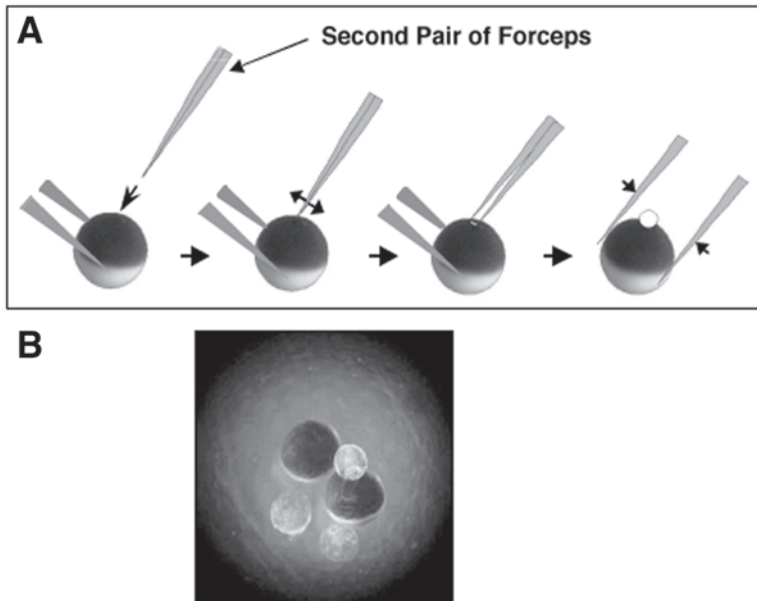


Fig. 7. Isolation of nuclei from *Xenopus* oocytes. (A) The diagram of the procedure. Use a pair of forceps to hold the oocyte and a second pair of forceps to make a small hole on the animal hemisphere of oocytes. Gently squeeze the oocyte with one pair of forceps until the nucleus emerges. The arrows indicate the force applied onto the oocytes during the process. (B) A photo of two isolated nuclei (on the side of the oocytes) and an emerging nucleus (on the top of an oocyte) is shown.

3. Using another pair of forceps, gently poke a small single hole on the top of the animal hemisphere (*see Note 18*).
4. Gently and slowly squeeze the oocyte in the middle. Slowly, the nucleus will emerge neatly without cytoplasmic contamination (**Fig. 7B**).
5. Pick up the nuclei using a 10- μ L pipet and put them in a microfuge tube. Store the tube in dry ice the whole time while working on nuclear isolation.
6. Repeat **steps 2 to 5** for all 20 oocytes.
7. Pipet the sample of nuclei up and down 10 times to completely break the nuclei.
8. Centrifuge briefly to spin down the membrane and debris.
9. Transfer the supernatant (nuclear extract) into a new tube (*see Note 19*).
10. Add 300 μ L of G50 buffer to the nuclear extract, and perform PCA extraction and ethanol precipitation.
11. Suspend the RNA pellet in 2 μ L of water.
12. Proceed with pre-mRNA splicing analysis.

3.5. Splicing Assay

To analyze pre-mRNA splicing, the nuclear RNA isolated above is resolved on a 8% polyacrylamide-8M urea gel and exposed to the PhosphorImager screen overnight, which allows for visualization of the splicing profile (spliced intermediates and prod-

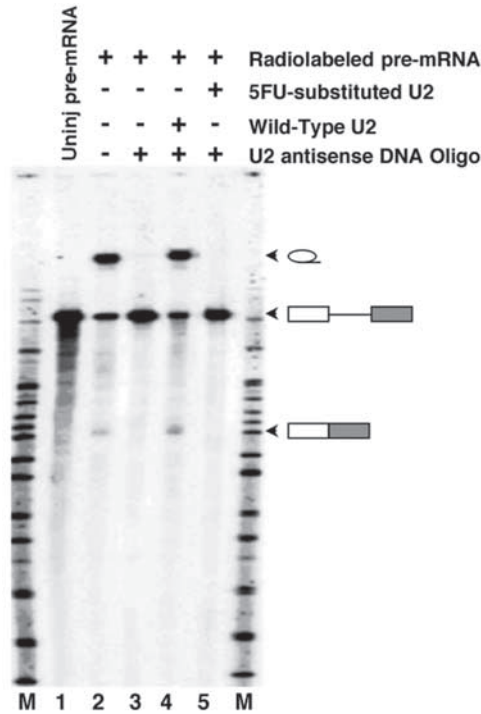


Fig. 8. Functional analysis of U2 snRNA. *Xenopus* oocytes are injected in the cytoplasm with 50.6 nL of water (**lane 2**) or with 50.6 nL of an antisense U2 DNA oligonucleotide (3 $\mu\text{g}/\mu\text{L}$) (**lanes 3–5**). After an overnight incubation, 50.6 nL of water (**lanes 2 and 3**) or 50.6 nL of 50 ng/ μL in vitro transcribed wild-type U2 (**lane 4**) or 5FU-substituted U2 (**lane 5**) are injected into the cytoplasm of the U2-depleted oocytes. Following overnight incubation, 13.8 nL of radiolabeled pre-mRNA (500,000 cpm/ μL) are injected into the nuclei of the oocytes. After 1 h, nuclei are isolated from the oocytes, and total nuclear RNA is recovered and resolved on an 8% polyacrylamide-8M urea gel. The transcribed pre-mRNA prior to the injection is shown (**lane 1**). The positions of spliced products, including the lariat-intron and mature mRNA as well as the pre-mRNA, are indicated on the right. **Lanes M** on both sides are size markers of MspI-digested pBR322 DNA.

ucts). An autoradiograph of a typical splicing gel is shown in **Fig. 8**. As indicated, spliced lariat-intron and mRNA are clearly visible. In fact, splicing occurs efficiently in the control oocytes (**Fig. 8, lane 2**). As expected, when the endogenous U2 snRNA is depleted, pre-mRNA splicing is completely abolished (**Fig. 8, lane 3**). Importantly, when the U2-depleted oocytes are supplemented with the in vitro transcribed wild-type U2 snRNA, splicing is completely restored (**Fig. 8, lane 4**). In contrast, the injection of 5FU-U2 into the U2-depleted oocytes fails to reconstitute pre-mRNA splicing (**Fig. 8, lane 5**). These results, together with previously published results (25), indicate that the uridines and the pseudouridines converted from uridines at certain positions in U2 snRNA are absolutely required for U2 function in pre-mRNA splicing.

3.6. Summary

Using the *Xenopus* oocyte microinjection system, we have presented a functional analysis of U2 snRNA in pre-mRNA splicing. In principle, not only can one specifically target a spliceosomal snRNA, but also one can effectively introduce a modified snRNA to study its function. In short, the versatility of this system provides a powerful tool for studying pre-mRNA splicing.

4. Notes

1. A trace amount of [α - 32 P]GTP is included in addition to the nonradioactive nucleotide GTP to allow calculation of the percentage incorporation and thereby accurate determination of the amount of RNA transcribed.
2. Glycogen is not recommended as a carrier when precipitating RNA to be injected since it can cause the samples to become sticky, thus complicating the injection procedure. Also, it is very important that the samples are pristine. Dust, a trace of debris, or any other contaminants can block the needle, making the injection procedure difficult.
3. The amount of time for anesthesia depends on the size of frog, but the total time should not exceed more than 15 min. Also, cover the container to ensure that the frog does not leap out.
4. Make an incision only at the lower abdomen. Inaccurate placement of the incision may cause damage to a major blood vessel, thus causing excessive bleeding.
5. Both manual or enzymatic separation of the oocytes are effective. However, the enzymatic approach grants certain advantages: (1) The enzymatic approach is relatively milder than manual isolation; (2) it is easier to perform injection with the enzyme-digested oocytes.
6. Sometimes, an incubation period of 20 min is not sufficient. In that case, hold the membrane with a pair of forceps and gently shake the vitelline membrane. If necessary, extend the incubation time. Alternatively, one can separate the oocytes manually using a pair of forceps. In manual isolation of the oocytes, hold the vitelline membrane firmly with a pair of forceps. Using another pair of forceps, grab the membrane where the oocyte is attached and gently tug away from the membrane. With practice, oocytes should release easily from the membrane.
7. Oocytes can be kept at temperatures ranging from 13 to 21°C. To obtain the maximum number of healthy oocytes, change the 1X MBS buffer at least once a day and discard dying or unhealthy oocytes.
8. This is an overestimation of the amount of oligonucleotide needed for the reaction. This is to ensure that, despite constant DNase activity, there will be enough oligonucleotide binding to endogenous U2 snRNA to cause its destruction.
9. Proceed slowly when filling the needle. Avoid trapping bubbles in the needle, which would cause inaccuracy.
10. The meshed Petri dish is used to help immobilize the oocytes. To make the meshed Petri dish, place a sheet of 800- μ m mesh Nitex (Tetko) at the bottom of a Petri dish and fix it in place by melting the bottom of the Petri dish with a few drops of chloroform. Before usage, the newly made meshed Petri dish must be washed extensively with ethanol, water, and buffers.
11. If the needle is blocked, the injection will not work. To ensure that the needle does not block, inject above the buffer to observe that a small drop of sample exits when pressing "inject." If you do not see the sample exiting, trim the tip by snapping off the end using a forceps.

12. To make oocytes less mobile, you may choose to decrease the volume of the buffer so that the top of each oocyte emerges above the surface of the buffer. However, it is important to finish the injection quickly to ensure that oocytes do not dry out.
13. Be gentle when taking out the needle. Pulling the needle out rapidly can cause the cytoplasm to leak out, an occurrence called *blebbing*. Adding 5% Ficoll to 1X MBS buffer helps prevent blebbing.
14. The purpose of this step is to check that the needle has not become blocked during the injection process and to ensure that all oocytes were injected with the sample.
15. To ensure that the endogenous U2 snRNA is completely depleted via endogenous RNase H activity and the antisense U2 oligonucleotide is completely degraded via endogenous DNase activity, the oocytes are incubated overnight.
16. To measure the amount of injected U2 snRNA accumulated in the nucleus, primer extension or Northern analysis on total nuclear RNA isolated from 5 to 10 oocytes can be carried out. The level of injected U2 accumulated in the nucleus should be similar to that of the endogenous U2 in mock-depleted oocytes.
17. Nuclear injection can be practiced using dye or even mineral oil by injecting and quickly opening up the oocytes to see if the dye or mineral oil is injected into the nucleus.
18. Sometimes, forceps will need sharpening. Sharpening should be kept to a minimum. When sharpening forceps, sharpen with both sides closed at the tip by holding it at a small angle from the surface of the sandpaper and by pulling it gently toward you. Do this in slow, gentle strokes.
19. At this step, an aliquot of the nuclear extract can be used directly for spliceosome assembly assays. The aliquot can be loaded directly on a 4% polyacrylamide native gel. After electrophoresis and autoradiography, the profile of splicing complexes can be visualized (26).

Acknowledgment

We thank Mei-Di Shu, Branda Peculis, and the members of the Yi Tao Yu laboratory for advice, technical support, and valuable discussions. The work carried out in our lab is supported by grant GM 62937 from the National Institutes of Health.

References

1. Sharp, P. A. (1994) Split genes and RNA splicing. (Nobel Lecture). *Cell* **77**, 805–815.
2. Burge, C. B., Tuschl, T. H., and Sharp, P. A. (1999) Splicing of precursors to mRNAs by the spliceosome, in *The RNA World*, 2nd ed. (Gesteland, R. F., Cech, T. R., and Atkins, J. F., eds.), Cold Spring Harbor Laboratory Press, Cold Spring Harbor, New York, pp. 525–560.
3. Yu, Y.-T., Scharl, E. C., Smith, C. M., and Steitz, J. A. (1999) The growing world of small nuclear ribonucleoprotein particles, in *The RNA World*, 2nd ed. (Gesteland, R. F., Cech, T. R., and Atkins, J. F., eds.). Cold Spring Harbor Laboratory Press, Cold Spring Harbor, New York, pp. 487–524.
4. Staley, J. P. and Guthrie, C. (1998) Mechanical devices of the spliceosome: motors, clocks, springs, and things. *Cell* **92**, 315–326.
5. Guthrie, C. (1988) Genetic analysis of yeast snRNAs, in *Structure and Function of Major and Minor snRNPs* (Birnstiel, M., ed.), Springer-Verlag, Berlin, Germany, pp. 196–211.
6. Lin, R. J., Newman, A. J., Cheng, S. C., and Abelson, J. (1985) Yeast mRNA splicing in vitro. *J. Biol. Chem.* **260**, 14,780–14,792.
7. Padgett, R. A., Hardy, S. F., and Sharp, P. A. (1983) Splicing of adenovirus RNA in a cell-free transcription system. *Proc. Natl. Acad. Sci. USA.* **80**, 5230–5234.

8. Grabowski, P. J., Padgett, R. A., and Sharp, P. A. (1984) Messenger RNA splicing in vitro: an excised intervening sequence and a potential intermediate. *Cell* **37**, 415–427.
9. Krainer, A. R., Maniatis, T., Ruskin, B., and Green, M. R. (1984) Normal and mutant human β -globin pre-mRNAs are faithfully and efficiently spliced in vitro. *Cell* **36**, 993–1005.
10. Ruskin, B., Krainer, A. R., Maniatis, T., and Green, M. R. (1984) Excision of an intact intron as a novel lariat structure during pre-mRNA splicing in vitro. *Cell* **38**, 317–331.
11. Rio, D. C. (1988) Accurate and efficient pre-mRNA splicing in *Drosophila* cell-free extracts. *Proc. Natl. Acad. Sci. USA* **85**, 2904–2908.
12. Spikes, D. and Bingham, P. M. (1992) Analysis of spliceosome assembly and the structure of a regulated intron in *Drosophila* in vitro splicing extracts. *Nucleic Acids Res.* **20**, 5719–5727.
13. Pan, Z. Q. and Prives, C. (1989) U2 snRNA sequences that bind U2-specific proteins are dispensable for the function of U2 snRNP in splicing. *Genes Dev.* **3**, 1887–1898.
14. Hamm, J., Dathan, N. A., and Mattaj, I. W. (1989) Functional analysis of mutant *Xenopus* U2 snRNAs. *Cell* **59**, 159–169.
15. Hannon, G. J., Maroney, P. A., Denker, J. A., and Nilsen, T. W. (1990) *Trans* splicing of nematode pre-messenger RNA in vitro. *Cell* **61**, 1247–1255.
16. Black, D. L. (1992) Activation of c-src neuron-specific splicing by an unusual RNA element in vivo and in vitro. *Cell* **69**, 795–807.
17. Yu, Y.-T., Shu, M.-D., and Steitz, J. A. (1998) Modifications of U2 snRNA are required for snRNP assembly and pre-mRNA splicing. *EMBO J.* **17**, 5783–5795.
18. Evans, J. P. and Kay, B. K. (1991) Biochemical fractionation of oocytes. *Methods Cell Biol.* **36**, 133–148.
19. Forbes, D. J., Kornberg, T. B., and Kirschner, M. W. (1983) Small nuclear RNA transcription and ribonucleoprotein assembly in early *Xenopus* development. *J. Cell Biol.* **97**, 62–72.
20. Hamm, J. and Mattaj, I. W. (1989) An abundant U6 snRNP found in germ cells and embryos of *Xenopus laevis*. *EMBO J.* **8**, 4179–4187.
21. Peculis, B. A. and Steitz, J. A. (1994) Sequence and structural elements critical for U8 snRNP function in *Xenopus* oocytes are evolutionarily conserved. *Genes Dev.* **8**, 2241–2255.
22. Peculis, B. A. and Steitz, J. A. (1993) Disruption of U8 nucleolar snRNA inhibits 5.8S and 28S rRNA processing in the *Xenopus* oocyte. *Cell* **73**, 1233–1245.
23. Tycowski, K. T., Shu, M.-D., and Steitz, J. A. (1994) Requirement for intron-encoded U22 small nucleolar RNA in 18S ribosomal RNA maturation. *Science* **266**, 1558–1561.
24. Mattaj, I. W. (1986) Cap trimethylation of U snRNA is cytoplasmic and dependent on U snRNP protein binding. *Cell* **46**, 905–911.
25. Zhao, X. and Yu, Y.-T. (2004) Pseudouridines in and near the branch site recognition region of U2 snRNA are required for snRNP biogenesis and pre-mRNA splicing in *Xenopus* oocytes. *RNA* **10**, 681–690.
26. Kornarska, M. M. (1990) Analysis of splicing complexes and small nuclear ribonucleoprotein particles by native gel electrophoresis. *Methods Enzymol.* **180**, 442–453.

Chromatin Immunoprecipitation for Studying Transcriptional Regulation in *Xenopus* Oocytes and Tadpoles

David Stewart, Akihiro Tomita, Yun-Bo Shi, and Jiemin Wong

Summary

Understanding the accurate temporal and spatial regulation of gene expression during development requires knowledge of the spectrum of transcription factors and cofactors involved and their functional interplay with chromatin. Chromatin immunoprecipitation (ChIP) has become a powerful technique that allows us to do so. A typical ChIP assay involves (1) treating cells or tissues with formaldehyde to rapidly crosslink chromatin-associated proteins to DNA, (2) shearing chromatin by sonication into small fragments, (3) immunoprecipitation of the proteins of interest, (4) reversal of crosslinking, and (5) quantitating the specific associated DNA sequences by PCR. Here we present and discuss the protocols we have developed over the years for ChIP assays using *Xenopus* oocytes and tadpole tissues as experimental materials.

Key Words: Chromatin immunoprecipitation (ChIP); tadpole; thyroid hormone receptor; transcription; *Xenopus* oocyte.

1. Introduction

Accumulating evidence indicates that chromatin structure has a profound effect on transcriptional regulation (1,2). It has become clear that transcription is a complex process involving a large number of sequence-specific transcription factors and cofactors that exert functions in remodeling of chromatin or recruitment of basal transcriptional machinery. Understanding the accurate temporal and spatial regulation of gene expression during development requires knowledge of the spectrum of transcription factors and cofactors involved (3,4). Although techniques such as gel mobility shift assay and deoxyribonuclease (DNase) I footprinting have long been used to analyze interactions between proteins and DNA in vitro, for years it proved to be challenging to demonstrate whether such interactions also occurred in vivo and whether they were physiologically relevant.

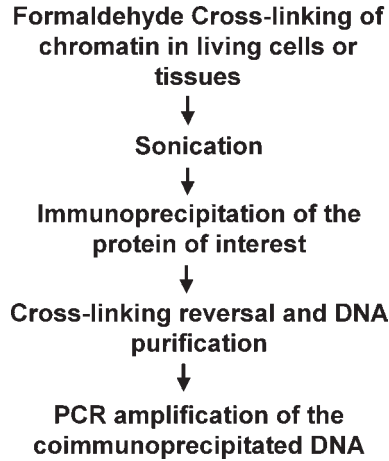


Fig. 1. Five major steps of ChIP assay. (1) Living cells or tissues are treated with formaldehyde to crosslink histone and nonhistone chromatin-associated proteins. (2) Sonication is used to solublize and shear chromatin into short fragments (0.5–1 kb). (3) Immunoprecipitation is performed with antibodies against the protein of interest. The chromatin fragments will be immunoprecipitated if associated with the protein of interest. Extensive washing is necessary to reduce nonspecific association of chromatin fragments with the beads. (4) Crosslinking is reversed and DNA is purified. (5) PCR is used to determine whether the specific sequences were coimmunoprecipitated with the protein of interest.

The development of assays that measure protein–DNA interactions and chromatin structure *in vivo* is therefore essential to understand better the mechanisms of transcriptional regulation *in vivo*. Chromatin immunoprecipitation (ChIP) is such an assay (5,6). ChIP has become a powerful technique that allows us to determine not only the status of histone modifications but also whether the transcription factors or coregulators of interest are associated with the specific target genes in living cells.

As illustrated in **Fig. 1**, the basic ChIP protocol can be generally divided into five major steps. In the first step, living culture cells or tissues are briefly treated with formaldehyde to covalently crosslink DNA with DNA-associated proteins. Formaldehyde is a tight (2 Å) crosslinking agent that efficiently crosslinks proteins to proteins and proteins to nucleic acids *in vivo* (6–8). Formaldehyde-induced crosslinking can occur between amino and imino groups of amino acids (lysines, arginines, and histidines) and of DNA (primarily adenines and cytosines). Its ability to crosslink proteins to proteins and proteins to DNA therefore allows detection of proteins that bind directly or indirectly to DNA in chromatin. Importantly, crosslinking by formaldehyde is a very rapid process (within minutes) and has been shown to preserve chromatin structure faithfully. Thus, crosslinking by formaldehyde is likely to provide a snapshot of the *in vivo* chromatin structure as well as the association of nonhistone proteins with chromatin. Another important feature of formaldehyde crosslinking is its full reversibility. The crosslinking can be reversed by mild heat treatment at low

pH, making it an ideal reagent for ChIP. This full reversibility is significant because it allows DNA fragments to be recovered from immunoprecipitated chromatin samples in a manner suitable for subsequent analysis by semiquantitative or quantitative real-time PCR.

After crosslinking with formaldehyde, the second step in a ChIP assay is to lyse the cells and shear chromatin by sonication to an average size of 0.5 to 1.5 kb. This step is essential to solubilize the chromatin and reduce the probability of immunoprecipitating distant DNA sequences along the linear chromatin.

The third step is immunoprecipitation of chromatin using antibodies against histones or nonhistone proteins of interest. In principle, if the protein of interest is associated with and crosslinked to a specific chromosomal region *in vivo*, the chromatin fragment containing this region will be coimmunoprecipitated with the protein of interest. After extensive washing to reduce nonspecific association, the precipitated chromatin is eluted from the beads.

The fourth step is to reverse the crosslinks by heat treatment in a buffer at low pH. This allows efficient recovery of DNA fragments from the precipitated chromatin. The final step is semi- or quantitative analysis of the precipitated DNA by PCR to determine whether a specific DNA sequence is present and therefore whether the protein was associated with the sequence in living cells.

Although the basic ChIP protocol for tissue culture cells has been extensively described (5,6), we present and discuss here the protocols we have developed over the years for ChIP assays using *Xenopus* oocytes (9–11) and tadpole tissues as experimental materials (12–14). *Xenopus* oocytes have been extensively used as a model system for studying transcriptional regulation in the context of chromatin because circular plasmid reporter DNA injected into the nucleus of a *Xenopus* oocyte is efficiently assembled into chromatin, and remodeling of chromatin structure by transcription factors such as thyroid hormone receptor (TR) can be studied by various assays, including DNase I hypersensitivity, regularity of the nucleosomal ladder, and DNA topology (15–17). The basic protocols for the chromatin remodeling assays described above have been extensively described (18) and thus are not covered here.

An example of the use of ChIP to examine recruitment of corepressors and coactivators by unliganded and liganded TR is illustrated in Fig. 2. In this experiment, a reporter containing four Gal4 binding sites upstream of the TR β A gene promoter was assembled into chromatin via the injection of ssDNA (Fig. 2A). A primer extension analysis of transcription from the 4XUAS-pTR β A reporter is also shown (Fig. 2B). From these data, it is quite clear that repression by unliganded TR is associated with recruitment of corepressors SMRT and N-CoR (Fig. 2C). In addition, chromatin under this condition is hypoacetylated and contains a relatively higher level of H3-K9 methylation in comparison to the control. Upon addition of T₃, SMRT and N-CoR dissociate from chromatin, and the coactivators SRC-3 and p300 are recruited. Associated with this exchange of cofactors is increased histone acetylation and decreased H3-K9 methylation. Furthermore, a significant increase in the association of RNA polymerase II is detected in the presence of T₃. Note that no significant change in the level of chromatin-associated Gal-TR was detected, as expected. The feasibility of the

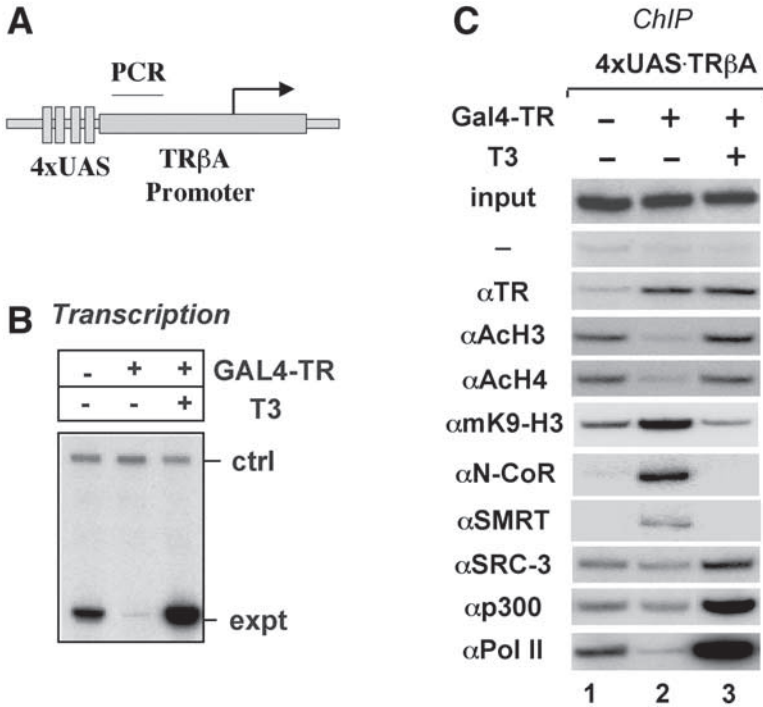


Fig. 2. TR recruits corepressors SMRT and N-CoR for repression in the absence of T₃ and coactivators SRC-1 and p300 for activation in the presence of T₃. (A) A simple illustration of the structure of the 4XUAS-pTRβA reporter. Groups of oocytes were injected with or without Gal4-TR [Gal4(DBD)-TR(LBD)] (200 ng/μL, 18.4 nL/oocyte) and the single-stranded 4XUAS-pTRβA reporter (100 ng/μL, 18.4 nL/oocyte). The oocytes were incubated at 18°C overnight with or without T₃ (50 nM) and processed for transcriptional analysis by (B) primer extension or (C) ChIP assay using antibodies against the proteins as indicated. Note that repression by unliganded Gal4-TR was correlated with histone deacetylation, increased H3-K9 methylation, a marker associated with transcriptional repression, and recruitment of corepressors SMRT and N-CoR. Addition of T₃ led to the release of SMRT and N-CoR and recruitment of SRC-1 and p300. In addition, the levels of histone acetylation increased and H3-K9 methylation decreased.

ChIP assay in this model system opens up an avenue to further investigate the cofactors involved and changes in histone modifications associated with transcriptional activation or repression processes.

2. Materials

2.1. Preparation and Microinjection of Xenopus Oocytes

- 10X OR2 buffer: 48.2 g NaCl (82.5 mM), 1.86 g KCl (2.5 mM), 2.03 g MgCl₂ (1 mM), 1.42 g Na₂HPO₄ (1 mM), 11.9 g HEPES (5 mM). The concentration shown is for final 1X solution. Adjust to pH 7.8 with 1N NaOH. Bring final volume to 1 L with distilled water.

2. 10X High salt modified Barth's solution (MBSH) buffer: dissolve first 23.8 g HEPES (10 mM), 51.3 g NaCl (88 mM), 0.75 g KCl (1 mM), 2 g NaHCO₃ (2.4 mM). Then, add 2 g MgSO₄·7H₂O (0.82 mM), 0.9 g CaCl₂·6H₂O (0.41 mM), and 0.78 g Ca(NO₃)₂·4H₂O (0.33 mM). The concentration shown is for a final 1 X solution. Adjust to pH 7.6 with 1 N NaOH. Bring final volume to 1 L with distilled water. Add the antibiotics penicillin and streptomycin to a final concentration of 100 µg/mL.
3. Stage VI *Xenopus laevis* oocytes. Oocytes are obtained surgically from adult female *Xenopus laevis* (Nasco, Wisconsin).
4. Nanoject II microinjection apparatus (Drummond Scientific Co.).
5. mMESSAGE mMACHINE kits (Ambion).
6. Forceps.
7. Microscope.
8. Glass capillary tubes for pulling injection needles (Drummond Scientific Co.).
9. Reporter DNA (single-stranded or double-stranded plasmids).
10. Thyroid hormone triiodothyronine (T₃; Sigma T-2752).

2.2. ChIP Assay for Investigating the Mechanism of Transcriptional Regulation by TR in *Xenopus* Oocytes

1. 37% Formaldehyde (Sigma).
2. 100 mM Tris-HCl, pH 9.4, and 10 mM dithiothreitol (DTT).
3. Oocyte homogenization buffer: 20 mM Tris-HCl, pH 7.6, 60 mM KCl, 15 mM NaCl, 1 mM ethylenediaminetetraacetic acid (EDTA), 1 mM DTT, 1 mM phenylmethane-sulfonyl fluoride (PMSF), 1 µg/mL aprotinin, 1 µg/mL leupeptin, 1 µg/mL pepstatin A.
4. Collagenase (cat. no. C-6885; Sigma).
5. Salmon sperm DNA/protein A or G agarose (Upstate 16-157); 2.5 mL packed beads containing 1 mg sonicated salmon sperm DNA, 2.5 mg bovine serum albumin, 1.5 mg recombinant protein A or G agarose as an 50% gel slurry in TE (10 mM Tris-HCl, pH 8.0, 1 mM EDTA) buffer containing 0.05% sodium azide.
6. ChIP I wash buffer (low salt): 0.1% sodium deoxycholate, 1% Triton X-100, 2 mM EDTA, 50 mM HEPES, pH 7.5, 150 mM NaCl, 1 mM DTT, and 0.4 mM PMSF.
7. ChIP II wash buffer (high salt): 0.1% sodium deoxycholate, 1% Triton X-100, 2 mM EDTA, 50 mM HEPES, pH 7.5, 500 mM NaCl, 1 mM DTT, and 0.4 mM PMSF.
8. ChIP III wash buffer: 0.25M LiCl, 0.5% NP-40, 0.5% sodium deoxycholate, 1 mM EDTA, 10 mM Tris-HCl, pH 8.0, 1 mM DTT, and 0.4 mM PMSF.
9. TE buffer: 10 mM Tris-HCl, pH 8.0, 1 mM EDTA, 1 mM DTT, and 0.4 mM PMSF.
10. ChIP elution buffer: 0.5% sodium dodecyl sulfate (SDS), 0.1M NaHCO₃.
11. 10 mg/mL Proteinase K (cat. no. 1 413 783; Roche).
12. PCR reaction: Taq DNA polymerase (Promega).
13. Antibodies: anti-SMRT and anti-N-CoR (9), anti-SRC3 and anti-p300 (11), antiacetyl-H3, anti-acetyl-H4, and anti-H3-methyl-K9 antibodies (Upstate).
14. PCR primers: thyroid hormone receptor β promoter (TRβA) promoter primers: forward 5'-TGCCAGGGCCTATTTTGAATC-3', reverse 5'-AGAGCCTGAGTGAAGACCCATAAG-3'.

2.3. Use of ChIP for Investigating TR Action in Development

1. Adults and premetamorphic tadpoles of the South African clawed frog *Xenopus laevis* were obtained from Nasco (Wisconsin). Developmental stages of tadpoles were determined according to ref. 19.
2. Nuclei extraction buffer A (buffers A–C should be prepared just before use): 0.5% Triton X-100, 10 mM Tris-HCl, pH 7.5, 3 mM CaCl₂, 0.25M sucrose, 1 mM DTT, 0.2 mM PMSF,

- and a protease inhibitor tablet (Complete, Mini, EDTA free; Roche) This should be dissolved freshly in double-distilled water (add DTT and protease inhibitors just before use).
3. Nuclei extraction buffer B: 0.5% Triton X-100, 10 mM Tris-HCl, pH 7.5, 3 mM CaCl₂, 2.2M sucrose, 1 mM DTT, 0.2 mM PMSF, and protease inhibitor tablet (Complete, Mini, EDTA free; Roche) This should be dissolved freshly in double-distilled water (add DTT and protease inhibitors just before use).
 4. Nuclei extraction buffer C: 10 mM Tris-HCl, pH 7.5, 3 mM CaCl₂, 2.2M sucrose, 1 mM DTT, 0.2 mM PMSF, and protease inhibitor tablet (Complete, Mini, EDTA free; Roche) This should be dissolved freshly in double-distilled water (add DTT and protease inhibitors just before use).
 5. SDS lysis buffer: 1% SDS, 10 mM EDTA, 50 mM Tris-HCl, pH 8.1, and 0.2 mM PMSF (add PMSF just before use).
 6. CHIP dilution buffer: 0.01% SDS, 1.1% Triton X-100, 1.2 mM EDTA, 16.7 mM Tris-HCl, pH 8.1, 167 mM NaCl, 0.2 mM PMSF, and protease inhibitor tablet (add PMSF and protease inhibitor tablet just before use).
 7. Salmon sperm DNA/protein A or G agarose (Upstate 16-157): 2.5 mL packed beads containing 1 mg sonicated salmon sperm DNA, 2.5 mg bovine serum albumin, and 1.5 mg recombinant protein A or G agarose as a 50% gel slurry in TE buffer containing 0.05% sodium azide.
 8. TE: 10 mM Tris-HCl, 1 mM EDTA, pH 8.0.
 9. Antibodies: anti-TR, SMRT, N-CoR, and TBLR1 antibody (**13,20,21**); anti-acetyl-histone-H3 and H4 (Upstate); anti-Flag M2 affinity gel (Sigma A2220).
 10. CHIP I SDS wash buffer (low salt): 0.1% SDS; 1% Triton X-100; 2 mM EDTA; 50 mM HEPES, pH 7.5; 150 mM NaCl; 1 mM DTT; 0.4 mM PMSF and proteinase inhibitor tablet (add DTT and protease inhibitors just before use).
 11. CHIP II SDS wash buffer (high salt): 0.1% SDS, 1% Triton X-100, 2 mM EDTA, 50 mM HEPES, pH 7.5, 500 mM NaCl, 1 mM DTT, 0.4 mM PMSF (add DTT and PMSF just before use).
 12. CHIP III wash buffer: 0.25M LiCl, 0.5% NP-40, 0.5% sodium deoxycholate, 1 mM EDTA, 10 mM Tris-HCl, pH 8.0, 1 mM DTT, and 0.4 mM PMSF (add DTT and PMSF just before use).
 13. PCR primers: TRβA promoter primers for tissue samples: forward 5'-TGT GTC TAT ACT GAT GGG ATG-3', reverse 5'-GAG GAA CTG AAG TAG CAG CG-3'; TH/bZIP promoter: forward 5'- TCT CCC TGT TGT GTA TAA TGG-3', reverse 5'-CTC CCA ACC CTA CAG AGT TCA-3'.
 14. CHIP elution buffer: 0.5% SDS, 0.1 M NaHCO₃.
 15. 10 mg/mL Proteinase K (cat. no. 1 413 783; Roche).
 16. Taq DNA polymerase (Promega) or Takara LA Taq polymerase (cat. no.; RR002A Takara).

3. Methods

3.1. Use of ChIP Assays to Analyze the Cofactors and Histone Modifications in Transcriptional Regulation by TR in Xenopus Oocytes

3.1.1. Preparation of Xenopus Oocytes

Xenopus oocytes have long been used for transcriptional studies by microinjection (**22–25**). *Xenopus* oocytes have a robust capability to translate injected mRNA into protein and contain a large storage of basal transcription machinery and proteins required for chromatin assembly (**26,27**). Plasmid DNA injected into the nucleus of

Xenopus oocytes is assembled into chromatin via one of two pathways depending on the type of DNA injected (28). When double-stranded DNA (dsDNA) is injected, it is assembled in a relatively slow replication-independent manner (5–6 h), which yields less-defined nucleosomal arrays that permit a relatively high level of basal transcription. However, when single-stranded DNA (ssDNA) is injected, it rapidly undergoes synthesis of the complementary strand and is assembled into chromatin via a replication-coupled pathway, mimicking the genomic chromatin assembly process in somatic cells (28).

These features allow reconstitution of a chromatin-based transcription system by expressing transcription factors or cofactors of interest through injection of their *in vitro* synthesized mRNAs and assembling reporter DNA into chromatin with regular spaced nucleosomes via a replication-coupled chromatin assembly pathway. For instance, by injecting mRNAs encoding TR and 9-*cis* retinoid acid receptor (RXR) into the cytoplasm and a single-stranded reporter plasmid containing the T₃-regulated promoter of the *Xenopus* TRβA gene into the nucleus, we were able to reconstitute both T₃-independent repression and T₃-dependent transcriptional activation by the TR/RXR heterodimer in *Xenopus* oocytes (16,20).

Xenopus laevis can be raised in the laboratory, as discussed in **ref. 29**, or purchased from commercial sources (Nasco). Because of the long life cycle of *X. laevis*, it is more convenient to purchase mature female frogs from commercial sources and maintain them in the laboratory. Because each mature female frog contains tens of thousand of oocytes, costs can be reduced by using each frog twice for obtaining stage VI oocytes. For oocyte collection, we use a modified protocol initially developed by Smith et al. to anesthetize the frog and surgically remove a sufficient amount of ovary (30). Then, the ovary is digested with collagenase to release individual oocytes and free them of follicle cells and blood vessels.

1. Once a sufficient quantity of ovary is obtained (30), cut the isolated ovary into small pieces with scissors and place into a 50-mL tube filled with 1X OR2 buffer.
2. Wash the oocytes five or six times with 30 to 40 mL 1X OR2 buffer.
3. Weigh 15 mg of collagenase, place in a 15-mL tube, and dissolve in approx 5 mL of 1X OR2 buffer. Pour off as much OR2 buffer from the oocytes as possible and then add the collagenase solution. Add more OR2 to a final volume of 15 mL (final collagenase concentration of 1 mg/mL).
4. Place the tube on a shaker platform and agitate for approx 1 h. This incubation time varies with different lots of collagenase. After 45 min, take a small sample of oocytes and examine the oocytes under a stereomicroscope. The majority should be separate from one another and be free of follicle cells and blood vessels. If not, continue the incubation and check again every 10 min. Do not overtreat with collagenase as this will damage the oocytes.
5. Wash oocytes six times with 1X OR2 buffer.
6. Wash oocytes twice with 1X MBSH plus antibiotics (100 μg/mL penicillin and 100 μg/mL streptomycin).
7. Transfer oocytes to a Petri dish containing 1X MBSH plus antibiotics and leave at 18°C for at least 3 h or overnight to allow recovery from collagenase treatment.

3.1.2. Microinjection of *Xenopus* Oocytes

After recovery, healthy stage VI oocytes are selected for microinjection. Stage VI *Xenopus* oocytes are quite large (about 1200 μm) and thus can be easily injected with different types of microinjectors. We prefer Nanoject II from Drummond Scientific Company because it allows injection of variable volumes ranging from 4.6 to 73.6 nL. It is relatively simple to inject mRNAs into the cytoplasm of oocytes for protein expression, whereas injection of reporter DNA into the nucleus (**Fig. 3**) requires some practice.

For preparation of mRNA in vitro, we routinely use the mMMESSAGE mMACHINE kit (Ambion) according to the manufacturer's instructions. This kit allows synthesis of approx 10 to 20 μg of mRNA containing a 5' cap from about 1 μg of template DNA. In addition to its role in mRNA stabilization, the 5' cap is known to increase the translation efficiency of injected mRNA in *Xenopus* oocytes at least fivefold. Because in general a poly(A) tail will increase the stability and translation efficiency of mRNA, we routinely clone all genes for oocyte expression into a pSP64poly(A) vector (Promega). Usually, the level of protein expression in the oocytes is correlated with the amount of mRNA injected until the translation capacity of the oocytes is saturated.

Either dsDNA or ssDNA can be used for injection. A good protocol for preparation of ssDNA from M13 or phagemid constructs can be found in *Current Protocols in Molecular Biology* (**31**). One advantage offered by injection of ssDNA reporter is that it will undergo a rapid, one-round complementary DNA strand synthesis and assemble into chromatin via a replication coupled-chromatin assembly. This feature makes injection of ssDNA reporter ideal for studying the transcriptional regulation in the context of chromatin.

1. Select a sufficient number of healthy stage VI oocytes with a dissecting microscope and transfer them to a new Petri dish with MBSH buffer.
2. Pull injection needles from glass tubes (3.5-in. Drummond 3-000-203-G/X) with a needle puller.
3. Open the end of needles by cutting with a razor blade. The size of the opening should be suitable for injection but not too large to cause oocyte damage.
4. Completely fill the glass needle with light mineral oil (Fisher Scientific) using a 10-mL syringe equipped with a 26-gage needle.
5. Assemble a needle onto the nanoinjector and fill the needle with a DNA or mRNA sample for injection (*see Note 1*).
6. Transfer oocytes to an injection plate with a plastic transfer pipet (Samco).
7. For injection of mRNA (e.g., mRNA for Gal4-TR or a mixture of TR and RXR mRNAs) into the cytoplasm of the oocytes, there is no need to orient oocytes in a specific position. Inject mRNA at a volume of 18.4 nL/oocyte or a desired volume ranging from 4.7 to 50 nL. The mRNA can be dissolved in distilled water, and the concentration of mRNA for injection should be determined experimentally (in a range from 10 ng/ μL to 5 $\mu\text{g}/\mu\text{L}$).
8. For injection of DNA (dsDNA or ssDNA) into the nucleus (*see Note 2*), use forceps to manually orient the oocytes under the microscope with the animal hemisphere (brown or dark pigment) facing up. As illustrated in **Fig. 3**, the nucleus of the *Xenopus* oocyte is located closer to the animal pole; therefore, the injection needle must be pushed into the oocyte from the center point of the animal pole in parallel with the axis of the animal-

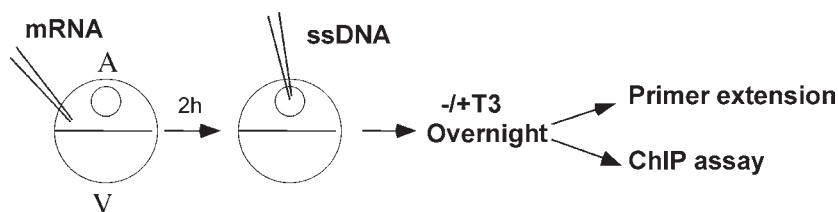


Fig. 3. Diagram illustrating how to inject DNA and mRNA into *Xenopus* oocytes for studying transcriptional regulation by TR. A, animal hemisphere; V, vegetal hemisphere; GV, germinal vesicle (nucleus).

vegetal pole and must penetrate only about one-fifth to one-fourth of the diameter of the oocyte to ensure successful injection of DNA into the nucleus. Because the nucleus (germinal vesicle) has a volume of approx 50 nL, we usually inject no more than 18.4 nL of DNA solution into each nuclei to reduce leakage of DNA into cytoplasm.

9. Transfer injected oocytes into 6- or 12-well plates. Add 2 to 3 mL MBSH buffer and incubate in a 18°C incubator for 1 to 6 h depending on the experimental design.
10. Transfer the injected oocytes to the injection plate again and inject them with RNA (if DNA is injected first) or reporter DNA (if mRNA is injected first) (*see Note 3*). In general, we inject mRNA first to allow protein synthesis before injection of reporter DNA. The time between two injections usually has little, if any, effect on the final results.
11. Treat the oocytes according to your experimental design. In our example, we incubate the injected oocytes (15–20 oocytes/group) with or without T₃ (50 nM) overnight.

3.1.3. Use of ChIP Assays to Analyze the Cofactors and Histone Modifications Involved in Transcriptional Regulation by TR in *Xenopus* Oocytes

1. After overnight incubation, select an equal number of healthy oocytes (10–15) from each group and crosslink histones or nonhistone proteins to DNA by adding formaldehyde (37%) to a final concentration of 1%. Shake for 10 to 15 min at room temperature.
2. Transfer each group of oocytes to a 1.5-mL tube. Wash the oocytes with 1 mL MBSH buffer twice. Resuspend oocytes in 1 mL 100 mM Tris-HCl, pH 9.4, and 10 mM DTT and incubate at 30°C for 15 min to stop formaldehyde activity.
3. Wash the oocytes once with 0.8 mL homogenization buffer and resuspend in 0.8 mL of homogenization buffer (*see Note 4*). Homogenize the oocytes by pipeting.
4. Place the tubes in a floating rack in a container filled with ice water. Sonicate using a Branson Sonifier 250 or equivalent machine. In our laboratory, 50 pulses at 40% duty cycle and 40% output repeatedly yields sheared DNA with an average length of 1 kb. The tip of the sonicator should almost touch the bottom of the tube.
5. Dilute the extracts with 0.6 mL cold ChIP I buffer. Centrifuge in a cold room at top speed for 10 min. Transfer clean supernatants to new tubes. From here, all steps should be performed at 4°C unless otherwise indicated.
6. To reduce nonspecific background, preclear the chromatin solution by adding 50 µL of salmon sperm DNA/protein A agarose or sepharose CL-4B beads (Amersham) and incubating 2 h at 4°C with rotation.
7. Pellet beads by brief centrifugation (1000 ref for 2 min) and collect supernatant fraction.
8. Keep a portion of this chromatin solution (20 µL) to check the amount of input DNA present in different samples before immunoprecipitation.

9. For ChIP assays using antibodies against histones or specific modified histones, mix 50 μL clean extracts with 150 μL ChIP I buffer, 1 μL antibody, and 5 μL salmon sperm DNA/protein A or G agarose (50% slurry) in a 0.5-mL tube. For cofactors such as corepressors SMRT and N-CoR, use 100 μL extract and add an appropriate amount of specific antibody (usually 1–2 μL of unpurified or purified antibody) and 5 μL of salmon sperm DNA/protein A agarose (*see Note 5*).
10. Incubate overnight with rotation in a cold room.
11. Pellet beads by centrifugation (1000 rcf, 1 min) and wash sequentially with 0.4 mL ChIP buffers I, II, and III and TE buffer in a cold room (10 min per wash) (*see Note 6*).
12. Add 100 μL elution buffer plus 0.5 μL of proteinase K (10 mg/mL) to each tube and to input samples. Vortex briefly and reverse crosslink in a 65°C incubator with rotation for at least 6 h or overnight.
13. Add 12 μL of 3M NaOAc, pH 5.2, and extract with phenol/chloroform once and chloroform once. Add 5 μg glycogen to each sample and precipitate DNA by addition of 3 volumes of ethanol. Incubate at –80°C for 20 to 30 min before centrifuging at 4°C for 15 min at top speed. Rinse pellets with 150 μL 70% ethanol and centrifuge at top speed for 5 min at room temperature. Remove all ethanol and allow the pellets to completely air-dry.
14. Dissolve DNA in 20 μL (80 μL for input samples) 10 mM Tris-HCl, pH 8.0. Use 4 μL of sample for PCR in a final volume of 20 μL . The conditions for PCR reactions have to be determined empirically (*see Note 7*).

Example: assemble a 20- μL reaction on ice as follows:

2 μL	10X Taq polymerase Mg^{2+} -free buffer
2 μL	25 mM MgCl_2
25 ng (0.1 μL)	Forward Primer
25 ng (0.1 μL)	Reverse Primer
0.1 μL	25 mM dNTPs
0.1 μL	Taq polymerase (5 u/ μL)
0.1 μL	$[\alpha\text{-}^{32}\text{P}]\text{-dCTP}$ or $[\alpha\text{-}^{32}\text{P}]\text{-dATP}$
4 μL	ChIP or Input DNA
11.5 μL	Water

PCR: 94°C for 30 s, 63°C for 45 s, 72°C for 45 s, 18 to 24 cycles depending on the intensity of signals, then 72°C for 5 min.

15. Add 4 μL 6X DNA loading buffer to each tube. Prepare a 5 to 6% polyacrylamide gel with 0.5X TBE. Load 3 to 4 μL of each PCR reaction per lane. Run the gel at 300 V for 40 min to 1 h. Dry the gel on chromatography paper and visualize the results by autoradiography. Also, real-time PCR (Applied Biosystems, 7000 sequence detection system) is quite useful for quantitative analysis of the ChIP assay.

3.2. Use of ChIP for Investigating TR Action in Development

Anuran metamorphosis is a postembryonic process controlled by T_3 (32,33). T_3 exerts its effects on various target tissues via binding to TRs. The presence of TRs in premetamorphic as well as metamorphosing tadpoles, but not embryos, suggests several testable hypotheses regarding TR binding and targeting chromatin remodeling, such as histone acetylation at its target sites in development. For example, as $\text{TR}\alpha$ and $\text{RXR}\alpha$ are known to be present in the premetamorphic tadpole before the onset of thyroid hormone synthesis, it has been hypothesized that unliganded TR/RXR heterodimers

recruit corepressors such as SMRT and N-CoR for repression through histone deacetylation in premetamorphic tadpoles to ensure proper animal growth before metamorphosis (12). Using the ChIP protocol described next, we have been able to investigate the binding of TR to DNA, the recruitment of transcriptional cofactors, and changes in histone acetylation at T_3 target genes in whole tadpoles or specific tissues during development (12–14). Such an approach should be applicable to other developmental systems as well.

An example of the use of ChIP assays to study changes in chromatin-associated proteins at TR-regulated promoters *in vivo* is illustrated in Fig. 4. Premetamorphic tadpoles do not produce T_3 ; therefore, TR-regulated genes are repressed by unliganded TR/RXR heterodimers. The data in Fig. 4B show that the corepressors N-CoR and SMRT associate with TR-regulated gene promoters in premetamorphic tadpoles; however, upon treatment with T_3 , the corepressors dissociate. Likewise, N-CoR and SMRT dissociate from TR target genes during natural metamorphosis (Fig. 4C).

3.2.1. Tadpole Treatment and Tissue Preparation

Keep 10 tadpoles at the same stage (stage 54 and/or 62) in a container with or without T_3 (~5–10 nM T_3). T_3 can be added directly to the tadpole-rearing water. After 24 to 48 h treatment, individual tissues, such as tail, intestine, liver, and hind limbs, or whole animals can be prepared for ChIP assay.

3.2.2. Nuclei Preparation From the Tissue Samples

3.2.2.1. CROSSLINKING AND NUCLEI PREPARATION FOR TAIL SAMPLES

1. Animals are anesthetized by placing them on ice for 20 min and then sacrificed by decapitation. To crosslink endogenous proteins and target genomic DNA, isolated tails are placed in 5 mL nuclei extraction buffer A and crushed gently in a 15 mL Dounce homogenizer (Kontes). Repeat douncing until the pestle can move smoothly (*see Note 8*).
2. Place the crushed sample into 15-mL tubes using wide-bore pipet tips (Stratagene) and add 134 μ L of 37% formaldehyde (final concentration is 1%). Mix well, place the samples on ice for 10 min, and follow by incubation at room temperature for 20 min.
3. Transfer the samples into 1.5-mL tubes (five tubes for each sample) and centrifuge at 6000 rcf for 5 min. Remove the supernatant and add 1 mL buffer B to each tube. Resuspend the pellet with wide-bore pipet tips and place in the extract back into the 15-mL Dounce homogenizer. Homogenize again (~10 strokes).
4. Transfer the samples into 10-mL centrifuge tubes (Beckman, 331372, 14 \times 89 mm). Add 1 mL buffer C, mix well, and add buffer B to 10 mL. A clear layer of buffer B should be seen at the bottom of the tubes. Centrifuge at 130,000 rcf for 3 h at 4°C to pellet the nuclei.

3.2.2.2. CROSSLINKING AND NUCLEI PREPARATION FOR INTESTINE AND LIVER SAMPLES

1. Use 1 mL nuclei extraction buffer A instead of 5 mL as for the tail. The tissues are crushed gently in a 2 mL Dounce homogenizer (Kontes). Continue homogenizing until the intestine fragments are ground to very small pieces.
2. Place the crushed samples into 1.5-mL tubes using wide-bore pipet tips and add 28 μ L of 37% formaldehyde (final concentration is 1%). Mix well, place the samples on ice for 10 min, and follow by incubation at room temperature for 20 min.

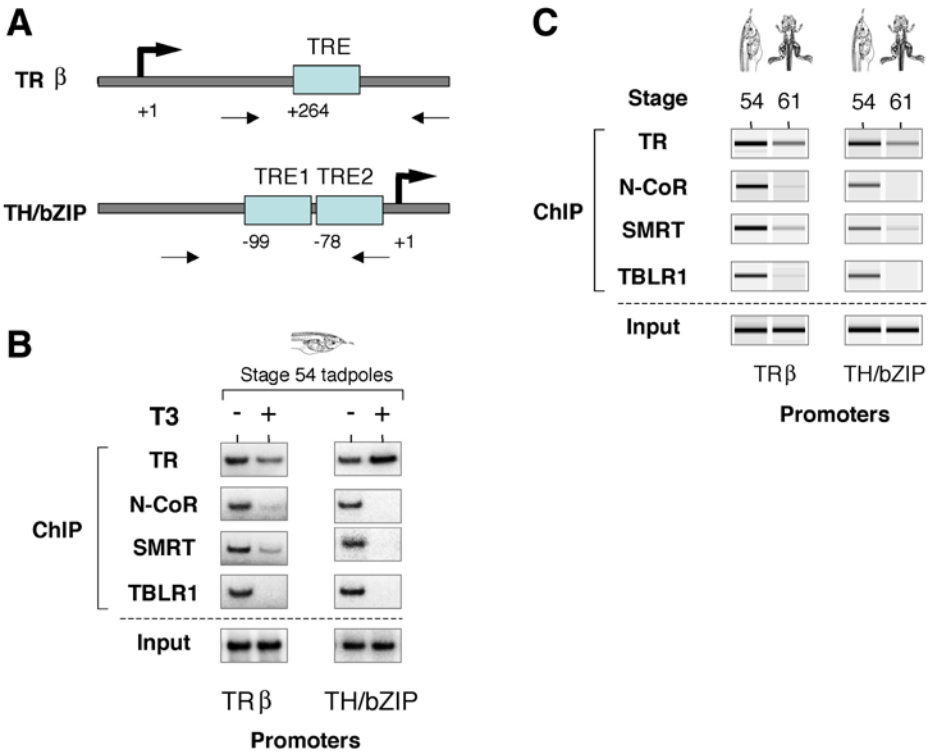


Fig. 4. N-CoR/SMRT-TBLR1 corepressor complexes associate with T_3 -dependent promoters in the intestine of premetamorphic but not metamorphosing tadpoles. **(A)** Schematic representation of the *Xenopus* TR β and TH/bZip promoters, which are directly regulated by TR (34,35). Each promoter has one or two TREs as indicated. PCR primers for ChIP are shown as thin arrows. Transcription start sites are indicated as +1. **(B)** T_3 treatment of premetamorphic tadpoles induces the dissociation of corepressors from TR target promoters. ChIP assays were carried on intestines isolated from premetamorphic stage 54 tadpoles treated with or without 5 nM T_3 for 24 h. Anti-TR, N-CoR, SMRT, and TBLR1 antibodies were used for immunoprecipitation. The precipitated DNA was amplified by PCR in the presence of [α - 32 P]-dCTP with primers specific for the TR β or TH/bZip promoter as indicated, and the 32 P-labeled products were analyzed on a 6% polyacrylamide gel. After drying the gel, the signals were detected using a PhosphorImager. **(C)** The dissociation of N-CoR/SMRT-TBLR1 corepressor complexes from TR target promoters is correlated with natural metamorphosis. Intestines from tadpoles at premetamorphic stage 54 and tadpoles at the climax of metamorphosis, stage 61, were isolated for ChIP. Anti-TR, N-CoR, SMRT and TBLR1 antibodies were used for immunoprecipitation. The precipitated DNA was amplified by PCR with primers specific for the TR β or TH/bZip promoter as indicated. The PCR products were analyzed with the DNA bioanalyzer system (Agilent Technologies). The digitized signals in each lane were converted into the digital gel-like images shown here. See ref. 13 for more details.

3. Centrifuge at 6000 rcf for 5 min. Remove the supernatant and add 1 mL buffer B. Mix the pellet well with a wide-bore pipet tip and transfer the sample into a 2-mL Dounce. Homogenize again (~10 strokes).
4. Transfer the sample into a 1.7-mL ultracentrifuge tube (Beckman, 357448) and centrifuge at 130,000 rcf for 3 h at 4°C.

3.2.3. Chromatin Preparation From Tail, Intestine, and Liver Samples

1. After the 3-h centrifugation, a pellet of nuclei should be seen at the bottom of each tube. Remove the supernatant and resuspend the pellet in 1 mL buffer C.
2. Centrifuge at 6000 rcf for 5 min and remove supernatant.
3. Add SDS lysis buffer (1 mL for tail, 500–800 μ L for intestine and liver samples). Incubate at room temperature for 15 min (*see Note 9*).
4. Sonicate the lysed samples on ice to reduce DNA fragments to 200 to 1000 bp. Duration of sonication time should be predetermined (from 20 s to 5 min). Centrifuge at 20,000 rcf for 15 min to remove the debris.
5. Transfer the supernatant (chromatin DNA/protein samples) into new tubes and check the DNA concentration by measuring the optical density at 260 nm. These chromatin samples can be stored at –80°C. Aliquot to avoid repeated freezing and thawing. Samples should be snap-frozen in liquid nitrogen.

3.2.4. ChIP Using Antibodies Against Histones or Nonhistone Proteins

1. Adjust the DNA concentration to 100 ng/ μ L. Use SDS lysis buffer for the dilution.
2. Dilute the samples to 10 ng/ μ L with ChIP dilution buffer. (For example, take 100 μ L of 100 ng/ μ L DNA/protein sample in a 1.5-mL tube and add 900 μ L of ChIP dilution buffer; *see Note 10*.)
3. To reduce nonspecific DNA/protein binding to the agarose, preclearing is helpful. Add 60 μ L salmon sperm DNA/protein A or G agarose (50% slurry) to 1 mL of diluted ChIP sample. Mix gently for 30 min at 4°C. After centrifugation at 1000 rcf for 1 min, the supernatant is ready for ChIP analysis using specific antibodies. For input controls, 20 μ L of each sample should be saved. These samples are used directly for elution and reverse crosslinking.
4. Place 1 mL of the precleared sample in a 1.5-mL slick tube (prelubricated polypropylene microcentrifuge tubes) and add appropriate volume of antibody (*see Note 11*). Incubate at 4°C with rotation for at least 4 h.
5. After incubation, add 40 μ L salmon sperm DNA/protein A or G agarose (50% slurry). Incubate for 1 h in a cold room to allow the binding of the antibodies to the beads.
6. Pellet the beads by centrifugation (1000 rcf, 1 min) and wash sequentially in a cold room with ChIP wash buffers I, II, III, and TE. Use 0.8 mL buffer for each wash and rotate for 10 to min.
7. After the fourth wash, completely remove the supernatant with flat capillary tips (Stratagene).
8. Elution and reverse crosslinking: add 100 μ L of elution buffer plus 0.5 μ L proteinase K (10 mg/mL) to each tube. Vortex briefly and mix using a rotator for 30 min at room temperature. For reverse crosslinking, incubate samples at 65°C for 6 h to overnight.
9. Purify DNA by phenol/chloroform extraction as described in Subheading 3.1.3. or using a Qiagen PCR purification kit.
10. Dissolve DNA in 50 μ L water or 10 mM Tris-HCl, pH 8.0. For each PCR reaction, 5 μ L (10%) of DNA solution can be used. Conventional PCR using [α -³²P]-dNTP followed by polyacrylamide gel electrophoresis can be applied for DNA amplification and detection. Gels are dried and the bands are visualized by autoradiography or phosphorimaging.

4. Notes

1. Based on our experience, almost any gene cloned into a vector containing a viral promoter such as SP6, T7, or T₃ can be transcribed into mRNA in vitro. However, our laboratory only uses the pSP64-poly(A) vector for in vitro mRNA synthesis because this vector provides a poly(A) tail. Before in vitro transcription, the expression construct must be linearized using an appropriate restriction enzyme that cuts downstream of the poly(A) tail. We normally inject mRNA at a concentration of 10 ng to 1 mg/mL in a volume of 18.4 nL per oocyte. It is easier to adjust the concentration of mRNA rather than the volume of injection by making a highly concentrated mRNA stock. The concentration of mRNA for injection should be determined experimentally by titration. We routinely use a series of threefold dilutions to determine the optimal mRNA concentration for each experiment. The concentration of DNA reporter injected ranges from 10 to 500 ng/μL depending on the strength of the promoter used and the purpose of the experiment.
2. To make plasmid ssDNA for injection, the promoters of interest must be cloned into an M13 or phagemid-based vector such as pBluescript II. The quality of plasmid dsDNA prepared using common miniprep or large-scale isolation kits is usually suitable for oocyte injection. The DNA for injection can be dissolved in distilled water. Because the levels of transcription vary from one promoter to another, the optimal concentration of DNA injected should be determined empirically. We routinely inject ssDNA or dsDNA at a concentration ranging from 10 to 100 ng/μL in a volume of 18.4 nL/oocyte. A more detailed discussion on how to inject mRNA and DNA into *Xenopus* oocytes can be found in **ref. 34**.
3. The order of injection of mRNA or DNA can be reversed. Although we normally inject mRNA before DNA, one can inject DNA first to assemble DNA into chromatin and then inject mRNA to express the protein of interest. This provides an opportunity to test whether a transcription factor has the capacity to bind to and regulate transcription of its target gene preassembled into chromatin. Using this strategy, we have demonstrated that TR and RXR have the capacity to bind to their recognition sequence (the thyroid response element [TRE]) preassembled into chromatin and repress or activate transcription depending on the absence or the presence of T₃ (**16**).
4. Unlike the protocol for ChIP assay using tadpoles or tissues, a buffer without SDS is used to homogenate oocytes. Inclusion of SDS in this buffer will solubilize storage yolk proteins and result in increased background. In addition, most antibodies work better in the absence of SDS.
5. Because there is always a certain level of nonspecific association of chromatin with protein A/G agarose beads, it is important to set up negative controls such as (1) without addition of antibody, (2) preimmune serum if a unpurified serum is used for ChIP, and (3) an unrelated antibody. In addition, the amount of antibody used must be carefully titrated. An insufficient amount of antibody may fail to reveal differences. Likewise, an excess amount of antibody may lead to high background. Both polyclonal and monoclonal antibodies may be used for ChIP, although polyclonal antibodies are preferred.
6. The ChIP wash buffers I, II, and III contain 0.1 to 0.5% deoxycholate instead of 0.1% SDS. From experience, we have found some antibodies do not work well in the presence of 0.1% SDS.
7. Primers are designed to yield a PCR product 100 to 200 bp in size. The specificity of primers should be verified before beginning a ChIP assay.
8. The purpose here is to disrupt the tissues into cells or tiny pieces to allow efficient crosslinking by formaldehyde and subsequently to isolate the nuclei. Preparation of nuclei helps to reduce nonspecific background in the ChIP assay.

9. The SDS lysis buffer is used here to help solubilize chromatin.
10. If it is difficult to obtain sufficient DNA, try lower concentrations; 5 ng/ μ L may also work fine. Make sure that the 10-fold dilution using ChIP dilution buffer is carried out to dilute the SDS concentration and adjust the salt condition.
11. Immunoprecipitation is done in samples with 0.1% SDS. It is thus recommended to test multiple different antibodies against the same protein and use the one that works well in the presence of 0.1% SDS. Again, both antiserum and purified antibodies can be used. Because efficiency and specificity of each antibody are different, antibody titration should be done before the experiment. Using preimmune serum as a negative control is helpful to ensure the specificity of each antiserum and wash condition.

References

1. Berger, S. L. (2002) Histone modifications in transcriptional regulation. *Curr. Opin. Genet. Dev.* **12**, 142–148.
2. Fischle, W., Wang, Y., and Allis, C. D. (2003) Histone and chromatin cross-talk. *Curr. Opin. Cell. Biol.* **15**, 172–183.
3. Levine, M. and Tjian, R. (2003) Transcription regulation and animal diversity. *Nature* **424**, 147–151.
4. Li, E. (2002) Chromatin modification and epigenetic reprogramming in mammalian development. *Nat. Rev. Genet.* **3**, 662–673.
5. Kuo, M. H. and Allis, C. D. (1999) In vivo cross-linking and immunoprecipitation for studying dynamic protein:DNA associations in a chromatin environment. *Methods* **19**, 425–433.
6. Orlando, V. (2000) Mapping chromosomal proteins in vivo by formaldehyde-crosslinked-chromatin immunoprecipitation. *Trends Biochem. Sci.* **25**, 99–104.
7. Jackson, V. (1978) Studies on histone organization in the nucleosome using formaldehyde as a reversible cross-linking agent. *Cell* **15**, 945–954.
8. Jackson, V. and Chalkley, R. (1981) A new method for the isolation of replicative chromatin: selective deposition of histone on both new and old DNA. *Cell* **23**, 121–134.
9. Li, J., Lin, Q., Wang, W., Wade, P., and Wong, J. (2002) Specific targeting and constitutive association of histone deacetylase complexes during transcriptional repression. *Genes Dev.* **16**, 687–692.
10. Li, J., Lin, Q., Yoon, H. G., Huang, Z. Q., Strahl, B. D., Allis, C. D., and Wong, J. (2002) Involvement of histone methylation and phosphorylation in regulation of transcription by thyroid hormone receptor. *Mol. Cell Biol.* **22**, 5688–5697.
11. Huang, Z. Q., Li, J., Sachs, L. M., Cole, P. A., and Wong, J. (2003) A role for cofactor-cofactor and cofactor-histone interactions in targeting p300, SWI/SNF and mediator for transcription. *EMBO J.* **22**, 2146–2155.
12. Sachs, L. M. and Shi, Y. B. (2000) Targeted chromatin binding and histone acetylation in vivo by thyroid hormone receptor during amphibian development. *Proc. Natl. Acad. Sci USA* **97**, 13,138–13,143.
13. Tomita, A., Buchholz, D. R., and Shi, Y. B. (2004) Recruitment of N-CoR/SMRT-TBLR1 corepressor complex by unliganded thyroid hormone receptor for gene repression during frog development. *Mol. Cell Biol.* **24**, 3337–3346.
14. Buchholz, D. R., Hsia, S. C., Fu, L., and Shi, Y. B. (2003) A dominant-negative thyroid hormone receptor blocks amphibian metamorphosis by retaining corepressors at target genes. *Mol. Cell Biol.* **23**, 6750–6758.

15. Wang, H. C., Beer, B., Sassano, D., Blume, A. J., and Ziai, M. R. (1991) Gene expression in *Xenopus* oocytes. *Int. J. Biochem.* **23**, 271–276.
16. Wong, J., Shi, Y. B., and Wolffe, A. P. (1995) A role for nucleosome assembly in both silencing and activation of the *Xenopus* TR β A gene by the thyroid hormone receptor. *Genes Dev.* **9**, 2696–2711.
17. Wolffe, A. P., Wong, J., Li, Q., Levi, B. Z., and Shi, Y. B. (1997) Three steps in the regulation of transcription by the thyroid hormone receptor: establishment of a repressive chromatin structure, disruption of chromatin and transcriptional activation. *Biochem. Soc. Trans.* **25**, 612–615.
18. Wong, J. (2002) Transcriptional regulation by thyroid hormone receptor in chromatin. *Methods Mol. Biol.* **202**, 177–194.
19. Nieuwkoop, P. D. and Faber, J. (1956) *Normal Table of Xenopus laevis*. North Holland Publishing, Amsterdam, The Netherlands.
20. Wong, J. and Shi, Y. B. (1995) Coordinated regulation of and transcriptional activation by *Xenopus* thyroid hormone and retinoid X receptors. *J. Biol. Chem.* **270**, 18,479–18,483.
21. Sachs, L. M., Jones, P. L., Havis, E., Rouse, N., Demeneix, B. A., and Shi, Y. B. Nuclear receptor corepressor recruitment by unliganded thyroid hormone receptor in gene repression during *Xenopus laevis* development. *Mol. Cell Biol.* **22**, 8527–8538.
22. De Robertis, E. M. and Mertz, J. E. (1977) Coupled transcription-translation of DNA injected into *Xenopus* oocytes. *Cell* **12**, 175–182.
23. Mertz, J. E. and Gurdon, J. B. (1977) Purified DNAs are transcribed after microinjection into *Xenopus* oocytes. *Proc. Natl. Acad. Sci. USA* **74**, 1502–1506.
24. Wang, H. C., Beer, B., Sassano, D., Blume, A. J., and Ziai, M. R. (1991) Gene expression in *Xenopus* oocytes. *Int. J. Biochem.* **23**, 271–276.
25. Etkin, L. D. (1982) Analysis of the mechanisms involved in gene regulation and cell differentiation by microinjection of purified genes and somatic cell nuclei into amphibian oocytes and eggs. *Differentiation* **21**, 149–159.
26. Laskey, R. A., Mills, A. D., and Morris, N. R. (1977) Assembly of SV40 chromatin in a cell-free system from *Xenopus* eggs. *Cell* **10**, 237–243.
27. Wickens, M. P., Woo, S., O'Malley, B. W., and Gurdon, J. B. (1980) Expression of a chicken chromosomal ovalbumin gene injected into frog oocyte nuclei. *Nature* **285**, 628–634.
28. Almouzni, G. and Wolffe, A. P. (1993) Replication-coupled chromatin assembly is required for the repression of basal transcription in vivo. *Genes Dev.* **7**, 2033–2047.
29. Wu, M. and Gerhart, J. Raising *Xenopus* in the laboratory. (1991) *Methods Cell Biol.* **36**, 3–18.
30. Smith, L. D., Xu, W. L., and Varnold, R. L. Oogenesis and oocyte isolation. (1991) *Methods Cell Biol.* **36**, 45–60.
31. Ausubel, F. M., Brent, R., Kingston, R. E., Moore, D. D., Seidman, J. G., Smith, J. A., Struhl, K. (2000) *Current Protocols in Molecular Biology*. John Wiley & Sons, Inc., Hoboken, NJ.
32. Dodd, M. H. I. and Dodd, J. M. (1976) The biology of metamorphosis, in *Physiology of the Amphibia* (Lofts, B., ed.), Academic Press, New York, pp. 185–223.
33. Shi, Y. B., Sachs, L. M., Jones, P., Li, Q., and Ishizuya-Oka, A. (1998) Thyroid hormone regulation of *Xenopus laevis* metamorphosis: functions of thyroid hormone receptors and roles of extracellular matrix remodeling. *Wound Repair Regen.* **6**, 314–322.
34. Kay, B. K. (1991) *Xenopus laevis*: practical uses in cell and molecular biology. Injections of oocytes and embryos. *Methods Cell Biol.* **36**, 663–669.

35. Ranjan, M., Wong, J., and Shi, Y. B. (1994) Transcriptional repression of *Xenopus* TR β gene is mediated by a thyroid hormone response element located near the start site. *J. Biol. Chem.* **269**, 24,699–24,705.
36. Furlow, J. D. and Brown, D. D. (1999) In vitro and in vivo analysis of the regulation of a transcription factor gene by thyroid hormone during *Xenopus laevis* metamorphosis. *Mol. Endocrinol.* **13**, 2076–2089.

Cytoplasmic mRNA Polyadenylation and Translation Assays

Maria Piqué, José Manuel López, and Raúl Méndez

Summary

Vertebrate development is directed by maternally inherited messenger RNAs that are synthesized during the very long period of oogenesis. These dormant mRNAs usually contain short poly(A) tails and are stored as mRNA ribonucleoproteins that preclude ribosomal recruitment. In *Xenopus laevis* oocytes treated with the meiosis-inducing hormone progesterone, their poly(A) tails are elongated, and the mRNAs are mobilized into polyosomes. This cytoplasmic polyadenylation is directed by *cis*-acting elements located in the 3' untranslated region of the mRNAs. However, the cytoplasmic polyadenylation of all the maternal mRNAs does not take place at once, but rather the translational activation of specific mRNAs is regulated in a sequential manner during meiosis and early development. This chapter describes the use of microinjected reporter mRNAs and radiolabeled RNAs into *Xenopus* oocytes to study the mRNA translational control by cytoplasmic polyadenylation. Cyclin B1 mRNA is used to illustrate the methods described.

Key Words: CPEB; cyclin B1; cytoplasmic polyadenylation; translational control; 3'-UTR; *Xenopus* oocytes.

1. Introduction

The role of the 3' untranslated regions (3'-UTRs) of specific messenger RNAs (mRNAs) in the regulation of the poly(A) tail length and translation has been known for over 20 yr (for a review, *see* **ref. 1** and references therein), but only recently have we begun to unveil the molecular mechanism governing this particular system of controlling gene expression. Most of our current understanding of cytoplasmic polyadenylation is derived from experiments performed in *Xenopus* oocytes, not only because this is a prominent mechanism in the control of maternal gene expression during meiosis and early development (**2–5**), but also because of the many technical advantages offered by *Xenopus* oocytes. The knowledge acquired in *Xenopus* oocytes has then been extrapolated to other systems, including oocytes from other species (**6–10**) and nongerm cells, such as neurons (**11,12**).

Fully grown oocytes (stage VI) are arrested at prophase I until progesterone induces resumption of meiosis (oocyte maturation). Maturation ends at metaphase II, when the

oocytes await fertilization before they can complete the final meiotic division and initiate the embryonic cell divisions.

Cytoplasmic polyadenylation and subsequent translational activation of maternal mRNAs is required in at least two steps during meiotic progression (13–18). First, at prophase I when Mos mRNA, and probably other as-yet-unidentified mRNAs (19), have to be translationally activated for the oocyte to enter metaphase I. Then, progression from metaphase I to metaphase II requires the cytoplasmic polyadenylation of a different subset of mRNAs, of which cyclin B1 is the best-characterized example (reviewed in ref. 2). These two events allowed discrimination between early (or Mos- and Cdc2-independent) and late (or Mos- and Cdc2-dependent) cytoplasmic polyadenylation (20–22).

Mos, cyclin B1, and several other dormant mRNAs in oocytes contain short poly(A) tails (~20–40 nucleotides), and it is only when these tails are elongated (to ~150 nucleotides) that translation takes place. Polyadenylation requires two elements in the 3'-UTR, the hexanucleotide AAUAAA and the nearby cytoplasmic polyadenylation element (CPE), which recruits the CPE-binding protein (CPEB). The induction of polyadenylation by this protein is regulated by two sequential phosphorylation events. First, the kinase Eg2 increases the affinity of CPEB for cleavage and polyadenylation specificity factor (CPSF) and mediates Mos polyadenylation (23,24); subsequently, Cdc2 induces hyperphosphorylation and partial degradation of CPEB and is required for cyclin B1 polyadenylation (22).

Prior to polyadenylation, the CPE-containing mRNAs, or at least some of them, are actively silenced by CPEB (25,26) through its interaction with another inhibitory protein called Maskin. Together, they block the cap-binding translation initiation factor eIF4E, preventing the recruitment of the small ribosomal subunit (27). Elongation of the poly(A) tail is both required and sufficient to release the Maskin-mediated translational repression (28).

A number of mRNAs have been shown to undergo translational control by cytoplasmic polyadenylation in both oocytes and embryos. Most of the examples correspond to mRNAs polyadenylated in oocytes in response to progesterone. From these, the consensus for CPE in *Xenopus* oocytes is derived as U₄A₁₋₂U, although alternative sequences can also be found. The CPE should be located close to the hexanucleotide, but it seems to admit a wide range of positions, from overlapping up to a distance of 100 nucleotides and even further if there is secondary structure in the 3'-UTR that effectively positions the CPE in the proximity of the hexanucleotide.

Different methods to analyze the poly(A) tail length of endogenous or injected mRNAs have been developed (29,30). *Xenopus* oocytes, in which RNA reporters can be injected into the cytoplasm, provide an ideal system to study cytoplasmic polyadenylation. By this method, it is possible to measure the functionality of any 3'-UTR in mediating translational repression and activation in response to progesterone, as well as cytoplasmic changes in the length of the poly(A) tail. Moreover, the use of exogenous transcripts means that variants can be generated to better define the functional elements in the 3'-UTR under study. Although this method is obviously best suited to study maternal *Xenopus* mRNAs, it has been successfully used to ana-

lyze the potential regulation of heterologous 3'-UTRs derived, for example, from neuronal mRNAs (11).

The study of the CPE-dependent translational repression, translational activation, and cytoplasmic polyadenylation mediated by the 3'-UTR of cyclin B1 mRNA is used to illustrate the methods described in this chapter.

2. Materials

2.1. DNA and RNA Manipulation

1. 6X DNA gel-loading buffer: 30% glycerol, 0.025% Orange G (Sigma).
2. Agarose gels in 1X TBE (see item 7) and 0.5 $\mu\text{g}/\text{mL}$ ethidium bromide.
3. Ethidium bromide solution (10 mg/mL) (Sigma); store protected from light.
4. Water-saturated phenol/chloroform/isoamyl alcohol (25/24/1).
5. Phenol/chloroform/isoamyl alcohol (25/24/1) saturated with 10 mM Tris-HCl, pH 8.0.
6. Diethyl pyrocarbonate (DEPC)-treated water: treat with 0.1% diethyl pyrocarbonate for at least 12 h at 37°C and autoclave twice.
7. 1X TBE: 90 mM Tris-borate and 2 mM ethylenediaminetetraacetic acid (EDTA), pH 8.3.
8. PAS buffer: 0.1 M Tris-HCl, 6% (w/v) *p*-aminosalicylic acid (PAS), 1% sodium dodecyl sulfate (SDS), 1 mM EDTA, pH 7.6.

2.2. Oocyte Isolation, Injection, and Treatment

1. 10X Modified Barth's solution (MBS): 880 mM NaCl, 10 mM KCl, 10 mM MgSO_4 , 50 mM of *N*-2-hydroxyethylpiperazine-*N*-2-ethanesulfonic acid (HEPES), 25 mM NaHCO_3 . Adjust pH to 7.8 with NaOH. Autoclave.
2. 1X MBS: prepare the final 1X MBS from the 10X stock and supplement with CaCl_2 to a 0.7 mM final concentration.
3. Progesterone (Sigma): prepare a 10 mM stock in 100% ethanol. Aliquot and store at -20°C .
4. Cycloheximide (Sigma): prepare a 100 mg/mL stock in 100% ethanol. Aliquot and store at -20°C .
5. Microinjection glass capillaries: 3.5 in. long, 0.53 mm internal diameter, and 1.14 mm external diameter (ref. 3-000-203-G/X, Drummond Scientific Co.).
6. Needle puller (model P-30, Sutter Instrument Co.).
7. Microinjector (automatic nanoliter injector, Nanoject II 2.3- to 96-nL variable volume, Drummond Scientific Co.).

2.3. Luciferase RNA Synthesis and Quantification

1. mMESSAGE mMACHINE kit (Ambion).
2. 2X RNA gel-loading buffer: 95% formamide, 18 mM EDTA, 0.025% SDS, 0.025% Orange G.

2.4. Dual-Luciferase Reporter Assay

1. Dual-Luciferase reporter assay kit (Promega).
2. Plate-reading luminometer equipped with two reagent injectors.

2.5. Synthesis of ^{32}P -Labeled RNA

1. 5X Transcription buffer: 200 mM Tris-HCl, pH 7.9, 30 mM MgCl_2 , 50 mM dithiothreitol, 50 mM NaCl, and 10 mM spermidine (MBI Fermentas).
2. 20 U/ μL Ribonuclease (RNase) inhibitor (MBI Fermentas).

3. 40 mM Cap analog (m⁷G(5')ppp(5')G, Ambion).
4. 800 Ci/mmol, 20 mCi/mL uridine 5'-[α-³²P] triphosphate (α-[³²P]-UTP; Amersham Pharmacia Biotech).
5. 20 U/μL T3, T7, or Sp6 RNA polymerase (MBI Fermentas).
6. 10X Ribonucleotide 5'-triphosphate mix: 5 mM adenosine 5'-triphosphate (ATP), 5 mM cytidine 5'-triphosphate (CTP), 1 mM uridine 5'-triphosphate (UTP), 0.5 mM guanosine 5'-triphosphate (GTP).
7. 2X RNA gel-loading buffer: 95% formamide, 18 mM EDTA, 0.025% SDS, 0.025% xylene cyanol, 0.025% bromophenol blue.

2.6. Denaturing Polyacrylamide Gel Electrophoresis

1. 40% Acrylamide solution (acryl/bis = 37.5/1) (BioRad).
2. 10% Ammonium persulfate. Store at 4°C protected from light.
3. 6% Polyacrylamide/8M urea gel solution in 1X TBE; store protected from light.

2.7. Oligonucleotides

1. T3Luc-s: GGAATTAACCTCACTAAAGGGGGCCAAGAAGGGCGGAAAGTC
2. B1-as: CCGGATCCGCTTTATTAAAACAGTAAAACATTAAAAACAC
3. B1(-CPE)-as: CCGGATCCGCTTTATTccAACCAGTccAACATcccAAACAC
4. c-mos antisense: TGGACATTGAGATACTGTACTAGAT

The T3Luc-s oligonucleotide contains the T3 promoter (nucleotides 3–22 of the primer) and a sequence matching the nucleotides 1670 to 1690 of the firefly luciferase Open Reading Frame (ORF; nucleotides 23–43 of the primer).

The B1-as oligonucleotide contains a sequence complementary to the 3'-UTR of *Xenopus laevis* cyclin B1 mRNA (nucleotides 1350–1382 of the Genbank accession number J03166; nucleotides 9–41 of the primer), and a *Bam*HI restriction site (nucleotides 3–8 of the primer).

The B1(-CPE)-as oligonucleotide contains a sequence partially complementary to the 3'-UTR of *X. laevis* cyclin B1 mRNA (nucleotides 1350–1382 of the Genbank accession number J03166; nucleotides 9–41 of the primer) with point mutations in the CPEs (indicated in lowercase) and a *Bam*HI restriction site (nucleotides 3–8 of the primer).

The c-mos antisense oligonucleotide is complementary to a sequence in the 3'-UTR of *X. laevis* c-mos mRNA (nucleotides 2265–2289 of the Genbank accession number X13311).

3. Methods

Particular precautions are required when working with RNA to eliminate RNase contamination. Whenever possible, solutions should be autoclaved or filtered and made with DEPC-treated water. Glassware must be baked at 180°C, and Eppendorf tubes and pipet tips should be RNase free. Filter tips are recommended. Powder-free gloves should be worn for the transcription reactions and manipulation of RNA.

3.1. Analysis of the Translational Effect of 3'-UTRs

To determine how translation is regulated by a 3'-UTR, fusion mRNAs containing the ORF of firefly luciferase followed by the 3'-UTR (luc-3'UTR) under study are generated (see Fig. 1A). These mRNAs are injected into oocytes, and their translational efficiency is determined by measuring the luciferase activity in oocyte extracts.

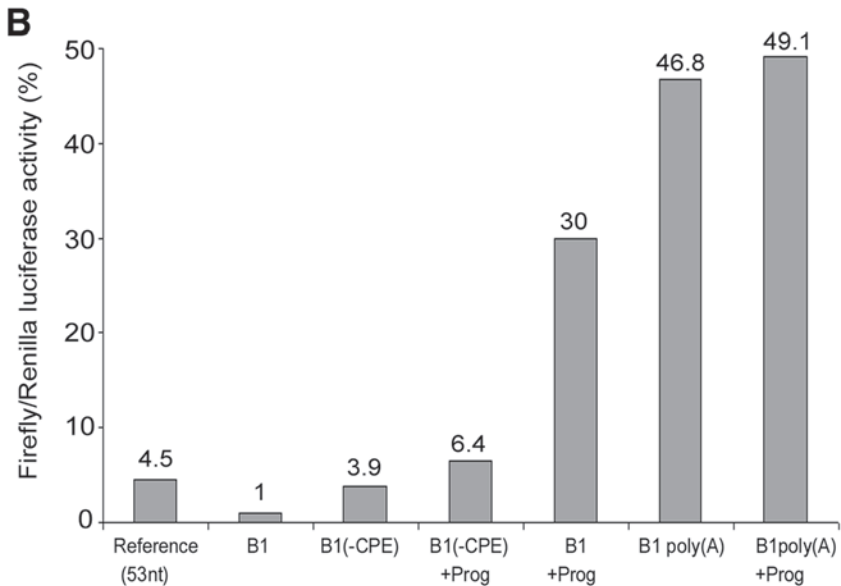
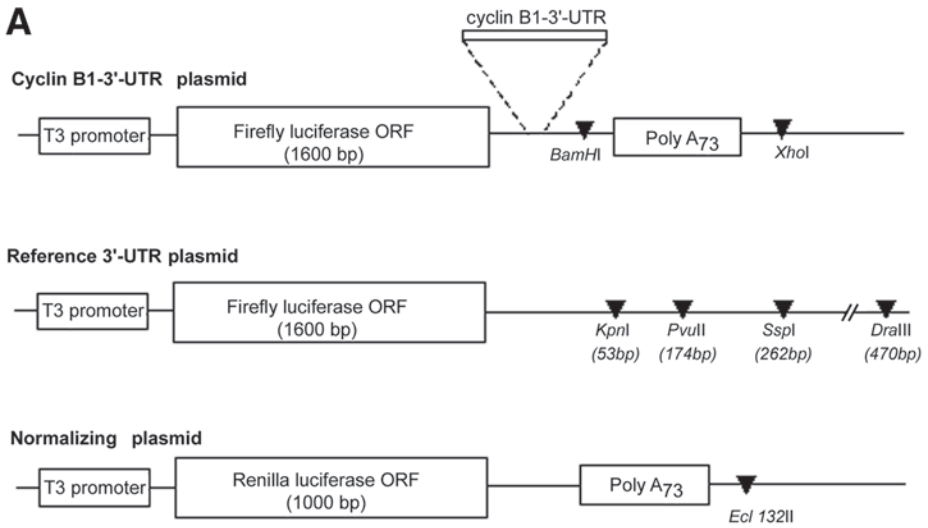


Fig. 1. (A) Schematic drawing of plasmids used for in vitro transcription. The arrows show positions of restriction sites used to linearize the plasmids. Positions of the T3 promoter, the firefly and *Renilla* luciferase Open Reading Frames (ORFs), the poly(A), and the inserted cyclin B1 3'-UTR are indicated. (B) Cyclin B1 3'-UTR-mediated translational repression and activation. Synthetic mRNAs containing luciferase coding sequences fused to the cyclin B1 3'-UTR (B1), cyclin B1 3'-UTR where the CPEs were rendered nonfunctional by point mutation [B1(-CPE)], cyclin B1 3'-UTR with a poly(A) tail [B1 poly(A)] or a control 3'-UTR of 53 nucleotides (reference 53) were coinjected with the *Renilla* luciferase normalizing mRNA. Oocytes were then incubated in the presence or absence of progesterone (Prog). The histogram plots the firefly/*Renilla* luciferase activity referred to the activity of the B1-mRNA.

To obtain a reliable measurement of the translational regulation by the 3'-UTR, two critical controls are needed. First, the activity of each studied 3'-UTR is compared with a control 3'-UTR (reference 3'-UTR) of equal length because the size of the 3'-UTR has a clear effect on translation, and this effect has to be discriminated from the activation by polyadenylation (31). Second, to control for microinjection accuracy as well as any possible mRNA degradation during the manipulation or general changes on the translational rate of individual oocytes, the fusion mRNAs containing the luc-3'UTR and reference 3'-UTR are coinjected with identical amounts of an mRNA encoding for *Renilla* luciferase as a second reporter (normalizing RNA).

To better define the role of the poly(A) tail in the translational efficiency of the reporters, use pBluescript (pBSK)-derived plasmids containing a stretch of 73 adenines 3' of the inserted 3'-UTR (6). Thus, the luc-3'UTR RNAs can now be synthesized containing 73 adenines. This additional control defines the expected degree of translational activation for an mRNA that is cytoplasmically polyadenylated. In addition, it also determines whether the poly(A) elongation is the only event responsible for the stimulation by comparing the luciferase activity of the transcribed polyadenylated mRNA in the presence and absence of progesterone.

An additional step can be incorporated to this assay to identify the time at which the translational activation takes place, early or late (see **Subheading 1.**). Both events can be easily discriminated by preventing Mos synthesis with the microinjection of a mos antisense oligonucleotide (32) (see **Note 1**) and then performing the assay as described. The progesterone-induced translational activation of the "early mRNAs" is not affected by the mos antisense oligonucleotide, whereas the activation of the "late mRNAs" is blocked (20,21).

Although the injected mRNAs are very stable in stage VI *Xenopus* oocytes, we routinely performed Northern blot analysis to confirm stability. Extract the RNA as described in **Subheading 3.2.3.** and perform the Northern blot according to standard methods (33).

For the cyclin B1 3'-UTR, we generated two fusion mRNAs containing the firefly luciferase ORF followed by the cyclin B1 3'-UTR, either wild type (B1) or a variant in which all the putative CPEs were rendered nonfunctional by point mutations [B1(-CPE)]. By studying the translational effects of the B1 and B1(-CPE) 3'-UTRs in prophase-arrested stage VI oocytes, compared with their reference 3'-UTR (control, 53 nt), we determined the CPE-dependent translational repression mediated by this 3'-UTR. As shown in **Fig. 1B**, the cyclin B1 3'-UTR, but not the cyclin B1(-CPE) 3'-UTR induced a 4.5-fold translational repression. An indirect, but quantitative, measurement of the translational activation by cytoplasmic polyadenylation was obtained by comparing the translation of the B1 and B1(-CPE) mRNAs in the absence and presence of progesterone. The cyclin B1 3'-UTR induced a 30-fold increase in translational activation after progesterone addition, which was not observed for the cyclin B1(-CPE) 3'-UTR. Cyclin B1 3'UTR plus poly(A) [B1 poly(A)] mRNA was already fully active in prophase-arrested stage VI oocytes and was not further activated by progesterone.

The methods described next outline the generation of the DNA templates (**Subheading 3.1.1.**), *in vitro* transcription (runoff method) and mRNA quantification (**Sub-**

heading 3.1.2.), RNA injection in oocytes and induction of maturation (**Subheading 3.1.3.**), and dual-luciferase reporter assay (**Subheading 3.1.4.**).

3.1.1. Generation of the DNA Templates for In Vitro Transcription

Three different plasmids are required to study the translational effects of a 3'-UTR: the luc-3'UTR plasmid, the reference 3'-UTR plasmid, and the normalizing plasmid.

The luc-3'UTR plasmid construct contains, in sequential order, the phage polymerase T3 promoter (T7 or SP6 promoters can also be used), the firefly luciferase ORF, a multicloning site, and a poly(A) stretch of 73 nucleotides followed by a unique restriction site. The multicloning site is used for the directional cloning of the 3'-UTR under study and to linearize the plasmid 5' of the poly(A) tail. The unique restriction site allows the linearization of the plasmid to generate transcripts containing the poly(A) tail (see **Fig. 1A**). This plasmid was generated as follows: the ORF of the firefly luciferase was obtained by polymerase chain reaction (PCR), adding a *SmaI* restriction site at the 5' end and *HpaI* and *BamHI* restriction sites at the 3' end. The resulting PCR product was cloned into *SmaI* and *BamHI* sites of the pBSK plasmid containing a poly(A) track of 73 residues (PBSK-A) (**6**).

To generate the cyclin B1 3'-UTR plasmid, we PCR amplified the 67 nucleotides corresponding to positions 1316 to 1380 of the *X. laevis* cyclin B1 mRNA (Genbank accession number J03166) (B1 3'-UTR in **Fig. 1A**) or a variant with the putative CPEs mutated [B1(-CPE) 3'-UTR], that were cloned into *HpaI* and *BamHI* sites of the 3'-UTR plasmid (for details of the point mutations, see **Subheading 2.7.**).

The reference 3'-UTR plasmid construct contains, in sequential order, the T3 promoter, the firefly luciferase ORF, and a polylinker sequence that is used to linearize the plasmid at different positions. The transcription of these templates generates reference mRNAs with 3'-UTRs of different lengths (see **Fig. 1A**). This plasmid was generated by inserting the firefly luciferase ORF into the *SacI* and *EcoRV* sites of the pBSK plasmid.

The normalizing plasmid construct contains, in sequential order, the T3 promoter, the *Renilla* luciferase ORF, a poly(A) stretch of 73 nucleotides, and a unique restriction site (*Ecl132 II*) (see **Fig. 1A**). The transcription of this linearized DNA will generate the normalizing mRNA. This plasmid was obtained as follows: the ORF of the *Renilla* luciferase was obtained by PCR adding a *SmaI* restriction site at the 5' end and *BglII*, *HpaI*, and *BamHI* restriction sites at the 3' end. The resulting PCR product was cloned into *SmaI* and *BamHI* sites of the pBSK plasmid. The poly(A) track of 73 residues was inserted as described by Gebauer et al. (**6**).

All, the luc-3'UTR plasmid, the reference 3'-UTR plasmid and the normalizing plasmid are linearized in the appropriate restriction site (see **Notes 2** and **3**) and purified by phenol/chloroform/isoamyl alcohol extraction and isopropanol precipitation (**33**).

3.1.2. In Vitro Transcription (Runoff Method) and mRNA Quantification

Although the method described in **Subheading 3.2.2.** can also be used for transcription of long 5'-capped mRNAs in vitro, a much better yield is obtained using commercial kits, such as the mMMESSAGE mMACHINE (Ambion). If the assay from **Subheading 3.2.2.** is performed, increase the final UTP concentration to 0.5 mM and the linearized DNA template to 1 µg. Scale up the reaction as needed.

Comparison of the translational efficiency of different transcripts requires accurate measurement of the concentration and integrity of the mRNAs. This step should be performed prior to each round of injections. An approximate measurement of the RNA concentration can be derived from the optical density (OD) at 260 nm, where 1 absorption unit equals 40 $\mu\text{g}/\text{mL}$ for single-stranded RNA (see **Note 4**). Typically, a 1/100 dilution of the transcription reaction will give an absorbance reading in the linear range of the spectrophotometer. However, any unincorporated nucleotide or partially degraded RNA or template DNA in the mixture will interfere with the measurement (see **Note 5**).

A more accurate determination of the concentration and integrity of the transcripts can be obtained by running the RNA samples in an agarose gel with ethidium bromide and quantifying the intensity of the bands. A normal 1X TBE gel is sufficient, although a formamide-loading buffer should be used and the samples heat denatured. This method is as accurate as the quantification by trace radiolabeling, with the additional advantage that the ratio of full transcript to partial products is also obtained (see **Note 6**).

1. Prepare a 2% agarose gel in 1X TBE and prerun it for 10 min at 9 V/cm to maintain the heated system, thus avoiding RNA renaturalization during electrophoresis. Denaturing gels with 1X MOPS and 10% formaldehyde may be run if secondary structures are a problem (see **Note 7**).
2. Dilute 1/20 each RNA sample (to approx 50–100 ng/ μL) and mix 3 μL of the dilutions with 3 μL of gel-loading buffer. Heat to 70°C for 5 to 10 min (see **Note 8**).
3. Load the RNAs under study and an RNA marker of known concentration as standard.
4. Run the gel for 10 min at 9 V/cm. Longer running times may result in the formation of secondary structures.
5. Photograph the gel using short-wavelength ultraviolet irradiation. Compare the intensity of fluorescence of the unknown RNA with that of the RNA standard and calculate the quantity of RNA in the samples (usually between 50 and 100 ng/ μL). An image analysis system, such as the Gel Doc 2000 hardware and the *Quantity One* software package (BioRad), will facilitate this step.
6. Make the firefly/*Renilla* mRNAs mix so the final concentration of each one is 30 ng/ μL . Check and verify this mixture by running an aliquot (5 μL) in a 2% agarose gel (as described in **steps 1–5**).

3.1.3. RNA Injection in Oocytes and Induction of Maturation

For a detailed protocol of the isolation of *Xenopus* oocytes, see Chapter 3, this volume, and refs. 34 to 36. We use 0.8 mg/mL collagenase and 0.48 mg/mL dispase II instead of collagenase alone to dissociate oocytes from follicles (see **Note 9**).

Although cytoplasmic polyadenylation seems to tolerate large quantities of substrate, the CPEB-mediated translational repression is overridden by the injection of more than 0.1 fmol of RNA per oocyte (25,26). Larger quantities of mRNA could competitively inhibit global translation and even prevent maturation. Injection of mRNAs in the order of 0.01 fmol produces enough luciferase activity that can be detected within the linear range (see **Fig. 2A,B**), ensuring that the limited masking capability of the oocytes is not overwhelmed.

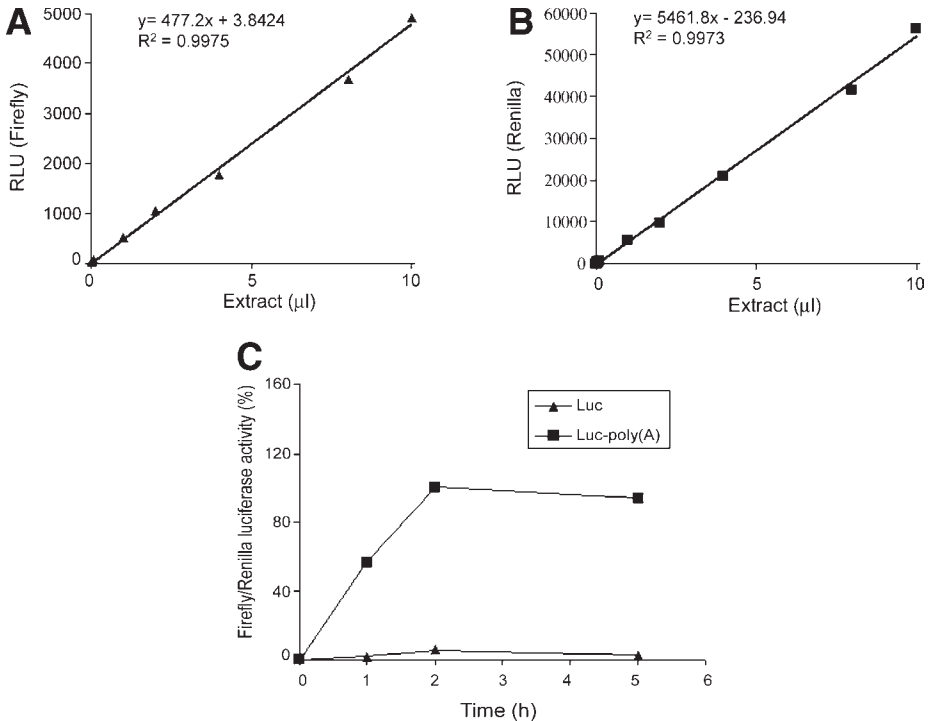


Fig. 2. Determination of the linear range of firefly and *Renilla* luciferase activities. *Xenopus* oocytes were coinjected with the luciferase/cyclin B1 3'-UTR fusion mRNA and the *Renilla* luciferase normalizing mRNA. Oocytes were then treated with progesterone, and luciferase activity was determined as described in **Subheadings 3.1.5.** and **3.1.6.** Panels display the (A) firefly and (B) *Renilla* relative luminescence units (RLU) as a function of extract volume. (C) Time-course of luciferase accumulation. The firefly luciferase mRNAs containing or not containing a 73-residue poly(A) [Luc poly(A) or (Luc), respectively] were coinjected with the *Renilla* normalizing mRNA. The oocytes were collected at the indicated times, and the luciferase activities were determined. The firefly/*Renilla* luciferase activity is plotted as a function of the incubation time, and the results are expressed as the percentage of the value at 2 h.

1. Prepare a fresh 1/66 dilution of each firefly/*Renilla* RNA mixture (0.5 ng/ μL). Heat the RNA samples to eliminate secondary structures and keep them on ice during the course of injection (*see Note 10*).
2. Prepare the microinjection needles from glass capillaries by setting the controls of the needle vertical puller at 750 for heat 1 and at 860 for the puller (*see Note 11*).
3. Backfill the needle with mineral oil using a syringe. Hold the needle with the micromanipulator at 45°. Break the needle tip with forceps to a diameter of approx 10 μm . Front-fill the needle with 1 to 2 μL of the RNA sample, avoiding the formation of air bubbles.
4. Set the automatic microinjector so that 27 nL/oocyte (0.025 fmol RNA/oocyte) is injected in fast-speed mode.

5. For each firefly/*Renilla* RNA mixture, inject 20 to 30 oocytes. The injection should be made in the middle equatorial line of the oocyte, avoiding the nucleus.
6. Separate the injected oocytes in two pools in glass dishes with 5 mL of 1X MBS. Add progesterone (10 μ M) to one of the pools (see **Note 12**).
7. Incubate the oocytes at 20°C. Check periodically and discard the unhealthy oocytes. Although the exact time of incubation varies according to the design of the experiment and the maturation rate of the oocytes, within 2 h luciferase activity reaches the steady state (see **Fig. 2C**). When analyzing the effect of progesterone, use oocytes synchronized for maturation (detected by the appearance of a white spot in the animal pole); usually more than 90% of the oocytes mature.
8. Collect the oocytes. Remove as much 1X MBS as possible and freeze the tubes in dry ice. At this step, the samples can be stored for several days at -80°C.

3.1.4. Dual-Luciferase Reporter Assay

In the dual-luciferase reporter assay, the activities of both firefly (*Photinus pyralis*) and *Renilla* (*Renilla reniformis*) luciferases are measured sequentially from the same sample. Each luciferase catalyzes a bioluminescent reaction with different substrate specificity, allowing for a clear discrimination between their expression levels. The levels of detection for each experimental condition should be determined to define the lower concentration of injected mRNA that results in a luciferase signal within the linear range (see **Fig. 2A,B**). For B1 and B1(-CPE) mRNAs, the assay was performed using the dual-luciferase reporter assay system of Promega and a plate-reading luminometer equipped with two reagent injectors and a computer for direct capture of data output.

1. Lyse the oocytes by adding 10 μ L/oocyte of 1X passive lysis buffer and pipeting up and down through a 200- μ L tip. Clear the samples by centrifugation at 16,000g for 15 min at 4°C. Collect the middle layer and discard the upper phase containing the lipids and yolk, as well as the pellet with the pigment granules. Perform this step on ice (see **Note 13**).
2. Dispense a 10- μ L aliquot of each cytoplasmic extract into an opaque 96-well plate and read in the luminometer programmed as follows:
 - a. Inject 50 μ L of luciferase assay reagent II.
 - b. Measure firefly luciferase activity for 10 s after a delay of 2.05 s.
 - c. Inject 50 μ L of Stop & Glo reagent.
 - d. Measure *Renilla* luciferase activity for 10 s.

3.2. Analysis of Changes in RNA Polyadenylation

This method allows the direct visualization of cytoplasmic poly(A) addition to small RNA probes. Radiolabeled RNAs containing the 3'-UTRs of interest are generated by *in vitro* transcription in the presence of α -[³²P]-UTP. Then, the RNAs are micro-injected in the cytoplasm, and the oocytes are incubated in the presence or absence of progesterone. Following the treatment, total RNA is extracted and resolved by polyacrylamide-urea gel electrophoresis, and the RNA probes are visualized by autoradiography. The polyadenylated RNAs will display slower gel mobility and a more heterogeneous size than the nonpolyadenylated RNAs (see **Fig. 3**).

In addition, to test whether the polyadenylation of the injected RNA probe is an "early" or a "late" event (see **Subheadings 1.** and **3.1.**), the protein synthesis inhibitor



Fig. 3. Cyclin B1 polyadenylation. Labeled RNAs derived from wild-type (B1) and CPE-mutated [B1(-CPE)] cyclin B1 3'-UTR were assayed for poly(A) addition, as described in **Subheading 3.2**.

cycloheximide may be used to prevent Mos synthesis. The oocytes injected with the labeled RNAs should be incubated in the presence of 100 $\mu\text{g/mL}$ cycloheximide for 1 h prior to the addition of progesterone. Note that oocytes treated with cycloheximide fail to undergo germinal vesicle breakdown.

The maximum recommended length of the RNA transcripts for this assay is 300 nucleotides (*see Note 14*).

To analyze whether the cyclin B1 3'-UTR was a target for CPE-dependent cytoplasmic polyadenylation, small RNAs containing either the wild-type (B1) or a mutant of the three putative CPEs [B1(-CPE)] were generated and processed. As shown in **Fig. 3**, progesterone-induced polyadenylation of the B1 probe but not of the B1(-CPE) probe.

The methods described in **Subheading 3.2.1**. outline the generation of a DNA template for in vitro transcription by PCR; **Subheading 3.2.2**. describes the preparation of radiolabeled RNA probe by in vitro transcription; **Subheading 3.2.3**. discusses RNA extraction from *X. laevis* oocytes; and **Subheading 3.2.4**. addresses visualization of poly(A) addition by RNA electrophoresis in polyacrylamide-urea gel and autoradiography.

The oocytes are injected as described in **Subheading 3.1.3**., with the single difference that more RNA can now be injected because polyadenylation has a higher toler-

ance to saturation than translational repression. Typically 4.6 fmol, equivalent to 14,000 cpm (Cerenkov), are injected.

3.2.1. Generation of DNA Template for In Vitro Transcription by PCR

The DNA template for in vitro transcription is generated by PCR, from the luc-3'UTR plasmid described in **Subheading 3.1.1.**, with a sense oligonucleotide that contains a phage promoter sequence (T3, T7, or Sp6) at its 5' end, thus generating a PCR product that can be used directly as a DNA template for in vitro transcription, and an antisense oligonucleotide complementary to the 3'-UTR under study. Following PCR, the DNA is purified by phenol/chloroform/isoamyl alcohol extraction and isopropanol precipitation (**33**).

For the study of cyclin B1 3'-UTR polyadenylation, the DNA templates were generated from the cyclin B1 3'-UTR and the cyclin B1(-CPE) 3'-UTR plasmids (see **Subheading 3.1.1.**) with the sense T3Luc-s oligonucleotide and the antisense B1-as or B1(-CPE)-as oligonucleotide, as described in **Subheading 2.7.**

3.2.2. Preparation of Radiolabeled RNA Probe by In Vitro Transcription

1. Set up a 10- μ L reaction containing the following components added sequentially as indicated:
 - a. 100 ng Linearized DNA template.
 - b. 2 μ L 5X Transcription buffer.
 - c. 1 μ L 10X rNTPs mix.
 - d. 0.5 μ L 20 U/ μ L RNase inhibitor.
 - e. 0.12 μ L 40 mM Cap analog.
 - f. 1.5 μ L 800 Ci/mmol \times 20 mCi/mL α -[32 P]-UTP.
 - g. 0.5 μ L T3 RNA polymerase (20 U/ μ L).
 - h. DEPC-treated water (10 μ L final volume of the reaction).
2. Mix well and incubate at 37°C for 1 to 2 h.
3. Once the transcription is complete, degrade the DNA template by adding 1 μ L of RNase-free DNase (2 U/ μ L) and incubating at 37°C for 15 min.
4. Purify the RNA probe from the unincorporated nucleotides, either by phenol/chloroform/isoamyl alcohol extraction and isopropanol precipitation or by filtration through Sephadex G-25 minicolumns (RNase free). The preparation and running of such columns is thoroughly described in **ref. 33**; however, the column should be equilibrated in water rather than in TE. Typically, the yield after purification is 200 to 300 ng of RNA with a specific activity of approx 10,000 cpm/ng.
5. Verify the quality of the RNA in a denaturing gel. Assemble a 6% polyacrylamide/8M urea minigel 7 cm long. Prerun it in 1X TBE buffer at 28 V/cm for 15 min. Mix the RNA (1 μ L) with gel-loading buffer and heat it at 70°C for 10 min. Load the samples and run the gel for 20 min (see **Note 15**). Determine the position of the transcript by brief autoradiography (5–10 min) without drying the gel. Excise the band and quantify the cpm (Cerenkov) (see **Note 6**).

3.2.3. RNA Extraction From *Xenopus laevis* Oocytes

1. Homogenize five oocytes (or fewer) by adding 500 μ L of PAS buffer; vortex and pipet the sample up and down through a 200- μ L tip. Add 500 μ L of phenol/chloroform/isoamyl alcohol and vortex thoroughly.

2. Centrifuge at 16,000g for 15 min at 4°C. Remove the aqueous (upper) phase to a clean tube, avoiding precipitated material from the interface. Add 1 volume of phenol/chloroform/isoamyl alcohol and repeat the extraction.
3. Again, remove the aqueous phase to a clean tube. Add 1/10 volume of 3 M ammonium acetate, pH 5.2, and 2.5 volume of 100% ethanol. Mix by inversion. Keep at -20°C for 30 min.
4. Recover the RNA by centrifugation at 16,000g for 30 min at 4°C. Discard the supernatant and wash the pellet with 70% ethanol, air dry, and resuspend in 10 µL DEPC-treated water (see **Note 4**).
5. Denature the total RNA sample by adding gel-loading buffer and heating at 70°C for 10 min.

3.2.4. Visualization of Poly(A) Addition by RNA Electrophoresis in Polyacrylamide-Urea Gel and Autoradiography

Total RNA extracted from oocytes is resolved by polyacrylamide-urea gel electrophoresis, and the labeled probe is detected by autoradiography. Because the expected size differences between the polyadenylated and nonpolyadenylated labeled RNAs range between 80 and 150 nucleotides, the resolution of the gel has to be adjusted according to the size of the injected RNA. For cyclin B1 3'-UTR, a 6% polyacrylamide/8 M urea gel 28 cm long was used, with a running time of 2 h. For RNAs 300 nucleotides long, a lower percentage of polyacrylamide (4–5%) and longer running times (up to 5 h) may be required.

1. Assemble a 1-mm thick polyacrylamide-urea gel making sure that one of the glass plates is silanized.
2. Prepare the gel with 6% polyacrylamide/8 M urea gel solution.
3. Prerun the gel in 1X TBE at 14 V/cm for 45 to 60 min at room temperature.
4. Load the denatured sample corresponding to two oocytes per well.
5. Run the gel at 14 V/cm for 2 h at room temperature.
6. Remove one of the glass plates and transfer the gel to a double layer of Whatman 3MM filter paper by overlaying and gently peeling it off. Note that these low-percentage gels are not easy to handle as they tend to be loose and sticky.
7. Dry the gel and expose to X-ray film in a cassette with an amplifying screen for 16 h at -80°C and develop the autoradiograph according to the manufacturer's instructions.

4. Notes

1. Inject 0.02 nmol (27 nL of a 6-ng/nL solution) of c-mos antisense per oocyte. Then, inject the RNAs of interest in both c-mos-injected and noninjected oocytes and treat with progesterone (10 µM) as required. Oocytes injected with c-mos antisense fail to undergo germinal vesicle breakdown, and a white spot is not observed, whereas control oocytes matured normally in response to progesterone.
2. It is preferable to linearize with restriction enzymes that produce a 5' overhang because enzymes leaving 3' overhanging ends may result in low levels of transcription (37).
3. Confirm that cleavage is complete by resolving an aliquot of the restriction reaction in a 1% agarose gel electrophoresis. Even a small amount of circular plasmid in a template preparation will generate a large proportion of incorrect transcripts.
4. An incubation for 5 to 10 min at 65 to 70°C may be required to resuspend the RNA.

5. Quantification can also be obtained by adding trace amounts of a radiolabeled NTP to the RNA transcription, followed by trichloroacetic acid (TCA) precipitation, filtration through a Whatman GF/C glass fiber filter, and measurement in a scintillation counter (33).
6. If necessary, the full-length mRNAs can be purified by cutting out the RNA band, crushing the gel slice in 0.5 M ammonium acetate and 1 mM EDTA, and incubating for 3 h at room temperature. The gel is separated from the eluate by a brief spin, and the RNA is recovered as described in **Subheading 3.2.2., step 4**, with the addition of 1 μ L of glycogen (20 mg/mL) as a carrier.
7. RNAs may be denatured by treatment with 2.5 M formaldehyde and 50% formamide in 1X MOPS (2 mM sodium acetate, 1 mM EDTA, 20 mM MOPS (3-(*N*-morpholino)-propanesulfonic acid), pH 7.0, and 10 ng/ μ L ethidium bromide and heated 10 min at 70°C. Samples are run in agarose gels containing 2.2 M formaldehyde and 1X MOPS.
8. The minimum amount of RNA that can be detected with ethidium bromide is on the order of 20 to 50 ng. Avoid the xylene cyanol and bromophenol blue dyes in the gel-loading buffer because they comigrate with the luciferases mRNAs, interfering with the quantification.
9. The presence of dispase allows the use of a lower collagenase concentration. It is advisable to select the oocytes the day before the experiment and leave them overnight in 1X MBS at 20°C. Manual isolation of the oocytes is also possible, and the resulting oocytes have a higher rate of protein synthesis (38).
10. RNAs on the nanomolar order are very susceptible to degradation and cannot be tested for integrity. Therefore, it is recommended to discard them after the injection and prepare new dilutions from the stock for each experiment.
11. For microinjection, the needle should be 50 to 75 mm long, and the tip must have steep shoulders followed by a gradual taper approx 5 to 10 mm long. The gradual taper allows the tip to be broken repeatedly to adjust the orifice or to reopen a clogged tip.
12. Progesterone adheres to plastic, and even traces of progesterone could induce oocyte maturation. Thus, plastic dishes or pipets should not be reused, and glassware must be cleaned thoughtfully.
13. Contamination with the lipid phase does not affect the luciferase activity. However, contamination with pigment granules must be avoided. If necessary, a second clearing step can be performed. Samples can be stored at -80°C for up to 1 mo.
14. Because, on average, 80 to 100 adenines are added to the polyadenylated RNAs, for probes longer than 300 nucleotides it becomes more difficult to detect differences in size caused by poly(A) tail elongation. If longer 3'-UTRs are studied, they can be shortened prior to electrophoresis by incubation with an antisense oligonucleotide followed by RNase H treatment, as described in **ref. 29**.
15. Before loading the sample, flush out the urea from the wells with a syringe and running buffer (1X TBE). A 100-nucleotide RNA comigrates with xylene cyanol.

Acknowledgments

We are grateful to Fátima Gebauer for the PBSK-A construct, the luciferase cDNAs, and advice with the dual-luciferase assay. We also thank Mercedes Fernandez for her assistance. Our work in the translational control and cytoplasmic polyadenylation of cyclin B1 mRNA is supported by the Ministerio de Ciencia y Tecnología (SAF2002-03201), by the Fundación La Caixa (ON03-13-0), and by the Fundación La Maratón de TV3.

References

1. Richter, J. D. (1999) Cytoplasmic polyadenylation in development and beyond. *Microbiol. Mol. Biol. Rev.* **63**, 446–456.
2. Mendez, R. and Richter, J. D. (2001) Translational control by CPEB: a means to the end. *Nat. Rev. Mol. Cell. Biol.* **2**, 521–529.
3. De Moor, C. H. and Richter, J. D. (2001) Translational control in vertebrate development. *Int. Rev. Cytol.* **203**, 567–608.
4. Stebbins-Boaz, B. and Richter, J. D. (1997) Translational control during early development. *Crit. Rev. Eukaryot. Gene Expr.* **7**, 73–94.
5. Gray, N. K. and Wickens, M. (1998) Control of translation initiation in animals. *Annu. Rev. Cell Dev. Biol.* **14**, 399–458.
6. Gebauer, F., Xu, W., Cooper, G. M., and Richter, J. D. (1994) Translational control by cytoplasmic polyadenylation of c-mos mRNA is necessary for oocyte maturation in the mouse. *EMBO J.* **13**, 5712–5720.
7. Bally-Cuif, L., Schatz, W. J., and Ho, R. K. (1998) Characterization of zebrafish Orb/CPEB-related RNA binding protein and localization of maternal components in the zebrafish oocyte. *Mech. Dev.* **77**, 31–47.
8. Chang, J. S., Tan, L., and Schedl, P. (1999) The *Drosophila* CPEB homolog, Orb, is required for Oskar protein expression in oocytes. *Dev. Biol.* **215**, 91–106.
9. Minshall, N., Walker, J., Dale, M., and Standart, N. (1999) Dual roles of p82, the clam CPEB homolog, in cytoplasmic polyadenylation and translational masking. *RNA* **5**, 27–38.
10. Luitjens, C., Gallegos, M., Kraemer, B., Kimble, J., and Wickens, M. (2000) CPEB proteins control two key steps in spermatogenesis in *C. elegans*. *Genes Dev.* **14**, 2596–2609.
11. Wu, L., Wells, D., Tay, J., et al. (1998) CPEB-mediated cytoplasmic polyadenylation and the regulation of experience-dependent translation of α -CaMKII mRNA at synapses. *Neuron* **21**, 1129–1139.
12. Theis, M., Si, K., and Kandel, E. R. (2003) Two previously undescribed members of the mouse CPEB family of genes and their inducible expression in the principal cell layers of the hippocampus. *Proc. Natl. Acad. Sci. USA* **100**, 9602–9607.
13. Wasserman, W. J. and Masui, Y. (1975) Effects of cyclohexamide on a cytoplasmic factor initiating meiotic maturation in *Xenopus* oocytes. *Exp. Cell. Res.* **91**, 381–388.
14. Gerhart, J., Wu, M., and Kirschner, M. (1984) Cell cycle dynamics of an M-phase-specific cytoplasmic factor in *Xenopus laevis* oocytes and eggs. *J. Cell. Biol.* **98**, 1247–1255.
15. McGrew, L. L., Dworkin-Rastl, E., Dworkin, M. B., and Richter, J. D. (1989) Poly(A) elongation during *Xenopus* oocyte maturation is required for translational recruitment and is mediated by a short sequence element. *Gene Dev.* **3**, 803–815.
16. McGrew, L. L. and Richter, J. D. (1990) Translational control by cytoplasmic polyadenylation during *Xenopus* oocyte maturation: characterization of *cis* and *trans* elements and regulation by cyclin/MPF. *EMBO J.* **9**, 3743–3751.
17. Sheets, M. D., Fox, C. A., Hunt, T., Vande Woude, G., and Wickens, M. (1994) The 3'-untranslated regions of c-mos and cyclin mRNAs stimulate translation by regulating cytoplasmic polyadenylation. *Genes Dev.* **8**, 926–938.
18. Sheets, M. D., Wu, M., and Wickens, M. (1995) Polyadenylation of c-mos mRNA as a control point in *Xenopus* meiotic maturation. *Nature* **374**, 511–516.
19. Barkoff, A., Ballantyne, S., and Wickens, M. (1998) Meiotic maturation in *Xenopus* requires polyadenylation of multiple mRNAs. *EMBO J.* **17**, 3168–3175.
20. De Moor, C. H. and Richter, J. D. (1997) The mos pathway regulates cytoplasmic polyadenylation in *Xenopus* oocytes. *Mol. Cell Biol.* **17**, 6419–6426.

21. Ballantyne, S., Daniel, D. L., and Wickens, M. (1997) A dependent pathway of cytoplasmic polyadenylation reactions linked to cell cycle control by c-mos and CDK1 activation. *Mol. Biol. Cell* **8**, 1633–1648.
22. Mendez, R., Barnard, D., and Richter, J. D. (2002) Differential mRNA translation and meiotic progression require Cdc2-mediated CPEB destruction. *EMBO J.* **21**, 1833–1844.
23. Mendez, R., Hake, L. E., Andresson, T., Littlepage, L. E., Ruderman, J. V., and Richter, J. D. (2000) Phosphorylation of CPE binding factor by Eg2 regulates translation of c-mos mRNA. *Nature* **404**, 302–307.
24. Mendez, R., Murthy, K. G., Ryan, K., Manley, J. L., and Richter, J. D. (2000) Phosphorylation of CPEB by Eg2 mediates the recruitment of CPSF into an active cytoplasmic polyadenylation complex. *Mol. Cell* **6**, 1253–1259.
25. De Moor, C. H. and Richter, J. D. (1999) Cytoplasmic polyadenylation elements mediate masking and unmasking of cyclin B1 mRNA. *EMBO J.* **18**, 2294–2303.
26. Barkoff, A. F., Dickson, K. S., Gray, N. K., and Wickens, M. (2000) Translational control of cyclin B1 mRNA during meiotic maturation: coordinated repression and cytoplasmic polyadenylation. *Dev. Biol.* **220**, 97–109.
27. Stebbins-Boaz, B., Cao, Q., de Moor, C. H., Mendez, R., and Richter, J. D. (1999) Maskin is a CPEB-associated factor that transiently interacts with eIF4E. *Mol. Cell* **4**, 1017–1027.
28. Cao, Q. and Richter, J. D. (2002) Dissolution of the maskin-eIF4E complex by cytoplasmic polyadenylation and poly(A)-binding protein controls cyclin B1 mRNA translation and oocyte maturation. *EMBO J.* **21**, 3852–3862.
29. Salles, F. J., Richards, W. G., and Strickland, S. (1999) Assaying the polyadenylation state of mRNAs. *Methods Companion Methods Enzymol.* **17**, 38–45.
30. Gebauer, F. (1997) Following up microinjected mRNAs: analysis of mRNA poly(A) tail length during mouse oocyte maturation, in *Microinjection and Transgenesis: Strategies and Protocols* (Cid-Arregui, A. García-Carrancá, A., ed.), Springer-Verlag, Berlin/Heidelberg, Germany, pp. 309–322.
31. Tanguay, R. L. and Gallie, D. R. (1996) Translational efficiency is regulated by the length of the 3' untranslated region. *Mol. Cell. Biol.* **16**, 146–156.
32. Sagata, N., Oskarsson, M., Copeland, T., Brumbaugh, J., and Vande Woude, G. F. (1988) Function of c-mos proto-oncogene product in meiotic maturation in *Xenopus* oocytes. *Nature* **335**, 519–525.
33. Sambrook, J. and Russell, D. W. (2001) *Molecular Cloning. A Laboratory Manual*, Cold Spring Harbor Laboratory Press, Cold Spring Harbor, NY.
34. Smith, L. D., Xu, W., and Varnold, R. L. (1991) Oogenesis and oocyte isolation, in *Methods in Cell Biology. Xenopus laevis: Practical Uses in Cell and Molecular Biology* (Kay, B. K., Peng, H. B., ed.), Academic Press, New York, pp. 45–60.
35. Sive, H. L., Grainger, R. M., and Harland, R. M. (2000) *Early Development of Xenopus laevis. A Laboratory Manual*, Cold Spring Harbor Laboratory Press, Cold Spring Harbor, NY.
36. Dumont, J. (1972) 4. Oogenesis in *Xenopus laevis* (Daudin). I. Stages of oocyte development in laboratory maintained animals. *J. Morphol.* **136**, 153–159.
37. Schenborn, E. T. and Mierendorf, R. C., Jr. (1985) A novel transcription property of SP6 and T7 RNA polymerases: dependence on template structure. *Nucleic Acids Res.* **13**, 6223–6236.
38. Wallace, R. A., Jared, D. W., Dumont, J. N. and Sega, M. W. (1973) Protein incorporation by isolated amphibian oocytes. III. Optimum incubation conditions. *J. Exp. Zool.* **184**, 321–334.

Xenopus Egg Extracts

A Model System to Study Proprotein Convertases

Kathleen I. J. Shennan

Summary

The *Xenopus* egg extract translation system has proved an ideal tool with which to study the biosynthesis of the prohormone convertases. It provides a robust coupled translation/translocation system capable of efficient translocation of any protein containing an N-terminal signal sequence into the lumen of its microsomal membranes, with cotranslational cleavage of the signal peptide. Its main advantage over rival in vitro translation systems is that it will also carry out posttranslational modification of proteins, such as N-glycosylation, and, in the case of the proprotein convertases, support autocatalytic proregion removal. The egg extract also contains an endogenous, acidic pH optimum enzyme activity, suggestive of a proprotein convertase, that can undertake limited proteolysis of precursors containing multibasic processing sites.

Key Words: In vitro translation; membrane association; proprotein convertase; protease protection.

1. Introduction

The proprotein convertases (PC) are a family of proteases related to bacterial subtilisins (**1**). They are capable of cleaving proproteins primarily at runs of basic amino acids to generate biologically active proteins. The seven mammalian members of this family are furin (**2,3**), PC1/3 (**4,5**), PC2 (**6,7**), PACE4 (paired amino acid converting enzyme) (**8**), PC4 (**9**), PC5/6 (**10,11**), and PC7/8/LPC (lymphoma proprotein convertase) (**12–14**). Together, this group of proteases is responsible for the processing of a wide variety of proproteins, including growth factors and their receptors, envelope glycoproteins of many retroviruses, and prohormones such as proinsulin and proglucagon (**1**).

All the members of this family share common structural features. They are synthesized with an N-terminal signal sequence that ensures their entry into the endoplasmic reticulum (ER), and they are all derived from precursor proteins through autocatalytic

cleavage of an N-terminal prodomain. In many cases, this prodomain acts as an intramolecular chaperone to aid the folding or transport of the proprotein convertase out of the endoplasmic reticulum (**1**). In the case of PC2, this function may be carried out by a chaperone and intermolecular inhibitor, 7B2 (**15,16**).

We have made extensive use of the *Xenopus* egg extract translation system to study various aspects of proprotein convertase biology, including their biosynthesis and, in the case of PC1/3 and PC2, their mechanism of sorting into secretory granules. The *Xenopus* egg extract constitutes a highly efficient, homologous translation/translocation system that is far more robust than other heterologous systems, such as rabbit reticulocyte lysate (RRL) supplemented with canine pancreatic microsomal membranes. It is ideally suited for studying the biosynthesis of secretory proteins containing an N-terminal signal sequence as there is almost 100% translocation of such newly synthesized proteins into the microsomal membranes of the extract coupled with signal peptide cleavage. In addition, using the protocols described in this chapter, post-translational modification of proteins such as glycosylation and propeptide removal can be studied. Because of the efficiency of translocation and the robustness of the system, other features, such as the potential for some proteins to aggregate and the ability of some proteins to insert into the membrane, can also be investigated.

2. Materials

1. pSP64T vector (**17**).
2. PC1/3 and PC2 complementary DNAs (cDNAs) were obtained from Professor D. F. Steiner, Howard Hughes Medical Institute, University of Chicago, Illinois; furin cDNA was from Dr. G. Matthews, Department of Surgery, University of Birmingham, UK; 7B2 cDNA was from Professor G. Martens, Department of Animal Physiology, University of Nijmegen, The Netherlands; and the α 1-antitrypsin cDNA was obtained from Dr. M. Spiess, Department of Medical Biochemistry and Genetics, University of Copenhagen, Denmark.
3. Restriction enzymes.
4. SP6 ribonucleic acid (RNA) polymerase (60 U/ μ L): use an SP6 RNA polymerase with as high specific activity as possible and avoid exposure to temperatures higher than -20°C . Dispense from a freezer block rather than an ice box to prevent the enzyme warming up to 4°C .
5. rNTPs (ribonucleoside 5'-triphosphates): ATP (adenosine 5'-triphosphate), CTP (cytidine 5'-triphosphate), GTP (guanosine 5'-triphosphate), UTP (uridine 5'-triphosphate), 10 mM each.
6. m7G(5')ppp(5')G cap structure analog (10 mM). Aliquot out the cap structure to reduce the chances of ribonuclease (RNase) contamination and avoid multiple freeze-thawings.
7. 10 U/ μ L RNase inhibitor.
8. Molecular biology grade phenol/chloroform/isoamyl alcohol (25/24/1).
9. Molecular biology grade chloroform.
10. Absolute ethanol: use high-grade ethanol, preferably RNase free.
11. 7 M Ammonium acetate; store at -20°C .
12. *Xenopus* egg extract (**18**). Store the extract in small aliquots at -70°C and avoid freeze-thawing.
13. 0.5 M Creatine phosphate.

14. 100 mM Spermidine: use free-base spermidine rather than spermidine phosphate as the latter is insoluble in water.
15. Nuclease-treated rabbit reticulocyte lysate (Promega, UK).
16. 25 to 50 μ Ci of radiolabeled amino acid (Amersham Biosciences, UK).
17. Phosphate-buffered saline (PBS) containing 10% (w/v) sucrose.
18. Triton X-100 (1% v/v).
19. TES (2-[[2-hydroxy-1,1-bis(hydroxymethyl)ethyl]amino]ethanesulfonic acid) at 1 M stock concentration, pH 7.0, 7.5, and 8.0.
20. Sodium acetate buffers at 1 M stock concentration, pH 4.5, 5.0, and 5.5.
21. MES (4-morpholineethanesulfonic acid) buffers at 1 M stock concentration, pH 5.5, 6.0, and 6.5.
22. (Acetyl)-Asn-Tyr-Thr-(amide): 500 mM stock solution made in dimethylsulfoxide (DMSO), diluted to 50 mM with water.
23. 100 mM CaCl_2 .
24. Proteinase K (10 mg/mL stock solution).
25. Phenylmethanesulfonyl fluoride at 10 mg/mL in absolute ethanol.

3. Methods

3.1. Preparation of cRNA: In Vitro Transcription

cDNAs encoding the prohormone convertases were subcloned into the *Xenopus* expression vector SP64T (17), which contains an SP6 promoter to drive RNA synthesis. The RNA produced is flanked by the 5' and 3' untranslated regions (UTRs) of β -globin RNA, resulting in increased stability in the egg extract. cRNA is transcribed from linearized SP64T vector using a restriction enzyme that cuts downstream from the *Xenopus* β -globin 3'-UTR sequences, in the remains of the polylinker, with the choice of enzyme determined by the insert sequence. Typically, 20 μ g of DNA is linearized, phenol:chloroform extracted, and ethanol precipitated using standard molecular biology techniques. The linearized DNA is resuspended in 20 μ L of sterile water, and 1 μ L is used in each transcription reaction. SP6 RNA polymerase is usually supplied with a 10X reaction buffer that contains high concentrations of spermidine. To prevent the precipitation of the DNA that can occur in high concentrations of spermidine, the DNA is added after all the other reagents have been added and mixed.

1. Add the following reagents to a 1.5-mL microcentrifuge tube at room temperature: 23.5 μ L water; 5 μ L each 10 mM ATP, CTP, and UTP; 1 μ L 10 mM GTP (see Note 1); 2.5 μ L 10 mM m7G(5')ppp(5')G cap structure analogue; 5 μ L 10X transcription buffer; 1 μ L (10 U) RNase inhibitor. Mix gently, then add: 1 μ L linearized DNA; 1 μ L (40–60 U) SP6 RNA polymerase
2. Mix gently and incubate at 37°C for 60 min (see Note 2).
3. Increase the volume of the reaction to 200 μ L with autoclaved water and phenol/chloroform extract using standard molecular biology techniques. Precipitate the RNA by adding 0.1 vol 7 M ammonium acetate and 2.5 vol absolute ethanol. Leave overnight at -70°C (see Note 3).
4. Centrifuge at 13,000g for 20 min at 4°C to pellet the RNA. Remove the ethanol and wash the pellet in 70% ethanol. Centrifuge as before, remove the ethanol, and air dry the pellet. Resuspend the RNA in 10 μ L water and store at -70°C.

3.2. Standard *Xenopus* Egg Extract Translation

Xenopus egg extract, made according to **ref. 18**, is generally aliquoted into either 50- μ L or 100- μ L lots prior to snap freezing. A 50- μ L aliquot, once prepared as described next, will allow translation of six separate RNAs using 10 μ L of extract for each RNA. The protocol described is specifically for any protein that contains an N-terminal signal sequence and would therefore be translocated into the lumen of the ER. RNAs that encode proteins that are not translocated can be translated in the egg extract by following **steps 1 to 4** and analyzing the translation reaction after **step 4**.

1. To one 50- μ L aliquot of extract add 1 μ L of 0.5 M creatine phosphate, 0.5 μ L of 100 mM spermidine, 5 μ L of nuclease-treated rabbit reticulocyte lysate (*see Note 4*) and 25 to 50 μ Ci of radioisotopically labeled amino acid (e.g., 35 S-methionine, 35 S-cysteine, or 3 H-leucine).
2. Mix gently but thoroughly by pipeting repeatedly up and down, taking care to avoid bubble formation.
3. Translation can be initiated by addition of 1 or 2 μ L of in vitro transcribed RNA to this mix (*see Note 5*).
4. Incubate reactions at room temperature (18–20°C) for 1 to 2 h.
5. After incubation, dilute the translation reaction 10-fold with PBS containing 10% (w/v) sucrose. Mix well, then centrifuge at 13,000g for 20 min at 4°C to spin down membranes.
6. Carefully remove and discard supernatant without disturbing the membrane pellet. Because the membrane pellet is not compact at this stage, it is best to leave 10 to 20 μ L of supernatant in the tube at this time.
7. Add 200 μ L of PBS/10% (w/v) sucrose, mix, and centrifuge at 13,000g for 20 min at 4°C as before.
8. Carefully remove and discard supernatant. The membranes are usually slightly more compact at this point, so more of the supernatant can be removed, but it is still advisable to leave some supernatant behind to ensure that no membranes are lost. If necessary, or desired, a further wash step can be done to remove as much nontranslocated material as possible.
9. Finally, resuspend membranes by adding PBS/10% (w/v) sucrose if further procedures are to be carried out or, if the proteins are to be analyzed immediately by SDS polyacrylamide gel electrophoresis (PAGE), add 10 mM TES buffer, pH 7.0, containing 1% (v/v) Triton X-100 (*see Note 6*).

3.3. Glycosylation of Proprotein Convertases

All members of the proprotein convertase family contain multiple potential glycosylation sites. On entering the ER, proteins with the glycosylation consensus sequence Asn-X-Ser/Thr can become modified by addition of a preformed carbohydrate moiety because of the action of oligosaccharide transferase. The glycosylated protein is modified by removal of some glucose residues before exit from the ER and then more complexly modified on transit through the Golgi complex. The *Xenopus* egg extract, the only in vitro translation system that will carry out posttranslational modifications on proteins that it synthesizes, is highly efficient at carrying out the initial glycosylation step but is less able to perform the complex modifications carried out in the Golgi complex (**18**), suggesting that ER-to-Golgi transport does not take place in this in vitro system.

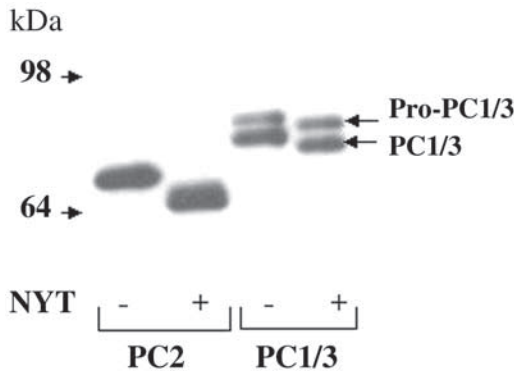


Fig. 1. Glycosylation of PC2 and PC1/3. PC2 and PC1/3 cRNAs were translated in the *Xenopus* egg extract containing ^{35}S -methionine in the presence or absence of a tripeptide (Asn-Tyr-Thr) that inhibits glycosylation. The equivalent of 5 μL of the translation reaction was analyzed by SDS-PAGE and fluorography. The position of SeeBlue prestained molecular weight markers (Invitrogen) are indicated on the left.

Although the *Xenopus* egg extract therefore will not modify a protein in absolutely the same way as a mammalian cell, its use will rapidly determine whether potential glycosylation sites are used and hence help determine the orientation of a transmembrane protein. The following protocol makes use of a tripeptide, (acetyl)-Asn-Tyr-Thr-(amide), that can be readily synthesized and added to the extract prior to translation without affecting translation efficiency. In the presence of this tripeptide, which acts as a substrate for oligosaccharide transferase, glycosylation of the nascent polypeptide is inhibited (19).

1. To one 50- μL aliquot of egg extract add creatine phosphate, spermidine, RRL, and radio-labeled amino acid as described in **Subheading 3.2., step 1**. Mix gently but thoroughly.
2. Divide extract into two equal portions. To one aliquot, add 0.6 μL of a 50 mM solution of tripeptide and mix thoroughly. To the other aliquot, add 0.6 μL of solvent (*see Note 7*).
3. Add RNA to both extracts and incubate at room temperature for 2 h. Spin down and wash membranes as described in **Subheading 3.2., steps 5 to 9** and analyze on SDS-PAGE.

Figure 1 shows the effect of the tripeptide on translation of PC2 and PC1/3 RNA. In the absence of the tripeptide, PC2 RNA synthesizes a single protein of approx 75 kDa corresponding to pro-PC2. If the Asn-Tyr-Thr tripeptide is included in the translation reaction, the efficiency of translation is unaffected, but the molecular weight of the pro-PC2 synthesized is reduced by approx 5 kDa.

After PC1/3 RNA is translated in the egg extract, in the absence of tripeptide a doublet of proteins is observed on SDS-PAGE. These bands correspond to pro-PC1/3 and to PC1/3 that has had the proregion removed (*see Subheading 3.4.*). Again, when translation occurs in the presence of the tripeptide both bands show reduced mobility. Proteins that do not become glycosylated show no such change in mobility when translated in the presence/absence of tripeptide (data not shown). Thus, the *Xenopus* egg

extract is able to perform at least the initial stages of glycosylation, and this can be effectively inhibited by a tripeptide of Asn-Tyr-Thr.

3.4. Autocatalytic Processing of the Prohormone Convertases

The proregion of the proprotein convertases is cleaved by autocatalysis on transit through the secretory pathway. Unlike other *in vitro* translation systems, the *Xenopus* egg extract is able to support this autocatalytic event. For proprotein convertases with a proregion that is removed in the ER, such as furin and PC1/3, autocatalytic processing occurs rapidly and is apparent within a 2-h translation period. The advantage of the egg extract system is that after translation the extract can be modified in terms of its pH and calcium ion concentration; this can allow assessment of where in the secretory pathway processing is likely to take place. Studies like those described here illustrate that PC2 autocatalytic processing occurs at acidic pH in a high concentration of calcium, indicative of the late secretory pathway (20).

1. Translate RNA as described in **Subheading 3.2., steps 1 to 4**, designated the pulse period (see **Note 8**). At the end of the translation period, split the translation reaction into 9- μ L aliquots in 0.5-mL microcentrifuge tubes.
2. Add 1 μ L 1 M buffer at the appropriate pH (i.e., sodium acetate, MES, or TES). Also, 1 μ L 100 mM CaCl₂ can be added to mimic the calcium concentrations in the late secretory pathway.
3. Continue incubation for 5 to 18 h at room temperature, designated the chase period.
4. Spin down and wash membranes in PBS/10% (w/v) sucrose as described in **Subheading 3.2., steps 5 to 9**, and analyze by SDS-PAGE.

Figure 2A shows a typical pH profile of pro-PC2 autocatalytic processing. In this case, a pulse period of 2 h was used, followed by a chase period of 20 h. The calcium concentration at each pH was adjusted by addition of CaCl₂ to a final concentration of 10 mM, and the pH was set to that shown by addition of sodium acetate, MES, or TES buffer. At the end of the pulse period, at 0 h of chase, only pro-PC2 with a molecular weight of 75 kDa is observed. However, after a 20-h chase at pH 5.5, 6.0, or 6.5, a lower molecular weight 66-kDa protein is observed, corresponding to mature PC2.

In contrast, autocatalytic processing of pro-PC3 occurs at neutral pH and is seen after a brief pulse period as a doublet of bands (**Fig. 2B**). Pro-PC3 proregion removal occurs early during transit through the secretory pathway, probably within the ER itself. However, it also undergoes a further cleavage event, removing C-terminal 116 amino acids, later in the secretory pathway (21). By using a chase period of 5 h at neutral pH to allow the majority of pro-PC3 to be processed to PC3 and then adjusting to pH 5.5 and chasing for an additional 18 h, C-terminal truncation of PC3 can be observed (**Fig. 2B**). Clearly, although C-terminal truncation of PC1/3 can be induced in the egg extract, it is much more inefficient than would occur *in vivo*.

3.5. Endogenous Proprotein Convertase Activity in the Egg Extract

Autocatalytic processing of prohormone convertases in the *Xenopus* egg extract was confirmed using catalytically inactive mutants (20,22), but the *Xenopus* egg extract also has endogenous proprotein convertase activity, allowing it to cleave some

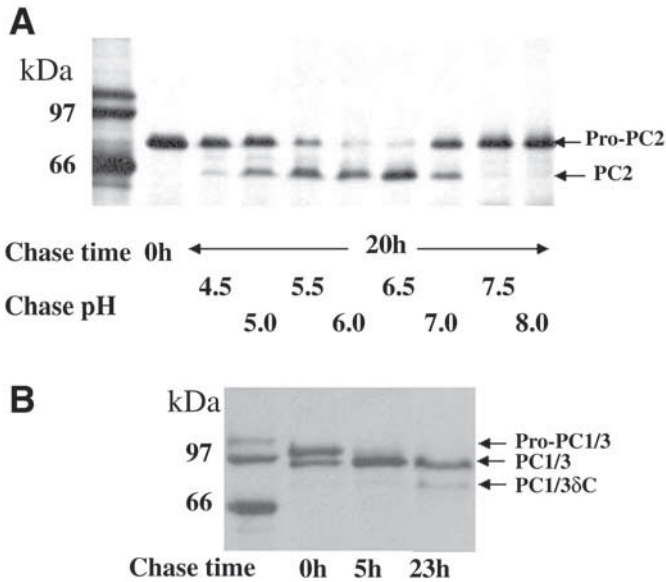


Fig. 2. Autocatalytic processing of PC2 and PC1/3. (A) PC2 cRNA was translated in the egg extract; after a 2-h translation period, the pH was adjusted to that indicated, and the calcium concentration was adjusted to 10 mM. The reactions were then chased for a period of 20 h before analysis by SDS-PAGE and fluorography. (B) PC1/3 cRNA was translated in the egg extract for 30 min before addition of cycloheximide to stop further translation. The reactions were initially chased for 5 h with no additions. After adjusting the pH to 5.5 and the calcium concentration to 10 mM, the reactions were chased for an additional 18 h. ^{14}C -labeled molecular weight markers are indicated on the left.

precursor proteins that contain basic amino acid cleavage sites. 7B2 is a specific chaperone protein for PC2 that aids in its folding and is thought to inhibit PC2 activity until late in the secretory pathway (15,16). 7B2 is synthesized as a 27-kDa precursor that is proteolytically processed in mammalian cells to a 21-kDa mature protein. Processing occurs at a basic quintuplet (Arg-Arg-Lys-Lys-Arg¹⁵⁵) and is probably carried out *in vivo* by furin (23).

Processing experiments similar to those described in **Subheading 3.4.** have been carried out using wild-type and mutant 7B2 RNA. When wild-type 7B2 RNA was translated in the *Xenopus* egg extract for a 2-h period then chased at different pH for 6 h, processing to a 21-kDa form was seen at acidic pH (Fig. 3A). That processing occurred at the basic quintuplet was shown by the fact that a mutant 7B2 protein where this sequence was mutated, SLQLS-7B2, showed no processing to the 21-kDa form (Fig. 3B).

The identity of the endogenous *Xenopus* egg extract proprotein convertase responsible for 7B2 processing is unknown. In mammalian cells, 7B2 is processed by furin, and two furin homologues have been identified in *Xenopus* eggs, Xen14 and Xen18

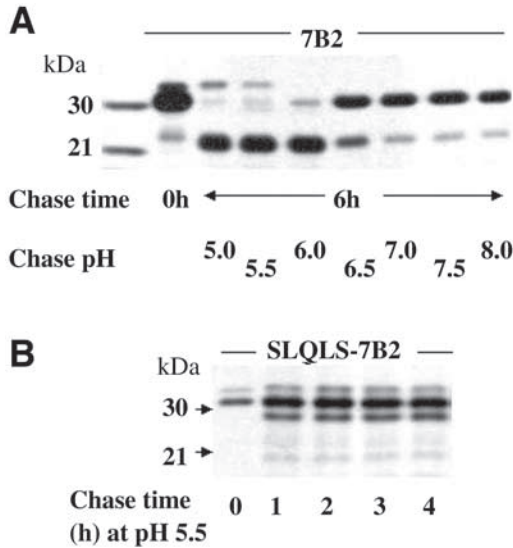


Fig. 3. *Xenopus* egg extract contains an endogenous proprotein convertase. (A) 7B2 cRNA was translated in the egg extract; after a 2-h translation period, the pH was adjusted to that indicated. The reactions were then chased for a period of 5 h before analysis by SDS-PAGE and fluorography. (B) A mutant 7B2 cRNA, containing a mutation in the basic quintuplet cleavage site, was translated in the egg extract for 2 h and chased at pH 5.5 for the indicated period of time before analysis by SDS-PAGE. ^{14}C -labeled molecular weight markers are indicated on the left.

(24). However, furin has a neutral pH optimum, whereas the activity observed against 7B2 has an acidic pH optimum. It remains to be determined whether 7B2 processing in the egg extract is carried out by Xen-14, Xen-18, or another unidentified proprotein convertase.

3.6. pH-Dependent Aggregation of the Prohormone Convertases

PC1/3 and PC2 are responsible for the processing of prohormones in the acidic environment of the immature secretory granule (1). Therefore, they need to be sorted into immature secretory granules on exit from the *trans*-Golgi network (TGN) along with the prohormone to be secreted by the regulated secretory pathway. Current views on how proteins become sorted into secretory granules as opposed to secreted in an unregulated, constitutive way propose that regulated secretory proteins become separated from constitutively secreted proteins in part because of their aggregation in the acidic environment of the TGN or immature granule (25). The following protocol can be used to determine whether proteins will aggregate in defined conditions and was used to determine that the proregion of PC2 contained a transferable aggregation domain (26):

1. Translate RNA as described in **Subheading 3.2., steps 1 to 4**. At the end of the translation period, pellet the membranes and wash as described in **Subheading 3.2., steps 4 to 8**.
2. Resuspend the membrane pellet from **Subheading 3.2., step 8**, in 10 mM TES buffer, pH 7.0, containing 1% (v/v) Triton X-100 to disrupt the membranes.

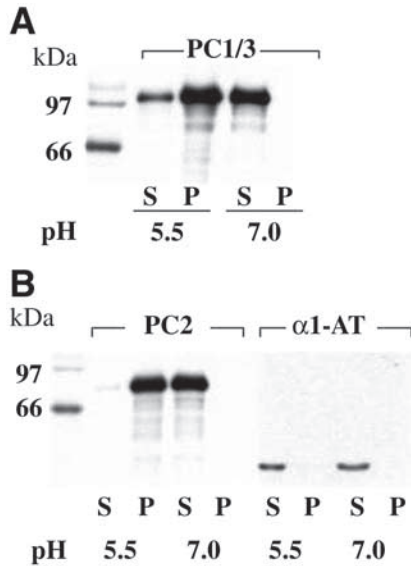


Fig. 4. PC1/3 and PC2 aggregate in vitro at acidic pH. (A) PC1/3 and (B) PC2 and α 1-antitrypsin (α 1-AT) cRNAs were translated in the egg extract. After purifying and lysing the membranes, the pH was adjusted to that indicated, and the reactions were incubated at 4°C for 60 min. Aggregated material was separated by centrifugation, and both the supernatants and pellets were analyzed by SDS-PAGE and fluorography. 14 C-labeled molecular weight markers are indicated on the left.

3. Buffer the extract by addition of either MES at pH 5.5 or TES at pH 7.0 to a final concentration of 100 mM.
4. Incubate at 4°C for 60 min and separate aggregated material by centrifugation at 20,000g for 15 min.
5. Resuspend the pellet in an equivalent volume of 10 mM TES/1% Triton X-100 as the volume of extract that was originally used in **step 3** and analyze both pellet and supernatant by SDS-PAGE.

Using this protocol, PC1/3 appears primarily in the pellet fraction at pH 5.5 and is completely soluble at pH 7.0 (**Fig. 4A**). This indicates that PC1/3 aggregates in the acidic environment of the TGN. Likewise, when PC2 RNA is translated in a similar experiment, PC2 protein is found primarily in the pellet fraction at acidic pH but is soluble at neutral pH (**Fig. 4B**). This aggregation of PC1/3 and PC2 at acidic pH is selective as a protein that is constitutively secreted, α 1-antitrypsin, remains soluble at both acid and neutral pH (**Fig. 4B**).

3.7. Protease Protection: Identification of Transmembrane Domains

Some of the proprotein convertases, such as furin, are integral membrane proteins and are oriented with their N-terminal, catalytically active region within the ER lumen and their C-terminus in the cytoplasm (27). PC1/3 and PC2 are generally considered

soluble proteins with the ability to associate peripherally with membranes, particularly at acidic pH (28,29). However, it was reported that PC1/3 functions as an integral membrane protein, with a transmembrane domain at the C-terminus, and that cleavage at this point occurs late in the secretory pathway to release PC1/3 from the membrane (30). Translation in the egg extract allows a transmembrane protein to achieve its correct membrane orientation, so any part of the protein that is not translocated into the lumen of the microsomal membranes will remain extralumenal and therefore will be accessible to proteases such as trypsin or proteinase K. Protease protection experiments such as that described next can be used to determine whether a protein contains a transmembrane domain and the orientation of that protein in the membrane.

1. Translate RNA in one 50- μ L aliquot of extract as described in **Subheading 3.2., steps 1 to 4**. At the end of the translation period, pellet the membranes and wash as described in **Subheading 3.2., steps 4 to 8**.
2. Resuspend the membranes in 50 μ L PBS containing 10% (w/v) sucrose and dispense 9 μ L of resuspended membranes into each of the following tubes:
 - a. No treatment control: containing 1 μ L of PBS containing 10% (w/v) sucrose and 10 mM CaCl_2 .
 - b. Proteinase K treated: containing 1 μ L of 0.4 mg/mL proteinase K in PBS containing 10% (w/v) sucrose and 10 mM CaCl_2 (see **Note 9**).
 - c. Proteinase K/Triton X-100 treated: containing 1 μ L proteinase K as in tube b plus 1 μ L of 1% (v/v) Triton X-100.
3. Incubate on ice for 30 min.
4. Add 1 μ L 10 mM phenylmethanesulfonyl fluoride and incubate for 5 min on ice.
5. Add 11 μ L of SDS-PAGE sample buffer and boil for 3 min.

This protocol was used to determine whether PC1/3 and PC2 proteins synthesized in the egg extract contained an observable transmembrane domain. As a control for the protease protection experiments, furin RNA was also translated in the egg extract, synthesizing a protein of approx 94 kDa (**Fig. 5**). Subsequent treatment with proteinase K in the absence of Triton X-100 led to a reduction in the size of the furin protein consistent with the cleavage of its exposed cytoplasmic domain. The proteinase K was fully active in the conditions used because addition of Triton X-100 to lyse the extract membranes during protease K digestion led to almost-complete degradation of the furin protein. This shows furin to be oriented in the membrane such that the major proportion of the protein is intralumenal, and thus protected from protease activity in the absence of detergent, and with a short cytoplasmic tail that is accessible to the protease.

In contrast, neither PC1/3 nor PC2 shows any alteration in size after proteinase K treatment, indicating that both proteins are either completely translocated into the microsomal membranes of the egg extract or that the “cytoplasmic tail” of these proteins is too small to see a size shift following proteinase K digestion. However, the potential transmembrane domain of PC1/3 is proposed to be located between amino acids 619 and 638 of this 735-amino acid protein (30). Protease K digestion would therefore be predicted to remove 97 amino acids, resulting in a size shift easily seen in this gel. Although this experiment illustrates that neither PC2 nor PC1/3 becomes an

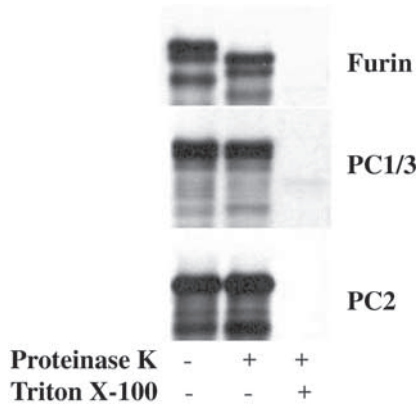


Fig. 5. Protease protection of translated proteins. Furin, PC1/3, or PC2 cRNAs were translated in the egg extract for 1 h. The translation reactions were then treated with buffer or proteinase K in the absence or presence of Triton X-100 before analysis by SDS-PAGE.

integral membrane protein on translocation into the ER, it is possible that membrane insertion requires other factors that are not present in the *Xenopus* egg extract. However, experiments like these illustrate the potential usefulness of the *Xenopus* egg extract translation system in determining membrane insertion and orientation.

4. Notes

1. Reducing the amount of GTP added helps incorporation of the cap analogue, which in turn increases translation of RNAs in the egg extract. However, it may also reduce the amount of RNA synthesized, and in some cases it may be better to add the same amount of GTP as the other nucleotides to improve RNA synthesis.
2. The reaction can continue for 2 h or more to increase the yield of RNA. Generally, after an incubation of 1 h, remove 2 μ L of the reaction and analyze on a 1.5% agarose gel. As RNA tends to diffuse easily out of these gels, it is best to run them for only a short period, say 15 min at 80 V, before visualizing the products by ethidium bromide staining. The RNA should be visible as a bright band running between the 500- and 1000-bp markers, depending on the size of the cDNA insert, with the DNA band barely visible. This gel is not a quantitative assessment of RNA produced but is merely a guide to show that the transcription reaction has been successful.
3. It is important to use 7 M ammonium acetate and not sodium acetate for precipitating the RNA to reduce the amount of unincorporated nucleotides precipitated. Generally leaving the precipitation reaction overnight at -70°C increases the amount of RNA recovered.
4. Addition of RRL to the translation reactions improves translation from extract that has been frozen (18). It is not necessary to add this if the extract is made and used immediately in translation reactions. The dilution of RRL in the egg extract is such that it is unlikely that translation will occur from the added RRL. However, to ensure that this does not occur, an S-100 fraction of the RRL can be made. Centrifuge the RRL at 100,000g for 2 h at 4°C in a Beckman TLA 100 Ultracentrifuge. Remove the supernatant, taking care not to disturb the pellet, and store the supernatant frozen in small aliquots at -70°C .

5. The translation reaction can be aliquoted into 10- μ L amounts at this stage, and up to 1 μ L of RNA can be added per 10 μ L extract. This allows multiple RNAs to be translated separately with the same translation mix. In practice, for many RNAs made as described, it is possible to dilute the RNA in sterile water up to fivefold without loss of translation. Addition of more than 1 μ L RNA to a 10- μ L aliquot of extract will reduce translation or translocation efficiency by overdilution of extract factors.
6. The volume used here depends on the volume of extract that was used in each translation. If 10- μ L aliquots of extract were used, addition of 10 μ L of TES/Triton will allow sufficient membrane lysis to allow analysis by SDS-PAGE. If a full 50- μ L aliquot of extract was used for the translation, then addition of 50 μ L of TES/Triton should be sufficient.
7. The tripeptide Asn-Tyr-Thr is dissolved in DMSO to make a stock concentration of 500 mM. This can then be diluted in water to the 50 mM working solution, and 0.6 μ L can be added to 30 μ L of extract. For the control tube without tripeptide, 0.6 μ L of DMSO, previously diluted 1 in 10 with water, should be added to 30 μ L of extract.
8. This translation period is designated the pulse period and can vary between 2 h for PC2 and 30 min for furin and PC1/3 that undergo rapid proregion removal at neutral pH. For proprotein convertases with proregion removal that occurs rapidly, the translation period has to be reduced to observe primarily the proprotein. To prevent further translation and allow observation of processing to the mature form, cycloheximide can be added to the translation reactions to a concentration of 1 mg/mL at the end of the translation period.
9. The concentration of proteinase K required to give complete, or near-complete, digestion of translocated products in the presence of Triton X-100, without compromising the integrity of the extract membranes in the absence of Triton, may vary depending on the batch of extract. Thus, a range of concentrations of proteinase K will have to be tested with each batch of membranes.

Acknowledgments

I would like to thank Kathleen Scougall for carrying out the 7B2 work. This work was supported by grants from the Royal Society, the Medical Research Council, Diabetes UK, and the Biotechnology and Biological Sciences Research Council.

References

1. Steiner, D. F. (1998) The proprotein convertases. *Curr. Opin. Chem. Biol.* **2**, 31–39.
2. Roebroek, A. J. M., Schalken, J. A., Leunissen, J. A. M., Onnekink, C., Bloemers, H. P. J., and Van de Ven, W. J. M. (1986) Evolutionary conserved close linkage of the c-fps/fps proto-oncogene and genetic sequences encoding a receptor-like protein. *EMBO J.* **5**, 2197–2202.
3. Van de Ven, W. J., Creemers, J. W., and Roebroek, A. J. (1991) Furin: the prototype mammalian subtilisin-like proprotein-processing enzyme. Endoproteolytic cleavage at paired basic residues of proproteins of the eukaryotic secretory pathway. *Enzyme* **45**, 257–270.
4. Seidah, N. G., Gaspar, L., Mion, P., Marcinkiewicz, M., Mbikay, M., and Chrétien, M. (1990) cDNA sequence of two distinct pituitary proteins homologous to Kex2 and furin gene products: tissue-specific mRNAs encoding candidates for pro-hormone processing proteinases. *DNA Cell Biol.* **9**, 415–424.
5. Smekens, S. P., Avruch, A. S., LaMendola, J., Chan, S. J., and Steiner, D. F. (1991) Identification of a cDNA encoding a second putative prohormone convertase related to PC2 in AtT20 cells and islets of Langerhans. *Proc. Natl. Acad. Sci. USA* **88**, 340–344.

6. Smeekens, S. P. and Steiner, D. F. 1990. Identification of a human insulinoma cDNA encoding a novel mammalian protein structurally related to the yeast dibasic processing protease Kex2. *J. Biol. Chem.* **265**, 2997–3000.
7. Seidah, N. G., Marcinkiewicz, M., Benjannet, S., et al. (1991) Cloning and primary sequence of a mouse candidate prohormone convertase PC1 homologous to PC2, Furin, and Kex2: distinct chromosomal localization and messenger RNA distribution in brain and pituitary compared to PC2. *Mol. Endocrinol.* **5**, 111–122.
8. Kiefer, M. C., Tucker, J. E., Joh, R., Landsberg, K. E., Saltman, D., and Barr, P. J. (1991) Identification of a second human subtilisin-like protease gene in the fes/fps region of chromosome 15. *DNA Cell Biol.* **10**, 757–769.
9. Nakayama, K., Kim, W., Torii, S., et al. (1992) Identification of the fourth member of the mammalian endoprotease family homologous to the yeast Kex2 protease. *J. Biol. Chem.* **267**, 5897–5900.
10. Lussou, J., Vieau, D., Hamelin, J., Day, R., Chrétien, M., and Seidah, N. G. (1993) cDNA structure of the mouse and rat subtilisin/kexin-like PC candidate proprotein convertase expressed in endocrine and nonendocrine cells. *Proc. Natl. Acad. Sci. USA* **90**, 6691–6695.
11. Nakagawa, T., Hosaka, M., Torii, S., Watanabe, T., Murakami, K., and Nakayama, K. (1993) Identification and functional expression of a new member of the mammalian Kex2-like processing endoprotease family: its striking structural similarity to PACE4. *J. Biochem.* **113**, 132–135.
12. Bruzzaniti, A., Goodge, K., Jay, P., et al. (1996) PC8, a new member of the convertase family. *Biochem. J.* **314**, 727–731.
13. Meerabux, J., Yaspo, M. L., Roebroek, A. J., Van de Ven, W. J., Lister, T. A., and Young, B. D. 1996. A new member of the proprotein convertase gene family (LPC) is located at a chromosome translocation breakpoint in lymphomas. *Cancer Res.* **56**, 448–454.
14. Seidah, N. G., Hamelin, J., Mamarbachi, A., et al. (1996) cDNA structure, tissue distribution, and chromosomal localization of rat PC7, a novel mammalian proprotein convertase closest to yeast kexin-like proteinases. *Proc. Natl. Acad. Sci. USA* **93**, 3388–3393.
15. Martens, G. J., Braks, J. A., Eib, D. W., Zhou, Y., and Lindberg, I. (1994) The neuroendocrine polypeptide 7B2 is an endogenous inhibitor of prohormone convertase PC2. *Proc. Natl. Acad. Sci. USA* **91**, 5784–5787.
16. Braks, J. A. and Martens, G. J. (1994) 7B2 is a neuroendocrine chaperone that transiently interacts with prohormone convertase PC2 in the secretory pathway. *Cell* **78**, 263–273.
17. Krieg, P. A. and Melton, D. A. (1984) Functional messenger RNAs are produced by SP6 in vitro transcription of cloned cDNAs. *Nucleic Acids Res.* **12**, 7057–7070.
18. Matthews, G. and Colman, A. (1991) A highly efficient, cell-free translation/translocation system prepared from *Xenopus* eggs. *Nucleic Acids Res.* **19**, 6405–6412.
19. Lau, J. T., Welply, J. K., Shenbagamartin, P., Naider, F., and Lennarz, W. J. (1983) Substrate recognition by oligosaccharyl transferase. Inhibition of co-translational glycosylation by acceptor peptides. *J. Biol. Chem.* **258**, 15,255–15,260.
20. Scougall, K., Taylor, N. A., Jermany, J. L., Docherty, K., and Shennan, K. I. J. (1998) Differences in the autocatalytic cleavage of pro-PC2 and pro-PC3 can be attributed to sequences within the propeptide and Asp(310) of pro-PC2. *Biochem. J.* **334**, 531–537.
21. Vindrola, O. and Lindberg, I. (1992) Biosynthesis of the prohormone convertase mPC1 in AtT-20 cells. *Mol. Endocrinol.* **6**, 1088–1092.
22. Matthews, G., Shennan, K. I., Seal, A. J., Taylor, N. A., Colman, A., and Docherty, K. (1994) Autocatalytic maturation of the prohormone convertase PC2. *J. Biol. Chem.* **269**, 588–592.

23. Paquet, L., Bergeron, F., Boudreault, A., et al. (1994) The neuroendocrine precursor 7B2 is a sulfated protein proteolytically processed by a ubiquitous furin-like convertase. *J. Biol. Chem.* **269**, 19,279–19,285.
24. Korner, J., Chun, J., O'Bryan, L., and Axel, R. (1991) Prohormone processing in *Xenopus* oocytes: characterisation of cleavage signals and cleavage enzymes. *Proc. Natl. Acad. Sci. USA* **88**, 11,393–11,397.
25. Blázquez, M. and Shennan, K. I. J. (2000) Basic mechanisms of secretion: sorting into the regulated secretory pathway. *Biochem. Cell Biol.* **78**, 181–191.
26. Jan, G., Taylor, N. A., Scougall, K. T., Docherty, K., and Shennan, K. I. (1998) The propeptide of prohormone convertase PC2 acts as a transferable aggregation and membrane-association signal. *Eur. J. Biochem.* **257**, 41–46.
27. Nakayama, K. (1997) Furin: a mammalian subtilisin/kex2p-like endoprotease involved in processing of a wide variety of precursor proteins. *Biochem. J.* **327**, 625–635.
28. Shennan, K. I., Taylor, N. A., and Docherty, K. (1994) Calcium- and pH-dependent aggregation and membrane association of the precursor of the prohormone convertase PC2. *J. Biol. Chem.* **269**, 18,646–18,650.
29. Blázquez, M., Docherty, K., and Shennan, K. I. J. (2001) Association of prohormone convertase PC3 with membrane lipid rafts. *J. Mol. Endocrinol.* **27**, 107–116.
30. Arnaoutova, I., Smith, A. M., Coates, L. C., et al. (2003) The prohormone processing enzyme PC3 is a lipid raft-associated transmembrane protein. *Biochemistry* **42**, 10,445–10,455.

Analysis of Molecular Chaperones Using a *Xenopus* Oocyte Protein Refolding Assay

John J. Heikkila, Angelo Kaldis, and Rashid Abdulle

Summary

Heat shock proteins (Hsps) are molecular chaperones that aid in the folding and translocation of protein under normal conditions and protect cellular proteins during stressful situations. A family of Hsps, the small Hsps, can maintain denatured target proteins in a folding-competent state such that they can be refolded and regain biological activity in the presence of other molecular chaperones. Previous assays have employed cellular lysates as a source of molecular chaperones involved in folding. In this chapter, we describe the production and purification of a *Xenopus laevis* recombinant small Hsp, Hsp30C, and an in vivo luciferase (LUC) refolding assay employing microinjected *Xenopus* oocytes. This assay tests whether LUC can be maintained in a folding-competent state when heat denatured in the presence of a small Hsp or other molecular chaperone. For example, microinjection of heat-denatured LUC alone into oocytes resulted in minimal reactivation of enzyme activity. However, LUC heat denatured in the presence of Hsp30C resulted in 100% recovery of enzyme activity after microinjection. The in vivo oocyte refolding system is more sensitive and requires less molecular chaperone than in vitro refolding assays. Also, this protocol is not limited to testing *Xenopus* molecular chaperones because small Hsps from other organisms have been used successfully.

Key Words: Aggregation; luciferase; microinjection; molecular chaperone; recombinant protein; refolding; small heat shock protein; *Xenopus* oocyte.

1. Introduction

Heat shock proteins (Hsps) are molecular chaperones that aid in the folding and translocation of cellular proteins under normal conditions and are upregulated when cells are exposed to environmental stress (e.g., elevated temperature, sodium arsenite, and heavy metals) (1–4). Hsps are composed of three major families, the high molecular weight (Hsp90), the Hsp70, and the small Hsp (SHsp) family. During environmental stress, SHsps bind to denatured or partially unfolded target proteins, prevent their aggregation, and maintain them in a soluble state until they can be refolded back into an active form by other molecular chaperones, including the Hsp70 family (5–11).

From: *Methods in Molecular Biology*, vol. 322: *Xenopus Protocols: Cell Biology and Signal Transduction*
Edited by: X. J. Liu © Humana Press Inc., Totowa, NJ

Protein aggregation is detrimental to a living cell and has been implicated in a variety of human diseases, including Alzheimer's disease, muscle myopathy, and multiple sclerosis (12,13). Various assays have been developed to monitor the ability of purified or recombinant SHsps to inhibit heat- or chemical-induced target protein aggregation in vitro using light scattering (14–18). The determination of whether an SHsp maintains its denatured target protein in a folding competent state has employed in vitro assays using either rabbit reticulocyte or wheat germ lysates as a source of molecular chaperones involved in refolding (15,19).

We developed an assay to assess the ability of a molecular chaperone, namely the *Xenopus* SHsp, Hsp30C, to maintain denatured client protein, firefly luciferase (LUC), in a folding competent state using microinjected *Xenopus* oocytes (19,20). Using the methods described here, we found that LUC when heat denatured and microinjected into oocytes regained very little enzyme activity. However, heat denaturation of LUC in the presence of *Xenopus* Hsp30C resulted in 100% enzyme reactivation following oocyte injection.

Xenopus oocytes contain a variety of molecular chaperones involved in protein folding, including Hsp70, but do not contain detectable levels of Hsp30 protein or messenger ribonucleic acid (RNA) (19,21–24). This in vivo refolding assay requires less molecular chaperone and substrate than in vitro refolding assays (19). Also, this protocol has been used successfully in our laboratory with SHsps from other organisms, including the American bullfrog *Rana catesbeiana* and the fruit fly *Drosophila melanogaster*. It is likely that this assay could be used with a wide variety of molecular chaperones. Coupling this assay with deletion or site-specific mutagenesis of the Hsp will allow the determination of protein domains essential for maintenance of the client protein in a folding-competent state (19,20).

2. Materials

1. pRSET vector and ProBond column system (Invitrogen; Burlington, ON, Canada).
2. Deoxyribonucleic acid (DNA) encoding *Xenopus* Hsp30C.
3. Isopropylthio- β -D-galactoside (IPTG).
4. Guanidinium lysis buffer: 6 M guanidinium hydrochloride, 20 mM sodium phosphate, and 500 mM sodium chloride, pH 7.8.
5. Protein dialysis buffer: 50 mM Tris-HCl at pH 8.0, 0.1 mM ethylenediaminetetraacetic acid (EDTA), and 25 mM NaCl.
6. Branson Sonifier 250 sonicator (VWR International; Mississauga, ON, Canada).
7. SDS-PAGE (sodium dodecyl sulfate-polyacrylamide gel electrophoresis) equipment.
8. Nanoject II oocyte microinjector with glass 3.5-in. (7.7-cm) capillary tubes (Drummond; Broomall, PA).
9. Penicillin and streptomycin.
10. Microsep 3K microconcentrator column (Pall Filtron; Northborough, MA).
11. Bicinchoninic acid (BCA) protein assay (Pierce; Rockford, IL).
12. Micropipet puller (Harvard Apparatus, Canada; Saint-Laurent, QC, Canada).
13. Variable-volume micropipeters (10 and 100 μ L).
14. Teflon homogenizer for 1.5-mL microfuge tubes.
15. Injection buffer: 50 mM HEPES-KOH at pH 7.5.
16. Mineral oil.

17. Modified Barth's solution (MBS): 88 mM NaCl, 1 mM KCl, 0.7 mM CaCl₂, 1 mM MgSO₄, 5 mM HEPES at pH 7.8, and 2.5 mM NaHCO₃.
18. Ficoll.
19. Firefly LUC and luciferase assay reagent (Promega, Madison, WI).
20. Homogenization buffer: 5 mM MgCl₂, 10 mM KCl, 2 mM dithiothreitol, 2 mM adenosine triphosphate (ATP), 2% protease inhibitor cocktail (Sigma, St. Louis, MO), and 125 mM HEPES-KOH at pH 7.5.
21. TD 20/20 luminometer (Turner Designs, Sunnyvale, CA).
22. *Xenopus laevis* females (Xenopus I, Ann Arbor, MI).
23. Dissecting microscope with fiber-optic lights.

3. Methods

The methods described outline the induction and purification of *Xenopus* Hsp30C recombinant protein as well as the protocol for the LUC enzyme reactivation assay using microinjected *Xenopus* oocytes.

3.1. Induction of *Xenopus* Recombinant Hsp30C Synthesis in *Escherichia coli*

Previously in our laboratory, the reading frame of *Xenopus* Hsp30C was cloned into a pRSETB (Invitrogen) expression vector that contains an N-terminal 6x-histidine tag (18) (see Note 1). The resultant Hsp30C-pRSETB vector was transformed into *Escherichia coli* BL21 (DE3) cells and stored as a glycerol stock at -80°C. The following protocol details the induction of recombinant Hsp30C expression with IPTG and purification of the resultant protein using a ProBond nickel affinity column (18,25-27):

1. Grow the transformed *E. coli* cells at 37°C in ZB media ((1% tryptone, 0.5% NaCl) overnight.
2. Inoculate 50 mL M9ZB media with 2.5 mL of the overnight culture and grow to an optical density of 0.6 to 0.8 at 600 nm.
3. Add IPTG to a final concentration of 0.4 mM and incubate for 4 h to induce Hsp30C gene expression (see Note 2).
4. Centrifuge the cells at 12,000g for 30 min at 4°C. Discard the supernatant, freeze the pellet in liquid nitrogen, and then thaw quickly at 37°C. Repeat the freezing and thawing step twice.
5. Resuspend the cells in 5 mL guanidinium lysis buffer (see Note 3).
6. Agitate the solution on an orbital shaker for 4 h at 22°C.
7. Place the tubes on ice and sonicate with 20 sets of three 1-s bursts (Output = 5; Duty cycle = 80%).
8. Centrifuge the sonicated mixture at 3000g at 4°C for 30 min, transfer the supernatant or bacterial lysate to a new tube, and store at -80°C.

3.2. Purification of Recombinant Hsp30C

1. The ProBond beads and columns are prepared and equilibrated with 5 mL denaturing buffer at pH 7.8 (see Note 3) according to manufacturer's instructions. Prior to use, the column is centrifuged, and the supernatant is discarded.
2. Add 5 mL bacterial lysate to the column and mix gently by inversion (see Note 4).
3. Centrifuge at 600g for 5 min and remove the unbound lysate.
4. Add 5 mL denaturing buffer at pH 7.8 to the column and mix gently by inversion.
5. Place the column on an orbital nutator and agitate for 2 min at room temperature.
6. Centrifuge at 1200g for 3 min and discard the supernatant.

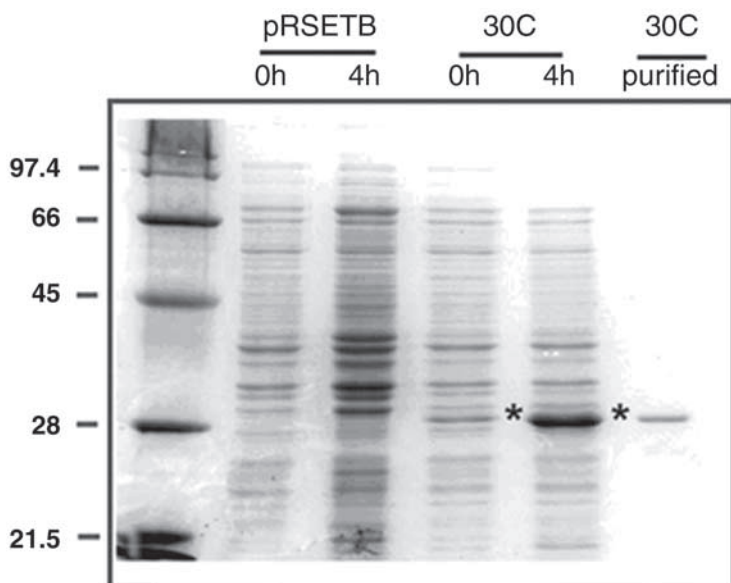


Fig. 1. Expression and purification of Hsp30C recombinant protein from *E. coli*. Total bacterial protein from *E. coli* BL21 (DE3) cells containing either the expression vector (pRSETB) or the vector with the Hsp30C gene insert (30C) were collected either before or after 4 h of IPTG addition. Protein was analyzed by Coomassie brilliant blue staining. Purified 30C after nickel affinity column chromatography is shown. The asterisks indicate the location of 30C. Molecular mass markers in kilodaltons are indicated on the left side of the figure.

7. Repeat **steps 5 to 7** three times each with 5 mL denaturing buffer at pH 6.0 and denaturing buffer at pH 5.3 and then twice with denaturing buffer at pH 5.0 (*see Note 5*).
8. After the last centrifugation, clamp the ProBond column in a vertical position and snap off the tip to allow the excess buffer to drain.
9. Cap the tip of the column and add 5 mL denaturing buffer at pH 4.0 and mix gently by inversion.
10. Centrifuge at 1200g for 30 s to pack the resin.
11. Clamp the column in a vertical position, remove the cap from the tip, and collect 1-mL fractions.
12. Repeat **steps 10 to 12** and freeze all fractions at -80°C .
13. Analyze 20 μL of each fraction by means of SDS-PAGE and staining with Coomassie brilliant blue.
14. Combine all fractions that contain the recombinant protein and dialyze for 15 h against protein dialysis buffer.
15. Concentrate the dialysate ($\sim 5\text{--}10$ mL) using a 3K Microsep microconcentrator column (*see Note 6*) to the desired volume (200–300 μL) and transfer to a microcentrifuge tube. Take a sample for SDS-PAGE to check the purity of the protein preparation (**Fig. 1**) and then store in aliquots at -80°C .
16. Determine the concentration of the protein using a BCA protein assay.

3.3. *Xenopus* Oocyte Isolation and Microinjection Apparatus

Xenopus oocytes are isolated according to standard procedures and maintained in covered Petri dishes containing MBS media with 100 U/mL penicillin and 100 $\mu\text{g}/\text{mL}$ streptomycin at 22°C. Only normal-appearing oocytes that have been incubated overnight should be used in this assay. Microinjection of protein is carried out with a Nanoject II system set up to deliver a volume of 27.6 nL according to manufacturer's instructions (*see Note 7*).

Microinjection needles or micropipets are made from glass capillary tubes using a micropipet puller. The tips of the needles are broken off with a pair of fine forceps and stored until needed. New microinjection needles are used for each sample. The placement of 10 to 20 μL of a sample on a strip of parafilm facilitates the filling of the micropipet with the Drummond Nanoject II. Prior to microinjection, oocytes were transferred to fresh MBS media containing 4% Ficoll to minimize cytoplasmic leakage after injection.

3.4. Luminometer Settings

The TD 20/20 luminometer is used to measure the production of light resulting from the enzymatic action of LUC on luciferin present in the luciferase assay reagent. This equipment is used according to the manufacturer's instructions employing a 12 mm adapter to hold 1.5 ml clear microcentrifuge tubes with the Sensitivity Adjust set to 100.

3.5. Preparation of LUC or Hsp30C Samples for Microinjection

Dilute a sample of the stock firefly LUC solution to 2.5 μM with injection buffer and store 4- μL aliquots at -80°C . Prepare recombinant Hsp30C by diluting it to concentrations ranging from 16.7 to 100.2 μM (depending on the final molar ratio of Hsp30C to LUC desired, namely, 5/1 to 30/1) using protein dialysis buffer and store at -80°C until needed.

3.6. Activity of Nondenatured LUC After Oocyte Injection

1. Place a microcentrifuge tube on ice with 24 μL of injection buffer (*see Note 8*).
2. Add 1.0 μL LUC to the tube followed by mixing and brief centrifugation at 12,000g for 20 s.
3. Incubate the solution at 22°C for 10 min in the dark (covered in aluminum foil).
4. Add 75 μL injection buffer and mix as above.
5. Transfer 20 μL of the sample onto parafilm and use the Drummond Nanoject II settings to fill the microinjection needle.
6. Place 10 oocytes into a dish for microinjection containing MBS with 4% Ficoll.
7. Inject 27.6 nL of the LUC mixture per oocyte.
8. Immediately after injection, divide the oocytes between two microcentrifuge tubes (five each) and remove all of the oocyte media using a Pasteur pipet.
9. Add 20 μL freshly prepared homogenization buffer to each tube and homogenize with a Teflon pestle made for microcentrifuge tubes.
10. Vortex each tube for 5 s and centrifuge at 12,000g for 5 min.
11. Take 2 μL of the clear supernatant, taking care to avoid the pellet and overlying pellicle, and transfer it to a 1.5-mL clear microcentrifuge tube.
12. Add 18 μL LUC reagent equilibrated at room temperature to the 2 μL oocyte extract and mix.

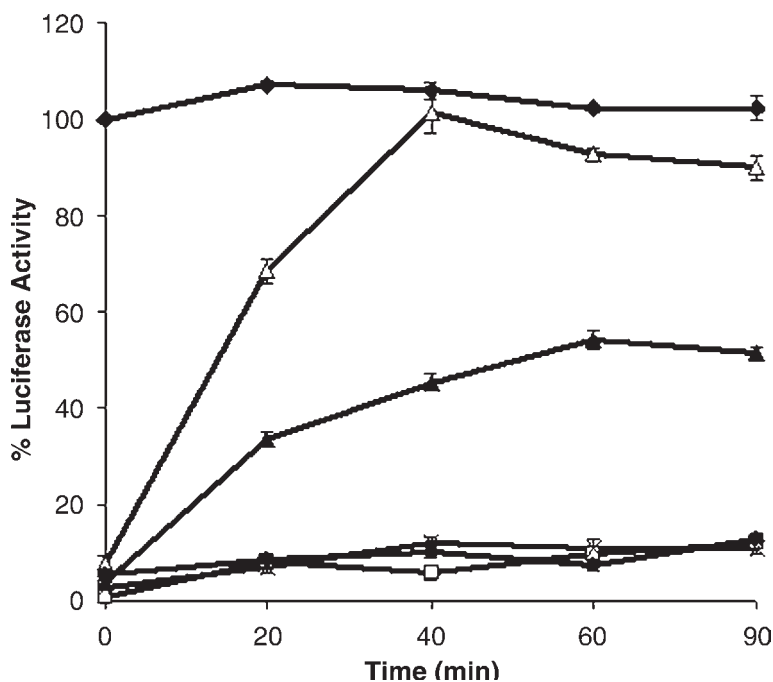


Fig. 2. LUC heat denatured in the presence of Hsp30C can be refolded *in vivo* after microinjection into *Xenopus* oocytes. LUC ($0.2 \mu\text{M}$) was incubated at 22°C (◆) or heat denatured alone (×) or in the presence of either $6 \mu\text{M}$ BSA (●) or 30C at 30C:LUC molar ratios of 1/1 (□), 10/1 (▲), or 30/1 (△). Mixtures (containing 1.38 fmol of LUC in 26.7 nL) were microinjected into *Xenopus* oocytes, and LUC activity in the oocytes was monitored over time. Data are representative of three to five trials and are shown as the mean \pm standard error.

13. Immediately place the tubes into the TD 20/20 luminometer and take readings for a period of 12 s following a 3-s delay. The average of the duplicate sample readings should be approx 800 to 1000 cpm or more and will be set as the 100% value against which all remaining samples will be compared.

3.7. Activity of Heat-Denatured LUC After Oocyte Injection

The next sample will determine the loss of LUC enzyme activity after heat denaturation and microinjection into oocytes.

1. Place a microcentrifuge tube on ice with $24 \mu\text{L}$ injection buffer.
2. Add $1.0 \mu\text{L}$ LUC to the tube, followed by mixing and brief centrifugation at $12,000g$ for 20 s.
3. Cover the tubes with aluminum foil and incubate at 42°C for 8 min, followed by 2 min at 22°C (see Note 9).
4. Follow **Subheading 3.6., steps 4 to 13**. The luminometer readings of this time-point are expressed as a percentage of nondenatured LUC value obtained in **Subheading 3.6**. Ideally, this time point should be 1 to 8% of the nondenatured LUC sample assayed previously. Furthermore, incubation of injected oocytes at 22°C for time periods ranging up to 100 min should show minimal LUC activity (Fig. 2).

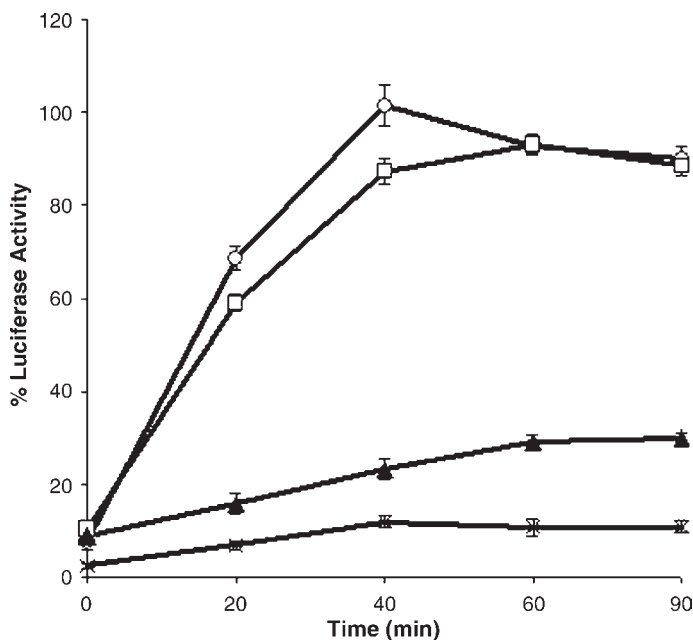


Fig. 3. LUC heat denatured in the presence of 30C and N-30C but not C-30C can be refolded in *Xenopus* oocytes. LUC ($0.2 \mu\text{M}$) was heat denatured alone (X) or with $6.0 \mu\text{M}$ of 30C (O), N-30C (□), or C-30C (▲) at 42°C . Samples containing 1.38 fmol of LUC in 26.7 nL were microinjected into *Xenopus* oocytes, and LUC activity was determined over time as indicated in **Subheadings 2.** and **3.** Data are representative of three to five trials and are shown as the mean \pm standard error.

3.8. Enzyme Activity of LUC Heat Denatured in the Presence of Hsp30C

This sample will determine whether Hsp30C can maintain heat-denatured LUC in a folding-competent state such that it can regain enzyme activity after injection of the complexes into *Xenopus* oocytes.

1. Place a microcentrifuge tube on ice with $22.5 \mu\text{L}$ injection buffer.
2. Add $1.5 \mu\text{L}$ of Hsp30C to the tube.
3. Add $1.0 \mu\text{L}$ LUC to the tube, followed by mixing and brief centrifugation at $12,000g$ for 20 s.
4. Cover the tubes with aluminum foil and incubate at 42°C for 8 min followed by 2 min at 22°C .
5. Follow **Subheading 3.6., steps 4 to 13.** However, with this sample it is essential to follow the enzyme activity of LUC over a period of 100 min at 22°C after injection into oocytes. The suggested incubation times are 0, 20, 40, 60, 80, and 100 min using a total of 10 oocytes per time-point. The injections of the oocytes are staggered to facilitate LUC enzyme analysis. The luminometer readings of these time-points are expressed as a percentage of nondenatured LUC value obtained in **Subheading 3.6.** A typical LUC enzyme reactivation curve is shown in **Fig. 2.** As mentioned in **Subheading 1.1.**, this assay can also be used to examine the various protein domains associated with Hsp30C to maintain LUC in a folding-competent state (19). As shown in **Fig. 3,** deletion of 17 amino acids

from the N-terminal end (N-30C) has no effect on LUC enzyme reactivation in *Xenopus* oocytes, but removal of 25 amino acids from the C-terminal end (C-30C) dramatically reduces the molecular chaperone function of Hsp30C.

4. Notes

1. As described in a previous publication, the entire open reading frame of *Xenopus* Hsp30C was obtained by polymerase chain reaction such that a *Bam*HI restriction site was created just 5' to the start codon and an *Eco*RI restriction site just 3' to the translation stop codon (18). This fragment was then cloned into a pRSETB vector. This type of approach can be used with any molecular chaperone gene, but it is essential that the chimeric plasmid is sequenced to ensure no mutations and that the coding sequence is in the correct reading frame.
2. With other molecular chaperones, it is necessary to determine the optimal conditions for recombinant protein induction. Preliminary experiments should vary the IPTG concentration from 0.4 to 1.0 mM for periods of time ranging from 2 to 10 h, followed by analysis by SDS-PAGE and Coomassie brilliant blue staining.
3. Because the pH of the guanidinium lysis buffer and denaturing buffer solutions tend to drift with time, they should be checked prior to use. In our experience, the inability to recover recombinant protein from the ProBond nickel affinity column can often be traced to incorrect pH of the denaturing buffer.
4. It is important not to exceed the binding capacity of the nickel affinity resin, which is between 1 and 5 mg/mL.
5. The application of denaturing buffer (pH 5.0) to the column may result in the elution of some bound SHsp from the resin, but this step is necessary to obtain a pure sample of Hsp30C. The ProBond beads can be reused at least two more times after the column has been recharged following manufacturer's instructions.
6. The Microsep Concentrator column can be reused to concentrate additional batches of Hsp30C protein by adding 2 mL of 20% ethanol onto the filter and storing it at 4°C until required.
7. Microinjection of 1.38 fmol of LUC plus 5- to 30-fold Hsp30C in 26.7 nL into oocytes appears to be optimal. Injection of higher amounts of LUC (e.g., 10.12 fmol) and accompanying SHsp results in reduced enzyme reactivation (19). It is likely that higher amounts may overload the available chaperone folding machinery in oocytes.
8. Because this assay is very sensitive, it is essential that all pipeters are calibrated on a regular basis.
9. The time required for heat denaturation of LUC at 42°C may vary between lot numbers of enzyme. Although our normal denaturation time is 8 min, we have found that with some batches of LUC, a longer heat denaturation time up to 15 min may be required to achieve a final enzyme activity of 1 to 8%.

Acknowledgments

This research was supported by Natural Science and Engineering Research Council grants to J. J. H., who is also the recipient of a Canada Research Chair in Stress Protein Gene Research.

References

1. Parsell, D. A. and Linquist S., (1994) The function of heat shock proteins in stress tolerance: degradation and reactivation of damaged proteins. *Annu. Rev. Genet.* **27**, 437–496.
2. Morimoto, R. I., Tissieres, A., and Georgopoulos, C. (eds.) (1994) *The Biology of Heat Shock Proteins and Molecular Chaperones*, Cold Spring Harbor Laboratory Press, Cold Spring Harbor, NY.
3. Feige, U., Morimoto, R. I., Yahara, I., and Polla, B. S. (1996) *Stress-inducible Cellular Responses*, Birkhauser Verlag, Basel, Switzerland.
4. Morimoto, R. I. (1998) Regulation of the heat shock transcriptional response: cross talk between a family of heat shock factors, molecular chaperones, and negative regulators. *Genes Dev.* **12**, 3788–3796.
5. Arrigo, A.-P. (1998) Small stress proteins: chaperones that act as regulators of intracellular redox state and programmed cell death. *J. Biol. Chem.* **379**, 19–26.
6. Ehrnsperger, M., Buchner, J., and Gaestel, M. (1998) Structure and function of small heat shock proteins, in *Molecular Chaperones in the Life Cycle of Proteins: Structure, Function and Mode of Action* (Fink, A. L. and Goto, Y., eds.), Marcel Dekker, New York, pp. 553–575.
7. MacRae, T. H. (2002) Structure and function of small heat shock/ α -crystallin proteins: established concepts and emerging ideas. *Cell. Mol. Life Sci.* **57**, 899–913.
8. Van Montfort, R., Slingsby, C., and Vierling, E. (2002) Structure and function of the small heat shock protein/ α -crystallin family of molecular chaperones. *Adv. Protein Chem.* **59**, 105–156.
9. Arrigo, A.-P. and Landry, J. (1994) Expression and function of the low-molecular-weight heat shock proteins, in *The Biology of Heat Shock Proteins and Molecular Chaperones*. (Morimoto, R. I., Tissieres, A., and Georgopoulos, C., eds.), Cold Spring Harbor Laboratory Press, Cold Spring Harbor, NY, pp. 335–373.
10. Waters, E., Lee, G., and Vierling, E. (1996) Evolution, structure and function of the small heat shock proteins in plants. *J. Exp. Biol.* **47**, 325–338.
11. Ehrnsperger, M., Graber, S., Gaestel, M., and Buchner, J. (1997) Binding of non-native protein to hsp25 during heat shock creates a reservoir of folding intermediates for reactivation. *EMBO J.* **16**, 221–229.
12. Quinlan, R. and Van Den Ijssel, P. (1999) Fatal attraction: when chaperones turn harlot. *Nat. Med.* **5**, 25–26.
13. Bova, M. P., Yaron, O., Huang, Q. L., et al. (1999) Mutation R120G in α B-crystallin, which is linked to a desmin-related myopathy, results in an irregular structure and defective chaperone-like function. *Proc. Natl. Acad. Sci. U. S. A.* **96**, 6137–6142.
14. Buchner, J., Grallert, H., and Jakob, U. (1998) Analysis of chaperone function using citrate synthase as nonnative substrate protein. *Methods Enzymol.* **290**, 323–338.
15. Lee, G. J. and Vierling, E. 2000. A small heat shock protein cooperates with heat shock protein 70 systems to reactivate a heat-denatured protein. *Plant. Physiol.* **122**, 189–198.
16. Lee, G. J., Roseman, A. M., Saibil, H. R., and Vierling, E. (1997) A small heat shock protein stably binds heat-denatured model substrates and can maintain a substrate in a folding-competent state. *EMBO J.* **16**, 659–671.
17. Smulders, R. H., Carver, J. A., Lindner, R. A., van Boekel, M. A., Bloemedal, H., and de Jong, W. W. (1996) Immobilization of the C-terminal extension of bovine α A-crystallin reduces chaperone-like activity. *J. Biol. Chem.* **271**, 29,060–29,066.

18. Fernando, P. and Heikkila, J. J. (2000) Functional characterization of *Xenopus* small heat shock protein, hsp30C: the carboxyl end is required for stability and chaperone activity. *Cell Stress Chaperones* **5**, 148–159.
19. Abdulle, R., Mohindra, A., Fernando, P., and Heikkila, J. J. (2002) *Xenopus* small heat shock protein hsp30C and hsp30D, maintain heat- and chemically denatured luciferase in a folding-competent state. *Cell Stress Chaperones* **7**, 6–16.
20. Fernando, P., Abdulle, R., Mohindra, A., Guillemette, J. G., and Heikkila, J. J. (2002) Mutation or deletion of the C-terminal tail affects the function and structure of *Xenopus laevis* small heat shock protein, hsp30. *Comp. Biochem. Physiol. Part B* **133**, 95–103.
21. Bienz, M. (1984) Developmental control of the heat shock response in *Xenopus*. *Proc. Natl. Acad. Sci U. S. A.* **81**, 3138–3142.
22. Krone, P. H. and Heikkila, J. J. (1989) Expression of microinjected *hsp70/cat* and *hsp30/cat* chimeric genes in developing *Xenopus laevis* embryos. *Dev. Biol.* **106**, 271–281.
23. Uzawa, M., Grams, J., Madden, B., Toft, D., and Salisbury, J. L. (1995) Identification of a complex between centrin and heat shock proteins in CSF-arrested *Xenopus* oocytes and dissociation of the complex following oocyte activation. *Dev. Biol.* **171**, 51–59.
24. Ali, A., Bharadwaj, S., O'Carroll, R., and Ovsenek, N. (1998) Hsp 90 interacts with and regulates the activity of heat shock factor 1 in *Xenopus* oocytes. *Mol. Cell. Biol.* **18**, 4949–4960.
25. Studier, F. W., Rosenberg, A. H., Dunn, J. J., and Dubendorf, J. W. (1990) Use of T7 RNA polymerase to direct expression of cloned genes. *Meth. Enzymol.* **185**, 60–89.
26. Kroll, D. J., Abdel-Malek Abdel-Hafiz, H., Marcell, T., et al. (1993) A multifunctional prokaryotic protein expression system: overproduction, affinity purification and selective detection. *DNA Cell Biol.* **12**, 441–453.
27. Sambrook, J., Fritsch, E. F., and Maniatis, T. (1998) *Molecular Cloning, a Laboratory Manual*, 2nd ed., Cold Spring Harbor Laboratory Press, Cold Spring Harbor, NY.

Ubiquitin-Mediated Protein Degradation in *Xenopus* Egg Extracts

Anna Castro, Suzanne Vigneron, Cyril Bernis,
Jean-Claude Labbé, and Thierry Lorca

Summary

Events controlling cell division are governed by the degradation of different regulatory proteins by the ubiquitin-dependent pathway. In this pathway, the attachment of a polyubiquitin chain to a substrate by an ubiquitin–ligase targets this substrate for degradation. *Xenopus* egg extracts present many advantages for the study of the cell cycle, including the availability of a large quantity of material synchronized at a particular phase of the cell cycle. In this chapter, we describe various protocols used in *Xenopus* egg extracts to study the ubiquitination and degradation of different cell cycle regulators. We first provide the method used to obtain interphase- and metaphase II-arrested egg extracts. Subsequently, we describe the protocol employed in these extracts to test the putative ubiquitination and degradation of a protein. Moreover, we describe a detailed practical procedure to test the role of different regulators in the ubiquitin-dependent degradation pathway of a specific protein. To that, we show how to eliminate some of these regulators from the extracts by immunodepletion and how to activate ectopically their function by the translation of their messenger ribonucleic acid. Finally, the Notes provide a series of practical details that explain the different problems that can occur and the possible solutions used to overcome them.

Key Words: Anaphase-promoting complex (APC); Cdc20; Cdh1; degradation; immunodepletion; mRNA translation; ubiquitination; *Xenopus* extracts.

1. Introduction

Since the first description of mitosis by Flemming in 1965 (1) until the production of the first *Xenopus* egg extract by Lohka and Masui in 1983 (2), studies of the mechanisms regulating cell division had been limited. The development of the *Xenopus* egg extract model has revolutionized cell cycle studies. The use of egg extracts allows the availability of a large quantity of biological material synchronized at specific phases of the cell cycle. Concentrated extracts retain the majority of the properties of intact

egg cytoplasm and mimic many of the biochemical and morphological changes associated with DNA replication and mitosis. The extracts can be easily and inexpensively prepared. They are widely used in cell biological studies. Moreover, these extracts permit the elimination of a specific cell cycle regulator by immunodepletion and its subsequent “rescue” by the ectopic translation of the corresponding messenger RNA (mRNA). This maneuver facilitates the analysis of the physiological role of different proteins in the cell cycle control.

Progress through mitosis is governed by the sequential degradation of different cell cycle proteins. This degradation is mediated by the ubiquitination pathway. In this process, an ubiquitin chain is covalently attached to the target protein, leading to its recognition and proteolysis by the 26S proteasome. Ubiquitination involves three major steps (3). First, the ubiquitin-activating enzyme (E1) forms a covalent bond to ubiquitin. Second, the activated ubiquitin is transferred to a second enzyme, the ubiquitin-conjugating enzyme (E2). Finally, E2, together with a third enzyme, the ubiquitin–ligase (E3), transfers the ubiquitin to the substrate protein. The E3 enzyme is a key component of this pathway because it confers substrate specificity. Two different ubiquitin–ligases play important roles in the cell cycle: the SCF (Skp1/Cullin/F-Box) and the anaphase-promoting complex (APC). SCF controls principally the degradation of cell cycle regulators at the G1/S and G2/M boundary, and APC is required for the progression and exit from mitosis.

In this chapter, we focus on the different methods used in *Xenopus* egg extracts to test the putative ubiquitination and degradation of a specific protein. We also describe in detail different practical procedures that demonstrate the functional role of the ubiquitin–ligase APC in this degradation.

2. Materials

2.1. Preparation of Cytostatic Factor and Interphase Egg Extracts

1. Pregnant mare serum gonadotropin (PMSG): 200 U/mL PMSG (Intervet, Boxmeer, Holland), dissolved in water and made freshly every time.
2. Human chorionic gonadotropin (hCG): 1333 U/mL hCG (Sigma CG-10, Steinheim, Germany) in water and stored at 4°C for as long as 1 wk.
3. Laying buffer: 100 mM NaCl.
4. Dejelling solution: 2% cysteine hydrochloride monohydrate (Sigma C-7880) titrated to pH 7.8 with NaOH.
5. Extract buffer (XB): 100 mM KCl, 0.1 mM CaCl₂, 1 mM MgCl₂, 50 mM sucrose, and 10 mM *N*-2-hydroxyethylpiperazine-*N*-2-ethanesulfonic acid (HEPES) at pH 7.7 (pH is titrated with KOH). We make two-fold (2X) concentrated XB and store it frozen. This stock is freshly diluted with water for every experiment.
6. Cytochalasin B: 10 mg/mL cytochalasin B (Sigma C-6762) in dimethyl sulfoxide (DMSO) and stored in aliquots of 10 to 20 µL at –20°C.
7. Aprotinin: 5 mg/mL aprotinin (Sigma A-1153) in water stored in aliquots of 200 µL at –20°C.

2.2. Protein Degradation Assay

2.2.1. mRNA Obtention

In vitro synthesis of mRNAs is carried out using the mMessage mMachine™ kit from Ambion for either SP6 (Ref: 1340), T7 (Ref: 1344) or T3 (Ref: 1348) promoters.

2.2.2. *In Vitro* Translation

1. In Vitro Translation System: rabbit reticulocyte lysate system nuclease treated (Promega L4960). Reticulocyte lysate should be stored in aliquots of 15 μ L at -80°C .
2. [^{35}S] Methionine: [^{35}S] methionine is from Amersham Biochemicals (AGQ 0080), and it is stored at -20°C in 20- μ L aliquots.

2.3. *In Vitro* Ubiquitination

1. 6-Histidine ubiquitin: recombinant 6-histidine ubiquitin was purified with a nickel-NTA column as previously described (4). 6-Histidine ubiquitin is eluted to a final concentration (FC) of 10 mg/mL (according manufacturer's protocols), dialyzed against 50 mM Tris buffer at pH 7.5 and stored in small aliquots at -20°C .
2. E2 enzyme (Ubch5): a pET3a-Ubch5 plasmid (described in ref. 5) was expressed in *Escherichia coli* BL21 and purified by a double chromatographic purification with a first 5 mL High S column (Bio-Rad) and a subsequent 24 mL Superose 12 column (Pharmacia). FC is 14 mg/mL. Protein preparation is dialyzed against 50 mM Tris buffer at pH 7.5, diluted with the same buffer to an FC of 4 mg/mL, and stored at -20°C in small aliquots.
3. Ubiquitin aldehyde: ubiquitin aldehyde (UW8450, Affiniti Research Products Limited) is dissolved in distilled water at an FC of 117 μM and stored in 10- μ L aliquots at -20°C .
4. Proteasome Inhibitor (MG132): proteasome inhibitor MG132 (ZW8440, Affiniti Research Products Limited) is dissolved in DMSO to an FC of 10 mM and stored at -20°C in 10- μ L aliquots.
5. Ubiquitin-activating enzyme (E1): *Xenopus* E1 protein was purified as previously described (6) except for the composition of the elution buffer (50 mM Tris buffer at pH 7.5, 1 mM dithiothreitol [DTT], 2 mM adenosine 3'-5'-cyclic monophosphate (AMP) and 2 mM inorganic pyrophosphate (PPi)). The sample was then dialyzed against the same elution buffer without AMP/PPi and stored in small aliquots at -20°C .
6. Ubiquitination buffer: 10 mM Tris buffer at pH 7.5, 5 mM MgCl_2 , 1 mM adenosine triphosphate (ATP). Ubiquitination buffer is prepared as 20X stock and stored in aliquots at -20°C .
7. Energy-regenerating system: 10 mM creatine phosphate, 80 $\mu\text{g}/\text{mL}$ creatine kinase, 1 mM ATP, 1 mM MgCl_2 . The energy-regenerating system is prepared as 20X stock and stored in small aliquots at -20°C .

2.4. Protein Immunodepletion and Translation in *Xenopus* Egg Extracts

2.4.1. Protein Immunodepletion in *Xenopus* Egg Extracts

1. Dynabeads–protein A: Dynabeads–protein A is from Dynal Biotech (Ref: 100.02).
2. Magnetic particle concentrator: magnetic rack to concentrate Dynabeads–protein A particles is from Dynal Biotech (Ref: MPC-P-12).

2.4.2. Protein Translation in *Xenopus* Egg Extracts

1. Pancreatic ribonuclease A (RNase A): 50 U/mg RNase A from bovine pancreas (cat. no. 109 142; Roche Diagnostics, Meylan, France) is diluted to 10 mg/mL in water, boiled for 30 min to inactivate contaminating DNAses, and centrifuged at 20 000g (14,000 rpm) for 20 min; the supernatant is diluted again to an FC of 40 $\mu\text{g}/\text{mL}$ and stored at -20°C .
2. 100 mM DTT solution made in water.
3. Placental RNase inhibitor (RNAguard): ribonuclease inhibitor from human placenta, 5000 U, 30 U/ μ L (cat. no. 27-0815-01; Amersham Bioscience).
4. Transfer RNA (tRNA): tRNA from bovine liver (Sigma R-4752) is diluted in water to an FC of 5 mg/mL and frozen at -20°C in small aliquots.

5. Phosphocreatine: stock solution of 1 M phosphocreatine (Sigma P 1937) is prepared with distilled water and stored in small aliquots at -20°C .
6. Spermidine: 100 mM Spermidine solution (Sigma S 0266) is prepared with distilled water and stored in small aliquots at -20°C .

3. Methods

3.1. Preparation of Interphase and Cytostatic Factor Egg Extracts

Immature oocytes are arrested in the female *Xenopus* ovary at late prophase of the first meiotic cycle. Progesterone primes ovulation and induces oocytes to resume meiosis I and to enter into meiosis II, at which they remain arrested at metaphase with a high cyclin B/cdk1 activity. The fluctuation of this kinase activity controls the cell cycle. Activation of cyclin B/cdk1 induces entry into mitosis or meiosis, whereas its inactivation triggers mitosis and meiosis exit. In laid eggs, metaphase II arrest is maintained by the cytostatic factor (CSF; reviewed in [ref. 7](#)) which prevents cyclin B/cdk1 inactivation by impairing ubiquitin-dependent degradation of cyclin B. On fertilization or parthenogenetic activation, a transient increase in the cytoplasmic free calcium levels triggers meiosis exit by releasing CSF arrest.

Two different *Xenopus* egg extracts can be obtained: interphase extracts and CSF extracts. Interphase extracts are obtained by lysing laid eggs in the absence of ethylene glycol *bis* (beta-aminoethyl ether)-*N,N,N',N'*-tetraacetic acid (EGTA). The presence of calcium in the extraction buffer leads to cyclin B degradation and as a consequence the release of the CSF arrest and exit of meiosis. When demembrated sperm nuclei are added to these extracts, the nuclear DNA decondense and initiate DNA replication, thus mimicking the events of the S phase of the cell cycle. These sperm-supplemented extracts have been widely used to investigate the mechanisms controlling DNA condensation ([8,9](#)) and replication ([10,11](#)). On the other hand, because they reproduce the events of meiosis/mitosis exit, they are also very useful for studying the ubiquitination and degradation of proteins during this phase of the cell cycle ([12,13](#)). CSF extracts are obtained by crushing metaphase II-arrested eggs in the presence of EGTA. In the absence of Ca^{2+} , these extracts maintain high cyclin B protein levels and cyclin B/cdk1 kinase activity. The addition of demembrated sperm to these extracts results first in chromosome condensation and subsequently in the formation of metaphase plates that will remain stable unless calcium is added. In these extracts, calcium addition will induce in vitro metaphase-to-anaphase transition and exit of the meiotic/mitotic state. Such extracts are very useful for the study of different aspects of the cell cycle, such as the mechanisms controlling the mitotic spindle assembly ([14](#)) or the regulation of the metaphase-to-anaphase transition ([15,16](#)), or the study of the ubiquitination pathway responsible for the degradation of different cell cycle regulators during this late phase of meiosis/mitosis ([17](#)).

3.1.1. Preparation of Interphase Extracts

The procedure for isolation of interphase *Xenopus* egg extracts is based in the method of Lohka and Masui ([2](#)).

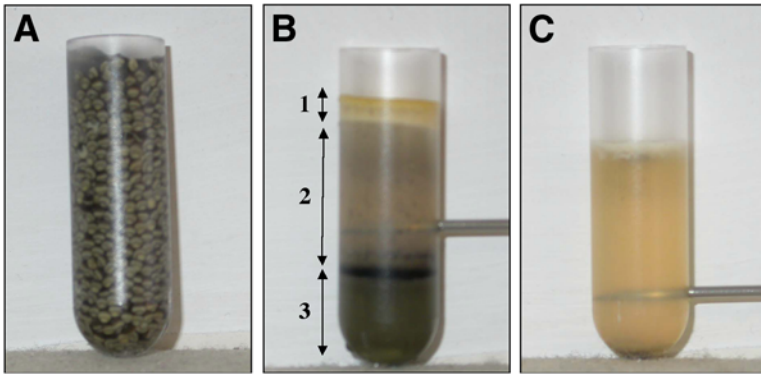


Fig. 1. Stages in the preparation of *Xenopus* egg extracts. **(A)** Dejellied oocytes transferred in a polyallomer centrifuge tube (Beckman). **(B)** The same tube after 15 min of centrifugation at 15,000 rpm at 4°C in a TLS 55 Beckman rotor. Three layers are formed: lipids (1), cytoplasm (2), and yolk (3). As shown, cytoplasmic fraction is recovered by puncturing above the yolk fraction. **(C)** The same tube after a second centrifugation. Cytoplasmic fraction is recovered again by a new puncturing above the yolk pellet.

1. Female frogs are primed for ovulation first by injection of 100 U of PMSG 3 to 14 d before egg collection. Ovulation is then induced by the subsequent injection of 660 U of hCG. Toads are then placed in a separate container containing the Laying Buffer in a room maintained at 19°C. Eggs are collected 18 h later.
2. Eggs are inspected visually. Only batches presenting a homogeneous population of regular shape–feature oocytes with a clear differentiated animal and vegetal pole will be chosen. Any batch containing an extensive number of lysed or activated (*see Note 1*) eggs will be discarded. Extracts should be prepared as promptly as possible to prevent egg lyses and activation.
3. Eggs are poured in a glass Petri dish. Lysed or pigment mottled eggs are then eliminated using a 3-mL plastic transfer pipet (Falcon) with a tip that has been cut to give a big enough orifice to avoid oocyte crushing. Eggs are rinsed twice in XB buffer and subsequently dejellied with 2% cysteine solution by gently swirling. Once dejellied (*see Note 1*), they are extensively rinsed with XB buffer to completely eliminate cysteine solution (*see Note 2*).
4. Eggs are then recovered from the Petri dish by a cut transfer pipet and transferred in a polyallomer centrifuge tube (11 × 34 mm, Beckman) previously filled with XB buffer. Once eggs are packed, the excess of XB buffer is discarded to avoid extract dilution.
5. Eggs are then crushed by centrifugation in a TLS 55 Beckman rotor for 15 min at 12,000g at 4°C. At the end of centrifugation, the tubes are recovered and maintained on ice. Three layers will be formed after centrifugation, from top to bottom: lipids, cytoplasm, and yolk (*see Fig. 1B*). It is important that from this point the extract should always be kept on ice.
6. The cytoplasm layer is collected by puncturing the side of the tube with an 18-gage needle attached to a syringe (*see Fig. 1B*). Cytochalasin B is then added to an FC of 50 µg/mL, and the mixture is centrifuged again for 15 min at 12 000g at 4°C in a TLS 55 rotor.

7. Recover the cytoplasmic fraction as in **step 6**; see **Fig. 1C**). Aprotinin is added to an FC of 5 $\mu\text{g}/\text{mL}$. Extracts are either used directly or frozen with liquid nitrogen in small aliquots.

3.1.2. Preparation of CSF Extracts

The preparation of the CSF-arrested extracts is similar to that of the interphasic extracts except for the differences noted next.

1. It is very important during the entire procedure to manipulate eggs gently to prevent egg activation.
2. Washing of eggs before and after cysteine treatment must be carried out with XB buffer containing an FC of 5 mM EGTA.
3. Eggs must be gently poured into centrifuge tubes previously filled with XB and EGTA.

3.2. Characterization of Cell Cycle Regulators Proteolyzed at the Metaphase-to-Anaphase Transition

3.2.1. Protein Degradation Assay

The protein degradation assay is useful for analysis of the degradation of a cell cycle regulator during the metaphase-to-anaphase transition. The degradation of several cell cycle proteins, such as cyclin B (**18**) and Xkid (**17,19**), has been characterized by this procedure.

In this assay, our putative substrate of ubiquitin-mediated degradation is translated *in vitro* in the presence or absence of [^{35}S] methionine and then added to CSF extracts. Once mixed, the extract, which is arrested at metaphase II of meiosis, is induced to exit meiosis by the addition of calcium. A sample of this mixture is recovered at different times following calcium addition, and the levels of the putative substrate are analyzed by either autoradiography (when ^{35}S is included) or immunoblotting. This analysis can also apply to endogenous substrates present in the extracts, employing immunoblotting to determine the levels of the proteins.

1. The plasmid containing the complementary DNA encoding the protein to be tested is linearized with a restriction enzyme downstream of the insert. Transcription is then developed with the mMessage mMachine as described by the manufacturer's recommendations.
2. Protein translation is performed by mixing 11.25 μL reticulocyte lysate solution and 0.75 μL amino acid mixture minus methionine solution from the rabbit reticulocyte lysate system (Promega) plus 1.5 μL [^{35}S] methionine and 1.5 μL of the mRNA transcript (1 $\mu\text{g}/\mu\text{L}$) (mRNA must be preheated at 63°C for 5 min and immediately placed on ice to avoid formation of secondary mRNA structures). This mixture is incubated for 1 h at 30°C. The protocol for translation of a nonlabeled protein is developed as described in **Note 3**. Protein translation is verified by sodium dodecyl sulfate–polyacrylamide gel electrophoresis (SDS–PAGE) and autoradiography.
3. To perform a degradation assay, 2 μL of the reticulocyte lysate containing the radiolabeled protein are mixed to 20 μL CSF extract. Subsequently, CaCl_2 is added to an FC of 0.5 mM to induce metaphase II exit (see **Note 4**). A positive control such as radiolabeled cyclin B protein (1 μL reticulocyte lysate) should be added to the same mixture prior to the addition of calcium to induce metaphase II exit (see **Notes 5** and **6**). The degradation mix is incubated at room temperature; 2- μL samples are removed at different times (0, 20, 40, 60, 120 min). The protein levels are analyzed by SDS–PAGE and autoradiog-

raphy. When endogenous or nonlabeled protein levels are studied, they are analyzed by SDS-PAGE and immunoblotting. The degradation of cyclin B is indicative of successful metaphase exit.

3.2.2. Protein Ubiquitination Assay

Most of the cell cycle-dependent protein degradation is carried out by the ubiquitination pathway (19–21). Ubiquitin-dependent degradation at the metaphase-to-anaphase transition is regulated by an ubiquitin–ligase named APC-Cdc20; this degradation is controlled by the ubiquitin–ligase APC-Cdh1 from anaphase to the end of mitosis and throughout the G1 phase (M/G1 phase).

Both E3 ubiquitin–ligases are composed of a multisubunit complex, the APC, and regulated by two different activators, Cdc20 and Cdh1. The addition of calcium to CSF extracts induces first metaphase II-to-anaphase II transition and subsequently meiosis exit. When a cell cycle protein is degraded in CSF extracts following the addition of calcium, it is likely that the degradation is mediated by ubiquitination and that it is dependent on the APC. Furthermore, APC-Cdc20 is likely responsible because Cdh1 is not present in *Xenopus* eggs in a sufficient amount to form an active APC-Cdh1 complex (16). The following assay is designed to test the involvement of APC-cdc20 in such a system:

1. APC-Cdc20 complexes are purified from CSF extracts by immunoprecipitation with antibodies against the APC structural component Cdc27. To that, 10 μL of Dynabeads–protein A are first washed twice with 100 μL ; Tris-HCl buffer (Tris 50 mM at pH 7.5) and subsequently incubated with 1 μg affinity-purified anti-Cdc27 antibodies in 100 μL of the same buffer for 30 min at 4°C (see Note 7). Antibody-bound Dynabeads are then extensively washed and subsequently incubated with 30 μL CSF extract. After 1-h incubation at 4°C, the APC-Cdc20 beads are washed five times with XB buffer supplemented with 500 mM KCl and 0.5% Nonidet P-40 and twice in XB buffer. This complex is kept on ice until use. APC-Cdc20 purification from CSF extracts must be freshly prepared for each in vitro ubiquitination assay.
2. Each ubiquitination assay is performed in a 20- μL volume. The reaction mixture contains the purified APC-Cdc20 beads, an energy-regenerating system (1 μL 20X stock), 125 μM 6-histidine-ubiquitin (2 μL of a 10-mg/mL solution), 1.2 μM of *Xenopus* E1 (3 μL of a 1-mg/mL solution), 30 μM Ubch5 (2.5 μL of a 4-mg/mL solution), 200 μM of the proteasome inhibitor MG132 (0.4 μL of a 10 mM solution), 5 μM of ubiquitin aldehyde (0.8 μL of a 117 μM solution) (see Note 8), 2 μL of a radiolabeled programmed reticulocyte lysate, 1 μL of ubiquitination buffer, and 7.3 μL of distilled water. The reaction is incubated at room temperature for 1 h, quenched with SDS sample buffer, and analyzed by SDS-PAGE followed by autoradiography. If the corresponding protein is ubiquitinated in these conditions, a slowly migrated smeared background corresponding to ubiquitinated forms will appear above the major protein band. Negative controls in which either APC-Cdc20 or Ubch5 is left out should be included to test the specificity of the ubiquitination reaction (see Fig. 2).

3.2.3. Immunodepletion and Rescue Assays in CSF Extracts

It is possible to demonstrate the function of an ubiquitin–ligase in the ubiquitination and degradation of a cell cycle regulator during metaphase-to-anaphase transition by

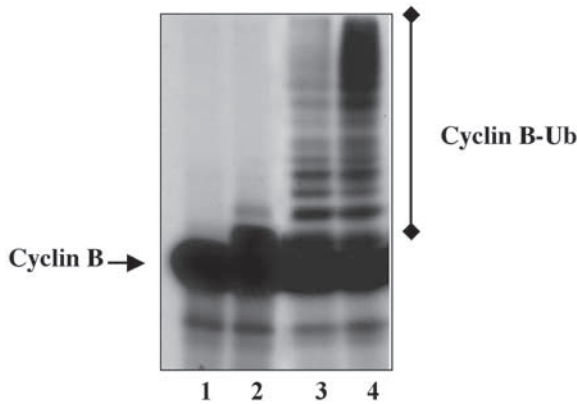


Fig. 2. Cyclin B ubiquitination assay. ^{35}S -radiolabeled cyclin B1 translated in reticulocyte lysate was incubated in the presence (*lanes 3 and 4*) or in the absence (*lanes 1 and 2*) of active APC complex. This complex was obtained by Cdc27 immunoprecipitation either in interphase *Xenopus* egg extracts preincubated with recombinant GST-cyclin B to activate cyclin B/cdk1 kinase (*lane 3*) or in CSF *Xenopus* egg extracts (*lane 4*). In *lanes 3 and 4*, the incubation buffer contains 6-histidine Ubiquitin, Ubch5, MG132, ubiquitin aldehyde, and the APC-Cdc27 beads. In *lane 2*, ^{35}S -radiolabeled cyclin B1 is incubated in the absence of APC-Cdc27 beads. In *lane 1*, the incubation buffer contains exclusively ^{35}S -radiolabeled cyclin B1. Ubiquitination pattern (cyclin B-Ub) was analyzed by SDS-PAGE and autoradiography.

immunodepletion of this complex from the CSF extracts. Subsequently, a rescue assay can be performed to demonstrate the specific effect of this immunodepletion. For example, the role of the APC-Cdc20 in the degradation of a cell cycle regulator during metaphase-to-anaphase transition can be verified by immunodepletion of either the APC structural component Cdc27 or the APC regulator Cdc20. In both cases, immunodepletion results in APC-Cdc20 inhibition and, as a consequence, should inhibit substrate degradation. Subsequently, the rescue assay can be performed by the translation of Cdc20 mRNAs in these Cdc20-immunodepleted extracts. This manipulation should restore APC-Cdc20 activity and protein degradation. In contrast, removal of Cdc27 in these extracts cannot be rescued by Cdc27 mRNA translation because the immunodepletion removes the entire APC complex from the extract.

3.2.3.1. IMMUNODEPLETION

1. 20 μL of CSF extracts are incubated with 2 μg of antibody-bound Dynabeads for 30 min at 4°C (antibody binding to Dynabeads is described in **Subheading 3.2.2**). The ability to deplete a specific protein from the extract is dependent on the quality of the antibodies; thus, we always use affinity-purified antibodies. We have also observed that for some antibodies, immunodepletion is only obtained when two successive immunoprecipitations are performed. In this case, we perform two antibody incubations of 15 min each. Extended incubations must be avoided because they can induce spontaneous metaphase II exit. At the end of the assay, a sample of the extract is taken to verify immunodepletion by SDS-PAGE and immunoblotting.

2. Following immunodepletion, a degradation assay is performed in these extracts to test the effect of the inactivation of the selected ubiquitin–ligase in the proteolysis pattern of a particular protein (the degradation assay is described in **Subheading 3.2.1.**).

3.2.3.2. RESCUE

1. Freshly prepared CSF extracts are mixed with antibody-bound Dynabeads (immunodepletion). Simultaneously, the extracts are first treated for 15 min at 16°C with RNase A at an FC of 0.2 µg/mL (please write here 0.2 µg/mL) to induce destruction of endogenous mRNAs, subsequently supplemented with DTT (1 nmol/µL FC) and finally treated 10 min at the same temperature with RNAGuard (0.37 U/µL FC) to inhibit RNase A.
2. Dynabeads are then removed from the extract using a magnetic rack (*see Subheading 2.*). Magnetic beads are tightly retained in the wall of the tube within the magnetic rack, thus allowing easy recovery of the depleted extracts in a fresh tube. This process can be repeated to obtain complete removal of the beads (*see Note 7*).
3. Clear supernatants are then supplemented with tRNA (0.1 µg/µL FC), phosphocreatine (20 nmol/µL FC), and spermidine (1 nmol/µL FC) and with the mRNA encoding the immunodepleted protein (0.1 µg/µL) and incubated for 2 h at 20°C. Please note that mRNA must be first preheated at 63°C for 3 min and rapidly placed on ice to prevent the formation of secondary mRNA structures. A sample of this extract is saved to analyze protein translation.
4. Once the protein is translated in the immunodepleted CSF extract, a degradation assay of a particular substrate can be performed as described in **Subheading 3.2.1.** A comparison between the immunodepleted extracts and the same extracts with exogenous mRNA should reveal the functional importance of the ubiquitin ligase activator (*cdc20*).

3.3. Characterization of Cell Cycle Regulators Proteolyzed at Mitosis Exit and G1 Phase

As described in **Subheading 3.2.2.**, the metaphase-to-anaphase and the M-G1 phases and are regulated by the sequential ubiquitin-dependent degradation of different cell cycle proteins by the APC-Cdc20 and APC-Cdh1 complexes. APC-Cdc20 mediates securin and cyclin B degradation, a prerequisite for progression through mitosis (**16,22**). APC-Cdh1 mainly controls anaphas–telophase transition and progression through G1 by ensuring the complete proteolysis of cyclin B and Cdc20 (**23–25**).

Early cell divisions in *Xenopus* embryos consist of alternating S and M phases without G1 and G2 gaps. Accordingly, the ubiquitin-dependent degradation mechanism controlling G1 phase is not active in these cells. This inactivation is the result of the presence of very low levels of Cdh1 incapable of activating APC. Similar to embryo cells, interphase egg extracts are devoid of APC-Cdh1 activity. This feature makes interphase extracts a powerful tool for the study of the APC-Cdh1-dependent degradation. Actually, activation of the APC-Cdh1 can be restored in these extracts by ectopic translation of *cdh1* mRNA. Using this approach, two new substrates of APC-Cdh1 have been identified, the proteins Aurora A and Xkid (**12,13,17**).

To test if a protein is a substrate of the APC-Cdh1 complex, interphase extracts are first translated with the mRNA encoding Cdh1 and subsequently used to develop a degradation assay. The protocol used is similar to that described for the CSF extracts:

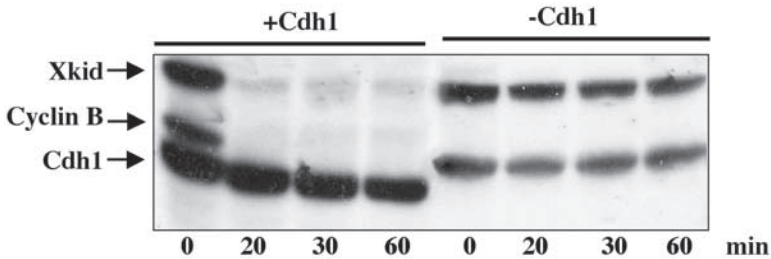


Fig. 3. The APC-Cdh1 complex mediates ubiquitin-dependent degradation of the chromokinesine Xkid. Cdh1 protein was translated in interphase egg extracts by the addition of the corresponding mRNA in the presence of [^{35}S]-methionine. Following a 1-h translation, 1 μL ^{35}S -cyclin B1 and 1 μL ^{35}S -Xkid translated in reticulocyte lysate were added to 20 μL Cdh1-containing extract (+Cdh1). At different times (0, 20, 30, and 60 min), 2- μL samples were removed, and the protein levels were analyzed by SDS-PAGE and autoradiography. As a control, the same degradation assay was performed in interphase egg extracts without exogenous cdh1 mRNA (-Cdh1).

1. Freshly prepared interphase extracts are treated with RNase A (0.2 $\mu\text{g}/\mu\text{L}$ FC) for 15 min at 16°C, subsequently supplemented with DTT (1 nmol/ μL FC), and finally treated with RNAgard (0.37 U/ μL FC) for 10 min.
2. Extracts are then supplemented with tRNA (0.1 $\mu\text{g}/\mu\text{L}$ FC), phosphocreatine (20 nmol/ μL FC), spermidine (1 nmol/ μL FC), and the mRNA encoding Cdh1 (0.1 $\mu\text{g}/\mu\text{L}$ FC) and incubated for 2 h at 20°C. A sample of this extract is saved to analyze Cdh1 translation.
3. Cdh1-containing interphase extracts are then used to perform a degradation assay with a putative APC-Cdh1 substrate as described in **Subheading 3.2.1**.

If this protein is degraded in interphase extracts in the presence but not in the absence of Cdh1, it is very likely that this protein is proteolysed by the APC-Cdh1 complex (see **Fig. 3**). However, to further demonstrate the role of this ubiquitin-ligase in this process, ubiquitination and immunodepletion assays similar to that described for CSF extracts can be performed.

4. Notes

1. Completion of the dejellinging process is easily confirmed because eggs that have lost their jelly coats pack as tight spheres with little space between (**Fig. 1A**). These dejellied eggs stick together and are more easily activated and lysed; thus, once dejellied they should be handled carefully. Activated eggs are easily recognized because activation induces animal pole retraction and thus a reduction of the pigmented zone.
2. We have noticed that dejellied eggs are very sensitive to the reducing effect of the cystein solution. These eggs are easily lysed when there is residual cystein. Thus, cystein solution must be completely removed from the media by extensively rinsing the eggs with XB buffer.
3. Translation of nonlabeled protein is performed by mixing 3.75 μL reticulocyte lysate solution, 0.25 μL amino acid mixture minus methionine solution, and 0.25 μL amino acid mixture minus leucine solution (so the two complement each other to make up a complete

set of amino acids) from the rabbit reticulocyte lysate system (Promega), and 0.5 μL of the mRNA transcript (1 $\mu\text{g}/\mu\text{L}$).

4. Newly prepared CaCl_2 solution must be calibrated for the capacity to induce metaphase II exit in every CSF extract. A degradation assay must be performed by mixing different volumes of this new CaCl_2 solution (from 0.5 to 2 μL) to 20 μL CSF extract to determine precisely the concentration that will induce cyclin B proteolysis and metaphase II exit. Some extracts need a higher concentration of CaCl_2 than others to induce metaphase II exit. Excess Ca^{2+} should be avoided as it may activate calpain proteases and cause nonspecific effects.
5. Care must be taken to avoid too much dilution of the extract when performing the degradation assay. Such dilution may inhibit ubiquitin-dependent degradation, so the smallest possible volume of radiolabeled cyclin B should be added.
6. Cyclin B can be used as a positive control for metaphase II exit because its proteolysis is easily observed between 10 and 15 min following calcium addition at the metaphase II-to-anaphase II transition.
7. It is very important to use the smallest possible quantity of beads to perform immunoprecipitation because the presence of beads in the extract interferes with protein degradation. The use of magnetic Dynabeads–protein A instead of protein A-Sepharose improves significantly the efficiency of these assays because Dynabeads are more efficiently removed. In the case that the Cdc27 immunoprecipitation does not bring enough active APC-Cdc20 complex to induce ubiquitination, it is preferable to add purified recombinant Cdc20 protein instead of using more anti-Cdc27 immunoprecipitate.
8. MG132 is used in the ubiquitination assay to inhibit the proteasome activity present in the reticulocyte lysate. Ubiquitin aldehyde is used to inhibit deubiquitination enzymes. Both are used to enhance protein ubiquitination and therefore facilitate detection of ubiquitinated substrates.

Acknowledgments

We thank Olivier Coux for the gift of the Ubch5, the 6-histidine ubiquitin, and the recombinant *Xenopus* ubiquitin-activating enzyme (E1). This work was supported by the Ligue Nationale Contre le Cancer (Equipe Labellisée).

References

1. Flemming, W. (1965) Contributions to the knowledge of the cell and its vital processes. Part II. *J. Cell Biol.* **25**, 3–69.
2. Lohka, M. J. and Masui, Y. (1983) Formation in vitro of sperm pronuclei and mitotic chromosomes induced by amphibian ooplasmic components. *Science* **220**, 719–721.
3. Hershko, A. and Ciechanover, A. (1998) The ubiquitin system. *Annu. Rev. Biochem.* **67**, 425–479.
4. Beers, E. P. and Callis, J. (1993) Utility of polyhistidine-tagged ubiquitin in the purification of ubiquitin–protein conjugates and as an affinity ligand for the purification of ubiquitin-specific hydrolases. *J. Biol. Chem.* **268**, 21,645–21,649.
5. Scheffner, M., Huibregtse, J. M., and Howley, P. M. (1994) Identification of a human ubiquitin-conjugating enzyme that mediates the E6-AP-dependent ubiquitination of p53. *Proc. Natl. Acad. Sci. USA* **91**, 8797–8801.
6. Tamura, T., Tanaka, K., Tanahashi, N., and Ichihara, A. (1991) Improved method for preparation of ubiquitin-ligated lysozyme as substrate of ATP-dependent proteolysis. *FEBS Lett.* **292**, 154–158.

7. Castro, A., Peter, M., Lorca, T., and Mandart, E. (2001) c-Mos and cyclin B/cdc2 connections during *Xenopus* oocyte maturation. *Biol. Cell* **93**, 15–25.
8. Losada, A., Hirano, M., and Hirano, T. (2002) Cohesin release is required for sister chromatid resolution, but not for condensin-mediated compaction, at the onset of mitosis. *Genes Dev.* **16**, 3004–3016.
9. Cuvier, O. and Hirano, T. (2003) A role of topoisomerase II in linking DNA replication to chromosome condensation. *J. Cell Biol.* **160**, 645–655.
10. Moore, J. D., Kirk, J. A., and Hunt, T. (2003). Unmasking the S-phase-promoting potential of cyclin B1. *Science* **300**, 987–990.
11. Vashee, S., Cvetic, C., Lu, W., Simancek, P., Kelly, T. J., and Walter, J. C. (2003) Sequence-independent DNA binding and replication initiation by the human origin recognition complex. *Genes Dev.* **17**, 1894–1908.
12. Castro, A., Vigneron, S., Bernis, C., Labbe, J. C., Prigent, C., and Lorca, T. (2002) The D-Box-activating domain (DAD) is a new proteolysis signal that stimulates the silent D-Box sequence of Aurora-A. *EMBO Rep.* **3**, 1209–1214.
13. Castro, A., Arlot-Bonnemains, Y., Vigneron, S., Labbe, J. C., Prigent, C., and Lorca, T. (2002) APC/Fizzy-related targets Aurora-A kinase for proteolysis. *EMBO Rep.* **3**, 457–462.
14. Horne, M. M. and Guadagno, T. M. (2003) A requirement for MAP kinase in the assembly and maintenance of the mitotic spindle. *J. Cell Biol.* **161**, 1021–1028.
15. Reimann, J. D. and Jackson, P. K. (2002) Emi1 is required for cytostatic factor arrest in vertebrate eggs. *Nature* **416**, 850–854.
16. Lorca, T., Castro, A., Martinez, A. M., et al. (1998) Fizzy is required for activation of the APC/cyclosome in *Xenopus* egg extracts. *EMBO J.* **17**, 3565–3575.
17. Castro, A., Vigneron, S., Bernis, C., Labbe, J. C., and Lorca, T. (2003) Xkid is degraded in a D-box, KEN-box, and A-box-independent pathway. *Mol. Cell Biol.* **23**, 4126–4138.
18. Murray, A. W. and Kirschner, M. W. (1989) Cyclin synthesis drives the early embryonic cell cycle. *Nature* **339**, 275–280.
19. Funabiki, H. and Murray, A. W. (2000) The *Xenopus* chromokinesin Xkid is essential for metaphase chromosome alignment and must be degraded to allow anaphase chromosome movement. *Cell* **102**, 411–424.
20. Glotzer, M., Murray, A. W., and Kirschner, M. W. (1991) Cyclin is degraded by the ubiquitin pathway. *Nature* **349**, 132–138.
21. Zou, H., McGarry, T. J., Bernal, T., and Kirschner, M. W. (1999) Identification of a vertebrate sister-chromatid separation inhibitor involved in transformation and tumorigenesis. *Science* **285**, 418–422.
22. Cohen-Fix, O., Peters, J. M., Kirschner, M. W., and Koshland, D. (1996) Anaphase initiation in *Saccharomyces cerevisiae* is controlled by the APC-dependent degradation of the anaphase inhibitor Pds1p. *Genes Dev.* **10**, 3081–3093.
23. Pflieger, C. M. and Kirschner, M. W. (2000) The KEN box: an APC recognition signal distinct from the D box targeted by Cdh1. *Genes Dev.* **14**, 655–665.
24. Yamano, H., Gannon, J., and Hunt, T. (1996) The role of proteolysis in cell cycle progression in *Schizosaccharomyces pombe*. *EMBO J.* **15**, 5268–5279.
25. Visintin, R., Prinz, S., and Amon, A. (1997) CDC20 and CDH1: a family of substrate-specific activators of APC-dependent proteolysis. *Science* **278**, 460–463.

Introduction to Nucleocytoplasmic Transport

Molecules and Mechanisms

Reiner Peters

Summary

Nucleocytoplasmic transport, the exchange of matter between nucleus and cytoplasm, plays a fundamental role in human and other eukaryotic cells, affecting almost every aspect of health and disease. The only gate for the transport of small and large molecules as well as supramolecular complexes between nucleus and cytoplasm is the nuclear pore complex (NPC). The NPC is not a normal membrane transport protein (transporter). Composed of 500 to 1000 peptide chains, the NPC features a mysterious functional duality. For most molecules, it constitutes a molecular sieve with a blurred cutoff at approx 10 nm, but for molecules binding to phenylalanine–glycine (FG) motifs, the NPC appears to be a channel of approx 50 nm diameter, permitting bidirectional translocation at high speed. To achieve this, the NPC cooperates with soluble factors, the nuclear transport receptors, which shuttle between nuclear contents and cytoplasm. Here, we provide a short introduction to nucleocytoplasmic transport by describing first the structure and composition of the nuclear pore complex. Then, mechanisms of nucleocytoplasmic transport are discussed. Finally, the still essentially unresolved mechanisms by which nuclear transport receptors and transport complexes are translocated through the nuclear pore complex are considered, and a novel translocation model is suggested.

Key Words: Nuclear envelope; nuclear pore complex; nuclear transport receptors; nucleocytoplasmic transport; nucleoporins.

1. Introduction

In 1949, the nuclear envelope of salamander oocytes was visualized by electron microscopy (*1*) which revealed a dense array of large pores occluded by “complexes.” Previous studies, initiated in the 19th century by Schleiden, Schwann, Purkinje, and others, had shown that the nucleus was a universal cell component of higher organisms and had provided evidence for a thin membrane surrounding the nucleus. But the

direct visualization of the nuclear envelope and nuclear pore complexes (NPC) fired the imagination, particularly when it became apparent that the nuclear envelope segregates genetic material from the protein-synthesizing apparatus. It appeared obvious, that the creation of the nucleus during evolution was not just one event among others but the decisive step toward higher complexity and that the exchange of matter between nucleus and cytoplasm would profoundly affect cell function. However, several decades of intensive work were required to substantiate such speculations. Only during recent years, fueled by the extraordinary progress in molecular biology and biophysics, could the close connections between nucleocytoplasmic transport and cellular networks be revealed. Links to nucleocytoplasmic transport were found, for instance, in gene expression, transcriptional silencing, chromatin organization, posttranscriptional modifications, cell cycle regulation, proliferation, differentiation, apoptosis, viral infections, cancer, and certain genetic diseases (2–6). Thus nucleocytoplasmic transport became a focus of biomedicine (for review, see refs. 7–17).

What are the fundamental parameters driving and regulating nucleocytoplasmic transport? Nucleocytoplasmic transport involves short distances. But on a molecular scale a pathway as short as 1 μm involves an incredibly large number of steps, particularly in an environment crowded with macromolecules, particles and membranes. The cell has developed systems to facilitate molecular transport in the cytoplasm by energy-dependent mechanisms involving filaments and motor proteins. It has been suggested (18) that analog systems occur also in the nucleus (for a recent critical review, see ref. 19). But most of the experimental evidence, including our early photobleaching studies (20), indicates (21–25) that the dissipation of macromolecules in the aqueous phase of the nucleus is usually based on simple diffusion. This holds also for large structures such as ribonucleoprotein particles (RNPs) (26) and ribosomal subunits (27).

Thus, diffusion seems to be the basis of nucleocytoplasmic transport. However, chemical reactions, specific association–dissociation processes, and compartmentalization by membranes play a decisive role in controlling and directing diffusion. In salivary gland cells of *Chironomus tentans* larvae the interplay between these factors could be visualized with exceptional clarity. These cells are dedicated to producing a giant peptide (~1 MDa) in large amounts. The premessenger ribonucleic acid (mRNA) (35–40 kb) is created on the puffs (Balbiani rings, BRs) of chromosome IV, a process that could be followed by electron microscopy, both in spreads (28) and in cells (29). In the course of transcription, a thin ribonucleoprotein fibril is formed. The fibril is initially loosely coiled but then tightly folded and bent into a partial ring. On release from the gene, the BR particle assumes an almost ring like conformation, which has been reconstructed by electron tomography (30). The compact BR particle is dissipated in the nuclear contents by diffusion (26). When encountering a NPC, it binds in a specific orientation to the nuclear basket of the NPC, unfolds into a fibril, and is translocated, 5' end first, through the NPC center (31). In the cytoplasm, the filament is further unfolded, bound by ribosomes, and translated. The pathway the BR particle takes when traveling from genes to ribosomes emphasizes the critical role of the nuclear envelope and NPC: the nuclear envelope confines diffusive dissipation to

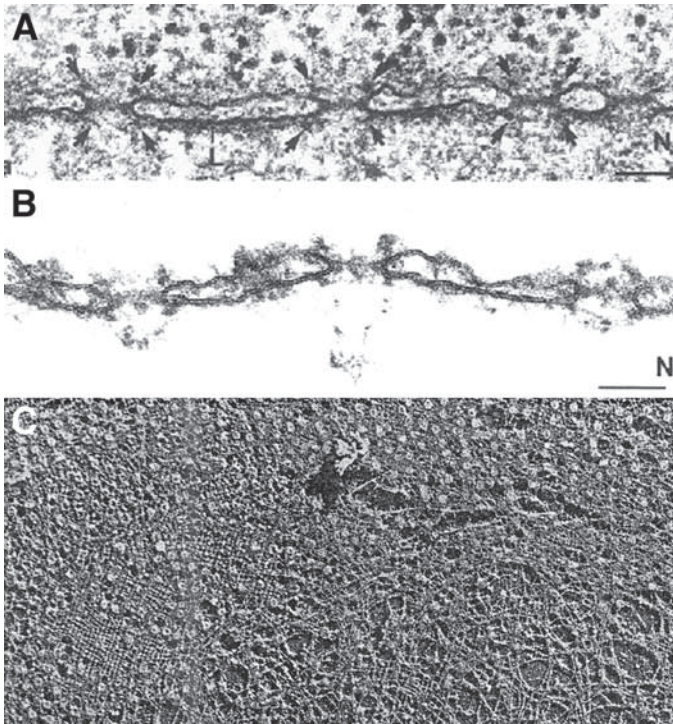


Fig. 1. Structure of nuclear envelope and nuclear lamina in amphibian oocytes. (A) Traverse section through the nuclear periphery of a growing oocyte of *Dytiscus marginalis*. The cytoplasmic and nuclear rings of the nuclear pore complexes are indicated by arrows. (B) Traverse section through an isolated nuclear envelope of a *Xenopus laevis* oocyte. (C) Nuclear face of a freeze-dried, metal-shadowed nuclear envelope of *Xenopus* oocytes that had been extracted with Triton X-100. **Figure 1A,B** from ref. 43 and **Fig. 1C** from ref. 34 with permission (<http://www.nature.com/>).

the aqueous phase of the nucleus, whereas the NPC selectively exports mature RNPs into the cytoplasm. Analogous relationships hold for proteins traveling from ribosomes to nuclear targets and thus are of general relevance.

In this chapter, we provide a brief introduction to nucleocytoplasmic transport. First, properties of nuclear envelope and NPC are summarized. Then, the transport of molecules from cytoplasm to nucleus and vice versa is considered. Finally, the core of nucleocytoplasmic, translocation through the NPC, is discussed.

2. Nuclear Envelope and Pore Complex

The nucleus is surrounded by a tripartite structure, the nuclear envelope (**Fig. 1**; reviewed in **ref. 2,32**). It consists of outer nuclear membrane (ONM), perinuclear space, and inner nuclear membrane (INM). ONM and INM fuse at many locations to form pores of approx 100 nm diameter and approx 50 nm length that harbor the NPCs. The nuclear envelope is connected to the endoplasmic reticulum (ER) by anastomoses

such that perinuclear space and ER lumen form a continuum. Little is known about the number, dynamics, and function of ER-nuclear envelope anastomoses.

The INM has a unique protein composition distinct from that of ONM and ER membrane. Most integral proteins of the INM such as lamin B receptor, lamin-associated peptides, and emerin bind directly to A- or B-type lamins and to chromatin. Furthermore, the INM is supported by a fibrous network, the nuclear lamina, made up in metazoans of four A-type lamins and three B-type lamins. The lamins display a domain structure typical for intermediate filaments (globular head domain, central α -helical coiled-coil dimerization domain, globular tail domain) and are thought (33) to be evolutionary progenitors of cytoplasmic intermediate filament proteins. In *Xenopus* oocytes (34), the lamins form a 2D orthogonal meshwork (Fig. 1C) that determines the shape and size of the nucleus, keeps the NPCs separated from each other by making direct contact (35) with NPC proteins (nucleoporins), and recruits proteins to the INM (36). Lamins have been found not only in the lamina but also in nuclear bodies (37) and might be involved in RNA processing and deoxyribonucleic acid (DNA) biosynthesis. In addition, lamins play an essential role in development (38) and have been linked with a range of genetic disorders (5).

The nuclear envelope is a dynamic structure (39). In *Xenopus* oocytes, the area of the nuclear envelope and the number of NPCs per nucleus increase by a factor of approx 5 during maturation. In HeLa cells, the surface area of the nuclear envelope increases during interphase by a factor of approx 1.4; the number of NPCs doubles. In cell types having open mitosis, the nuclear envelope is disintegrated at the onset and reformed at the end of mitosis. The number of NPCs per nucleus varies within wide limits, amounting to 40×10^6 in stage VI *Xenopus* oocytes but only 100 in adult chicken red blood cells. All components of the nuclear envelope, including lamina and NPCs, not only can be newly synthesized and inserted into the nuclear envelope, but also can be removed, rearranged, and remodeled according to cellular needs.

The NPC (Fig. 2) has been extensively studied by electron microscopic methods (1,11,32,39–43). Three-dimensional (3D) reconstructions of detergent-treated NPCs have been obtained employing negative staining (44) or freeze–dehydration (45). Recently (46), 3D reconstructions have been also obtained from NPCs embedded in amorphous ice, in the absence of detergents. It is generally accepted that the NPC consists of five major parts: the central framework, also referred to as the spoke complex; the cytoplasmic ring; eight filaments attached to the cytoplasmic ring; the nuclear ring; and the nuclear basket, consisting of eight filaments that emanate from the nuclear ring and fuse at their distal endings to form the distal ring. The central framework consists of eight spokes that have a twofold symmetry regarding the plane of the nuclear envelope.

The most controversial part of the NPC structure is the central granule, a large elongated particle in the center of the NPC. Early studies (summarized in ref. 39) reported that the central granule occurred only in variable fractions of NPCs and seemed to be composed of RNPs. It was therefore suggested that the central granule represents large cargo such as RNPs and ribosomal subunits in transit rather than a genuine component of the NPC. Later (47,48), the central granule was considered a

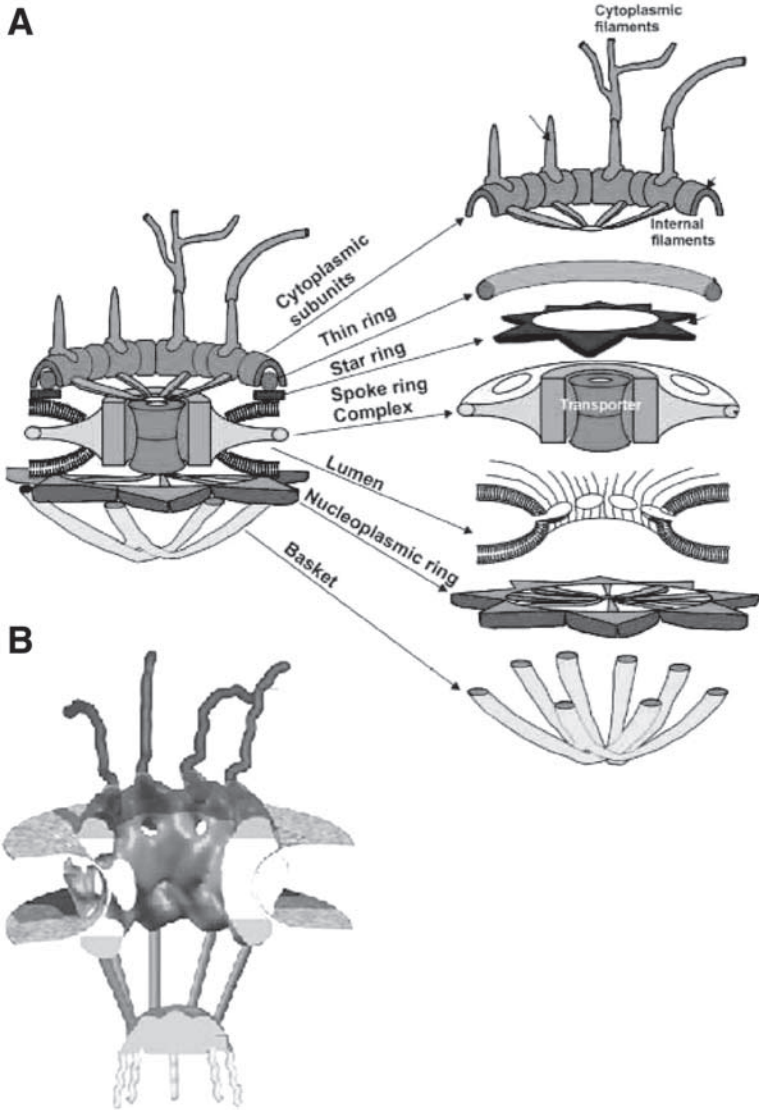


Fig. 2. Alternative structural models of the nuclear pore complex. (A) Structural model of the nuclear pore complex of *Xenopus* oocytes based on field emission in-line scanning electron microscopy of both proteolytically treated nuclear pore complexes and pore complexes reconstituted in *Xenopus* egg extracts. Modified from [ref. 42](#) with permission. (B) A 3D reconstruction of the nuclear pore complex of *Xenopus* oocytes obtained by electron microscopy of native nuclear pore complexes embedded in thick amorphous ice. (A) From [ref. 42](#); (B) from [ref. 11](#) with permission.

genuine part of the NPC, and its structure was worked out in considerable detail (Fig. 2A). Recently, it appears (11) that the central granule is composed mainly of the distal ring of the nuclear basket, projected or collapsed into the NPC center, and, to a lesser extent, of cargo in transit. Accordingly (Fig. 2B), the cargo-free NPC would contain an hourglass-shaped patent channel with a length of approx 70 nm and a smallest diameter of 40 to 50 nm. This contention is supported by a recent 3D reconstruction (49) of the NPC of *Dictyostelium discoideum*.

A number of nucleoporins have been known for some years. But only recently progress in NPC isolation (50,51) and protein characterization techniques yielded complete inventories of yeast (52) and rat liver cell (53) nucleoporins. In both yeast and rat liver cells, approx 30 different nucleoporins were found (Table 1), substantially fewer than previously estimated.

From the relative abundance of nucleoporin species in gel bands and on the assumption that each nucleoporin species occurs in eight copies per NPC or multiples thereof, the total molecular mass of the NPC was estimated to be approx 40 MDA for yeast and approx 60 MDA for liver cells. Previous determinations of the NPC mass by scanning transmission electron microscopy yielded values of 55 to 72 MDA for the yeast NPC (54) and 125 MDA for the *Xenopus* oocyte NPC (55). The difference between new and previous values was explained by assuming that transport factors and cargoes were essentially removed from biochemical but largely retained in electron microscopic preparations. From the total mass of the NPC, the number of protein molecules per NPC can be estimated as 500 to 1000.

Members of the vertebrate (v) and yeast (y) nucleoporin families are frequently named according to molecular weight, which varies between approx 30 and approx 360 kDa. In spite of that monotonous nomenclature, each member has its own distinct biogenesis, character, and function. Most nucleoporins occur in both the nuclear and cytoplasmic half of the NPC (symmetric nucleoporins), and only a few occur only on the cytoplasmic (vNup358, vNup214) or nuclear (Tpr) side (asymmetric nucleoporins). Some nucleoporins, such as vNup98 and vNup50, appear to be dynamic or mobile in the sense that their location within the NPC varies and that they can occur at cellular locations other than the NPC. Thus, vNup98 was found in intranuclear bodies and vNup107, vNup133, and vNup358 in kinetochores.

A particularly striking feature of nucleoporins is the frequent occurrence of repetitive domains (52,53). About one-third of nucleoporins contain so-called FG (phenylalanine glycine) repeats, which consist of small hydrophobic clusters of the amino acid residues FG, FXFG, or GLFG spaced by 20 to 70 hydrophilic residues. In yeast, the spacer sequences of FXFG repeats are highly charged and rich in serine and threonine; the spacers of GLFG repeats are rich in serine, threonine, and glutamine but lack acidic residues. FG repeats (cf. Fig. 3 in ref. 10 for vertebrate and Fig. 1B in ref. 56 for yeast nucleoporins) are frequently clustered at either the N-terminus (vNup98), C-terminus (vNup214), or both (vNup45, vNup58). The number of FG repeats per nucleoporin varies between approx 5 and approx 50, so that the total number of FG repeats amounts to 2,500 to 10,000 per NPC.

Table 1
Catalog of Nuclear Pore Complex Proteins

Yeast protein	Suggested vertebrate homolog	Localization	Motifs
Nup1	Nup153	Nuclear	FXFG
Nsp1 (87)	Nup62	Symmetric	FG, FXFG
Nup2	Nup50	Nuclear biased	FXFG
Nup42	NLP1/hCG1 (45)	Cytoplasmic	FG
Nup49	Nup58, Nup45	Symmetric	GLFG, FG
Nup53	Nup35	Symmetric	
Nup59	Nup35	Symmetric	
Nup57	Nup54	Symmetric	GLFG
Nup82	Nup88	Cytoplasmic	
Nup84	Nup107	Symmetric	
Nup85	Nup75/Nup85	Symmetric	
Nic96	Nup93	Symmetric	
Nup100	Nup98	Cytoplasmic biased	GLFG
Nup116	Nup98	Cytoplasmic-biased	FG, GLFG
Nup145N (60)	Nup98	Nuclear biased	GLFG
Nup120	Nup160	Symmetric	
Nup133	Nup133	Symmetric	
Nup145C	Nup96	Symmetric	
Nup157	Nup155	Symmetric	
Nup170	Nup155	Symmetric	
Nup159	Nup214/CAN	Cytoplasmic	FG
Nup188	Nup188	Symmetric	
Nup192	Nup205	Symmetric	
Gle1 (62)	hG11 (85)	Cytoplasmic biased	
Gle2 (41)	Rae1/Gle2 (41)	Symmetric	WD
Mlp1 (218)	Trp (266)	Nuclear	
Mlp2	Trp (266)	Nuclear	
Seh1 (39)	Seh1 (40)	Symmetric	WD
Nup60	-	Nuclear	FXF
Ndc1 (74)	-	Pore membrane	TM
Pom34	-	Pore membrane	TM
Pom152	-	Pore membrane	TM
-	Pom121	Pore membrane	FG, TM
-	Gp210	Pore membrane	TM
-	Nup358/RanBP2	Cytoplasmic	FXFG
-	ALADIN (60)	?	WD
-	Nup37	?	WD
-	Nup43	?	WD

Source: Modified from ref. 15, © 2003, with permission from Elsevier.

FG repeat-containing nucleoporins belong to the class of natively unfolded proteins (57), which are characterized by low overall hydrophobicity, substantial lack of α -helical or β -sheet secondary structure, high flexibility, large hydrodynamic radius, and hypersensitivity for proteases. A large body of experimental data indicates that FG repeats are the primary docking sites of karyopherins and thus play a fundamental role in selective translocation through the NPC (*see Subheading 4.*).

By systematically deleting FG motifs in yeast nucleoporins, a differentiated view of the role FG repeats in nucleocytoplasmic transport was obtained (56). FG motifs of asymmetric nucleoporins could be completely deleted without affecting growth parameters. Of the remaining FG motifs in symmetric nucleoporins (70% of total) another 20% could be deleted without inducing lethality, although growth rates were severely reduced. At those conditions, transport was also affected. But the type and degree of the transport defect depended on the specific combination of deletions.

In addition to FG repeats, nucleoporins contain Ran-binding domains, zinc fingers, and leucine zippers. Two vertebrate nucleoporins (gp210, POM121) and one yeast nucleoporin (POM152) have transmembrane (TM) domains anchoring the NPC in the nuclear membrane. Another subset of nucleoporins contains so-called WD domains (53), thought to mediate the assembly of large multiprotein complexes.

The molecular architecture of the NPC is not very well understood. It is clear that the NPC is largely built up from subcomplexes (58). The central part of the vertebrate NPC seems to be composed mainly of the vNup62 complex (vNup44, vNup54, vNup58, vNup62); the vNup107 complex (vNup85, vNup96, vNup107, vNup133, vNup160); and the vNup93-vNup188-vNup205 complex. The yeast homolog of vNup107 complex, the yNup84 complex, has been reconstituted *in vitro* and shown by electron microscopy to have a y-shaped structure (59). The cytoplasmic filaments seem to be essentially composed of vNup358, vNup214 and vNup88, while the nuclear basket is made up from mainly from Tpr (60) and vNup153 (61), which is apparently attached to the nuclear basket by its N-terminus but can extend its free C-terminus through the central channel of the NPC to the nuclear side.

3. Nucleocytoplasmic Transport

The NPC is not a "normal" transporter: It does not span a lipid bilayer to provide a pathway between topologically different compartments but occupies a large pore in the nuclear envelope connecting two topologically identical aqueous phases, cytosol and karyosol. This suggests that the evolutionary roots of the NPC and other transporters are fundamentally different (62). In line with that contention, the transport properties of the NPC are also unusual.

First, the NPC displays a remarkable functional duality: for "inert" molecules, which do not interact with nucleoporins, it constitutes a molecular sieve with a blurred cutoff at approx 10 nm, but for nuclear transport receptors, which bind specifically to nucleoporins via interaction with FG repeats, it provides a passageway of approx 50 nm diameter. Second, macromolecules containing nuclear transport signals can be selectively "pumped" from cytoplasm to nucleus or vice versa, but the NPC is not a pump.

Rather, the energy-consuming step of pumping is dissociated from the NPC and occurs in the aqueous phases of cytoplasm and nucleus.

In the following (**Subheading 3.1.**), the transport of inert molecules through the NPC is summarized. Subsequently (**Subheading 3.2.**), signal-mediated transport of proteins involving nuclear transport receptors of the karyopherin family is described. Finally (**Subheading 3.3.**), the export of messenger RNPs by nuclear export factors (NXF) is dealt with.

3.1. Permeability of the NPC for Inert Molecules

The NPC has a large passive permeability for small inert molecules that depends inversely on the molecular size of the permeant. In microinjected *Xenopus* oocytes, the NPC was found (63) to have a relative permeability of 1, 0.03, and 0.0004 for dextrans of 3.6-kDa (1.20-nm Stokes' radius), 10-kDa (2.33-nm radius), and 24.0-kDa (3.55-nm radius), respectively. When such data were interpreted employing a hydrodynamic theory for the restricted diffusion through cylindrical pores (64,65), which takes into account the steric hindrance at the pore entrance and the friction inside the pore, a pore radius of approx 9 nm diameter was derived. That figure was confirmed by many studies (reviewed in ref. 20), including permeability measurements on single NPCs (66).

Thus, the NPC is an almost negligible permeability barrier for inorganic ions and small metabolites. In contrast, the permeation of small polymers is severely restricted. Green fluorescent protein (30 kDa), for instance, can permeate passively through the NPC and is distributed in live cells approximately evenly between cytoplasm and nucleus. However, measurement of transport kinetics showed (67,68) that the permeability of the NPC for green fluorescent protein is approx 50 times smaller than that for a nuclear transport receptor of the same size. Several small nuclear proteins, such as histones (~10 kDa), contain nuclear transport signals. Apparently, in these cases slow transport by restricted diffusion is enhanced by fast receptor-mediated translocation.

For large inert proteins such as β -galactosidase proteins (~500 kDa), the nuclear envelope is virtually impermeable. In contrast, antibodies, when injected into the cytoplasm of oocytes, can be recovered from the nucleus, although after extended times at minute concentrations only. This suggests that the diffusion pathway through the NPC is not a rigid but somewhat flexible tube.

3.2. Karyopherin-Mediated Transport

A general scheme of karyopherin-mediated transport is given in Fig. 3: in the cytoplasm, a cargo molecule containing a nuclear localization sequence (NLS) binds to an importing karyopherin (importin). The import complex docks at the cytoplasmic side of an NPC and is translocated into the nucleus. By interaction with the active, guanosine 5'-triphosphate (GTP)-loaded form of the small guanosine nucleotide-binding protein Ran, i.e. with RanGTP, the import complex is dissociated, and the cargo is set free to search the nuclear contents for a specific binding partner. In the nucleus, a cargo containing a nuclear export signal (NES) forms a trimeric export complex with an exporting karyopherin (exportin) and RanGTP. The export complex docks at the nuclear side of an NPC and is translocated into the cytoplasm. In the cytoplasm,

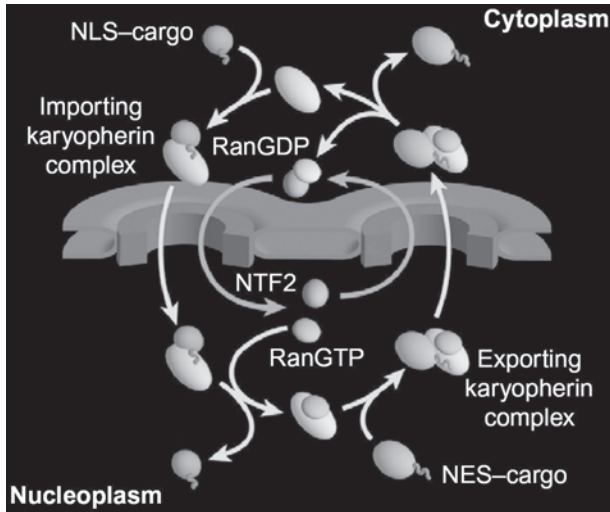


Fig. 3. Scheme of karyopherin-mediated nucleocytoplasmic transport. For details, *see* text. From **ref. 12** with permission; © 2003, with permission from Elsevier.

Ran-bound GTP is hydrolyzed, inducing the dissociation of the complex. Importing and exporting karyopherins, although quite large (~100 kDa), can freely pass through the NPC. In contrast, the import of Ran into the nucleus is facilitated by NTF2, a nuclear transport receptor belonging to the NXF family of nuclear transport receptors.

NLSs, first identified in the large T antigen of the SV40 virus (69), consist frequently of short stretches of predominantly basic residues such as PKKKRKV or of bipartite sequences of basic residues such as KRPAATKKAGQAKKKKLD (70). NESs (71,72) are leucine-rich stretches with the consensus sequence L-X_{2,3}-(L,I,M,F,M)-X_{2,3}-L-X-(L,I,V). In addition, more complex signal sequences exist, some of which confer both import and export (73). In all cases, NLSs and NESs are permanent constituents of the cargo not removed during transport. They can be located at any site within a polypeptide and frequently occur in more than one copy per molecule (for a database of nuclear transport signals, *see* **ref. 74**).

The karyopherin family (reviewed in **refs. 14,75–77**) has about 14 known members in yeast and more than 20 in vertebrates. Major members are listed in **Table 2**. All karyopherins are modular molecules composed of 18 to 20 motifs called HEAT repeats (HEAT is an acronym of four proteins related to Huntingtons disease (78)). HEAT repeats are stretches of approx 40 amino acid residues forming two α -helices (A and B helix) connected by a short turn. In karyopherins the HEAT repeats are joined by short linkers to yield a rather flexible (79) spiral with an N-terminal and a C-terminal arch which are able to bind RanGTP or nuclear transport signals, respectively. The interaction between karyopherins and FG repeats occurs at the convex surface of the spiral by insertion of phenylalanine residues thus yielding a binding surface with a spread of affinities.

Table 2
Major Mammalian Nuclear Transport Receptors

Name	Alternative name	Function
Kap α	Importin- α	Mediates import by functioning as an adaptor between proteins containing NLSs of the SV40 T antigen or nucleoplasmin type and Kap β 1
Kap β 1	Importin- β	Mediates import of proteins containing basic stretches
Kap β 2a	Transportin 1	Mediates import of mRNA-binding proteins, ribosomal proteins
CRM1	Exportin 1	Mediates export of proteins containing leucine-rich NESs
CAS		Mediates export of Kap α
Exportin-t		Mediates export of t-RNAs

Karyopherins bind signal-containing cargoes in a selective manner. For instance, the importing karyopherin Kap α selectively binds the NLS of the SV40 T antigen type, whereas the exporting karyopherin CRM1 binds the NES of the leucine-rich type (80), thereby mediating the export of proteins and several classes of RNAs (13) but not mRNAs. The diversity of interactions between signal-containing cargoes and karyopherins is further increased by the fact that the binding of a cargo to a karyopherin may be mediated by an adaptor molecule. Thus, in the “classical” or “canonical” import pathway, an NLS-containing cargo is bound first by karyopherin- α . In a second step, the cargo–karyopherin- α complex is bound by karyopherin- β 1 and only the trimeric complex is translocated into the nucleus.

In addition to cargo, karyopherins bind RanGTP. However, RanGTP has opposite effects on importing and exporting karyopherins. When RanGTP binds to an import complex, consisting of an NLS-containing cargo and an importing karyopherin, the cargo is released. The importin-RanGTP complex persists until Ran-bound GTP is hydrolyzed. In contrast, when RanGTP binds to an exporting karyopherin the additional binding of an NES-containing cargo is favored, that is, cargo and RanGTP binding are cooperative. The export complex dissociates into its three components when the GTP-bound Ran is hydrolyzed.

Ran belongs to the large and abundant family of guanosine nucleotide-binding proteins (GNBP; reviewed in ref. 81), which occur in two forms: the inactive guanosine 5'-diphosphate (GDP) and the active GTP forms. By switching between these states, GNBP regulate a large variety of cellular processes, ranging from cell growth and differentiation to protein synthesis and vesicular transport. For the activation of GNBP, the exchange of bound GDP for GTP is required. This process is intrinsically very slow but is speeded up by guanine nucleotide exchange factors (GEFs). The GDP–GTP exchange is a reversible process with an equilibrium favoring the GDP state. Thus, even in the presence of GEFs, a large surplus of GTP over GDP is required to drive the system into the GTP form. The inactivation of GNBP occurs by hydrolysis of bound GTP, an essentially irreversible but intrinsically also very low process.

Hydrolysis is activated by GTPase-activating proteins (GAPs). Besides the main regulators of GHBPs, GEFs, and GAPs, further accessory regulators are known.

The regulatory factors of Ran, RanGEF, and RanGAP are asymmetrically distributed between nucleus and cytoplasm. Thus, RanGEF, a donut-shaped molecule also known as RCC1, is a nuclear protein directly bound to histones H2A and H2B. On the other hand, RanGAP, a crescent-shaped molecule, occurs only in the cytoplasm. A large fraction of RanGAP, modified by the 8-kDa peptide SUMO, is covalently attached to the cytoplasmic filaments of the NPC (82). An accessory regulator of Ran, Ran-binding protein1, which increases the hydrolytic activity of RanGAP by a factor of approx 10, is found in both cytoplasm and nucleus. But Nup358, a constituent of the cytoplasmic filaments, also has RanGAP-activating properties. The asymmetric distribution of the regulatory factors of Ran led to the hypothesis (83) that a steep gradient of RanGTP exists between nuclear contents and cytoplasm, providing the driving force for karyopherin-dependent nucleocytoplasmic transport. Using a fluorescence indicator system, the nuclear-cytoplasmic concentration ratio of RanGTP could be measured (84) and was found to be more than 200 during interphase.

The transport scheme shown in Fig. 3 implies that the passage of empty transport receptors and transport complexes through the NPC is a purely passive and thus reversible process driven by concentration gradients alone. Only by interaction with RanGTP in the nucleus, both the import of NLS cargoes and the export of NES cargoes can be rendered irreversible if a gradient of RanGTP between nucleus and cytoplasm is maintained. At this condition, NPC and RanGTP gradient cooperate to yield a system that can pump cargo molecules into and out of the nucleus, probably even simultaneously. The necessary energy is provided by hydrolysis of Ran-bound GTP with a minimum of one GTP hydrolyzed per translocation of one cargo molecule. To achieve that theoretical maximum efficiency, the coupling of RanGTP gradient to transport complex dissociation or formation would have to be perfect. Also, the NPC would have to be completely impermeable for (karyopherin-free) cargoes. The actual energy requirement and transport efficiency of karyopherin-mediated nucleocytoplasmic transport have yet to be determined.

3.3. NXF-Mediated Export of mRNPs

A central function of the nucleus is the biosynthesis of mRNA and its release into the cytoplasm (for review, see refs. 12,85,86). Because the primary transcript of a gene (pre-mRNA) is usually a patchwork of coding regions (exons) and noncoding regions (introns) the export apparatus has to be able to recognize fully processed, mature mRNA and to translocate it selectively through the NPC into the cytoplasm while retaining nonprocessed and partially processed, immature mRNAs as well as excised introns and other noncoding RNA sequences. In this process, proteins that bind to pre-mRNA or mature mRNA play a decisive role (87).

In vertebrates, more than 20 major and many minor pre-mRNP and mRNP proteins are known. Some of these proteins, such as A1 and C1/C2, are abundant (~100 million copies per nucleus); others occur in small amounts only. It is assumed that each mRNA species carries a unique combination of proteins that are specifically distributed along

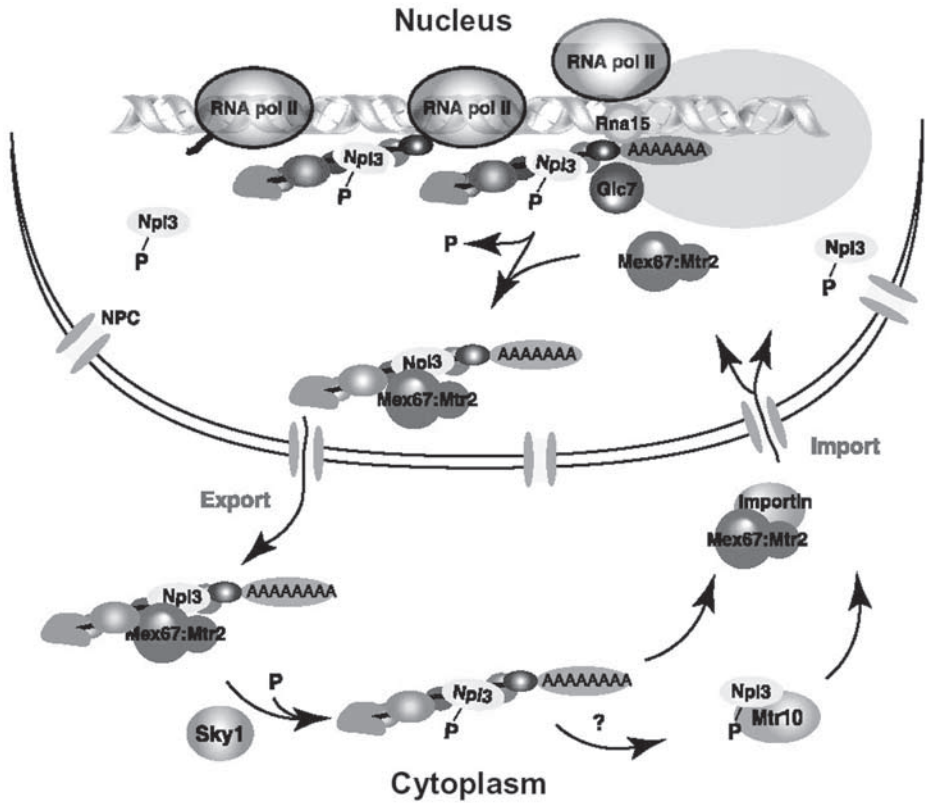


Fig. 4. Scheme of NXF-mediated mRNA export. For details, *see* text. From **ref. 91** with permission (<http://www.nature.com>).

the length of the mRNA molecule, thus providing each mRNA molecule with an “identity” that determines its fate. Most proteins are bound to pre-mRNAs already during transcription. In the process of splicing, the overall number of proteins bound to the pre-mRNA is greatly reduced, but at the same time a complex consisting of at least five proteins, called the exon junction complex, is deposited approx 20 nucleotides upstream of exon–exon junctions (88,89). The exon junction complex contains proteins that can directly bind to NXFs, thus signaling to the nuclear export machinery that the mRNA molecule has been spliced and is ready for export.

A current scheme of mRNA export in yeast (90,91) is given in **Fig. 4**. The Npl3 protein is shown to be the adaptor between exon junction complex and export receptor Mex67/Mtr 2. Other components of the exon junction complex, particularly Sub2 (vertebrate homolog UAP56) and Yra1 (vertebrate homologue ALY) have been previously implied as adaptors (92,93). Additional mRNA export pathways, independent of the exon junction complex, seem to exist also ([94]; for review, *see* **ref. 95**).

The yeast protein Mex67 (85) and its vertebrate ortholog TAP (77,93) are major representatives of the evolutionary conserved multigene NXF family (96,97). Normally, NXFs bind mRNAs via Mlp3, Aly/Yra, or other adaptors in a sequence-unspecific manner. Certain viral RNAs known as constitutive transport elements (CTEs) can bind directly to Tap in a sequence-specific manner. Very similarly to karyopherins, NXFs bind to FG repeats and rapidly permeate through the NPC.

Both Mex67 and TAP form heterodimeric complexes with small proteins called Mtr2 and p15/NXT1 (98), respectively. p15 is a homolog of NTF2, the nuclear transport receptor of RanGDP. Although p15 and Mtr2 have no sequence homology their 3D structure is similar (99) and their function equivalent. 3D structures have been determined for several fragments of TAP (100–103) but not for the complete molecule.

Together, the following picture of the domain structure of TAP arises (cf. Fig. 3 of ref. 104): the N-terminal domain of TAP (residues 1–100), for which a crystal structure is not available, contains a NLS. This is followed by an RNA-binding domain (RBD, residues 119–198) and a leucine-rich repeat domain (residues 203–362), which are connected by a short linker of restricted flexibility. Further C-terminal, an NTF2-like domain (residues 371–551) and an UBA (ubiquitin-associated fold) domain (residues 566–608) are found. The RBD and leucine-rich repeat domains of TAP bind (101,105) Mex67/Tap and viral CTEs. The NTF-like domain of TAP and p15 combine by coiled-coil interaction similarly to NTF2 homodimers (106). The NTF2 dimer can bind directly to FG repeats and so can the domain formed in TAP by the NTF2-like domain and p15. The UBA domain of TAP also binds FG repeats. Interestingly, efficient mRNA export requires two FG repeat-binding domains in Tap/p15, but instead of one NTF2-like domain and one UBA domain, two UBA domains are sufficient.

Neither Mex67 nor Tap bind Ran. Therefore, it is not clear how directionality is conferred in mRNA export. Helicases have been implied to disrupt mRNA–protein interactions in cytoplasmic mRNPs, thus preventing reimport of mRNAs (107). Alternatively, ribosomes may attach to mRNPs emerging from the NPC and strip them of transport factors (108). Recent results suggest (90) that the phosphorylation of Npl3 in the cytoplasm by the kinase Sky1 induces the dissociation of Mex67/Mtr2 from the mRNA (Fig. 4). In this model, the cytoplasmic localization of Sky1, complemented by nuclear localization of the corresponding phosphatase Glc7p, provides for the directionality of mRNA export, in analogy to the nucleocytoplasmic gradient of RanGTP in karyopherin-mediated nucleocytoplasmic transport. The energy would be provided by adenosine triphosphate (i.e., the transfer of phosphate groups from adenosine triphosphate to Mlp3).

4. Translocation Through the Nuclear Pore Complex

As pointed out, the NPC displays a puzzling functional duality with regard to inert and FG-binding molecules. The fact that translocation through the NPC is enhanced by binding appears mysterious and, in essence, has remained unresolved. Nevertheless, several models have been described to account for the transport properties of the NPC (8,11,44,47,48,52,67,109–117). Here, some recent translocation models (Fig. 5) are briefly described and discussed.

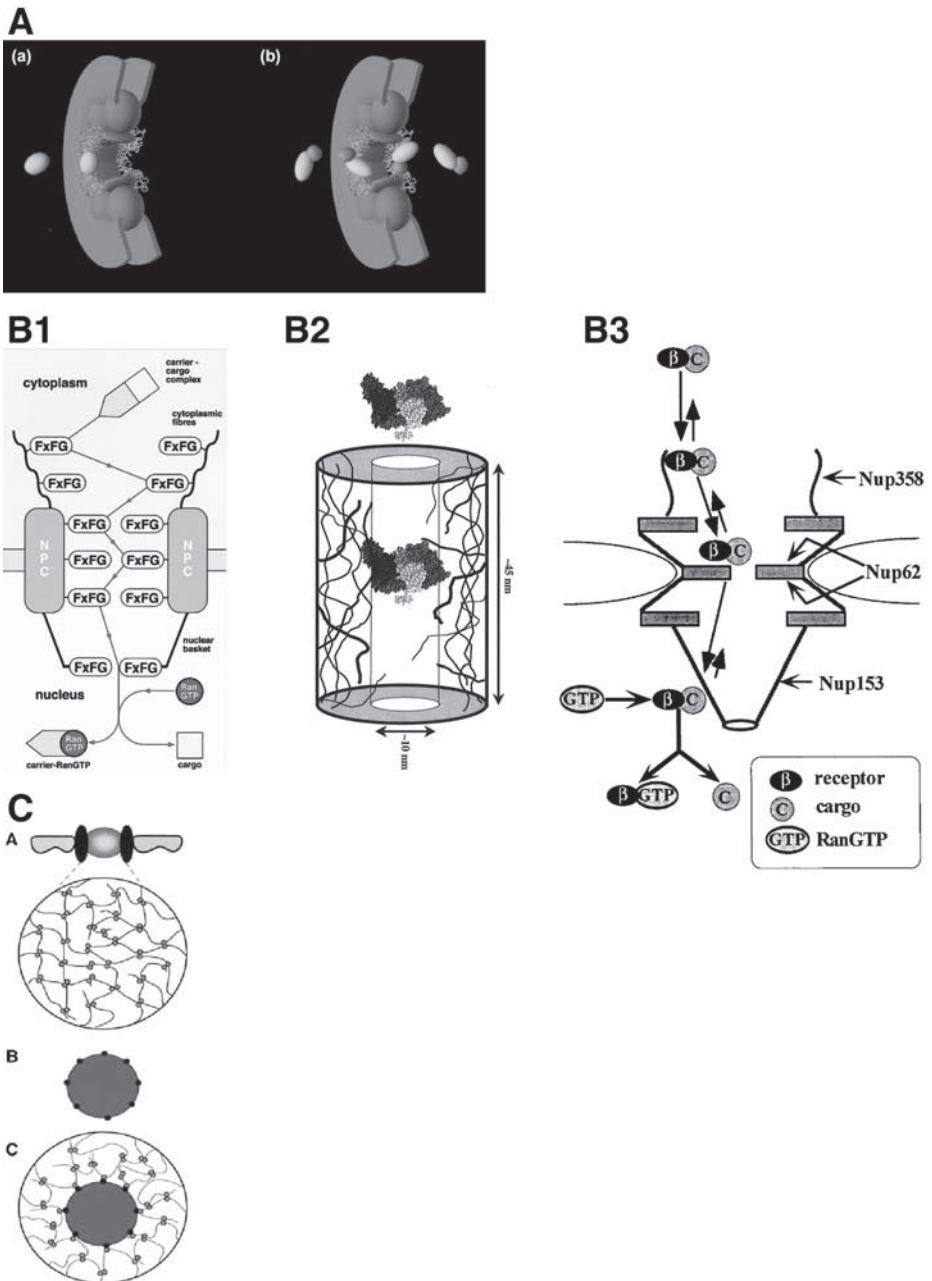


Fig. 5. Current models of translocation through the nuclear pore complex. (A) The virtual gating model of Rout et al. (12); (B1) the model of Stewart et al. (111); (B2) the oily spaghetti model of Macara (8); (B3) the affinity gradient model of Ben-Efraim and Gerace (112); and (C) the selective phase model of Ribbeck and Görlich (67). (A) From ref. 12, © 2003, with permission from Elsevier; (B1) from ref. 111; (B2) from ref. 8 with permission; (B3) from ref. 112, with permission from The Rockefeller University Press; (C) from ref. 67 (<http://www.nature.com>).

In the “virtual gating model” (Fig. 5A) it is assumed (12,52) that the NPC contains a large patent channel of approx 50 nm diameter. The channel entrance but not the channel wall is thought to be decorated with a large number of small flexible protein filaments carrying an abundance of binding sites, i.e. FG motifs. The channel would constitute a large energy barrier for the translocation of inert molecules, even if they are much smaller than the channel diameter. In addition, the small, flexible FG repeat containing filaments would push away inert molecules by thermal motion. In contrast, transport receptors or transport complexes which would be concentrated at the channel entrance by binding to FG repeats. This would reduce the energy barrier for entering the channel and thus enhance translocation. Experimentally, little is known about the distribution of FG motifs along the axis of the NPC. Data we have obtained by immunogold electron microscopy (118) and by single-molecule fluorescence microscopy (119) suggest that binding sites of transport receptors occur all along the NPC axis. Deletion experiments have shown (56) that in yeast the FG motifs of asymmetric nucleoporins can be completely removed without compromising growth properties.

Stewart et al. (111,120) also assume that the NPC contains a large channel. However, in their model (Fig. 5B1) binding sites (i.e. FG repeats) are distributed along the complete transport pathway, that is, from the tips of the cytoplasmic filaments throughout the channel down to the nuclear basket. An import complex, for instance, would bind to FG repeats of the cytoplasmic filaments, jump from one FG repeat to the next, and thus pass through the central channel. In arriving in the nuclear basket, it would encounter RanGTP and dissociate. Similarly, in the “oily-spaghetti model” (8) (Fig. 5B2) the wall of the central channel is decorated with a loose and highly flexible meshwork of FG repeats. The filaments extend into the channel lumen but leave free a diffusion tube approx 10 nm in diameter. Thus, the passage of inert molecules would be restricted to the diffusion tube but transport receptors and transport complexes would be able to use the complete cross section of the channel because of their affinity for FG repeats.

Ben-Efraim and Gerace (112) found that the nucleoporins vNup358, vNup62, and vNup153, which localize to cytoplasmic filament, central scaffold, and nuclear basket, respectively, display increasing affinities for karyopherin β 1. They suggested that the gradient of increasing affinity found *in vitro* using purified proteins also exists *in vivo*. Thus (Fig. 5B3), import complexes would be handed over from a nucleoporin with a lower affinity to an neighboring nucleoporin with higher affinity until they arrive in the nuclear basket where they are dissociated by interaction with RanGTP. Recent experiments (121) in which the FG domains of asymmetric cytoplasmic and nuclear yeast nucleoporins were either deleted or exchanged did not revealed, however, any effect of these modifications on transport.

In the selective-phase model (67) the NPC contains a large channel which is occluded by a gel. That gel is thought to be formed by FG domains such that the hydrophobic FG motifs interact with each other to yield “knots” while the hydrophilic linker sequences provide the connections between knots. To permeate through the NPC inert molecules would have to slip through the rather small meshes of the gel. In contrast, transport receptors and transport complexes would be able to interact with FG motifs and thus to temporarily open the knots. In accordance with the model small

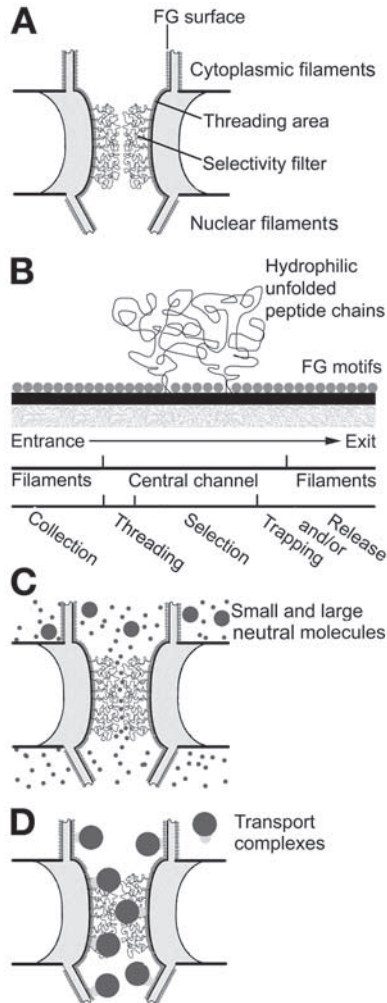


Fig. 6. Reduction-of-dimensionality model of translocation through the nuclear pore complex. (A) The nuclear pore complex (NPC) is assumed to contain a large channel. The channel wall is lined with phenylalanine glycine (FG) motifs (i.e., binding sites for nuclear transport receptors). FG repeats form a surface that extends onto filaments. (B) The channel wall is decorated with a loose network of unfolded hydrophilic peptide chains, here referred to selectivity filter. The selectivity filter is very gentle and flexible. (C) Inert molecules, which do not bind to FG motifs, permeate the pore by diffusion in the aqueous phase. The selectivity filter restricts the passage to an inner tube with a diameter of 5 to 10 nm. (D) Transport complexes, which consist of a nuclear signal containing cargo and a nuclear transport receptor, first bind to FG motifs on filaments and then search the FG surface by a 2D random walk for the site with highest affinity. From **ref. 116**.

alcohols that perturb hydrophobic interactions were found to cause a large increase in the passive permeability of the NPC (122).

Results obtained by optical transport measurements (16) and single-molecule fluorescence microscopy (119) prompted us suggested a translocation model (116) in which the enhancement of transport by binding is accounted for by the fundamental differences (123) existing between diffusion in two and three dimensions. In the model (Fig. 6) it is assumed that the wall of the channel traversing the NPC is covered with a dense array of FG motifs forming one, coherent hydrophobic surface. The FG surface is thought to continue on cytoplasmic filaments and on parts of the nuclear filaments (Fig. 6A). In addition to the FG surface, the model includes a loose network of flexible, hydrophilic, possibly glycosylated peptide chains decorating the central part of the channel wall (Fig. 6B). The loose network extends into the pore lumen but leaves free a central tube with a approx 10-nm diameter.

Inert molecules (Fig. 6C) are thought to permeate the NPC by diffusing through the inner water-filled central tube. In contrast, transport receptors and transport complexes (Fig. 6D) would bind to the FG surface on filaments and then rapidly search the FG surface for the channel exit by a two-dimensional random walk. At the exit the transport complexes would encounter either RanGTP (import) or RanBP and RanGAP and thus be dissociated. Further properties, implications, and predictions of the model are discussed elsewhere (116).

5. Concluding Remarks

The elucidation of nucleocytoplasmic transport has made tremendous progress. Excitingly, the full power of the eukaryotic building plan, segregating genetic material from protein synthesis, is in gradual disclosure. Better understanding of nucleocytoplasmic transport will have important implications for both medicine and biotechnology. Already, the role of nucleocytoplasmic transport in the biogenesis of pathological conditions and the possibilities for new therapeutic strategies are intensively studied. Apart from this, the NPC provides an intriguing paradigm for a molecular machine able to sort native protein molecules at high speed.

References

1. Callan, H. G., Randall, J. T. and Tomlin, S. G. (1949) An electron microscope study of the nuclear membrane. *Nature* **163**, 280.
2. Hutchison, C. J. (2002) Lamins: building blocks or regulators of gene expression? *Nat. Rev. Mol. Cell Biol.* **3**, 848–858.
3. Kau, T. R., Way, J. C. and Silver, P. A. (2004) Nuclear transport and cancer: from mechanism to intervention. *Nat. Rev. Cancer* **4**, 106–117.
4. Smith, J. M. and Koopman, P. A. (2004) The ins and outs of transcriptional control: nucleocytoplasmic shuttling in development and disease. *Trends Genet.* **20**, 4–8.
5. Mounkes, L., Kozlov, S., Burke, B. and Stewart, C. L. (2003) The laminopathies: nuclear structure meets disease. *Curr. Op. Genet. Dev.* **13**, 223–230.
6. Cronshaw, J. M. and Matunis, M. J. (2004) The nuclear pore complex: disease associations and functional correlations. *Trends Endocrinol. Metabol.* **15**, 34–39.

7. Gorlich, D. and Mattaj, I. W. (1996) Protein kinesis–Nucleocytoplasmic transport. *Science* **271**, 1513–1518.
8. Macara, I. G. (2001) Transport into and out of the nucleus. *Microbiol. Mol. Biol. Rev.* **65**, 570–594.
9. Weis, K. (2003) Regulating access to the genome: nucleocytoplasmic transport throughout the cell cycle. *Cell* **112**, 441–451.
10. Bednenko, J., Cingolani, G. and Gerace, L. (2003) Nucleocytoplasmic transport: navigating the channel. *Traffic* **4**, 127–135.
11. Fahrenkrog, B. and Aebi, U. (2003) The nuclear pore complex: Nucleocytoplasmic transport and beyond. *Nat. Rev. Mol. Cell Biol.* **4**, 757–766.
12. Rout, M. P., Aitchison, J. D., Magnasco, M. O. and Chait, B. T. (2003) Virtual gating and nuclear transport: the hole picture. *Trends Cell Biol.* **13**, 622–628.
13. Cullen, B. R. (2003) Nuclear RNA export. *J. Cell Sci.* **116**, 587–597.
14. Fried, H. and Kutay, U. (2003) Nucleocytoplasmic transport: taking an inventory. *Cell. Mol. Life Sci.* **60**, 1659–1688.
15. Suntharalingam, M. and Wenthe, S. R. (2003) Peering through the pore: Nuclear pore complex structure, assembly, and function. *Dev. Cell* **4**, 775–789.
16. Peters, R. (2003) Optical single transporter recording: Transport kinetics in microarrays of membrane patches. *Annu. Rev. Biophys. Biomol. Struct.* **32**, 47–67.
17. Peters, R., Lang, I., Scholz, M., Schulz, B. and Kayne, F. (1986) Fluorescence Microphotolysis to Measure Nucleocytoplasmic Transport In vivo and In vitro. *Biochem. Soc. Trans.* **14**, 821–822.
18. Nelson, W. G., Pienta, K. J., Barrack, E. R. and Coffey, D. S. (1986) The Role of the Nuclear Matrix in the Organization and Function of DNA. *Ann. Rev. Biophys. Biophysic. Chem.* **15**, 457–475.
19. Pederson, T. (2000) Half a century of “the nuclear matrix”. *Mol. Biol. Cell* **11**, 799–805.
20. Peters, R. (1986) Fluorescence Microphotolysis to Measure Nucleocytoplasmic Transport and Intracellular Mobility. *Biochim. Biophys. Acta* **864**, 305–359.
21. Luby-Phelps, K. (2000) Cytoarchitecture and physical properties of cytoplasm: Volume, viscosity, diffusion, intracellular surface area. *International Review of Cytology—A Survey of Cell Biology, Vol 192* **192**, 189–221.
22. Verkman, A. S. (2002) Solute and macromolecule diffusion in cellular aqueous compartments. *Trends Biochem. Sci.* **27**, 27–33.
23. Misteli, T. (2001) Nuclear structure–Protein dynamics: Implications for nuclear architecture and gene expression. *Science* **291**, 843–847.
24. Kues, T., Peters, R. and Kubitscheck, U. (2001) Visualization and tracking of single protein molecules in the cell nucleus. *Biophys. J.* **80**, 2954–2967.
25. Kues, T., Dickmanns, A., Luhrmann, R., Peters, R. and Kubitscheck, U. (2001) High intranuclear mobility and dynamic clustering of the splicing factor U1 snRNP observed by single particle tracking. *Proc. Natl. Acad. Sci. USA* **98**, 12021–12026.
26. Singh, O. P., Bjorkroth, B., Masich, S., Wieslander, L. and Daneholt, B. (1999) The intranuclear movement of Balbiani ring premessenger ribonucleoprotein particles. *Exp. Cell Res.* **251**, 135–146.
27. Politz, J. C. R., Tuft, R. A. and Pederson, T. (2003) Diffusion-based transport of nascent ribosomes in the nucleus. *Mol. Biol. Cell* **14**, 4805–4812.
28. Lamb, M. M. and Daneholt, B. (1979) Characterization of Active Transcription Units in Balbiani Rings of *Chironomus Tentans*. *Cell* **17**, 835–848.

29. Andersson, K., Bjorkroth, B. and Daneholt, B. (1980) The In situ Structure of the Active 7S-RNA Genes in Balbiani Rings of *Chironomus-Tentans*. *Exp. Cell Res.* **130**, 313–326.
30. Skoglund, U., Andersson, K., Strandberg, B. and Daneholt, B. (1986) 3-Dimensional Structure of A Specific Pre-Messenger RNP Particle Established by Electron-Microscope Tomography. *Nature* **319**, 560–564.
31. Mehlin, H., Daneholt, B. and Skoglund, U. (1992) Translocation of a Specific Pre-messenger Ribonucleoprotein Particle Through the Nuclear-Pore Studied with Electron-Microscope Tomography. *Cell* **69**, 605–613.
32. Franke, W. W. and Scheer, U. (1974) Structures and functions of the nuclear envelope. *Cell Nucleus* **1**, 219–347.
33. Doring, V. and Stick, R. (1990) Gene Structure of Nuclear Lamin-LIII of *Xenopus-Laevis*—A Model for the Evolution of IF Proteins from A Lamin-Like Ancestor. *EMBO J.* **9**, 4073–4081.
34. Aebi, U., Cohn, J., Buhle, L. and Gerace, L. (1986) The Nuclear Lamina Is A Meshwork of Intermediate-Type Filaments. *Nature* **323**, 560–564.
35. Smythe, C., Jenkins, H. E. and Hutchison, C. J. (2000) Incorporation of the nuclear pore basket protein Nup 153 into nuclear pore structures is dependent upon lamina assembly: evidence from cell-free extracts of *Xenopus* eggs. *EMBO J.* **19**, 3918–3931.
36. Senior, A. and Gerace, L. (1988) Integral Membrane-Proteins Specific to the Inner Nuclear-Membrane and Associated with the Nuclear Lamina. *J. Cell Biol.* **107**, 2029–2036.
37. Jagatheesan, G., Thanumalayan, S., Muralikrishna, B., Rangaraj, N., Karande, A. A. and Parnaik, V. K. (1999) Colocalization of intranuclear lamin foci with RNA splicing factors. *J. Cell Sci.* **112**, 4651–4661.
38. Stick, R. and Hausen, P. (1985) Changes in the Nuclear Lamina Composition During Early Development of *Xenopus-Laevis*. *Cell* **41**, 191–200.
39. Maul, G. G. (1977) The nuclear and cytoplasmic pore complex: Structure, dynamics, distribution, and evolution. *Int. Rev. Cytol. Suppl.* **6**, 76–187.
40. Akey, C. W. (1989) Interactions and Structure of the Nuclear-Pore Complex Revealed by Cryo-Electron Microscopy. *J. Cell Biol.* **109**, 955–970.
41. Goldberg, M. W. and Allen, T. D. (1993) The Nuclear-Pore Complex—3-Dimensional Surface-Structure Revealed by Field-Emission, In-Lens Scanning Electron-Microscopy, with Underlying Structure Uncovered by Proteolysis. *J. Cell Sci.* **106**, 261–274.
42. Allen, T. D., Cronshaw, J. M., Bagley, S., Kiseleva, E. and Goldberg, M. W. (2000) The nuclear pore complex: mediator of translocation between nucleus and cytoplasm. *J. Cell Sci.* **113**, 1651–1659.
43. Scheer, U., Dabauvalle, M. C., Merkert, H. and Benavente, R. (1988) The nuclear envelope and the organization of the pore complex. *Cell Biol. Int. Rep.* **12**, 669–689.
44. Unwin, P. N. T. and Milligan, R. A. (1982) A Large Particle Associated with the Perimeter of the Nuclear-Pore Complex. *J. Cell Biol.* **93**, 63–75.
45. Akey, C. W. and Radermacher, M. (1993) Architecture of the *Xenopus* Nuclear Pore Complex Revealed by 3-Dimensional Cryoelectron Microscopy. *J. Cell Biol.* **122**, 1–19.
46. Stoffler, D., Feja, B., Fahrenkrog, B., Walz, J., Typke, D. and Aebi, U. (2003) Cryo-electron tomography provides novel insights into nuclear pore architecture: Implications for nucleocytoplasmic transport. *J. Mol. Biol.* **328**, 119–130.
47. Akey, C. W. (1990) Visualization of Transport-Related Configurations of the Nuclear-Pore Transporter. *Biophys. J.* **58**, 341–355.

48. Kiseleva, E., Goldberg, M. W., Allen, T. D. and Akey, C. W. (1998) Active nuclear pore complexes in *Chironomus*: visualization of transporter configurations related to mRNP export. *J. Cell Sci.* **111**, 223–236.
49. Beck, M., Forster, F., Ecke, M., et al. (2004) Nuclear pore complex structure and dynamics revealed by cryoelectron tomography. *Science* **306**, 1387–1390.
50. Rout, M. P. and Blobel, G. (1993) Isolation of the Yeast Nuclear-Pore Complex. *J. Cell Biol.* **123**, 771–783.
51. Miller, B. R., Powers, M., Park, M., Fischer, W. and Forbes, D. J. (2000) Identification of a new vertebrate nucleoporin, Nup188, with the use of a novel organelle trap assay. *Mol. Biol. Cell* **11**, 3381–3396.
52. Rout, M. P., Aitchison, J. D., Suprapto, A., Hjertaas, K., Zhao, Y. M. and Chait, B. T. (2000) The yeast nuclear pore complex: Composition, architecture, and transport mechanism. *J. Cell Biol.* **148**, 635–651.
53. Cronshaw, J. A., Krutchinsky, A. N., Zhang, W. Z., Chait, B. T. and Matunis, M. J. (2002) Proteomic analysis of the mammalian nuclear pore complex. *J. Cell Biol.* **158**, 915–927.
54. Yang, Q., Rout, M. P. and Akey, C. W. (1998) Three-dimensional architecture of the isolated yeast nuclear pore complex: Functional and evolutionary implications. *Mol. Cell* **1**, 223–234.
55. Reichelt, R., Holzenburg, A., Buhle, E. L., Jarnik, M., Engel, A. and Aebi, U. (1990) Correlation Between Structure and Mass-Distribution of the Nuclear-Pore Complex and of Distinct Pore Complex Components. *J. Cell Biol.* **110**, 883–894.
56. Strawn, L. A., Shen, T. X., Shulga, N., Goldfarb, D. S. and Wente, S. R. (2004) Minimal nuclear pore complexes define FG repeat domains essential for transport. *Nature Cell Biol.* **6**, 197–206.
57. Denning, D. P., Patel, S. S., Uversky, V., Fink, A. L. and Rexach, M. (2003) Disorder in the nuclear pore complex: The FG repeat regions of nucleoporins are natively unfolded. *Proc. Natl. Acad. Sci. USA* **100**, 2450–2455.
58. Powers, M. A. and Dasso, M. (2004) Nuclear transport erupts on the slopes of Mount Etna. *Nat. Cell Biol.* **6**, 82–86.
59. Lutzmann, M., Kunze, R., Buerer, A., Aebi, U. and Hurt, E. (2002) Modular self-assembly of a Y-shaped multiprotein complex from seven nucleoporins. *EMBO J.* **21**, 387–397.
60. Krull, S., Thyberg, J., Bjorkroth, B., Rackwitz, H. R. and Cordes, V. C. (2004) Nucleoporins as components of the nuclear pore complex core structure and Tpr as the architectural element of the nuclear basket. *Mol. Biol. Cell* **15**, 4261–4277.
61. Fahrenkrog, B., Maco, B., Fager, A. M., et al. (2002) Domain-specific antibodies reveal multiple-site topology of Nup153 within the nuclear pore complex. *J. Struct. Biol.* **140**, 254–267.
62. Devos, D., Dokudovskaya, S., Alber, F., et al. (2004) Components of coated vesicles and nuclear pore complexes share a common molecular architecture. *PLoS Biol.* **2**, e380.
63. Paine, P. L., Moore, L. C. and Horowitz, S. B. (1975) Nuclear envelope permeability. *Nature* **254**, 109–114.
64. Pappenheimer, J. R., Renkin, E. M. and Borrero, L. M. (1951) Filtration, Diffusion and Molecular Sieving Through Peripheral Capillary Membranes A Contribution to the Pore Theory of Capillary Permeability. *Am. J. Physiol.* **167**, 13–46.
65. Renkin, E. M. and Curry, F. E. (1979) Transport of water and solutes across endothelium. In *Transport Organs* (Giebisch, G., ed), Springer-Verlag, Berlin, pp. 1–45.

66. Keminer, O., Siebrasse, J. P., Zerf, K. and Peters, R. (1999) Optical recording of signal-mediated protein transport through single nuclear pore complexes. *Proc. Natl. Acad. Sci. USA* **96**, 11,842–11,847.
67. Ribbeck, K. and Gorlich, D. (2001) Kinetic analysis of translocation through nuclear pore complexes. *EMBO J.* **20**, 1320–1330.
68. Siebrasse, J. P. and Peters, R. (2002) Rapid translocation of NTF2 through the nuclear pore of isolated nuclei and nuclear envelopes. *EMBO Reports* **3**, 887–892.
69. Kalderon, D., Richardson, W. D., Markham, A. F. and Smith, A. E. (1984) Sequence requirements for nuclear location of simian virus-40 large-T-antigen. *Nature* **311**, 33–38.
70. Dingwall, C., Robbins, J., Dilworth, S. M., Roberts, B. and Richardson, W. D. (1988) The Nucleoplasmin nuclear location sequence is larger and more complex than that of Sv40 large T-antigen. *J. Cell Biol.* **107**, 841–849.
71. Wen, W., Meinkoth, J. L., Tsien, R. Y. and Taylor, S. S. (1995) Identification of a signal for rapid export of proteins from the nucleus. *Mol. Biol. Cell* **6**, 471.
72. Fischer, U., Huber, J., Boelens, W. C., Mattaj, I. W. and Luhrmann, R. (1995) The Hiv-1 Rev activation domain is a nuclear export signal that accesses an export pathway used by specific cellular RNAs. *Cell* **82**, 475–483.
73. Michael, W. M., Choi, M. Y. and Dreyfuss, G. (1995) A nuclear export signal in hnRNP a1—a signal-mediated, temperature-dependent nuclear-protein export pathway. *Cell* **83**, 415–422.
74. Nair, R., Carter, P. and Rost, B. (2003) NLSdb: database of nuclear localization signals. *Nucleic Acids Res.* **31**, 397–399.
75. Gorlich, D. and Kutay, U. (1999) Transport between the cell nucleus and the cytoplasm. *Annu. Rev. Cell Dev. Biol.* **15**, 607–660.
76. Chook, Y. M. and Blobel, G. (2001) Karyopherins and nuclear import. *Curr. Opin. Struct. Biol.* **11**, 703–715.
77. Conti, E. and Izaurralde, E. (2001) Nucleocytoplasmic transport enters the atomic age. *Curr. Opin. Cell Biol.* **13**, 310–319.
78. Andrade, M. A. and Bork, P. (1995) Heat repeats in the Huntingtons-disease protein. *Nat. Genet.* **11**, 115–116.
79. Fukuhara, N., Fernandez, E., Ebert, J., Conti, E. and Svergun, D. (2004) Conformational variability of nucleo-cytoplasmic transport factors. *J. Biol. Chem.* **279**, 2176–2181.
80. Fornerod, M., Ohno, M., Yoshida, M. and Mattaj, I. W. (1997) CRM1 is an export receptor for leucine-rich nuclear export signals. *Cell* **90**, 1051–1060.
81. Vetter, I. R. and Wittinghofer, A. (2001) Signal transduction—The guanine nucleotide-binding switch in three dimensions. *Science* **294**, 1299–1304.
82. Matunis, M. J., Wu, J. A. and Blobel, G. (1998) SUMO-1 modification and its role in targeting the Ran GTPase-activating protein, RanGAP1, to the nuclear pore complex. *J. Cell Biol.* **140**, 499–509.
83. Gorlich, D., Pante, N., Kutay, U., Aebi, U. and Bischoff, F. R. (1996) Identification of different roles for RanGDP and RanGTP in nuclear protein import. *EMBO J.* **15**, 5584–5594.
84. Kalab, P., Weis, K. and Heald, R. (2002) Visualization of a Ran-GTP gradient in interphase and mitotic *Xenopus* egg extracts. *Science* **295**, 2452–2456.
85. Reed, R. and Hurt, E. (2002) A conserved mRNA export machinery coupled to pre-mRNA splicing. *Cell* **108**, 523–531.
86. Vinciguerra, P. and Stutz, F. (2004) mRNA export: an assembly line from genes to nuclear pores. *Curr. Opin. Cell Biol.* **16**, 285–292.

87. Dreyfuss, G., Kim, V. N. and Kataoka, N. (2002) Messenger-RNA-binding proteins and the messages they carry. *Nat. Rev. Mol. Cell Biol.* **3**, 195–205.
88. Le Hir, H., Izaurralde, E., Maquat, L. E. and Moore, M. J. (2000) The spliceosome deposits multiple proteins 20–24 nucleotides upstream of mRNA exon-exon junctions. *EMBO J.* **19**, 6860–6869.
89. Kataoka, N., Yong, J., Kim, V. N., et al. (2000) Pre-mRNA splicing imprints mRNA in the nucleus with a novel RNA-binding protein that persists in the cytoplasm. *Mol. Cell* **6**, 673–682.
90. Gilbert, W. and Guthrie, C. (2004) The Glc7p nuclear phosphatase promotes mRNA export by facilitating association of Mex67p with mRNA. *Mol. Cell* **13**, 201–212.
91. Izaurralde, E. (2004) Directing mRNA export. *Nature Struct. Mol. Biol.* **11**, 210–212.
92. Strasser, K. and Hurt, E. (2000) Yra1p, a conserved nuclear RNA-binding protein, interacts directly with Mex67p and is required for mRNA export. *EMBO J.* **19**, 410–420.
93. Kang, Y. B. and Cullen, B. R. (1999) The human Tap protein is a nuclear mRNA export factor that contains novel RNA-binding and nucleocytoplasmic transport sequences. *Genes Develop.* **13**, 1126–1139.
94. Rodriguez-Navarro, S., Fischer, T., Luo, M. J., et al. (2004) Sus1, a functional component of the SAGA histone acetylase complex and the nuclear pore-associated mRNA export machinery. *Cell* **116**, 75–86.
95. Erkmann, J. A. and Kutay, U. (2004) Nuclear export of mRNA: from the site of transcription to the cytoplasm. *Exp. Cell Res.* **296**, 12–20.
96. Katahira, J., Strasser, K., Podtelejnikov, A., Mann, M., Jung, J. U. and Hurt, E. (1999) The Mex67p-mediated nuclear mRNA export pathway is conserved from yeast to human. *EMBO J.* **18**, 2593–2609.
97. Herold, A., Suyama, M., Rodrigues, J. P., et al. (2000) TAP (NXF1) belongs to a multigene family of putative RNA export factors with a conserved modular architecture. *Mol. Cell Biol.* **20**, 8996–9008.
98. Black, B. E., Levesque, L., Holaska, J. M., Wood, T. C. and Paschal, B. M. (1999) Identification of an NTF2-related factor that binds Ran-GTP and regulates nuclear protein export. *Mol. Cell Biol.* **19**, 8616–8624.
99. Fribourg, S. and Conti, E. (2003) Structural similarity in the absence of sequence homology of the messenger RNA export factors Mtr2 and p15. *EMBO Rep.* **4**, 699–703.
100. Liker, E., Fernandez, E., Izaurralde, E. and Conti, E. (2000) The structure of the mRNA export factor TAP reveals a cis arrangement of a non-canonical RNP domain and an LRR domain. *EMBO J.* **19**, 5587–5598.
101. Ho, D. N., Coburn, G. A., Kang, Y. B., Cullen, B. R. and Georgiadis, M. M. (2002) The crystal structure and mutational analysis of a novel RNA-binding domain found in the human Tap nuclear mRNA export factor. *Proc. Natl. Acad. Sci. USA* **99**, 1888–1893.
102. Fribourg, S., Braun, I. C., Izaurralde, E. and Conti, E. (2001) Structural basis for the recognition of a nucleoporin FG repeat by the NTF2-like domain of the TAP/p15 mRNA nuclear export factor. *Mol. Cell* **8**, 645–656.
103. Grant, R. P., Hurt, E., Neuhaus, D. and Stewart, M. (2002) Structure of the C-terminal FG-nucleoporin binding domain of Tap/NXF1. *Nat. Struct. Biol.* **9**, 247–251.
104. Stutz, F. and Izaurralde, E. (2003) The interplay of nuclear mRNP assembly, mRNA surveillance and export. *Trends Cell Biol.* **13**, 319–327.
105. Gruter, P., Taberero, C., von Kobbe, C., et al. (1998) TAP, the human homolog of Mex67p, mediates CTE-dependent RNA export from the nucleus. *Mol. Cell* **1**, 649–659.

106. Bullock, T. L., Clarkson, W. D., Kent, H. M. and Stewart, M. (1996) The 1.6 angstrom resolution crystal structure of nuclear transport factor 2 (NTF2) *J. Mol. Biol.* **260**, 422–431.
107. Snay-Hodge, C. A., Colot, H. V., Goldstein, A. L. and Cole, C. N. (1998) Dbp5p/Rat8p is a yeast nuclear pore-associated DEAD-box protein essential for RNA export. *EMBO J.* **17**, 2663–2676.
108. Maquat, L. E. (2004) Nonsense-mediated mRNA decay: Splicing, translation and mRNP dynamics. *Nat. Rev. Mol. Cell Biol.* **5**, 89–99.
109. Rexach, M. and Blobel, G. (1995) Protein import into nuclei: association and dissociation reactions involving transport substrate, transport factors, and nucleoporins. *Cell* **83**, 683–692.
110. Feldherr, C. M. and Akin, D. (1997) The location of the transport gate in the nuclear pore complex. *J. Cell Sci.* **110**, 3065–3070.
111. Bayliss, R., Corbett, A. H. and Stewart, M. (2000) The molecular mechanism of transport of macromolecules through nuclear pore complexes. *Traffic* **1**, 448–456.
112. Ben-Efraim, I. and Gerace, L. (2001) Gradient of increasing affinity of importin beta for nucleoporins along the pathway of nuclear import. *J. Cell Biol.* **152**, 411–417.
113. Bickel, T. and Bruinsma, R. (2002) The nuclear pore complex mystery and anomalous diffusion in reversible gels. *Biophys. J.* **83**, 3079–3087.
114. Kustanovich, T. and Rabin, Y. (2004) Metastable network model of protein transport through nuclear pores. *Biophys. J.* **86**, 2008–2016.
115. Fahrenkrog, B., Koser, J. and Aebi, U. (2004) The nuclear pore complex: a jack of all trades? *Trends Biochem. Sci.* **29**, 175–182.
116. Peters, R. (2005) Translocation through the nuclear pore complex: Selectivity and speed by reduction-of-dimensionality. *Traffic* **6**, 421–427.
117. Shulga, N. and Goldfarb, D. S. (2003) Binding dynamics of structural nucleoporins govern nuclear pore complex permeability and may mediate channel gating. *Mol. Cell. Biol.* **23**, 534–542.
118. Grote, M., Kubitscheck, U., Reichelt, R. and Peters, R. (1995) Mapping of Nucleoporins to the Center of the Nuclear-Pore Complex by Postembedding Immunogold Electron-Microscopy. *J. Cell Sci.* **108**, 2963–2972.
119. Kubitscheck, U., Grünwald, D., Hoekstra, A., et al. (2005) Nuclear transport of single molecules: Dwell times at the nuclear pore complex. *J. Cell Biol.* **168**, 233–243.
120. Stewart, M., Baker, R. P., Bayliss, R., et al. (2001) Molecular mechanism of translocation through nuclear pore complexes during nuclear protein import. *FEBS Lett.* **498**, 145–149.
121. Zeitler, B. and Weis, K. (2004) The FG-repeat asymmetry of the nuclear pore complex is dispensable for bulk nucleocytoplasmic transport in vivo. *J. Cell Biol.* **167**, 583–590.
122. Ribbeck, K. and Gorlich, D. (2002) The permeability barrier of nuclear pore complexes appears to operate via hydrophobic exclusion. *EMBO J.* **21**, 2664–2671.
123. Berg, O. G. and von Hippel, P. H. (1985) Diffusion-controlled macromolecular interactions. *Annu. Rev. Biophys. Chem.* **14**, 131–160.

Use of *Xenopus laevis* Oocyte Nuclei and Nuclear Envelopes in Nucleocytoplasmic Transport Studies

Reiner Peters

Summary

In this chapter, two techniques for the analysis of transport through the nuclear pore complex are described. In the first technique, nuclei isolated manually from *Xenopus laevis* oocytes are used to measure the import kinetics of fluorescent substrates by confocal fluorescence microscopy. In the second technique, referred to as optical single transporter recording (OSTR), isolated *Xenopus* oocyte nuclei, perforated nuclei, or isolated nuclear envelopes are tightly bound to planar transparent substrates containing arrays of nanoscopic-to-microscopic cavities. Transport through membrane patches spanning these cavities is recorded by confocal microscopy. By these means, the transport through single nuclear pore complexes or populations of pore complexes can be quantitatively measured.

Key Words: Membrane transport kinetics; nuclear envelope; nuclear pore complex; nucleocytoplasmic transport; optical single transporter recording.

1. Introduction

A complete analysis of a membrane transporter usually requires identification and characterization *in vivo*; solubilization and characterization *in vitro*; expression in heterologous systems and reconstitution in spherical or planar lipid bilayers, functional characterization by electrical and optical techniques; and ultimately structural characterization at atomic resolution by crystallization and X-ray diffraction.

The nuclear pore complex (NPC) has resisted such strategies to a considerable extent. Sheer size and complexity (500–1000 protein molecules/NPC) are reasons for that, an intimate integration into the cellular network on both the structural and functional level is another. Fundamentally, difficulties in applying strategies developed for “normal” transporters to the NPC may relate to the fact that the NPC is not a normal transporter: It does not span a lipid bilayer separating topologically different phases but provides a gate between topologically identical phases, cytosol and karyosol. Only in cooperation with soluble transport factors does it achieve selectivity and directionality.

From: *Methods in Molecular Biology*, vol. 322: *Xenopus Protocols: Cell Biology and Signal Transduction*
Edited by: X. J. Liu © Humana Press Inc., Totowa, NJ

In the beginning, nucleocytoplasmic transport could be studied exclusively by microinjection of live cells (1). Meanwhile, in vivo studies of nucleocytoplasmic transport have been much refined by a diversity of molecular genetic techniques including the green fluorescent protein (GFP) technology (2), photobleaching techniques (3), and cell fusion methods (4). Early attempts to employ isolated nuclei (5) or nuclear envelope vesicles (6) for nucleocytoplasmic transport studies were soon abandoned, leaving behind the widespread feeling that the NPC cannot be removed from the cellular context in functional form. “Artificial” nuclei, created by incubation of demembranized sperms with *Xenopus* egg extracts (7,8), played a crucial role in studies analyzing the assembly and disassembly of nuclear envelope and NPC but were less successful in transport studies.

A breakthrough was achieved in 1990 (9) by establishing conditions at which digitonin renders the plasma membrane permeable for macromolecules but does not affect nuclear envelope and NPC. Application of digitonin-permeabilized cells led to the discovery of karyopherins and Ran and thus triggered great progress. However, digitonin permeabilization yields little control over the nuclear content, a parameter of crucial importance in nuclear export studies.

In this chapter, two novel assays of nuclear transport are described. In the first assay (10), confocal fluorescence microscopy is employed to measure the import of fluorescent substrates into isolated *Xenopus* oocyte nuclei, thus proving that nuclei can be isolated in functional form. In the second assay, optical single transport recording (OSTR) (11) is employed to measure transport through the NPC in isolated intact nuclei, perforated nuclei, or isolated nuclear envelopes. In OSTR, membranes are firmly attached to flat, transparent, solid substrates containing a dense array of microscopic or nanoscopic cavities, here referred to as test compartments (TCs). Transport across TC-spanning membrane patches is induced by changing the concentration of transport substrates in the OSTR chamber and monitored by recording the fluorescence of transport substrates in the TCs. As described elsewhere in more detail (12), OSTR permits analysis of all sorts of transporters, such as the very fast (e.g., ion channels) and the very slow (e.g., translocases, ABC pumps). Furthermore, it features a variable membrane patch size, substrate multiplexing, and parallel data acquisition and thus ideally complements electrical single-channel recording.

2. Materials

1. Fresh sample of *Xenopus laevis* ovary.
2. Amphibian Ringer's: 88 mM NaCl, 1 mM KCl, 0.8 mM MgSO₄, 1.4 mM CaCl₂, 5 mM HEPES, pH 7.4.
3. Stereomicroscope with “cold” (glass fiber) light source.
4. Small glass dishes, 30-mm diameter, 5-mm rim height, for *Xenopus* oocyte isolation.
5. Forceps for *Xenopus* oocyte isolation (e.g., Dumont no. 5).
6. Pasteur pipets, tip diameter larger than 1.5 mm, for transfer of *Xenopus* oocytes from one dish to another and the like.
7. Mock 3, a mock intracellular medium buffered to 3 μ M free Ca²⁺, 90 mM KCl, 10 mM NaCl, 2 mM MgCl₂, 0.1 mM CaCl₂, 1.0 mM *N*-(2-hydroxyethyl)ethylene-diaminetriacetic acid, 10 mM HEPES, pH 7.3.

8. Transfer pipet: a normal microliter pipet set to a volume of approx 3 μL with a tip diameter increased to approx 2 mm.
9. Glass capillary with a tip briefly exposed to a flame to form a blunt and bent end, similar in shape to a hockey club, for manual purification of isolated *Xenopus* oocyte nuclei and their attachment to TC arrays.
10. Plastic dishes (Falcon 353004) for construction of microchambers or OSTR chambers.
11. Drills, 2.5- and 3.5-mm diameter, for creation of microchambers or OSTR chamber, respectively.
12. Sandpaper, finest grade.
13. Cover slips, 15 \times 15 mm, for creation of microchambers and OSTR chambers.
14. Transport solution 1 (*see* **ref. 10**), for studying import into isolated intact nuclei: 0.5 μM PK4 (a β -galactosidase fusion protein containing a nuclear localization sequence, NLS) or 0.5 μM GG-NLS (a fusion protein of GFP, GST, and an NLS); 0.5 μM karyopherin- α ; 0.5 μM karyopherin- β 1; 2 μM Texas-red-labeled 70-kDa dextran (TRD70); energy mix (final concentrations of 2 mM adenosine triphosphate [ATP], 25 mM phosphocreatine, 30 U/mL creatine phosphokinase, 200 μM GTP; 20 g/L bovine serum albumin (BSA); in mock 3.
15. Preformed TC arrays, custom made by excimer laser irradiation of approx 100- μm thick polycarbonate, may be ordered from Bartels Mikrotechnik, Dortmund, Germany. These arrays are available with TC diameters, depths, and pitches between approx 5 and 100 μm
16. Eastman Instant Adhesive no. 910 (SERVA, Heidelberg, Germany).
17. Brush for applying adhesive.
18. Polycarbonate track-etched membrane filters, type Cyclopure Transparent[®] (Whatman, Maidstone, Kent, UK), for creating random TC arrays. These filters are available with pore diameters of 0.1, 0.2, 0.4, 0.6, 0.8, 1.0, 3.0, 5.0, and 8.0 μm . Filter thickness varies between 20 μm (0.1- μm pore diameter) and 12 μm (8.0- μm pore diameter), pore density between 200 pores/(100 \times 100) μm^2 (0.1- μm pore diameter) and 10 pores/(100 \times 100) μm^2 (8.0- μm pore diameter).
19. Double-sticky tape, referred to as optically clear adhesive, type 8141, 3M Company.
20. Ultrasound bath.
21. Stainless steel pins no. 26002-10 and holder no. 26018-17, Fine Science Tools, Heidelberg, Germany.
22. Transport solution 2 for OSTR measurements (*see* **ref. 13**): 4 μM Alexa488-labeled NTF2 or 4 μM GFP, 100 mM sucrose in mock 3.
23. GELoader Tips (Eppendorf, Hamburg, Germany), which are very fine plastic pipet tips for injection of transport substrate into OSTR chamber.
24. Confocal laser scanning system based on an inverted microscope.
25. Software for image processing (e.g., *ImageJ*).

3. Methods

3.1. Confocal Fluorescence Microscopic Measurement of Nucleocytoplasmic Transport Using Isolated *Xenopus* Oocyte Nuclei

3.1.1. Isolation of *Xenopus* Oocyte Nuclei

1. Use two fine forceps to remove a stage VI oocyte (~1.2-mm diameter; **Fig. 1A**) from a piece of *Xenopus* ovary (*see* **Notes 1** and **2**).
2. Use a Pasteur pipet to transfer the oocyte into a small glass dish (**Subheading 2., item 4**) containing mock 3 at ambient temperature.

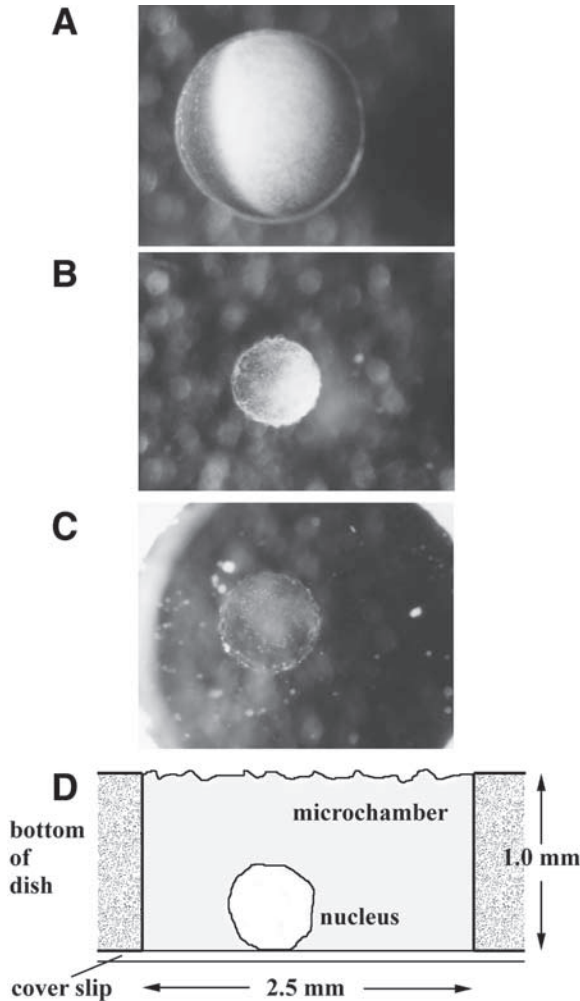


Fig. 1. Isolation and purification of *Xenopus* oocyte nuclei for nucleocytoplasmic transport measurements. A stage VI *Xenopus* oocyte (A) was manually dissected. The nucleus was (B) isolated, (C) cleaned of adhering yolk particles, and (D) deposited in a microchamber. From ref. 10.

3. Place the dish on the stage of a stereomicroscope and adjust the illuminating glass fibers such that the light beams enter the dish almost horizontally. This yields a darkfield effect, facilitating visualization of isolated nuclei otherwise virtually invisible.
4. At approx 16 \times total magnification, grip the oocyte at the equator by forceps. Tear the oocyte gently apart. Try to spot the nucleus, which initially is visible only as a hole in the yolk (see Notes 3 and 4). Gently isolate the nucleus.

5. Dip the tip of the transfer pipet into mock 3 and extrude the air from the pipet tip (see **Note 5**). Aspirate the nucleus. Place another small glass dish containing fresh mock 3, not contaminated by Ringer's solution and yolk, on the stage of the stereomicroscope and release the nucleus into mock 3.
6. Further purify the nucleus from adhering yolk particles (**Fig. 1C**) by repeatedly touching the nucleus with the blunt end of a microcapillary (**Subheading 2., item 9**). Isolation and purification of a nucleus should be completed within 1 to 2 min.

3.1.2. Preparation of Microchambers

1. Drill a hole of 2.5-mm diameter into the bottom of a tissue culture dish. Remove ridges using sandpaper. Use a jet of compressed air to remove debris and dust.
2. Attach a regular cover slip to the bottom of the dish using any glue appropriate. We prepare a batch of approx 20 chambers at a time, which lasts for many experiments because each microchamber can be used several times.

3.1.3. Deposition of an Isolated Nucleus in a Microchamber

1. Fill a microchamber with mock 3 (requires ~5 μL). Mock 3 should be kept at ambient temperature (see **Note 5**).
2. Employing the transfer pipet, aspirate an isolated clean nucleus prepared in advance according to **Subheading 3.1.1.** (but see **Note 2**). Deposit the nucleus in the microchamber (**Fig. 1C**). The nucleus will sink to the bottom of the microchamber and rest on the cover slip (**Fig. 1D**).

3.1.4. Addition of Transport Solution

1. Aspirate 10 μL transport solution 1 into a GELoader tip.
2. Dip the GELoader tip into the microchamber and place it on top of the oocyte nucleus. Slowly expel the transport solution. Because of its BSA content, the transport solution will sink to the bottom of the microchamber. Mock 3 will be displaced and gather at the top of the microchamber.
3. After addition of import solution, aspirate surplus of mock 3 from the top of the microchamber.

3.1.5. Recording of Transport Kinetics

1. Mount the microchamber on the stage of a confocal laser scanning microscope. Visualize the nucleus in through-light using a 10 \times objective. Bring the largest perimeter of the nucleus into the focal plane. Adjust laser power, filter settings, multiplier voltages, confocal aperture, and so on so that the brightness of both transport substrate (NLS protein) and control substrate (TRD70) is about equal.
2. Start scanning and acquire scans at intervals, properly resolving import kinetics (**Fig. 2**). The nucleus should be perfectly impermeable for the control substrate. If that is not the case, the nuclear envelope may have been damaged during isolation and purification of the nucleus. The experiment has then to be discarded.
3. Alternatively, to reduce the time lag between substrate addition and confocal scanning, adjust the confocal microscope in advance using a test specimen. Place the microchamber on the stage of the confocal microscope, start scanning, and inject transport solution into the OSTR chamber (see **Note 6**).

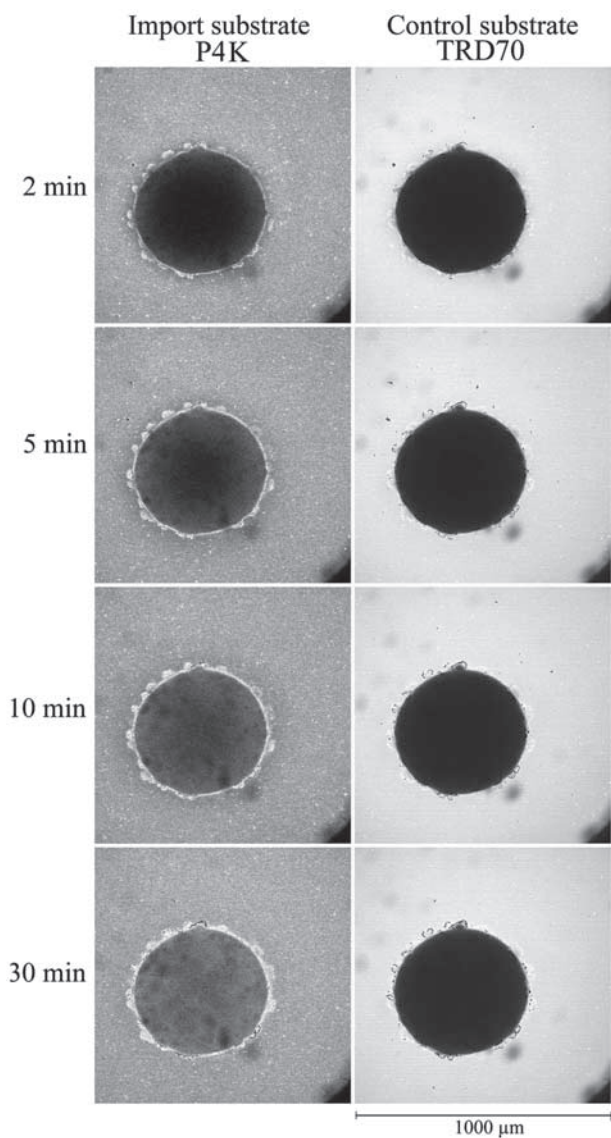


Fig. 2. Measurement of nucleocytoplasmic transport using isolated *Xenopus* oocyte nuclei. In a microchamber, an isolated *Xenopus* oocyte nucleus was incubated with transport solution 1 containing an NLS protein (P4K) and a control substrate (TRD70). Scans were taken after addition of the transport solution at indicated times. From [ref. 10](#).

3.2. OSTR Measurement of Nucleocytoplasmic Transport Using Isolated Intact Nuclei, Perforated Nuclei, or Nuclear Envelopes of Xenopus Oocytes

For OSTR experiments, various protocols are available (see **Note 7**). Here, a particularly convenient, fast, and robust procedure for *Xenopus* oocytes (**13**) employing comparatively large TCs is described. Alternative protocols and a discussion of single-transporter analysis may be found in refs. **11, 12**, and **14**.

3.2.1. Isolation and Purification of Xenopus Oocyte Nuclei

Isolate a nucleus as described in **Subheading 3.1.1.**, but take special care to remove yolk particles from the nucleus.

3.2.2. Preparation of OSTR Chambers

1. Drill a 3.5-mm diameter hole into the bottom of a tissue culture dish and clean the dish of debris.
2. Cut a preformed TC array (**Subheading 2., item 15**) into pieces approx 5×5 mm using a scalpel or sharp scissors. Apply Eastman Instant Adhesive no. 910 around the edges of the hole in the culture dish with a fine brush. Use forceps to place the array on the hole, with TCs facing the chamber volume.
3. Alternatively, TC arrays may be created from track-etched membrane filters (**Subheading 2., item 18**). Apply a piece the optically clear, double-sticky tape (adhesive 8141, **Subheading 2., item 19**) to a clean cover slip (15×15 mm). Cut a track-etched membrane filter into small pieces (5×5 mm) and place a filter piece, shiny side up (see **Note 8**), on the tape. Attach the cover slip and track-etched filter assembly to the culture dish such that the membrane filter forms the bottom of the hole.

3.2.3. Attachment of Nuclei to TC Arrays and Preparation of Nuclear Envelopes

1. Fill an OSTR chamber with 10 μ L mock 3. Place the OSTR chamber on the water surface in an ultrasonic bath and sonicate for a few seconds. This fills the TCs with mock 3, which does not occur spontaneously. Remove the OSTR chamber from the ultrasonic bath and wipe off water droplets from the bottom.
2. Under the stereomicroscope, using the transfer pipet, deposit an isolated nucleus in the OSTR chamber as indicated in **Fig. 3**. Employ the blunt-end glass capillary (**Subheading 2., item 9**) to press the nucleus against the TC array. The nucleus will adopt a domelike shape. Its lower part will attach firmly to the TC array. For parameters that may affect attachment, see **Notes 9** and **10**.
3. If desired, repeatedly perforate the TC-attached nucleus using the sharp steel pin (**Subheading 2., item 21**).
4. Alternatively, employ the steel pin to completely open the nucleus, to fold back the free-floating parts of nuclear envelope, and to remove the nuclear contents. Employ a GELoader tip to rinse the nuclear envelope three times with 15 μ L mock 3.
5. Prevent drying out of the OSTR chamber (which has a small volume) by including in the dish containing the OSTR chamber a wet "collar" of filter paper and putting on a lid during measurements.

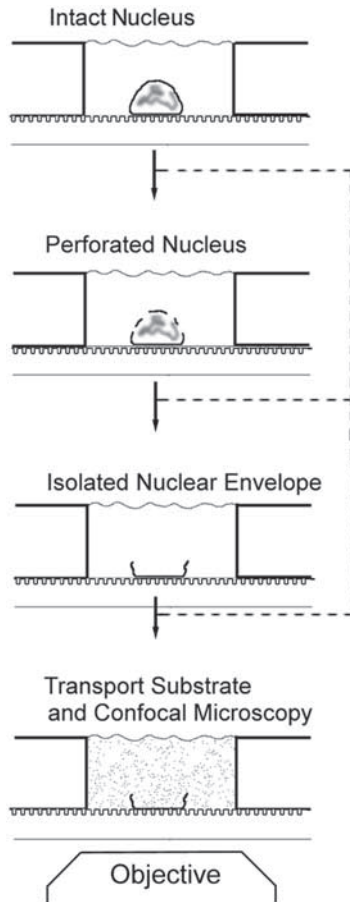


Fig. 3. Preparation of *Xenopus* oocyte nuclei and nuclear envelopes for nucleocytoplasmic transport measurements by optical single transporter recording (OSTR). An isolated *X.* oocyte nucleus is deposited in an OSTR chamber. The bottom of the OSTR chamber consists of a thin transparent foil containing an array of small cavities (test compartments, TCs). The nucleus is firmly attached to the TC array and may be perforated or completely dissected. A fluorescent transport substrate is added to the OSTR chamber and the appearance of transport substrate in the cavities is monitored by confocal fluorescence microscopy. From [ref. 14](#).

3.2.4. Recording of Export and Import Kinetics

1. Place the OSTR chamber on the stage of the confocal microscope. Visualize the nucleus or nuclear envelope in through-light at low magnification (10-fold objective lens) and position it in the center of the field of vision.
2. Depending on the TC diameter, continue with the 10-fold objective or change to a higher magnification. A 10-fold objective (air) or a 16-fold objective (water immersion, numerical aperture 0.5) is appropriate for TCs with 10- to 100- μm diameters. A 40-fold objective (oil immersion, numerical aperture 1.0) is required for TCs with 0.1- to 1.0- μm diameters.

3. After choosing the appropriate objective lens, position the nucleus or nuclear envelope such that the edge of the nucleus/nuclear envelope runs through the field of vision (**Fig. 4A**). This yields two populations of TCs: measuring TCs, which are covered by the nuclear envelope, and reference TCs, which are not covered.
4. Focus on the bottom of the TCs (**Fig. 4B**). Adjust the confocal system regarding filter settings, laser power, high voltage, scan speed, and zoom factor (*see Note 11*). It is advantageous to do these adjustments beforehand using an OSTR chamber filled with transport solution but void of a nucleus/nuclear envelope. If the microscope system is able to execute time-lapse programs, design a program to suit the transport kinetics.
5. Start the time-lapse program or activate the scanner manually. Use a GELoader tip to inject 20 μL transport solution 2 into the OSTR chamber between two scans (*see Note 6*). The transport solution, containing 100 mM sucrose, will displace mock 3, which spills over the edge of the OSTR chamber. Record transport kinetics until substrate has equilibrated between OSTR chamber and TCs. The transport solution used in OSTR measurements contains a transport substrate (e.g., NTF2) and a control substrate (e.g., TRD70). The control substrate permits following the kinetics of solution exchange and checking for a tight seal of the nuclear envelope to the TC array and the integrity of the nuclear envelope. Thus (**Fig. 4B**), after injection of transport solution, the measuring TCs should be filled by the transport substrate in a time-dependent manner and remain void of control substrate. In contrast, control TCs should be filled immediately with both transport substrate and control substrate.
6. After completion of export, import may be recorded by restarting the time-lapse program and injecting approx 50 μL mock 3 supplemented with 100 mM sucrose into the OSTR chamber.
7. For a second round of export and import measurements, remove the specimen from the confocal microscope. Under the stereomicroscope, wash the nucleus or nuclear envelope with a surplus of mock 3 (e.g., $3 \times 50 \mu\text{L}$). Then, place the specimen back on the stage of the confocal microscope and start an export measurement.

3.3. Data Evaluation

1. Employ an image analysis program (*see Note 12*) to derive the integral time-dependent fluorescence of single intact nuclei (if performing measurements according to **Subheading 3.1.**) or of all the TCs in a scan series (if performing measurements according to **Subheading 3.2.**). Plot the fluorescence of isolated nuclei or individual TCs vs time, as illustrated in **Fig. 4C,D**.
2. Fit the experimental OSTR data by Eq. 6 to obtain the rate constant k , which can be used to derive P according to Eq. 8 (*see Note 13*).
3. With large TCs (or nuclei), the assumptions made for deriving Eq. 6 may not hold. In that case, a deconvolution method (**13**) can be applied to separate membrane transport from intra-TC (intranuclear) diffusion and substrate mixing and to recover, within certain limits, true k and P values.

4. Notes

1. *Xenopus* ovary can be used for about a week if kept at 10°C and medium is changed daily.
2. Use a freshly isolated nucleus for each experiment. Isolated nuclei will rapidly swell in mock 3. This is desirable to a certain extent because the nuclear surface is made smoother, and protusions (*see Note 10*) are reduced. Osmotic swelling of nuclei can be prevented by addition of approx 20% (w/v) BSA to mock 3.

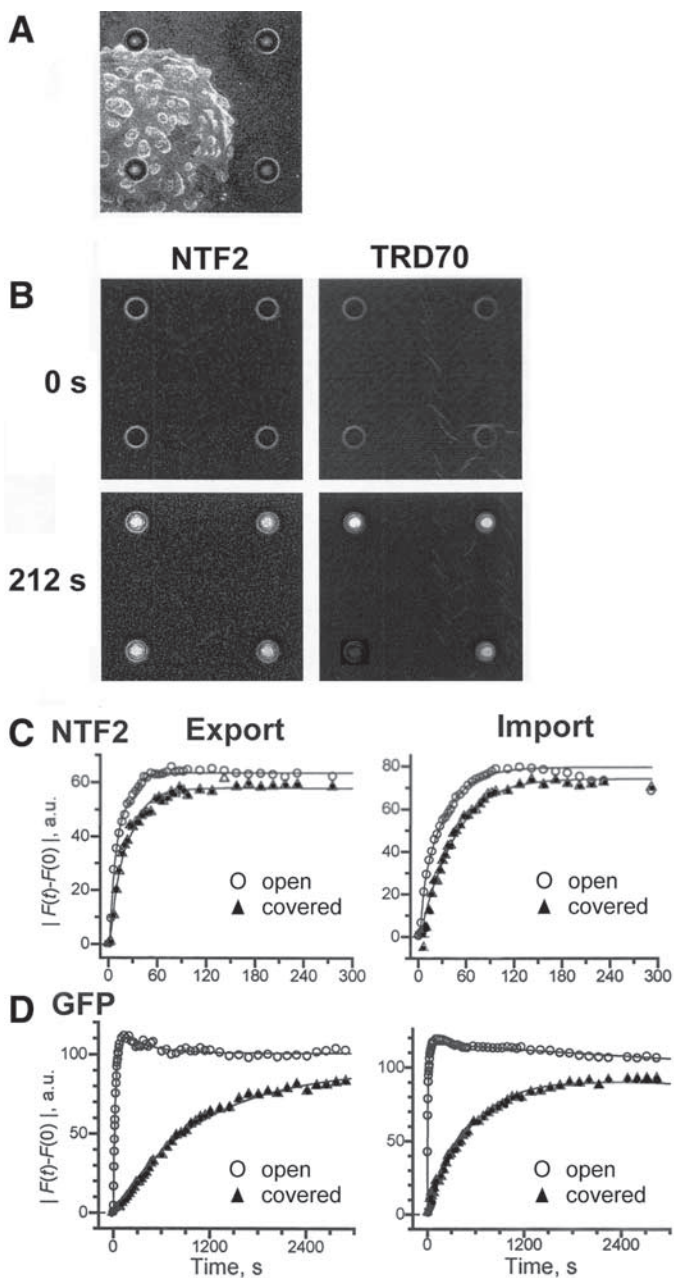


Fig. 4. Measurement of nucleocytoplasmic transport by optical single transporter recording (OSTR). (A) In an OSTR chamber, a nuclear envelope was attached to an array of test compartments (TCs). The nuclear envelope covers only one of the four TCs contained in the field of view. (B) Transport solution 2, containing the nuclear transport receptor NTF2 and the control

3. Ease by which *Xenopus* oocyte nuclei can be isolated and purified varies largely from batch to batch.
4. Isolated purified nuclei are very sticky. To avoid sticking of nuclei to glass surfaces, apply a BSA solution (1 mg/mL) to the surface for a few minutes, then wash with mock 3. Also, do not wash glass dishes used for nuclear isolation extensively but rinse with distilled water only. Furthermore, use always the same “dirty” tip on the transfer pipet and never clean the blunt-end glass pipet used for cleaning isolated nuclei from yolk particles and attaching isolated nuclei to TC arrays.
5. Isolated nuclei will be destroyed when coming into contact with the air–water interface. Make sure that pipet tips do not contain air bubbles when aspirating a nucleus. Keep mock 3 at room temperature during experiments to avoid the formation of air bubbles in dishes and chambers.
6. Injection of transport solution during scanning is facilitated by attaching a magnifying glass to the microscope stage.
7. In OSTR experiments, transport across TC-spanning membrane patches is usually induced by changing the concentration of transport substrates in the OSTR chamber and monitored by recording the fluorescence of transport substrates in the TCs. Within this frame, a number of specific protocols exist:
 - a. In OSTR experiments with isolated intact nuclei, the addition of transport substrate to the microchamber will induce the import of the substrate from the chamber into the nucleus and, after a lag time, the export from the nucleus into TCs.
 - b. If in such experiments the substrate has equilibrated among the chamber, nucleus, and TCs, removal of substrate from the OSTR chamber will induce the import from the TCs into the nucleus and simultaneously export from the nucleus into the OSTR chamber.
 - c. In OSTR experiments with isolated nuclear envelopes, the addition of substrate to the chamber will induce export. After equilibration of the substrate, its removal from the chamber will induce import.
 - d. In case of two transport substrates with different emission wavelengths (e.g., green and red), addition to and removal from the OSTR chamber can be arranged such that either both substrates are exported or imported or one is exported and the other imported.
 - e. If a transport substrate has been equilibrated between OSTR chamber and TCs, transport can be induced by photobleaching of individual TCs (**14**). Neighboring TCs will remain essentially unaffected. Similarly, photoactivation of a substrate by an ultraviolet flash can be used to induce import from single TCs.
 - f. The transport of nonfluorescent substrates can be monitored by substrate-specific fluorescent indicators. Such indicators are available not only for many inorganic ions but also for certain proteins (e.g., **ref. 15**). For a transport measurement, the OSTR chamber is filled with a solution containing an indicator. Then, a nucleus/nuclear envelope

(caption continued from previous page) substrate TRD70, was added to the OSTR chamber, and the TCs were observed by confocal microscopy. NTR2 rapidly entered the nuclear envelope-covered TC; TRD70 was excluded. Open TCs were immediately filled with both NTF2 and TDR70. (**C, D**) From a series of confocal scans, the import and export kinetics were derived for NTF2 and GFP. The transport kinetics of the two compounds differ drastically, although their molecular dimensions are virtually identical. From **ref. 13**.

is attached to the TC array, and the residual indicator is washed out of the OSTR chamber. Transport substrate is added to the OSTR chamber, and fluorescence of the indicator in the TCs is recorded.

- g. Usually, substrate fluorescence is monitored by confocal x - y sections. The confocal plane is adjusted to pass through TCs close to their bottom and parallel to the plane of the TC array. This has the advantage that many TCs can be recorded in parallel. However, it is also possible to employ vertical (x - z) sectioning. In that case, a single TC or a line of TCs can be imaged along the TC axis together with nuclear envelope and chamber volume. Thus, the fluorescence of TCs, nuclear envelope, and chamber contents can be monitored simultaneously. In principle, stacks of x - y scans can also be acquired and used to reconstruct substrate flux in three dimensions and time
 - h. Depending on the area density of transporters and the TC diameter, TC-spanning membrane patches will contain one, few, or many transporters. By employing TC arrays with different TC diameters, it is thus possible to measure on the same membrane the flux through single transporters or transporter populations. In the *Xenopus* oocyte nuclear envelope, the area density of NPCs is approx $50/\mu\text{m}^2$, and the single NPC occupies approx $0.02 \mu\text{m}^2$, corresponding to the cross section of a cylindrical TC with a $0.160\text{-}\mu\text{m}$ diameter. Therefore, for the single-transporter analysis of the *Xenopus* oocyte NPC, TCs with approx $0.2\text{-}\mu\text{m}$ diameter are appropriate.
8. When employing track-etched membrane filters to create TC arrays, it is important to choose filters designated as transparent. In this filter type, the pore density is small, and all pores are oriented perpendicular to the filter plane. It is also essential to note that filters have a shiny, smooth side and a less-shiny, rough side. When creating OSTR chambers, the smooth side of the filter should face the chamber volume.
 9. Parameters influencing the tightness of seal between nuclear envelope and TC arrays are (1) clean surfaces of both nuclei and TC arrays and (2) Ca^{2+} concentration. Prepare a fresh charge of mock 3 every day. Take care that the Ca^{2+} concentration of all solutions is $3 \mu\text{M}$. Dialyze BSA stock solution (100 g/L) against mock 3 overnight.
 10. The oocyte nuclear envelope carries numerous large protrusions (cf, **Fig. 4A**). The protrusions collapse in an onionlike manner when the nuclear envelope is attached to a TC array. For transport measurements use, only TCs void of protrusions.
 11. Recording of transport kinetics by confocal microscopy may induce fluorescence photobleaching. Reduce laser power and number of scans as much as possible. If necessary, increase transport substrate concentration or the labeling ratio. Check for absence of photobleaching by making confocal scans on TC arrays that are filled with transport solution and sealed with immersion oil as described in **ref. 16**.
 12. We have developed (**I3**) a plug-in for *ImageJ* (public domain Java version by W. Rasband; available at <http://rsb.info.nih.gov/ij/>) that permits automatic localization of TCs in confocal scans to derive their average fluorescence intensities and to correct the readings for local background. In the case of export experiments (i.e., net transport from chamber into TCs), the initial TC fluorescence, measured before addition of the transport solution to the chamber, is subtracted from the data set; for import, all measurements are subtracted from the initial bright level, thus creating standardized curves rising with time from near-zero initial values, as illustrated in **Fig. 4C,D**.
 13. To evaluate the experimental data in terms of transport coefficients, both the isolated-nucleus system and the OSTR system are considered two-compartment systems in which a "large" compartment (microchamber, OSTR chamber) and one or many "small" compartments (isolated nucleus, TCs) are separated by a thin membrane (the nuclear envelope).

lope) containing discrete transporters (the NPCs). It is furthermore assumed, as a first approximation, that the transport substrate is instantaneously added to or removed from the chamber at zero time, that the chamber is well stirred so that the transport substrate concentration in the chamber C_{Ch} is constant, and that the TC (or nucleus) is so small that the transport substrate is rapidly dissipated by diffusion and the intranuclear TC concentration C_{TC} is a function of time only. For a purely passive, diffusional membrane transport process in which the substrate is not absorbed or produced anywhere in the system and its equilibration across the membrane is very fast (thin membrane approximation), the flux of substrate per unit membrane area ($\text{mol}/\mu\text{m}^2/\text{s}$) is quasi stationary at any time and can be expressed as

$$\phi(t) = P[C_{Ch} - C_{TC}(t)] \quad (1)$$

where P is the permeability coefficient ($\mu\text{m}/\text{s}$). The total flux through a TC-spanning membrane patch is the sum of the unitary fluxes through individual NPCs, each having the average single-transporter permeability P_{NPC} ($\mu\text{m}^3/\text{s}$). For a membrane of surface area S containing a large number n of NPCs at an average density σ ($\text{NPC}/\mu\text{m}^2$)

$$P = nP_{NPC}/S = \sigma P_{NPC} \quad (2)$$

For a constant concentration difference ΔC across the membrane (e.g., $1 \mu\text{M}$), the flux and permeability described by Eq. 1 can be linked to the single-transporter permeability and expressed using Avogadro's number N_A as a unitary flux (molecules/s/NPC)

$$\phi_{NPC} = P_{NPC}N_A\Delta C = PN_A\Delta C/\sigma \quad (3)$$

OSTR chamber and TC shall have volumes V_{Ch} and V_{TC} , respectively; the membrane patches covering the TCs shall have surface area S . The mean time of substrate diffusion inside the TC is proportional to $(TC \text{ dimension})^2/D$ where D is the diffusion coefficient of the substrate. If the TC is a few micrometers only in size, the intra-TC diffusion time is very small, the TC can be considered well stirred, and the concentration C_{TC} will be a function of time only. Then, the kinetics of substrate accumulation in the TC caused by the flux through the membrane patch is given by

$$\frac{dC_{TC}(t)}{dt} + PS \frac{V_{Ch} + V_{TC}}{V_{Ch}V_{TC}} C_{TC}(t) = \frac{PSM(t)}{V_{Ch}V_{TC}} \quad (4)$$

where $M(t) = V_{Ch}C_{Ch}(t) + V_{TC}C_{TC}(t)$ is the total amount of substrate. In the typical OSTR specimen, the volume of the chamber is large ($V_{Ch} \gg V_{TC}$), and the amount of substrate in the TC is negligible, so that Eq. 4 simplifies to

$$\frac{dC_{TC}(t)}{dt} = \frac{PS}{V_{TC}} [C_{Ch}(t) - C_{TC}(t)] = k[C_{Ch}(t) - C_{TC}(t)] \quad (5)$$

For a constant concentration of the substrate in the chamber $C_{Ch}(t) = C_{max}$, the solution of Eq. 5 is

$$C_{TC}(t) = C_{max}[1 - \exp(-kt)] \quad (6)$$

The rate constant k is given by

$$k = PS/V_{TC} = nP_{NPC}/V_{TC} \quad (7)$$

For cylindrical TCs with length L and $V_{TC} = SL$, the rate constant is

$$k = PIL = \sigma P_{NPC}/L \quad (8)$$

References

1. Feldherr, C. M. and Feldherr, A. B. (1960) The nuclear membrane as a barrier to the free diffusion of proteins. *Nature* **185**, 250–251.
2. Lippincott-Schwartz, J., Snapp, E., and Kenworthy, A. (2001) Studying protein dynamics in living cells. *Nat. Rev.* **2**, 444–456.
3. Peters, R. (1986) Fluorescence microphotolysis to measure nucleocytoplasmic transport and intracellular mobility. *Biochim. Biophys. Acta* **864**, 305–359.
4. Michael, M., Choi, M., and Dreyfuss, G. (1995) A nuclear export signal in hnRNP A1: a signal-mediated, temperature-dependent nuclear protein export pathway. *Cell* **83**, 415–422.
5. Paine, P. L., Austerberry, C. F., Desjarlais, L. J., and Horowitz, S. B. (1983) Protein loss during nuclear isolation. *J. Cell Biol.* **97**, 1240–1242.
6. Riedel, N., Bachmann, M., Prochnow, D., Richter, H.-P., and Fasold, H. (1987) Permeability measurements with closed vesicles from rat liver nuclear envelopes. *Proc. Natl. Acad. Sci. USA* **84**, 3540–3544.
7. Forbes, D. J., Kirschner, M. W., and Newport, J. W. (1983) Spontaneous formation of nucleus-like structure around bacteriophage DNA microinjected into *Xenopus* eggs. *Cell* **34**, 13–23.
8. Lohka, M. J. and Masui, Y. (1983) Formation in vitro of sperm pronuclei and mitotic chromosomes induced by amphibian ooplasmic components. *Science* **220**, 719–721.
9. Adam, S., Sterne-Marr, R., and Gerace, L. (1990) Nuclear protein import in permeabilized mammalian cells requires soluble cytoplasmic factors. *J. Cell Biol.* **111**, 807–816.
10. Radtke, T., Schmalz, D., Coutavas, E., Soliman, T. M., and Peters, R. (2001) Kinetics of protein import into isolated *Xenopus* oocyte nuclei. *Proc. Natl. Acad. Sci. U. S. A.* **98**, 2407–2413.
11. Tschödrich-Rotter, M. and Peters, R. (1998) An optical method for recording the activity of single transporters in membrane patches. *J. Microsc.* **192**, 144–125.
12. Peters, R. (2003) Optical single transporter recording: transport kinetics in microarrays of membrane patches. *Annu. Rev. Biophys. Biomol. Struct.* **32**, 47–67.
13. Kiskin, N., Siebrasse, J. P., and Peters, R. (2003) Optical micro-well assay of membrane transport kinetics. *Biophys. J.* **85**, 2311–2322.
14. Siebrasse, J. P., Coutavas, E., and Peters, R. (2002) Reconstitution of nuclear protein export in isolated nuclear envelopes. *J. Cell Biol.* **158**, 849–854.
15. Kalab, P., Weis, K., and Heald, R. (2002) Visualization of a Ran-GTP gradient in interphase and mitotic *Xenopus* egg extracts. *Science* **295**, 2452–2456.
16. Siebrasse, J. P. and Peters, R. (2002) Rapid translocation of p10/NTF2 through the nuclear pore of isolated nuclei and nuclear envelopes. *EMBO Rep.* **3**, 887–892.

Nuclear Pore Complex Structure and Plasticity Revealed by Electron and Atomic Force Microscopy

Bohumil Maco, Birthe Fahrenkrog, Ning-Ping Huang, and Ueli Aebi

Summary

To study the ultrastructure of nuclear pore complexes (NPCs), a wide spectrum of different electron microscopy (EM) or atomic force microscopy (AFM) techniques can be employed. The combination of these methods can reveal new insights into the structural and functional organization of this important supramolecular machine through which nucleocytoplasmic transport occurs. Negative staining, quick freezing/freeze-drying/rotary metal shadowing, embedding and thin sectioning, cryoelectron microscopy and tomography, scanning electron microscopy, or combination with immunolabeling techniques are tools for collecting data and information about the three-dimensional structure and architecture of the NPCs. AFM enables investigation of the functional dynamics of native NPCs under physiological conditions.

Key Words: Atomic force microscopy; electron microscopy; nuclear pore complex; nucleus; *Xenopus laevis*.

1. Introduction

Nuclei of *Xenopus laevis* oocytes, which are typically a fraction of a millimeter in diameter, can be easily isolated manually and manipulated, and they have a high density of nuclear pore complexes (NPCs). This makes *Xenopus* oocytes the system of choice to study the ultrastructure and molecular architecture of NPCs. NPCs are embedded in the double membrane of the nuclear envelope (NE), and they provide the sole gateways for molecular trafficking between the cytoplasm and the nucleus of interphase eukaryotic cells.

A consensus model of the three-dimensional (3D) architecture of the NPC has evolved from extensive electron microscopic (EM) and tomographic studies (1–4). Accordingly, the vertebrate NPC, which has a total mass of approx 125 MDa (5), consists of an eightfold symmetric central framework that in turn is composed of two identical halves that are put together back to back in the midplane of the NE (6,7).

From: *Methods in Molecular Biology*, vol. 322: *Xenopus Protocols: Cell Biology and Signal Transduction*
Edited by: X. J. Liu © Humana Press Inc., Totowa, NJ

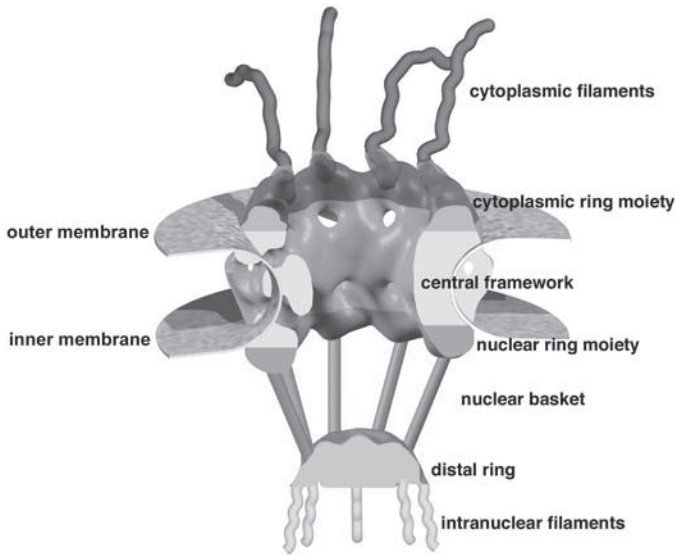


Fig. 1. Representation of the 3D consensus model of the NPC. The main structural components of the NPC include the central framework embedded in NE membrane, the cytoplasmic ring moiety and cytoplasmic filament, and the nuclear ring moiety and nuclear basket. The reconstructions of the central framework and the distal ring of the nuclear basket have been adapted from a tomographic reconstruction of native NPCs embedded in thick amorphous ice (4). Figure was modeled with a visual programming environment (ViPER) at the Scripps Research Institute (<http://www.scripps.edu>). Reproduced with permission from ref. 7 (<http://www.nature.com/nrm>).

The cytoplasmic ring moiety of the central framework is decorated with eight cytoplasmic filaments, whereas the nuclear ring moiety is topped with eight more tenuous filaments that join distally into a massive distal ring and thereby form a distinct nuclear basket (6,7; Fig. 1). Here, we describe the basic EM techniques to study the ultrastructure of the NPC: negative staining, quick freezing/freeze-drying/rotary metal shadowing, embedding and thin sectioning, and preembedding immunogold labeling. Furthermore, we provide protocols to study NPC dynamics by atomic force microscopy (AFM).

2. Materials

All chemicals used were analytical grade, and all buffer solutions were prepared with double-distilled water. All experimental procedures were performed at room temperature unless otherwise stated.

2.1. Basic Materials

1. Female *Xenopus laevis*.
2. Anesthetic and surgical equipment for the isolation of oocytes.
3. Modified Barth's solution (MBS): 10 mM HEPES, pH 7.5, 88 mM NaCl, 1 mM KCl, 0.82 mM MgSO₄, 0.33 mM Ca(NO₃)₂, 0.41 mM CaCl₂, and 100 U/mL of penicillin-streptomycin.

4. Low-salt buffer (LSB): 10 mM HEPES, pH 7.5, 1 mM KCl, 0.5 mM MgCl₂, and trace amounts of phenylmethylsulfonyl fluoride (PMSF; *see Note 1*).
5. 10% Stock solution of bovine serum albumin (BSA) stored in aliquots at -20°C.
6. Poly-L-lysine, 0.1% w/v in water (Sigma Diagnostics Inc., St. Louis, MO).
7. Fine glass needles pulled from micropipets on a microelectrode puller.
8. Small Petri dishes, 35-mm diameter.
9. Binocular dissection stereomicroscope with adjustable top or side illumination.
10. Fine Dumont forceps.
11. Glow-discharge apparatus.
12. Copper grids, 200 mesh per inch.

2.2. Fixation, Extraction, and Contrasting Solutions (see Note 2)

1. 25% Stock solution of glutaraldehyde, EM grade (GA; Fluka Chemie AG, Buchs, Switzerland); store at 4°C.
2. 4% Stock solution osmium tetroxide (OsO₄; Electron Microscopic Sciences, Fort Washington, PA); store at 4°C.
3. 20% Stock solution of Triton X-100; store at 4°C.
4. 2% Stock solution of tannic acid prepared fresh.
5. 6% Stock solution of uranyl acetate (UA; Fluka Chemie AG); make fresh as required from uranyl acetate salt.

2.3. Negative Staining

A 2% solution of UA in double-distilled water is freshly prepared from a 6% stock solution.

2.4. Quick Freezing/Freeze-Drying/Rotary Metal Shadowing

1. Pneumatically operating plunging device for rapid freezing.
2. Propane gas (dangerous, explosive).
3. Isopentane (cryoprotectant; Fluka Chemie AG); store at 4°C.
4. Liquid nitrogen.
5. Freeze-drying device (e.g., BAF-300 freeze-fracture apparatus, Baltec, Liechtenstein).

2.5. Thin Sectioning

1. Materials described in **Subheading 2.1**.
2. Solutions described in **Subheading 2.2**.
3. Epoxy resin (Epon 812, Fluka Chemie AG).
4. Ultramicrotome (e.g., Reichert Ultracut microtome, Reichert-Jung Optische Werke, Vienna, Austria).
5. Diamond knife (Diatome, Biel, Switzerland).

2.6. Atomic Force Microscopy

1. Materials described in **Subheading 2.1**.
2. AFM imaging buffer: 10 mM HEPES, pH, 7.5, 100 mM KCl.
3. Poly-L-lysine hydrobromide (molecular weight 1000–4000; Sigma-Aldrich, Buchs, Switzerland).
4. AFM (e.g., Nanoscope IIIa-Multimode AFM, Digital Instruments, Santa Barbara, CA).
5. All buffer solutions for AFM are sterile filtered (0.22- μ m Durapore filter).

3. Methods

The methods described next outline (1) the isolation of nuclei from *Xenopus laevis* stage VI oocytes; (2) the spreading of *Xenopus* NEs on EM grids; (3) negative staining

of spread NEs; (4) quick freezing/freeze-drying/rotary metal shadowing of spread NEs; (5) the embedding and thin sectioning of isolated nuclei from *Xenopus* oocytes, including immunogold labeling; and (6) the preparation of isolated nuclei from *Xenopus* oocytes for AFM.

3.1. Isolation of Nuclei From *Xenopus* Oocytes

A piece of ovary containing mature (stage VI) oocytes is surgically removed from female *X. laevis* and stored in MBS at 4°C for a maximum of 5 d. Before isolation of the nuclei, individual oocytes are placed (with 1-mL pipet with cut off tip's end; see **Note 3**) in a small Petri dish containing LSB to equilibrate them at room temperature. This buffer is commonly used to keep nuclei intact and partially swollen (nuclei are easily popped out) during the isolation. Nuclei are manually isolated either by opening the oocytes at their animal (dark) pole or by disrupting the oocytes with fine Dumont forceps along the line separating the two hemispheres. The released nuclei are cleaned from yolk and other materials by sucking them gently up and down into the tip of a 20- μ L pipet (adjusted to 5 μ L; see **Note 3**) in LSB containing a trace amount of PMSF (see **Note 1**) (5,8).

3.2. Spreading Nuclear Envelope

For all EM techniques (except for thin sectioning and AFM), single isolated and cleaned nuclei are transferred onto an EM grid (with a 20- μ L pipet). Next, the NE needs to be spread on the EM grid without damaging its NPCs. Two different strategies to open a nucleus and to spread its NE are used, depending on which side of the NE should be observed.

3.2.1. Visualization of the Nucleoplasmic Face of the NE

The 200-mesh copper EM grids covered with a carbon-coated parlodion support film are glow-discharged or alternatively coated with poly-L-lysine (0.1%; see **Note 4**). To adsorb the cytoplasmic face of the NE to the grid (i.e., to visualize the nuclear surface of the NE), the nucleus is opened manually by inserting two sharp, finely drawn glass needles into the top of the nucleus and peeling it like a banana. By touching the glass needle with NE to the support film of the grid, part of the NE is released and attaches to the grid. This technique ends up with a spread NE in the form of a four-arm star.

3.2.2. Visualization of the Cytoplasmic Face of the NE

The 200-mesh copper EM grids are covered with a carbon-coated parlodion support film. To adsorb the nuclear face of the NE to the carbon surface, a nucleus is opened by inserting two sharp, fine glass needles into the sides of the nucleus. The size of the resulting hole is gently increased until half of the nucleus is opened. Next, such a half-opened nucleus is turned over so that the hole/opening faces the support film of the grid. Quickly, before the nucleus collapses, the NE is spread on the carbon/parlodion surface. By this procedure, at least half of the NE is properly spread with its nuclear surface adsorbed to the support film.

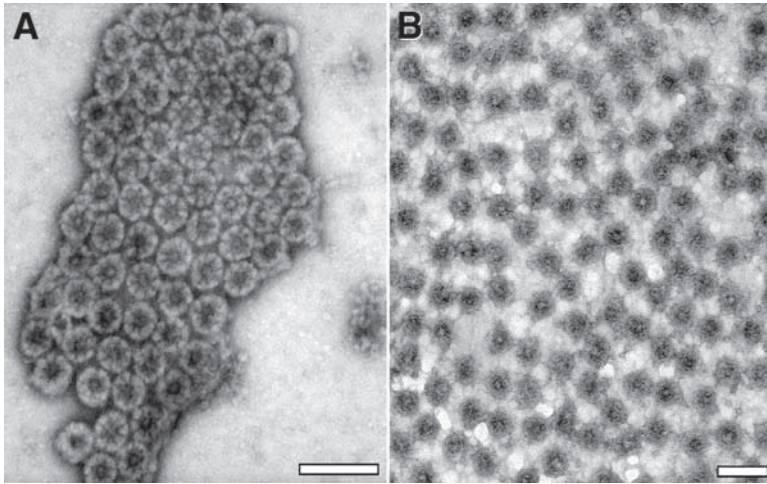


Fig. 2. Two different views of negatively stained and air-dried spread NEs. (A) Small NE patches that have been adsorbed to the support with their nuclear face revealing well-preserved NPCs are usually found along the edges of large poorly preserved areas. (B) Large area of NE with poorly preserved NPCs has been adsorbed to the support with its cytoplasmic face. Scale bars 200 nm.

3.3. Negative Staining

Negative staining is the easiest and fastest technique to briefly check the sample quality (5,8,9). However, excess staining solution (e.g., UA, uranyl formate, ammonium molybdate) leads to an increase in contrast of the background rather than the sample (for more details, see ref. 10). Well-preserved NPCs are typically found in small, evenly stained NE patches (Fig. 2A), whereas larger pieces of the NE are irregularly stained and contain no well-preserved NPCs (Fig. 2B).

A clean, intact nucleus is transferred onto a 5- μ L droplet of LSB placed on a carbon-/parlodion-coated EM grid (if the cytoplasmic face should be visualized; treat with poly-L-lysine or glow-discharge if the nuclear face should be visualized). Next, the nucleus is spread on the grid as described in Subheadings 3.2. and 3.2.2. All the following manipulations are performed with 5- μ L droplets directly on the grid (see Note 5).

1. Wash spread NE twice with LSB.
2. Fix with 2% GA in LSB for 2 min.
3. Wash twice with LSB.
4. Postfix with 1% OsO₄ in LSB for 2 min.
5. Wash twice with LSB.
6. Negative staining with 2% UA in double-distilled water (prepared fresh from 6% stock solution and centrifuged for 10 min at 16,000g) for 1 min.
7. Air dry by sucking off residual staining solution on the grid with filter paper.

3.3.1. Negative Staining of Detergent-Extracted NPCs

Triton X-100 extraction of the NE leads to differential dissociation of NPCs into distinct components and subcomplexes (**Fig. 3**).

1. Wash spread NE twice with LSB.
2. Incubate NE with 0.1% Triton X-100 plus 0.5% GA in LSB for 1 min.
3. Wash three times with 0.1% ethanol in LSB.
4. Fix with 2% GA in LSB for 2 min.
5. Wash twice with LSB.
6. Postfix with 1% OsO₄ in LSB for 2 min.
7. Wash twice with LSB.
8. Negative staining with 2% UA in double-distilled water (prepared fresh from 6% stock solution and centrifuged for 10 min at 16,000 g) for 1 min.
9. Air dry by sucking off residual staining solution on the grid with filter paper.

3.4. Quick Freezing/Freeze-Drying/Rotary Metal Shadowing

Quick freezing/freeze-drying/rotary metal shadowing is a technique that allows observation of the surface topography of the NPCs, comparable to scanning electron microscopy (**11–13**). The major advantage of the quick freezing/freeze-drying/rotary metal shadowing technique is easy sample preparation, with only very gentle and short fixation, without the need of air drying or critical point drying of the sample. Instead, the sample is frozen and freeze-dried, and the surface is coated with a very thin metal layer. The 3D effect of the obtained images can be enhanced by recording stereo pairs of the sample at tilt angles of $\pm 6^\circ$ or $\pm 10^\circ$ using a goniometer stage. Examples of quick frozen/freeze-dried/rotary metal shadowed NEs are shown in **Fig. 4** (cytoplasmic view) and in **Fig. 5** (nucleoplasmic side). All peripheral structural components of the NPC, such as the cytoplasmic filaments, the cytoplasmic ring moiety, the nuclear ring moiety, and the nuclear basket with its distal ring are visible (**Figs. 4B–D** and **5B–D**).

All the following manipulations were performed with 5- μ L droplets directly on the grid (*see Note 5*).

1. Wash spread NE twice with LSB.
2. Fix with 2% GA in LSB for 2 min.
3. Wash twice with LSB.
4. Postfix with 1% OsO₄ in LSB for 2 min.
5. Wash twice with LSB.
6. Wash six times with double-distilled water for 10 s each (at this stage, the sample can be transported to the site where the plunge freezing and freeze-fracture devices are located).
7. Fix the grid in Dumont forceps and mount it to a pneumatically operating plunging device for rapid freezing. Remove excess water with filter paper and quick-freeze the specimen immediately in a 3/1 (v/v) mixture of liquid propane–isopentane cooled to approx -185°C by liquid nitrogen (*see Notes 6* and **7**).
8. After transferring the frozen specimen to a freeze-fracture device (e.g., a BAF-300 apparatus), freeze-dry at -80°C at a vacuum of 2×10^{-7} torr for 3 to 4 h (*see Note 8*).
9. Rotary shadow at an elevation angle of 40° with 50 to 80 Hz of Pt/C or Ta/W.
10. Deposit an additional thin layer of carbon on top of the metal-shadowed sample.
11. Store all freeze-dried samples in a desiccator under vacuum and view them in the EM as soon as possible.

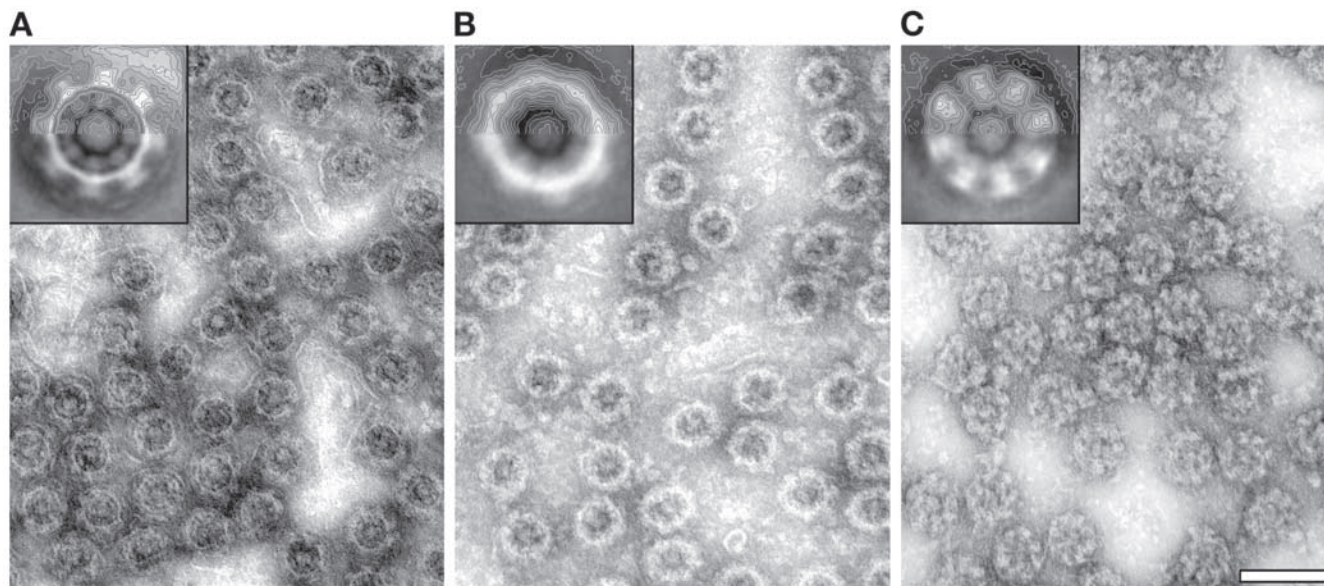


Fig. 3. Electron micrographs and averages (upper insets; computed from 100 particles) of chemically fixed (GA/OsO_4) and negatively stained/air-dried NPCs. Extraction of the NPCs with 0.1% Triton X-100 in LSB results in partial dissociation of the NPCs to distinct subcomplexes: (A) cytoplasmic rings obtained after treatment of intact nuclei with detergent prior to spreading the NEs on EM grids; (B) nuclear rings; and (C) central frameworks embedded in the NE, both obtained on treatment of spread NEs with detergent. Scale bar 200 nm.

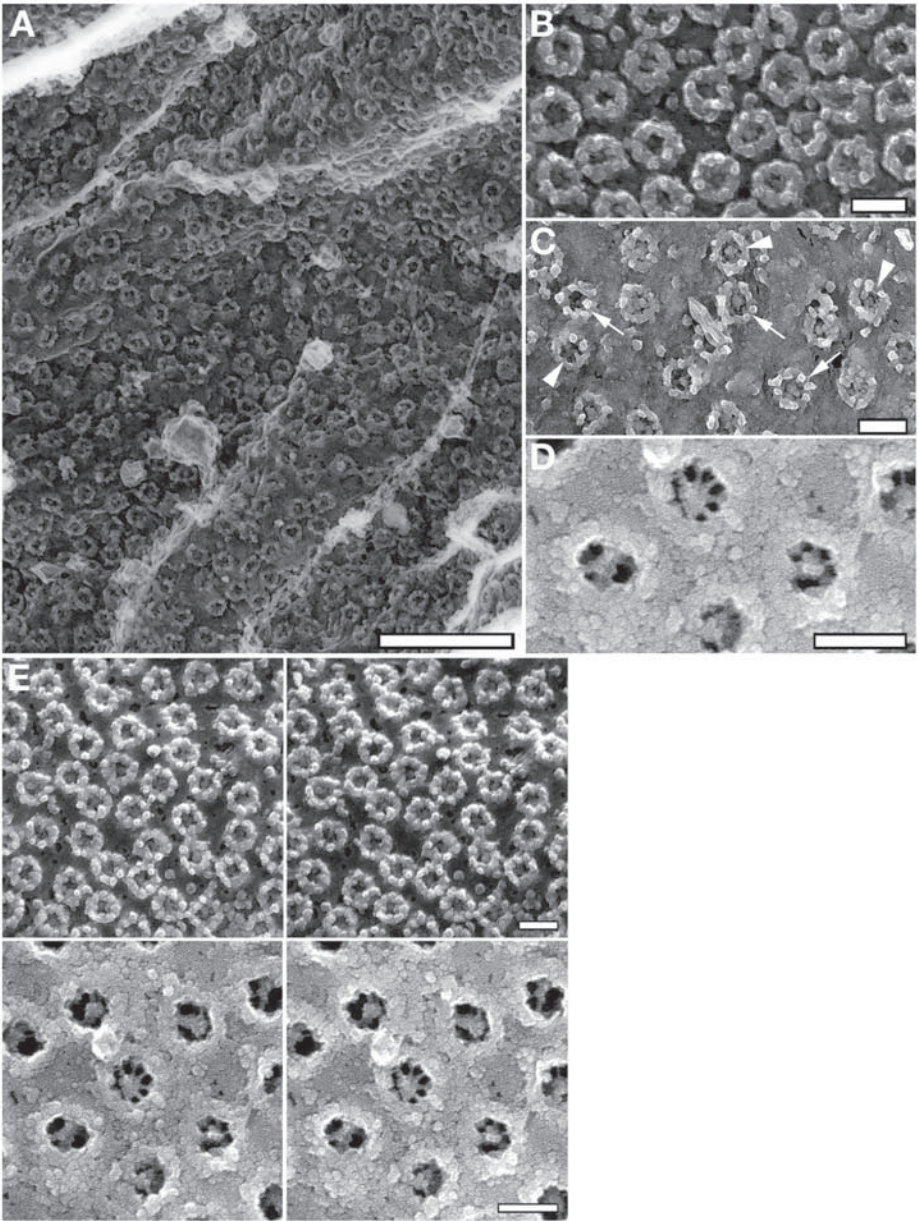


Fig. 4. Cytoplasmic view of NPCs that were quick frozen/freeze-dried/rotary metal shadowed. (A) Low-magnification overview and (B–D) higher magnification of the cytoplasmic ring moiety of the NPCs revealing the anchorage of the cytoplasmic filaments (arrows). Note some nuclear baskets that can be depicted through the central channel of the NPCs (D and arrowheads in C). (E) Stereo pair images of the cytoplasmic face-spread NE. Scale bars: (A) 0.5 μm and (B–E) 100 nm.

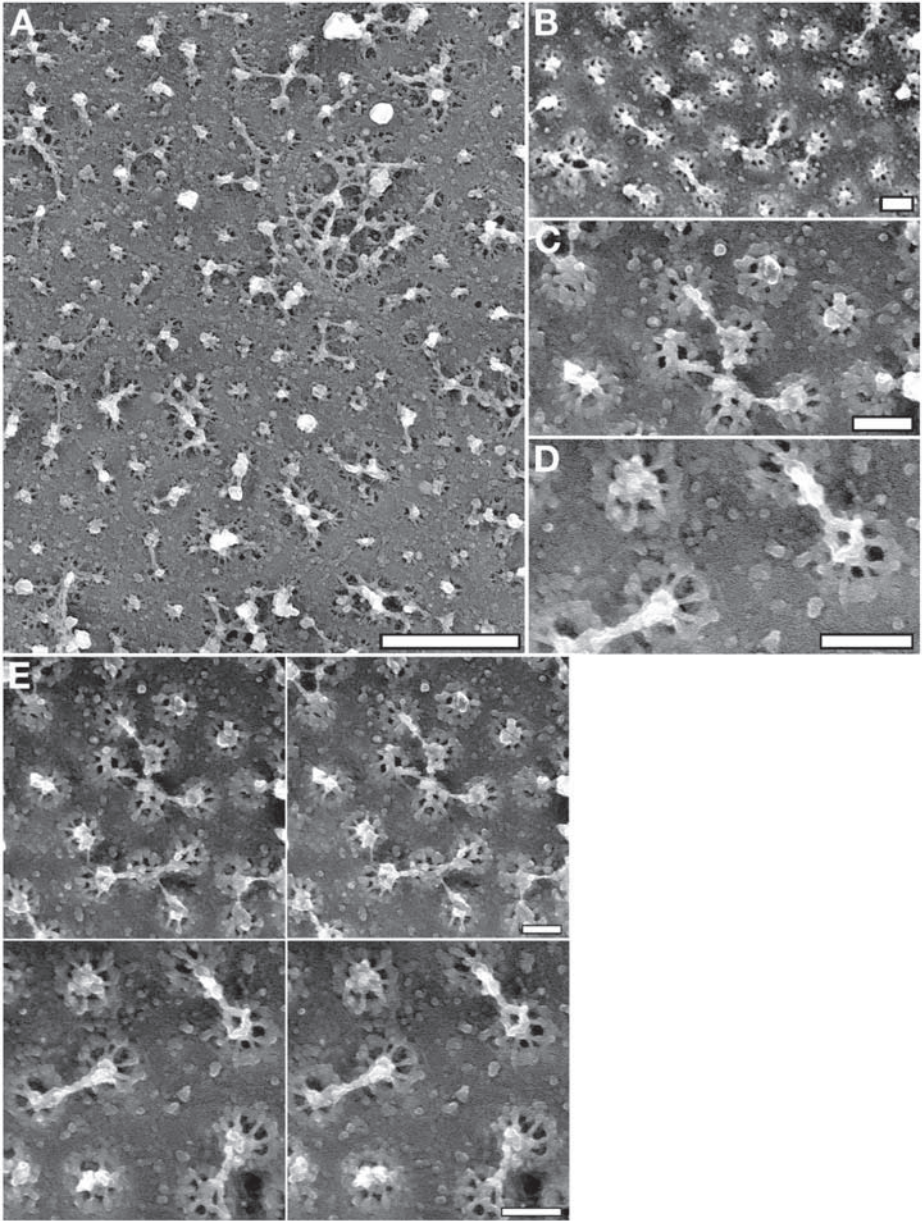


Fig. 5. Nuclear view of NPCs. A spread NE was adsorbed with its cytoplasmic face on the grid and prepared by quick freezing/freeze-drying/rotary metal shadowing. (A) Low-magnification overview and (C–D) higher magnification view of the nuclear baskets with their nuclear ring moiety (base of the basket) and the distal ring (top of the basket). Note that some distal rings appear open; others are closed (C,D). (E) Stereo pair images of nuclear side-spread NE. Scale bars: (A) 0.5 μm and (B–E) 100 nm.

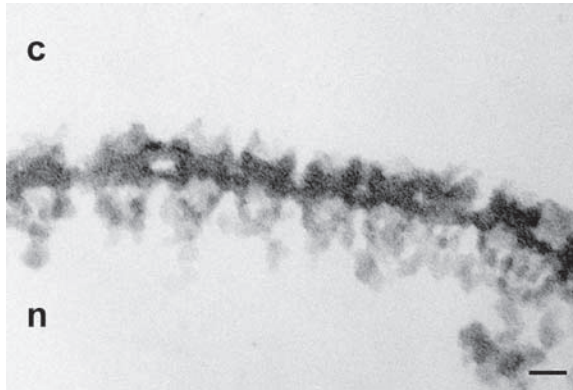


Fig. 6. Cross-sectioned view of NEs studded with NPCs. Isolated nuclei were prepared for EM by Epon embedding and thin sectioning. c, cytoplasm; n, nucleus. Scale bar 100 nm.

3.5. Embedding and Thin Sectioning

Thin sectioning is another technique that is used to investigate the 3D architecture of the NPCs (Fig. 6). Moreover, thin sectioning, negative staining, and quick freezing/freeze-drying/rotary metal shadowing in combination with immunogold labeling enable determination of the localization of individual nucleoporins within the 3D NPC architecture (14,15).

1. Prefix freshly isolated nuclei in 2% GA/0.3% tannic acid for 1 h.
2. Wash twice for 5 min with LSB.
3. Transfer washed nuclei on a microslide with cavity.
4. Embed nuclei in a drop of 2% low-melting agarose (*see Note 9*).
5. Cut small blocks of embedded nuclei out of the agarose and fix nuclei in 1% OsO₄ for 1 h.
6. Wash twice with LSB.
7. Dehydrate the fixed samples in a series of increasing ethanol concentrations: 50% ethanol for 10 min, 70% ethanol for 10 min, 90% ethanol for 10 min, followed by 100% ethanol three times for 10 min each, and finally acetone for 10 min.
8. Infiltrate the dehydrated samples with mixtures of Epon and acetone at 1/1 for 1 h and 2/1 for 1 h and finally in pure Epon for 3 to 4 h.
9. Place samples into gelatin capsules filled with fresh pure Epon resin and polymerize overnight at 60°C.
10. Cut thin sections (50–70 nm) on an ultramicrotome (e.g., a Reichert Ultracut microtome) using a diamond knife.
11. Collect the sections on parlodion-coated copper grids and stain them with 6% UA for 1 h followed by 2% lead citrate for 2 min.

3.6. Colloidal Gold Immunolabeling

For immunogold labeling, antibodies directly coupled to colloidal gold can be used to determine the localization of distinct nucleoporins within the NPC (16,17). The labeling is performed prior to the embedding of the sample (i.e., preembedding labeling).

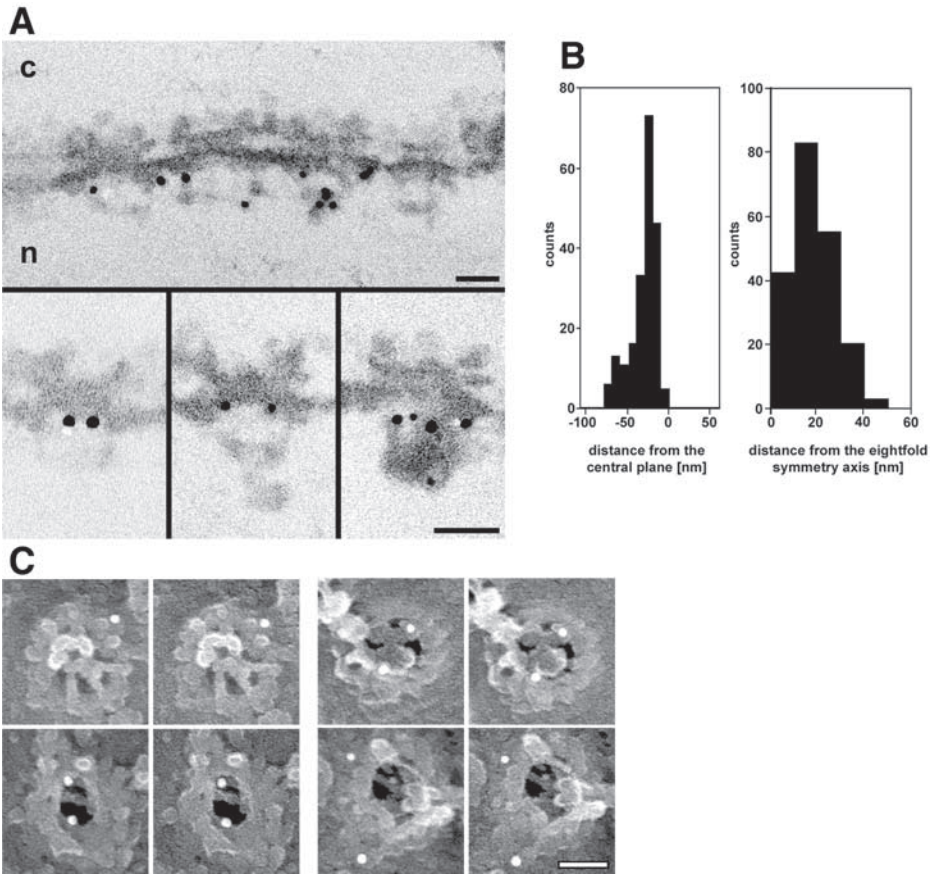


Fig. 7. Localization of the N-terminal domain of Nup153 in isolated *Xenopus* nuclei. (A) Intact isolated nuclei were immunolabeled with the anti-Nup153-N antibody conjugated directly to 8-nm colloidal gold and prepared for EM by Epon embedding and thin sectioning. Shown are an overview along the NE with labeled NPCs (top), and a gallery of selected examples of gold-labeled NPCs (bottom). c, cytoplasm; n, nucleus. (B) Histograms show distribution of the gold particles associated with the NPC along its central plane as well as its eight-fold symmetry axis. (C) Selected gallery of stereo pair images from the sample prepared as in (A) but processed by quick freezing/freeze-drying/rotary metal shadowing. The 8-nm colloidal gold particles are white because of inversion of the images. Scale bars: (A) 100 nm and (C) 50 nm. Parts A and B reprinted with permission from ref. 15. © 2002, Elsevier.

Figure 7 shows examples of thin sections along the NE, with NPCs labeled with an antibody against the N-terminal domain of the nucleoporin Nup153.

1. Incubate freshly isolated nuclei in LSB containing the appropriate antibody directly conjugated to colloidal gold for 2 h at room temperature.
2. Wash the nuclei with LSB containing 0.1% BSA for 5 min (see **Note 10**).

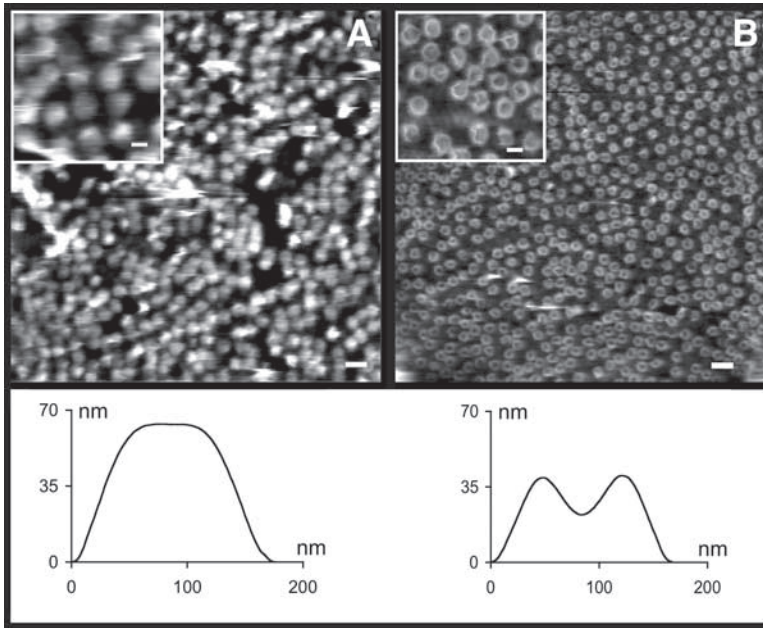


Fig. 8. Imaging native *Xenopus* NPCs by AFM in contact mode. (A) The nuclear face of the NPCs appears dome-like, whereas the cytoplasmic face (B) exhibits a donut-like morphology. The average radial height profiles of both the cytoplasmic and the nuclear faces were computed from 80 NPCs each. Scale bar 250 nm; insets 100 nm.

3. Process samples for negative staining (**Subheading 3.3.**), quick freezing/freeze-drying/rotary metal shadowing (**Subheading 3.4.**), or thin sectioning (**Subheading 3.5.**).

3.7. Atomic Force Microscopy

The advantage of AFM in biological research is the possibility of obtaining the surface topography of biological specimens at molecular detail under native or near-native conditions, that is, the sample is imaged in physiological buffer without any chemical fixation, detergent treatment, or dehydration. Moreover, time-lapse AFM enables investigation of the dynamic features of native NPCs *in situ* and direct correlation of structural changes with distinct functional states. The steps for preparing and scanning native NEs on a solid support by AFM are outlined in detail in **Subheading 3.7.1.** (see **Note 11**). Most significantly, AFM images reveal a distinct morphology for the cytoplasmic and the nuclear face of NPCs (**Fig. 8**).

3.7.1. Imaging Native NPCs

1. Surgically remove oocytes from female *X. laevis* ovaries as described in **Subheading 3.1.** Place individual oocytes in a Petri dish filled with LSB.
2. Clean silicon wafers ($5 \times 5 \text{ mm}^2$) by immersing in a 1/1 mixture of 30% H_2O_2 and 98% H_2SO_4 (use caution as this solution can explode in contact with organic matter) for

- 1 h at room temperature, extensively rinsing with pure water and drying in a nitrogen stream.
3. Incubate the pretreated silicon wafers with a poly-L-lysine solution (0.5 mg/mL in LSB) for 15 min, rinse with pure water, and dry under nitrogen, then glue using double-sided tape onto steel disks covered with Teflon (*see Note 12*).
 4. Manually isolate nuclei and transfer with 5 μ L LSB onto the poly-L-lysine-coated silicon wafer.
 5. Manually open the nucleus and spread the NE over the silicon wafer with the nuclear face or the cytoplasmic face exposed as described in **Subheading 3.2**. Gently wash the sample with LSB using a micropipet and cover with a 20- μ L droplet of imaging buffer.
 6. Mount samples on a Nanoscope IIIa-MultiMode AFM equipped with a “J” (120 μ m) scanner. No O-ring seal is used.

Images are recorded in contact mode using oxide-sharpened silicon nitride tips attached to cantilevers with a nominal force constant of 0.06 N/m. The applied force is kept at the lowest possible value by continuously adjusting the set point during scanning.

3.7.2. Imaging Reversible Calcium-Mediated Structural Changes of Individual NPCs by Time-Lapse AFM

1. Prepare and image a sample of native NPCs as described in **Subheading 3.7.1**.
2. Perform buffer changes by adding an equal volume of buffer containing either 0.2 mM CaCl₂ or 2 mM EGTA (Ethylene glycol-bis(β -aminoethyl ether)-*N,N,N',N'*-tetraacetic acid; a calcium chelator), while keeping the AFM tip engaged but without applying a force onto the sample surface.
3. After buffer addition, equilibrate the sample for 5 min before rescanning.

Time-lapse AFM images of the nuclear face of NPCs (**Fig. 9**) depict the reversible opening and closing of the nuclear basket of individual NPCs at its distal end (i.e., via its distal ring), which may act as an iris-like diaphragm in response to adding or removing calcium (**18**).

3.7.3. Imaging Temperature-Dependent Plugging and Unplugging of Individual NPCs by Time-Lapse AFM

1. Prepare and image sample of native NPCs in a cold room at 4°C according to the procedures described in **Subheading 3.7.1**.
2. Scan sample first at 4°C and rescan the same area after warming the imaging buffer and equilibrating it at 25°C.

Time-lapse AFM images of the cytoplasmic face of NPCs (**Fig. 10**) depict the temperature-dependent appearance (at 4°C) and disappearance (at 25°C), respectively, of a plug in the central pore of the NPC, suggesting that a direct correlation exists between the transport state of the NPCs, which is strongly attenuated at 4°C and fully resumes at 25°C, respectively, and the amount of cargo obstructing the central pores (**4**).

4. Notes

1. The protease inhibitor PMSF is dissolved in ethanol and stored at 4°C. Trace amounts are added to LSB immediately before use.

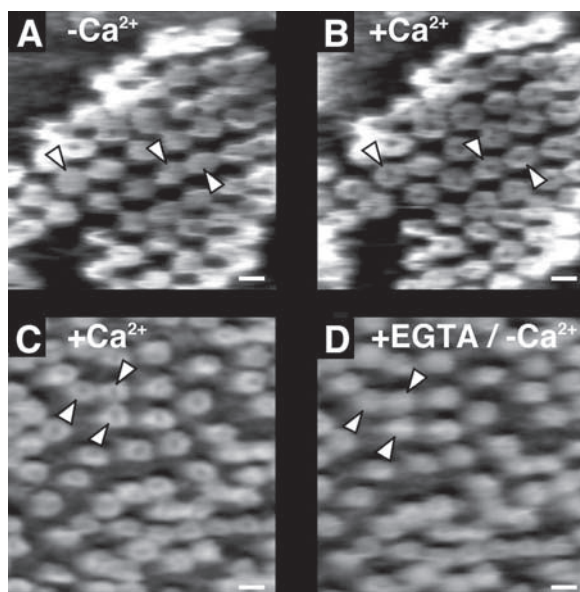


Fig. 9. Visualization of the reversible calcium-mediated opening and closing of the nuclear baskets by time-lapse AFM. (A,B) The same NPCs with closed baskets (i.e., $-Ca^{2+}$) (A) could be opened after addition of $0.1\text{ mM } Ca^{2+}$ (B). The opposite is true in C and D; the same NPCs with open baskets (i.e., $+0.1\text{ mM } Ca^{2+}$) (C) could be closed after addition of 1 mM EGTA (i.e., $-Ca^{2+}$) (D). Three corresponding NPCs in (A,B) and (C,D), respectively, are marked by arrowheads for better comparison. Scale bars: 100 nm . Reprinted with permission from ref. 18. © 1999 Elsevier.

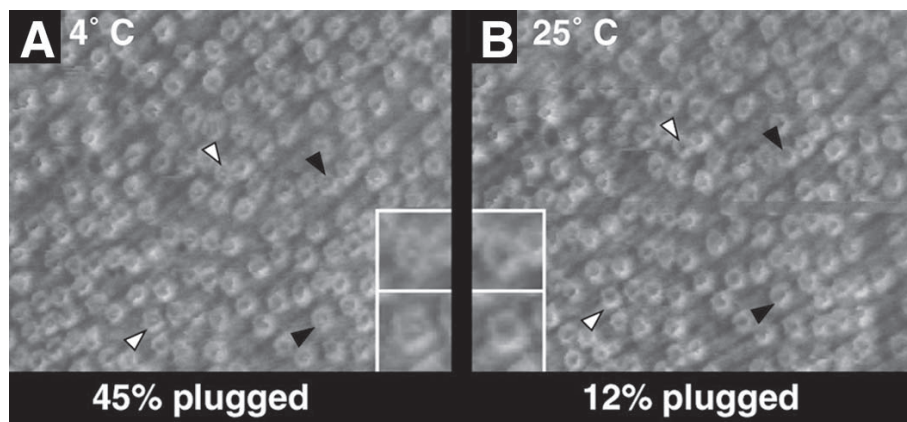


Fig. 10. Imaging temperature-dependent plugging or unplugging of individual NPCs by time-lapse AFM. (A,B) The same area of cytoplasmic face of NPCs on NE area was imaged by AFM in contact mode at 4°C (A) and after warming the system to 25°C (B). Previously plugged NPCs (A) became unplugged on increasing the temperature (B). Four corresponding NPCs are marked by arrowheads for better comparison. Reprinted with permission from ref. 4. © 2003 Elsevier.

2. Because most of the chemical fixatives used for EM are highly toxic (especially vapors of GA and OsO₄), it is absolutely necessary to work in a ventilated hood. Not only is UA radioactive but also aqueous solutions are light sensitive. Hence, light-protected storage is required, either in dark flasks or in bottles that are wrapped in aluminum foil.
3. Because the diameter of an Eppendorf pipet tip is smaller than the diameter of both oocytes and isolated nuclei, the end of the tip has to be cut off, for example, with a sharp razor blade.
4. Adsorption of the NE to the support strongly depends on the physical properties of the support. If the grids are glow-discharged (i.e., in a reduced atmosphere of air yielding a net negative charge), NEs tend to adsorb with their cytoplasmic face to the support so that their nuclear side is exposed for observation. Coating the grids with 0.1% poly-L-lysine has the same effect.
5. We prefer to perform all preparation steps on a grid. Changes of solution are followed by very quick touching of the edge of the EM grid with filter paper but without drying it completely. After blotting, immediately add a drop of the next solution. As an alternative, you may move the grids upside down from one solution drop to the next.
6. Proper freezing of the sample is crucial for obtaining good quality vitrified ice. To achieve this, the blotting time is critical: If it is too long, the sample becomes air dried, and the NPCs collapse before they are frozen. On the other hand, if the blotting time is too short, the water layer is too thick for freezing into a vitrified ice film. Instead, cubic ice is formed, which in turn causes mechanical damage (for more details, see [ref. 10](#)).
7. It is important from which side the grid is blotted. For a delicate sample such as the NE, the blotting should be done from the back side of the grid to minimize mechanical damage of the sample.
8. The principle of freeze-drying is that the vitrified ice is directly sublimated in the vacuum chamber of the freeze-fracture machine. Sublimation of vitreous ice occurs at temperatures ranging from -120 to -80°C at a vacuum of 2×10^{-7} torr or less.
9. This step is important for easier manipulation of the sample during its embedding into Epon resin. With a piece of filter paper, the excess water is removed, and a few drops of melted 2% agarose are added on top of the sample. When the agarose has hardened, small blocks containing sample are cut out of the agarose under a binocular microscope.
10. 0.1% BSA is used to block unspecific binding of the antibodies.
11. This section describes the use of a poly-L-lysine-coated silicon wafer as a stable support for imaging NEs by AFM. A carbon-coated copper grid is also a good support for the same purpose ([18](#)). However, the preparation of poly-L-lysine-coated silicon wafers is more straightforward, and both the cytoplasmic and the nuclear faces of the NE are relatively easily and reproducibly imaged by AFM on these wafers.
12. The step of rinsing silicon wafers with pure water after incubation with poly-L-lysine is important. Without that, it may cause distal openings of the nuclear baskets of NPCs because of the strong immobilization of NEs.

Acknowledgments

This work was supported by a National Center of Competence in Research (NCCR) program, Nanoscale Science by the Swiss National Science Foundation, and by research grants from the Swiss National Science Foundation (B. F.) and the Human Frontier Science Program (U. A.). Additional funds were provided by the Maurice E. Müller Foundation and by the Kanton Basel Stadt.

References

1. Unwin, P. N. and Milligan, R. A. (1982) A large particle associated with the perimeter of the nuclear pore complex. *J. Cell Biol.* **93**, 63–75.
2. Hinshaw, J. E., Carragher, B. O., and Milligan, R. A. (1992) Architecture and design of the nuclear pore complex. *Cell* **69**, 1133–1141.
3. Akey, C. W. and Radermacher, M. (1993) Architecture of the *Xenopus* nuclear pore complex revealed by 3-dimensional cryo-electron microscopy. *J. Cell Biol.* **122**, 1–19.
4. Stoffler, D., Feja, B., Fahrenkrog, B., Walz, J., Typke, D., and Aebi, U. (2003) Cryo-electron tomography provides novel insights into nuclear pore architecture: implications for nucleocytoplasmic transport. *J. Mol. Biol.* **328**, 119–130.
5. Reichelt, R., Holzenburg, A., Buhle, E. L., Jr., Jarnik, M., Engel, A., and Aebi, U. (1990) Correlation between structure and mass distribution of the nuclear pore complex and of distinct pore complex components. *J. Cell Biol.* **110**, 883–894.
6. Fahrenkrog, B., Köser, J., and Aebi, U. (2004) The nuclear pore complex: a jack of all trades? *Trends Cell Biol.* **29**, 175–182.
7. Fahrenkrog, B. and Aebi, U. (2003) The nuclear pore complex: nucleocytoplasmic transport and beyond. *Nat. Rev. Mol. Cell Biol.* **4**, 757–766.
8. Jarnik, M. and Aebi, U. (1991) Toward a more complete 3-D structure of the nuclear pore complex. *J. Struct. Biol.* **107**, 291–308.
9. Hinshaw, J. E. and Milligan, R. A. (2003) Nuclear pore complexes exceeding eightfold rotational symmetry. *J. Struct. Biol.* **141**, 259–268.
10. Harris, J. R., ed. (1997) *Negative Staining and Cryoelectron Microscopy: The Thin Film Techniques*, BIOS Scientific Publishers Limited, Oxford, UK.
11. Goldberg, M. W. and Allen, T. D. (1992) High resolution scanning electron microscopy of the nuclear envelope: demonstration of a new, regular, fibrous lattice attached to the baskets of the nucleoplasmic face of the nuclear pores. *J. Cell Biol.* **119**, 1429–1440.
12. Goldberg, M. W. and Allen, T. D. (1993) The nuclear pore complex: three-dimensional surface structure revealed by field emission, in-lens scanning electron microscopy, with underlying structure uncovered by proteolysis. *J. Cell Sci.* **106**, 261–274.
13. Goldberg, M. W., Wiese, C., Allen, T. D., and Wilson, K. L. (1997) Dimples, pores, star-rings, and thin rings on growing nuclear envelopes: evidence for structural intermediates in nuclear pore complex assembly. *J. Cell Sci.* **110**, 409–420.
14. Panté, N., Bastos, R., McMorrow, I., Burke, B., and Aebi, U. (1994) Interactions and three-dimensional localization of a group of nuclear pore complex proteins. *J. Cell Biol.* **126**, 603–617.
15. Fahrenkrog, B., Maco, B., Fager, A. M., Köser, J., Sauder, U., Ullman, K.S., and Aebi, U. (2002) Domain-specific antibodies reveal multiple-site topology of Nup153 within the nuclear pore complex. *J. Struct. Biol.* **140**, 254–267.
16. Slot, J. W. and Geuze, H. J. (1985) A new method of preparing gold probes for multiple-labeling cytochemistry. *Eur. J. Cell Biol.* **38**, 87–93.
17. Baschong, W. and Wrigley, N. G. (1990) Small colloidal gold conjugated to Fab fragments or to immunoglobulin G as high-resolution labels for electron microscopy: a technical overview. *J. Electron Microsc. Tech.* **14**, 313–323.
18. Stoffler, D., Goldie, K. N., Feja, B., and Aebi, U. (1999) Calcium-mediated structural changes of native nuclear pore complexes monitored by time-lapse atomic force microscopy. *J. Mol. Biol.* **287**, 741–752.

In Vitro Study of Nuclear Assembly and Nuclear Import Using *Xenopus* Egg Extracts

Rene C. Chan and Douglass J. Forbes

Summary

Nuclear import is a critical process for the cell: molecules are selectively permitted into the nuclear interior where the sheltered genome resides. The process of nuclear import can be biochemically studied in vitro using nuclei reconstituted from *Xenopus* egg extract components and *Xenopus* sperm chromatin. This in vitro system allows for the visualization of nuclear import by monitoring the accumulation of fluorescent nuclear import substrates in the reconstituted nuclei. A powerful aspect of the system is that “biochemically mutant” nuclei can be readily generated, either by immunodepletion of proteins from or addition of proteins to the reaction. This ability allows ascertainment of the role of specific proteins in nuclear import.

Key Words: In vitro nuclear reconstitution; nuclear assembly; nuclear import; nuclear import substrate; nuclear pore; nuclear transport; nucleus; sperm chromatin; *Xenopus* egg extract.

1. Introduction

Study of the nucleus and its molecular functions has been greatly aided by a system capable of assembling nuclei in vitro (1–4). This system takes advantage of the fact that each *Xenopus* oocyte contains a very large nucleus with tens of millions of nuclear pores. As the interphase oocyte matures into the metaphase egg, it disassembles its large nucleus and pores into their component parts. Unfertilized *Xenopus* eggs thus serve as bountiful storehouses of disassembled nuclear components. In nature, these components would be used to assemble the nuclei needed for the thousands of cells formed in the early embryonic divisions.

Experimentally, when *Xenopus* eggs are lysed, the disassembled components can be combined with added deoxyribonucleic acid (DNA) or chromatin and will spontaneously form nuclear structures. *Xenopus* egg extract thus allows one to study the steps of nuclear assembly, including nuclear envelope and nuclear pore assembly. The assembled nuclei can further be used to study nuclear import in vitro. Transport is

assayed by the accumulation of fluorescent nuclear import substrates in the reconstituted nuclei (5–8). The effect of individual cytosolic factors on nuclear import can be determined either by adding an excess amount of the protein to the extract or by removing the factor from the extract by immunodepletion (9,10).

In a different type of experiment, a specific structural component of the pore can be removed from the extract while in the disassembled state by immunodepletion (11–13). Assembly of nuclei lacking the component can then be performed in the immunodepleted egg extract. The resultant “biochemically mutant” nuclei can then be tested for function. The ability to assemble nuclei lacking a specific protein in vitro has been used to reveal proteins involved in nuclear import, nuclear envelope assembly, nuclear pore assembly, and DNA replication.

2. Materials

1. *Xenopus laevis* frogs, female and male.
2. Pregnant mare serum gonadotropin (12.5X stock; cat. no. 367222; Calbiochem, La Jolla, CA): 5000 U/2 mL sterile filtered water.
3. 1X Stock human chorionic gonadotropin (cat. no. CG-10; Sigma, St. Louis, MO): 10,000 U/10 mL sterile filtered water.
4. 27 × 0.5-in. Gage needles.
5. 18 × 1.5-in. Gage needles.
6. Plastic Pasteur pipet.
7. Egg lysis buffer (ELB): 250 mM sucrose, 2.5 mM MgCl₂, 50 mM KCl, 10 mM HEPES, pH 7.8.
8. Sucrose cushion: 1X ELB with 500 mM sucrose.
9. 10X Marc’s Modified Ringer’s solution (MMR) wash buffer: 1M NaCl, 20 mM KCl, 10 mM MgSO₄, 20 mM CaCl₂, 1 mM ethylenediaminetetraacetic acid (EDTA), 100 mM HEPES, pH 7.8.
10. 2% Cysteine in water, pH 7.8.
11. 1000X Dithiothreitol (DTT): 1 M in water.
12. 1000X Cytochalasin B stock: 5 mg/mL in dimethylsulfoxide.
13. 200X Cycloheximide stock: 10 mg/mL in water.
14. 1000X Aprotinin/leupeptin stock: 10 mg/mL in water.
15. IEC clinical tabletop centrifuge.
16. Sorvall swinging bucket rotor (HB-4 or HB-6): adaptors for 18 × 100-mm tubes (cat. no. 00367; Sorvall, Asheville, NC).
17. Beckman TL100 ultracentrifuge with TLS55 rotor: 11 × 34-mm Ultra-Clear tubes (cat. no. 347356; Beckman, Fullerton, CA).
18. Tricaine methanesulfonate (MS-222; cat. no. E10521; Sigma).
19. 10X buffer X: 100 mM HEPES, pH 7.4, 0.8 M KCl, 150 mM NaCl, 50 mM MgCl₂, 10 mM ethylenediaminetetraacetic acid (EDTA).
20. Large-orifice 200-μL pipet tips (cat. no. 1011-8406; USA Scientific, Ocala, FL).
21. Energy mix stocks: 5 mg/mL creatine phosphokinase (cat. no. C3755; Sigma; in 10 mM HEPES, pH 7.5, 50% glycerol, 50 mM NaCl); 1 M phosphocreatine (cat. no. P7936; Sigma; in 10 mM KH₂PO₄, pH 7.0); 0.2 M adenosine triphosphate (cat. no. A2382; Sigma; in water, pH 7.0); store all frozen at –20°C.
22. Fix: 70 μL 16% paraformaldehyde plus 25 μL 1 M sucrose plus 1 μL 1 mg/mL Hoechst 33258 DNA dye (cat. no. 861405; Sigma).

23. 18 × 18 mm glass cover slips.
24. Zeiss Axioskop 2 microscope: 63× objective, connected to charge-coupled device (CCD) camera, images captured on computer.
25. Human serum albumin (HSA; cat. no. 126658; Calbiochem).
26. Tetramethylrhodamine isothiocyanate Isomer R (TRITC; cat. no. T3163; Sigma).
27. Synthetic nuclear localization sequence (NLS) peptide (CTPPKKKRKV).
28. MBS (*m*-maleimidobenzoyl-*N*-hydroxysuccinimide ester; cat. no. 22310; Pierce, Rockford, IL).
29. Transport substrate buffer: 20 mM HEPES, pH 7.5, 50 mM KCl.
30. Desalting column: a Poly-Prep chromatography column (0.8 × 4 cm; cat. no. 731-1550; Bio-Rad, Hercules, CA) filled with 10 mL P-6 DG desalting gel (cat. no. 150-0738; Bio-Rad) hydrated with phosphate-buffered saline (PBS).
31. Bio-Rad protein assay: dye reagent concentrate (cat. no. 500-0006; Bio-Rad).
32. Protein A-Sepharose beads (cat. no. 17-528001; Amersham, Piscataway, NJ).

3. Methods

3.1. *Xenopus* Egg Extracts

In vitro-assembled nuclei can be reconstituted using cytoplasmic extracts of the eggs of female *X. laevis*, combined with chromatin from the demembrated sperm of male *X. laevis*. The reconstituted nuclei are capable of nuclear import as well as a complete round of DNA replication.

Female frogs are induced to lay unfertilized eggs (**Subheading 3.1.1.**). These eggs are then fractionated to obtain cytosol and membrane fractions (**Subheading 3.1.2.**). The cytosol fraction is a concentrated solution of egg proteins (~40 mg/mL). The high concentration of protein in *Xenopus* egg cytosol greatly facilitates biochemical studies, such as assaying the effect on nuclear assembly and nuclear import (**Subheadings 3.3.** and **3.4.**) and immunodepletions to remove specific proteins of interest (**Subheading 3.5.**). The membrane fraction, when combined with the cytosol fraction, contributes membranes for forming nuclear membranes, endoplasmic reticulum networks, and annulate lamellae (cytoplasmic membrane stacks with nuclear pore complexes; **14–16**).

3.1.1. Priming Frogs and Inducing Egg Laying

To prime frogs for ovulation and to induce egg laying, female frogs are injected with hormones. After the frogs are used for egg laying, they are allowed to rest for approx 3 to 6 mo before being used again (*see* **Note 1**).

1. Prime each female frog with 0.5 mL pregnant mare serum gonadotropin (dilute 1 mL stock with 11.5 mL water to make a working dilution) 2 d to 2 wk before you wish to induce egg laying (*see* **Note 2**). Inject the frogs in the thigh region, underneath the skin, using a 27 × 0.5 in. gauge needle. Place them in a container with distilled water at room temperature.
2. Schedule the chorionic gonadotropin injection to induce egg laying approx 24 h before you wish to collect eggs. Preferably do this injection in the morning so that the eggs can be collected the following morning, and the remainder of the second day will be used for fractionating the egg extracts. Inject 0.5 mL human chorionic gonadotropin per frog in the thigh region underneath the skin using a 27 × 0.5 in. gauge needle. Place each frog in a separate container filled with distilled water containing 30 mM NaCl at room temperature (*see* **Note 3**).

3. After frogs have laid their eggs, transfer the frogs into a large storage bin of water. Keep the frogs in the storage bin overnight to allow them to finish laying eggs before returning them to their long-term housing. Collect laid eggs in 500-mL glass beakers. Do not mix eggs from different frogs.

3.1.2. Fractionation of *Xenopus* Egg Extracts

Two major fractions are isolated from *Xenopus* eggs: (1) the clear cytosol, which contains soluble proteins of the disassembled nuclei and soluble cytoplasmic proteins; and (2) the cloudy membrane fraction, which consists of endoplasmic reticulum, Golgi, and nuclear membranes (12).

1. Prepare these solutions fresh at room temperature before collecting eggs (see Note 4):
 - a. 2% Cysteine, pH 7.8: 100 mL per frog.
 - b. 1/4 X MMR wash buffer (prepared from 10X stock): 300 mL per frog.
 - c. ELB containing 1 mM DTT and 50 µg/mL cyclohexamide: prepare 100 mL per frog.
2. Pour out the excess water from the collected eggs (see Note 5). At this point, the eggs are treated with 2% cysteine, pH 7.8, to remove the gelatinous coat around the eggs. For this, add 100 mL 2% cysteine, pH 7.8, into each beaker of eggs. Gently mix with a plastic Pasteur pipet until the eggs settle to bottom of beaker and the gelatinous coats of the eggs are removed. The eggs will occupy a smaller volume when dejellied. Let the eggs sit in the cysteine solution for a maximum of 5 min. If the gelatinous coats are not removed after 5 min, replace the solution with fresh cysteine solution. Pour out the cysteine solution after the eggs are dejellied. The eggs are very fragile after the gelatinous coat is removed, so use care in pouring solutions out of and into the beaker.
3. Wash the dejellied eggs three times with 1/4 X MMR wash buffer by swirling gently and pouring out the wash buffer.
4. Next, incubate the eggs in ELB with DTT and cycloheximide for 5 min. Cycloheximide inhibits protein synthesis, which includes inhibiting new cyclin synthesis. The eggs and the resulting extract are thus arrested in an interphase state.
5. Pour the eggs into a 14-mL plastic round-bottom tube. Remove as much of the buffer as possible with a plastic Pasteur pipet. This prevents the dilution of the extract. Spin in an IEC clinical tabletop centrifuge at 185 rcf (1350 rpm) for 30 s to pack the eggs (Fig. 1A). Keep the lysed eggs on ice at all times after this spin. Again, remove as much buffer from on top of the lysed eggs as possible. Add aprotinin/leupeptin and cytochalasin B to a final concentration of 1X to the top of the tubes of packed eggs to prevent protein degradation. No mixing is necessary.
6. Next, spin the packed eggs in a swinging bucket rotor (HB-4 or HB-6) at 13200 rcf (9000 rpm) for 20 min at 4°C. The eggs will separate into distinct layers: a top bright yellow layer that contains lipids, a middle golden layer containing cytoplasm and membranes, and a bottom dark layer that consists of pigment and yolk granules (Fig. 1B).
7. Using an 18 × 1.5 in. needle, puncture the tube just above the bottom dark layer (Fig. 1B). Quickly place a preassembled 10-mL syringe with an 18 × 1.5 in. needle into the hole and collect the middle golden layer and a bit of the top lipid layer for a total of approx 9.6 mL. This is termed *crude egg extract* and can be used directly for nuclear assembly as described in refs. 18 and 19. Transfer the crude extract to Ultra-Clear tubes (11 × 34 mm) for the TLS55 rotor (Beckman TL100 ultracentrifuge). Each tube holds a maximum of 2.4 mL. Spin the extract in a TLS55 rotor at 260,000 rcf (55,000 rpm) for 1.5 h at 2°C.

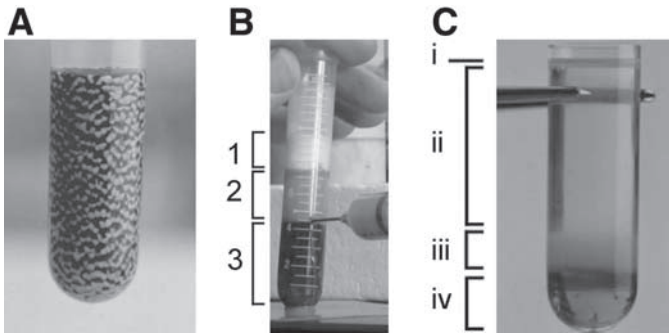


Fig. 1. (A) *Xenopus* eggs are packed. Notice that the vegetal (light) and animal (dark) poles of each egg are aligned in the same direction. (B) The eggs are separated into distinct fractions after centrifugation: the yellow lipid layer at the top (1), followed by the golden crude extract (2), which contains cytosol and membranes, and the black pigments and yolk granules at the bottom (3). A syringe is used to collect the crude extract by puncturing through the tube right above the bottom dark layer. (C) High-speed centrifugation of the golden crude extract results in the separation of the lipids (i, topmost thin yellow layer) from the cytosol (ii, clear layer) and membranes (iii, cloudy yellow layer). The gelatinous pellet with dark and clear layers at the bottom consists of mitochondria and glycogen (iv).

8. After centrifugation, separate cytosol and membrane fractions become apparent, topped with a thin lipid layer (*see Note 6; Fig. 1C*). Loosen the topmost yellow lipid layer with a thin micropipet tip and then aspirate this layer off using a large-orifice pipet tip. Next, remove the layer of clear cytosol with a 200- μ L pipet tip, avoiding the cloudy membrane layer below, by gently swirling while pipeting up. Collect all of the clear cytosol into a tube. Next, pipet the cloudy pale yellow membrane layer with a large-orifice pipet tip into a 15-mL plastic conical tube, avoiding the dark brown layer beneath it, which contains mitochondria. To salt wash the membranes, fill the tube to a total volume of 8 mL with a final concentration of 1X ELB and 0.5 M KCl. Keep the tube of salt-washed membranes on ice while the cytosol goes through another spin in the next step.
9. Spin the cytosol in Ultra-Clear tubes (11 \times 34 mm) at 260,000 rcf (55,000 rpm) for 30 min at 2°C in a TLS55 rotor to remove the majority of residual contaminating membranes (note that some will still remain; *see Discussion in Harel, A. et al., 2003, ref. 9*). Avoid pipeting up the residual membrane pellet at the bottom. Aliquot the cleared cytosol into 100- μ L aliquots and quick-freeze it in liquid nitrogen. Store at -80°C.
10. Next, the salt-washed membranes are isolated through a sucrose cushion. After placing 400 μ L sucrose cushion in each of four Ultra-Clear tubes (11 \times 34 mm), slowly layer 2 mL of the salt-washed membranes on top of the cushion. Spin at 77,000 rcf (30,000 rpm) for 30 min at 2°C in a TL100 ultracentrifuge. Remove most of the supernatant by suctioning, leaving the minimum amount of liquid (~10–20 μ L) at the bottom of the tube to allow membranes to be pipeted up. Any further dilution of the membranes at this stage will affect the nuclear reconstitution reaction because the cytosol is sensitive to dilution. Flick the tube to loosen the membranes. With the tube tilted, pipet up the membranes with a large-orifice pipet tip. Leave behind the dark-color pellet at the bottom of the tube. Aliquot the concentrated membranes (to be used as an ~20X stock) into 10- μ L aliquots and quick-freeze it in liquid nitrogen. Store at -80°C.

3.2. Demembrated Sperm Chromatin

Sperm chromatin from male frogs is used as a source of DNA for nuclear reconstitution reactions (3). Each sperm, when demembrated, releases a “packet” of chromatin containing all the chromosomes. These chromosomes remain associated and are capable of forming a functional nucleus that can import and replicate its DNA when incubated with egg cytosol and membranes.

All procedures should be carried out at room temperature unless stated otherwise.

1. Prepare these solutions a day before preparing the sperm chromatin because the high-concentration sucrose solutions take time to dissolve. Store at 4°C.
 - 100 mL Buffer X plus 0.2 M sucrose
 - 2 mL buffer X–0.2 M sucrose plus 0.4% TX-100 (add aprotinin/leupeptin and DTT fresh)
 - 10 mL buffer X–0.2 M sucrose plus 3% BSA (add aprotinin/leupeptin and DTT fresh)
 - 5 mL buffer X–0.5 M sucrose plus 3% BSA (add aprotinin/leupeptin and DTT fresh)
 - 5 mL buffer X–2.0 M sucrose
 - 10 mL buffer X–2.3 M sucrose
 - 5 mL buffer X–2.5 M sucrose
2. Place four or five male frogs in an ice bath. The frogs are anesthetized in 1 g/L tricaine methanesulfonate dissolved in water, buffered with NaHCO₃ to a final pH of 7.0 to 7.5. Then, cervical dislocation is performed by a sharp blow to the neck, and the brain stem is ruptured by double pithing. Place the frog on its back and cut through the abdomen to expose the organs. Isolate the testes, which are white, oval-shaped structures about 0.5 to 1 cm long. Blot the blood off the testes by rolling on paper towels. Place the testes in a small Petri dish containing buffer X–0.2 M sucrose. Remove as much blood and fat as possible before mincing the testes in fresh buffer X–0.2 M sucrose. Mince the testes into small, 1- to 2-mm pieces by pulling with two pairs of sharp forceps. Transfer the minced testes and buffer into a 15-mL plastic conical tube. Rinse the Petri dish with 2 to 3 mL buffer X–0.2 M sucrose into the same conical tube.
3. The release of sperm from the testes is maximized by mashing the testes with a spatula in the conical tube. In addition, vortex vigorously for 1 min. Pellet the larger pieces of tissue at 100 rcf (1000 rpm) for 10 s in an IEC clinical tabletop centrifuge. Remove the supernatant containing released sperm to a new 15-mL conical tube. Add 2 to 3 mL of buffer X–0.2 M sucrose to the pellet, vortex for 1 min, and recentrifuge as above. Combine the supernatants into the 15-mL conical tube and repeat the extraction of the pellets two or three times until the supernatant is no longer cloudy. Centrifuge the combined supernatants in the 15-mL conical tube at 185 rcf (1350 rpm) for 50 s to pellet any remaining pieces of tissue. Transfer the supernatant, containing released sperm, to a 14-mL plastic, round-bottom tube. Pellet the sperm in a Sorvall swinging bucket rotor at 2600 rcf (4000 rpm) for 10 min at 4°C. Resuspend the sperm pellet very well in 0.8 mL of buffer X–2 M sucrose.
4. To separate the sperm from red blood cells, prepare sucrose step gradients in four Ultra-Clear tubes (11 × 34 mm) for the TLS55 rotor. To each tube add 0.25 mL buffer X–2.5 M sucrose. Slowly and gradually overlay with 1.7 mL buffer X–2.3 M sucrose. Be sure not to disturb the interface between the buffer X–2.5 M sucrose and buffer X–2.3 M sucrose layers. Next, overlay the sucrose gradient in each tube with 0.2 mL of the resuspended sperm. Stir the interface well between the sperm and the buffer X–2.3 M sucrose layer

with a Pasteur pipet tip. Spin in the TL100 ultracentrifuge at 93,000 rcf (33,000 rpm) for 25 min at 2°C.

5. Aspirate off the top half of the gradient containing contaminating red blood cells, which will fractionate at the interface between the 2 M and 2.3 M sucrose layers. Carefully transfer the entire lower half of the gradient containing the sperm to a 14-mL round-bottom tube. Be careful not to take any red blood cells left from the top half of the gradient. Rinse the bottom half of the tube with 1 mL buffer X–0.2 M sucrose three times and combine the washes with the sperm in the 14-mL round-bottom tube.
6. Dilute the sperm solution to a total volume of 12 mL with buffer X–0.2 M sucrose. Pellet the sperm by centrifugation in a Sorvall swinging bucket rotor at 4000 rcf (5000 rpm) for 10 min. The membranes surrounding the sperm and its nucleus are then removed by resuspending the sperm pellet in 1 mL buffer X, 0.2 M sucrose, 0.4% Triton X-100, 1X aprotinin/leupeptin, 1 mM DTT for 30 min on ice, with occasional agitation of the solution.
7. After demembration of the sperm, residual Triton X-100 is removed by a series of spins. Prepare two 1.5-mL tubes containing 0.5 mL Buffer X with 0.5M sucrose, 3% BSA, 1X aprotinin/leupeptin, and 1 mM DTT. Overlay each sucrose cushion with half the demembrated sperm solution. Centrifuge in an IEC clinical tabletop centrifuge at 360 rcf (1900 rpm) for 10 min at room temperature.
8. Remove the supernatant and resuspend the sperm pellet in 0.1 mL buffer X, 0.2 M sucrose, 3% BSA, 1X aprotinin/leupeptin, and 1 mM DTT. Avoid the sides of the tubes, which may have residual Triton X-100. Transfer the sperm chromatin into a new 1.5-mL tube, dilute to 1 mL with the same buffer mix, and centrifuge in an IEC clinical tabletop centrifuge at 360 rcf (1900 rpm) for 10 min at room temperature. Repeat this wash two times.
9. Resuspend the sperm chromatin pellet in 0.5 mL buffer X with 0.2 M sucrose, 3% BSA, 1X aprotinin/leupeptin, and 1 mM DTT. Count the sperm using a hemocytometer. Dilute to 150,000 U sperm chromatin/microliter and 50,000 U sperm chromatin/microliter and freeze 5- μ L to 10- μ L aliquots in liquid nitrogen. Store at –80°C.

3.3. Reconstitution of Nuclei

In vitro nuclear reconstitution reactions using *Xenopus* egg extract and sperm chromatin are generally set up as described next (20). However, with different batches of extracts, the ratio of cytosol to membranes used to form functional nuclei may vary because of differences in preparing the extract and variation between the eggs of different frogs. Each batch of extract should be tested for the optimum ratio of cytosol to membranes to form nuclei. The shape and size of the nuclei, along with the functional test of nuclear import, are indications of how robust the nuclear reconstitution reaction is. The standard is to start with a ratio of 1 μ L of membranes to 20 μ L of cytosol and then to vary the amount of membranes from 0.5 to 2 μ L. The amount of sperm chromatin added can also be varied.

In this in vitro system, exogenous proteins can be added at the start of the reaction up to 10% of the final volume. Further dilution of the reaction, however, may decrease the extract's ability to form nuclei.

1. Quick-thaw a tube of cytosol (100 μ L), a tube of membranes (10 μ L), and a tube of sperm chromatin (~50,000 U sperm chromatin/microliter) at room temperature. Also, thaw components for the energy regeneration system at room temperature. Immediately place all tubes on ice after thawing.

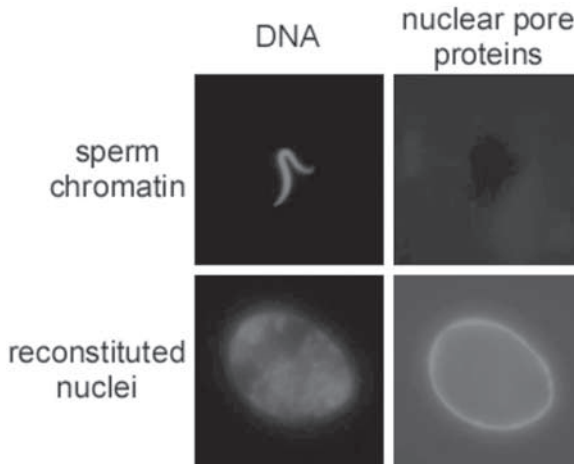


Fig. 2. Immunofluorescence of sperm chromatin and reconstituted nuclei, stained with Hoechst DNA dye and a tetramethylrhodamine -directly labeled monoclonal antibody against nuclear pore proteins (TAMRA-mAb414). mAb414 recognizes four nuclear pore proteins: Nup358, Nup214, Nup153, and Nup62. After incubation with cytosol, membranes, and energy, the sperm chromatin decondenses and acquires a nuclear envelope containing nuclear pores.

2. Prepare a fresh energy mix from the stock solutions using a ratio of 1 μL creatine kinase to 0.5 μL phosphocreatine to 0.5 μL adenosine triphosphate. Keep the energy mix on ice.
3. For each reaction, mix 20 μL cytosol with 1 μL energy mix and 2 μL ELB (or 2 μL exogenous protein) in a 0.5-mL tube. Then add 1 μL membranes. Immediately after adding the membranes, pipet the reaction four or five times to mix the membranes well (*see Note 7*). Avoid introducing air bubbles into the reaction. Sharp tapping of the tube on a hard surface helps remove air bubbles. Keep the reactions on ice until all the components have been added.
4. Last, add 1 μL sperm chromatin ($\sim 50,000$ U sperm chromatin/microliter) using a large-orifice pipet tip. After adding the sperm chromatin, any pipeting of the reaction is to be done with large-orifice pipet tips to prevent the shearing of the chromatin. Pipet up and down slowly, with the pipet set to about half the volume of the reaction. Let the reaction incubate at room temperature for 40 min to 1 h for complete nuclear assembly.
5. If reactions are to be assayed for nuclear import, *see Subheading 3.4*. If nuclei are only to be assessed for assembly and the growth of the nuclei, prepare fix and keep on ice. Aliquots of 2 μL can be removed from the reaction at intervals and mixed with 0.5 μL fix on a slide to assess the progress of assembly. Care should be taken when putting on the 18 \times 18 mm glass cover slip so as not to damage the reconstituted nuclei (*see Note 8*). If samples are to be viewed later, fix the sample at a ratio of 2 μL fix to 8 μL sample (ideal volume for mixing with pipet) on ice. The fixed samples (2.5 μL /cover slip) should be viewed as soon as possible, within 1 to 2 h on ice. The samples cannot be stored at 4°C overnight. View the nuclei on a fluorescence microscope with a 63 \times objective (*see Note 9*; [Fig. 2](#)).

3.4. Assaying Nuclear Import

Reconstituted nuclei are capable of robust nuclear import. This is assayed by the accumulation of nuclear import substrates in the reconstituted nuclei. Nuclear import substrates commonly used are either fluorescently labeled or green fluorescent protein (GFP) fusion proteins containing NLSs (7,8).

3.4.1. Preparing Nuclear Import Substrate

Nuclear import substrates are expressed recombinantly (GFP-nucleoplasmin) or, alternatively, synthesized by crosslinking NLS peptides to fluorescently labeled carrier protein (TRITC-NLS-HSA) (5,6). Both substrates are actively imported into reconstituted nuclei.

GFP fusion import substrates are expressed in bacteria, then purified via the protein's tag, such as a 6-His tag. Alternatively, NLS peptides can be covalently coupled onto carrier proteins that are conjugated to a fluorophore. The NLS peptide-carrier protein conjugate can be labeled with different fluorophores. The method to generate the second type of nuclear import substrate, specifically, NLS-HSA-TRITC, is described next.

1. To conjugate the fluorescent TRITC group to HSA, incubate 0.5 mL HSA (10 mg/mL in 0.1 M Na₂CO₃) with 30 μL of 1 mg/mL TRITC at room temperature for 1 h in the dark. All subsequent reactions should be done in the dark, by covering the reaction with foil, to prevent the quenching of the fluorophore TRITC. Next, add 0.25 mL of 0.1 M sodium phosphate and 250 μL MBS (10 mg/mL in dimethyl formamide) and incubate for 1 h at room temperature with rocking. This will quench the unreacted TRITC in the reaction.
2. Unreacted TRITC and MBS are removed by running the sample through a desalting column. Set up a desalting column with 10 mL P-6 DG desalting gel and equilibrate it with 0.1M sodium phosphate. Load the reaction onto the top of the column and use 0.1M sodium phosphate to run the column. Collect 1 mL for the first fraction, followed by 0.25-mL fractions. Pool the fractions of HSA-TRITC that have the most protein as determined by the Bio-Rad protein assay.
3. Dilute 2.5 mg of the synthesized NLS peptide (CTPPKKKRKV) with 475 μL of 0.1 M sodium phosphate, pH 6.0. Add the NLS peptide solution drop by drop into the pooled fractions of HSA-TRITC in **step 2**. The solution may become turbid as more peptide is added, and precipitate can be seen after adding in the NLS solution. Incubate at room temperature with rocking for 1 h.
4. Uncoupled NLS peptides are then removed from TRITC-NLS-HSA by running the reaction through two desalting columns. Spin the reaction in an IEC clinical tabletop centrifuge at 2800 rpm for 1 min. Split the supernatant in two. Equilibrate two desalting columns (each with 10 mL P-6 DG desalting gel) with transport substrate buffer. Run each half of the supernatant over a separate column. Use 0.1M sodium phosphate to run the columns. Collect 1 mL for the first fraction, followed by 0.25-mL fractions. Pool fractions that have the most protein as determined by the Bio-Rad protein assay. Concentrate the transport substrate to a concentration of 1 mg/mL. Aliquot into 5- to 10-μL aliquots and quick-freeze with liquid nitrogen. Store at -80°C.

3.4.2. Assaying Nuclear Import in Reconstituted Nuclei

1. Reconstitute nuclei as in **Subheading 3.3.**, up to **step 4**. After 40 min to 1 h, functional nuclei are formed.

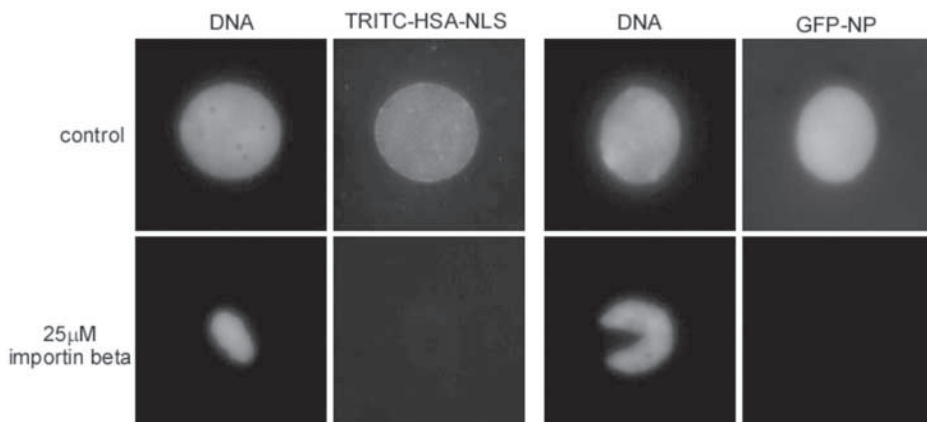


Fig. 3. Nuclear import of fluorescently labeled HSA conjugated to NLS peptide (TRITC-HSA-NLS) as well as GFP-nucleoplasmin (GFP-NP) are seen in control nuclei. The addition of 25 mM importin beta at the beginning of an assembly reaction, however, blocks the assembly of nuclear pores and thus prevents nuclear import (9).

2. Add 1.5 to 2 μg import substrate to 10 μL of the reconstituted nuclei. Classical nuclear import substrates include GFP-nucleoplasmin or TRITC-NLS-HSA. Mix the transport reaction gently two or three times with large-orifice pipet tips. Cover the tubes with foil to prevent the fluorescence of the import substrate from being quenched. Incubate the reaction at room temperature. Substantial import should be seen by 40 min.
3. Prepare fix and keep on ice. After the reaction is completed, fix the sample at a ratio of 2 μL fix to 8 μL sample. Keep the fixed nuclei on ice. View the nuclei with a fluorescence microscope as soon as possible (Fig. 3).

3.5. Assaying Nuclear Import in Nuclei Depleted of Specific Proteins

The function of particular proteins in nuclear assembly, nuclear pore assembly, or nuclear import can be elucidated by the removal of specific proteins from the cytosol by immunodepletion, followed by addition of membranes and sperm chromatin. The immunodepleted nuclei can then be assayed for various functions simultaneously, such as nuclear import, or for the ability to assemble a correct nucleus (11–13).

1. Incubate 300 to 600 μg affinity-purified antibody to a protein of interest (or an equal amount of preimmune antibody) with 60 μL protein A-Sepharose at 4°C overnight. Block the antibody beads with 20 mg/mL BSA in PBS buffer for 30 min at room temperature and wash two or three times with ELB buffer.
2. Immunodeplete or mock deplete 200 μL of cytosol by incubating them with 30 μL of the antibody-protein A-Sepharose two consecutive times, each time for 1 h at 4°C.
3. The immunodepleted and mock-depleted cytosol can be quickly frozen with liquid nitrogen in 20- μL aliquots and stored at -80°C (see Note 10).
4. The immunodepleted or mock-depleted cytosols can then be used to form nuclei as in Subheading 3.3. Nuclear import can be assayed as described in Subheading 3.4.

4. Notes

1. The quality of extract varies with the time of the year. In the summer months, the frogs do not lay eggs as well. It is advisable, if possible, to make egg extracts during cooler months and freeze them for later use.
2. It is ideal for frogs to be primed with pregnant mare serum gonadotropin at least 2 to 3 d before injecting with chorionic gonadotropin to induce egg laying. If frogs are primed more than 2 wk before egg laying, apoptotic extracts will result (17).
3. The temperature of the distilled water plus 30 mM NaCl that is used for housing the frogs after the chorionic gonadotropin injection should not be warmer than room temperature. If the distilled water is warmer than room temperature, place the salt in the water and then cool the water by placing securely tied plastic bags filled with ice into the water. After the water has reached room temperature, remove the plastic bags with ice.
4. On the morning that the frogs have laid their eggs, check the number of frogs that have laid and the approximate volume of eggs each has laid. With these numbers in hand, the amount of each solution (2% cysteine, pH 7.8, 1/4 X MMR wash buffer, ELB containing DTT and cyclohexamide) needed for processing the eggs can more easily and accurately be prepared.
5. Avoid processing batches of eggs for which a majority of eggs that are entirely white (a sign of the eggs having been activated) or have lysed (causing the solution around them to be cloudy) at any stage before the eggs are lysed by centrifugation. In our experience, eggs that have activated before packing have generated extracts that did not assemble nuclei well or were apoptotic.
6. After spinning in the ultracentrifuge, the outside of the 11 × 34 mm Ultra-Clear tubes may fog up. To clearly see the boundary between layers after centrifugation, use a squirt bottle of ethanol to run ethanol on the outside of the 11 × 34 mm Ultra-Clear tubes (not close to the top of the tube) to remove condensation that is clouding the outside of the tube. Use a Kimwipe to remove excess ethanol from the side of the tube. Hold the tube up to a source of light to see the distinct layers in the tube.
7. In reconstituting nuclei, the mixing of the reaction is crucial for achieving homogeneity. After the membranes are added, the reaction needs to be mixed immediately, otherwise the membranes will clump in the reaction. We pipet the reaction around five times until there are no visible clumps of membranes, which are yellow color compared to the clear cytosol.
8. The preparation of the slide affects the appearance of the nuclei. Nuclei are more fragile than cells, thus care needs to be taken in the manner in which the samples are prepared on the slide. After the fixed sample (2.5 μL final volume) is placed on a glass slide, place one edge of the glass cover slip next to the droplet of sample at a 45° angle. Slowly lower the cover slip so the solution is wicked up to encompass the area underneath the cover slip. If a bubble is developing, raise the cover slip slowly, keeping one edge of the cover slip on the slide at all times, and then lower the cover slip again. To avoid drying of the samples under the cover slip, only prepare one slide at a time for viewing (with a maximum of two cover slips per slide).
9. When nuclei are placed between the slide and cover slip, there may be regions on the slide where the nuclei have dried (when an air bubble is present over the nuclei) or, alternately, have been broken by the cover slip. These defects may also occur after long periods of fixing. Such nuclei are not to be included in your data set, especially in assaying for import, as the presence of import substrate in these nuclei is not reflective of the actual amount of import. When stained with a DNA dye, nuclei that have dried look flat or two dimensional; nuclei that have broken appear wrinkled or collapsed.
10. Immunodepleted extracts are to be freeze-thawed once only.

References

1. Newport, J. (1987) Nuclear reconstitution in vitro: stages of assembly around protein-free DNA. *Cell* **48**, 205–217.
2. Blow, J. J. and Laskey, R. A. (1986) Initiation of DNA replication in nuclei and purified DNA by a cell-free extract of *Xenopus* eggs. *Cell* **47**, 577–587.
3. Lohka, M. J. and Masui, Y. (1984) Roles of cytosol and cytoplasmic particles in nuclear envelope assembly and sperm pronuclear formation in cell-free preparations from amphibian eggs. *J. Cell Biol.* **98**, 1222–1230.
4. Lohka, M. J. and Masui, Y. (1983) Formation in vitro of sperm pronuclei and mitotic chromosomes induced by amphibian ooplasmic components. *Science* **220**, 719–721.
5. Newmeyer, D. D. and Forbes, D. J. (1998) Nuclear import can be separated into distinct steps in vitro: nuclear pore binding and translocation. *Cell* **52**, 641–653.
6. Newmeyer, D. D. and Forbes, D. J. (1990) An *N*-ethylmaleimide-sensitive cytosolic factor necessary for nuclear protein import: requirement in signal-mediated binding to the nuclear pore. *J. Cell Biol.* **110**, 547–557.
7. Newmeyer, D. D., Finlay, D. R., and Forbes, D. J. (1986) In vitro transport of a fluorescent nuclear protein and exclusion of non-nuclear proteins. *J. Cell Biol.* **103**, 2091–2102.
8. Finlay, D. R., Newmeyer, D. D., Price, T. M. and Forbes, D. J. (1987) Inhibition of in vitro nuclear transport by a lectin that binds to nuclear pores. *J. Cell Biol.* **104**, 189–200.
9. Harel, A., Chan, R. C., Lachish-Zalait, A., Zimmerman, E., Elbaum, M. and Forbes, D. J. (2003) Importin beta negatively regulates nuclear membrane fusion and nuclear pore complex assembly. *Mol. Biol. Cell* **14**, 4387–4396.
10. Hachet, V., Kocher, T., Wilm, M. and Mattaj, I. W. (2004) Importin alpha associates with membranes and participates in nuclear envelope assembly in vitro. *EMBO J.* **23**, 1526–1535.
11. Harel, A., Orjalo, A. V., Vincent, T., et al. (2003) Removal of a single pore subcomplex results in vertebrate nuclei devoid of nuclear pores. *Mol. Cell* **11**, 853–864.
12. Powers, M. A., Macaulay, C., Masiarz, F. R. and Forbes, D. J. (1995) Reconstituted nuclei depleted of a vertebrate GLFG nuclear pore protein, p97 (Nup98), import but are defective in nuclear growth and replication. *J. Cell Biol.* **128**, 721–736.
13. Walther, T. C., Alves, A., Pickersgill, H., et al. (2003) The conserved Nup107-160 complex is critical for nuclear pore complex assembly. *Cell* **113**, 195–206.
14. Campanella, C., Andreuccetti, P., Taddei, C. and Talevi, R. (1984) The modifications of cortical endoplasmic reticulum during in vitro maturation of *Xenopus laevis* oocytes and its involvement in cortical granule exocytosis. *J. Exp. Zool.* **229**, 283–293.
15. Dabauvalle, M. C., Loos, K., Merkert, H. and Scheer, U. (1991) Spontaneous assembly of pore complex-containing membranes (“annulate lamellae”) in *Xenopus* egg extract in the absence of chromatin. *J. Cell Biol.* **112**, 1073–1082.
16. Meier, E., Miller, B. R. and Forbes, D. J. (1995) Nuclear pore complex assembly studied with a biochemical assay for annulate lamellae formation. *J. Cell Biol.* **129**, 1459–1472.
17. Newmeyer, D. D., Farschon, D. M., and Reed, J. C. (1994) Cell-free apoptosis in *Xenopus* egg extracts: inhibition by Bcl-2 and requirement for an organelle fraction enriched in mitochondria. *Cell* **79**, 353–364.
18. Newport, J. (1987) Nuclear reconstitution in vitro: stages of assembly around protein-free DNA. *Cell* **48**, 205–217.
19. Newmeyer, D. D. and Wilson, K. L. (1991) Egg extracts for nuclear import and nuclear assembly reactions. *Methods Cell Biol.* **36**, 607–634.
20. Macaulay, C. and Forbes, D. J. (1996) Assembly of the nuclear pore: biochemically distinct steps revealed with NEM, GTP gamma S, and BAPTA. *J. Cell Biol.* **132**, 5–20.

Use of Intact *Xenopus* Oocytes in Nucleocytoplasmic Transport Studies

Nelly Panté

Summary

Because of its large nucleus, the *Xenopus laevis* oocyte offers an excellent system to study nucleocytoplasmic transport. This system, in combination with electron microscopy, has provided much of our insight into the mechanisms of nuclear import and export. In a typical experiment, the nuclear transport substrate is first labeled with colloidal gold, and the resulting complex is injected into the cytoplasm (to study nuclear import) or the nucleus (to study nuclear export) of *Xenopus* oocytes. The oocytes are then fixed, dehydrated, infiltrated, and embedded into an epoxy resin. Following resin polymerization, thin sections of oocyte nuclei are obtained and examined under an electron microscope. Subsequent evaluation of the position and distribution of the gold-labeled substrate reveals whether the substrate has undergone nuclear import (or export) and the position of rate-limiting events. This chapter describes in detail the protocols for performing electron microscopy import assays with *Xenopus* oocytes and presents some data illustrating the types of experiments possible using this system.

Key Words: Electron microscopy; microinjection; nuclear import; nuclear pore complex; *Xenopus* oocyte.

1. Introduction

Microinjection of *Xenopus laevis* oocytes has provided an excellent in vivo system to study nucleocytoplasmic transport. They are a popular model because the large size of the oocytes and their nuclei (~0.4 mm) make their manipulation and injection relatively easy. Moreover, detection of transport substrate after the transport assay involves well-established techniques. The use of intact *Xenopus* oocytes to study nucleocytoplasmic transport also has advantages over in vitro systems (e.g., *Xenopus* egg extract reconstitution system [1], digitonin-permeabilized cells [2]) in that all the essential protein factors necessary for transport are present in high amounts in the oocyte. Therefore, one only requires oocytes and the transport probe or substrate.

To study nuclear transport in *Xenopus* oocytes, normally a transport substrate is microinjected into the cytoplasm of the oocyte (for a study of nuclear import) or the nucleus (for a study of nuclear export). After the transport reaction occurs (10–60 min after the injection depending on the site of injection), the transported substrate is detected in the individual compartments (cytoplasm and nucleus). Studies using radioactively labeled substrates require manual isolation of the nucleus and cytoplasm of the injected oocytes. The transported substrate is then detected by sodium dodecyl sulfate-polyacrylamide gel electrophoresis and autoradiography (3–6). However, detection of the transported molecules by electron microscopy (EM) offers more information about the transport process because the structure of the nuclear pore complex (NPC) of *Xenopus* oocyte nuclei is highly preserved. Thus, EM detection allows visualization of the transport of particular ligands through single NPCs at the level of distinct NPC components (see Fig. 1). This chapter describes the methods of studying nucleocytoplasmic transport of microinjected *Xenopus* oocytes using EM.

The EM transport assay in the *Xenopus* oocyte requires the transport substrate to be labeled with electron-opaque particles. Feldherr was the first to use embedding and thin-sectioning EM of amphibian oocytes microinjected with colloidal gold particles (7). His pioneer studies using colloidal gold coated with nucleoplasmin (a nuclear protein from *X. laevis* that contains two nuclear localization signals [NLSs]) were fundamental in demonstrating that proteins enter the nucleus through the NPC (8). Using the same approach, in vivo interactions between the nucleoplasmin-coated gold particles and structural components of the NPC have been depicted (9,10). For example, interactions of the nucleoplasmin-gold particles with filaments that protrude from the NPC were documented by EM visualization of nuclear import in *Xenopus* oocytes (9,10).

Experimental designs using inhibitors of nuclear transport have also been explored to map intermediates arrested at the NPC of *Xenopus* oocytes (10,11; see Fig. 2). For example, the lectin wheat germ agglutinin (WGA) is known to inhibit nuclear import (12,13). When WGA is preinjected in *Xenopus* oocytes to inhibit nuclear import of gold particles coated with nucleoplasmin, the gold-nucleoplasmin particles are arrested at the terminal end of the cytoplasmic filaments of the NPC (10; see Fig. 2A). Similarly, we have arrested NLS-import substrates at the nuclear side of the NPC when oocytes are coinjected with a mutant form of the transport factor importin- β , which does not bind Ran (11; see Fig. 2C). This importin- β mutant failed to deliver the NLS-import substrate into the nucleus, which indicates that the Ran binding site in importin- β is essential for the last step of the nuclear import of cNLS-bearing proteins. Thus, these EM studies revealed the distinct molecular steps of the mechanism of protein import into the nucleus.

Nuclear transport assays using *Xenopus* oocytes have also been very valuable for the study of nuclear import of other substrates, including viral capsids (14,15). In particular, nuclear import of the spliceosomal uridine-rich small nuclear ribonucleoprotein particles (U snRNPs) has been extensively studied in *Xenopus* oocytes (5,16–20). Most of these studies involved detection of radioactively labeled probes. However, EM in combination with colloidal gold has also been used to follow the nuclear import of U1 snRNPs (20).

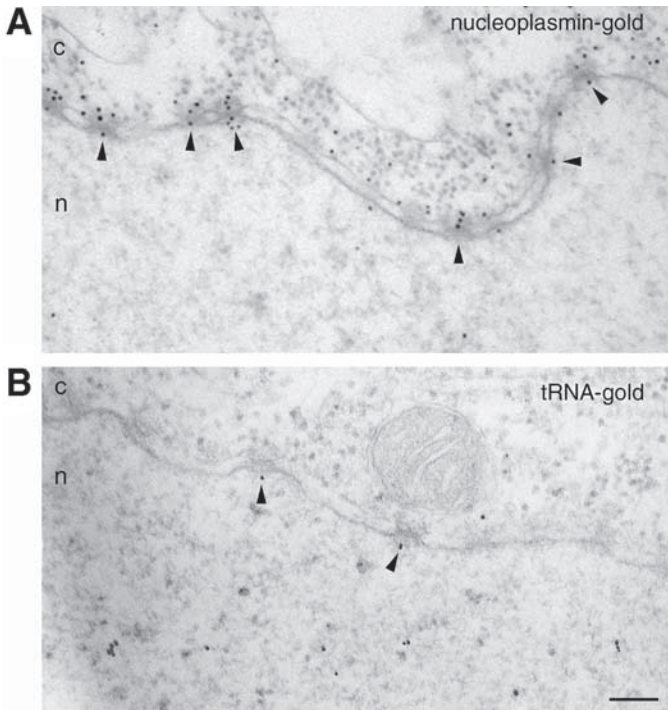


Fig. 1. EM visualization of nucleocytoplasmic transport of gold particles coated with transport substrate in *Xenopus* oocytes. (A) Nuclear import of nucleoplasmin-coated gold particles. The 8-nm diameter gold particles were coated with nucleoplasmin (as indicated in **Subheading 3.1.2.**) and injected into the cytoplasm of *Xenopus* oocytes. After incubation for 1 h at room temperature, the oocytes were processed for embedding and thin-sectioning EM, as indicated in **Subheading 3.3.** (B) Nuclear export of transfer RNA-coated gold particles. The 8-nm diameter gold particles were coated with transfer RNA (as indicated in **Subheading 3.1.3.**), and injected into the nucleus of *Xenopus* oocytes. After incubation for 30 min at room temperature, the oocytes were processed for embedding and thin-sectioning EM, as indicated in **Subheading 3.3.** Shown are views of nuclear envelope cross sections with adjacent cytoplasm (c) and nucleoplasm (n). Arrowheads point to NPCs that are actively transporting the transport substrate-coated gold particles. Scale bar 200 nm.

Xenopus oocytes are the system of choice for the study of nuclear export, and most of our insight into the mechanism of ribonucleic acid (RNA) nuclear export has come from these studies. A summary of these studies, as well as the methods for nuclear export of RNAs, was presented (21). Again, most of these studies were performed with ^{32}P -labeled RNAs. However, although less popular, gold-conjugated RNAs have also been used (22,23).

For EM analysis of the injected oocytes, conventional embedding and thin sectioning is normally used, and the samples are examined by transmission EM. This meth-

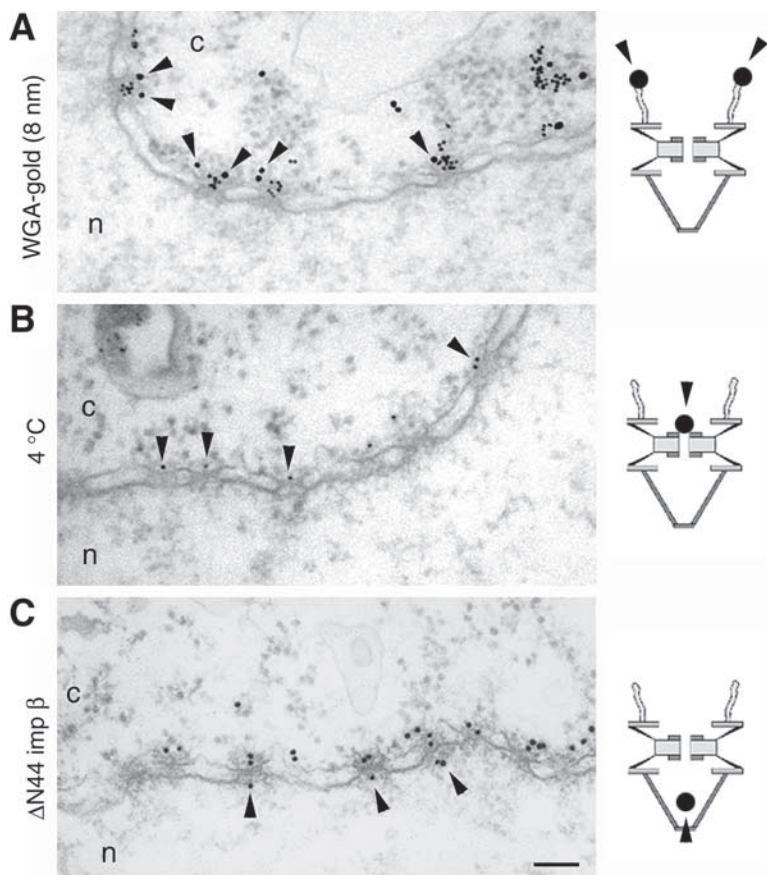


Fig. 2. EM visualization of transport-arrested intermediates at the NPC depicted with three different inhibitors of nuclear import. (A) WGA inhibits translocation of nucleoplasm-coated gold particles through the NPC but not its initial binding to the NPC cytoplasmic filaments. For these experiments, 8-nm gold particles were coated with WGA and preinjected into the cytoplasm of *Xenopus* oocytes. After incubation for 1 h at room temperature, the oocytes were injected with 14-nm gold particles coated with nucleoplasm, incubated for 1 h at room temperature, and processed for embedding and thin-sectioning EM. The 8-nm WGA-gold particles bind to the center of the NPC, and the 14-nm nucleoplasm-gold particles are found at a distance corresponding to the distal end of the cytoplasmic NPC filaments (arrowheads). (B) Inhibition of nuclear import by chilling arrests nucleoplasm-coated gold particles at the cytoplasmic entrance of the NPC central channel. Oocytes were cooled at 4°C for 1 h before injection with 8-nm gold particles coated with nucleoplasm. During injection, oocytes were kept on an ice bath. After injection, the oocytes were incubated for 1 h at 4°C and then processed for embedding and thin-sectioning EM. (C) Gold particles coated with import substrates are arrested at the nuclear side of the NPC, when nuclear import is followed in the presence of

odology reveals side views of the NPCs (*see* **Figs. 1,2**). However, other EM specimen preparations and even visualizations by atomic force microscopy (**24**) or field emission scanning EM (**25**) are possible. The preparation of injected oocytes using unconventional EM techniques, including cryo-EM (**26**), metal shadowing (**27**), and quick freezing/freeze-drying/rotary metal shadowing (**10**), was used in the past to detect nuclear import of gold-labeled nucleoplasm after microinjection into *Xenopus* oocytes. However, these state-of-the-art EM techniques are not accessible to most researchers because they require specialized instrumentation. Therefore, the current chapter focuses on the methods used to analyze the injected oocytes by conventional embedding and thin-sectioning EM. They require equipment commonly present in many EM facilities and laboratories, thereby increasing the usefulness of this research.

2. Materials

1. HAuCl₄ (Sigma).
2. Sodium citrate.
3. Tannic acid.
4. KCO₃.
5. 10% NaCl.
6. Specimen EM grids: 200-mesh/in, copper grids coated with a specimen support film (collodion/carbon or formvar/carbon).
7. Import substrate (e.g., nucleoplasm, bovine serum albumin [BSA] coupled to the peptide CGGGPKKKRKVED [a classical NLS], U1 snRNP).
8. BSA (Sigma).
9. Beckman tabletop ultracentrifuge and rotor TLA 120.2.
10. Th(NO₃)₄.
11. Export substrate (e.g., messenger RNA, transfer RNA, U1 RNA, proteins containing nuclear export signal).
12. Uranyl acetate.
13. *Xenopus laevis*.
14. Tricaine methane sulfonate MS222 (Sigma).
15. Sodium bicarbonate.
16. Modified Barth's saline (MBS) buffer: 88 mM NaCl, 1 mM KCl, 0.82 mM MgSO₄, 0.33 mM Ca(NO₃)₂, 0.41 mM CaCl₂, 10 mM HEPES, pH 7.5.
17. Collagenase (Sigma).

(caption continued from previous page) a mutant form of importin- β lacking the first 44 amino acid residues (Δ N44-imp β). For these experiments, the importin β -binding domain of importin- α (the IBB domain, which is a monovalent substrate) was used as the import substrate. Gold particles 14 nm in diameter were first coated with the IBB domain, and the IBB-coated gold particles were preincubated at 4°C for 1 h with Δ N44-imp β at a 1/1 molar ratio. This mixture was then injected into the cytoplasm of *Xenopus* oocytes. After injection, the oocytes were incubated at room temperature for 2 h and then processed for embedding and thin-sectioning EM. The electron micrographs show cross sections of nuclear envelopes with NPC-arrested intermediates (arrowheads). The c and n indicate the cytoplasm and nucleus, respectively. On the right are schematic diagrams of the NPC indicating the distinct arrested intermediates (arrowheads) visualized by EM. Scale bar, 200 nm.

18. Calcium-free MBS: MBS without $\text{Ca}(\text{NO}_3)_2$ and CaCl_2 .
19. Penicillin/streptomycin (Sigma).
20. Oocyte microinjector.
21. Dissecting microscope.
22. Dissecting forceps.
23. Glutaraldehyde.
24. Low-salt buffer (LSB): 1 mM KCl, 0.5 mM MgCl_2 , 10 mM HEPES, pH 7.5.
25. Low-melting agarose.
26. OsO_4 .
27. Ethanol.
28. Acetone.
29. Epon 812 (Fluka).
30. Ultramicrotome.
31. Lead citrate.
32. Electron microscope.

3. Methods

In general, the methods for the study of nucleocytoplasmic transport in *Xenopus* oocyte by EM include (1) gold conjugation of transport substrates, (2) microinjection of oocytes with gold-conjugated transport substrate, (3) preparation of injected oocytes for EM, and (4) EM visualization and image recording. The details of these procedures are outlined next.

3.1. Gold Conjugation of Transport Substrates

Colloidal gold particles have been utilized for both nuclear import (7–10) and nuclear export (22,23). These particles are very electron dense and easy to visualize on the EM. They can also be used in different sizes to study nuclear transport of different substrates at the same time or to visualize biochemical inhibitors of nuclear transport (i.e., WGA, antibodies; see Fig. 2). Colloidal gold in a variety of sizes is commercially available or can be easily produced using a procedure described in Subheading 3.1.1. After the gold particles are obtained, they are coated with the transport substrate. Outlined next are the methods for coating colloidal gold particles with proteins (Subheading 3.1.2.) and RNAs (Subheading 3.1.3.).

3.1.1. Preparation of Colloidal Gold

Our standard procedure to make gold particles 8 nm in diameter is through reducing tetrachloroauric acid with sodium citrate and tannic acid (28). Described here are the steps to make 100 mL of 8-nm gold particles (see Note 1). For 15-nm gold particles, we used 0.1 mL 1% tannic acid and 0.1 mL 25 mM KCO_3 .

1. Make an 80-mL solution (solution A) of 0.01% HAuCl_4 by diluting 1% stock solution of HAuCl_4 (Sigma).
2. Make the reduction solution (solution B) by mixing the following: 4 mL 1% sodium citrate (freshly made), 0.5 mL 1% tannic acid (freshly made), 0.5 mL 25 mM KCO_3 (freshly made), and 15 mL distilled water
3. Pour solution A into a 250-mL Erlenmeyer flask and heat to 60°C while stirring.

4. When solution A reaches 60°C, immediately add solution B and boil for about 2 min while stirring. The solution will become red when it boils.
5. Cool the solution. Pour the colloidal gold solution into a sterile container (e.g., a tissue culture flask) and store in the dark at room temperature.
6. Check the quality and size of the gold particles by EM. For this purpose, a 5- μ L drop of the colloidal gold solution is placed onto a specimen copper EM grid. After 2 to 5 min, blot the excess liquid by gently touching the grid with filter paper. Let the grid dry. Examine the grid using EM.

3.1.2. Conjugation of Proteins With Colloidal Gold

Colloidal gold particles are negatively charged. Positively charged proteins are adsorbed by noncovalent binding (i.e., ionic and hydrophobic interactions) on the surface of gold particles. During the reaction, protein molecules are added to the surface of the gold particle until its negative charge is stabilized. However, if not enough molecules are available, the gold particles will not be electrically stable and will interact with molecules in the cell on microinjection. It is also very important not to have an excess of proteins because the free proteins inhibit the import of the gold-conjugated protein and cause competition.

Thus, the first step in the preparation of gold-protein conjugates is determining the minimal amount of protein required for the stabilization of gold particles. This is accomplished by mixing small amounts of colloidal gold with varied (decreasing) amounts of protein. The stability of gold particles is monitored by a red-to-blue color change on the addition of an electrolyte (NaCl). This color shift is caused by aggregation (flocculation) of the unstable gold particles. This test is called a *flocculation test*. The following steps compose a flocculation test:

1. Centrifuge the protein suspension at full speed in an Eppendorf centrifuge for 10 min to eliminate aggregates.
2. Spread a sheet of parafilm on a white background (e.g., white tray) and place 5- μ L drops of serially diluted protein suspension (to dilute the protein, use phosphate-buffered saline or a buffer in which the protein is usually kept).
3. Add 25 μ L colloidal gold to each drop of protein suspension. Mix each drop well by repeated pipeting up and down with a 50- μ L pipetor.
4. Add 25 μ L 10% NaCl to each drop and mix well again by pipeting up and down.
5. Visually check the color of the drops. The slightest change of color (from red to blue) indicates the instability of the gold complex.
6. The amount of protein required to stabilize 25 μ L of colloidal gold can be estimated as twice the concentration of the point at which the color change was observed. For example, if the color changed at a protein concentration of 0.05 mg/mL, 5 μ L of protein at 0.1 mg/mL is the right amount to stabilize 25 μ L of colloidal gold. Note, however, that it is not necessary to know the exact concentration of the protein. For example, if the color changed when the dilution of the protein was 1/20, 5 μ L of a 1/10 dilution would be the right amount of protein to stabilize 25 μ L of colloidal gold (see **Note 2**).

To finalize the preparation of the protein-coated gold particles, the amount of protein necessary to mix with 0.5 to 1 mL of gold (0.5 mL is more than enough for a couple of experiments) needs to be scaled. Then, follow this procedure:

1. Add the colloidal gold to an Eppendorf tube.
2. Add the protein to the tube in the ratio determined by the flocculation test.
3. Slowly stir for 5 min.
4. Add BSA to a final concentration of 0.1% and stir for 10 min (*see Note 3*).
5. Centrifuge for 15 min at 32,000 rpm at 4°C in a Beckman tabletop ultracentrifuge (rotor TLA 120.2). After centrifugation, the supernatant will be clear, and the pellet will consist of red sediment on the bottom of the centrifuge tube.
6. Carefully remove the supernatant and resuspend the loose sediment in a small volume (20–100 μL) of a convenient buffer (phosphate-buffered saline or the normal buffer in which the protein is usually kept) containing 0.1% BSA. Store in the dark at 4°C (*see Note 4*).
7. Check the quality of the protein-coated gold particles by negative-staining EM. For this purpose, a 5- μL drop of the gold-protein solution is placed onto a specimen EM grid. After 2 to 5 min of adsorption, blot the excess liquid by gently touching the grid with a filter paper. Wash grids on 4 drops of distilled water by placing the grid on top of the drops. Remove excess water from the grid and add 5 μL 1% uranyl acetate. After 1 min, remove the drop of uranyl acetate and let the grid dry. Examine the grid using EM.

3.1.3. Conjugation of RNA With Colloidal Gold

To conjugate RNA with colloidal gold, first positively charged colloidal gold is prepared using $\text{Th}(\text{NO}_3)_4$. The amount of $\text{Th}(\text{NO}_3)_4$ required to reverse the charge of colloidal gold depends on the size of the gold particles and changes from batch to batch of colloidal gold. Thus, the following test needs to be done to determine the right amount of $\text{Th}(\text{NO}_3)_4$ necessary to reverse the charge of colloidal gold:

1. On a sheet of parafilm spread on a white background, place 5- μL drops of decreasing concentration of $\text{Th}(\text{NO}_3)_4$, starting with a 1 M concentration.
2. Add 50 μL colloidal gold to each drop of $\text{Th}(\text{NO}_3)_4$. Mix each drop well by suctioning up and down with a 50- μL pipetor.
3. Visually check the color of the drops. At higher concentrations of $\text{Th}(\text{NO}_3)_4$, the color of the drop changes from red to blue. At decreasing concentrations of $\text{Th}(\text{NO}_3)_4$, the color of the drop turns lilac and then red, corresponding to positively charged gold particles.
4. Estimate the amount of $\text{Th}(\text{NO}_3)_4$ necessary to reverse the charge of the gold particles by determining the concentration at which the drop changed color to lilac and then to red. Scale up this amount to make 5 to 20 mL of positively charged colloidal gold.

The method of conjugating RNA to positively charged colloidal gold particles is similar to that of conjugating protein described in **Subheading 3.1.2**. First, a flocculation test is performed to determine the amount of RNA required to stabilize the gold particles. This amount is scaled up to make large amounts of RNA-gold conjugates. After conjugation, the quality of the gold-RNA particles is checked by negatively staining as described in **Subheading 3.1.2**.

3.2. Oocyte Preparation and Microinjection

3.2.1. Oocytes

1. Surgically remove oocytes from narcotized female *X. laevis*. (To narcotize a frog, place the frog in a solution of 300 mg/L of Tricaine methane sulfonate MS222 [Sigma] that has been buffered to a pH of 7.5 with about 600 mg/L sodium bicarbonate for 45 min.)

2. Wash oocytes two or three times with MBS to remove traces of blood and debris.
3. Defolliculate oocytes by treating them with 5 mg/mL collagenase (Sigma) in calcium-free MBS for 1 h. For this purpose, place oocytes into a 50-mL Falcon centrifuge tube together with 20 mL of 5 mg/mL collagenase in calcium-free MBS. Gently rock the tube for 1 h at room temperature (*see Note 5*).
4. Wash the oocytes three times with MBS.
5. Resuspend oocytes in MBS containing 1% penicillin/streptomycin with MBS.
6. Transfer oocytes to a sterile Petri dish and keep at 4°C.
7. Microinject the oocytes within the next 5 d.

3.2.2. Microinjection

1. Using a dissecting microscope select oocytes at developmental stage VI. These oocytes are large, with good contrast between the black animal hemisphere and the creamy color vegetal hemisphere (*see Fig. 3*). If the oocytes were at 4°C, let them warm to room temperature before microinjection.
2. Transfer mature stage VI oocytes into a microwell plate (Nalge Nunc, 10- μ L well volume) filled with MBS (*see Fig. 3*). This should be done carefully, using a 50- μ L pipettor with a pipet tip that has been cut at the end to allow undisrupted suction of the oocytes.
3. Place one oocyte into each well and properly orient it for cytoplasmic or nuclear injection (*see Fig. 3*).
4. For cytoplasmic injection, inject 50 nL gold-conjugated import substrate into each oocyte. For consistency between each injection, inject each oocyte in its vegetal hemisphere, very close to the animal hemisphere.
5. For nuclear injection, position the oocyte in each well with the black animal pole (which contains the nucleus) facing upward (*see Fig. 3*). Cover the microwell plate with a lid, place it on a low-speed centrifuge, and centrifuge at 500g for 15 min. After centrifugation, the nucleus will be visible through the animal pole, thus increasing the accuracy of nuclear injection. If the nucleus is not visible, recentrifuge for 10 min (*see Note 6*). Inject 10 nL gold-conjugated export substrate into the nucleus of each oocyte.
6. Transfer injected oocytes into a small (35-mm diameter) Petri dish filled with MBS and incubate at room temperature for 1 h (*see Note 7*).

3.3. Preparation of Injected Oocytes for Embedding and Thin-Sectioning EM

1. After incubation of injected oocytes as indicated above, fix the oocytes overnight at 4°C with 2% glutaraldehyde in MBS.
2. The next day, rinse the oocytes with MBS three times for 5 min each.
3. Place the oocytes into a small Petri dish (35-mm diameter) filled with LSB. Using dissecting forceps and a dissecting microscope, manually dissect the animal pole of the oocytes (*see Note 8* and *Fig. 4*). At this point, the success of the microinjection can be evaluated by the presence of red color in the cytosol (for cytosolic injections) or a red nucleus (for nuclear injection). Follow the protocol only for the oocytes that were injected successfully.
4. Fix the dissected oocytes again with 2% glutaraldehyde in LSB for 1 h at room temperature.
5. Rinse the dissected oocytes three times in LSB for 5 min each and embed them in 2% low-melting agarose. Using a razor blade, cut small pieces of agar containing the dissected oocyte (*see Fig. 4*).
6. Postfix the agar-embedded oocytes with 1% OsO₄ in LSB for 1 h.

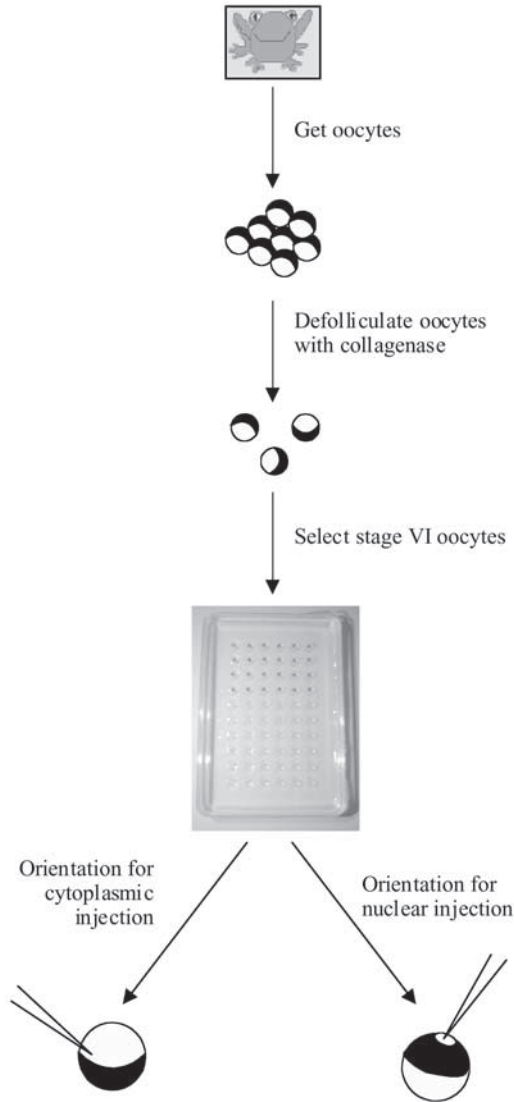


Fig. 3. Steps for preparing *Xenopus* oocytes for microinjection. For detail, see **Subheading 3.2**.

7. Rinse three times in LSB for 5 min each. If necessary, oocytes can be stored overnight at 4°C, and the protocol can be continued the next day.
8. Sequentially dehydrate the agar-embedded oocytes in an ascending series of ethanol and embed in Epon (Fluka) as follows: dehydrate samples in 50, 70, and 90% ethanol for 20 min each. Follow this with two changes in 100% ethanol for 20 min each. Finally, dehydrate with 100% acetone for 20 min. Infiltrate with mixtures of Epon and acetone at a 1:1 ratio for 1 h and at a 2:1 ratio for 2 h and finally in pure Epon for at least 6 h.

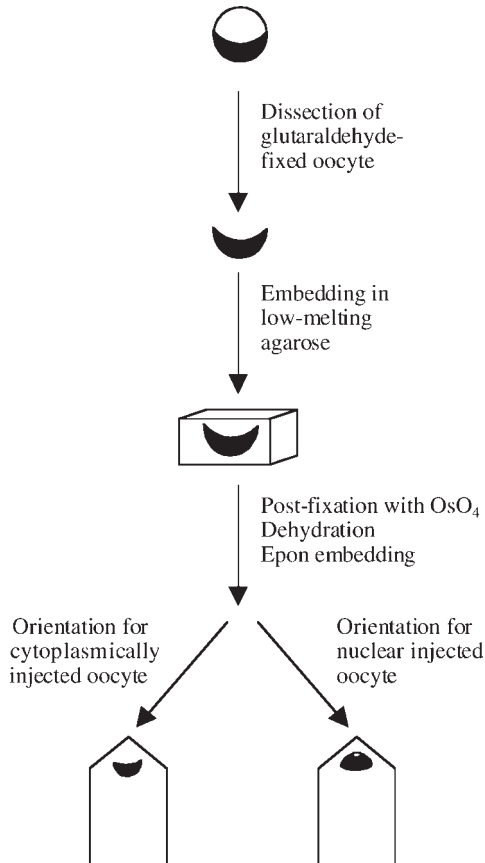


Fig. 4. Steps for preparing injected *Xenopus* oocytes for embedding in Epon. For detail, see **Subheading 3.3**.

9. Place samples on flat molds filled with fresh pure Epon. Orient the oocytes in such a way that the side of the nucleus closer to the injection site is trimmed and sectioned first (see **Fig. 4**). This is done with the help of a dissecting microscope.
10. Polymerize for 2 d at 60°C.
11. Trim the specimen block so that sections can be made through the area of the oocyte that includes the nucleus.
12. With an ultramicrotome, obtain sections that are 50 nm thin. Transfer sections onto specimen EM grids. Stain grids with 2% uranyl acetate for 30 min and wash grids on 4 drops of distilled water. Stain with 2% lead citrate for 5 min. Wash grids again on 4 drops of distilled water and let them dry. Examine grids using the EM.

4. Notes

1. The quality of colloidal gold depends on the cleanliness of the glassware and the freshness of the solution used. Even a minimal amount of contamination on the glassware or in the solutions used can interfere with the formation of the gold particles.

2. Conjugation of proteins with colloidal gold depends on the charge of the protein. It is recommended to perform the reaction at a pH higher than the isoelectrical point of the protein to be conjugated. If this value is not known and the reaction does not work at neutral pH, the pH of both the protein solution and the colloidal gold should be adjusted to 8.0 to 9.0, and the flocculation test should be done again. Alternatively, the flocculation test can be performed at different pH levels.
3. BSA is used as a stabilizer. It adsorbs to bare areas on the surface of the gold particles and prevents the aggregation of the gold complexes.
4. Although the binding of proteins to colloidal gold is irreversible, freezing the gold-protein complexes is not recommended because the protein might dissociate at low temperatures. The gold-protein complexes can be stored for weeks at 4°C. However, it is advised not to use old gold-protein complexes for transport assays.
5. Some batches of oocytes require longer collagenase treatments. It is advised to check whether after 1 h of collagenase treatment a glass needle (the needle used for microinjection) can be easily inserted into the oocyte. If this is not possible or if the oocytes still have follicles, they should be kept in the collagenase solution for an additional 15 to 30 min.
6. Alternatively, instead of centrifugation, the microwell plate containing the oocytes (properly oriented, with the animal pole facing upward) can be left overnight at 4°C. The next day, the nuclei should be visible in the animal pole.
7. Time-course experiments can also be performed by incubating different oocytes for different time lengths (i.e., 15, 30, 60, 120 min, etc.) (10,23). Experiments in which nuclear transport is inhibited through chilling are performed by precooling the oocytes at 4°C for at least 1 h before microinjection. The oocytes are then kept on an ice bath during microinjection, and after injection they are incubated at 4°C for 1 h. Inhibition experiments with WGA or antibodies are performed by first cytoplasmically injecting the inhibitor (10–20). After incubation for 2 h at room temperature, the gold-conjugated transport substrate is injected into the preinjected oocytes.
8. The purpose of this dissection is to eliminate most of the cytoplasm (so that a cross section through the nucleus of the Epon-embedded oocyte can easily be performed after the polymerization of Epon) and to help in the orientation of the sample during embedding (see Fig. 4). This dissection should be done before fixation in OsO₄ because after this fixation the vegetal hemisphere becomes black, and it is indistinguishable from the animal hemisphere.

Acknowledgments

This work was supported by grants from the Canadian Institutes of Health Research (CIHR) and the Natural Sciences and Engineering Research Council of Canada (NSERC).

References

1. Newmeyer, D. D. and Wilson, K. L. (1991) Egg extracts for nuclear import and nuclear assembly reactions. *Methods Cell Biol.* **36**, 607–634.
2. Adam, S. A., Sterne-Marr, R., and Gerace, L. (1990) Nuclear protein import in permeabilized mammalian cells requires soluble cytoplasmic factors. *J. Cell Biol.* **111**, 807–816.
3. Dingwall, C., Sharnick, S. V., and Laskey, R. A. (1982) A polypeptide domain that specifies migration of nucleoplasmin into the nucleus. *Cell* **30**, 449–458.

4. Dabauvalle, M. C. and Franke, W. W. (1982) Karyophilic proteins: polypeptides synthesized in vitro accumulate in the nucleus on microinjection into the cytoplasm of amphibian oocytes. *Proc. Natl. Acad. Sci. USA* **79**, 5302–5306.
5. Michaud, N. and Goldfarb, D. S. (1991) Multiple pathways in nuclear transport: the import of U2 snRNP occurs by a novel kinetic pathway. *J. Cell Biol.* **112**, 215–223.
6. Jarmolowski, A., Boelens, W. C., Izaurralde, E., and Mattaj, I. W. (1994) Nuclear export of different classes of RNA is mediated by specific factors. *J. Cell Biol.* **124**, 627–635.
7. Feldherr, C. M. (1969) A comparative study of nucleocytoplasmic interactions. *J. Cell Biol.* **42**, 841–845.
8. Feldherr, C. M., Kallenbach, E., and Schultz, N. (1984) Movement of a karyophilic protein through the nuclear pores of oocytes. *J. Cell Biol.* **99**, 2216–2222.
9. Richardson, W. D., Mills, A. D., Dilworth, S. M., Laskey, R. A., and Dingwall, C. (1988) Nuclear protein migration involves two steps: rapid binding at the nuclear envelope followed by slower translocation through nuclear pores. *Cell* **52**, 655–664.
10. Panté, N. and Aebi, U. (1996) Sequential binding of import ligands to distinct nucleopore regions during their nuclear import. *Science* **273**, 1729–1732.
11. Görlich, D., Panté, N., Kutay, U., Aebi, U., and Bischoff, F. R. (1996) Identification of different roles for RanGDP and RanGTP in nuclear protein import. *EMBO J.* **15**, 5584–5594.
12. Finlay, D. R., Newmeyer, D. D., Price, T. M., and Forbes, D. J. (1987) Inhibition of in vitro nuclear transport by a lectin that binds to nuclear pores. *J. Cell Biol.* **104**, 189–200.
13. Dabauvalle, M. C., Schulz, B., Scheer, U., and Peters, R. (1988) Inhibition of nuclear accumulation of karyophilic proteins in living cells by microinjection of the lectin wheat germ agglutinin. *Exp. Cell Res.* **174**, 291–296.
14. Panté, N. and Kann, M. (2002) Nuclear pore complex is able to transport macromolecules with diameters of about 39 nm. *Mol. Biol. Cell.* **13**, 425–434.
15. Rabe, B., Vlachou, A., Panté, N., Helenius, A., and Kann, M. (2003) Nuclear import of hepatitis B virus capsids and release of the viral genome. *Proc. Natl. Acad. Sci. USA* **100**, 9849–9854.
16. Fischer, U., Darzynkiewicz, E., Tahara, S. M., Dathan, N. A., Lührmann, R., and Mattaj, I. W. (1991) Diversity in the signals required for nuclear accumulation of U snRNPs and variety in the pathways of nuclear transport. *J. Cell Biol.* **113**, 705–714.
17. Fischer, U., Sumpter, V., Sekine, M., Satoh, T., and Lührmann, R. (1993) Nucleo-cytoplasmic transport of U1 snRNPs: definition of a nuclear location signal in the SM core domain that binds a transport receptor independently of the m₃G-cap. *EMBO J.* **12**, 573–583.
18. Michaud, N. and Goldfarb, D. S. (1992) Microinjected U snRNAs are imported to oocyte nuclei via the nuclear pore complex by three distinguishable targeting pathways. *J. Cell Biol.* **116**, 851–861.
19. Huber, J., Cronshagen, U., Kadokura, M., et al. (1998) Snurportin1, an m3G-cap-specific nuclear import receptor with a novel domain structure. *EMBO J.* **17**, 4114–4126.
20. Rollenhagen, C., Muhlhauser, P., Kutay, U., and Panté, N. (2003) Importin β -depending nuclear import pathways: role of the adapter proteins in the docking and releasing steps. *Mol. Biol. Cell* **14**, 2104–2115.
21. Terns, M. P. and Goldfarb, D. S. (1998) Nuclear transport of RNAs in microinjected *Xenopus* oocytes. *Methods Cell Biol.* **53**, 559–89.
22. Dworetzky, S. I. and Feldherr, C. M. (1988) Translocation of RNA-coated gold particles through the nuclear pores of oocytes. *J. Cell Biol.* **106**, 575–584.

23. Panté, N., Jarmolowski, A., Izaurralde, E., Sauder, U., Baschong, W., and Mattaj, I. W. (1997) Visualizing nuclear export of different classes of RNA by electron microscopy. *RNA* **3**, 498–513.
24. Goldie, K. N., Panté, N., Engel, A., and Aebi, U. (1994) Exploring native nuclear pore complex structure and conformation by scanning force microscopy in physiological buffers. *J. Vac. Sci. Technol. B* **12**, 1482–1485.
25. Allen, T. D., Rutherford, S. A., Bennion, G. R., et al. (1998) Three-dimensional surface structure analysis of the nucleus. *Methods Cell Biol.* **53**, 125–138.
26. Akey, C. W. and Goldfarb, D. S. (1989) Protein import through the nuclear pore complex is a multistep process. *J. Cell Biol.* **109**, 971–982.
27. Stewart, M., Whytock, S., and Mills, A. D. (1990) Association of gold-labelled nucleoplasmin with the centres of ring components of *Xenopus* oocyte nuclear pore complexes. *J. Mol. Biol.* **213**, 575–582.
28. Slot, J. W. and Geuze, H. J. (1985) A new method of preparing gold probes for multiple-labeling cytochemistry. *Eur. J. Cell Biol.* **38**, 87–93.

Studying the Mechanosensitivity of Voltage-Gated Channels Using Oocyte Patches

Catherine E. Morris, Peter F. Juranka,
Wei Lin, Terence J. Morris, and Ulrike Laitko

Summary

The mechanosensitivity of voltage-gated (VG) channels is of biophysical, physiological, and pathophysiological interest. *Xenopus* oocytes offer a critical advantage for investigating the electrophysiology of recombinant VG channels subjected to membrane stretch, namely, the ability to monitor macroscopic current from membrane patches. High-density channel expression in oocytes makes for macroscopic current in conventional-size, mechanically sturdy patches. With the patch configuration, precisely the same membrane that is voltage-clamped is the membrane subjected to on-off stretch stimuli. With patches, meaningful stretch dose responses are possible. Experimental design should facilitate within-patch comparisons wherever possible. The mechanoresponses of some VG channels depend critically on patch history. Methods for minimizing and coping with interference from endogenous voltage-dependent and stretch-activated endogenous channels are described.

Key Words: Activated; current; gadolinium; mechanosensitive; patch clamp; stretch; tension; voltage dependent.

1. Introduction

Mechanosensitive (MS) channels, that is, channels sensitive to membrane stretch, are found in most channel families, including the voltage-gated (VG) channel superfamily. The MS responses of VG channels are biophysically significant and putatively are of physiological and pathophysiological interest. When membrane stretch alters membranes, a new equilibrium distribution of channel conformations may result. The process of relaxation to that new equilibrium can loosely be termed MS gating of the VG channel. If stretch exerts an irreversible effect on gating, it is more appropriate to speak of the VG channel as mechanosusceptible.

Both reversible and irreversible mechanoresponses of VG channels have been studied in *Xenopus* oocyte patches, a preparation often used for recombinant VG channels.

From: *Methods in Molecular Biology*, vol. 322: *Xenopus Protocols: Cell Biology and Signal Transduction*
Edited by: X. J. Liu © Humana Press Inc., Totowa, NJ

Stretch of the oocyte patch has been examined in connection with the cell's endogenous cation-permeant stretch channels (**1**). It is assumed that the reader is familiar with patch clamp recording and its application to VG channels.

2. Materials

1. Molecular biology facility for expressing recombinant VG channels in oocytes and for modifying channel constructs as required.
2. Standard patch clamp laboratory with rig suitable for recording from oocyte patches.
3. Optional: two-microelectrode voltage clamp suitable for oocytes.
4. ALA Scientific Instruments high-speed pressure clamp on patch clamp rig (other less-sophisticated options are listed).

3. Criteria for Choosing *Xenopus* Oocytes vs Mammalian Cells to Study Mechanosensitivity of Recombinant Voltage-Gated Channels

Biophysical studies of recombinant VG channel mechanosensitivity are mostly performed with oocytes (**2–6**) rather than mammalian cells. It is important to uniformly stretch precisely the same membrane area that is generating current. The high-density channel expression of oocytes allows for macroscopic VG channel currents from cell-attached and excised patches; pipet suction can uniformly and reversibly stretch the channel-bearing membrane. For macroscopic current in mammalian cells (**7–9**), in contrast, mechanical stimuli take the form of whole-cell inflation or shear flow. Adherent and nonadherent membrane will both be clamped yet will experience different mechanical stimuli. Inflation, moreover, is extremely difficult to control and to reverse; shear, although physiologically interesting, is hard to standardize.

For single-channel recordings of VG channels before, during, and after stretch, oocytes are suitable for VG potassium and sodium but not for VG calcium channels; the reason is that the endogenous stretch channel can be selectively blocked (*see Sub-heading 3.*) for study of potassium- and sodium- but not calcium-selective unitary current. Mammalian cells have sporadic endogenous stretch conductances (e.g., *see ref. 10*), but they pass no current with the high-divalent pipet solutions used for unitary VG calcium channel current (**7**).

4. Expressing Voltage-Gated Channels at Appropriate Densities for Stretch Studies

Macroscopic patch current in the 0.1- to 1-nA range provides good signal-to-noise ratio without worries of saturating the current amplifier during capacitive transients. Use of one of the many available expression vectors specialized to produce *Xenopus* oocyte-friendly complementary ribonucleic acid (cRNA) helps achieve current density in this range.

When obtaining a channel construct from another lab, check if it expresses in oocytes. Not all do; bacterial VG channels are a particularly disappointing case in point.

Every construct is different, but an optimum level of VG channel expression is sought by controlling the amount of cRNA injected plus the duration and temperature of incubation. This is hardly an exact science. Some VG channel will be spontaneously active once expressed, and this may stress the oocyte. To increase the number of

days an oocyte batch can be used, we sometimes transfer some or all of a batch of injected oocytes (plus some uninjected controls) from our usual incubation temperature (18°C) to 4°C after approx 24 h.

Certain VG channels express poorly in oocytes even though closely related channels express well. The skeletal muscle VG sodium channel, for example, is unproblematic in oocytes, whereas seemingly similar central nervous system VG sodium channels only sporadically express well. Oocytes from different individual frogs are not all equally effective as expression machines. When a capricious expresser construct cannot be avoided, inject some oocytes in each batch with an “easy” channel construct to serve as a positive control. This is useful, for example, for different sodium channels isoforms (e.g., NaV1.4 plus the more difficult NaV1.6) as well as for mutant vs wild-type constructs of a given channel isoform (e.g., Shaker).

Some channels are reputed to express at higher density in the pigmented animal pole half of the *Xenopus* oocyte (where we usually patch) than in the unpigmented vegetal pole. Although we have not noticed differences, it is advisable to patch consistently at one pole or the other. Cortical structures differ in the two areas, and for cell-attached patches, this might have mechanical consequences.

Access to a two-microelectrode clamp (in addition to the patch clamp) is desirable for checking expression levels of new or difficult-to-express constructs (as well as for testing drug effects on the VG channels).

5. Microscopy During Patch Recording

A standard rig for patch clamping oocytes can be used. This involves a dissecting microscope and fiber-optic illumination. Typically, the micropipet approaches the oocyte surface at an acute angle. Cell-attached patches will be essentially invisible given the low-power objectives of the dissecting scope.

An inverted microscope-based patch clamp rig fitted with a low-power objective (4×), a digital camera, and a video monitor is also suitable. The pipet approach to the oocyte is more horizontal than with the dissecting scope rig.

High-resolution images of patch curvature before, during, and after stretch are not feasible for the small cell-attached patches we generally use (i.e., conventional-size tips, ~1- to 2- μm , diameter prior to heavy fire polishing). Long-shank, thin-wall pipets would be needed for imaging of small patches. These pipets have large capacitances, and because of their parallel inner walls, the gigaseal tends to move tens of microns up the tip. Macropatches appropriate for imaging have a disadvantage in that they are mechanically fragile. Moreover, their large VG currents may swamp the linear subtraction capacity of the amplifier.

The oocyte membrane is microvillar, but as Zhang and Hamill (*I*) showed by measuring the area and capacitance of large patches (**Fig. 1C**), making a gigaohm seal smoothes the membrane. Flat patches like that shown are expected if the pipet has little taper. “Omega-shaped” patches that stabilize near the pipet tip, such as the excised oocyte patch shown in **Fig. 1A**, can be expected for small-diameter, heavily fire-polished, thick-wall pipets. More stable gigaohm seals result, but imaging of patches in brightfield (**Fig. 1A**) is almost impossible. Fluorescence can be used to

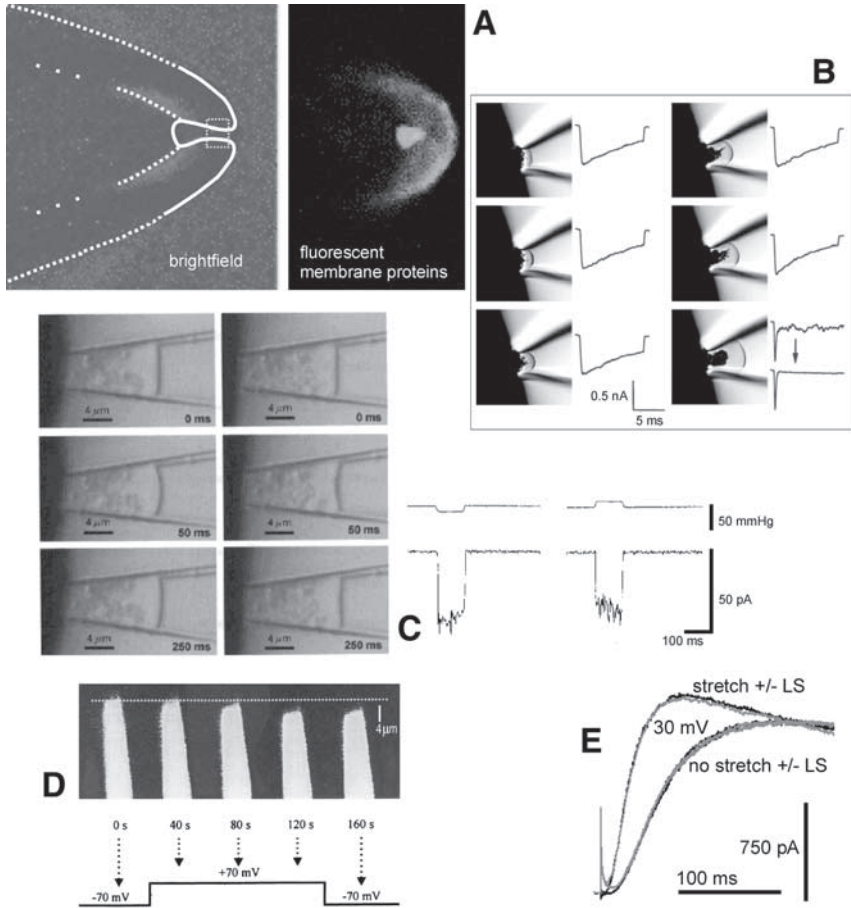


Fig. 1. (A) Simultaneous brightfield/fluorescence images of an excised oocyte patch. The solid white overlay in brightfield is our interpretation of the location of the fluorescent excised patch; the dotted white line is the pipet (our interpretation) in brightfield. In the boxed area, the pipet orifice presumably veered out of the confocal plane. Membrane was stained with a cysteine-specific rhodamine reagent. Modified from ref. 45. (B) A very large oocyte patch and traces showing VG sodium currents. See text for explanation. Adapted from ref. 3. (C) A very large oocyte patch and traces showing macroscopic current from the endogenous SACat. Adapted from ref. 1. (D) Fluorescent images over time during voltage clamp of a large oocyte patch. The pipet solution has a fluorescent label and so demarcates the position of the cell-attached patch, which is seen to undergo progressive displacement during the depolarizing step whose time course is depicted. Adapted from ref. 13. (E) Outward potassium currents from a Shaker channel mutant. Adapted from ref. 6. Currents (at 30 mV) are shown with and without stretch, as well as with and without linear subtraction (LS); a P/4 procedure was used. The inherently slow gating kinetics of this mutant ensure that even if LS had not been used, there would be little difficulty extracting kinetic information. This is not true in the case of activation for the wild type, for which activation occurs within several milliseconds, when the capacitive transient would still be settling.

locate either small or large patches by staining the oocyte membrane (**Fig. 1A**) or adding dye to the pipet solution (**Fig. 1D**). To image patch location via pipet solution fluorescence, use pipets with a shank that is bent in a microforge to allow a horizontal approach to the oocyte.

6. Micromanipulator Adjustments and Oocyte Flattening

We use water-hydraulic or motorized micromanipulators (Narishige and Burlington, respectively). Remotely controlled low-drift micromanipulators are critical for cell-attached patch recording. Excised patches are indifferent to drift but considerably more fragile. We use them only when no-cytoplasm conditions are called for in the experimental design.

Devitellinated oocytes are used for patching. A mechanical consequence of removing the vitelline support is the slow flattening of the oocyte under gravity. (To devitellinate, shrink oocyte in hyperosmotic K-aspartate in the recording chamber, pull away the vitelline with forceps, wash with recording bath saline, and place chamber in the rig with the preferred oocyte pole oriented for pipet approach.)

If possible, use an already-flattened oocyte for several patches, exchanging bath solution as needed to avoid evaporation and recording information on patches per oocyte. If waiting for flattening is impractical, monitor the pipette/oocyte contact as recording proceeds, using the micromanipulator fine control to keep the tip at a fixed position with respect to the oocyte surface. Pushing a sealed pipet tip into or pulling it away from cytoplasm could alter resting patch tension, so avoid large adjustments. If they are unavoidable, record them as an aspect of “patch history.”

7. Patch History

Patches have “history” because plasma membrane is not just bilayer, but an ill-defined structure of bilayer plus adherent membrane skeleton and any residual extracellular matrix adhering to membrane lipids and proteins. In addition to producing a far-field tension in the plane of the membrane, stretch will irreversibly alter patch microstructure. For some aspects of VG channel behavior, these changes will matter; for some, they will not. In terms of patch history, spontaneously formed cell-attached patches and excised patches represent opposite extremes of mechanical gentleness. See **refs. 2** and **4** for references and discussion. The mechanical status of membrane skeleton in cell-attached patches changes with repeated or prolonged stretch (**1,10**), so keep notes on ease of seal formation and other aspects of patch history. We generally assume that excised patch structure is essentially a bilayer without long-range load-bearing membrane skeleton. Vesicle shedding may occur at high stretch.

Illustrated in **Fig. 1B** is one example of oocyte patch history for an exceptionally large (10- μm inner tip diameter) cell-attached patch. The time series shows the patch-stretch-induced release of membrane-attached strands (presumably mixed cytoskeleton and endoplasmic reticulum). Release *coincides* with an irreversible gating-mode transition for the recombinant VG sodium channels. Note that the membrane is not puckered, so force normal to the membrane presumably was having relatively little impact compared to tension in the plane of the bilayer. Strand release, therefore, is

likely an epiphenomenon: a secondary event occurring as the overtensed actin-spectrin mesh, which is coplanar with the bilayer, suddenly disassembles (*see* **ref. 11** regarding this phenomenon in amoebae). To reiterate, we think the critical patch historical event seen here occurred in the plane of the bilayer, not normal to the bilayer.

A point of technical interest is seen in the bottom right of **Fig. 1B**. Suction was present in the first but not the second trace, and endogenous stretch current (*see* **Subheading 14.**) is evident during the first trace only. This current provides a useful internal metric for the application of an adequate stretch stimulus. A “positive control” for stretch intensity can be valuable in a case like that illustrated here for which stretch irreversibly changes the VG sodium current.

8. Recording Pipets

Patch stretch is controlled by micropipet pressure. For very small patches, pressures exceeding -100 mmHg may be needed. Micropipet holder gaskets must therefore tighten securely so the applied pressure does not bleed and so pipets do not move during pressure steps. To avoid cut-glass damage to the gaskets during pipet insertion, lightly firepolish the pipet blanks before pulling.

Thick-walled glass and heavily fire-polished pipet tips maximize the membrane-pipet tip contact area during seal formation. We use borosilicate (Garner N51A 1.65-mm outside diameter, 1.15-mm inside diameter, Garner Glass, Claremont, CA). We do not use soda glass as it yields higher capacitance pipets and may affect the kinetics of VG channels (*see* **ref. 12**). However, for reasons discussed in **Subheading 15. (13)**, it is strongly recommended to coat borosilicate with vaporized soda glass (simply melt soda glass onto the filament used for fire polishing). There is no single pipet parameter prescription for studying VG channel mechanosensitivity, but parameters should be monitored and not varied without reason. We used different tip sizes for macroscopic and unitary Shaker currents (**4**). As expected, larger suction stimuli were required for MS Shaker gating with smaller pipet tips, and rupture suctions also varied accordingly. Because pipet tip size, and therefore patch size (and hence tension for a given pressure), varies, asserting that channels are insensitive to stretch requires testing the entire pressure range up to rupture. As mentioned, endogenous stretch current can serve as a bioassay or positive control for membrane tension in the range expected to affect channel function. Usually, however, it is desirable to block that current.

9. Bath and Pipet Solutions

So that oocyte $V_m = 0$ mV (and hence so that $V_{\text{transpatch}}$ will be known during cell-attached patch recording), an isotonic high potassium (usually K-aspartate- or K-glucuronate-based) bath solution is used. Bear in mind, however, that prolonged exposure to the high-potassium bath may affect the cytoplasm (signaling molecules, cytoskeletal arrangements, etc.), so it could be useful to check if a stretch-induced VG channel behavior is different with physiological bath solution.

If excised patches are used, note that the choice of major anion in the bath solution can matter. Chaotropic anions like Cl^- promote loss of squid axon membrane skeleton

as determined by scanning electron microscopy (14). Excising a patch into chloride-based saline should therefore disassemble the membrane skeleton. If reversible stretch effects on gating are the same in cell-attached patches and patches excised into a high-chloride saline, the mechanoresponses likely depend exclusively on bilayer mechanics (see ref. 4) rather than membrane skeleton, auxiliary proteins, or other modulators.

The major pipet solution constituents are chosen in accordance with the permeation and gating characteristics of the VG channel and with the gating parameters under investigation (e.g., activation rate, tail current magnitude). Recall that VG channel kinetics will shift in the depolarizing direction on the voltage axis if multivalent cation concentrations are increased.

The pipet and bath solutions must not precipitate pharmacological agents; this is discussed below with respect to lanthanide blockers of the endogenous stretch channel. Pipet and bath solutions are in direct contact prior to seal formation (a few millimeters of mercury of positive pressure is maintained in the pipet until the pipet contacts the oocyte membrane); precipitates forming at the tip will prevent gigaohm seal formation.

10. Mechanostimulator

For sustained patch stretch, suction can be applied to the pipette's suction port by a simple syringe with manual valves and a pressure gage (e.g., ref. 2). An electronic pressure gage is preferable, but U-tube manometers (configured correctly, i.e., one arm open to atmosphere) can be used.

A slow (hundreds of milliseconds rise time) pressure stepper can be contrived by modifying a pair of pressure transducer testers (4,15).

A commercial stepper is now available at a reasonable price (ALA Scientific Instruments' version of the Sachs lab high-speed pressure clamp) (16). This computer-driven pressure servo allows for precise timing of stretch stimuli (steps, families of steps, or ramps as desired) during voltage clamp protocols run under *pClamp* (Axon Instruments) or a comparable program. We initially configured the pressure clamp using house vacuum and a compressed air tank. This works, but the dynamic response improved using the motorized pump/compressor supplied by ALA. Use thick-wall tubing, keep lines short and avoid rigid coupling to the micropipet holder. The dynamic response of this device depends on pressure; each 10 mmHg increment adds 1 to 2 ms to the rise time. Larger membrane patches experience larger tensions for smaller pressures (a Laplace's law effect), so given this limitation, it would be advisable to use patches as large as possible to examine how channel kinetics respond to pressure jumps.

11. Stretch/Voltage Clamp Protocols

Membrane tension (T_m ; given in mN/m or dyn/cm), unlike V_m , is not under absolute control between patches. Between-patch size variation is inevitable; hence, a given pressure will produce different tensions in accordance with Laplace's law (for spherical membrane, $T_m = \text{Pressure} \times \text{Radius of curvature}/2$). Normalizing patches for channel density is not enough because the issue is which tension is associated with the applied pressure. Design the protocols, whenever possible, therefore, around within-patch comparisons (e.g., kinetic parameter before vs during stretch) and do signifi-

cance testing via paired *t*-tests on these within-patch comparisons. An unpaired comparison for a parameter (e.g., current amplitude before and during stretch) measured from a population of patches would likely show no significant effect of stretch even when the same data set analyzed as paired comparisons yielded a highly significant effect.

Membrane stretch is a somewhat casual term that refers to any force that generates a T_m . T_m is a more precise concept for artificial bilayers than for plasma membranes, for which membrane skeleton shares in load bearing (17–19). In designing stretch/clamp protocols for oocyte membrane stretch, therefore, use a variety of protocols that include acutely applied and prolonged stretch and keep track of patch history.

For voltage step protocols, time is required for automated linear subtraction for each step (see Fig. 1E); during stretch, this will contribute to patch history.

In designing stretch protocols for VG channels, it is too simple to assume only that channel conformations that displace more bilayer volume will be favored by stretch (17). The widespread and diverse nature of channel mechanosensitivity surely reflects diverse stretch-sensitive channel/bilayer and channel/protein interactions. The interactions could be short or long range (e.g., for short range, channel/boundary lipid or channel/G protein; for long range, channel/far-field tension or channel/spectrin-skeleton). The bilayer-embedded part of a channel embedded feels large lateral forces described variously in the language of line tensions (20) or lateral pressure profiles (21,22). How these forces alter with stretch is unclear. In a bilayer under stretch, the mean area per head group increases, hydrocarbon tails become more disordered, surface charge density decreases, water penetration deepens, and certain lipids may leaflet-flip or diffuse away; thinning at the channel/lipid boundary may produce hydrophobic mismatch.

Stretch/clamp protocols depend on the nature of gating in each VG channel, but there are two broad approaches involving, not surprisingly, sustained voltage and sustained tension. In both approaches, the aim is to maximize the use of within-patch comparisons.

1. Sustained voltage: Obtain a steady-state current baseline at $V_{\text{transpatch}} = X$, then apply negative (usually) pipet pressure to stretch the membrane. The pressure application can be a series of steps (for a dose–response), a ramp of pressure, or, for time course data, an intermittently repeated step or ramp. Return to zero pressure as frequently as possible to test for reversibility and repeatability.
2. Sustained tension: Without applied pressure, obtain currents using voltage steps (individual steps, pulse trains, or a family) or do a voltage ramp, then apply a sustained level of pressure, then repeat voltage stimulus, release pressure, and repeat the voltage commands.

When VG channels show progressive and irreversible stretch-induced changes, time-course data are needed during sustained or repeated stretch stimuli and possibly under various conditions (e.g., without and with cytoskeleton-disrupting reagents). Design the voltage protocol to generate information on several gating parameters in the same experiment to determine if the membrane stretch has pervasive effects on the channel or acts selectively on particular aspects of gating.

12. Dose–Responses and Between-Patch Comparisons

Within a patch, a pipet pressure series (or pressure ramp) corresponds to a membrane tension series (or tension ramp), yielding a semiquantitative dose–response that can be “calibrated” at zero and rupture tension (the latter corresponding to ~ 10 mN/m, i.e., the lytic tension typical of cellular bilayers; *see* **ref. 23**). Tension dose–responses reported for Shaker mutants (**5**) illustrate this point: Stretch-induced left shift (in mV) of the ramp current was determined between zero and rupture tension for a series of channel constructs. Gearing this experiment (a series of within-patch measurements) to the two tensions (zero and rupture) that are knowable between patches was particularly helpful. It allowed for an among-patches mean value (for the stretch-induced hyperpolarizing shift at rupture tension) that, critically, was then compared statistically (unpaired test) between channel constructs.

13. Single-Channel Measurements of Voltage-Gated Channel Mechanosensitivity in Oocytes

Endogenous stretch-activated (SA) cation channels need to be blocked for single-channel studies of VG channels and stretch. Because the nonspecific blockers of the endogenous stretch channel also block VG calcium channels, oocyte patches offer no benefits over mammalian cell patches for these channels (e.g., **ref. 7**). For VG potassium and sodium channels, however, oocytes can be used because lanthanide effects on these channels are tolerable (e.g., **ref. 4**).

Single-channel recording has inherent problems of statistical sampling error. These problems may be exacerbated in stretched patches, which seldom last long enough to provide enough unitary events for complex kinetic analyses of at least two or more stretch intensities and at several voltages. We limit single-channel studies to experiments that pose questions for which unitary event information is explicitly required (e.g., whether stretch alters mean open time, the channel’s unitary conductance, or the distribution of its subconductance states).

14. Dealing With Endogenous Currents

Oocytes express no endogenous VG sodium and potassium channels, but L-type calcium current has been reported (**24**), and other unidentified hyperpolarization-activated conductances can occur (*see* **Table 1**). A channel of particular concern is the weakly voltage-sensitive MS channel or SACat (stretch-activated cation nonselective), which occurs at approx 1 channel/ μm^2 (**1,25**). Conductances other than SACat should interfere only at extreme hyperpolarization and possibly when divalent cations are very low or absent. A general caution is to avoid VG channel constructs, which have interesting behavior that occurs at extremely hyperpolarized voltages.

14.1. Endogenous SACats

1. For macroscopic VG channel current, SACat current density is low enough to be ignored in some, but not all, cases.
2. SACats reverse at approx 0 mV in most solutions. For sodium and potassium channels that activate at 0 mV, a narrow selection of protocols is available for SACat-free data even in the absence of SACat blockers.

Table 1
Endogenous Voltage-Dependent Conductances in *Xenopus* Oocytes

Description	References	Comments
Stretch-activated cation selective channel (SACat)	25,27,34,38	~30 pS, open time increases with depolarization; exhibits adaptation that is hyperpolarization induced and patch history dependent; can be spontaneously active; blocked by diverse multivalent cations; interference between voltage and stretch effects has been reported (13)
Depolarization-induced P _{Na}	39	Activation midpoint ~ 0 mV; persistent in cell-attached patches; in excised without MgATP, it runs down (but Mg ²⁺ alone blocks it); time dependence is voltage dependent (fastest at deeply hyperpolarized levels); noise analysis suggests a unitary conductance <1 pS if the P _{Na} is channel based
Depolarization-activated Ca-induced g _{Na}	40	Induction depends on calcium from intracellular stores
Hyperpolarization- and acid-activated divalent cation conductance	41	Induced by heterologous expression of certain membrane proteins; this conductance stimulates the endogenous Ca-activated g _{Cl} ; activates at extreme hyperpolarizations; blocked by lanthanide/calcium combinations
Hyperpolarization-dependent nonselective (cation/anion) nonlinear conductance	42,43	Induced by expression of single-spanning membrane proteins, extremely slow kinetics (activation τ ; <1 s at -100 mV); inhibited by extracellular divalent cations in millimolar range; permeable to inulin (MW ~5000) but not dextran-70 (MW ~70,000); similar conductances activated by extreme hyperpolarization (≥ 150 mV) of uninjected oocytes
Voltage-dependent anion-selective porin	44	Presence inferred indirectly from detection of porin by immunofluorescence
L-type VG calcium	24	Up to several hundred nanoamperes from whole oocytes when recording in 20 mM barium

3. SACats can be blocked by lanthanides and various cationic organic compounds, including amiloride, streptomycin, and gentamicin (26). GdCl_3 almost completely blocks the oocyte SACats at $10 \mu\text{M}$ (27). The active form of gadolinium is not known. The common assumption is that it is Gd^{+3} , but Gd^{+2} also exists in solution, as do various hydroxide complexes. See comments in **Subheading 14.2.** below on gadolinium carbonate and **refs. 28** and **29**. Lanthanides, antibiotics, and amiloride are all nonspecific inhibitors with effects on VG channels, but for VG sodium and potassium, the crossreactions are tolerable. Blocker effects on the VG channel under study (e.g., activation curve right shifts, diminished maximal conductance) need to be characterized. For these tests, two-micro-electrode voltage clamp of the oocyte is appropriate as it facilitates wash on/wash off of the blocking reagent (4) for gadolinium effects on Shaker in oocytes; the bath solution should be identical to the pipet solution of patch/stretch experiments, and the full voltage range should be tested.
4. Lanthanides adsorb strongly to phospholipids in bilayers (30,31). To determine if effects of stretch on VG channels are confounded by lanthanide effects on the bilayer, controls without lanthanides are needed.
5. The Sachs lab has identified a tarantula peptide toxin, GsMTx-4, that inhibits some SA cation channels (32). The affinity is not high, but importantly, in spite of the toxin's similarity to voltage sensor toxins, it is thought not to interfere with VG channel activity (33). GsMTx-4 has just become commercially available (PCB-4393-S, Peptides International, Pepnet.com) and needs to be tested on oocyte SACats.

14.2. Gadolinium Carbonate: A Problem

Gadolinium and lanthanum ions readily precipitate with divalent or polyvalent anions. Consequently, to produce the desired level of free lanthanide, pipet and bath solutions must be kept free of carbonate, phosphate, sulfate (e.g., gentamicin sulfate), and similar anions. Residual carbonate in pipet solutions probably underlies the large disparities (reported and unreported) in gadolinium's effectiveness as an SACat channel blocker (e.g., **refs. 4,28,34**, although *see* **ref. 29**). By *residual*, we mean carbonate originating from CO_2 in the air both before and after solutions are made. Water film on hygroscopic crystals will contain CO_2 and hence carbonic acid, bicarbonate, and carbonate. Exposure of the highly hygroscopic crystals of $\text{GdCl}_3 \cdot 6\text{H}_2\text{O}$ to atmospheric CO_2 may therefore result in gadolinium carbonate precipitates admixed with the GdCl_3 . On first opening a bottle of $\text{GdCl}_3 \cdot 6\text{H}_2\text{O}$, therefore, make an acidified concentrated stock solution (say 100 mM GdCl_3 in 0.1 N HCl) and store it under N_2 , under vacuum, or in frozen aliquots.

Even with this precaution, a major source of residual carbonate is likely the recording pipet solution. When open to the atmosphere, HEPES-rich pipet solutions, buffered as they are to a slightly alkaline pH, will continually take up CO_2 . Although this CO_2 converts only slowly to bicarbonate and carbonate, the solubility of $\text{Gd}_2(\text{CO}_3)_3$ is vanishingly small, so the equilibrium favors precipitation of Gd^{3+} ; hence, the concentration of free $[\text{Gd}^{3+}]$ will progressively fall. Therefore, keep pipet solutions degassed; vacuum conditions will drive off dissolved CO_2 . Just prior to recording, dilute acidified GdCl_3 from the stock solution into degassed pipet solution. Discard gadolinium-containing pipet solutions within a few hours.

15. Assorted Considerations

Applying stretch to a cell-attached patch might alter series resistance and thus the transpatch voltage during a given command voltage. If a stretch-induced change in gating is seen with both negative and positive pressure stimuli or for both cell-attached and excised patches, a series resistance effect is ruled out.

For a fast VG current, passive capacitive transients may overlap with activation, and subtle differences in the effectiveness of linear subtraction with and without stretch might be suspected. Determine if the stretch effect persists when gating is sufficiently slow not to overlap appreciably with the capacitive transient (e.g., at smaller depolarizations, in slower-gating mutants, at reduced temperatures).

Silberberg and colleagues ([13,35](#)) found that with Corning 7740 borosilicate (or equivalent) pipets, sustained depolarization displaced the membrane patch and elevated membrane tension. Displacements did not occur with a soft lead phosphate glass (Corning 8161) or for borosilicate tips coated with soft glass. SACat activity is the primary assay for elevated tension, but displacement can be detected visually (*see* [Fig. 1D](#)). The nature of the lipid–glass interaction is unclear. Displacement was observed with and without divalent cations and using organic and inorganic anions.

We generally block SACat activity, but even without gadolinium, we have not observed SACat channels becoming hyperactive during depolarizing steps. On the other hand, we may have had soda glass melted on the fire-polishing filament (although not always, until recently). Although the phenomenon has not been reported by others for oocytes or replicated in other preparations (e.g., [36,37](#)), in protocols calling for prolonged depolarization rather than brief steps, it should be watched for as a possible source of error. Unless there is a specific reason not to vaporize soda glass during fire polishing, do so and report it explicitly. We emphasize this because we had trouble recently with seal stability during stretch application and realized that the newly replaced fire-polishing filament had not been soda glass coated. Adding the soda glass dramatically improved seal stability, even though it seems difficult to believe one coats very far into the pipet during the few seconds of fire polishing.

16. Conclusion

Oocyte patches are useful for studying stretch effects on recombinant VG sodium and potassium channels. They would be unsuitable for studying the mechanosensitivity of L-type VG calcium channels. Difficulties exist in connection with endogenous currents and with patch history. Both reversible and irreversible effects of stretch on VG channels can be studied. Dose-response data (i.e., tension dose) that are impossible to acquire for VG channels expressed in cell lines can be routinely obtained for macroscopic currents in oocyte patches because of the ease of reversibly and repeatedly stretching a patch of voltage-clamped membrane using precisely controlled pipet suction.

Note Added in Proof

The endogenous stretch-activated cation channel of *Xenopus* oocytes has now been shown to be based on TRPC1 subunits (46).

References

1. Zhang, Y., and Hamill, O. P. (2000) On the discrepancy between whole-cell and membrane patch mechanosensitivity in *Xenopus* oocytes. *J. Physiol.* **523**, 101–115.
2. Tabarean, I. V., Juranka, P., and Morris, C. E. (1999) Membrane stretch affects gating modes of a skeletal muscle sodium channel. *Biophys. J.* **77**, 758–774.
3. Shcherbatko, A., Ono, F., Mandel, G., and Brehm, P. (1999) Voltage-dependent sodium channel function is regulated through membrane mechanics. *Biophys. J.* **77**, 1945–1959.
4. Gu, C. X., Juranka, P. F., and Morris, C. E. (2001) Stretch-activation and stretch-inactivation of Shaker-IR, a voltage-gated K⁺ channel. *Biophys. J.* **80**, 2678–2693.
5. Tabarean, I. V. and Morris, C. E. (2002) Membrane stretch accelerates activation and slow inactivation in Shaker channels with S3-S4 linker deletions. *Biophys. J.* **82**, 2982–2994.
6. Laitko, U. and Morris, C. E. (2004) Membrane tension accelerates rate-limiting voltage-dependent activation and slow inactivation steps in a Shaker channel. *J. Gen. Physiol.* **123**:135–154.
7. Calabrese, B., Tabarean, I. V., Juranka, P., and Morris, C. E. (2002) Mechanosensitivity of N-type calcium channel currents. *Biophys. J.* **83**, 2560–2574.
8. Lyford, G. L., Strege, P. R., Shepard, A., et al. (2002) $\alpha(1C)$ (Ca(V)1.2) L-type calcium channel mediates mechanosensitive calcium regulation. *Am. J. Physiol. Cell Physiol.* **283**, C1001–C1008.
9. Ou, Y., Strege, P., Miller, S. M., et al. (2003) Syntrophin $\gamma 2$ regulates SCN5A gating by a PDZ domain-mediated interaction. *J. Biol. Chem.* **278**, 1915–1923.
10. Wan, X., Juranka, P., and Morris, C. E. (1999) Activation of mechanosensitive currents in traumatized membrane. *Am. J. Physiol.* **276**, C318–C327.
11. Keller, H., Rentsch, P., and Hagmann, J. (2002) Differences in cortical actin structure and dynamics document that different types of blebs are formed by distinct mechanisms. *Exp. Cell Res.* **277**, 61–72.
12. Cota, G. and Armstrong, C. M. (1988) Potassium channel “inactivation” induced by soft-glass patch pipettes. *Biophys. J.* **53**, 107–109.
13. Gil, Z., Silberberg, S. D., and Magleby, K. L. (1999) Voltage-induced membrane displacement in patch pipettes activates mechanosensitive channels. *Proc. Natl. Acad. Sci. USA* **96**, 14,594–14,599.
14. Terakawa, S. and Nakayama, T. (1985) Are axoplasmic microtubules necessary for membrane excitation? *J. Membr. Biol.* **85**, 65–77.
15. Small, D. and Morris, C. E. (1994) Delayed activation of single mechanosensitive channels in *Lymnaea* neurons. *Am. J. Physiol.* **267**, C598–C606.
16. Besch, S. R., Suchyna, T., and Sachs, F. (2002) High-speed pressure clamp. *Pflugers Arch.* **445**, 161–166.
17. Sachs, F. and Morris, C. E. (1998) Mechanosensitive ion channels in nonspecialized cells. *Rev. Physiol. Biochem. Pharmacol.* **132**, 1–77.
18. Morris, C. E. and Homann, U. (2001) Cell surface area regulation and membrane tension. *J. Membr. Biol.* **179**, 79.
19. Manno, S., Takakuwa, Y., and Mohandas, N. (2002) Identification of a functional role for lipid asymmetry in biological membranes: phosphatidylserine-skeletal protein interactions modulate membrane stability. *Proc. Natl. Acad. Sci. USA* **99**, 1943–1948.

20. Dan, N. and Safran, S. A. (1998) Effect of lipid characteristics on the structure of transmembrane proteins. *Biophys. J.* **75**, 1410–1414.
21. Cantor, R. S. (1999) Lipid composition and the lateral pressure profile in bilayers. *Biophys. J.* **76**, 2625–2639.
22. Gullingsrud, J. and Schulten, K. (2003) Gating of MscL studied by steered molecular dynamics. *Biophys. J.* **85**, 2087–2099.
23. Morris, C. E. (2001) Mechanosensitive ion channels in eukaryotic cells, in *Cell Physiology Source Book*, 3rd ed. (Sperelakis, N., ed.), Academic Press, New York, pp. 745–760.
24. Chahine, M., Bibikova, A., and Sculptoreanu, A. (1996) Okadaic acid enhances prepulse facilitation of cardiac α 1-subunit but not endogenous calcium channel currents in *Xenopus laevis* oocytes. *Can. J. Physiol. Pharmacol.* **74**, 1149–1156.
25. Methfessel, C., Witzemann, V., Takahashi, T., Mishina, M., Numa, S., and Sakmann, B. (1986) Patch clamp measurements on *Xenopus laevis* oocytes: currents through endogenous channels and implanted acetylcholine receptor and sodium channels. *Pflugers Arch.* **407**, 577–588.
26. Hamill, O. P. and McBride, D. W., Jr. (1996) The pharmacology of mechanogated membrane ion channels. *Pharmacol. Rev.* **48**, 231–252.
27. Yang, X. C. and Sachs, F. (1989) Block of stretch-activated ion channels in *Xenopus* oocytes by gadolinium and calcium ions. *Science* **243**, 1068–1071.
28. Caldwell, R. A., Clemo, H. F., and Baumgarten, C. M. (1998) Using gadolinium to identify stretch-activated channels: technical considerations. *Am. J. Physiol.* **275**, C619–C621.
29. Yeung, E. W., Head, S. I., and Allen, D. G. (2003) Gadolinium reduces short-term stretch-induced muscle damage in isolated mdx mouse muscle fibres. *J. Physiol.* **552**, 449–458.
30. Ermakov, Y. A., Averbakh, A. Z., Yusipovich, A. I., and Sukharev, S. (2001) Dipole potentials indicate restructuring of the membrane interface induced by gadolinium and beryllium ions. *Biophys. J.* **80**, 1851–1862.
31. Tanaka, T., Tamba, Y., Masum, S. M., Yamashita, Y., and Yamazaki, M. (2002) La(3+) and Gd(3+) induce shape change of giant unilamellar vesicles of phosphatidylcholine. *Biochim. Biophys. Acta* **1564**, 173–182.
32. Suchyna, T., Besch, S. R., and Sachs, F. (2004) Dynamic regulation of mechanosensitive channels; capacitance used to monitor patch tension in real time. *Phys. Biol.* **1**, in press.
33. Bode, F., Sachs, F., and Franz, M. R. (2001) Tarantula peptide inhibits atrial fibrillation. *Nature* **409**, 35–36.
34. Reifarh, F. W., Clauss, W., and Weber, W. M. (1999) Stretch-independent activation of the mechanosensitive cation channel in oocytes of *Xenopus laevis*. *Biochim. Biophys. Acta* **1417**, 63–76.
35. Silberberg, S. D. and Magleby, K. L. (1997) Voltage-induced slow activation and deactivation of mechanosensitive channels in *Xenopus* oocytes. *J. Physiol.* **505**, 551–569.
36. Franco-Obregon, A. and Lansman, J. B. (2002) Changes in mechanosensitive channel gating following mechanical stimulation in skeletal muscle myotubes from the mdx mouse. *J. Physiol.* **539**, 391–407.
37. Suchyna, T. M., Johnson, J. H., Hamer, K., et al. (2000) Identification of a peptide toxin from *Grammostola spatulata* spider venom that blocks cation-selective stretch-activated channels. *J. Gen. Physiol.* **115**, 583–598.
38. Hamill, O. P. and McBride, D. W., Jr. (1992) Rapid adaptation of single mechanosensitive channels in *Xenopus* oocytes. *Proc. Natl. Acad. Sci. USA* **89**, 7462–7466.
39. Rettinger, J. (1999) Novel properties of the depolarization-induced endogenous sodium conductance in the *Xenopus laevis* oocyte. *Pflugers Arch.* **437**, 917–924.

40. Charpentier, G. and Kado, R. T. (1999) Induction of Na⁺ channel voltage sensitivity in *Xenopus* oocytes depends on Ca²⁺ mobilization. *J. Cell Physiol.* **178**, 258–266.
41. Kuruma, A., Hirayama, Y., and Hartzell, H. C. (2000) A hyperpolarization- and acid-activated nonselective cation current in *Xenopus* oocytes. *Am. J. Physiol. Cell Physiol.* **279**, C1401–C1413.
42. Tzounopoulos, T., Maylie, J., and Adelman, J. P. (1995) Induction of endogenous channels by high levels of heterologous membrane proteins in *Xenopus* oocytes. *Biophys. J.* **69**, 904–908.
43. Sha, Q., Lansbery, K. L., Distefano, D., Mercer, R. W., and Nichols, C. G. (2001) Heterologous expression of the Na(+),K(+)-ATPase γ subunit in *Xenopus* oocytes induces an endogenous, voltage-gated large diameter pore. *J. Physiol.* **535**, 407–417.
44. Steinacker, P., Awni, L. A., Becker, S., et al. (2000) The plasma membrane of *Xenopus laevis* oocytes contains voltage-dependent anion-selective porin channels. *Int. J. Biochem. Cell Biol.* **32**, 225–234.
45. Zheng, J. and Zagotta, W. N. (2003) Patch-clamp fluorometry recording of conformational rearrangements of ion channels. *Sci. STKE.* **176**, PL7.
46. Maroto, R., Raso, A., Wood, T. G., Kurosky, A., Martinac, B., and Hamill, O. P. (2005), TRPC1 forms the stretch-activated cation channel in vertebrate cells. *Nat. Cell Biol.* **7**, 179–185.

Oocytes as an Expression System for Studying Receptor/Channel Targets of Drugs and Pesticides

Steven David Buckingham, Luanda Pym, and David Barry Sattelle

Summary

The *Xenopus laevis* oocyte offers one of the most convenient expression systems for assaying the actions of candidate ligands on cloned ionotropic neurotransmitter receptors (also known as ligand-gated ion channels [LGICs]). Their large size makes injection of complementary ribonucleic acid or complementary deoxyribonucleic acid and electrophysiological recording very easy. Furthermore, *Xenopus* oocytes translate messages very efficiently, resulting in the detection of large-amplitude ligand-induced currents from expressed, recombinant LGICs. Compared to other electrophysiological techniques, recording from oocytes is not difficult and requires only a basic electrophysiological recording setup. Oocytes can be used for two-electrode voltage clamp, as well as cell-attached patch and inside- or outside-out patch clamp recordings. A variety of protocols allows the experimenter to determine the actions of ligands on cloned receptors and parameters, such as their affinity, efficacy, rates of association and desensitization, and reversibility, to be estimated. Here, we present protocols for using *Xenopus* oocytes in assaying candidate ligands acting against cloned targets of drugs and pesticides.

Key Words: Drug assay; expression system; oocyte; two-electrode voltage clamp; *Xenopus laevis*.

1. Introduction

The *Xenopus laevis* oocyte is arguably the simplest receptor/channel expression system in use. Oocytes are very convenient for both the introduction of genetic material and the application of voltage clamp electrophysiology for investigating novel ligands and drugs. There are numerous examples of studies of potential drugs or pest control agents acting on cloned ionotropic receptors (**Table 1**).

In addition, using cell-attached or inside-out patch clamp allows estimation of single-channel properties such as unitary conductance, opening probability, and mean open and closed times (**1**). The large volume (~1-mm diameter) and consequent large

Table 1
Examples of *Xenopus* Oocytes as an Expression Vehicle
in Defining the Actions of Drugs and Pest Control Agents
Against a Wide Variety of Cloned Receptor/Channel Targets

Drug pest control agent	Reference
Avermectin/ivermectin	<i>3,4</i>
Fipronil	<i>5,6</i>
Propofol	<i>7-9</i>
Benzodiazepines	<i>10,11</i>
Levamisole	<i>12</i>
Nereistoxin	<i>13</i>
Neonicotinoids	<i>14,15</i>
Analgesics	<i>11,16,17</i>

membrane area can present problems when a very rapid voltage clamp is needed, such as in the measurement of some voltage-gated currents. However, this does not usually present difficulty when studying drugs acting on ligand-gated ion channels (LGICs) or other receptor-activated channels because the onset of the response is much slower than the membrane time constant.

Compared to other electrophysiological approaches, little training is required, and the availability of electronic amplifiers specifically designed for oocyte work makes the task even easier. Here, we present a variety of protocols for using oocytes to assay drugs on functional LGICs. These protocols can also be readily adapted to assay drug actions on expressed voltage-gated ion channels.

Medium-throughput assays using large numbers of oocytes have been made possible through a number of automated or semiautomated systems. For example, OpusXpress™ is a parallel voltage clamp system offered by Axon Instruments (Union City, CA) that automates the simultaneous recording of up to 8 oocytes and controls the applications of drugs from 96-well plates. The Roboocyte™ system (Multi Channel Systems, MCS GmbH, Germany) automates messenger RNA (mRNA) or complementary DNA (cDNA) injection, incubation, and two-electrode voltage clamp (TEVC) analysis using 96-well plates. Driven by a special graphical user software package, the Roboocyte is capable of unsupervised assays and is provided with an 8- or 16-channel perfusion system. Details of these devices are available on the company Web sites (<http://www.roboocyte.com/products/roboocyte/robointro.htm>, <http://www.multichannel.com/>, <http://www.axon.com>).

2. Materials

1. The basic recording solution (standard oocyte saline [SOS]) is given in **Table 2**. This can be made up as a 10X stock for storage for up to 1 wk (**Table 3**). Some laboratories use Barth's medium, the composition of which is given in **Table 4**. Both media have been used successfully by many laboratories. The incubation medium is a supplemented SOS (**Table 5**) to which penicillin, streptomycin, and gentamicin are added to counteract bacterial growth, and sodium pyruvate is added to provide a source of metabolic energy.

Table 2
Composition of Standard Oocyte Saline (SOS)

SOS composition	Per liter	mM	MW
NaCl	5.844 g	100	58.44
KCl	149.1 mg	2	74.55
CaCl ₂	264.6 mg	1.8	147
MgCl ₂	203.3 mg	1	203.3
HEPES	1.1915 g	5	238.3

Adjust to pH 7.6 with NaOH.

Table 3
Composition of 10X SOS

10X SOS composition	mM	MW	1 L
NaCl	1000	58.44	58.44 g
KCl	20	74.55	1.491 g
CaCl ₂	18	147	2.646 g
MgCl ₂	10	203.3	2.033 g
HEPES	50	238.3	11.915 g

Adjust pH 7.6 with 10 M NaOH. Can be stored up to 1 wk in a refrigerator.

Table 4
Composition of Barth's Medium: An Alternative to SOS

Composition	mM	MW	1 L
NaCl	88	58.44	5.143 g
KCl	1	74.55	74.5 mg
NaHCO ₃	2.4	84.01	0.202 g
MgSO ₄	0.82	120.37	98.7 mg
Tris-HCl	7.5	157.60	11.82 g

Adjust to pH 7.4.

Table 5
Composition of Incubation Medium

Composition	Additions to SOS for incubation medium		
	mM	MW or stock	Per 500 mL
Sodium pyruvate	2.5	110	138 mg
Penicillin	100 U/mL	10 000 U/mL	5 mL
Streptomycin	100 µg/mL	10 mg/mL	5 mL
Gentamicin	50 µg/mL	10 mg/mL	1 mL

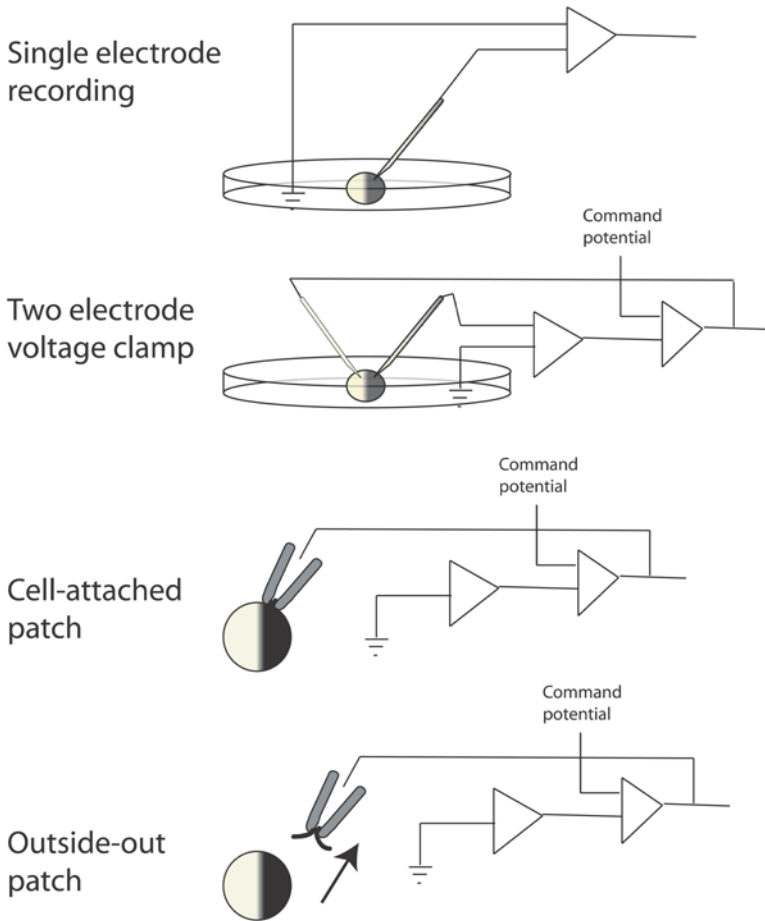


Fig. 1. Electrophysiological recordings can be made from oocytes using a number of recording configurations. The simplest (A) is to record membrane potential using a single intracellular electrode. This is of limited usefulness, however, as the membrane potential varies from oocyte to oocyte and is often quite low. (B) A two-electrode voltage clamp is not much more difficult and allows easy control of the oocyte membrane potential. Three patch configurations are feasible: cell attached (C), inside out (not shown) and outside out (D). For each of these configurations, the vitelline membrane has to be removed. Whole-cell patch clamp is made impractical owing to the large capacitance associated with these cells.

2. Voltage clamp amplifier: recordings can be made from oocytes in a number of configurations (Fig. 1). In principle, any voltage clamp amplifier can be used for TEVC of oocytes, providing it is capable of delivering the large currents required to charge the membrane capacitance rapidly. A number of models specifically designed for oocyte TEVC are available. Examples of two widely used devices are the Warner OC series and the Axon Geneclamp. The latter is particularly easy to use because many functions (such as testing

the electrode resistance and controlling feedback gain) are taken care of by the circuitry of the amplifier. For patch clamp, no special demands are placed on the clamp amplifier beyond those of any patch clamp experiment (the whole-cell configuration is the exception, but this is not feasible for oocytes anyway), so any patch clamp amplifier can be used. The Axon Geneclamp amplifiers are capable of doing TEVC, patch, or both simultaneously. There are many very effective alternatives, so the experimenter has an excellent choice of options.

3. Analog-to-digital (A/D) converter: data are most conveniently acquired, stored, and analyzed using a personal computer. A computer is also convenient for controlling the execution of experiments. The output of voltage clamp amplifiers, however, is an analog signal in which the amplitude of the parameter read from the amplifier (such as the clamp current in voltage clamp experiments) is encoded by a direct current voltage. This must therefore be converted into a digital signal to be of use to the computer. The output of the amplifier is therefore passed to the input port of an analog to digital converter. The A/D converter is connected to the computer through the supplied on-board card or through conventional computer interface ports. Similarly, for the computer to control the amplifier, the digital output from the alternating current converter must be connected to the "command input" or similar port on the amplifier. The experimenter must choose the acquisition parameters suitable for the experiment being performed, but a discussion of signal digitization is beyond the scope of this book. An accessible account can be found in **ref. 2**.
4. The recording chamber: an illustration of a recording setup suitable for TEVC of oocytes is provided in **Fig. 2A**.

Accurate assay of agonist actions requires rapid drug delivery, thereby minimizing errors caused by receptor desensitization. Therefore, the chamber must be as small as possible and the flow of physiological saline as rapid as possible. The dimensions of a suitable chamber are provided in **Fig. 2B**. A Perspex chamber with about a 0.5-mL volume with Sylgard lining the base is widely used. A basket of four to six entomological pins inserted into the Sylgard base arranged vertically around the oocyte retains it securely.

The speed of solution exchange can be gauged subjectively by testing the chamber with a dye. A more accurate and objective measure is to clamp an oocyte and challenge it with SOS with the potassium concentration increased 10-fold (adjusting the concentration of sodium ions to preserve osmotic balance). The time-course of the change in holding current will exactly match the exchange at the oocyte membrane. For patch, use a normal patch clamp rig with phase-contrast microscope optics.

Perfusion is most simply applied using a gravity-fed system. Particular problems can arise when application and wash need to be rapid because the large volume of the oocytes places restrictions on how rapidly drugs can be applied. For many expression experiments, the onset of the responses is slower than the solution exchange rate, but this is not always the case. Responses mediated by $\alpha 7$ -nicotinic acetylcholine receptors, for instance, desensitize very quickly, and this can lead to errors in the construction of dose-response curves unless the drug is applied very rapidly. This can be accomplished by increasing the flow rate (but not so that the flow moves the oocyte) and decreasing the chamber volume. In addition, allowing an air bubble to enter the perfusion line immediately before the test drug prevents mixing within the perfusion line and can help speed the application of the test drug.

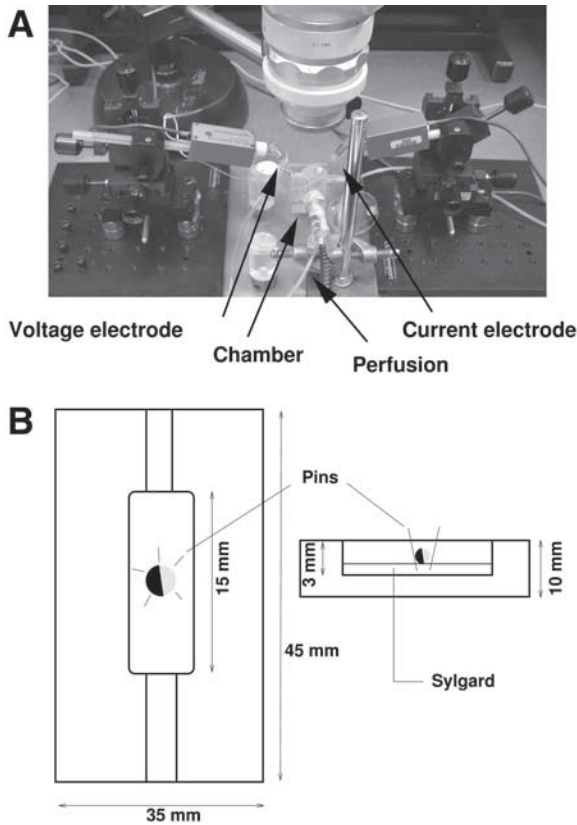


Fig. 2. An oocyte recording setup suitable for two-electrode voltage clamp. (A) A basic oocyte recording setup. Visualization of the oocytes requires a binocular dissecting microscope. Salines are supplied by gravity, and the two recording electrodes are placed on either side of the recording chamber. (B) The recording chamber is constructed from a plastic block. Its volume allows rapid solution exchange without excessive friction forces.

3. Methods

3.1. Defolliculation

Ovary tissue contains oocytes at all developmental stages (stage I is the most immature, and stage VI is the most mature), but only stages V and VI (the largest oocytes) are normally used for expression of ion channels. Each oocyte is surrounded by a vitelline membrane and a layer of follicle cells. There are several ways to remove the follicular layer surrounding the oocytes when they have been freshly removed from the frog. Removal is essential because the follicular layer contains receptors that may respond to the compounds under test, and they are electroconically connected to the oocyte. It is possible to remove the follicular layer manually without enzymatic

treatment, but this is not easy and frequently results in damaged or bruised oocytes. The stages in the defolliculation process are as follows:

1. Separate the ovarian tissues into clumps of about 100 oocytes each.
2. Wash three times in normal SOS, then three times in calcium-free SOS (this is most simply and effectively done by a transfer through containers of SOS and picking up clumps of oocytes with forceps and taking them through the air–water interface does no damage at this stage).
3. Transfer them to 2-mg/mL collagenase IA in calcium-free SOS.
4. Agitate for 5 min (*see Note 1*) on a rocking table.
5. Wash the enzyme-treated oocytes three times in calcium-free SOS, then three times in normal SOS.
6. Remove oocytes from their follicle cell layer using two pairs of finely sharpened forceps (*see Notes 2 and 3*). The forceps must be sharpened so that both halves form a point and the points meet together. This is achieved using an Arkansas stone.

Alternatively, the oocytes can be left in collagenase for up to 1 h, after which many will have shed their follicular cell layer. To avoid potential dangers arising from excessive enzyme treatment, oocytes should be removed into incubation medium when about half of them have shed their follicular layer. Usually, most of the oocytes that still retain their follicular layer will have shed it following overnight incubation at 11°C.

3.2. Injection

Oocytes can be injected with either DNA (into the nucleus) or mRNA (into the cytoplasm). Expression of receptors is usually faster following RNA injection compared to nuclear injection with cDNA, and mRNA of course does not involve expression failures caused by missing the nucleus. Conversely, DNA is more robust than RNA and is therefore easier to handle without the danger of degradation.

If RNA is the message to be used, the usual precautions in handling RNA must be followed. All materials coming in contact with the RNA must be autoclaved and kept sterile to prevent the action of ubiquitous ribonucleases. Gloves must also be used.

The appropriate message volumes for injection are 50 nL for cytoplasmic injections and 20 nL for nuclear injections. Therefore, to deliver the appropriate amount of message, the concentration of the injected material must vary. The amount of message for optimum expression can only be determined by titrating the concentration or mass injected (10-fold steps) and assaying the amplitude of responses. A reasonable starting concentration is 1 $\mu\text{g}/\mu\text{L}$, so titration one or two log units above and below this concentration is recommended. Injecting too much message can paradoxically result in underexpression. The following procedure works well:

1. Place the oocytes into a Petri dish (*see Note 4*).
2. Injection can be done using any system capable of delivering small volumes. We have used Drummond pipeters and purpose-built oocyte injectors (Drummond nanoject, Drummond Scientific Co., USA). These dispensers have a wire plunger that comes into contact with oil in the injecting needle and must be replaced if any kink or bend develops. Care is needed to prevent damage to the needle.

3. Pull the injection pipets from the glass capillaries that are made for the dispenser. They can be pulled on any pipet puller.
4. Break the pipets at the tip using a pair of forceps (*see Note 5*).
5. Backfill the pipets with mineral oil using a syringe and hypodermic needle (*see Note 6*). Fill the whole pipet.
6. Load the injection pipet onto the plunger of the dispenser and tighten the collet into position (*see Note 7*). Once filled, expel some oil as if you were injecting to make sure that the tip is clear.
7. Transfer 1 μ L message onto a clean piece of parafilm or a sterile Petri dish. Advance the injection needle into the message.
8. Fill by withdrawing the plunger (*see Note 8*).
9. Once the pipet is filled, withdraw it from the remaining message droplet and do several dummy injections in the air to confirm that droplets of message are expelled and that no draw-back of material into the pipet occurs. Should draw-back occur, it is quicker in the long run to replace the pipet and refill it with message.
10. Position the dish containing the oocytes under the injection pipet.
11. For RNA injection, advance the tip of the pipet against the vegetal (yellow) pole of the cell. Keep advancing the tip, dimpling the cell, until the pipet has clearly entered the cell. Inject and continue with the remaining oocytes. For nuclear DNA injections, advance the pipet against the middle of the animal pole and inject as for RNA injections (*see Note 9*).
12. Transfer the injected oocytes to clean SOS in a Petri dish on ice for 30 min.
13. After about 30 min, transfer to an incubator set at 18°C.

3.3. Incubation

Oocytes can survive many days in incubation medium (*see Table 5*) at 18°C, provided the incubation medium is changed daily. They can be incubated in an under-bench or smaller bench-top incubator. Once expression has been obtained, the oocytes can then be incubated at 4°C in a refrigerator to extend their usable lifetime. In this case, appropriate time must be allowed for the cells to acclimatize to the change in temperature before beginning experiments.

3.4. Electrophysiology

3.4.1. Two-Electrode Voltage Clamp

3.4.1.1. WIRING THE RIG

1. The basic wiring of the essential components of an oocyte rig can be very simple. The leads to the microelectrodes are connected to their respective connections in the amplifier.
2. The analog output (referred to as the scaled output in the Geneclamp 500 and as V_{out} in the Warner OC50) is connected to the analog in port of an A/D converter.
3. The voltage command port of the amplifier must also be connected to the analog output of the A/D converter.
4. The connection from the A/D converter is usually a proprietary connection to a card supplied with the A/D converter.
5. Calibration is performed through the data acquisition software and should be checked by measuring the output of the amplifier with an oscilloscope and comparing that to the reading in the data acquisition software.

3.4.1.2. PREPARING THE ELECTRODES

1. In preparing the electrodes, bear in mind that the current electrode must be able to pass large currents, whereas the purpose of the voltage electrode is to record the membrane potential stably and accurately. Thin-wall, fiber-filled borosilicate glass is used in both cases.
2. Pull to 1 to 5 M Ω for the voltage electrode and 0.5 to 1 M Ω for the current electrode (see **Note 10**). Fill both with 0.22- μ m-filtered 3 M KCl (see **Note 11**).
3. Keep in a large Petri dish on two parallel strips of wax and keep covered until used. These will last for several hours, but new pipets should be pulled each day.

3.4.1.3. ELECTROPHYSIOLOGICAL RECORDING

1. Reject cells that have a blotchy appearance or that are obviously unhealthy. Reject cells in which the animal (dark) pole does not form a sharp boundary with the vegetal (light) pole.
2. Establish the SOS perfusion and then place an oocyte into the basket of pins using a wide-mouth Pasteur pipet without sharp edges or a plastic Pasteur pipet. The wide-mouth pipet is made by cutting back a normal Pasteur pipet using a diamond glass cutter followed by flaming to smooth the edges.
3. Place the two electrodes on their holders and advance them into the SOS.
4. Check the resistance of both electrodes. On Warner amps, this is done by pressing the “electrode resistance” button and reading the size of the voltage trace displacement. On Geneclamp, this is done by pressing “V1 resistance” or “V2 resistance.”
5. Wait until the voltage recorded by both is stable. If this is not achieved (see **Note 12**).
6. Position both electrodes over the oocyte.
7. Zero the value of the voltage electrode.
8. Advance the voltage electrode onto the oocyte at a position about one-third of the diameter inward. You will see a dimple.
9. Watching the voltage trace, slowly advance the electrode until there is a sharp jump in the voltage. You can even use the coarse control of the micromanipulator for this.
10. Wait until a stable membrane potential is observed (see **Note 13**).
11. Repeat for the current electrode.
12. If you are going to be recording rapid changes in current, tune the electrode (see **Note 14**).
13. Select an appropriate holding potential on the voltage clamp amplifier (such as -70 mV) and enter voltage clamp mode.

3.4.2. Patch

Patch clamp amplifiers are not capable of delivering the large, rapid currents that would be required to patch an oocyte in whole-cell mode, so only inside-out and outside-out modes (for an example, see **Fig. 3A**) are available for these cells.

Oocytes are surrounded by a vitelline membrane that prevents access to the plasma membrane and must therefore be removed if cells are to be patched. This is done by “hypertonic” stripping.

1. Place the oocyte in hypertonic SOS (we have simply used a 10X SOS stock).
2. Wait until the cell is seen coming away from the vitelline membrane. This usually takes about 5 to 10 min.
3. Carefully remove the vitelline membrane. This can be done using two pairs of very fine forceps and must be done with extreme care to avoid damaging the underlying cell.

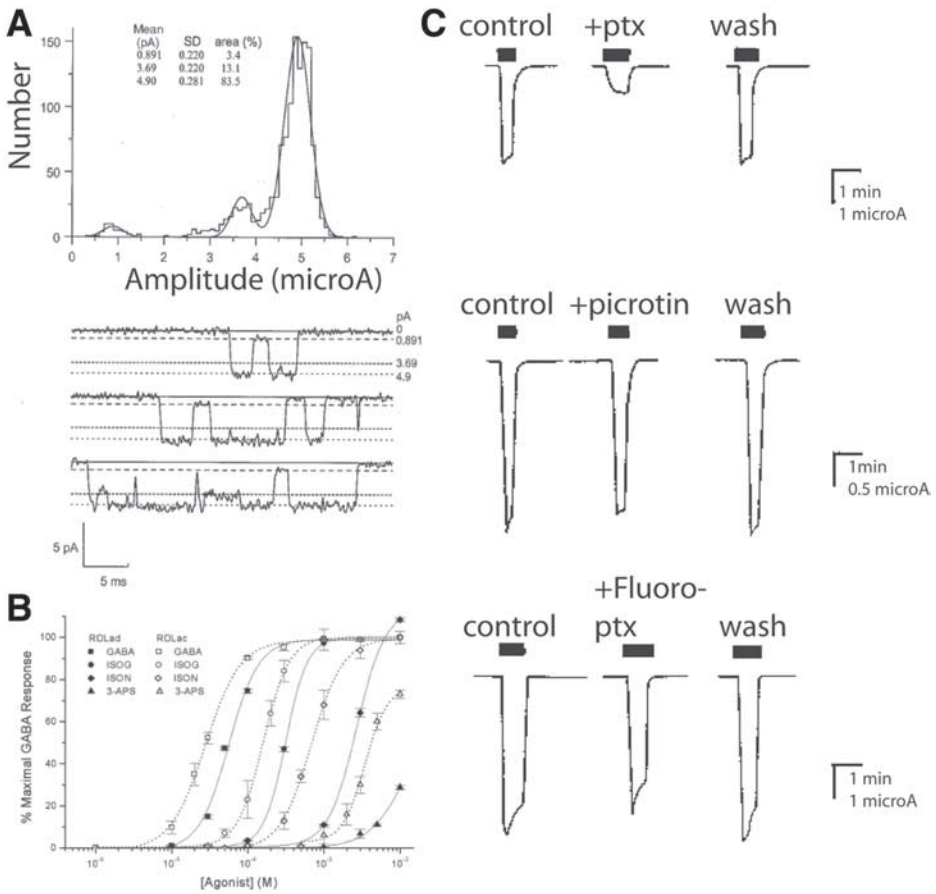


Fig. 3. (A) Single channels can be recorded from outside-out patches of oocytes expressing neurotransmitter receptors. In this example, amplitude histograms of events were recorded from an outside-out patch obtained from an oocyte expressing NR1a and NR2A subunits. In the lower panel is a sample of single-channel recordings used to generate such histograms. From ref. 18. (B) A dose–response curve for an agonist (in this case γ -aminobutyric acid [GABA] and three other GABA receptor agonists acting on two splice variants of the insect GABA receptor, RDL) is derived from measuring the amplitudes of the responses to a series of challenges of agonist at different concentrations. Data can be normalized to a standard response, usually the maximum response to a standard agonist. Here, a set of dose–response curves to a series of GABA agonists is constructed for two splice variants of RDL, an insect GABA receptor. From ref. 19. (C) The action of antagonists is best assayed using triplet challenges of the form agonist, agonist plus antagonist, wash. The actions of three picrotoxin analogs are assayed for their actions on GABA responses mediated by the insect GABA receptor RDL. From ref. 20. ptx, picrotoxinin.

4. Transfer to the recording chamber using a wide-mouth pipet. Once the vitelline membrane has been removed, the oocyte is very fragile and must be transferred with great care. Any contact with the SOS-air interface will destroy the cell.
5. Fill the pipet with SOS containing a low (EC_{10} , the concentration that elicits 10% of the maximum response to that agonist) dose of agonist.
6. Focus on the edge of the cell.
7. Advance the pipet against the cell membrane and release the positive pressure. Seal formation can be helped by applying very gentle negative pressure, but seals that form without negative pressure often seem to be more stable.
8. Cancel the capacitance of the pipet using the amplifier's compensation circuitry.
9. The cell is now in cell-attached mode, and the appropriate experiments can be performed.

The assay of ligands, however, is much more conveniently performed using outside-out recordings, the procedure for which is as follows:

1. Once in cell-attached configuration, apply gentle negative pressure to obtain whole-cell recording configuration. Establishment of whole-cell configuration is marked by the appearance of large capacitative transients (see **Note 15**).
2. Establish outside-out configuration by slowly withdrawing the pipet away from the oocyte. The membrane will eventually yield, marked by a disappearance of the transients and an increase in the resistance of the patch.
3. Move the patch into the stream of SOS. Confirm that the patch is properly placed by applying a pulse of high-potassium SOS, which should result in a rapid increase in holding current. Note that the response to high-potassium SOS can be quite small.
4. Dose-response curves are then constructed as described in **Subheading 3.5.1**.

3.5. Protocols for Assaying Ligands

The following protocols are designed for TEVC but can be adapted to patch.

3.5.1. Neurotransmitter Receptors

3.5.1.1 AGONISTS

The determination of the EC_{50} of agonists is accomplished as described next. An example of the data obtained using this approach is provided in **Fig. 3B**.

1. Establish a stable voltage clamp.
2. Determine which concentration of the drug elicits a maximum response. If there is no response to the drug at all, or if the response is very small (<100 nA), see **Note 16**.
3. Determine the interval required to eliminate the effects of desensitization by applying the above-determined concentration of the agonist at decreasing intervals, starting from a reasonably high value (e.g., 10 min). This will give an indication of the interval required to minimize possible interference from desensitization. In all assays, keep this as a minimum interval between challenges.
4. To construct a dose-response curve, establish an oocyte in voltage clamp.
5. Apply the drug at different concentrations in random order (see **Note 17**) and at appropriate intervals to avoid desensitization.

3.5.1.2. ANTAGONISTS AND MODULATORS

1. To determine the IC_{50} of an antagonist or negative allosteric modulator (see **Fig. 3C**), first determine the EC_{50} (the concentration of the drug that elicits the half maximal response) of the agonist.

2. Make a series of dilutions (10- or 3-fold intervals) of the antagonist or modulator.
3. For each antagonist or modulator concentration, the action of the antagonist is then assayed using a three-challenge protocol consisting of challenges with agonist, agonist plus antagonist, and finally agonist. The third challenge is designed to test for reversibility and is not essential if only one oocyte is used for each test. If the antagonist is rapidly reversible, the third challenge can be used to confirm recovery of the agonist response prior to a subsequent test.
4. Plot the percentage decrease in the amplitude of the agonist response against the antagonist concentration.
5. The IC_{50} and Hill slope are determined by fitting a Hill function to this curve. This can be done using most scientific data visualization programs, such as *SigmaPlot* (SPSS Inc., Chicago, IL, www.spss.com) or *Graphpad Prism* (GraphPad Software Inc., San Diego, CA, www.graphpad.com) for Windows- or Macintosh-based computers or *Gnuplot* or *Grace* for Linux computers.
6. To determine whether an antagonist or allosteric modulator is competitive or noncompetitive, the IC_{50} of the antagonist must first be determined.
7. Construct a dose-response curve for the agonist in normal SOS, then again in SOS containing the antagonist at its IC_{50} concentration.
8. The two agonist dose-response curves constructed in **step 7** are then fitted to a Hill equation, and a shift in EC_{50} indicates a competitive component to the antagonist's action.

4. Notes

1. How long should the oocytes be in collagenase? The time of exposure to enzyme varies from batch to batch of both oocytes and enzyme. Clumps of oocytes can be removed from the enzyme every 10 min or so, washed, and tested to see if they are ready.
2. Defolliculation is a tricky process that requires some practice. One method is to remove the follicle cell layer manually with two pairs of highly sharpened forceps. Grab an oocyte with forceps around the "stalk" where it joins the ovary. With a second forceps, pinch the membrane very close to the first forceps. Pulling away can release the oocyte. Alternatively, if the enzyme treatment has been thorough, the oocyte can be secured at the stalk with a pair of forceps, and a heat-blunted glass probe (made simply by heating a Pasteur pipet) is used to squeeze the oocyte out of its follicular cell layer. This is much quicker than manual defolliculation. A third approach is to heat the tip of a Pasteur pipet so that its opening is slightly smaller than the oocytes. Sucking oocytes into this pipet often leaves the follicle cell layer behind. A final alternative preferred by many labs is to treat the oocytes much longer (up to 2 h) in collagenase, under agitation, until they are released from the follicular cell layer under the action of the collagenase alone. The treated ovaries are then washed thoroughly and left overnight. Oocytes that have lost their follicular layer are then picked out and used. Although simpler, we have found the oocytes treated in this way are much more fragile and less likely to tolerate injection.
3. Defolliculated oocytes are easy to distinguish from those still having their follicular layer. If blood vessels are present, the oocyte has not been defolliculated. The follicular layer imparts a shiny appearance to the cells, whereas defolliculated oocytes are duller. However, if the cells looked like a deflated beach ball, you have removed the vitelline layer.
4. Injection is considerably easier if the dish is scored with a hot wire to make channels in which the oocytes can settle. This is particularly useful for nuclear injection of DNA because it keeps the oocytes with their animal (dark) pole facing upward.

5. For preparing the injection electrode, if RNA is used, the forceps must be flame sterilized before each use. The size of the broken-back tip depends on the material injected and the purity of the message. It should be as small as possible without the danger of small particles in the message solution blocking the tip. Larger pipets are easier to use because they do not block, but they are more likely to damage the oocyte. The choice of tip size therefore depends on how healthy the batch of oocytes is and how clean the message solution is. It is better to err on the finer side because blocked tips can easily be broken back further during the injection.
6. Clean oil: if RNA is used, this oil needs to be heat sterilized and kept sterile. We load a 1-mL syringe with sterilized oil with a $279 \times 3/4$ -in gage needle kept capped when not in use.
7. Make sure you can fill the injection pipet adequately. Make sure the plunger is almost, but not quite, at its most extended position, so that there is as much room as possible for filling the injection pipet.
8. Monitor the filling of the injection needle continuously. While the pipet is filling, attention must be paid to ensure that the pipet is filling properly. By alternately focusing on the oil-message interface as it moves back up the pipet and the tip of the pipet, the experimenter will know that the pipet is filling correctly. The tip can become plugged with impurities in the message. The plunger will keep on withdrawing, and air will make its way into the oil. If this happens, expel the contents until all the bubbles are gone and try again. If the problem persists, break the pipet back and try again.
9. The nucleus occupies a large proportion of the animal pole, and injections aimed at the middle of this half of the oocyte will usually hit the nucleus. Novice users can gain confidence and train themselves by practicing using a toluidine blue, concentrated methylene blue, or neutral red solution. Subsequent dissection of the oocytes using two pairs of forceps will release the nuclei, revealing the hit rate.
10. The current electrode can be made by breaking back a higher resistance electrode but do not overdo it so that KCl is visibly leaking from the pipet.
11. Fill the current-injecting pipet with 3 M KCl. This high concentration will make it easier to achieve the low resistance required for the current electrode. Particles in the filling medium or too fine a tip in the current electrode can cause blockage of the current electrode, which will give odd currents when you voltage clamp.
12. If the voltage recordings of the pipets are not stable, you need to determine which electrode is drifting. If both are changing in the same way, the problem is with the earthing circuit. Take out the bath electrodes and rechloride them. If only one electrode is drifting, rechloride the silver wire (if you are using factory-made electrode holders with incorporated silver chloride pellets, take them apart and clean with distilled water). If both are drifting but the drifts are uncoordinated, clean or rechloride both pipet holders.
13. Regarding stability of the membrane potential, there may be some background fluctuations in the potential. Typically, the cell loses some potential immediately after impaling but then recovers.
14. Fine-tuning of the clamp is not as important for most ligand-evoked responses as for recording voltage-gated currents, but some receptors, such as the $\alpha 7$ -nicotinic acetylcholine receptor, can support responses that are fast enough for clamp tuning to be of concern. Before entering voltage clamp mode, a square oscillation is applied to the voltage electrode. The capacitance compensation is adjusted until the pulses are squared off without ringing. Note that the capacitance of the electrodes changes with changing levels of SOS. As the SOS level often changes during solution changes, this can mean that an

- electrode can become transiently overcompensated during solution changes. During a voltage clamp experiment, this will appear as the trace goes off the screen during a solution change. For this reason, it is better to have the electrode slightly undertuned.
15. For capacitative transients in whole-cell mode, experienced patch users will notice the extremely large transients associated with the large volume of the cells, which can lead inexperienced users to conclude that the patch has been lost. You can increase the duration of the test pulses to confirm that these are indeed transient capacitance artifacts. It is useless to attempt to cancel these transients.
 16. If there is no expression, the failure to express must result from an inability of the oocyte to express the channel, a failure to inject properly, or a problem with the message. If previous successful expression sessions have shown that the oocytes are capable of expressing the message, the first can be eliminated. Expression failure because of degradation of the message is more likely for RNA than for DNA and can result from careless manipulation of the material, so that at some stage ribonucleases have been introduced. The quality of the message can be confirmed to some extent by running a gel to look for smears. If a gradual decline is noticed over several expression runs, it may be worthwhile to produce fresh message.
 17. The duration of drug applications depends on the dynamic properties of the response and can only be determined by vicarious trial and error. The number of challenges required to obtain accurate dose-response data must be greater than six, and the experimenter must ensure that clear minima and maxima are obtained for each curve if accurate estimates of the EC_{50} and Hill slope are to be obtained.

References

1. Methfessel, C., Witzemann, V., Takahashi, T., Mishina, M., Numa, S., and Sakmann, B. (1986) Patch clamp measurements on *Xenopus laevis* oocytes: currents through endogenous channels and implanted acetylcholine receptor and sodium channels. *Pflugers Arch.* **407**, 577–588.
2. Dempster, J. (1993) *Computer Analysis of Electrophysiological Signals*, Academic Press, London.
3. Arena, J. P., Liu, K. K., Paress, P. S., Schaeffer, J. M., and Cully, D. F. (1992) Expression of a glutamate-activated chloride current in *Xenopus* oocytes injected with *Caenorhabditis elegans* RNA: evidence for modulation by avermectin. *Brain Res. Mol. Brain Res.* **15**, 339–348.
4. Njue, A. I., Hayashi, J., Kinne, L., Feng, X. P., and Prichard, R. K. (2004) Mutations in the extracellular domains of glutamate-gated chloride channel $\alpha 3$ and β subunits from ivermectin-resistant *Cooperia oncophora* affect agonist sensitivity. *J. Neurochem.* **89**, 1137–1147.
5. Hosie, A. M., Baylis, H. A., Buckingham, S. D., and Sattelle, D. B. (1995) Actions of the insecticide fipronil, on dieldrin-sensitive and -resistant GABA receptors of *Drosophila melanogaster*. *Br. J. Pharmacol.* **115**, 909–912.
6. Buckingham, S. D., Hosie, A. M., Roush, R. L., and Sattelle, D. B. (1994) Actions of agonists and convulsant antagonists on a *Drosophila melanogaster* GABA receptor (RDL) homo-oligomer expressed in *Xenopus* oocytes. *Neurosci. Lett.* **181**, 137–140.
7. Bali, M. and Akabas, M. H. (2004) Defining the propofol binding site location on the GABA_A receptor. *Mol. Pharmacol.* **65**, 68–76.
8. Murasaki, O., Kaibara, M., Nagase, Y., Mitarai, S., Doi, Y., Sumikawa, K., and Taniyama, K. (2003) Site of action of the general anesthetic propofol in muscarinic M1 receptor-mediated signal transduction. *J. Pharmacol. Exp. Ther.* **307**, 995–1000.

9. Do, S. H., Ham, B. M., and Zuo, Z. (2003) Effects of propofol on the activity of rat glutamate transporter type 3 expressed in *Xenopus* oocytes: the role of protein kinase C. *Neurosci. Lett.* **343**, 113–116.
10. Davies, M., Newell, J. G., Derry, M., Martin, I. L., and Dunn, S. M. Characterization of the interaction of zopiclone with γ -aminobutyric acid type A receptors. *Mol. Pharmacol.* **58**, 756–762.
11. Okamoto, T., Minami, K., Uezono, Y., et al. (2003) The inhibitory effects of ketamine and pentobarbital on substance P receptors expressed in *Xenopus* oocytes. *Anesth. Analg.* **97**, 104–110.
12. Levandoski, M. M., Picket, B., and Chang, J. (2003) The anthelmintic levamisole is an allosteric modulator of human neuronal nicotinic acetylcholine receptors. *Eur. J. Pharmacol.* **471**, 9–20.
13. Raymond Delpuch, V., Ihara, M., Coddou, C., Matsuda, K., and Sattelle, D. B. (2003) Action of nereistoxin on recombinant neuronal nicotinic acetylcholine receptors expressed in *Xenopus laevis* oocytes. *Invert. Neurosci.* **5**, 29–35.
14. Nishiwaki, H., Nakagawa, Y., Kuwamura, M., et al. (2003) Correlations of the electrophysiological activity of neonicotinoids with their binding and insecticidal activities. *Pest. Manag. Sci.* **59**, 1023–1030.
15. Ihara, M., Matsuda, K., Otake, M., et al. (2003) Diverse actions of neonicotinoids on chicken α 7, α 4 β 2 and *Drosophila*-chicken SAD β 2 and ALS β 2 hybrid nicotinic acetylcholine receptors expressed in *Xenopus laevis* oocytes. *Neuropharmacology* **45**, 133–144.
16. Ogata, J., Minami, K., Uezono, Y., et al. (2004) The inhibitory effects of tramadol on 5-hydroxytryptamine type 2C receptors expressed in *Xenopus* oocytes. *Anesth. Analg.* **98**, 1401–1406.
17. Wagner, L. E., Gingrich, K. J., Kulli, J. C., and Yang, J. (2001) Ketamine blockade of voltage-gated sodium channels: evidence for a shared receptor site with local anesthetics. *Anesthesiology* **95**, 1406–1413.
18. Cheffings, C. M. and Colquhoun, D. (2000) Single channel analysis of a novel NMDA channel from *Xenopus* oocytes expressing recombinant NR1A, NR2A and NR2D subunits. *J. Physiol.* **526 Pt. 3**, 481–491.
19. Hosie, A. M., Buckingham, S. D., Presnail, J. K., and Sattelle, D. B. (2001) Alternative splicing of a *Drosophila* GABA receptor subunit gene identifies determinants of agonist potency. *Neuroscience* **102**, 709–714.
20. Shirai, Y., Hosie, A. M., Buckingham, S. D., Holyoke, C. W., Jr., Baylis, H. A., and Sattelle, D. B. (1995) Actions of picrotoxinin analogs on an expressed, homo-oligomeric GABA receptor of *Drosophila melanogaster*. *Neurosci. Lett.* **189**, 1–4.

Microtransplantation of Neurotransmitter Receptors From Cells to *Xenopus* Oocyte Membranes

New Procedure for Ion Channel Studies

Ricardo Miledi, Eleonora Palma, and Fabrizio Eusebi

Summary

The *Xenopus* oocyte is largely used as a cell expression system for studying both structure and function of transmitter receptors and ion channels. Messenger RNA extracted from the brain and injected into oocytes leads to the synthesis and membrane incorporation of many types of functional ion channels. A new method was developed further to transplant neurotransmitter receptors from human brain or cultured cell lines to the membrane of *Xenopus* oocytes. This method represents a modification of the method used many years ago of injecting into oocytes membrane vesicles from *Torpedo* electroplaques, yielding the expression of functional *Torpedo* acetylcholine receptors. We describe this approach by extracting membrane vesicles from human hippocampus or temporal neocortex and from mammalian cell lines stably expressing glutamate or neuronal nicotinic receptors. Because the human neurotransmitter receptors are “microtransplanted” with their native cell membranes, this method extends the usefulness of *Xenopus* oocytes as an expression system for addressing issues in many fields, including channelopathies.

Key Words: Epilepsy; human brain tissues; transfected cell lines; voltage clamp; *Xenopus* oocytes.

1. Introduction

The heterologous expression of ligand-gated and voltage-gated ion channels in the oolemma of *Xenopus* oocytes is regarded as one of the most powerful and convenient tools available to study the properties of receptors and ion channels. This experimental approach is particularly useful when the native cells (i.e., human nerve cells) are not easily accessible for extensive investigations.

Two methods with similar efficacy may be used to express ion channels in the oocyte membrane. The first method consists of either cytoplasmic injections into *Xenopus* oocytes with poly(A⁺) messenger RNAs (mRNAs) extracted from native tissues (1–4) or intranuclear injections of complementary DNAs (cDNAs) encoding for

ion channels (5–7). The second method consists of injecting into the oocyte membrane vesicles extracted from the native tissue (8–11). A detailed description of the first method is beyond the scope of this chapter because many reviews have already addressed this issue (1,3–6,12–14).

This chapter describes the method of membrane transplantation from cells to oocytes, as used particularly for cultured cells. This procedure is relatively new and overcomes some of the problems associated with oocyte injections of mRNAs or cDNAs. For example, with the latter procedure, the proteins are synthesized and posttranslationally processed by the oocyte's own machinery, and the receptors are assembled in oocyte membranes. In contrast, when the foreign membranes are injected into the oocyte, the *original* ion channels, still embedded in their native cell membrane, are transplanted to the oocyte plasma membrane (see **Note 1**).

2. Materials

1. Anesthetic (2% 3-aminobenzoic acid ethyl ester; Sigma, St. Louis, MO).
2. *Xenopus laevis* frogs.
3. Oocytes ringer (OR): 82.5 mM NaCl, 2.5 mM KCl, 5 mM HEPES, pH 7.4. To prepare 1 L of 10-fold concentrated OR (OR 10X) without Ca^{2+} and Mg^{2+} , weigh 48.2 g NaCl, 1.86 g KCl, 11.9 g HEPES, pH 7.2 with 5M NaOH, add 5 mL phenol red. Store at 4°C and use within 3 to 4 wk. To make 1 L of the final OR, take 100 mL OR 10X, add 1 mL 1 M MgCl_2 and 2.5 mL 1 M CaCl_2 , complete to 1 L with water, check pH, and store at 18°C.
4. Sterile filter system for oocyte Ringer (Corning, NY).
5. Collagenase type I (Sigma).
6. Stereomicroscope.
7. Spinner flask (100 mL; Bellco Glass, NJ).
8. Barth's modified saline solution: 88 mM NaCl, 1 mM KCl, 2.4 mM NaHCO_3 , 10 mM HEPES, 0.82 mM MgSO_4 , 0.33 mM $\text{Ca}(\text{NO}_3)_2$, 0.41 mM CaCl_2 . Prepare 500 mL of Barth's 10X stock solution. Weigh 25.67 g NaCl, 0.37 g KCl, 1 g NaHCO_3 , 11.9 g HEPES, 1 g $\text{MgSO}_4 \cdot 7 \text{H}_2\text{O}$, 0.39 g $\text{Ca}(\text{NO}_3)_2$, 0.3 g $\text{CaCl}_2 \cdot 2 \text{H}_2\text{O}$ at pH 7.2 with 5 M NaOH. Filter and store at 4°C in sterilized glass bottle. To prepare 500 mL Barth's medium for experiments, take 50 mL Barth's 10X, add 5 mL penicillin/streptomycin and 1 mL kanamycin solution (100 U/100 µg penicillin/streptomycin and 100 µg of kanamycin solution), complete to 500 mL with water, and store at 18°C.
9. Antibiotics: 100 U/100 µg penicillin/streptomycin; 100 µg kanamycin solution (Gibco-BRL).
10. Glycine buffer: 200 mM glycine, 150 mM NaCl, 50 mM ethyleneglycolbistetraacetic acid (EGTA), 50 mM ethylenediaminetetraacetic acid (EDTA), 300 mM sucrose plus protease inhibitor solution (100 µL/10 mL homogenized tissue). Prepare 20 mL glycine buffer: solution made with 4 mL 1 M glycine, 0.6 mL 5 M NaCl, 5 mL 0.2 M EGTA, 2 mL 0.5 M EDTA, 6 mL 1 M sucrose, 2.4 mL water at pH 9.0 with NaOH. Keep in 5-mL aliquots at 4°C.
11. Protease inhibitor: for stock solution, protease inhibitor cocktail (Sigma P2714) in 100 mL water; keep 5-mL aliquots at –20°C.
12. Homogenizer (Ultra-Turrex T8; metal tip S8N-5G and S8N-8G; IKA, Staufen, Germany).
13. Ultracentrifuge (Beckmann centrifuge with F 241.5 rotor, CA).
14. Assay buffer: 20 mL 5 mM glycine; keep 5-mL aliquots at 4°C.
15. BCA Protein Assay Reagents Kit (Pierce, Rockford, IL).
16. Vertical micropipet puller.

17. Microinjection apparatus (Harvard Apparatus, www.harvardapparatus.com; 6.66- μ L glass micropipets, Drummond, www.drummondsci.com; micromanipulator, Singer Instruments, Roadwater, UK).
18. Frog ringer: 115 mM NaCl, 2 mM KCl, 1.8 mM CaCl₂, 5 mM HEPES. To prepare 1 L of solution, weigh 6.72 g NaCl, 0.149 g KCl, 0.265 g CaCl₂·2 H₂O at pH 7.2 with 1 M NaOH and store at 18°C.
19. Microelectrode solution (3 M KCl) stored in a sterile bottle at 4°C.
20. 1 M CaCl₂ and 1 M MgCl₂ stock solutions (stored at 4°C in sterile glass bottles).
21. Micromanipulators for voltage clamp recording (Leica, Wetzlar, Germany).
22. Voltage clamp amplifier (GeneClamp 500B; Axon Instruments).
23. Recording chamber (Automate Scientific, CA).
24. Perfusion system (Biologique RSC-200; Claix, France) (see **Note 2**).

3. Methods

The methods described here outline the procedures for: (1) oocyte preparation and the expression of ligand-gated and voltage-gated channels in *Xenopus* oocytes following the extraction of membranes from either (2) native brain tissue or (3) cell lines; (4) membrane cytoplasmic injections into oocytes; and (5) voltage clamp recordings from oocytes.

3.1. Preparation of *Xenopus* Oocytes

Preparation of oocytes are detailed elsewhere (7,15,16) and are summarized here. Adult female frogs can be obtained from commercial suppliers. The steps for preparing oocytes are as follows:

1. Anesthetize the frog with 0.2% 3-aminobenzoic acid ethyl ester and sacrifice it by decapitation.
2. Cut part of the ovary into small pieces using a razor blade and thin forceps and place the segments in OR solution without CaCl₂.
3. Weigh 0.1 g of collagenase type I, and dissolve in 50 mL OR solution.
4. Add the collagenase solution and place the pieces of ovary in 100-mL spinner flask under slow agitation at 18°C for 2 to 3 h.
5. Check visually if the oocytes are isolated and defolliculated and wash three or four times with OR plus 2.5 mM CaCl₂ or frog Ringer.
6. Transfer the oocytes in Barth's modified saline solution plus antibiotics and incubate at 18°C.
7. Inject oocytes with membrane preparation 12 to 24 h after collagenase treatment (procedures for injections are described in **Subheading 3.4**).

3.2. Membrane Preparation From Mammalian Brain Tissues

The general method of membrane preparation has been described and used to extract membranes from the electric organ of *Torpedo* and the rat and human brains (8–10,17). The following protocol describes the procedures we have used for isolating membranes from, with minor modifications, (1) human temporal lobe (TL) and hippocampus of medically intractable epileptic patients who underwent surgical TL resection; (2) TL of patients affected by oligodendroglioma; (3) TL of P60 DBA mice; and (4) the cortex of P0-P12 BDF1 mice. **Figure 1** is a diagram illustrating the main steps used to obtain nervous tissue membranes for injection into oocytes. **Figure 2**

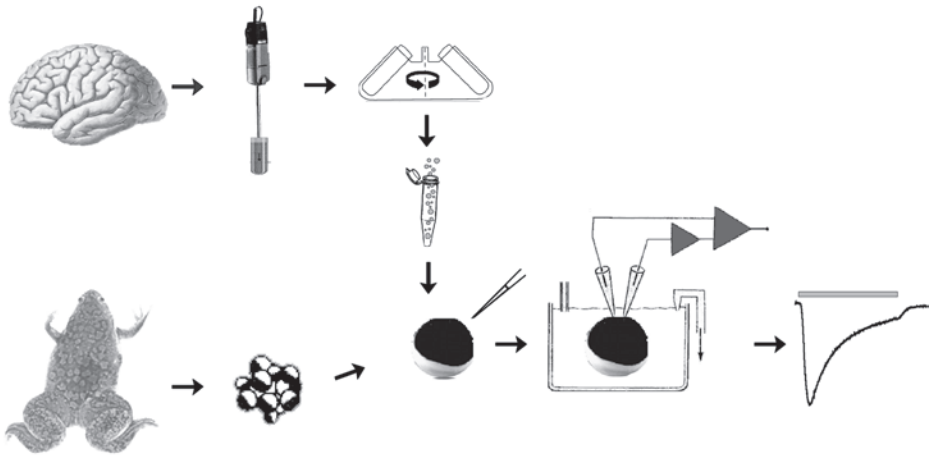


Fig. 1. Neurotransmitter receptors from the human brain microtransplanted to the *Xenopus* oocyte plasma membrane to study their functional properties. Two alternative procedures can be used to incorporate receptors in the oolemma: (1) injecting the oocytes with brain cell membranes (as shown) or (2) by injecting mRNA extracted from surgically removed brain tissues.

shows examples of responses obtained with this method. The steps for isolating membranes are as follows:

1. Prepare 4 mL glycine buffer by adding 40 μ L protease inhibitor stock solution immediately before use.
2. Clean the metal tip (S8N-8G; IKA, Germany) of the homogenizer by rinsing twice with ethanol (EtOH) 70% and water.
3. Homogenize the tissue in a 50-mL Falcon tube with 4 mL glycine buffer. Take care to keep the Falcon tube on ice during the homogenization (*see Note 3*).
4. Transfer the filtrate to 1.5-mL vials and centrifuge at 9500g for 15 min at 4°C.
5. Centrifuge the supernatant at 100,000g for 2 h at 4°C in a Beckmann centrifuge TL-100 (rotor TLA-100).
6. Withdraw the supernatant.
7. Wash the pellet twice with water.
8. Resuspend the pellet in 400 μ L assay buffer (5 mM glycine). Use when necessary an Eppendorf micropipet with a 1-mL plastic tip cut to enlarge three or four times the original opening to facilitate resuspension. Take 1 μ L sample and measure the amount of total proteins using a standard BCA Protein Assay Reagent Kit.
9. Prepare 10- to 50- μ L aliquots to use directly and to store frozen at -80°C for later use.

3.3. Membrane Preparation From Cell Lines

The procedure described next has been used to prepare membranes from the following cell lines: (1) human HEK (human embryonic kidney) stably expressing functional rat homomeric aminohydroxymethyl-isoxazole-propionic acid (AMPA)-type glutamate receptor type 1 (GluR1); (2) human HEK stably expressing functional human neuronal nicotinic acetylcholine receptor $\alpha 4\beta 2$ (AChR- $\alpha 4\beta 2$); (3) rat GH4-C1

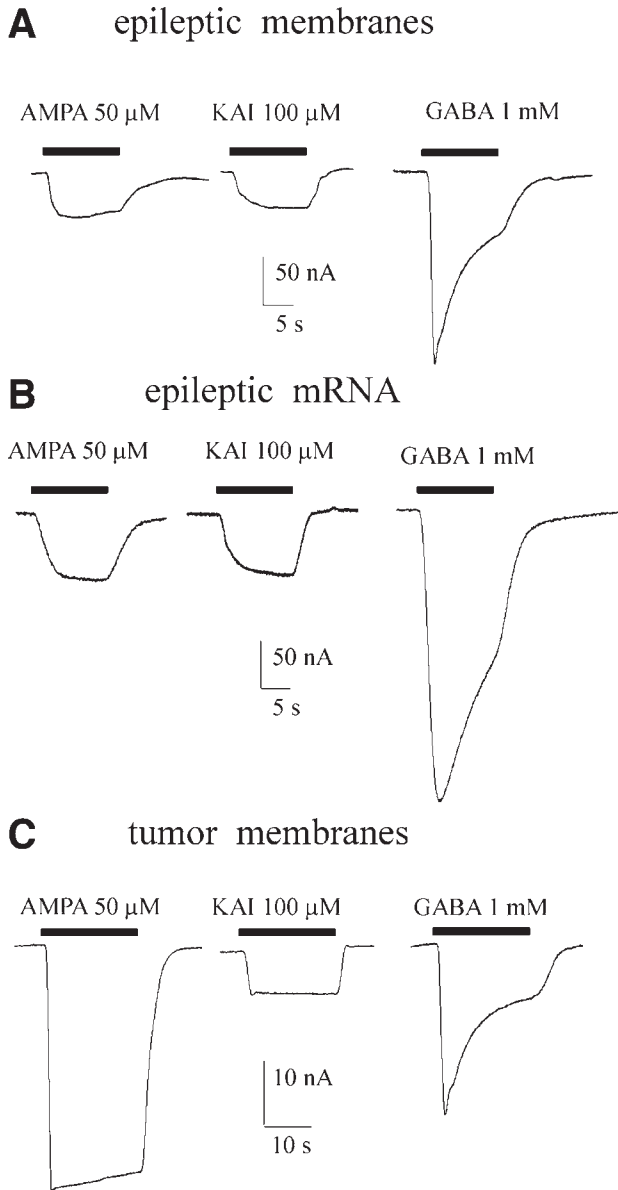


Fig. 2. Examples of currents evoked by different neurotransmitters (as indicated) in *Xenopus* oocytes injected with membranes (A), or mRNA (B) extracted from human mesial temporal lobe epilepsy (MTLE), or with membranes extracted from human oligodendroglioma (C). The responses to AMPA were evoked in the presence of 50 μ M cyclothiazide. GABA, γ -aminobutyric acid. KAI, kainic acid.

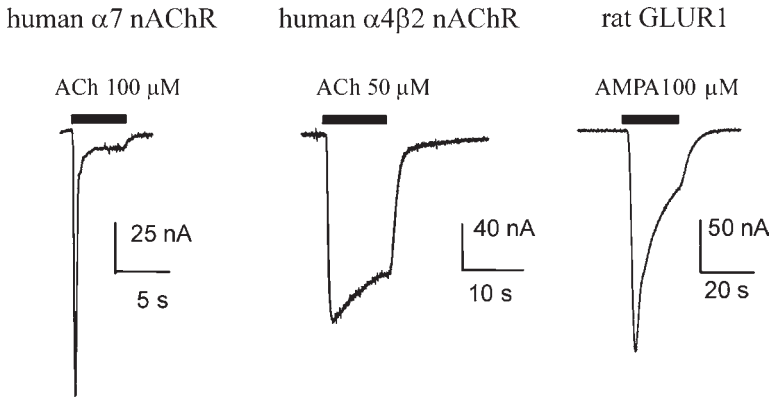


Fig. 3. Examples of currents evoked by acetylcholine (ACh) and AMPA as indicated, from *Xenopus* oocytes injected with membranes extracted from **left**, GH(4)C1 cells stably transfected with human $\alpha 7$ -nAChR subunit; **middle**, HEK293 cells stably transfected with human $\alpha 4$ - and $\beta 2$ -nAChR subunits; **right**, HEK293 cells stably transfected with rat flip variant of glutamate type 1 receptor subunit. The AMPA response was evoked as in Fig. 2.

pituitary cells expressing functional human neuronal $\alpha 7$ -AChR (see Fig. 3 and ref. 11). The steps for extracting membranes are as follows:

1. Collect 1 to 8×10^8 cells in 2 mL glycine buffer by scraping the cells.
2. Homogenize the cells in a 15-mL Falcon tube using the Ultra-Turrex T8 homogenizer with a small metal tip (S8N-5G; IKA, Germany) to match the small amount of cells (see Note 4).
3. Follow the protocol described in Subheading 3.2., steps 4 to 7.
4. Resuspend the pellet in 200 μ L assay buffer and, after measuring the protein concentration (10–15 mg/mL), use directly or store 5- μ L aliquots at -80°C for subsequent use.

3.4. Cytoplasmatic Injection Into Oocytes

For membrane injection, it is convenient to use only oocytes at stages V–VI of development, with a 1- to 1.5-mm diameter, and with a tough membrane. The steps for cytoplasmatic injection are as follows:

1. Pull the glass micropipets (6.66 μ L) for the injection using a standard puller.
2. Break slightly the micropipet tip under a stereomicroscope (20 \times ; Zeiss, Germany) and insert the micropipet in a standard holder connected to a pressure microinjector.
3. Fill the glass micropipet with 4 to 5 μ L membrane samples placed on a clean piece of parafilm.
4. Calibrate the injector according to the diameter of the glass micropipet, setting both duration and injecting pressure.
5. Inject each oocyte with about 100 nL membrane preparation (1–2 mg proteins/mL; see Notes 5 and 6).
6. After the injection, maintain the oocytes in Barth's solution at 18°C until the electrophysiological recordings are performed.

3.5. Voltage Clamp Recordings From Oocytes

Full-size currents are recorded about 12 h after the membrane injections. Membrane currents are recorded using two conventional voltage clamp electrodes as previously reviewed (5,6,14,15,18). One electrode is used to record the transmembrane potential of the oocyte. The amplifier compares the resting potential recorded by the voltage electrode to the desired holding potential, and the current is injected into the oocytes from the second electrode to keep the potential stable at this value. Both the electrodes are filled with 3 M KCl (19). The steps for voltage clamp recordings are as follows:

1. Prepare glass microelectrodes with filament, pulling them with a single-step vertical pipet puller. Bend the electrodes with a Bunsen flame to get electrodes more stably into the oocyte.
2. Transfer the oocyte to the recording chamber using a blunt and fire-polished Pasteur pipet.
3. Plunge the voltage and current electrode tips in the solution of the recording chamber and check their resistance (see Note 7).
4. Insert the voltage-recording electrode into the oocyte to measure its resting potential, then insert the passing current electrode. The resting potential of healthy membrane-injected oocytes ranges from -25 to -70 mV. After inserting the microelectrodes, there is a drop in membrane potential, which usually recovers after superfusing with the standard solution (OR) for a few minutes.
5. Superfuse with the standard solution.
6. Shift to voltage clamp configuration and hold the oocyte at -60 mV. Measure the transmembrane resistance of the oocyte (best conditions at 1- to 5-M Ω resistance).
7. Start recording membrane currents (Fig. 2; see Note 8).

4. Notes

1. The method of transplantation of receptors by injecting membranes is very powerful and has some advantages over the expression of receptors by mRNA injections, such as: (1) faster appearance of functional receptors in the oocyte plasma membrane; (2) problems with ribonuclease contamination are avoided; (3) small amounts of tissue are used to obtain abundant membrane preparations; (4) the same aliquots of membrane preparation can be used after thawing and freezing without much precaution. However, the main advantage is that the receptors are the original ones already assembled and in their original cell membranes.
2. Solution exchange is conveniently achieved using electromagnetic valves and a computer-controlled perfusion system consisting of 18 syringes (50 mL) connected with polythene tubing to 18 valves mounted directly on the Faraday cage and grounded. The aspiration of the solution from the recording chamber is achieved using a small plastic tube connected to a vacuum through an air pump for an aquarium in which the flux of the air has been inverted.
3. The amount of tissue to be used for membrane extraction can be variable. Its wet weight may be as low as 0.2 g to produce a membrane pellet suitable for many experiments.
4. Convenient membrane preparations from cultured cells are obtained using more than 10^8 cells.
5. It is easier and faster to inject oocytes using a dark background, such as a black plastic chamber.

6. If the membrane preparation is too viscous or dishomogeneous at visual inspection, it is necessary to sonicate the sample for 10 s before the injection.
7. Optimal electrode resistance is between 0.5 and 2 M Ω .
8. There is usually large variability in the number of receptors transplanted and consequently in the values of the recorded transmembrane currents. To reduce this variability, we recommend sonicating the membrane preparation just before injection and to inject in the equatorial region.

Acknowledgments

We thank Zulma Duenas and Flavia Trettel for help and discussion. This work was supported in part by FIRB and COFIN grants from MIUR (to F. E.) and NSF (Neuronal and Glial Mechanisms; to R. M.).

References

1. Gundersen, C. B., Miledi, R., and Parker, I. (1983) Voltage-operated channels induced by foreign messenger RNA in *Xenopus* oocytes. *Proc. R. Soc. Lond. BBiol. Sci.* **220**, 131–140.
2. Gundersen, C. B., Miledi, R., and Parker, I. (1984) Messenger RNA from human brain induces drug- and voltage-operated channels in *Xenopus* oocytes. *Nature* **308**, 421–424.
3. Miledi, R., Parler, I., and Sumikawa, K. (1989) Transplanting receptors from brain into oocytes, in *Fidia Award Lectures*, Vol. 3 (Smith, J., ed.), Raven Press, New York, pp. 57–90.
4. Arellano, R. O., Woodward, R. M., and Miledi, R. (1996) Ion channels and membrane receptors in follicle-enclosed *Xenopus* oocytes, in *Ion Channels*, Vol. 4 (Narahashi, T., ed.), Plenum Press, New York, pp. 203–259.
5. Bertrand D., Cooper, E., Valera, S., Rungger, D., and Ballivet, M. (1991) Electrophysiology of neuronal nicotinic acetylcholine receptors expressed in *Xenopus* oocytes following nuclear injection of genes or cDNAs, in *Methods in Neurosciences*, Vol. 4, edited by P. Michael Conn, Academic Press, NY, pp. 174–193.
6. Quick, M. W. and Lester, H. A. (1994) Methods for expression of excitability proteins in *Xenopus* oocytes, in *Methods in Neurosciences*, Vol. 19, edited by P. Michael Conn, Academic Press, NY, pp. 261–279.
7. Palma, E., Mileo, A. M., Eusebi, F., and Miledi, R. (1996) Threonine-for-leucine mutation within domain M2 of the neuronal $\alpha 7$ nicotinic receptor converts 5-hydroxytryptamine from antagonist to agonist. *Proc. Natl. Acad. Sci. USA* **93**, 11,231–11,235.
8. Marsal, J., Tigyi, G., and Miledi, R. (1995) Incorporation of acetylcholine receptors and Cl⁻ channels in *Xenopus* oocytes injected with *Torpedo* electroplaque membranes. *Proc. Natl. Acad. Sci. USA* **92**, 5224–5228.
9. Morales, A., Aleu, J., Ivorra, I., Ferragut, J. A., Gonzalez-Ros, J. M., and Miledi, R. (1995) Incorporation of reconstituted acetylcholine receptors from *Torpedo* into *Xenopus* oocyte membrane. *Proc. Natl. Acad. Sci. USA* **92**, 8468–8472.
10. Miledi, R., Eusebi, F., Martinez-Torres, A., Palma, E., and Trettel, F. (2002) Expression of functional neurotransmitter receptors in *Xenopus* oocytes after injection of human brain membranes. *Proc. Natl. Acad. Sci. USA* **99**, 13,238–13,242.
11. Palma, E., Trettel, F., Fucile, S., Renzi, M., Miledi R., and Eusebi, F. (2003) Microtransplantation of membranes from cultured cells to *Xenopus* oocytes: a method to study neurotransmitter receptors embedded in native lipids, *Proc. Natl. Acad. Sci. USA* **100**, 2896–2900.

12. Barnard, E. A., Miledi, R., and Sumikawa, K. (1982) Transplantation of exogenous messenger RNA coding for nicotinic acetylcholine receptors produces functional receptors in *Xenopus* oocytes. *Proc. R. Soc. Lond. B Biol. Sci.* **215**, 241–246.
13. Sumikawa, K., Parker, I., and Miledi, R. (1984) Partial purification and functional expression. *Proc. Natl. Acad. Sci. USA* **81**, 7994–7998.
14. Smart, T. G. and Krishek, B. J. (1995) *Xenopus* oocyte microinjection and ion-channel expression, in *Patch-Clamp Applications and Protocols* (Boulton, A. A., Baker, G. B., and Walz, W., eds.), Humana Press, Totowa, NJ.
15. Miledi, R. (1982) A calcium-dependent transient outward current in *Xenopus laevis* oocytes. *Proc. R. Soc. Lond. B Biol. Sci.* **215**, 491–497.
16. Miledi, R. and Woodward, R. M. (1989) Effects of defolliculation on membrane current responses of *Xenopus* oocytes. *J. Physiol.* **416**, 601–621.
17. Palma, E., Esposito, V., Mileo, A. M., et al. (2002) Expression of human temporal lobe neurotransmitter receptors in *Xenopus* oocytes: an innovative approach to study epilepsy. *Proc. Natl. Acad. Sci. USA* **99**, 15,078–15,083.
18. Kusano, K., Miledi, R., and Stinnakre, J. (1982) Cholinergic and catecholaminergic receptors in the *Xenopus* oocyte membrane. *J. Physiol.* **328**, 143–170.
19. Miledi, R. (1980) Intracellular calcium and desensitization of acetylcholine receptors. *Proc. R. Soc. Lond. B Biol. Sci.* **209**, 447–452.

Reconstitution of Golgi Disassembly by Mitotic *Xenopus* Egg Extract in Semi-Intact MDCK Cells

Fumi Kano, Katsuya Takenaka, and Masayuki Murata

Summary

Semi-intact cells are cells with plasma membranes that have been permeabilized by bacterial pore-forming toxins or surfactants. The addition of mitotic *Xenopus* egg extract to semi-intact cells can reconstitute a number of intracellular events that occur specifically at the onset of mitosis. In this chapter, we describe methods for reconstituting the disassembly of the Golgi apparatus by introducing mitotic *Xenopus* egg extract into semi-intact Mardin-Darby canine kidney (MDCK) cells. The Golgi apparatus was visualized in the cells by expression of green fluorescence protein (GFP)-tagged galactosyltransferase, a marker of trans-Golgi cisternae. *Xenopus* egg extracts arrested at mitosis or interphase were then prepared and added to the semi-intact MDCK cells. Disassembly of the Golgi apparatus was induced by mitotic *Xenopus* egg extract. This system can be used not only to elucidate the factors that are involved in the reconstitution process, but also to dissect the process into several elementary steps morphologically and biochemically.

Key Words: GFP; Golgi apparatus; kinase; mitosis; reconstitution; semi-intact cell; *Xenopus* egg extract.

1. Introduction

Semi-intact cells are cells with plasma membranes that have been permeabilized by bacterial pore-forming toxins or detergents. Various intracellular events can be functionally reconstituted in semi-intact cells by incubation with cytosol and adenosine triphosphate (ATP; **Fig. 1**). Because semi-intact cells allow direct access of chemicals and antibodies to the cytoplasm of the cells, they permit study of the molecular mechanisms of the reconstituted process biochemically. We used a bacterial cytolysin, streptolysin O (SLO), to permeabilize the cells (**1-3**). SLO binds to cholesterol in plasma membranes at 4°C. At warmer temperatures, SLO assembles to form amphiphilic hexamers, resulting in the generation of small, stable transmembrane pores (**4**).

SLO-induced pores are 30 nm in diameter, which is sufficient to allow entry of immunoglobulin into the cells (immunoglobulin G; 150 kDa) (**5**). We can minimize

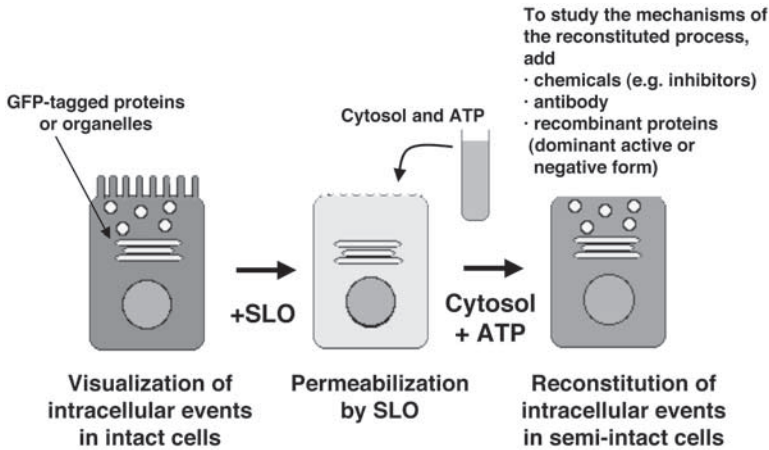


Fig. 1. Scheme of semi-intact cells.

the damage to membranes of intracellular organelles caused by passage of SLO through the SLO-induced pores in the plasma membrane into the cytoplasm by washing away any excess SLO at 4°C before the initiation of pore formation. In contrast, it is difficult to avoid damage to intracellular structures when cells are permeabilized with digitonin because digitonin permeabilization is insensitive to temperature. SLO-mediated semi-intact cells have thus proven useful for the reconstitution of transport to apical or basolateral membranes in polarized cells (6,7), the import of proteins to peroxisomes (8), and so on.

This chapter presents protocols for the reconstitution of the disassembly of the Golgi apparatus by mitotic *Xenopus* egg extract in SLO-induced, semi-intact Mardin-Darby canine kidney (MDCK) cells.

2. Materials

1. Marc's modified Ringer's (MMR): 100 mM NaCl, 2 mM KCl, 1 mM MgSO₄, 2 mM CaCl₂, 5 mM Na-HEPES, pH 7.8, 0.1 mM ethylenediaminetetraacetic acid.
2. EGFP-N1 vector (Clontech; Palo Alto, CA).
3. LipofectAMINE PLUS (Invitrogen; Carlsbad, CA).
4. Geneticin (Gibco-BRL).
5. Transwell (24-mm diameter, 0.4- μ m pore size; Corning Costar).
6. Transport buffer (TB): 25 mM HEPES-KOH, pH 7.4, 115 mM potassium acetate, 2.5 mM MgCl₂, 1 mM dithiothreitol, and 2 mM *O,O*-9-bis(2-aminoethyl)ethyleneglycol-*N,N,N',N'*-tetraacetic acid (EGTA); store at 4°C.
7. ATP (Sigma): 100 mM stock in water; store at -30°C.
8. Creatine phosphate (Sigma): 800 mM stock in water; store at -30°C.
9. Creatine kinase (Sigma): 5-mg/mL stock in 50 % glycerol; store at -30°C.
10. PD98059 (New England Biolabs): 50-mg/mL stock in dimethyl sulfoxide (DMSO); store at -30°C.
11. Staurosporine (Wako): 25 mg/mL stock in DMSO; store at -30°C.
12. SB203580 (Calbiochem): 20 mg/mL stock in DMSO; store at -30°C.

13. Butyrolactone I (Affiniti Research Products): 100 mg/mL stock in DMSO; store at -30°C .
14. Protease inhibitors (Sigma): chymostatin and pepstatin A, 5-mg/mL stock in water; leupeptin and antipain, 5 mg/mL stock in DMSO; store at -30°C .
15. Paclitaxel (Taxol) (Sigma): final concentration 5 $\mu\text{g}/\text{mL}$, prepared just before experiments.
16. SLO (purchased from Dr. Bhakdi, Meintz University, Germany).
17. Propidium iodide (Molecular Probes): 1.0-mg/mL stock in water; store at 4°C
18. Mouse anti-cdc2 kinase antibody (Santa Cruz Biotechnology).
19. Protein G and protein A-Sepharose (Amersham Pharmacia).
20. 33°C incubator.
21. Zeiss LSM510 confocal microscope (Carl Zeiss Inc.).
22. OptimaTM TLX (Beckman Instruments Inc.).

3. Methods

3.1. Preparation of Xenopus Egg Extracts

Xenopus egg extracts were prepared as previously described except that cytochalasin B was omitted (9,10).

1. M phase (cytostatic factor arrested) extracts are prepared from unfertilized eggs, and interphase extracts are prepared from parthenogenetically activated eggs that are electrically stimulated in 0.2X MMR by two 1-s pulses of 12 V alternating current followed by incubation for 10 min at room temperature. Eggs can also be activated with 0.1 $\mu\text{g}/\text{mL}$ A23187 in 0.5X MMR for 3 min.
2. Dilute the prepared extracts sevenfold with transport buffer containing protease inhibitors.
3. Centrifuge the extracts in the Optima TLX at 100,000g for 60 min at 4°C .
4. The supernatant is collected and stored at -80°C (see Note 1).

3.2. Visualization of the Golgi Apparatus in MDCK Cells

The Golgi apparatus in mammalian cells consists of stacked cisternae and tubular networks in the perinuclear region during interphase but diffuses throughout the cytoplasm at the onset of mitosis (11,12). In polarized MDCK cells, the Golgi apparatus appears as a ribbonlike structure adjacent to the nucleus during interphase. To visualize the Golgi apparatus in MDCK cells, we stably express galactosyltransferase (GT), a marker for trans-Golgi cisternae and the trans-Golgi network, fused to GFP (green fluorescence protein; GT-GFP).

3.2.1. Cloning

1. Complementary DNA (cDNA) encoding the first 60 amino acids of mouse GT is amplified from a mouse liver cDNA library using the polymerase chain reaction (PCR).
2. Insert the PCR fragment in-frame upstream of the EGFP cDNA in the EGFP-N1 vector.
3. MDCK cells are transfected by LipofectAMINE PLUS according to the manufacturer's instructions.

3.2.2. Selection of MDCK Cell Lines Stably Expressing GT-GFP

1. Select stable transfectants (MDCK-GT) in complete medium containing 300 $\mu\text{g}/\text{mL}$ Geneticin.
2. After 10 d, surviving cell colonies are isolated and screened visually for Golgi-localized fluorescence. Several positive clones are identified and expanded into cell lines for further experiments.

3.3. Reconstitution of Golgi Disassembly in Semi-Intact MDCK Cells

3.3.1. Preparation of Semi-Intact Cells (see **Note 2**)

1. Add 1×10^6 MDCK-GT cells to the upper chamber of each Transwell. Add 2.5 mL culture medium (Dulbecco's modified Eagle's medium supplemented with 10% fetal calf serum) to the lower chamber. The cells are incubated in a 37°C/5% CO₂ incubator for 3 to 4 d to form a tight polarized monolayer.
2. Incubate the cells with 5 µg/mL Taxol for 30 min at 37°C to stabilize microtubules.
3. Transfer the upper chamber to a 6-cm dish. Add 0.5 mL of 500 ng/mL preactivated SLO to the upper chamber for 20 min at 4°C.
4. After washing out the excess SLO three times with ice-cold phosphate-buffered saline, add 1 mL prewarmed TB containing 3 µg/mL propidium iodide for 20 min at 37°C to form pores in the plasma membranes. Of the total cytosol, 60% leaks out under these conditions, as determined by measurement of the leakage of cytosolic lactate dehydrogenase (**I3**; see **Note 3**). SLO-induced pores can be resealed with Ca²⁺ (see **Note 4**).

3.3.2. The Golgi Disassembly Assay

1. Incubate the permeabilized MDCK-GT cells with 1 M KCl in TB for 5 min at 4°C to remove peripheral membrane proteins.
2. Remove the polycarbonate membrane from the plastic side wall of the upper chamber with a knife and immerse it in TB with the cells facing upward. Cut the membranes into fragments 10 × 6 mm² and cut the lower right-hand corner of the pieces of the membranes to identify the surface on which the cells are cultured.
3. Incubate the fragments with 20 µL reaction mixture at 33°C for 80 min (see **Note 5**). The reaction mixture contains mitotic *Xenopus* egg extract (diluted to 4.5 to 5.5 mg proteins/milliliter in TB), ATP-regenerating system (1 mM ATP, 8 mM creatine kinase, and 50 µg/mL creatine phosphate), 1 mM guanosine 5'-triphosphate (GTP), and 1 mg/mL glucose.
4. Fix cells with 1% formaldehyde in TB for 20 min at room temperature.
5. View cells with an LSM 510 confocal microscope system.

3.4. Morphometric Analysis

1. The disassembly of the Golgi apparatus can be classified into three stages based on the fluorescence microscopic observations and the morphological properties of the Golgi membranes at each stage are easily distinguished in the same manner (**Fig. 2**):
 - a. Stage I (intact): a ribbonlike structure of the Golgi apparatus at the apical side of the cell.
 - b. Stage II (punctate): fragmented, punctate Golgi membranes. By electron microscopic observation, the punctate structures have an 0.8-µm average length and associate with microtubules at the apical side of the cells.
 - c. Stage III (dispersed): completely dispersed profiles of Golgi membranes. The Golgi membranes disperse throughout the cytoplasm. Some of the GT-GFP relocates to the endoplasmic reticulum (ER) membranes, which are identified by colocalization of GT-GFP with protein disulfide isomerase, a specific ER marker.
2. Count the number of cells at each stage. Be careful not to include nonpermeabilized cells, which are not stained by propidium iodide. We usually perform three independent experiments and calculate the means and standard deviations of the number of cells at stages I to III. Morphological changes of Golgi membranes can be expressed as the percentage of cells at stages I to III.

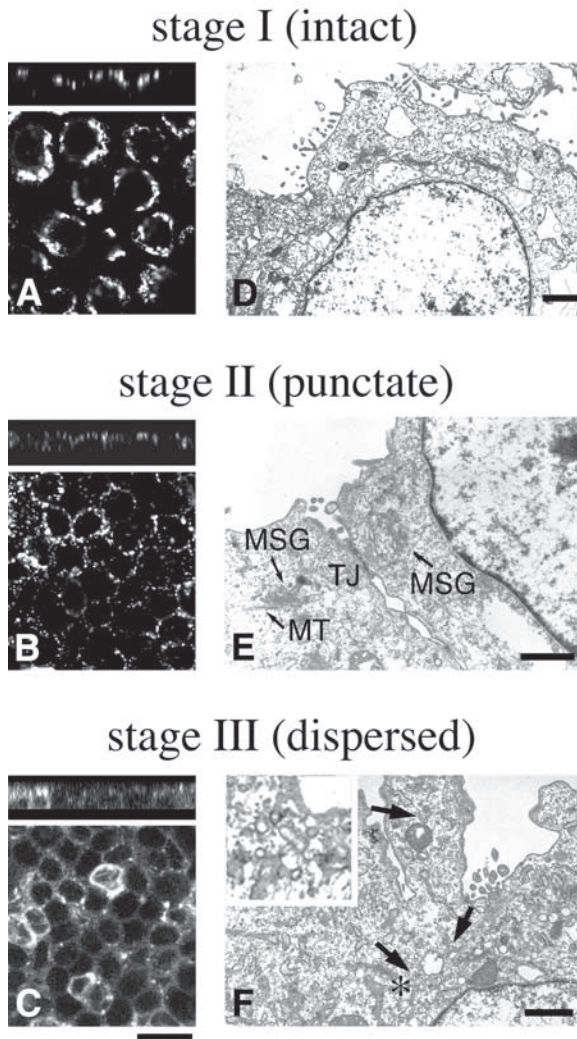


Fig. 2. Morphological dissection of the Golgi disassembly in semi-intact cells. Cells at stages I (intact), II (punctate), and III (dispersed) were observed by confocal (A–C) and electron (D–F) microscopy. In A–C, the lower panels show *x-y* images at the apical side of the cell, and the upper panels show *x-z* sectioning images. (A,D) Stage I (intact). Semi-intact MDCK-GT cells were incubated with TB and ATP at 33°C for 80 min. A large stack of cisternae of the Golgi apparatus is seen at the apical side of the cell. (B,E) Stage II (punctate) after 80-min incubation with mitotic *Xenopus* egg extracts containing *cdc2* kinase inhibitor (stage II). Ministacked Golgis (MSG) are seen at the apical side of the cell, where tight junction (TJ) is observed. Ministacked Golgi associates with microtubules (MT). (F) Stage III (dispersed) 80 min after incubation with mitotic *Xenopus* egg extracts. No stacked structure of the Golgi apparatus is observed, and only tubulovesicular structures (arrows), which probably derived from the Golgi, are seen. Inset represents the tubulovesicular structures (asterisk) at a higher magnification. Bars: (A–C) 20 μm ; (D–F) 1 μm . Reproduced with permission from **ref. 2**. © 2000 The Rockefeller University Press.

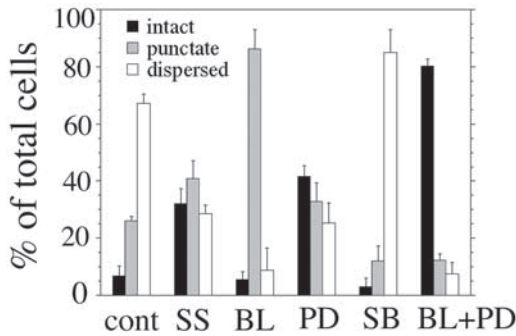


Fig. 3. Effect of protein kinase inhibitors on the Golgi disassembly. Semi-intact MDCK-GT cells were incubated with mitotic *Xenopus* egg extracts and ATP containing no inhibitor (control, cont), staurosporine (SS), butyrolactone 1 (BL), PD98059 (PD), SB203580 (SB), or BL + PD, respectively, at 33°C for 80 min. The cells were fixed, and morphometric analysis was performed. Reproduced with permission from ref. 2. © 2000 The Rockefeller University Press.

3.5. Biochemical Analysis for the Golgi Disassembly

3.5.1. Kinase Inhibitors

1. Incubate 1 M KCl-washed, semi-intact MDCK-GT cells with mitotic *Xenopus* extract, ATP-regenerating system, GTP, and glucose in the presence of protein inhibitors, 25 μ M staurosporine (protein kinase inhibitor), 20 μ M SB203580 (p38 mitogen-activated protein kinase inhibitor), 50 μ M PD98059 (mitogen-activated protein kinase kinase [MEK] inhibitor), 30 μ M butyrolactone I (cdc2 kinase inhibitor) at 33°C for 80 min.
2. Fix the cells with 1% formaldehyde and view by confocal microscopy.
3. Count the number of cells at stages I to III and calculate the percentage of cells at each stage (Fig. 3).

3.5.2. Immunodepletion of Kinases From Mitotic *Xenopus* Extracts

1. Incubate 20 μ L mouse anti-cdc2 antibody and 30 μ L protein G-Sepharose or 30 μ L of rabbit anti-MEK serum and 30 μ L of protein A-Sepharose at 4°C for 1 h with rotation.
2. Wash antibody-coupled beads with TB containing protease inhibitors (25 μ g/mL chymostatin, pepstatin A, leupeptin, and antipain) three times.
3. Incubate 150 μ L of mitotic *Xenopus* egg (4.5–5.5 mg proteins/mL) extracts with antibody-coupled beads at 4°C for 1 h with rotation.
4. Remove the beads by centrifugation (2300g or 5000 rpm, 4°C, 30 s) and transfer the supernatant to a new tube.
5. Add fresh antibody-coupled beads to the supernatant and incubate at 4°C for 1 h with rotation.
6. Repeat steps 4 and 5 twice in preparation of cdc2-depleted mitotic *Xenopus* extracts.
7. Remove the beads. Store the supernatant (cdc2- or MEK-depleted mitotic *Xenopus* extracts) at –80°C.
8. Check the depletion of cdc2 or MEK from mitotic *Xenopus* extracts by Western blotting.
9. Incubate 1M KCl-washed, semi-intact MDCK-GT cells with cdc2- or MEK-depleted *Xenopus* extract, ATP-regenerating system, GTP, and glucose at 33°C for 80 min.

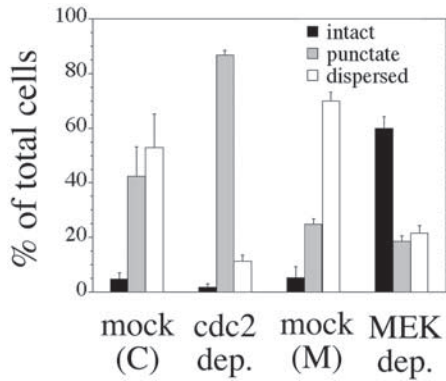


Fig. 4. Inhibition of the Golgi disassembly by *cdc2*- or MEK-depleted *Xenopus* egg extracts. Mock, *cdc2*- or MEK-depleted *Xenopus* egg extracts were applied to semi-intact cells and incubated at 33°C for 80 min. The cells were fixed, and morphometric analysis was performed. *Cdc2*-depleted extracts arrested the disassembly process at stage II (punctate), and MEK-depleted extracts did so at stage I (intact). Reproduced with permission from ref. 2. © 2000 The Rockefeller University Press.

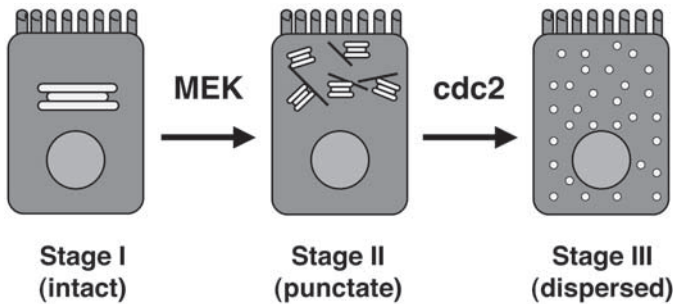


Fig. 5. Schematic model of Golgi disassembly.

10. Fix the cells with 1% formaldehyde and view by confocal microscopy.
11. Count the number of cells at stages I to III and calculate the percentage of cells at each stage (Fig. 4).

From the results using the Golgi disassembly assay based on the semi-intact cell system, Golgi disassembly is dissected into two sequential elementary steps, morphologically and biochemically (Fig. 5). The Golgi apparatus appears as a ribbonlike structure at the apical side of the cell but then fragments to form punctate structures in a MEK-dependent manner (stage I to II), followed by dispersion of the Golgi membranes and relocation to the ER in a *cdc2*-dependent manner (stage II to III).

4. Notes

1. MPF (M phase-promoting factor) activity varies between extracts. It can be measured by assaying phosphorylation of histone H1 (9,10).
2. The permeability of the cells can be altered by various experimental conditions: cell density, temperature, incubation time, cell type, and so on. It is important to maximize permeabilization before starting the experiments.
3. We use propidium iodide to check the permeability of the cells. Propidium iodide is a cell-impermeable dye that stains nucleic acids and can be excited with either mercury or xenon arc lamps or with an argon ion laser (Ex/Em = 535/617 [nm/nm]), making it suitable for two-color imaging in combination with GFP or fluorescein derivatives. Other impermeable dyes or fluorescence-labeled proteins, such as trypan blue, eosin, azure A, or tetramethylrhodamine isothiocyanate isomer R (TRITC)-labeled phalloidin, can be used to check the permeability of the cells (1,14,15). Leakage of endogenous cytosol can be examined by monitoring the activity of lactate dehydrogenase (135 kDa), a cytoplasmic enzyme, as described in refs. 8 and 13.
4. SLO-induced pores can be resealed with Ca^{2+} as demonstrated in refs. 16 and 17. By resealing pores after exposure of semi-intact cells with nuclear extracts and cytosol prepared from different cell types, the properties and fates of cells could be altered to other ones (17,18).
5. Because the assay is performed in 20 μL reaction mixture, we need to remove the TB from the membranes completely before incubation with the reaction mixture. We usually place a fragment of the membrane on a Kimwipe for a short time to absorb the TB and then transfer it on parafilm before quickly applying the reaction mixture. To avoid drying during the incubation at 33°C, it is necessary to cover the fragments with the lid of the culture dish. In addition, we place small pieces of wet Kimwipe under the cover to minimize moisture loss.

References

1. Kano, F., Takenaka, K., Yamamoto, A., Nagayama, K., Nishida, E., and Murata, M. (2000) MEK and Cdc2 kinase are sequentially required for Golgi disassembly in MDCK cells by the mitotic *Xenopus* extracts. *J. Cell Biol.* **149**, 357–368.
2. Kano, F., Sako, Y., Tagaya, M., Yanagida, T., and Murata, M. (2000) Reconstitution of brefeldin A-induced golgi tubulation and fusion with the endoplasmic reticulum in semi-intact Chinese hamster ovary cells. *Mol. Biol. Cell.* **11**, 3073–3087.
3. Kano, F., Nagayama, K., and Murata, M. (2000) Reconstitution of the Golgi reassembly process in semi-intact MDCK cells. *Biophys. Chem.* **84**, 261–268.
4. Bhakdi, S., Tranum-Jensen, J., and Sziegoleit, A. (1985) Mechanism of membrane damage by streptolysin-O. *Infect. Immunol.* **47**, 52–60.
5. Bhakdi, S., Weller, U., Walev, I., Martin, E., Jonas, D., and Palmer, M. (1993) A guide to the use of pore-forming toxins for controlled permeabilization of cell membranes. *Med. Microbiol. Immunol. (Berl.)* **182**, 167–175.
6. Lafont, F., Burkhardt, J. K., and Simons, K. (1994) Involvement of microtubule motors in basolateral and apical transport in kidney cells. *Nature* **372**, 801–803.
7. Pimplikar, S. W., Ikonen, E., and Simons, K. (1994) Basolateral protein transport in streptolysin O-permeabilized MDCK cells. *J. Cell Biol.* **125**, 1025–1035.
8. Wendland, M. and Subramani, S. (1993) Cytosol-dependent peroxisomal protein import in a permeabilized cell system. *J. Cell Biol.* **120**, 675–685.

9. Murray, A. W. and Kirschner, M. W. (1989) Cyclin synthesis drives the early embryonic cell cycle. *Nature* **339**, 275–280.
10. Chen, R. H. and Murray, A. W. (1997) Characterization of spindle assembly checkpoint in *Xenopus* egg extracts. *Methods Enzymol.* **283**, 572–584.
11. Shorter, J. and Warren, G. (2002) Golgi architecture and inheritance. *Annu. Rev. Cell Dev. Biol.* **18**, 379–420.
12. Rossanese, O. W. and Glick, B. S. (2001) Deconstructing Golgi inheritance. *Traffic* **2**, 589–596.
13. Schnaar, R. L., Weigel, P. H., Kuhlenschmidt, M. S., Lee, Y. C., and Roseman, S. (1978) Adhesion of chicken hepatocytes to polyacrylamide gels derivatized with *N*-acetylglucosamine. *J. Biol. Chem.* **253**, 7940–7951.
14. Ahnert-Hilger, G., Bhakdi, S., and Gratzl, M. (1985) Minimal requirements for exocytosis. A study using PC 12 cells permeabilized with staphylococcal alpha-toxin. *J. Biol. Chem.* **260**, 12,730–12,734.
15. Ahnert-Hilger, G., Bader, M. F., Bhakdi, S., and Gratzl, M. (1989) Introduction of macromolecules into bovine adrenal medullary chromaffin cells and rat pheochromocytoma cells (PC12) by permeabilization with streptolysin O: inhibitory effect of tetanus toxin on catecholamine secretion. *J. Neurochem.* **52**, 1751–1758.
16. Walev, I., Bhakdi, S. C., Hofmann, F., et al. (2001) Delivery of proteins into living cells by reversible membrane permeabilization with streptolysin-O. *Proc. Natl. Acad. Sci. USA* **98**, 3185–3190.
17. Hakelien, A. M., Landsverk, H. B., Robl, J. M., Skalhegg, B. S., and Collas, P. (2002) Reprogramming fibroblasts to express T-cell functions using cell extracts. *Nat. Biotechnol.* **20**, 460–466.
18. Gaustad, K. G., Boquest, A. C., Anderson, B. E., Gerdes, A. M., and Collas, P. (2004) Differentiation of human adipose tissue stem cells using extracts of rat cardiomyocytes. *Biochem. Biophys. Res. Commun.* **314**, 420–427.

Exploring RNA Virus Replication in *Xenopus* Oocytes

Andrea V. Gamarnik and Raul Andino

Summary

Microinjection of poliovirus RNA in *Xenopus* oocytes initiates a complete and authentic viral replication cycle that yields newly synthesized infectious virus. This system can be used to study the molecular mechanism of the different steps involved in virus replication. Interestingly, viral replication only occurs if poliovirus RNA is coinjected with factors present in HeLa extracts. We have determined that two HeLa cell factors are required for viral replication in oocytes, one involved in initiation of translation (polio translation factor) and the other in RNA synthesis. Thus, microinjection in oocytes provides a strategy to identify and further analyze the function of these host cell factors and to biochemically dissect the mechanism of initiation of poliovirus translation and RNA synthesis. Here, we review protocols, approaches, and potential issues that can be addressed using the oocyte system.

Key Words: *Xenopus* oocytes; RNA virus; viral RNA replication; negative strand RNA detection; viral protein synthesis; HeLa cell factors; infectious viral particles; IRES-dependent translation.

1. Introduction

Microinjection of viral RNAs into *Xenopus* oocytes constitutes a powerful system to study mechanistic aspects of viral replication. We have previously demonstrated that stage VI oocytes support replication of different members of the Picornaviridae family (1–4). These viruses followed a replication strategy common to other positive-strand RNA viruses (Fig. 1; ref. 5). After entry, the genomic RNA is released in the cytoplasm of the cell and functions as messenger RNA (mRNA) directing the synthesis of a large polypeptide, which is proteolytically processed to yield mature viral proteins.

The same RNA molecule is then amplified in a two-step process: first, its complementary negative strand is synthesized, and then the negative-strand RNA is used as a template to generate new molecules of positive-strand RNA (for review, see ref. 6). The synthesis of both negative- and positive-strand RNA is catalyzed by the viral RNA-dependent RNA polymerase. All these steps of replication, including the forma-

From: *Methods in Molecular Biology*, vol. 322: *Xenopus Protocols: Cell Biology and Signal Transduction*
Edited by: X. J. Liu © Humana Press Inc., Totowa, NJ

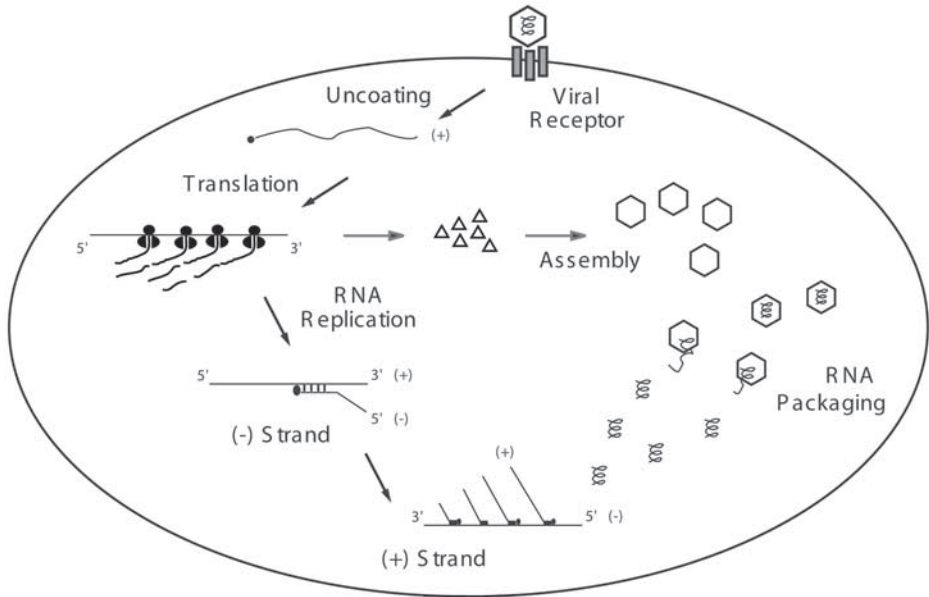


Fig. 1. Schematic representation of the replication of a positive-strand RNA virus. Infection starts with the binding of the virus to specific receptors on the cell surface. The viral RNA is uncoated and delivered into the cytoplasm. Viral RNA is translated to yield the structural and nonstructural viral proteins. Subsequently, cellular and viral proteins enable replication of the genomic RNA, which serves as a template to synthesize a complementary negative-strand RNA, which is employed to amplify the viral genome. Finally, the newly synthesized positive-strand RNA is packaged into newly synthesized virions.

tion of new infectious particles, can be faithfully reproduced in the oocyte system. Infectious virus is detected as early as 6 h postinjection (100 PFU/oocyte), and the amount of virus increases exponentially, reaching a maximum of 5×10^5 PFU/oocyte after 15 h.

This chapter describes the methods and techniques routinely used in our laboratory to analyze each step of poliovirus replication and provides some practical suggestions to identify and characterize host factors involved in these processes. We believe that this methodology could be easily extrapolated to study the replication of other RNA viruses.

2. Materials

1. Collagenase type I, 250 U/mg (CLS 1; Worthington Biochemical Corp.).
2. Proteinase K, stock solution (2 mg/mL); keep at -20°C .
3. Actinomycin D, 5-mg/mL stock solution in ethanol. Store the stock solution in a foil-wrapped vial at -20°C (it is light sensitive).
4. Phenol/chloroform (1/1) buffer equilibrated to pH 6.7.
5. [^{35}S] methionine 15 mCi/mL.
6. [α - ^{32}P] Guanosine 5'-triphosphate (GTP) 10 mCi/mL.

7. Buffer H (10X stock solution keep at -4°C): 100 mM HEPES, pH 7.9, 500 mM KCl, 20 mM ethylenediaminetetraacetic acid (EDTA), 5 mM phenylmethylsulfonyl fluoride (PMSF), 10 mM dithiothreitol (DTT), 5 mM Triton X-100.
8. Modified Barth's solution (MBS): 7.5 mM Tris-HCl at pH 7.6, 88 mM NaCl, 1 mM KCl, 2.4 mM NaHCO_3 , 8.2 mM MgSO_4 , 0.33 mM $\text{Ca}(\text{NO}_3)_2$, 0.4 mM CaCl_2 , 100 U/mL penicillin, 100 $\mu\text{g}/\text{mL}$ streptomycin. 2% Ficoll-400.
9. Buffer H: 10 mM HEPES at pH 7.9, 50 mM KCl, 2 mM EDTA, 0.5 mM PMSF, 1 mM DTT, 0.5 mM Triton X-100.
10. Hypotonic buffer: 20 mM HEPES at pH 7.4, 10 mM KCl, 1.5 mM $\text{Mg}(\text{CH}_3\text{CO}_2)_2$, 2 mM DTT.
11. TENSK: 50 mM Tris-HCl, pH 7.5, 5 mM EDTA, 100 mM NaCl, 1% sodium dodecyl sulfate (SDS), 200 $\mu\text{g}/\text{mL}$ proteinase K.
12. TSE buffer: 50 mM Tris-HCl, pH 7.5, 100 mM NaCl, 0.1 mM EDTA.
13. TE buffer: 10 mM Tris-HCl, pH 7.5, 1 mM EDTA.
14. Restriction enzymes.
15. T7 RNA polymerase.
16. SP6 RNA polymerase.
17. 10 mM Nucleotide triphosphate (NTP) mix.
18. Cap analog GpppG (10 mM).
19. Nitrocellulose membranes.
20. Electrophoresis equipment.
21. Dounce homogenizer.
22. HeLa S3 cells. 21. Tissue culture facilities.

3. Methods

3.1. Translation of Viral RNAs in *Xenopus Oocytes*

The first step of positive-strand RNA virus replication is the translation of the genomic RNA. Viral RNAs either resemble cellular mRNAs by having a cap structure at the 5' end or have different RNA elements, which initiate translation by cap-independent mechanisms (7). In the case of picornaviruses, the 5' untranslated region (UTR) bears an internal ribosomal entry site (IRES) that directs the landing of the ribosomes internally without scanning from the 5' end (8,9). A set of canonical and noncanonical (IRES-specific) translation factors is required for efficient IRES-mediated translation (10).

The requirement of specific proteins during internal initiation of translation varies in different viruses, and the identification of such proteins is an important step in understanding the molecular mechanism of the process. Furthermore, it has been proposed that the interaction with some of these factors determines tissue tropism and pathogenesis (11–13). Therefore, an initial and important question to be addressed is whether the oocyte translation machinery is capable of recognizing and translating the viral RNA of interest. As an example, we describe below a procedure to isolate poliovirus RNA from infected cells and to test the ability of oocytes to translate this viral RNA.

3.1.1. Purification of Poliovirus RNA From Virions

1. Infect a suspension culture of HeLa S3 cells (2×10^7 cells, about 50 mL of confluent culture) by adding 500 μL poliovirus stock (1×10^8 viruses).

2. Harvest cells 15 h postinfection and lyse the cells (50 mL) by three cycles of freezing and thawing in the same tissue culture medium.
3. Clarify the lysate by centrifugation at 9000g for 5 min and use the total volume to infect a suspension culture of 4×10^8 cells (1 L).
4. Incubate the infected cells at 37°C for 7 h and harvest them by centrifugation at 2000g for 10 min.
5. Wash the cell pellet with cold phosphate-buffered saline (PBS) and lyse the cells in 10 mM Tris-HCl, pH 7.5, 10 mM NaCl, and 0.1% Nonidet P-40. Nuclei and cellular insoluble debris are removed by centrifugation at 10,000g for 10 min. SDS is added to the supernatant to a final concentration of 0.5%.
6. Precipitate viruses by centrifugation for 1 h at 200,000g. Precipitated viruses should be resuspended overnight in 2 mL TSE buffer.
7. Purify viruses by CsCl gradient. To prepare 10 mL gradient, mix 1 mL of nonionic detergent Brij 10%, CsCl to final density $\delta = 1.33$ g/cc in TSE-0.5% SDS, and 2 mL viral pellets. Spin the gradient 17 h at 35,000 to 40,000g at 20°C. Collect 500- μ L fractions and measure optical density (OD) at 280 nm. The virus will be recovered in the middle of the gradient ($\delta = 1.35$ g/cc). Pool fractions containing the virus and dialyze against TSE buffer. Treat the sample with proteinase K (200 μ g/mL) to release the RNA.
8. Extract viral RNA with phenol-chloroform (1/1). Add 2.5 volumes of ethanol, 1/10 volumes of 3M sodium acetate, incubate 5 min on dry ice, and spin at 14,000 rpm for 5 min in a microfuge. Resuspend the pellet in TE buffer and store at -70°C. It is recommended to confirm the integrity of the RNA by electrophoresis of an aliquot on 0.7 to 1% agarose gels and visualize by ethidium bromide.

Similar procedures can be used to purify RNA from other picornaviruses using the appropriate host cell.

3.1.2. Microinjection of Viral RNA Into Oocytes

Oocytes are surgically isolated and enzymatically defolliculated by incubation with 2 mg/mL collagenase for 3 h at room temperature. Defolliculated oocytes are washed five times with MBS and kept in MBS at 17°C. Stage VI oocytes should be sorted for microinjection. Examine the oocytes under the dissecting microscope and separate good oocytes, which are large and have a symmetrical, even pigmentation. The animal hemisphere should be dark brown or black without white spots. The vegetal hemisphere should be yellow to pale white. To evaluate translation of the viral RNA, the oocytes can be labeled with [³⁵S] methionine as follows:

1. Microinject about 100 oocytes with 25 nL viral RNA (0.5 μ g/ μ L) each using a standard microinjection apparatus (we use the Nanoliter 2000, which delivers variable volumes from 5 to 60 nL).
2. For protein labeling, microinjected oocytes should be incubated in MBS containing 400 μ Ci [³⁵S] methionine per milliliter of media.
3. Take 20 oocytes at different times after microinjection (from 2 to 24 h) and lyse them “mechanically” in 200 μ L buffer H.
4. Remove debris by centrifugation at 5000g for 5 min, and proteins can be immunoprecipitated using antibodies directed against viral proteins using standard procedures (see **Note 1**).
5. Immunoprecipitated complexes should be resuspended in Laemmli sample buffer, incubate at 100°C for 5 min, and analyze by SDS polyacrylamide gel electrophoresis (PAGE).

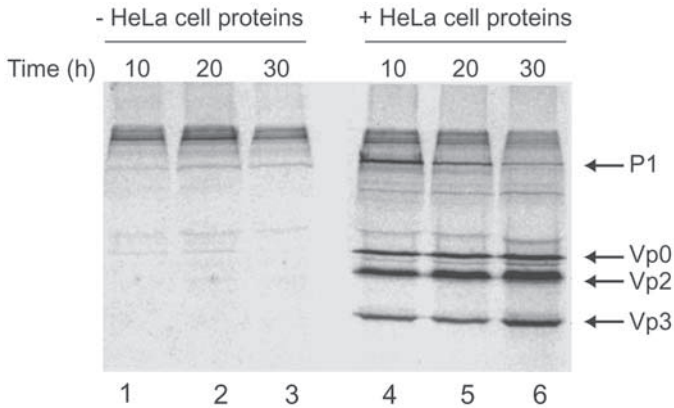


Fig. 2. Translation of poliovirus RNA in *Xenopus* oocytes requires additional host factors. SDS-PAGE analysis of [³⁵S]-labeled viral proteins synthesized in oocytes is shown. Oocytes were microinjected with poliovirus RNA in the absence (lanes 1–3) or presence (lanes 4–6) of HeLa cell extracts and incubated with [³⁵S] methionine at 22°C for 10 h (lanes 1 and 4), 20 h (lanes 2 and 5), or 30 h (lanes 3 and 6). Cytoplasmic extracts were immunoprecipitated with antiserum directed against capsid proteins and analyzed on gels. The relative migration of poliovirus capsid proteins (P1, Vp0, Vp2, and Vp3) is indicated.

To analyze whether specific host factors are required for viral RNA translation in oocytes, cytoplasmic extracts obtained from specific cell lines can be coinjected with the viral RNA. Next, we describe the procedure to prepare cytoplasmic extracts from HeLa cells.

1. Harvest 4×10^7 cells (100 mL suspension culture) by centrifugation and wash three times with cold PBS.
2. Resuspend the cell pellet in 2 vol of hypotonic buffer, incubate on ice for 20 min, and then disrupt cells with 20 strokes with a glass Dounce homogenizer.
3. Obtain a postnuclei supernatant by centrifugation at 5000g for 10 min at 4°C. This supernatant is submitted to a second centrifugation (15,000g for 20 min). The resulting supernatant contains approx 10 µg/µL of cytoplasmic proteins.
4. Transfer the supernatant to a clean tube and store at –70°C.

To evaluate the effect of cytoplasmic extracts on viral translation efficiency, the viral RNA is mixed with different amounts of the cytoplasmic extract just before microinjection. In the case of HeLa cell extracts, it is possible to mix viral RNA with cytoplasmic proteins up to a ratio of 1/1 v/v; however, different cell lines may contain variable amounts of ribonucleases that could degrade the RNA during the microinjection process. In those cases, two microinjections into the same oocytes, one with the viral RNA and a second one with the cell cytoplasmic extract, is recommended. The PAGE analysis of poliovirus protein synthesized in microinjected oocytes in the presence and absence of cytoplasmic extracts is shown in [Fig. 2](#).

3.2. Replication of Viral RNA in Oocytes

If appropriate and efficient synthesis and processing of viral proteins takes place in oocytes, the next step is to evaluate whether efficient viral RNA replication takes place in the oocytes supplemented with HeLa cell extracts. To determine *de novo* synthesis of viral RNA in oocytes, we developed two different methods. One method examines *de novo* synthesis of all viral RNAs in oocytes, and the other method is specifically designed to evaluate negative-strand RNA synthesis (3). We describe next a typical protocol for each of the two methods using poliovirus.

3.2.1. To Measure All Newly Synthesized Viral RNA in Oocytes

1. Microinject about 100 oocytes with 50 nL viral RNA (0.5 $\mu\text{g}/\mu\text{L}$) each together with HeLa cell cytoplasmic extracts (10 $\mu\text{g}/\mu\text{L}$) and mix in a 1/1 ratio.
2. After 30 min, microinject the oocytes a second time with 20 nL [α - ^{32}P] GTP 10 mCi/mL and incubate in MBS buffer containing 50 $\mu\text{g}/\text{mL}$ of actinomycin D (see Note 2).
3. Incubate the oocytes between 28 and 30°C and remove about 25 oocytes at different times between 6 and 20 h.
4. Prepare oocyte extracts by mechanical disruption in 400 μL TENS buffer and keep the extract at -20°C until all time-points are collected (see Note 3).
5. After the last sample is collected, incubate the extracts at 37°C for 1 h. Clarify the samples by centrifugation for 5 min at 14,000g. Take the supernatant carefully without disrupting the pellet. Extract the RNA from the supernatant with an equal volume of phenol-chloroform (1/1) and precipitate with ethanol.
6. Resuspend the RNA in 50 μL of TE buffer, load 25- μL aliquots of each sample on a native agarose 0.7% gel, dry the gel (using low heating, below 65°C) on top of a nitrocellulose membrane and autoradiograph (see Note 4). Ribosomal RNA, visualized by ethidium bromide before drying the gel, can be used as an internal loading control for RNA extraction.

Typically, two defined radiolabeled bands will be observed (see Fig. 3). The band of lower mobility (upper band) corresponds to the double-stranded RNA, containing both the genomic RNA and the complementary negative strand. This double-stranded RNA is an intermediate of viral replication (known as the replicative form) and is stable in oocytes. The second band, with faster mobility, corresponds to the positive-strand RNA that is synthesized in large excess relative to the negative-strand RNA.

3.2.2. To Detect Viral Negative-Strand RNA Synthesis in Oocytes

In this assay, ^{32}P -labeled RNA is synthesized *in vitro* using a plasmid encoding the full-length poliovirus as template (pXpA). This plasmid contains the T7 RNA polymerase promoter and can be used for runoff transcription as follows:

1. Linearize 5 to 10 μg of DNA plasmid with the restriction enzyme *MluI*, which cleaves at a single site at the 3' end of the poliovirus sequence.
2. Prepare transcription reaction by mixing 10 μL 5X transcription buffer, 5 μL ribonucleotide mix (10 mM adenosine triphosphate [ATP], uridine triphosphate [UTP], and cytidine triphosphate [CTP] and 2 mM GTP), 5 μL of linearized DNA (0.2 $\mu\text{g}/\mu\text{L}$), 2 μL ^{32}P GTP 10 mCi/mL, 2 μL ribonuclease inhibitor (20 U), 5 μL T7 RNA polymerase (100 U), and water to a final volume of 50 μL . Mix the components and incubate the reaction for 1 h at 37°C.

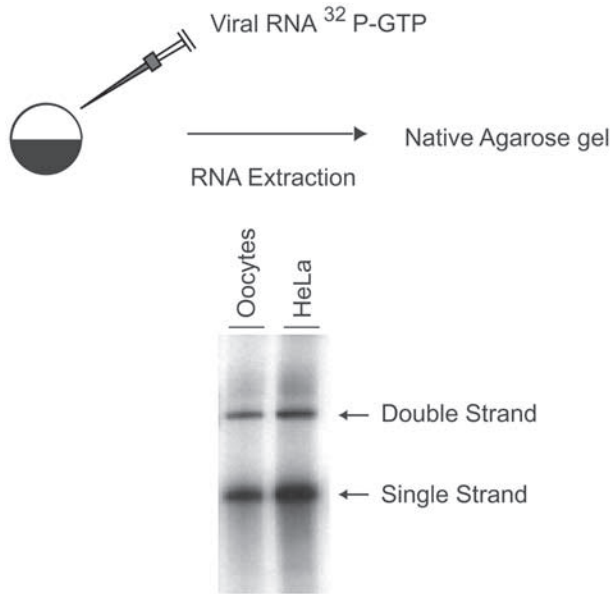


Fig. 3. *De novo* synthesis of poliovirus RNA in oocytes. Oocytes were microinjected with poliovirus RNA, HeLa cell extracts, and [α -³²P] GTP. Injected oocytes were incubated for 10 h at 27°C, and total cytoplasmic RNA was analyzed on an agarose gel. For comparison, poliovirus RNA was synthesized *in vitro* using viral-infected HeLa cell crude replication complex.

3. After incubation, add 50 μ L water and extract with 100 μ L phenol-chloroform. Precipitate the RNA with 2.5 volumes of ethanol and recover the RNA by centrifugation at 14,000 rpm for 5 min after addition of 1/10 volume of 3 M sodium acetate and incubate for 5 min on dry ice.
4. Resuspend the radiolabeled RNA in 50 μ L TE and examine the incorporation of GTP by loading 1 μ L of the sample in a 0.7% agarose gel. Run the gel 30 min at 100 V, dry the gel, and expose to film. The radiolabeled RNA should be visible after 1 to 10 min of exposure.
5. Microinject about 300 oocytes with 50 nL of the radiolabeled RNA per oocyte together with HeLa cell extracts (10 μ g/ μ L) (*see Note 5*).
6. Incubate oocytes between 28 and 30°C, take 30 oocytes every 2 to 3 h, ranging from 0 to 20 h, and lyse them in 400 μ L TENS buffer. Each lysed sample should be frozen until all the samples are taken.
7. Incubate the extracts at 37°C for 1 h for proteinase K digestion. Clarify the extract by centrifugation for 5 min at 14,000 rpm. Transfer the supernatant carefully to a new tube without disrupting the pellet. Extract the RNA with an equal volume of phenol-chloroform (1/1) and precipitate with ethanol.
8. Resuspend samples in 50 μ L TE and analyze 25 μ L by electrophoresis through 0.7% native agarose gel. Dry on a nitrocellulose membrane and autoradiograph as described in **Subheading 3.2.1.** (*see Note 4*).

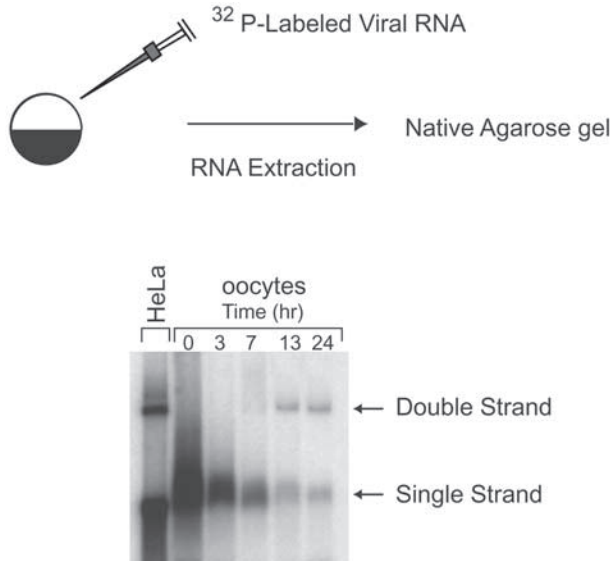


Fig. 4. Synthesis of viral negative-strand RNA in *Xenopus* oocytes. Oocytes were microinjected with in vitro transcribed ^{32}P -labeled poliovirus RNA together with HeLa extracts, and the conversion of the input RNA into a double-stranded form was analyzed as a function of time by native agarose gel electrophoresis, as indicated on the top. Single-stranded viral RNA (ssRNA) and the double-stranded replicative form (RF) are indicated on the left.

In this assay, the input RNA is first used for translation, then when enough viral proteins are made, the viral polymerase produces negative-strand RNAs complementary to the input RNA. These negative strands will anneal to the radiolabeled positive strands and will be detected by a shift in the mobility of the radiolabeled RNA on the agarose gel. This method only detects newly synthesized negative strand because the new positive strand produced by the viral polymerase will be unlabeled and therefore not visible on the autoradiograph. In **Fig. 4**, we see a typical analysis of negative-strand synthesis using poliovirus. In this case, the input RNA is degraded as a function of the time; after 6 h, a new RNA species appears that corresponds to the double-stranded RNA.

3.3. Production of Infectious Viral Particles in Oocytes

The next replication step that can be analyzed is the production of infectious viral particles.

1. Microinject about 100 oocytes with 50 nL purified viral RNA ($0.5 \mu\text{g}/\mu\text{L}$) together with HeLa cell extracts ($10 \mu\text{g}/\mu\text{L}$) (*see Note 6*). Mix the RNA and proteins 1/1 (v/v) just before microinjection.
2. Incubate oocytes at 30°C and remove about 20 oocytes per time-point up to 20 h.
3. Disrupt the oocytes mechanically with $200 \mu\text{L}$ PBS and remove cell debris by centrifugation at $5000g$ 5 min.

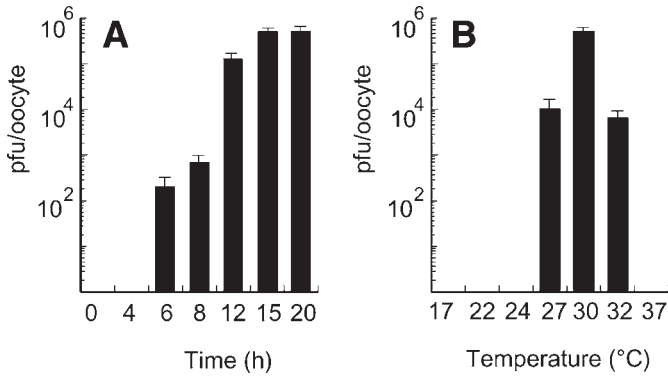


Fig. 5. Microinjection of poliovirus RNA into oocytes yields newly synthesized infectious virus. (A) Poliovirus RNA was injected into oocytes and incubated at 30°C for 0, 4, 6, 8, 12, 15, and 20 h. Infectious poliovirus titers were determined by plaque assay in HeLa cells. Viral titers are expressed as the logarithm of plaque forming units (PFUs) per oocyte. (B) Essentially as described in (A), but the microinjected oocytes were incubated for 20 h at 17, 22, 24, 27, 30, 32, and 37°C.

4. Sterilize the oocyte cytoplasmic extract by passage through a 0.22- μ m pore-size filter. The presence of infectious particles should be determined by plaque assays using standard procedures.

Viral particle formation in oocytes can be detected as soon as 6 h after microinjection, and the viral titer increases for up to 20 h at 30°C (see Fig. 5).

3.4. Requirements for Viral IRES-Dependent Translation in Oocytes

Microinjection of viral RNA into oocytes provides a powerful tool to characterize host proteins involved in viral RNA translation. Here, we describe a protocol to test the requirement of specific host factors for IRES-dependent viral translation using a reporter gene flanked by viral sequences.

1. Insert a luciferase gene into the commercially available vector pSP64T between the 5' and 3' UTRs of the *Xenopus* β -globin sequences using standard molecular biology techniques (14). This pSP64-Luc vector will be used to produce Cap-Luc-RNA that will serve as a control for microinjections. In addition, this vector will be used to insert the viral sequences of interest.
2. Replace the 5' UTR of β -globin in pSP64-Luc by the viral sequence of choice downstream of the SP6 RNA polymerase promoter (see Note 7). In some viruses, the 3' UTR could modulate the efficiency of translation. Therefore, it could be of interest to replace the 3' UTR of β -globin by the 3' UTR of the respective virus.
3. Linearize 5 to 10 μ g of the plasmid pSP64-IRES-Luc and pSP64-Luc with an appropriate restriction endonuclease that cleaves downstream of the insert (such as Sal I).
4. Prepare transcription reaction by mixing 10 μ L 5X transcription buffer, 5 μ L ribonucleotide mixture (10 mM), 5 μ L linearized DNA encoding the IRES-Luc (0.2 μ g/ μ L), 2 μ L of ribonuclease inhibitor (20 U), SP6 RNA polymerase (10 U), and water to a final vol-

ume of 50 μL . Mix the components gently and incubate the reaction 1 h at 37°C. For capped RNA, replace the ribonucleotide mixture by a solution containing 10 mM adenosine triphosphate, 10 mM UTP, 10 mM CTP, and 4 mM GTP and add 5 μL cap analog GpppG (10 mM) (see **Note 7**).

5. Extract the RNA with phenol-chloroform and precipitate with ethanol. Aliquot the RNA and store at -70°C . Typically, this transcription reaction would yield about 20 to 50 μg RNA.
6. Inject 50 oocytes with 50 nL IRES-Luc or Cap-Luc RNA (0.5 $\mu\text{g}/\mu\text{L}$) mixed 1/1 with buffer or cytoplasmic cell extracts. Incubate oocytes at 25°C.
7. Measure translation of microinjected RNAs as a function of the time between 4 and 20 h. For each time-point, take 10 oocytes and lyse them mechanically in 100 μL buffer H. Remove debris by centrifugation at 5000g for 5 min, and luciferase activity can be measured in 20 to 100 μL of the supernatant using luciferase substrate as recommended by the manufacturer.

Translation in oocytes of IRES-Luc RNAs carrying sequences from different viruses is illustrated in **Fig. 6**. The absolute requirement of additional host proteins is evident for poliovirus, rhinovirus, and coxsackievirus IRES elements.

3.4.1. Characterization of cis- and trans-Acting Factors Involved in IRES Activity

The common approach to identifying factors that participate in IRES-mediated translation has been to analyze RNA-binding proteins by either ultraviolet crosslinking or mobility shift assays. A major limitation of this approach is the assumption that the specific translation factor binds directly to the RNA. We have pursued a functional approach using *Xenopus laevis* oocytes. In previous experiments, we showed that microinjection of poliovirus RNA into oocytes leads to a complete replication cycle, provided that HeLa cell extract is coinjected with the viral RNA. Using this system, we determined that at least two different activities from HeLa cells are required for poliovirus replication in oocytes, one participating in viral translation and the other in RNA synthesis (2).

We have further characterized the activity necessary for translation of poliovirus RNA in *Xenopus* oocytes (poliovirus translation factor [PTF]) by examining the dependence of different picornavirus IRES elements on PTF and found that enteroviruses and rhinoviruses require PTF, whereas cardioviruses can function efficiently in the oocyte system without further supplementation (unpublished data, 1999). Using standard protein chromatography we found that fractions containing PTF activity do not contain canonical or noncanonical translation factors that participate in IRES-mediated translation. Furthermore, we can show that PTF activity is part of an initiation complex formed by interaction through the ribosome rather than binding to the viral RNA itself. This example demonstrates that the oocyte system can be used as a bioassay to study factors required for IRES-mediated translation.

In addition, the oocyte system can be used to investigate the role of proteins even if they are already present in the oocytes. In this case, it would be possible to coinject the IRES-Luc RNA with antibodies, decoy RNAs, peptides, or other molecules (2,15).

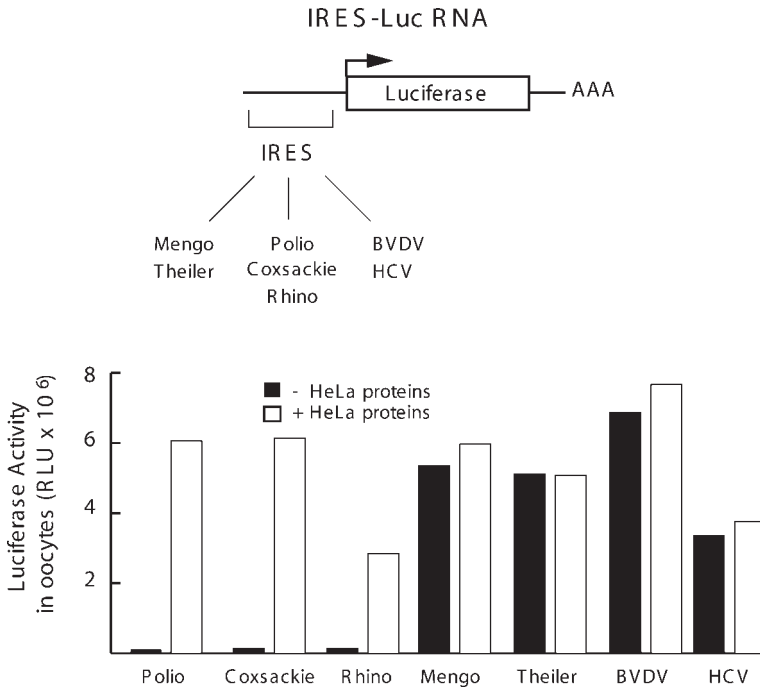


Fig. 6. Translation activity of different viral IRES in *Xenopus* oocytes. On the top is a schematic representation of the RNA constructs used. IRES sequences from poliovirus, rhinovirus, coxsackievirus, mengovirus, Theiler's virus, bovine viral diarrhea virus (BVDV), and hepatitis C virus (HCV) were incorporated upstream of the luciferase gene. Each RNA construct was microinjected in oocytes in the presence or absence of HeLa cell extracts, and luciferase activity was expressed in relative light units (RLUs).

4. Notes

1. A large amount of endogenous proteins will be also labeled in the oocytes, which results in high background. Therefore, immunoprecipitations rather than analysis of the total labeled proteins by SDS-PAGE followed by autoradiography are recommended for analysis of viral protein synthesis in oocytes.
2. Actinomycin D inhibits the RNA synthesis from any DNA-dependent RNA polymerase, which reduces the amount of oocyte RNA synthesis and favors the synthesis of viral RNA.
3. Add fresh proteinase K (5 mg) just before use.
4. Before loading the gel, it is optional but recommended to briefly treat the samples containing the radiolabeled RNA with ribonuclease-free deoxyribonuclease (5 min at room temperature). This procedure results in gels with fewer undesired bands.
5. Replication of purified viral RNA from virions is more efficient than from in vitro transcribed RNA. This difference is because of the presence of two additional Gs at the 5' end of the in vitro transcript that are part of the T7 RNA polymerase promoter. To increase efficiency of positive-strand synthesis, a hammerhead ribozyme could be incorporated to remove the additional nucleotides after RNA synthesis (16).

6. The initiation of translation of certain viruses requires sequences present inside the coding sequences (such as the IRES of hepatitis C virus and bovine viral diarrhea virus); therefore, if the IRES of interest is not well defined, it is recommended to design constructs including different segments of the coding sequence.
7. Synthetic RNAs can be capped by incorporation of the cap analogs G(5')pppG(5') or the methylated m7G(5')pppG(5') by the RNA polymerase during *in vitro* transcription. As oocytes will methylate the microinjected capped RNA, the use of the less-expensive G(5')pppG(5') is sufficient.

References

1. Gamarnik, A. V. and Andino, R. (1996) Replication of poliovirus in *Xenopus* oocytes requires two human factors. *EMBO J.* **15**, 5988–5998.
2. Gamarnik, A. V. and Andino, R. (1997) Two functional complexes formed by KH domain containing proteins with the 5' noncoding region of poliovirus RNA. *RNA* **3**, 882–892.
3. Gamarnik, A. V. and Andino, R. (1998) Switch from translation to RNA replication in a positive-stranded RNA virus. *Genes Dev.* **12**, 2293–1304.
4. Gamarnik, A. V., Boddeker, N., and Andino, R. (2000) Translation and replication of human rhinovirus type 14 and mengovirus in *Xenopus* oocytes. *J. Virol.* **74**, 11,983–11987.
5. Baltimore, D. (1984) Molecular genetics of poliovirus. *Rev. Infect. Dis.* **6(Suppl. 2)**, 484–486.
6. Johnson, K. A. and Sarnow, P. (1995) Viral RNA synthesis, in *Human Enterovirus Infections* (Rotbart, H., ed.), IASM, Washington, DC, pp. 95–112.
7. Gale, M., Jr., Tan, S. L., and Katze, M. G. (2000) Translational control of viral gene expression in eukaryotes. *Microbiol. Mol. Biol. Rev.* **64**, 239–280.
8. Chen, C. Y. and Sarnow, P. (1995) Initiation of protein synthesis by the eukaryotic translational apparatus on circular RNAs. *Science* **268**, 415–417.
9. Trono, D., Pelletier J., Sonenberg N., Baltimore D. (1988) Translation in mammalian cells of a gene linked to the poliovirus 5' noncoding region. *Science* **241**, 445–448.
10. Andino, R., Boddeker, N., Silvera D., Gamarnik, A. V. (1999) Intracellular determinants of picornavirus replication. *Trends Microbiol.* **7**, 76–82.
11. Gromeier, M., Alexander, L., and Wimmer, E. Internal ribosomal entry site substitution eliminates neurovirulence in intergeneric poliovirus recombinants. *Proc. Natl. Acad. Sci. USA* **93**, 2370–2375.
12. Kauder, S. E. and Racaniello, V. R. (2004) Poliovirus tropism and attenuation are determined after internal ribosome entry. *J. Clin. Invest.* **113**, 1743–1753.
13. Pilipenko, E. V., Pestova, T. V., Kolupaeva, V. G., et al. (2000) A cell cycle-dependent protein serves as a template-specific translation initiation factor. *Genes Dev.* **14**, 2028–2045.
14. Krieg, P. A. and Melton, D. A. (1984) Functional messenger RNAs are produced by SP6 *in vitro* transcription of cloned cDNAs. *Nucleic Acids Res.* **12**, 7057–7070.
15. Silvera, D., Gamarnik, A. V., and Andino, R. (1999) The N-terminal K homology domain of the poly(rC)-binding protein is a major determinant for binding to the poliovirus 5'-untranslated region and acts as an inhibitor of viral translation. *J. Biol. Chem.* **274**, 38,163–38,170.
16. Herold, J. and Andino, R. (2000) Poliovirus requires a precise 5' end for efficient positive-strand RNA synthesis. *J. Virol.* **74**, 6394–6400.

Study of Apoptosis In Vitro Using the *Xenopus* Egg Extract Reconstitution System

Paula Deming and Sally Kornbluth

Summary

It was first shown by Newmeyer and colleagues in the 1990s that the molecular events of apoptosis could be reconstituted in vitro using *Xenopus* egg extracts. When the egg extract is allowed to incubate at room temperature for an extended time, the biochemical events of apoptosis are activated spontaneously. The features of apoptosis in the *Xenopus* reconstitution system mimic those that occur in mammalian cells: Cytochrome c is released from the mitochondria, caspases are activated, cellular substrates are cleaved, and added nuclei are fragmented. Moreover, these apoptotic events can be inhibited by addition of antiapoptotic proteins such as Bcl-2 and conventional caspase inhibitors (e.g., ZVAD-fmk). The mitochondria, which are triggered to release cytochrome c by as-yet-unknown signals in the extract, are essential for induction of the spontaneous apoptotic program in these extracts. However, one can study the apoptotic events that occur downstream of mitochondrial cytochrome c release by preparing extracts devoid of membrane components (including mitochondria). When purified cytochrome c is added to such cytosolic extracts, biochemical markers of apoptosis (e.g., activation of caspases) can be monitored. The egg extract therefore offers a tractable system for studying either separately or together the events of apoptosis occurring upstream and downstream of the mitochondria.

Key Words: Apoptosis; caspase; cytochrome c; mitochondria.

1. Introduction

Newmeyer et al. noted in the early 1990s that crude *Xenopus* interphase egg extracts spontaneously activate apoptosis on prolonged incubation on the benchtop (1). This spontaneous apoptosis program is thought to mirror the process of oocyte atresia, by which mature eggs that have not been laid are reabsorbed by apoptosis.

Apoptosis in *Xenopus* egg extracts mimics the biochemical events of apoptosis observed in other systems: Cytochrome c is released from the mitochondria, caspases are activated, and added nuclei undergo condensation and fragmentation. Moreover, known regulators of apoptosis behave similarly in the extract as has been reported for

other systems. For example, addition of the antiapoptotic Bcl-2 protein to egg extracts is able to completely block apoptosis (**1**), whereas addition of proapoptotic proteins such as Reaper and cytochrome c accelerate apoptosis (**2,3**). Thus, the egg extract provides a model that faithfully reconstitutes the molecular pathways of apoptosis in vitro.

There are multiple advantages of using the egg extract to study apoptotic processes as the egg extract: (1) is highly concentrated with proteins that are poised for cellular events such as apoptosis; (2) can be made in abundance because of the large amount of eggs each frog lays; (3) provides a means to study the function of a particular protein by depletion of that protein, supplementation of the extract with recombinant protein, or inhibition of the protein by the addition of neutralizing antibodies; and (4) can be separated to allow for the study of pathways at particular loci in the apoptotic program.

2. Materials

2.1. Collection of Eggs and Preparation of Sperm Chromatin

2.1.1. Injection of Frogs and Collection of Eggs

1. Mature female frogs (e.g., Nasco, *Xenopus* I, or *Xenopus* Express).
2. 100 mM NaCl (25 g NaCl per 5 L water).
3. 200 U/mL Pregnant mare serum gonadotropin (PMSG; Calbiochem): Reconstitute in sterile water to allow a final injection volume of 0.5 mL (e.g., 200 U/mL Final concentration); store in aliquots at -20°C .
4. 1000 U/mL Human chorionic gonadotropin (hCG; Sigma or Amersham/USB): reconstitute in sterile water to allow a final injection volume of 0.5 mL (e.g., 1000 U/mL final concentration); store at 4°C .
5. 10X Modified Ringer's solution (MMR) at pH 7.7: 1 M NaCl, 20 mM KCl, 10 mM MgSO_4 , 25 mM CaCl_2 , 5 mM HEPES, pH 7.8, 0.8 mM ethylenediaminetetraacetic acid (EDTA); store at room temperature.
6. Water tanks.
7. 1-mL Syringes.
8. 25-Gage needles.

2.1.2. Preparation of Sperm Chromatin for Synthetic Nuclei

1. Four or five male *Xenopus* frogs (Nasco).
2. 0.1% Tricaine: 3-Aminobenzoic acid ethyl ester (Sigma); dissolve in water.
3. Extraction buffer: 10 mM HEPES at pH 7.4, 80 mM KCl, 15 mM NaCl, 5 mM MgCl_2 , 1 mM EDTA; store at 4°C .
4. Extraction buffer containing 200 mM, 2 M, 2.3 M, and 2.5 M sucrose.
5. 5 mg/mL Aprotinin.
6. 5 mg/mL Leupeptin.
7. 1 M Dithiothreitol (DTT).
8. Triton X-100.
9. Ultrapure sucrose.
10. Bovine serum albumin (BSA; fraction V).
11. Dissecting tools, including scissors and two pairs of sharp forceps.
12. 60 mM Glass Petri dish.
13. 15-mL Conical polypropylene tubes.

14. Tabletop centrifuge.
15. Refrigerated centrifuge with Sorvall HB-4 swinging bucket rotor or equivalent.
16. 2.5-mL Beckman Ultra-Clear centrifuge tubes
17. TL-100 tabletop centrifuge and TLS-55 rotor (Beckman) or equivalent.
18. Hemacytometer.

2.2. Preparation of Crude Interphase Egg Extract

1. Eggs obtained from injected frogs, in 100 mM NaCl.
2. 2% (w/v) L-Cysteine (free base; Sigma).
3. 0.25X MMR, pH 7.7 (*see Subheading 2.1.1.*).
4. Egg lysis buffer (ELB), pH 7.7: 250 mM sucrose, 2.5 mM MgCl₂, 1 mM DTT, 50 mM HCl, 10 mM HEPES; prepare fresh.
5. 5 mg/mL Cytochalasin B (Calbiochem) in dimethyl sulfoxide.
6. 5 mg/mL Aprotinin (Roche Diagnostics) in water.
7. 10 mg/mL Leupeptin (Roche Diagnostics) in water.
8. 200-mL Beaker.
9. 100 mM Glass Petri dish.
10. Pasteur pipets.
11. 15-mL Conical polypropylene centrifuge tubes.
12. IEC clinical microfuge.
13. Sorvall HB-4 swinging bucket rotor.
14. 18-Gage needle attached to 5-mL syringe.

2.3. Assessment of Apoptosis in the Interphase Extracts

2.3.1. Assessment of Cytochrome c Release

1. Interphase extract.
2. 0.2 M Phosphocreatine.
3. 5 mg/mL Creatine kinase.
4. 0.2 M Adenosine triphosphate (ATP).
5. 0.1 mM Ultrafree-MC filters (Millipore).
6. Anti-cytochrome c antibody (Pharmingen).
7. 17.5% Acrylamide gel for sodium dodecyl sulfate–polyacrylamide gel electrophoresis.

2.3.2. Assessment of In Vitro Caspase Activity

1. Interphase extract.
2. 0.2 M Phosphocreatine.
3. 5 mg/mL Creatine kinase.
4. 0.2 M ATP.
5. Caspase assay buffer: 50 mM HEPES, pH 7.4, 100 mM NaCl, 0.1% CHAPS, 1 mM EDTA, 10% glycerol; store at 4°C and just before use add 10 mM DTT.
6. Ac-DEVD-pNA substrate (Biomol): 2 mM (1.3 mg/mL) Ac- DEVD-pNA in assay buffer (store in light-blocking tube at –20°C).
7. 20X Inhibitor stock (Ac-DEVD-CHO, Biomol): Biomol stock is 0.1 mM (0.05 mg/mL) in dimethyl sulfoxide; dilute 1/50 in assay buffer for 20X stock; store at –20°C.

2.3.3. Monitoring of Nuclear Morphology

1. Interphase extract.
2. 0.2 M Phosphocreatine.

3. 5 mg/mL Creatine kinase.
4. 0.2 M ATP.
5. Sperm chromatin.
6. Hoechst 33258 (Bizbenzimidazole 33258): 100 μ L sucrose (from 1 M stock), 300 μ L Formaldehyde, 4 μ L HEPES, pH 8.0 (from 1 M stock), 4 μ L Hoechst 33258.
7. Microscope slides.
8. Cover slips.

2.4. Fractionated Interphase Egg Extract

2.4.1. Preparation of Cytosolic and Light Membrane Fractions

1. Crude interphase extract.
2. 2.5-mL Ultra-Clear centrifuge tubes.
3. TLS centrifuge and TLS-55 rotor (Beckman) or equivalent.

2.4.2. Preparation of Mitochondria-Rich Heavy Membrane Fraction

1. Mitochondrial buffer (MIB) concentrate: prepare fresh; the following makes approx 14.5 mL of 4X MIB:
 - a. 3.6 mL Sucrose (from 1 M stock).
 - b. 600 μ L Adenosine 5'-diphosphate (from 100 mM stock).
 - c. 240 μ L KCl (from 2.5 M stock).
 - d. 30 μ L DTT (from 1 M stock).
 - e. 600 μ L Succinate (from 1 M stock).
 - f. 600 μ L HEPES, KOH, pH 7.5 (from 1 M stock).
 - g. 600 μ L Ethylene glycol bis(2-aminoethyl ether)-*N,N,N',N'*-tetraacetic acid (EGTA; from 0.5 M stock).
 - h. 8.4 μ L Mannitol (from 1.5 M stock).
2. Percoll (Sigma).
3. Beckman TL-100 tabletop ultracentrifuge.
4. TLS-55 swinging bucket rotor.

2.5. Assessment of Apoptosis in Fractionated Extract

2.5.1. Reconstituted Extract:

Cytosolic and Mitochondria/Heavy Membrane Fractions

1. Cytosolic extract.
2. Mitochondria/heavy membrane fraction.
3. 0.2 M Phosphocreatine.
4. 5 mg/mL Creatine kinase.
5. 0.2 M ATP.

2.5.2. Assessment of Cytochrome c-Induced Apoptosis

1. Cytosolic extract.
2. 0.2 M Phosphocreatine.
3. 5 mg/mL Creatine kinase.
4. 0.2 M ATP.
5. Purified cytochrome c (from equine heart; Sigma); make stock solution in water at 1 mg/mL and store at -80°C for up to 1 mo.

2.6. Immunodepletion, Addition of Recombinant Proteins, and Antibody Neutralization

1. Antibody/antiserum.
2. Preimmune serum or immunoglobulin G (IgG).
3. Protein A/G-Sepharose.
4. Phosphate-buffered saline PBS: 8 g NaCl, 0.2 g KCl, 0.1 g CaCl₂, 0.1 g MgCl₂·6 H₂O, 1.15 g NaH₂PO₄·H₂O, 0.2 g KH₂PO₄; add water to 1 L; store at room temperature.
5. BSA, fraction V.
6. Bio-Spin Disposable 1-mL chromatography columns (Bio-Rad).
7. Extract buffer (XB): 50 mM sucrose, 100 mM KCl, 0.1 mM CaCl₂, 1 mM MgCl₂, 10 mM potassium HEPES, pH 7.7; prepare fresh.
8. Recombinant protein of interest.

3. Methods

The methods described in this chapter summarize: (1) how to obtain eggs for interphase extract preparation and how to prepare sperm chromatin for nuclear formation to monitor nuclear morphology during apoptosis; (2) the preparation of crude interphase egg extract and assessment of apoptosis in the interphase egg extract; (3) the separation of the crude interphase extract into cytosolic and membrane fractions and the assessment of apoptosis using fractionated extract; (4) the modification of the extract through immunodepletion or supplementation with recombinant proteins of interest or neutralizing antibodies.

3.1. Collection of *Xenopus* Eggs and Preparation of Sperm Chromatin for Nuclei Formation

3.1.1. Collection of Eggs

Xenopus laevis mature females are housed in clean, dechlorinated tap water at a maximal density of one frog per liter (lower densities are desirable). Dechlorination can be achieved by passing tap water through a carbon filter. If chloramines are absent in the tap water, it can be stored in an open tank for 24 h with aeration. The frogs should be housed at 18°C to achieve optimal egg production. To promote egg laying, frogs are first primed with PMSG, and 2 d later are injected with hCG (see **Note 1**).

1. Prepare a tank containing 100 mM NaCl to house frogs after injection. Keep frog density at one frog per liter.
2. Using a 25-gage needle attached to a 1-mL syringe, inject frogs subcutaneously into the dorsal lymph sac (the upper part of the frog leg) with 0.5 mL of 200 U/mL PMSG (total 100 U) (see **Fig. 1**). Place the frogs in the tank containing 100 mM NaCl. The frogs will be ready to induce egg laying in 2 to 3 d. Alternatively, the PMSG-injected frogs can be housed for up to 10 d before induction of egg laying with hCG.
3. To induce egg laying, inject the frogs as described in **step 2** with 0.5 mL of 1000 U/mL hCG (a total of 500 U).
4. Place the injected frog into a tank containing 5 L of 100 mM NaCl. Each injected frog should be housed in a separate tank as the quality of eggs varies between frogs.
5. At 16 to 22 h after injection of hCG, the eggs will be ready to collect. Remove the frog to a clean tank containing 100 mM NaCl and pour the eggs into a 500-mL beaker.



Fig. 1. Injection of frogs to obtain eggs. The frog is first primed with 100 U PMSG by subcutaneous injection into the dorsal lymph sac, marked by the asterisk in the picture. A second subcutaneous injection into the dorsal lymph sac (this time with 500 U hCG) 2 to 3 d later induces egg laying.

3.1.2. Preparation of Demembrated Sperm Chromatin

Fully functional nuclei are formed within 30 min of adding sperm chromatin to interphase egg extract. The formation of nuclei is driven by the binding and fusion of membrane vesicles to the chromatin. The resultant synthetic nuclei incorporate nuclear pore components and are competent to undergo bidirectional nuclear transport, DNA replication, mitosis, and apoptosis ([1,4,5](#)).

1. Anesthetize four or five male frogs by immersion in 0.1% Tricaine and sacrifice either by cervical dislocation or by pithing, followed by cutting through the spinal cord. Using dissecting scissors, cut through the skin into the peritoneum along the midline of the frog. The testes are beige 0.5-cm organs located along the midline in the center of the abdominal cavity.
2. After pushing the liver aside, grasp the fatty material at midabdomen and pull gently. The testes will emerge on either side of the midline. Gently cut them free of adherent tissue with either forceps or scissors and place in a 60-mm glass Petri dish containing extraction buffer.
3. Using two pairs of sharp forceps, mince the testes into small pieces and transfer them to a 15-mL conical polypropylene tube.
4. Vortex the minced testes vigorously and pellet the larger pieces by gentle centrifugation (~10 s at 200g in a clinical centrifuge).

5. Transfer the supernatant to a new tube and add 3 mL extraction buffer supplemented with 200 mM sucrose to pellet. Vortex for 1 min and recentrifuge for 10 s at 200g. Combine the supernatants and repeat the extraction of the pellets two or three times until the supernatant is no longer cloudy.
6. Centrifuge the combined supernatants 50 s at 450g at room temperature to pellet any remaining large pieces of tissue. Transfer the supernatants to a 15-mL tube and centrifuge 10 min at 2600g (4000 rpm in a Sorvall HB4 rotor).
7. Prepare gradients by adding 0.2 mL extraction buffer containing 2.5 M sucrose to each of four 2.5-mL Beckman Ultra-Clear tubes and overlaying with 1.7 mL extraction buffer containing 2.3 M sucrose.
8. Resuspend sperm in 0.8 mL extraction buffer containing 2 M sucrose and overlay gently on the top of the sucrose gradients (0.2 mL per tube). After stirring the interface between the sperm and the 2.3 M sucrose with a pipet tip, centrifuge the sucrose gradients in a TL-100 tabletop ultracentrifuge, 25 min at 93,000g (33,000 rpm in a TLS-55 rotor) at 4°C.
9. Aspirate the top half of the gradient, which contains contaminating red blood cells. Transfer the lower half of the gradient to a new tube (*see Note 2*).
10. Dilute sperm to 12 mL with extraction buffer containing 200 mM sucrose and centrifuge for 10 min in a swinging bucket rotor at 4100g (5000 rpm in a Sorvall HB4 or HB6 rotor or equivalent).
11. To demembranate the sperm, resuspend the pellet in 1 mL extraction buffer supplemented with 200 mM sucrose, 5 µg/mL aprotinin, 5 µg/mL leupeptin, 1 mM DTT, 0.4% (v/v) Triton X-100. Incubate on ice for 30 min.
12. Prepare sucrose cushions by adding 0.5 M sucrose, 3% (w/v) BSA fraction V, 5 µg/mL aprotinin, 5 µg/mL leupeptin, and 1 mM DTT to the extraction buffer. Prepare the sucrose cushion in two 1.5-mL microcentrifuge tubes and then overlay them with one-half of the sperm preparation from **step 11**. Pellet the sperm by centrifugation for 10 min in a clinical tabletop centrifuge at 870g at room temperature.
13. Prepare extraction buffer containing: 200 mM sucrose, 3% (w/v) BSA fraction V, 5 µg/mL aprotinin, 5 µg/mL leupeptin, and 1 mM DTT.
14. After centrifugation, remove the supernatant from the pellets and resuspend the sperm in 0.1 mL freshly prepared extraction buffer (**step 13**). Transfer the resuspended sperm to a clean microcentrifuge tube. Be very careful not to contaminate the sperm with residual Triton X-100 from the sides of the original tube.
15. Add extraction buffer prepared in **step 13** so that the final volume of the sperm preparation is 0.25 mL. Count the sperm using a hemacytometer and dilute to $1 \times 10^5/\mu\text{L}$ (this is 100X). Snap freeze the sperm in small aliquots in liquid nitrogen and store at -70°C . Usually, a sperm preparation yields 1 to 2×10^7 sperm per frog.

3.2. Preparation of Crude Interphase Egg Extract and Assessment of Apoptosis

The preparation and assessment of apoptosis in crude interphase egg extracts is described in **Subheadings 3.2.1. to 3.2.4.** The mature *Xenopus* eggs are arrested in metaphase of meiosis II and therefore have high mitotic kinase (cyclin B/cdc2) activity. On crushing of the eggs by centrifugation, there is a transient release of Ca^{2+} from intracellular stores. This release of Ca^{2+} promotes the degradation of cyclin B, subsequent loss of cdc2 kinase activity, and entry into interphase of the cell cycle. The extract is retained in interphase by addition of cycloheximide, which prevents new

protein synthesis. When the egg extract is prevented from entering interphase by the addition of EGTA so Ca^{2+} release is not allowed, the resultant cytostatic factor (CSF) is extremely refractory to apoptosis (6). This is attributed to the high levels of mitogen-activated protein kinase, which phosphorylates and inhibits the activity of caspase 9 (6,7). Prolonged incubation of the crude interphase extract (containing mitochondria) at room temperature induces a spontaneous apoptosis program that is characterized by the release of cytochrome c from the mitochondria, activation of apoptotic proteases (caspases), and condensation and fragmentation of added DNA.

3.2.1. Preparation of Crude Interphase Egg Extract and Induction of Spontaneous Apoptosis Program

1. Collect eggs in a 200-mL glass beaker and pour off any excess solution.
2. Rinse eggs once in 2% L-cysteine, pH 8.0, then continue to incubate in 100 mL 2% L-cysteine solution per frog for approx 5 min (or until the eggs pack very closely) at room temperature, gently swirling the eggs periodically (*see Note 3*).
3. Pour the cysteine solution off the dejellied eggs and wash the eggs in 0.25X MMR (1/40 dilution of 10X stock) by adding buffer, swirling the eggs, then pouring off the buffer. Repeat twice. Pour eggs into a 100-mm glass Petri dish.
4. Remove the “bad eggs” with a Pasteur pipet. Bad eggs appear as white puffy balls, with an obscure boundary between the dark and light hemispheres. This is in contrast with a “good egg,” which has an even unmottled appearance and a tiny white spot (indicative of oocyte maturation) in the center of the darkly pigmented hemisphere of the mature egg (*see Note 4*).
5. Wash the eggs three times with ELB by swirling the eggs in buffer, then pouring off the buffer.
6. Transfer the eggs with an inverted Pasteur pipet (the bulb on the pointed end so the eggs are not prematurely lysed) into a 15-mL polypropylene tube.
7. To pack the eggs, centrifuge for 15 s in a clinical centrifuge at 400g. Remove any extra buffer from the top of the packed eggs with a Pasteur pipet. It is critical to remove as much buffer as possible to ensure a concentrated egg extract. Sacrifice eggs to achieve this.
8. Determine the volume of the packed eggs, then add 5 $\mu\text{g}/\text{mL}$ aprotinin (1/1000), 5 $\mu\text{g}/\text{mL}$ leupeptin (1/1000), 5 $\mu\text{g}/\text{mL}$ cytochalasin B (1/1000), 5 $\mu\text{L}/\text{mL}$ of 10 mg/mL cyclohexamide (50 $\mu\text{g}/\mu\text{L}$ final) directly to the top of the packed eggs. For example, if you have 8 mL packed eggs, add 8 μL of each of these items.
9. Crush the eggs by centrifuging for 15 min at 12,000g, 4°C, in a Sorvall HB-4 swinging bucket rotor. The lysed eggs will be separated into three layers: a yellow lipid layer on top, the crude interphase extract in the middle, and a dark pellet containing pigment granules (*see Fig. 2A*).
10. Remove the crude extract by piercing the side of the polypropylene tube with an 18-gage needle attached to a 5-mL syringe (*see Note 5*).
11. Add 1/10 dilution of 0.2 M phosphocreatine (20 mM final) and 1/100 of 0.5 mg/mL creatine kinase (50 $\mu\text{g}/\text{mL}$ final) and 0.2 M ATP (20 μM final) to create an ATP-regenerating system and sperm nuclei to a concentration of 1000/ μL (1/100 dilution). Incubate this extract at room temperature for 4 to 8 h. The onset of apoptosis can be assayed in this system by observing the morphology of sperm nuclei stained with Hoechst 33528 (**Subheading 3.2.4.**), measuring cytochrome c release (**Subheading 3.2.2.**) or assessing caspase activity (**Subheading 3.2.3.**).

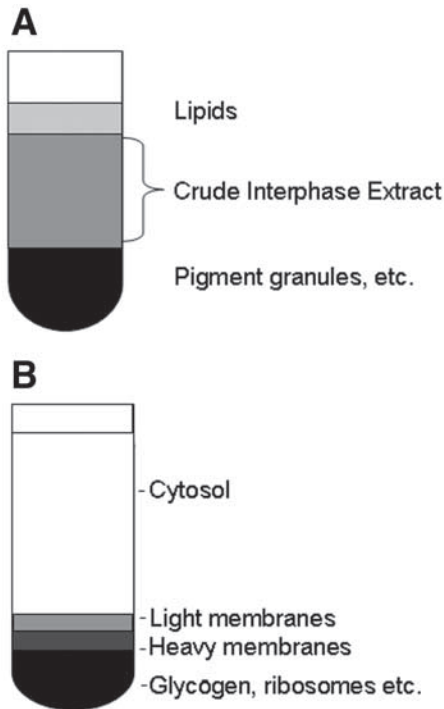


Fig. 2. (A) Crude interphase extract. After the eggs are crushed by centrifugation at 12,000 rpm, the eggs are separated into three layers. The top yellow layer consists of lipids, and the middle layer contains the cytosol and membrane fractions; the dark bottom layer contains pigment granules and yolk proteins and glycogen. (B) After ultracentrifugation of the crude extract, it is separated into cytosolic and membrane fractions. The light membrane fraction, which is pale yellow, lies just beneath the cytosolic fraction. The heavy membrane fraction enriched in mitochondria lies just beneath the light membrane layer; glycogen, ribosomes, and the like pellet at the bottom of the tube.

3.2.2. Cytochrome *c* Release Assays

Execution of the intrinsic apoptotic program depends on the release of cytochrome *c* from the mitochondria. Once released, cytochrome *c* is involved in the formation of a large proapoptotic proteolytic complex, known as the *apoptosome*. The apoptosome promotes apoptosis by activating caspases. Because cytochrome *c* serves to activate caspases, the transit of cytochrome *c* from the mitochondria to cytosol is indicative of apoptosis. This release can be monitored directly by immunoblotting of cytochrome *c* in the cytosolic fraction after removal of mitochondria by filtration.

1. Remove 25 μ L egg extract containing ATP-regenerating mix (**Subheading 3.2.1.**) at timed intervals (30- to 60-min intervals) and pass through a 0.1 mM Ultrafree MC filter. This process removes the mitochondria. The supernatant that flows through the filter will contain any cytochrome *c* that has been released into the cytosol.

2. Subject 7 μL of sample to sodium dodecyl sulfate-polyacrylamide gel electrophoresis analysis using a 17.5% acrylamide gel.
3. Immunoblot with anti-cytochrome c antibody (*see Note 6*).

3.2.3. Biochemical Assessment of Apoptosis: Measuring Caspase Activation

The apoptotic program culminates in the activation of proteases, known as caspases, that cleave intracellular substrates, resulting in orderly dismantling of the cell. Caspase activity can be measured easily *in vitro* using a colorimetric assay and thus provides a quantitative readout of apoptosis in the egg extract. The *in vitro* caspase assay described here measures the cleavage of a synthetic peptide substrate (Ac-DEVD-pNA) of caspase 3 that is linked to a chromophore (*see Note 7*). When the egg extract, containing active caspase 3, is incubated with the substrate, the substrate is cleaved. Caspase-mediated cleavage results in the release of the chromophore from the substrate, causing a color change which is measured spectrophotometrically.

1. Add 85 μL assay buffer to a well of a 96-well microtiter plate for each sample/time-point to be assayed. Keep this plate at room temperature.
2. Add 5 μL egg extract containing ATP-regenerating mix (**Subheading 3.2.1.**) to the well.
3. Add 10 μL caspase substrate (Ac-DEVD-pNA). Tap the sides of the plate to mix and incubate at 37°C for 1 h (*see Note 8*).
4. Read the plate at 405 nm using a microplate reader.

3.2.4. Nuclear Morphology

A hallmark of apoptosis is nuclear condensation and fragmentation. This apoptotic phenotype can be readily observed in synthetic nuclei formed in the egg extract because apoptotic nuclei appear as condensed and fragmented (*see Fig. 3*).

1. Prepare crude interphase egg extract with ATP-regenerating mix (**Subheading 3.2.1.**).
2. Add sperm chromatin to the egg extract at a 1/100 dilution (1000 sperm/ μL) and incubate at room temperature. Nuclei will start to form after 20 min and should be well formed after 30 min. The sperm chromatin will change shape from coiled and stringy to kidney bean shape and round. Well-formed nuclei appear round and are homogeneous (*see Fig. 3*).
3. Nuclei should be observed at 30-min intervals after 2.5 h of incubation in egg extract at room temperature because extracts undergo spontaneous apoptosis at varying rates. Remove 2 μL extract and mix with 2 μL Hoechst dye on a microscope slide and then add a cover slip. Observe nuclei using the ultraviolet filter on a fluorescent microscope. Apoptotic nuclei are condensed and fragmented or blebbed (*see Fig. 3*).

3.3. Fractionation of Interphase Extracts

The mitochondria are required for execution of the spontaneous apoptotic program as they are triggered to release cytochrome c, which serves as a cofactor for downstream apoptotic events. It is possible to study apoptosis in the interphase extract at distinct phases of the apoptotic pathway, particularly prior to and following mitochondrial cytochrome c release. Cytosolic extract alone is not able to support apoptosis because of the lack of mitochondria. However, addition of a mitochondria-rich heavy membrane fraction to the isolated cytosol leads to cytochrome c release and apoptosis. Therefore, it is possible to study the upstream cytosolic factors required to induce mitochondrial cytochrome c release using cytosolic extract.

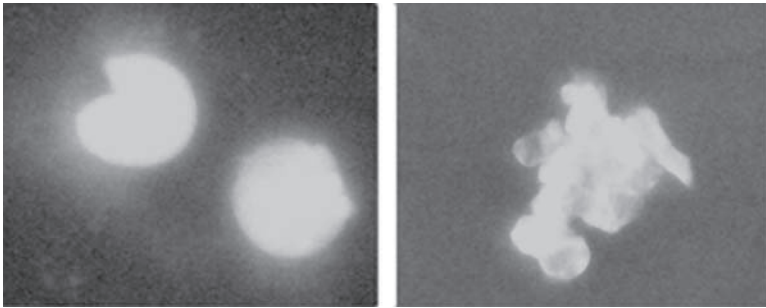


Fig. 3. Apoptotic nuclei in the egg extract. Sperm chromatin was added 1/100 to crude interphase extract supplemented with ATP-regenerating mix. The extract was then incubated at room temperature for 30 min to allow for nuclei formation. Soluble cytochrome c (10 ng/ μ L final) was then added, and the egg extract was allowed to incubate at room temperature for an additional 30 min. Nuclei are stained with Hoechst dye. The picture on the left depicts typical synthetic nuclei in the egg extract; the picture on the right is representative of apoptotic nuclei.

Moreover, addition of purified cytochrome c alone to a cytosolic extract (lacking mitochondria) results in caspase activation, allowing for the investigation of apoptotic signaling downstream of mitochondrial cytochrome c release. Thus, the egg extract offers a tractable system in which to examine events that occur at different loci in the apoptotic program.

3.3.1. Separation of Cytosolic, Light Membrane, Heavy Membrane, and Glycogen Fractions

1. Supplement the crude interphase egg extract (*see Subheading 3.1.2.*) with aprotinin, leupeptin, and cytochalasin B (1/1000 dilution).
2. Transfer the extract to a 2.5-mL Ultra-Clear centrifuge tube and centrifuge for 70 min at 4°C in a Beckman TLS-100 centrifuge at 250,000g (55,000 rpm in TLS-55 rotor).
3. After centrifugation, the extract will separate into a clear cytosolic portion with the membrane fractions below. Lying immediately below the cytosolic layer is the light membrane fraction, which is light yellow. Below this is a darker heavy membrane fraction consisting of mitochondria and other organelles (*see Fig. 2B*). Place the extract on ice and remove the clear cytosolic fraction with a 200- μ L pipet tip. Be extremely careful not to remove any of the light membrane layer. Hold the light membrane layer on ice and centrifuge the cytosolic fraction again in a new 2.5-mL Ultra-Clear tube and divide into aliquots. Use the extract fresh or snap freeze in liquid nitrogen and store at -80°C until ready for use.
4. To prepare light membrane, carefully remove the light membrane fraction from the membrane layer using a wide-bore pipet tip. Leave the darker heavy membranes undisturbed. Dilute the light membrane in 1.5 mL ELB.
5. Add 0.42 g sucrose to 5 mL ELB to create 2X sucrose/ELB.
6. Place the diluted membranes (**step 5**) into a new 2.5-mL Ultra-Clear centrifuge tube. Underlay the membranes with 2X sucrose/ELB by releasing it from a Pasteur pipet at the bottom of the membrane-containing tube. Add buffer until the tube is full.

7. Centrifuge for 20 min at 26,000g (20,000 rpm) at 4°C in the TLS-55 rotor. Centrifugation will result in a membrane pellet at the bottom of the tube.
8. Remove all buffer and, with a wide-bore tip, aliquot the membranes into microcentrifuge tubes (5–10 µL per tube) and snap freeze in liquid nitrogen. Store at –80°C (see **Note 9**).

3.3.2. Isolating Mitochondria From *Xenopus* Egg Extract

1. Prepare a fractionated interphase extract as described in **Subheading 3.3.1**.
2. After removing the light membranes, gently remove the heavy membrane fraction using a wide-bore pipet tip. Place the heavy membranes in a 2.5-mL Ultra-Clear centrifuge tube. The heavy membrane enriched in mitochondria is the brown opaque layer that lies directly below the light membrane layer. The translucent brown layer directly below the heavy membrane consists of glycogen and pigment granules.
3. Prepare Percoll solutions as follows:
 - a. 42%: 0.612 mL 4X MIB concentrate, 1.05 mL Percoll, 0.838 mL water.
 - b. 37%: 0.612 mL 4X MIB concentrate, 0.92 mL Percoll, 0.969 mL water.
 - c. 30%: 0.612 mL 4X MIB concentrate, 0.75 mL Percoll, 1.14 mL water.
 - d. 25%: 0.612 mL 4X MIB concentrate, 0.625 mL Percoll, 1.263 mL water.
4. Prepare step gradients by successively adding 0.45 mL of each of the Percoll solutions (**step 3**) to the heavy membrane fraction. Carefully layer the solutions on top of each other.
5. Centrifuge for 25 min at 24,430g (25,000 rpm) in the Beckman TL-100 centrifuge without the brake.
6. After centrifugation, any contaminating light membranes will lie at the top of the Percoll gradient. The heavy membranes/mitochondria will form a discrete band at the interface between different Percoll gradients. Withdraw the heavy membranes using a Pasteur pipet and resuspend in 50 vol 1X MIB buffer. Gently invert the tube to mix.
7. Centrifuge at 1700g to pellet the mitochondria.
8. Resuspend the mitochondria in an equal volume of 1X MIB buffer. The resulting mitochondria preparation can be used as a 10 to 20X stock for addition to the reconstituted extract. Do not freeze–thaw the mitochondria as this may rupture the mitochondrial membranes and release proapoptotic factors such as cytochrome c.

3.4. Assay of Apoptosis Using Fractionated Interphase Egg Extracts

3.4.1. Reconstitution Extract: Cytosolic and Heavy Membrane Fractions

1. Add ATP-regenerating mix (1/10 dilution of 0.2 M phosphocreatine and 1/100 of 0.5 mg/mL creatine kinase and 0.2 M ATP) to 170 µL of cytosolic extract.
2. Add 14 µL freshly prepared heavy membrane fraction enriched in mitochondria (**Subheading 3.3.2**).
3. Incubate at room temperature. Withdraw samples at 30-min intervals to assess cytochrome c release and caspase activity (**Subheadings 3.2.2.–3.2.3.**; see **Note 10**).

3.4.2. Assessment of Cytochrome c-Induced Apoptosis

1. Thaw 50 to 100 µL cytosolic egg extract and add ATP-regenerating mix (1/10 dilution of 0.2 M phosphocreatine, 1/100 dilution of 0.5 mg/mL creatine kinase, and 1/100 dilution of 0.2 M ATP).
2. Prepare 10X working solutions of soluble cytochrome c to be added to the extract. Final concentrations of cytochrome c in the extract should range between 0.6 and 2 µg/mL (see **Note 11**).

3. Incubate at room temperature for 30 to 180 min.
4. Assess caspase activity as described in **Subheading 3.2.3.**

3.5. Modification of the Egg Extract Through Immunodepletion of Proteins, Addition of Recombinant Proteins, or Neutralizing Antibodies

The *Xenopus* egg extract in vitro reconstitution systems provide the opportunity to easily study the function of proteins through their removal, addition, or inhibition. Complete immunodepletion of proteins from the egg extract often requires multiple rounds of depletion using a high-affinity antibody. To ensure that the process of immunodepletion has had no effect on the process of apoptosis in the extract, it is critical to use preimmune or IgG-depleted extract as a control. It is also imperative that the extract not be diluted during the depletion process so the function of the extract is not compromised.

Supplementation of the extract with wild-type or mutant recombinant proteins offers an easy assessment of their apoptotic function. For example, preincubation of a cytosolic extract with recombinant MAPK, a known inhibitor of apoptosis, inhibits cytochrome c-induced caspase activity (6); addition of Reaper to a crude interphase extract induces rapid full-blown apoptosis (2).

Although depletion of proteins from the egg extract can provide a very useful means to assess the function of a particular protein factor, sometimes it is not possible to remove sufficient protein from the egg extract. In this case, addition of an antibody specific for the protein of interest may act to neutralize the function of the protein. For example, addition of an antibody to Wee1, a protein required for the spontaneous apoptosis program in the egg extract, completely inhibited caspase activity in the crude interphase extract (8). The protocols described next outline how to deplete or supplement the egg extract without compromising the ability of the extract to function properly.

3.5.1. Immunodepletion From the Egg Extract

1. Precouple the antibody to the beads by incubating the antibody with protein A (or protein G) Sepharose in PBS containing 2 mg/mL BSA fraction V. (Incubation times and temperature vary depending on the antibody used.) Prepare control beads (preimmune or IgG) in the same manner. Although approximate volumes may vary depending on the antisera used, approx 15 μ L packed beads can be incubated with approx 10 μ g of IgG in 200 μ L PBS containing 2 mg/mL BSA.
2. Pellet the beads using an ultracentrifuge; wash twice with ELB. Remove all of the buffer from the beads using a 25-gage needle attached to a 1-mL syringe.
3. Add 100 μ L extract to be depleted to the packed antibody beads and rotate at 4°C for 40 min.
4. Pellet the beads by centrifugation and remove the supernatant to a new tube of prewashed antibody beads.
5. Rotate for an additional 40 min at 4°C
6. Rinse a Bio-Spin column with ELB. Be very careful to dry the column after rinsing to prevent dilution of the extract.
7. Transfer the extract/beads to the Bio-Spin column and spin for 3 min at high speed in a clinical centrifuge. This step ensures the removal of the beads from the extract.
8. The depleted extract is now ready to be used to assess apoptosis as described in **Subheadings 3.2.** and **3.4.** At this point, the extract has been depleted twice. Depending on the

protein of interest and the antibody, the number of depletions and length of incubation of extract with antibody beads will vary. You will have to optimize the depletion protocol for each protein of interest. To assess how well the depletion worked, perform an immunoblot for the protein of interest.

3.5.2. Addition of Recombinant Protein and Neutralizing Antibodies to Egg Extracts

3.5.2.1. ADDITION OF RECOMBINANT PROTEINS

1. It is best if the recombinant protein is dialyzed into XB buffer. To maintain the integrity of the egg extract, add the protein at a 1/5 dilution or greater into the egg extract (1/10 or more is best).
2. Incubate the protein in the extract and assess apoptosis as described in previous subheadings.

3.5.2.2. ADDITION OF NEUTRALIZING ANTIBODY

1. To inhibit the protein of interest with antibody, add 0.5 to 1 mg/mL antibody into the egg extract. Rotate the extract/antibody for 20 min at 4°C (see **Note 12**).
2. Add ATP-regenerating mix and assess apoptosis as described in previous subheadings.

4. Notes

1. It is common practice to refrain from feeding the frogs once they have been primed because regurgitated food and stomach contents will destroy the eggs.
2. The red blood cells band at the top of the 2.3 M sucrose layer. The sperm lie in a band at the top of the 2.5 M sucrose layer.
3. This step is critical because leaving the eggs in cysteine for too long will cause the eggs to lyse. As the eggs dejelly, they pack down. When the eggs are packed very tightly, with no visual space between them, remove the cysteine and start washing in 0.25X MMR.
4. It is important to remove bad eggs without lysing them. The lysis of one egg will cause nearby eggs to lyse, which compromises the function of the extract.
5. While piercing the side of the tube with the needle to withdraw the interphase extract, be sure to puncture the tube at the bottom of the extract with the needle bevel up.
6. It is suggested to cut the membrane after transfer to probe only the region around 14 kDa because the commercial cytochrome c antibodies seem to crossreact with other proteins in the extract. Because cytochrome c is used as a standard in molecular weight markers, it used as a convenient positive control for the immunoblot. Alternatively, purified cytochrome c can be used.
7. Synthetic caspase substrates linked to fluorophores rather than chromophores are also available. The use of a fluorophore-linked substrate increases the sensitivity of the assay. A fluorometer must be used to quantitate caspase activity with this assay. There are multiple caspase substrates available, each with varying specificity for particular caspases.
8. To read the plate at once at the end of the experiment, 5 mL of the inhibitor peptide AcDEVD-CHO can be added after the 1 h incubation at 37°C. Alternatively, the microtiter plate can be incubated on ice during the time-course of the experiment with the samples in assay buffer. Substrate can be added at the end of the experiment to each sample well and then incubated at 37°C for 1 h.
9. It is critical to avoid contaminating the light membrane with the heavy membrane fraction. If there is contaminating mitochondria/heavy membrane in the light membrane preparation, they will appear as a dark spot in the middle of the light membrane pellet.

It is possible to dislodge the light membrane from the mitochondria/heavy membrane by gently flicking the tube as the mitochondrial pellet will remain adhered to the tube.

10. It is also possible to monitor nuclear morphology using this reconstitution assay. To do this, simply add a 1/10 dilution of light membrane and a 1/100 dilution of sperm chromatin to the cytosolic and heavy membrane fractions. Assay nuclear morphology as described in **Subheading 3.2.4**.
11. The stock cytochrome c is made in water at a concentration of 1 mg/mL. Do not freeze-thaw. Perform serial dilutions to obtain 10X concentrations to be added to the egg extract. It is best to use larger volumes (e.g., 1 mL or greater ending volumes) when diluting to ensure homogeneous distribution of cytochrome c.
12. As commercial antibodies may be prepared with sodium azide, it is often necessary to dialyze the antibodies into XB buffer to prevent sodium azide from inhibiting extract function. In addition, it is often necessary to add high concentrations of antibody (in excess of 0.5 mg/mL final concentration).

References

1. Newmeyer, D. D., Farschon, D. M., and Reed, J. C. (1994) Cell-free apoptosis in *Xenopus* egg extracts: inhibition by Bcl-2 and requirement for an organelle fraction enriched in mitochondria. *Cell* **79**, 353–364.
2. Evans, E. K., Kuwana, T., Strum, S. L., Smith, J. J., Newmeyer, D. D., and Kornbluth, S. (1997) Reaper-induced apoptosis in a vertebrate system. *EMBO J.* **16**, 7372–7381.
3. Kluck, R. M., Martin, S. J., Hoffman, B. M., Zhou, J. S., Green, D. R., and Newmeyer, D. D. (1997) Cytochrome c activation of CPP32-like proteolysis plays a critical role in a *Xenopus* cell-free apoptosis system. *EMBO J.* **16**, 4639–4649.
4. Smythe, C. and Newport, J. W. (1991) Systems for the study of nuclear assembly, DNA replication, and nuclear breakdown in *Xenopus laevis* egg extracts. *Methods Cell Biol.* **35**, 449–468.
5. Newmeyer, D. D. and Wilson, K. L. (1991) Egg extracts for nuclear import and nuclear assembly reactions. *Methods Cell Biol.* **36**, 607–634.
6. Tashker, J. S., Olson, M., and Kornbluth, S. (2002) Post-cytochrome C protection from apoptosis conferred by a MAPK pathway in *Xenopus* egg extracts. *Mol. Biol. Cell* **13**, 393–401.
7. Allan, L. A., Morrice, N., Brady, S., Magee, G., Pathak, S., and Clarke, P. R. (2003) Inhibition of caspase-9 through phosphorylation at Thr 125 by ERK MAPK. *Nat. Cell Biol.* **5**, 647–654.
8. Smith, J. J., Evans, E. K., Murakami, M., et al. (2000) Wee1-regulated apoptosis mediated by the crk adaptor protein in *Xenopus* egg extracts. *J. Cell Biol.* **151**, 1391–1400.

Studying Fertilization in Cell-Free Extracts

Focusing on Membrane/Lipid Raft Functions and Proteomics

**Ken-ichi Sato, Ken-ichi Yoshino, Alexander A. Tokmakov,
Tetsushi Iwasaki, Kazuyoshi Yonezawa, and Yasuo Fukami**

Summary

Xenopus oocytes, eggs, and embryos serve as an ideal model system to study several aspects of animal development (e.g., gametogenesis, fertilization, embryogenesis, and organogenesis). In particular, the *Xenopus* system has been extensively employed not only as a “living cell” system but also as a “cell-free” or “reconstititional” system. In this chapter, we describe a protocol for studying the molecular mechanism of egg fertilization with the use of cell-free extracts and membrane/lipid rafts prepared from unfertilized, metaphase II-arrested *Xenopus* eggs. By using this experimental system, we have reconstituted a series of signal transduction events associated with egg fertilization, such as sperm–egg membrane interaction, activation of Src tyrosine kinase and phospholipase C γ , production of inositol trisphosphate, transient calcium release, and cell cycle transition. This type of reconstititional system may allow us to perform focused proteomics (e.g., rafts) as well as global protein analysis (i.e., whole egg proteome) of fertilization in a cell-free manner. As one of these proteomics approaches, we provide a protocol for molecular identification of *Xenopus* egg raft proteins using mass spectrometry and database mining.

Key Words: Calcium release; cell-free system; CSF extract; egg; egg activation; embryogenesis; expressed sequence tag; fertilization; gametogenesis; in vitro reconstitution; mass spectrometry; proteome; proteomics; raft; reproduction; signal transduction; sperm; Src; tyrosine phosphorylation; unigene.

1. Introduction

For the past several decades, much progress has been made in understanding the biological detail of early development in several organisms, such as worms, sea invertebrates, fish, amphibians, birds, and mammals. Among them, amphibian species, particularly frogs (e.g., *Xenopus laevis*) have been an excellent model for the study of

early development at the molecular and cell biological levels. This is mainly because the frog can provide a large amount of gametes (i.e., egg and sperm) and zygotes (i.e., embryos). The frog egg/embryo is also characterized as a “big” cell that gives a large amount of biochemical material (e.g., protein, messenger RNA [mRNA]) and that is easy to manipulate (e.g., by microinjection). Such advantages in the frog system have been well recognized, especially after the discovery of MPF (maturation-promoting or mitosis-promoting factor) and cytostatic factor (CSF) (1).

Use of the frog system has become fruitful in the study of fertilization (2). Fertilization is a key event that gives rise to the birth of a newborn. Fertilization works as a biological bridge connecting one generation and the next or, more biologically, gametogenesis (i.e., spermatogenesis and oogenesis) and embryogenesis (3). Principle features of fertilization involve species-specific gamete interaction and fusion, sperm-induced transient increase of intracellular Ca^{2+} concentration within the egg, and Ca^{2+} -dependent cellular events; collectively, these are called *egg activation* events. Egg activation events include formation of fertilization envelope, blocking of polyspermy, and the resumption of cell cycle (metaphase of second meiotic stage in frog and many mammals, including humans) (4). The goal of fertilization is to form a diparental, unique zygotic nucleus via the union of haploidic gamete nuclei. After the formation of the zygotic nucleus, the resulting diploidic embryo will initiate somatic cell division and early development.

We have been interested in the molecular mechanism of *Xenopus* egg fertilization with special focus on the role of the egg protein-tyrosine kinase Src, a proto-oncogene product. Src is well known as a component of transmembrane signal transduction in several cell systems (5). We have demonstrated that *Xenopus* egg Src is activated within 1 min of fertilization, and that the activated Src may be responsible for the sperm-induced Ca^{2+} transient and subsequent egg activation (6–9). In addition, we have demonstrated that membrane microdomains or “rafts” contain a specific subset of egg proteins, including Src, and may function as a platform for sperm–egg interaction and subsequent Src-dependent egg activation signaling (10).

Based on the fact that egg rafts can be isolated as “active” biochemical materials, we have attempted to construct an experimental system that allows us to analyze the signal transduction pathway of sperm–egg interaction and egg activation in a cell-free manner. In this chapter, we describe methods for preparation of rafts and cell-free extracts from unfertilized *Xenopus* eggs (**Subheading 3.1.**). The addition of living sperm or other appropriate activators to the mixture of rafts and cell-free extracts can promote several fertilization-signaling events, and the addition of inhibitors or protein depletion study will suggest the importance of Src and other cellular components of interest (**Subheading 3.2.**). Such cell fractionation-oriented “focused proteomics” strategy is useful not only for analyzing a series of fertilization events as a whole, but also for identifying a novel component in fertilization. Thus, we also present methods for identifying a raft-associated, fertilization-related protein with the use of mass spectrometry (MS; **Subheading 3.3.**).

2. Materials

1. Frogs: *Xenopus* adults were obtained from regional dealers.
2. Frog maintenance: *Xenopus* adults were maintained in chloride-free tap water (1.2–1.5 L/animal) at 18 to 22°C and fed artificial, floating snack once a week.
3. Pregnant mare serum gonadotropin (PMSG) and human chorionic gonadotropin (hCG) were obtained from Teikokuzoki (Tokyo, Japan), dissolved in the solvent provided, and kept at –30°C and 4°C, respectively.
4. 1X DeBoer's solution (DB): 110 mM NaCl, 1.3 mM KCl, and 0.44 mM CaCl₂ titrated to pH 7.2 with NaHCO₃; 20X stock can be stored at 4°C.
5. Dejelling solution: DB containing 2% (w/v) cysteine-HCl titrated to pH 7.8 with NaOH.
6. 0.33X Modified Ringer's solution: 33.3 mM NaCl, 0.6 mM KCl, 0.33 mM MgCl₂, 0.66 mM CaCl₂, and 1.67 mM HEPES-NaOH, pH 7.8.
7. Ficoll: molecular weight 400,000 (Sigma; St. Louis, MO).
8. Nuclear preparation buffer: 250 mM sucrose, 15 mM HEPES-NaOH, 1 mM ethylenediaminetetraacetic acid (EDTA), 0.5 mM spermidine trihydrochloride, 0.2 mM spermidine tetrahydrochloride, 1 mM dithiothreitol (DTT), 3% bovine serum albumin (BSA), 10 µg/mL leupeptin, 20 µM 4-amidinobenzylsulfonyl fluoride hydrochloride (APMSF), pH 7.4.
9. 0.5X Steinberg solution (SB): 29 mM NaCl, 0.34 mM KCl, 0.17 mM CaCl₂, 0.43 mM Mg₂SO₄, and 2.3 mM Tris-HCl, pH 7.4.
10. BSA: fraction V, crystalline (Calbiochem; San Diego, CA).
11. Lysolecithin: 10 mg/mL stock solution in distilled water, prepared fresh.
12. A23187 (Sigma): stock at 10 mM in dimethylsulfoxide; store at –80°C.
13. H₂O₂: Santoku Chemical Industries (Tokyo, Japan).
14. Raft buffer: 20 mM Tris-HCl, 1 mM EDTA, 1 mM ethylenebis(oxyethylenenitrilo)tetraacetic acid (EGTA), 10 mM β-mercaptoethanol; 10X stock can be stored at 4°C.
15. Sucrose buffer: stock at 85% (w/v) solution in raft buffer; store at 4°C.
16. Na₃VO₄ (Wako, Osaka, Japan): stock at 500 mM in distilled water; store at 4°C.
17. Leupeptin: stock at 100 mg/mL in distilled water; store at –30°C.
18. APMSF (Wako): stock at 100 mM in distilled water; store at –30°C.
19. Triton X-100 (Sigma): Stock at 25% (v/v) in distilled water; store at 4°C.
20. Extraction buffer: 100 mM KCl, 0.1 mM CaCl₂, 1 mM MgCl₂, 5 mM EGTA, 50 mM sucrose, and 50 mM HEPES-NaOH titrated to pH 7.8.
21. Cytochalasin B (Calbiochem): stock at 100 mg/mL in ethanol; store at –30°C.
22. Pepstatin (Calbiochem): stock at 10 mg/mL in dimethylsulfoxide (DMSO); store at –30°C.
23. Chymostatin (Calbiochem): stock at 10 mg/mL in DMSO; store at –30°C.
24. Energy mix: 20X stock consisting of 150 mM creatine phosphate, 20 mM adenosine triphosphate (ATP), and 20 mM MgCl₂; store at –30°C.
25. ATP (Calbiochem): stock at 100 mM in distilled water containing 1 mM DTT; store at –30°C. [γ -³²P]ATP (7000 Ci/mmol) was purchased from ICN Biomedicals (Costa Mesa, CA); store at –80°C.
26. DTT (Nacalai, Kyoto, Japan): stock at 1 M in distilled water; store at –30°C.
27. 5X Laemmli's sodium dodecyl sulfate (SDS) sample buffer: 200 mM Tris-phosphate, pH 6.7, 5% SDS, 100 mM DTT, 50% sucrose, 0.025% bromophenol blue.
28. Protein-tyrosine kinase (PTK) inhibitors: PP2 and its inactive analog PP3 (Calbiochem) are dissolved in DMSO to a 5-mM stock; store at –80°C.
29. Phospholipase C (PLC) inhibitors: U-73122 and its inactive analog U-73343 (BIOMOL International; Plymouth Meeting, PA) are dissolved in DMSO to a 5-mM stock; store at –80°C.

30. Other activators/inhibitors: a synthetic Arg-Gly-Asp-Ser (RGDS) peptide was from Sigma. Cyclic adenosine monophosphate (20 mM in water at -80°C), GTP γ S (20 mM in water at -80°C), and heparin (100 mg/mL in water at -30°C) were from Calbiochem.
31. Synthetic peptides: a tyrosine kinase substrate peptide, Cdc2 peptide, and Src inhibitor peptide, peptide A7 (sdsiqaeewyfgkitrre), and its inactive derivative, peptide A9 (sdsiqaeewyfgkit), were prepared as described previously (7).
32. Antibodies: Anti-Src tyrosine kinase polyclonal antibody (anti-pepY antibody), which has been shown to recognize *Xenopus* Src, was raised against a synthetic peptide that corresponds to residues 410 to 428 of the chicken c-Src according to the described method (6). Anti-phospho Src Y416 antibody, which recognizes the activated and tyrosine-phosphorylated form of Src, was purchased from Biosource. A monoclonal antibody against mammalian PLC γ was purchased from Upstate Biotechnology. Monoclonal antiphosphotyrosine antibody PY99 was from Santa Cruz Biotechnology. An antibody against phosphorylated MAPK (mitogen-activated protein kinase) was from New England Biolabs (Beverly, MA). Anti-FLAG antibody (M2 clone) was from Sigma.
33. Protein A-Sepharose (Amersham-Pharmacia; Piscataway, NJ): Sepharose beads were extensively washed with PBS, and the 50% slurry was kept at 4°C .
34. Radioimmunoprecipitation assay (RIPA) buffer: 0.1% SDS, 1% Triton X-100, 1% deoxycholate sodium salt, 0.15 M NaCl, 50 mM Tris-HCl, pH 7.5.
35. Hoechst 33342 (Calbiochem): stock at 10 mg/mL in water; store at 4°C .
36. Fura-2 (Molecular Probes): stock at 1 mM in distilled water; store at -30°C .
37. Bioimaging instrument: BAS2000 Bioimaging Analyzer (Fujifilm, Tokyo, Japan).
38. Immunoblotting instrument: Trans Blot Semidry Transfer Cell (Bio-Rad).
39. Calcium monitoring instrument: ratio-imaging microscopy using high-frame digital charge-coupled device (CCD) imaging ARGAS/HISCA system (Hamamatsu Photonics, Hamamatsu, Shizuoka, Japan).
40. Mammalian cultured cells: COS7 cells were grown in Dulbecco's modified Eagle's medium (Sigma) supplemented with 10% fetal bovine serum. Subconfluent cells were used for transfection experiments.
41. *Xenopus* Src complementary DNAs (cDNAs): reverse transcriptase polymerase chain reaction was carried out to generate the first-strand cDNA encoding *Xenopus* Src2 gene using SuperScript First-strand Synthesis System (GibcoBRL). Template mRNAs were purified from *Xenopus* liver using the QuickPrep Micro mRNA Purification Kit (Amersham Bioscience). Oligonucleotide-mediated mutagenesis was done to generate cDNAs encoding either kinase-active or kinase-inactive version of *Xenopus* Src2 gene.
42. DNA polymerase: *PfuTurbo* DNA polymerase was obtained from Stratagene (La Jolla, CA) and used for preparation of *Xenopus* Src cDNAs.
43. Expression vectors: cDNA constructs were inserted into p3xFLAG-CMV-14 vector (Sigma) by which *Xenopus* Src2 gene products are expressed as carboxyl-terminal FLAG-tagged protein. A bacterial strain DH5 α was used to perform large-scale purification of the expression vectors.
44. Transfection reagent: Effectene (Qiagen, Germany) was used according to the manufacturer's instruction.
45. Proteases: lysyl-endopeptidase (*Achromobacter lyticus* protease I) (Wako); store at 4°C . Asp-N endoprotease (Boehringer Mannheim; Mannheim, Germany); store at 4°C .
46. Other reagents used were purchased from Nacalai (Kyoto, Japan), Sigma, or Wako (Osaka, Japan).

3. Methods

3.1. Preparation of the Egg Samples, Raft Fractions, and Egg Extracts

3.1.1. Unfertilized Eggs

1. Fully grown, adult female *X. laevis* are injected with 40 U PMSG. Within 7 d of the PMSG injection, the same females are induced to ovulate by injection of 500 U hCG. Usually, ovulation begins 6 to 8 h after the hCG injection. Frogs are maintained at ambient temperature in water containing 0.1 M NaCl, which prevents spontaneous activation of ovulated eggs.
2. Ovulated eggs are collected and washed once with 1X DB to remove debris.
3. Add more than three times the volume of dejelling solution. Agitate the egg suspension gently occasionally by swirling for 3 to 4 min. Monitor successful removal of egg jelly coats, and when this has occurred, wash gently several times in 1X DB. The resulting jelly coat-free eggs are regarded as unfertilized eggs.

3.1.2. Sperm

3.1.2.1. LIVING SPERM

1. Living sperm for insemination or addition to the cell-free system are prepared as follows: remove testes surgically from male frogs that have been injected with 40 U/animal of PMSG 1 to 2 d before the experiment. Testes can be kept intact at 4°C in a microfuge tube filled with 1X DB supplemented with 3 mg/mL BSA and used within 1 wk.
2. To obtain sperm, a pair of testes is minced and washed twice with ice-cold 1X DB.
3. The washed sperm (about 10^8 sperm from one animal) are incubated with an excess volume of *Xenopus* egg jelly water (see **Subheading 3.1.2.1., step 5**) for 10 min. After the incubation, centrifuge the mixture at 2000g for 10 min.
4. Resuspend the pellet with 1 mL 1X DB. The resulting suspension is designated as jelly water-treated sperm.
5. Egg jelly water is prepared by gentle rocking of jelly-intact eggs (5 g) in a 60-mm plastic culture dish filled with 10 mL 0.33X modified Ringer's solution. After 60 min of rocking, soluble material is collected, and Ficoll is added to give a final concentration of 10% (w/v). The Ficoll-supplemented egg jelly water can be stored in aliquots at -30°C and used within 2 mo after preparation.

3.1.2.2. DEMEMBRANATED SPERM

1. Sperm for the determination of the cell cycle in egg extracts (see **Subheading 3.1.5.**) are prepared according to the method as described in **ref 11**.
2. Resuspend washed sperm pellet with 1 mL nuclear preparation buffer.
3. Add lysolecithin (0.5 mg/mL) and incubate for 5 min. After the incubation, add 10 mL ice-cold nuclear preparation buffer and centrifuge at 2000g for 10 min at 4°C.
4. Resuspend the pellet fraction with 1 mL nuclear preparation buffer containing 30% glycerol and store at -80°C until required.

3.1.3. Fertilized or Artificially Activated Eggs (see **Note 1**)

1. For insemination, groups of 20 dejellied eggs are placed in a plastic culture dish (35-mm diameter) filled with fresh 0.5X SB.
2. Add jelly water-treated sperm (100 μ L, see **Subheading 3.1.2.1., steps 1-4**) near the top surface of the eggs.

3. For parthenogenetic egg activation with calcium ionophore or H_2O_2 , dejellied eggs are transferred to a 35-mm dish filled with 0.5X SB or 1X DB supplemented with either 0.2 μM A23187 or 10 mM H_2O_2 .
4. At the specified time after activation treatment (e.g., 5 min following either insemination or parthenogenetic activation treatment), eggs are washed three times with 0.5X SB, immediately frozen by liquid nitrogen, and stored at -80°C .

3.1.4. Preparation of the Raft Fractions (see **Note 2**)

1. Egg samples are mixed with fivefold volume of ice-cold raft buffer supplemented with 1 mM Na_3VO_4 , 10 $\mu\text{g}/\text{mL}$ leupeptin, 20 μM APMSF, 150 mM NaCl, and 250 mM sucrose and homogenized with a 7-mL Dounce tissue grinder (Wheaton; Millville, NJ).
2. The homogenates are centrifuged at 500g for 10 min, and the supernatants are collected and centrifuged at 150,000g for 20 min (see **Note 2**).
3. Concentrated Triton X-100 (25%) is then added to the fluffy layer of the pellet (crude membranes) to yield a final 1% concentration of Triton X-100.
4. The mixtures are homogenized again, incubated on ice for 10 min, and mixed with equal volumes of ice-cold raft buffer containing 150 mM NaCl and 85% sucrose (sucrose buffer).
5. The resulting mixtures (5 mL) are layered first with 19 mL 30% sucrose and second with 12 mL 5% sucrose in the same buffer.
6. The samples are centrifuged at 144,000g for 20 to 24 h in an SW28 rotor (Beckman; Palo Alto, CA).
7. After the centrifugation, 3-mL aliquots of 12 fractions are collected from the top to the bottom of the tubes. Fractions 3 to 6 are pooled as egg rafts (LD-DIMs: low-density, detergent-insoluble membranes), whereas fractions 10 to 12 are pooled as detergent-soluble nonraft fractions.
8. In some experiments, egg rafts are diluted with water more than fourfold and centrifuged at 150,000g for 30 min. Such concentrated rafts are resuspended with 200 μL raft buffer containing 150 mM NaCl and used for experiments.

3.1.5. Preparation of the Egg Extracts (CSF Extracts)

1. Unfertilized eggs are washed extensively with extraction buffer.
2. Then, the eggs are transferred to the centrifuge tubes containing extraction buffer plus 100 $\mu\text{g}/\text{mL}$ cytochalasin B and 10 $\mu\text{g}/\text{mL}$ each of leupeptin, pepstatin, and chymostatin.
3. Centrifuge for 30 s at 500g, then for 30 s at 1000g at 4°C .
4. Remove all the buffer from the top of the tubes and crush eggs by centrifugation for 15 min at 15,000g rpm.
5. Collect the cytoplasmic part.
6. Centrifuge under the same conditions as the first centrifugation.
7. Add 10% volume of cytochalasin B, protease inhibitors, and energy mix to the extracts.
8. The extracts are kept on ice until use.

3.2. Reconstitution of Signaling Events of Egg Fertilization

In vitro reconstitution system involves both rafts and CSF extracts prepared from *Xenopus* eggs, and a series of biochemical and cell biological events associated with fertilization can be examined (**Fig. 1**).

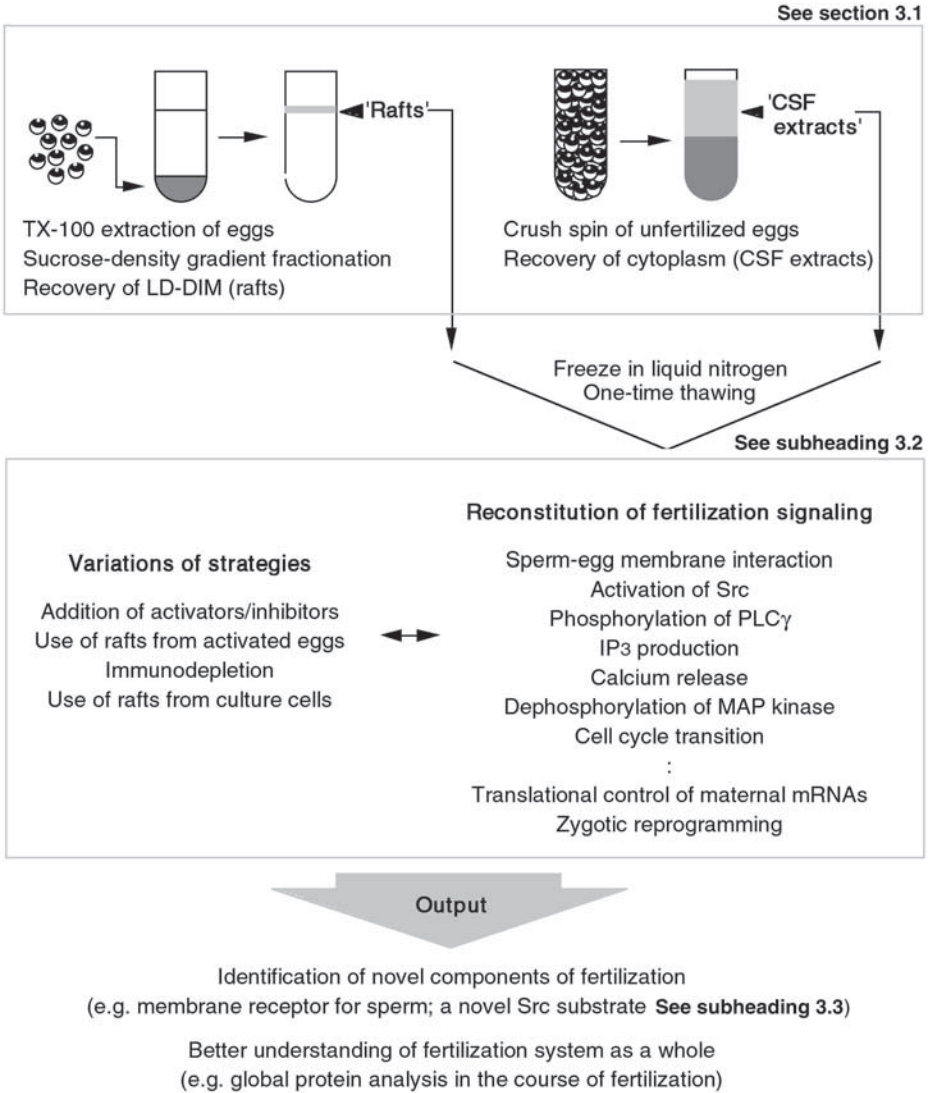


Fig. 1. Schematic representation of a reconstitution system of *Xenopus* egg fertilization signaling. This system involves the membrane/lipid rafts and cell-free extract that are prepared from unfertilized eggs. By combining these two different egg fractions, a series of events associated with fertilization, from the sperm-egg membrane interaction through the Ca²⁺-dependent cell cycle transition, can be reproduced in vitro. Because of its cell-free nature, this system enables us to perform specific targeting of signaling molecules of interest (e.g., pharmacological activation or activation, immunochemical depletion) that would contribute to identifying crucial components for fertilization signaling. A systematic as well as a pin-point approach to characterize egg proteins with use of mass spectrometric analysis certainly would be helpful to validate this strategy.

3.2.1. *In Vitro* Protein–Tyrosine Kinase Assay of the Isolated Raft Fraction

1. Raft fractions (10 μL , an equivalent of 30–60 eggs) were preincubated with or without activators such as $10^6/\text{mL}$ sperm, 1 mM GTP γS , 1 mM cAMP, 1 mM RGDS peptide, or 1 mM CaCl_2 at a final volume of 12.5–25 μL for 10 min at 30°C.
2. The mixtures were further incubated at 30°C for 10 min in the presence of 5 mM MgCl_2 , 20 mM Tris-HCl, 1 mM DTT, 2 μM [γ - ^{32}P]ATP (10 μCi), and 1 mM Cdc2 peptide at a final volume of 50 μL .
3. The reaction was stopped by the addition of 50 μL of Laemmli's SDS sample buffer followed by heat treatment at 98°C for 5 min.
4. Phosphorylated samples were separated by SDS polyacrylamide gel electrophoresis (PAGE) on 16% gels (see **Subheading 3.3.3.**). ^{32}P -labeled Cdc2 peptide was visualized and quantified by a BAS2000 Bioimaging analyzer (Fuji Film).

3.2.2. Tyrosine Phosphorylation of Src, Phospholipase C γ , and MAPK (see **Note 3**)

1. Rafts alone (3 μL : 10–20 egg equivalent), CSF extracts alone (27 μL : 30 egg equivalent), or a mixture of the both are incubated in the absence or presence of 1.5 μL of the activators (e.g., sperm) or 1.5 μL of various inhibitors for 10 min at 30°C. Inhibitors used are 10 μM PP2, PP3, U73122, or U73343; 100 μM heparin; or 5 mM EGTA.
2. The mixtures are then incubated with 5 mM MgCl_2 and 1 mM ATP for 10 min at 30°C.
3. The kinase reaction was terminated by the addition of 30 μL of 10 mM EDTA on ice.
4. Proteins are solubilized by incubation in the presence of 0.1% SDS and 1 mM sodium orthovanadate at 37°C for 10 min and collected as the supernatant fractions after centrifugation at 150,000g for 10 min at 4°C.
5. To assess tyrosine phosphorylation of Src and MAPK, protein samples (10–30 μg) are separated by SDS-PAGE on 8% gels and analyzed by immunoblotting (see below) with either antiphospho Src Y416 antibody (1 $\mu\text{g}/\text{mL}$) or antiphospho MAPK antibody (0.5 $\mu\text{g}/\text{mL}$). For tyrosine phosphorylation of PLC γ , protein samples (50–500 μg) are subjected to immunoprecipitation with anti-PLC γ antibody (1 $\mu\text{g}/\text{mL}$) followed by immunoblotting with antiphosphotyrosine antibody PY99 (1 $\mu\text{g}/\text{mL}$) or anti-PLC γ antibody (0.5 $\mu\text{g}/\text{mL}$).

3.2.3. Immunoprecipitation, SDS-PAGE, and Immunoblotting

1. Protein samples (50–500 μg at 1 $\mu\text{g}/\mu\text{L}$) are immunoprecipitated with 1–5 μL appropriate antibody for 3 h at 4°C.
2. After centrifugation at 10,000g for 10 min at 4°C, the immune complexes are adsorbed onto 10 μL protein A-Sepharose beads by gentle agitation for 30 min at 4°C.
3. The beads are washed three times with 500 μL RIPA buffer, washed once with extraction buffer containing 1% Triton X-100, and used as immunoprecipitates.
4. The immunoprecipitates prepared as above are treated with Laemmli's SDS sample buffer at 98°C for 5 min.
5. SDS-PAGE and immunoblotting of the SDS-denatured proteins are done as described previously using SDS-PAGE apparatus (Atto, Tokyo, Japan) and semidry blotting apparatus (Bio-Rad; Hercules, CA), respectively.

3.2.4. Calcium Release Assay

1. Ultraviolet-excitabile ratiometric fluorescent calcium indicator Fura-2 is added to the CSF extracts at the time 3 to 10 min prior to the initiation of reconstitution of signaling events to a final concentration of 2 μM .

2. The level of free calcium in the extracts is continuously monitored by ratio-imaging microscopy using the high-frame digital CCD imaging ARGUS/HISCA system from Hamamatsu Photonics. Excitation wavelengths are set at 340 and 380 nm; monitoring of the emission was made at 510 nm. The basal level of fluorescent signal was monitored over several minutes at 21 to 23°C prior to the initiation of the reactions.
3. The reaction was initiated by the administration of the effectors (e.g., rafts) that had been preincubated in the absence or the presence of various inhibitors or activators.
4. Further monitoring of the fluorescent signal was made at intervals of 10 to 15 s. Initial time of the calcium rise, its peak height, and duration of the rise are determined. Samples that showed no calcium rise during 40 min of the reaction are recorded as negative. *Calcium rise* is defined for the fluorescent signal that gives more than 0.04 unit of the 340/380 ratio, which persists for more than 30 s. **Table 1** summarizes results of calcium release assay obtained with several conditions involving rafts, activators/inhibitors, and CSF extracts.

3.2.5. Cell Cycle Transition Assay

1. Demembrated sperm nuclei (1 μ L: a final concentration of 10^5 /mL) are added to the CSF extracts (27 μ L) on ice prior to the initiation of reconstitution experiments.
2. Reaction is initiated by the addition of raft fractions as described above. Nuclear morphology of the added sperm nuclei are observed and scored by fluorescent microscopy after withdrawing 1 μ L of extract at appropriate time intervals and adding 4 μ L 0.33X modified Ringer's solution containing 1 μ g/mL Hoechst 33342 (Sigma), 10% formaldehyde, and 50% glycerol.

3.2.6. Immunodepletion of Phospholipase C γ From CSF Extracts

1. Depletion of PLC γ is done by incubating CSF extracts (100 μ L) with anti-PLC γ antibody (1 μ L) for 3 h at 4°C followed by the adsorption of the immune complexes onto protein A-Sepharose beads.
2. The resulting supernatant fractions are used as CSF extracts depleted of PLC γ (CSF/ Δ PLC γ). The efficiency of the depletion is determined by densitometry scanning of the anti-PLC γ immunoblotting results (see **Subheading 3.3.3.**) for intact CSF extracts and CSF/ Δ PLC γ .

3.2.7. Effect of Cultured Cell Raft Fractions

Containing Overexpressed *Xenopus Src* (see **Note 4**)

1. COS7 cells are maintained in Dulbecco's modified Eagle's medium supplemented with 10% fetal calf serum at 37°C in a humidified 5% CO₂ atmosphere. Cells of 20–30% confluence in 100-mm dishes are transfected with the expression vector of FLAG-epitope tagged *Xenopus Src* (2 μ g DNA/dish) using Effectene™ reagent (Qiagen) according to the manufacturer's standard protocol.
2. The transfection treatment proceeds for 24 h at 37°C. The resultant transfected cells are harvested, extracted with raft buffer, and subjected to sucrose density gradient ultracentrifugation as described above.
3. After ultracentrifugation, raft fractions are collected. The expression of *Xenopus Src* is verified by immunoblotting of the fractions with either anti-pepY antibody or anti-FLAG antibody.
4. The effect of the raft fraction containing *Xenopus Src* on the reconstitution of fertilization signaling events (e.g., tyrosine phosphorylation of PLC γ , calcium release) is analyzed as described above.

Table 1
Effect of Rafts Incubated With Sperm or GTP γ S on the Ca $^{2+}$ Release in CSF Extracts

Activators/inhibitors/rafts	% Ca $^{2+}$ rise ^a	Time to Ca $^{2+}$ rise ^b	Peak amplitude ^b	Duration of Ca $^{2+}$ rise ^b
IP $_3$ (10 μ M)	100 (8)	0.9 \pm 0.1	0.44 \pm 0.04	2.4 \pm 0.2
+ heparin (500 μ M)	14 (7)	1.1 (1)	0.07 (1)	1.8 (1)
U rafts	20 (5)	2.1 (2)	0.04 (2)	2.8 (2)
U rafts + sperm (10 ⁶ /mL)	82 (11)	1.7 \pm 0.2 (9)	0.08 \pm 0.11 (9)	5.5 \pm 1.1 (9)
+ PP2 (10 μ M)	13 (8)	2.1 (1)	0.04 (1)	2.6 (1)
+ PP3 (10 μ M)	100 (3)	2.0 \pm 0.4 (3)	0.11 \pm 0.03 (3)	9.1 \pm 3.8 (3)
+ U-73122 (10 μ M)	50 (4)	17.2 (2)	0.06 (2)	1.8 (2)
+ U-73343 (10 μ M)	100 (2)	1.6	0.07	10.3
+ heparin (500 μ M)	0 (3)	-	-	-
U rafts + GTP γ S (1 mM)	100 (3)	1.4 \pm 0.4	0.04 \pm 0.01	3.4 \pm 0.1
U rafts + RGDS (1 mM)	0 (2)	-	-	-
F rafts	50 (4)	2.8 (2)	0.07 (2)	3.7 (2)
A rafts	0 (4)	-	-	-
H rafts	100 (6)	2.4 \pm 0.2	0.20 \pm 0.03	6.5 \pm 1.1
+ PP2 (10 μ M)	0 (5)	-	-	-
+ PP3 (10 μ M)	100 (2)	2.1	0.30	13.0
+ peptide A7 (15 μ M)	0 (3)	-	-	-
+ peptide A9 (15 μ M)	67 (3)	2.3 (2)	0.19 (2)	23.3 (2)
+ U-73122 (10 μ M)	20 (5)	2.9 (1)	0.07	2.8
+ U-73343 (10 μ M)	100 (2)	3.2	0.28	10.2
CSF/ Δ PLC γ + IP $_3$ (10 μ M)	100 (3)	0.6 \pm 0.1	0.38 \pm 0.02	2.5 \pm 0.4
CSF/ Δ PLC γ + U rafts	25 (4)	2.2 (1)	0.06 (1)	5.3 (1)
+ sperm (10 ⁶ /mL)				
CSF/ Δ PLC γ + H rafts	75 (4)	2.1 \pm 0.6 (3)	0.24 \pm 0.03 (3)	5.2 \pm 0.9 (3)
+ PP2 (10 μ M)	0 (3)	—	—	—
+ U-73122 (10 μ M)	0 (4)	—	—	—

U rafts, rafts from unfertilized eggs; F rafts, A rafts, and H rafts indicate rafts from unfertilized, fertilized (5-min insemination), Ca $^{2+}$ ionophore-activated (5-min treatment with A23187), and H $_2$ O $_2$ -activated eggs (5-min treatment), respectively. CSF/ Δ PLC γ indicates CSF extracts depleted of PLC γ . IP $_3$, inositol 1,4,5-triphosphate.

^aNumber of samples tested indicated in parentheses.

^bData (minutes in Time to Ca $^{2+}$ rise and Duration of Ca $^{2+}$ rise columns or ratio unit in Peak amplitude column) shown are means \pm standard deviations of more than three independent experiments, average values of two experiments, or an exact value from one experiment, all of which are dependent on the numbers of samples with Ca $^{2+}$ rise.

3.3. Identification of Raft-Associated Proteins by MS

To explore the role of protein-tyrosine phosphorylation in fertilization, we have been interested in identifying tyrosine-phosphorylated proteins in fertilized or parthenogenetically activated *Xenopus* eggs. We have demonstrated that Src, PLC γ , and the adaptor protein Shc become tyrosine-phosphorylated following egg activation. We have found that a 30-kDa raft-associated protein is a major tyrosine-phosphorylated protein

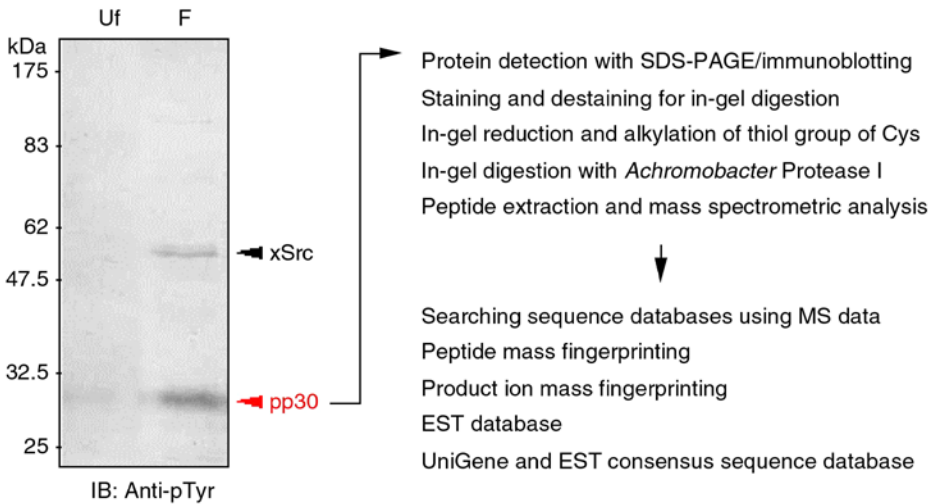


Fig. 2. Molecular identification of egg raft-associated proteins that are tyrosine-phosphorylated at fertilization of *Xenopus* eggs by mass spectrometry and data mining. Immunoblotting analysis (IB) with antiphosphotyrosine antibody (anti-pTyr) of the raft fractions that was prepared from unfertilized eggs (Uf) and fertilized eggs (F, 5 min after insemination) revealed that in addition to *Xenopus* Src (xSrc), a 30-kDa protein is predominantly phosphorylated on tyrosine residue(s). According to the experimental scheme shown in this figure and described in the text, we have characterized this protein, termed pp30, and it turns out to be uroplakin III, a single-transmembrane protein that contains a tyrosine phosphorylation site in the carboxyl-terminal cytoplasmic region (20) and that is a potential target of sperm-derived protease, which is believed to be essential for sperm-induced egg activation (21).

in the membrane/lipid raft fraction of activated *Xenopus* eggs (Fig. 2). In this subheading, we describe molecular identification of such raft-associated proteins using MS, with special emphasis on how to use sequence database to identify unknown *Xenopus* gene product.

3.3.1. In-Gel Digestion for MS Identification of Proteins

3.3.1.1. STAINING AND DESTAINING FOR IN-GEL DIGESTION

1. Visualize proteins in SDS polyacrylamide gels by the silver staining method using a Wako Silver Stain MS Kit for MS protein identification.
2. Excise bands or spots corresponding to proteins.
3. Destain proteins in gel pieces by treating with 0.1 mL of the destaining solution provided by the kit for 15 min according to the instructions.
4. Pull off solution and discard.
5. Add 0.2 mL 20 mM EDTA/100 mM NH_4HCO_3 and incubate at room temperature for 15 min.
6. Wash gel pieces by incubation with 1 mL water at room temperature for 3 min.
7. Pull off solution and discard.
8. Repeat steps 6 and 7.

3.3.1.2. IN-GEL REDUCTION AND ALKYLATION OF THIOL GROUPS OF CYS

1. Dry gel pieces in a centrifugal concentrator.
2. Prepare a fresh solution for reduction: 10 mM DTT/10 mM EDTA/100 mM NH_4HCO_3 .
3. Cover dried gel pieces with the solution for reduction to allow dried gel pieces to swell at room temperature.
4. Reduce proteins in gel pieces at 50°C on a heating block for 1 h.
5. Remove tubes from a heating block and let cool to room temperature.
6. Pull off solution and discard.
7. Dry gel pieces in a centrifugal concentrator.
8. Prepare a fresh solution for alkylation: 40 mM iodoacetamide/10 mM EDTA/100 mM NH_4HCO_3 and keep it in the dark.
9. Cover dried gel pieces with the solution for reduction to allow dried gel pieces to swell at room temperature.
10. Allow reaction to proceed in the dark at room temperature for 30 min.
11. Pull off solution and discard.
12. Wash gel pieces by incubation with 1 mL water at room temperature for 3 min.
13. Pull off solution and discard.
14. Repeat **steps 12 and 13**.

3.3.1.3. IN-GEL DIGESTION WITH *ACHROMOBACTER* PROTEASE I

1. Dry gel pieces in a centrifugal concentrator.
2. Prepare a stock solution of *Achromobacter* protease I (Lysyl endopeptidase[®]) with 0.05 amide unit (AU) (~20 µg) of enzyme/µL of 100 mM Tris-HCl, pH 8.9, and keep at 4°C.
3. Dilute 1 µL stock solution to 3 mL 100 mM Tris-HCl, pH 8.9, to prepare a working solution of *Achromobacter* protease I and keep on ice.
4. Swell dried gel pieces with working solution of *Achromobacter* protease I on ice.
5. Incubate at 37°C for 15 h.

3.3.1.4. PEPTIDE EXTRACTION AND MS ANALYSIS

1. Add 40 µL (or enough to cover gel pieces) 5% formic acid and incubate at room temperature for 10 min.
2. Centrifuge gel pieces, collect supernatant, and save it in on ice.
3. Add 40 µL (or enough to cover gel pieces) 50% acetonitrile/5% formic acid and incubate at room temperature for 10 min.
4. Centrifuge gel pieces, collect supernatant, and combine it with the supernatant from **step 2**.
5. Add 40 µL (or enough to cover gel pieces) of 95% acetonitrile/5% formic acid and incubate at room temperature for 10 min.
6. Centrifuge gel pieces, collect supernatant, and transfer it into a tube to which supernatant from **step 4** has been added to supernatant from **step 2**.
7. Evaporate organic solvent and reduce volume by a centrifugal concentrator until desired volume for desalting with ZipTip (Millipore) or liquid chromatography/MS has been reached.
8. Analyze peptide fragments by MS followed by desalting with ZipTip or liquid chromatography.

3.3.2. Searching Sequence Databases Using MS Data

Searching amino acid or nucleotide sequence database by using MS data of in-gel digests of unknown proteins is well established as a method for the rapid identification

of proteins. At present, several computer programs with different algorithms for protein identification by database searching using MS data have been developed. There are two major approaches for MS-based protein identification. One is the approach called peptide mass fingerprinting, and another is the product ion mass fingerprinting approach, which uses uninterpreted tandem mass spectrometry (MS/MS) data ([12,13](#)).

3.3.2.1. PEPTIDE MASS FINGERPRINTING

In peptide mass fingerprinting, experimental data used for searching are observed mass values of peptide fragments obtained by the digestion of a protein by an enzyme with high residue specificity. Several search engines for peptide mass fingerprinting can be freely accessed across the World Wide Web at uniform resource locators (URLs). Some examples follow. It is possible to obtain licenses to operate some of them for your in-house server.

Peptide Mass Fingerprint in *MASCOT* by Matrix Science: http://www.matrixscience.com/search_form_select.html

MS-fit in *ProteinProspector* by University of California, San Francisco: <http://prospector.ucsf.edu/ucsfhtml4.0/msfit.htm>

ProFound in *PROWL* by Rockefeller University: http://prowl.rockefeller.edu/profound_bin/WebProFound.exe

ProFound in *PROWL* by Genomic Solutions: <http://65.219.84.5/service/prowl/profound.html>

PeptideSearch by European Molecular Biology Laboratory: www.narrador.embl-heidelberg.de/GroupPages/PageLink/peptidesearchpage.html

PeptIdent in *ExPASy* by Swiss Institute of Bioinformatics: <http://us.expasy.org/tools/peptident.html>

PepMAPPER by the University of Manchester Institute of Science and Technology: <http://wolf.bms.umist.ac.uk/mapper/>

3.3.2.2. PRODUCT ION MASS FINGERPRINTING

Another major approach for MS-based protein identification uses uninterpreted MS/MS data (product ion mass lists) from one or more peptide fragments obtained from the digestion of a protein by an enzyme with high residue specificity ([14](#)). In principle, this is similar to peptide mass fingerprinting. The experimental data are compared with calculated mass values of peptide fragments or product ions, obtained by applying appropriate cleavage rule of protease or gas phase fragmentation. Several tools for product ion mass fingerprinting are available on the Internet sites. Some examples follow. It is possible to run a local copy of some of them for your in-house server.

MS/MS Ions Search in *MASCOT* by Matrix Science: http://www.matrixscience.com/search_form_select.html

MS-tag in *ProteinProspector* by University of California, San Francisco: <http://prospector.ucsf.edu/ucsfhtml4.0/mstag.htm>

PepFrag in *PROWL* by Rockefeller University: <http://prowl.rockefeller.edu/PROWL/pepfragch.html>

Cocoozo (National Institute of Advanced Industrial Science and Technology): <http://www.cbrc.jp/cocoozo/>

Sonor ms/ms™ in PROWL by Genomic Solutions: <http://65.219.84.5/service/prowl/sonar.html>

3.3.2.3. EXPRESSED SEQUENCE TAG DATABASE

The protein sequence database searched on servers for MS-based protein identification is mainly nr of the National Center for Biotechnology Information (NCBI) and SwissProt.

Unlike yeast and fly, all information on amino acid sequences of gene products of *Xenopus* is not registered in any database. Unfortunately, at present, the number of entries of *Xenopus* protein sequence in public databases is poor. The current MS-based protein identification approach largely depends on quality of sequence database. If a protein sequence database used in a search does not contain any information on sequence of an “unknown protein,” a particular protein match will be missed.

As product ion mass fingerprinting using uninterpreted MS/MS data can be performed on short stretches of sequence, it is possible to search, instead of an amino acid sequence, a short nucleotide sequence from an expressed sequence tag (EST) that contains a “single-pass” cDNA sequence (15,16). In general, as the reading frame for translation is unknown, the nucleotide sequence is translated to an amino acid sequence in all six reading frames by a search engine prior to searching. If the MS/MS data did not match any sequence in protein databases, the same data set should be searched against an EST database.

A public EST database, dbEST, is a division of GenBank. Currently, NCBI has compiled three databases of est_human, est_mouse, and est_others from the dbEST. These three EST databases are included in available sequence databases on MASCOT (MS/MS ions search) and ProteinProspector (MS-tag) servers that can be freely accessed on Web sites. In general, the est_others database should be used for *Xenopus* protein identification. If you can access to an in-house server for product ion mass fingerprinting, your MS/MS data is able to search against independent EST databases of *Xenopus* obtained from various *Xenopus* EST projects.

3.3.2.4. UNIGENE AND EST CONSENSUS SEQUENCE DATABASE

EST databases are invaluable resources for protein identification and characterization. This allows novel proteins to be identified in the absence of entry in a protein sequence database. However, there are a few drawbacks of using an EST database in proteomics:

1. In general, there are very few long sequences, and each EST translation does not correspond to full-length protein. Therefore, if MS/MS data from multiple peptides derived from the same protein are searched against an EST database, peptide matches are scattered over a number of database entries. With limited exceptions, peptide mass fingerprinting cannot be applied to short stretches of EST.
2. An EST identification is not a real protein identification. Sequence information obtained from the EST is helpful for protein mining. However, it is hard to identify a novel protein

using only the information obtained from the EST without using molecular biological strategy, which is time consuming and complicated.

There have been a number of attempts to identify unique genes and transcripts represented by EST data, such as UniGene of NCBI and The Institute of Genomic Research (TIGR) Gene Index (TGI). In both UniGene and TGI, EST sequences are grouped into a set based on overlapping sequence, in which each set theoretically represents a unique expressed gene. Such nonredundant sets are represented by sequence clusters in the UniGene and by assembled sequences (tentative consensus, TC) sequences in the TGI.

UniGene cluster is an index created by automatically partitioning GenBank sequences into a nonredundant set of gene-oriented clusters. Each UniGene cluster is a list of the nucleotide sequences registered in GenBank that represents a unique gene.

As there are very few long sequences in an EST database, in searching against the EST database using MS/MS data from multiple peptides derived from the same protein, peptide matches are scattered over a number of EST entries. It would be time consuming and not easy to find a connection among a number of matched EST entries. This difficulty can be improved with UniGene. There is an option to group-matched EST entries according to UniGene in one of the product ion mass fingerprinting search engines, a MS/MS ions search of MASCOT (17).

The other solution is using an EST consensus sequence database, instead of an EST database, as a database for product ion mass fingerprinting. The TIGR African clawed frog (*Xenopus*) Gene Index (XGI) uses assembly algorithms to produce consensus sequences (TC sequences) that represent the underlying mRNA transcripts (http://www.tigr.org/tigr-scripts/tgi/T_index.cgi?species=xenopus). UniGene does not attempt to assemble EST sequences within each cluster to produce a consensus sequence. *Xenopus* TC sequence database is a set of virtual transcripts of *Xenopus*. Therefore, peptide mass fingerprinting can be applied to EST consensus sequences. The TC sequence database from XGI is an invaluable resource for protein identification and characterization in MS-based identification of *Xenopus* proteins.

4. Notes

1. This procedure takes about 30 s between the start of the wash treatment and freezing. Only batches of eggs that showed a successful egg activation rate of more than 80% within 20 min of the activation treatment were used for experiments. The successful egg activation rate was determined by monitoring the occurrence of cortical contraction of the pigmented area—a hallmark of successful egg activation—in another group of the same batch of eggs.
2. In the initial procedure, which we used for the preparation of egg raft fractions (10), egg samples were directly mixed with Triton X-100-containing buffer, homogenized, and fractionated. However, we have found that, under these conditions, the resulting raft fractions contained mitochondria or mitochondrial membranes, as judged by the detection of some mitochondria-associated proteins (e.g., cytochrome c oxidase subunits) with the use of MS. The present protocol, which utilizes detergent-free extraction of egg samples and isolation of low-density membrane fraction followed by its solubilization with Triton X-100, essentially excludes the contamination of such nonplasma membranous components in the raft fractions.

3. Tyrosine phosphorylation of Src, PLC γ , and MAPK could also be determined in rafts and nonrafts that had been prepared from unfertilized, fertilized, and parthenogenetically activated egg samples. In this case, 10 μ g of protein from the SDS-solubilized rafts and 500 μ g of proteins from the Triton X-100-soluble nonrafts were subjected to immunoprecipitation and immunoblotting with the same antibodies used for in vitro reconstitution experiments (see refs. 18,19).
4. We also used the raft fractions of COS7 cells expressing different versions of *Xenopus* Src; wild type, kinase inactive, and kinase active. The kinase-inactive version was made by amino acid substitution of Lys-294 in the ATP-binding site with Met. The kinase-active version was made by substitution of Tyr-526 in the carboxyl-terminal tail to Phe. As expected, the COS7 cell rafts containing kinase-active Src induced calcium release in the CSF extracts, whereas those containing kinase-inactive Src did not show such effect (see ref. 19).

References

1. Masui, Y. (2000) The elusive cytostatic factor in the animal egg. *Nat. Rev. Mol. Cell. Biol.* **1**, 228–232.
2. Iwao, Y. (2000) Mechanisms of egg activation and polyspermy block in amphibians and comparative aspects with fertilization in other vertebrates. *Zool. Sci.* **17**, 699–709.
3. Yanagimachi, R. (1994) Fertilization, in *The Physiology of Reproduction* (Knobil, E. and Neill, J. D., eds.), Raven, New York, pp. 189–317.
4. Runft, L. L., Jaffe, L. A., and Mehlmann, L. M. (2002) Egg activation at fertilization: where it all begins. *Dev. Biol.* **245**, 237–254.
5. Sato, K., Iwasaki, T., Hirahara, S., Nishihira, Y., and Fukami, Y. (2004) Molecular dissection of egg fertilization signaling with the aid of tyrosine kinase-specific inhibitor and activator strategies. *Biochim. Biophys. Acta* **1697**, 103–121.
6. Sato, K., Aoto, M., Mori, K., et al. (1996) Purification and characterization of a src-related p57 protein-tyrosine kinase from *Xenopus* oocytes. *J. Biol. Chem.* **271**, 13,250–13,257.
7. Sato, K., Iwao, Y., Fujimura, T., et al. (1999) Evidence for the involvement of a Src-related tyrosine kinase in *Xenopus* egg activation. *Dev. Biol.* **209**, 308–320.
8. Sato, K., Tokmakov, A. A., Iwasaki, T., and Fukami, Y. (2000) Tyrosine kinase-dependent activation of phospholipase C γ is required for calcium transient in *Xenopus* egg fertilization. *Dev. Biol.* **224**, 453–469.
9. Sato, K., Ogawa, K., Iwasaki, T., Tokmakov, A. A., and Fukami, Y. (2001) Hydrogen peroxide induces Src family tyrosine kinase-dependent activation of *Xenopus* eggs. *Dev. Growth Differ.* **43**, 55–72.
10. Sato, K., Iwasaki, T., Ogawa, K., Konishi, M., Tokmakov, A. A., and Fukami, Y. (2002) Low density detergent-insoluble membrane of *Xenopus* eggs: subcellular microdomain for tyrosine kinase signaling in fertilization. *Development* **129**, 885–896.
11. Murray, A. W. (1991) Cell cycle extracts. *Methods Cell Biol.* **36**, 581–605.
12. Pappin, D. J. C., Hojrup, P., and Bleasby, A. J. (1993) Rapid identification of proteins by peptide-mass fingerprinting. *Curr. Biol.* **3**, 327–332.
13. James, P., Quadroni, M., Carafoli, E., and Gonnet, G. (1994) Protein identification in DNA databases by peptide mass fingerprinting. *Protein Sci.* **3**, 1347–1350.
14. Eng, J. K., McCormack, A. L., and Yates, J. R., III (1994) An approach to correlate tandem mass spectral data of peptides with amino acid sequences in a protein database. *J. Am. Soc. Mass Spectrom.* **5**, 976–989.

15. Yates, J. R., III, Eng, J. K., and McCormack, A. L. (1995) Mining genomes: correlating tandem mass spectra of modified and unmodified peptides to sequences in nucleotide databases. *Anal. Chem.* **67**, 3202–3210.
16. Neubauer, G., King, A., Rappsilber, J., et al. (1998) Mass spectrometry and EST-database searching allows characterization of the multi-protein spliceosome complex. *Nat. Genet.* **20**, 46–50.
17. Choudhary, J. S., Blackstock, W. P., Creasy, D. M., and Cottrell, J. S. (2001) Interrogating the human genome using uninterpreted mass spectrometry data. *Proteomics* **1**, 651–667.
18. Tokmakov, A. A., Sato, K., Iwasaki, T., and Fukami, Y. (2002) Src kinase induces calcium release in *Xenopus* egg extracts via PLC γ and IP $_3$ -dependent mechanism. *Cell Calcium* **32**, 11–20.
19. Sato, K., Tokmakov, A. A., He, C.-L., et al. (2003) Reconstitution of Src-dependent PLC γ phosphorylation and transient calcium release by using membrane rafts and cell-free extracts from *Xenopus* eggs. *J. Biol. Chem.* **278**, 38,413–38,420.
20. Sakakibara, K., Sato, K., Yoshino, K., et al. (2005) Molecular identification and characterization of *Xenopus* egg uroplakin III, an egg raft-associated transmembrane protein that is tyrosine-phosphorylated upon fertilization. *J. Biol. Chem.* **280**, 15,029–15,037.
21. Mahbub Hasan, A. K. M., Sato, K., Sakakibara, K., et al. (2005) Uroplakin III, a novel Src substrate in *Xenopus* egg rafts, is a target for sperm protease essential for fertilization. *Dev. Biol.* in press.

Localized Sampling, Electrophoresis, and Biosensor Analysis of *Xenopus laevis* Cytoplasm for Subcellular Biochemical Assays

Christopher E. Sims, Veronica Luzzi, and Nancy L. Allbritton

Summary

The *Xenopus* oocyte is a widely used model cell for studies of signal transduction mechanisms. Advances in microanalytical methods have made it feasible to perform rapid, localized collection of cytoplasm from individual *Xenopus* oocytes. Analytes contained in the cytoplasmic sample are separated by electrophoresis in a capillary and simultaneously transferred to a detection region. The development of bioengineered cells as sensitive detectors of intracellular components made quantitative measurements of native signaling molecules within the electrophoresed sample possible. Local determination of the second messenger inositol 1,4,5-trisphosphate is described to illustrate the methods for the sampling, electrophoresis, detection, and quantification of signaling molecules in single oocytes.

Key Words: Capillary; capillary electrophoresis; detector cell; inositol 1,4,5-trisphosphate; oocytes; single cell; subcellular sampling; *Xenopus laevis*.

1. Introduction

Chemical separation strategies are invaluable tools for analyzing biological samples. Among these strategies, capillary electrophoresis (CE) has proven a powerful method for the study of complex biologic mixtures (1,2). The small dimensions and a variety of sensitive detection schemes make CE especially useful for the study of extremely small samples, particularly for single-cell analyses. The use of a biological cell as the detector has proven a robust and sensitive means for identification and quantification of specific compounds by CE (3–8). Such a detector cell/CE system has been used to measure the concentration of inositol 1,4,5-trisphosphate (IP₃) in subcellular cytoplasmic samples of single *Xenopus laevis* oocytes (5,7,8).

By virtue of its large dimensions, the oocyte serves as an experimentally desirable model system for subcellular measurements of cytoplasmic components. Picoliter-to-nanoliter quantities of cytoplasm can be extracted from an intact, living oocyte or

matured egg (8–10). By manipulating the sampling device with a piezo element (a device formed from layered ceramic material that moves rapidly on application of an electric field), sampling can be performed in subsecond times for the fast temporal resolution desired in measuring dynamic cellular processes, such as the production of second messengers.

With the sampling technique described here, it is also possible to define a spatial resolution to such measurements. The spatial resolution depends on the volume sampled, the capillary's internal diameter (id), and the insertion depth of the capillary into the oocyte. Typical spatial resolutions of 50 to 250 μm are achievable (8–10). This micron-size spatial resolution enables gradients of metabolites across the 3-mm circumference of the oocyte to be identified (8). The determination of IP_3 is used to illustrate the combination of rapid subcellular sampling, electrophoresis, and detection with a biological cell for the measurement of a specific analyte within the complex cytoplasmic milieu of the *Xenopus* oocyte.

It should be noted that the approach is compatible with other techniques, such as confocal fluorescence microscopy, so that measurement of calcium concentration or other cellular properties of the oocyte can be performed in tandem with the electrophoretic determination (7,8). By selecting or engineering the detector cell, determinations of calcium-releasing second messengers other than IP_3 should also be possible.

2. Materials

1. BHK21 cell line (ATCC, Bethesda, MD).
2. Minimum essential medium supplemented with 10% fetal bovine serum, penicillin G (100 U/mL), streptomycin (100 $\mu\text{g}/\text{mL}$), and L-glutamine (2 mM).
3. Collagen, type IV (Sigma, St. Louis, MO).
4. Silicon "O" rings, 11/16-in. id, 7/8-in. outer diameter (od) (McMaster Carr, Los Angeles, CA).
5. Round glass cover slips, no. 1, 25-mm diameter (Fisher Scientific, Los Angeles, CA).
6. Stages V to VI *X. laevis* oocytes.
7. Capillaries: 50-, 75-, and 100- μm id, 360- μm od capillary tubing (Polymicro Technologies, Phoenix, AZ).
8. Capillary coating materials: 3-Methacryloxypropyltrimethoxysilane and 3-aminopropyltriethoxysilane (United Chemical Technologies, Bristol, PA); *N,N,N',N'*-tetramethyl-ethylenediamine (TEMED) and ammonium persulfate (Bio-Rad, Hercules, CA); methanol; TBE buffer (44.5 mM Tris base, 44.5 mM boric acid at pH 8.3, 10 mM ethylenediamine-tetraacetic acid).
9. Hydrofluoric acid (Sigma).
10. Compressed nitrogen gas.
11. IP_3 standard (Alexis Corp., San Diego, CA).
12. Digitonin (Sigma).
13. Mag-fura-2 (Molecular Probes, Eugene, OR).
14. [α - ^{32}P] Adenosine triphosphate (ATP; PerkinElmer, Boston, MA).
15. Ethylene glycol-*bis*(2-aminoethylether)-*N,N,N',N'*-tetraacetic acid (EGTA) "puriss" grade (Fluka, Ronkonkoma, NY).
16. Collagenase (Sigma).
17. Buffer A: 135 mM KCl, 5 mM NaCl, 2 mM ATP, 10 mM HEPES.

18. Buffer A with 900 nM Ca^{2+} . To establish a free Ca^{2+} concentration of 900 nM, a mixture of 1 mM EGTA and 1 mM EGTA with 1 mM Ca^{2+} must be prepared (**11,12**) (see **Note 1**).
19. Buffer A with 100 μM Ca^{2+} (**11,12**) (see **Note 1**)
20. ND96 buffer solution: 96 mM NaCl, 2 mM KCl, 1.8 mM CaCl_2 , 1 mM MgCl_2 , 5 mM HEPES at pH 7.6, 2.5 mM sodium pyruvate.
21. Electrically nonconductive stage containing “V”-shaped depression and reservoir.
22. Upright or dissection microscope for oocyte imaging.
23. Inverted fluorescence microscope for detector cell imaging.
24. Piezo element ($1.3 \times 3.8 \times 0.05$ cm) and power supply (Piezo Systems, Cambridge, MA).
25. Three-axis micromanipulators (2).
26. “T” junction, zero dead volume (Valco Instruments, Houston, TX).
27. Three-way valve (Lee Co., Westbrook, CT).
28. Relay switch: ODC-05 output module (Keithly-Metrabyte, Cleveland, OH).
29. 12-V power supply.
30. CE power supply (Spellman, Hauppauge, NY).
31. Computer with analog-to-digital (A/D) board for control of CE/sampling system and data acquisition.
32. Oocyte injection apparatus (Drummond, Broomall, PA).
33. Liquid scintillation counter.

3. Methods

The methods outlined next describe the basic techniques for (1) localized sampling of oocyte cytoplasm, (2) electrophoresis of cytoplasmic analytes, (3) the use of a cell as a biosensor for IP_3 , and (4) performance of a typical experiment integrating these various subcomponents. **Figure 1** provides a schematic overview of the integrated system.

3.1. Localized Sampling of Oocyte Cytoplasm

3.1.1. Oocyte Preparation

1. Surgically remove stages V and VI oocytes from *X. laevis* frogs.
2. Isolate individual oocytes after collagenase digestion (**13**).
3. Maintain oocytes at 18°C in ND96 until use.
4. Make a 0.5-mm “V”-shaped depression within a shallow (1–2 mm) reservoir created in a block of electrically nonconductive material such as delrin. The shallow reservoir should be contiguous with a deeper reservoir of 1 to 2 mL total volume (**Fig. 2**).
5. In preparation for sampling of oocyte cytoplasm into a capillary, place a single oocyte into the “V”-shaped depression (see **Note 2**).

3.1.2. Construction of Capillary Sampling Apparatus

For aspiration of sample volumes in the picoliter range, a capillary possessing a sharpened tip (see **Subheading 3.1.2., step 1**) can be inserted and withdrawn from the oocyte. Coring action extracts a sample proportional to the depth of insertion (**9**). For rapid, computer-controlled insertion and extraction, the capillary is attached to the end of a piezoelectric motor element with a custom-made mount (**Fig. 3**).

1. Etch the tip of the capillary to a sharp tip with concentrated hydrofluoric acid (HF). Appropriate caution must be taken as the HF solution is highly caustic, and all steps

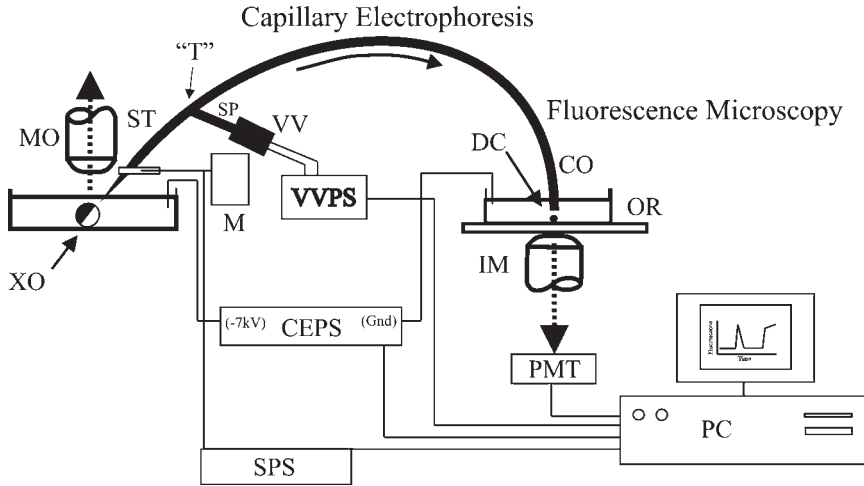


Fig. 1. Schematic representation of the equipment to measure $[IP_3]$. The stage of an upright microscope contains the custom-built delrin holder with a “V”-shaped depression to hold the *Xenopus* oocyte (XO). A microscope objective (MO) is used for viewing the oocyte and positioning the sampling tip (ST). A micromanipulator (M) on the stage of the microscope holds the sampling tip. The micromanipulator is mounted on a rail so that it can be translated and readily removed from the stage. The sampling tip is spliced into a “T” junction connected to the capillary outlet (CO) and a side port (SP) capillary. The side port capillary is attached to a vacuum valve (VV). The vacuum valve power supply (VVPS), the capillary electrophoresis power supply (CEPS), and the sampling power supply (SPS) are controlled through a data input/output board in a personal computer (PC). The capillary outlet is placed in the outlet reservoir (OR) on the stage of an inverted microscope (IM). The outlet reservoir is made from an “O” ring cemented to a cover slip on which the IP_3 -detector cell (DC) is plated. The fluorescence of the detector cell is measured with a photomultiplier tube (PMT) or intensified CCD camera. The fluorescence signal from the PMT is digitized by an A/D board and monitored, and the data are stored in the personal computer.

should be performed in a chemical fume hood. Etching is performed as follows: A 1-cm region of polyimide coating is burned from the capillary at a point 5 cm from one end and cleaned with ethanol to expose the fused silica. The capillary is connected to a nitrogen tank and purged with 10 psi of nitrogen to prevent diffusion of HF into the capillary. The capillary is threaded through a 1000- μ L disposable pipet tip (e.g., Rainin Pipetman P-1000) containing 200 μ L HF. The region of exposed fused silica is positioned within the HF solution, and the capillary is fixed in place on its short end. The other end of the capillary is weighted with a small weight (35 g) and allowed to hang from the pipet tip. The HF will etch the exposed glass until the weighted capillary breaks free (~20–30 min). On completion of the etching process, the capillary will typically be sharpened to a tip retaining the original inner diameter of the lumen, but which now possesses a 2- to 5- μ m wall.

2. Position the piezoelectric-mounted capillary adjacent to the oocyte using a three-axis micromanipulator. Typically, the tip of the capillary is placed at the upper pole of the oocyte, very nearly touching the cell membrane.

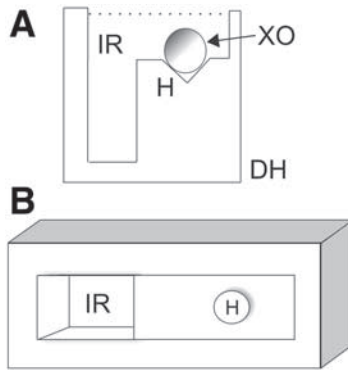


Fig. 2. Diagram of the custom-made delrin oocyte holder (DH) and reservoir. (A) Side view and (B) top view of the holder for the *Xenopus* oocyte (XO) and inlet buffer reservoir (IR). The “V”-shaped depression drilled in the holder is shown on the right (H). The deeper section of the inlet buffer reservoir is shown on the left. The microscope stage is modified to rigidly maintain the holder in place. The dimensions of the oocyte holder are as follows: 4.5 cm high, 4 cm wide, and 5 cm long.

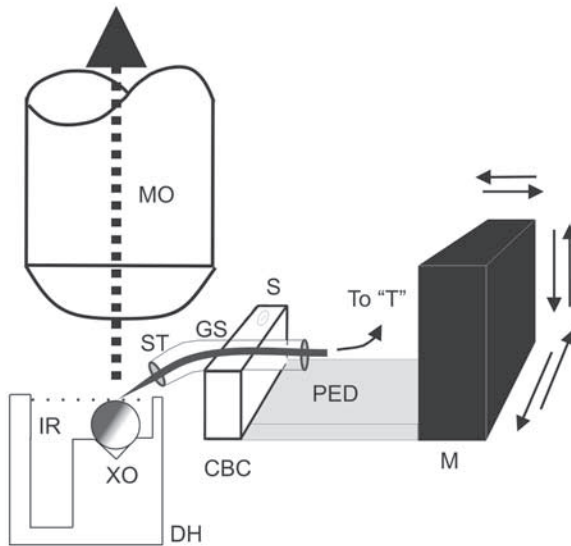


Fig. 3. Diagram of the sampling tip. The custom-built delrin holder (DH) with a “V”-shaped hole holds the *Xenopus* oocyte (XO) in the inlet buffer reservoir (IR). The sampling tip (ST) is cemented to the ends of a glass sleeve (GS). A nylon screw (S) is used to hold the glass sleeve in place in the custom-built clamp (CBC) connected to an “x-y-z” micromanipulator (M) through a piezoelectric device (PED). The oocyte and sampling tip are imaged through the microscope objective (MO).

3. At the desired time, insert the sharpened capillary tip into the oocyte to the desired depth (60–300 μm), followed by withdrawal of the tip into the solution surrounding the oocyte using the computer-controlled piezo element. The buffer solution serves as the buffer for electrophoresis (*see Note 3*).
4. Initiate electrophoresis.
5. Apply a vacuum to the capillary during the insertion to aspirate nanoliter volumes of cytoplasm if desired. This aspiration is accomplished by attaching a valve-operated vacuum line to the capillary at a position 7 cm from the capillary inlet. The inlet capillary should be of 75- μm id and 7 cm long to improve sample aspiration. This capillary is attached to the zero dead volume “T” junction. The separation capillary (50- μm id, 360- μm od, 45 cm long) is connected to the “T” on the straight-through position corresponding to the inlet capillary. To connect the vacuum line to the junction, a capillary (100- μm id, 360- μm od, 5 cm long) is attached to the perpendicular third leg of the “T.” A length of Teflon tubing (2 cm, 0.38-mm id) is connected to the capillary, and is cemented to the common outlet of the three-way valve. The normally open inlet of the valve is open to atmospheric pressure; the normally closed inlet is connected to a vacuum (709 mmHg). To remotely open the valve for application of a vacuum to the inlet capillary during the sampling procedure, a relay switch is interposed between the valve and a 12-V power supply. This relay is controlled by the personal computer PC via the A-to-D board.
6. Perform the cytoplasmic sampling. This is accomplished using a customized software program written to control the piezoelectric motor, the valve, time delays between piezoelectric motor movement and valve opening and closing, and the initiation of electrophoresis. After positioning the capillary tip adjacent to the desired sampling location (*see Subheading 3.1.2., step 2*), a series of software-controlled events are triggered: (1) movement of the piezoelectric motor downward, driving the capillary tip into the oocyte; (2) a variable time delay; (3) opening of the vacuum valve, causing aspiration of cytoplasm into the capillary; (4) closing of the vacuum valve; (5) another time delay; (6) upward movement of the piezoelectric element, withdrawing the capillary tip from the oocyte; (7) a third time delay; and (8) initiation of electrophoresis by application of a voltage across the capillary. Typical time delays are 100 ms.

3.1.3. Determination of the Volume of Cytoplasm Sampled

The detector cell acts primarily as a detector of the mass of IP_3 in the sample rather than its concentration (6). Because the heterogeneity of the oocyte cytoplasm can lead to significant variation in the volume sampled, it becomes imperative to accurately quantify the sample volume for each measurement to determine the IP_3 concentration (6,9). This is accomplished by loading a radioactive marker into the oocyte prior to sampling.

1. Load the oocyte with [α - ^{32}P] ATP (50 nL, ~ 105 cpm) 15 to 30 min prior to experiments to allow adequate time for diffusion of the injectate throughout the oocyte.
2. After sampling (*see Subheading 3.1.2., step 3*), immediately transfer the oocyte to a liquid scintillation vial.
3. After electrophoresis, flush the capillary with buffer and collect this buffer in a second scintillation vial. The [α - ^{32}P] ATP migrates more slowly than IP_3 and is retained in the capillary. Thus, the buffer flushed from the capillary contains that portion of the [α - ^{32}P] ATP sampled from the oocyte.

4. Determine the sample volume. Assuming an oocyte cytoplasmic volume of 0.5 μL (14), the volume sampled is determined by the following equation:

$$([\text{cpm buffer}]/[\text{cpm oocyte} + \text{cpm buffer}]) \times 0.5 \mu\text{L}$$

3.2. Electrophoresis of Cytoplasmic Analytes

3.2.1. Preparation of Capillaries

To reduce adsorption of biological molecules to the capillary walls and increase capillary lifetimes, it is desirable to prepare the capillaries with a neutral surface coating. Polymerized dimethylacrylamide has proven a consistent and robust surface coating for CE-based chemical separations of biological mixtures (15). To prepare a capillary coated with this material, the capillary is flushed with the appropriate solutions for the indicated times in the following procedure:

1. 0.1 *M* NaOH for 12 h.
2. Water for 30 min.
3. 0.1 *M* HCl for 4 h.
4. Water for 30 min.
5. 50% Methanol for 2 h.
6. 100% Methanol for 2 h.
7. 5% (v/v) 3-Methacryloxypropyltrimethoxysilane in methanol for 8 h.
8. 100% Methanol for 1 h.
9. 50% Methanol for 1 h.
10. Air dry for 30 min.
11. 3% (v/v) *N,N*-dimethylacrylamide in TBE buffer: degas by bubbling nitrogen through the solution for 10 min. To initiate polymerization, add 5 mg ammonium persulfate and 20 μL TEMED to 10 mL of the solution and mix immediately prior to flushing the capillary. Continually flush the capillary overnight with the polymerization solution.
12. Water for 3 h or longer.

3.2.2. Electrophoresis Conditions

CE is typically performed in capillaries (50- μm id, 360- μm od, 30–45 cm long) with the neutral surface coating described above.

1. Place ND96 in the inlet reservoir.
2. Place buffer A with 900 nM free Ca^{2+} in the detector cell dish and capillary.
3. Maintain the fluid level in the inlet reservoir 4 to 5 cm above that in the detector cell dish to prevent upward fluid flow from affecting the detector cell (see Note 4).
4. Apply a voltage of 5 to 7 kV (20–30 μA) to the capillary to initiate electrophoresis (see Note 5).

3.2.3. Standards

1. Prepare an IP_3 standard by dissolving a known concentration in buffer A.
2. Load the standard into the capillary by gravitational fluid flow. The volume of the sample loaded per unit time V_t (nL/s) is calculated by the Poiseuille equation (16):

$$V_t = (\rho g \Delta h D^4 \Pi) / 128 \eta L$$

where ρ is the density of the sample solution (typically 1 g/cm^3 for an aqueous buffer), g is the gravitational constant (980 g/cm^2), Δh is the height difference between the sample

and outlet reservoir, D is the inner diameter of the capillary, η is the viscosity (typically $0.801 \text{ g/cm}^2/\text{s}$), and L is the length of the capillary.

3. Bring the capillary inlet in contact with the standard solution for a given amount of time.
4. Place the capillary inlet in the inlet reservoir.
5. Initiate electrophoresis.
6. Monitor detector cell fluorescence over time to determine migration time of the IP_3 in the capillary.
7. Prepare a calibration curve correlating detector cell response to the IP_3 dose as described in **Subheading 3.3.4**.

3.3. Biosensor Detection of Cytoplasmic Analytes

3.3.1. Preparation of Detector Cell

Cells to be used as IP_3 detectors are prepared as follows (5–8,17):

1. Plate BHK21 cells 24 to 48 h prior to experiments in an open cell chamber made by attaching a silicon “O” ring to a no. 1 glass cover slip.
2. Coat the cover slip with collagen to improve cell adherence to the glass by pipeting $200 \mu\text{L}$ collagen solution onto the cover slip followed by air drying. If desired, the coated cover slip can be sterilized by a 70% ethanol wash.
3. Maintain the cells in a humidified 37°C , 5% CO_2 incubator in minimum essential medium (MEM) until use.
4. Prior to the experiments, the cells are incubated for 1 h in Mag-fura-2 ($25 \mu\text{M}$) and washed.
5. Incubate the cells for 5 min with digitonin ($20 \mu\text{g/mL}$) in buffer A with $100 \mu\text{M}$ Ca^{2+} (see **Note 6**).
6. Wash the cells five times in buffer A with 900 nM Ca^{2+} .
7. Maintain the detector cells in buffer A with 900 nM free Ca^{2+} during electrophoresis.

3.3.2. Positioning of Capillary Outlet With Respect to the Cell

Place the capillary the specified distance above the cell as follows:

1. Bring the upper portion of the cell into focus by visualizing the cell through the microscope eyepiece.
2. Use the micrometer markers on the focusing knob of the microscope to move the focal plane of the microscope lens ($100\times$, 1.3 numerical aperture) above the cell by the required distance.
3. Lower the capillary outlet mounted to a three-axis micromanipulator until the bottom (or outlet) end of the lumen is in focus.
4. Return the micrometer to its previous setting to ensure that the cell remains focused in the original focal plane of the capillary once the capillary outlet is lowered to the specified height above the cell.

3.3.3. Imaging of Detector Cell

1. Mount the dish containing the cells on the stage of an inverted fluorescence microscope.
2. Center a single detector cell under the capillary and illuminate at 380 nm (D380x filter, Chroma Technologies, Brattleboro, VT). The intensity of the excitation light is adjusted so that negligible photobleaching occurs during the time of experiments. Emission light from the cell is spectrally filtered (D510/40 filter, Chroma Technologies) and collected with a photomultiplier tube (PMT) or intensified charged coupled device (CCD) camera. Data points are acquired by integrating the fluorescence signal from the cell over 5 s.

3.3.4. Construction of a Calibration Curve for IP_3

The detector cell for IP_3 functions as a detector of the mass of eluted IP_3 (6). To quantify the amount of IP_3 in a sample, a calibration curve must be constructed that correlates the detector cell fluorescence change with the amount of IP_3 in the sample.

1. Electrophorese a known quantity of IP_3 onto a detector cell and measure the fluorescence increase of the cell (5).
2. After the fluorescence has returned to baseline, add a maximally stimulating concentration of IP_3 ($5 \mu M$) to the chamber containing the cell. The calibrated response is defined as the ratio of the peak area of the electrophoresed IP_3 to the peak height after the $5\text{-}\mu M$ calibration exposure.
3. Repeat this process using varying quantities of IP_3 to establish the calibration curve. The response of an unknown sample is compared to the curve to determine the number of moles of IP_3 in the sample. This value is divided by the sample volume (see **Subheading 3.1.2., step 4**) to calculate the concentration of IP_3 in the sample.

3.4. Performing an Analysis

Incubation of detector cells with Mag-fura-2 is performed initially. Fluorescent loading of cells in individual chambers is done serially every 30 to 60 min to have freshly loaded cells prepared for each run. While cells are incubating with Mag-fura-2, an isolated oocyte is injected with [$\alpha\text{-}^{32}P$] ATP and allowed to recover. The detector cells are permeabilized and washed on the stage of the microscope. On completion of the permeabilization step, a cell is chosen to act as the detector cell, and the capillary is positioned directly above that cell. The capillary is then raised 2 to 3 mm above the detector cell in preparation for electrophoresis. The oocyte is placed in the sampling reservoir, and the sharpened capillary inlet is positioned adjacent to the oocyte.

Computer-controlled sampling and electrophoresis are initiated. The oocyte is removed for scintillation counting. At 1 to 2 min prior to the expected elution time of IP_3 (as determined from a standard run at the beginning of the day), the capillary outlet is lowered 200 μm above the detector cell, and fluorescence imaging is begun. Once the detector cell's response to the eluted IP_3 returns to baseline, electrophoresis is terminated, and the $5\text{-}\mu M$ IP_3 calibration dose is added.

After the maximal fluorescence intensity from this calibration dose is achieved, fluorescence imaging is stopped, and the capillary is washed. The fluid from the capillary wash is collected in a scintillation vial, and the counts per minute are determined. Sample volume is calculated, and the number of moles of IP_3 is assessed from the calibration curve. The concentration of IP_3 in the cytoplasmic sample is then determined.

Results from a typical experiment are shown in **Fig. 4**. In this experiment, the intracellular concentration of IP_3 was measured in local regions of *Xenopus* oocytes after stimulation with the agonist lysophosphatidic acid (LPA) (5). Maximal IP_3 concentrations were seen within 2 min after the addition of a maximally stimulating dose of LPA. A range of 40 nm to $1.8 \mu M$ IP_3 was measured at this time-point. This variability is most likely the result of differences in the latency of response of individual oocytes to the LPA, which has been shown to vary between 30 s and longer than 3 min (18).

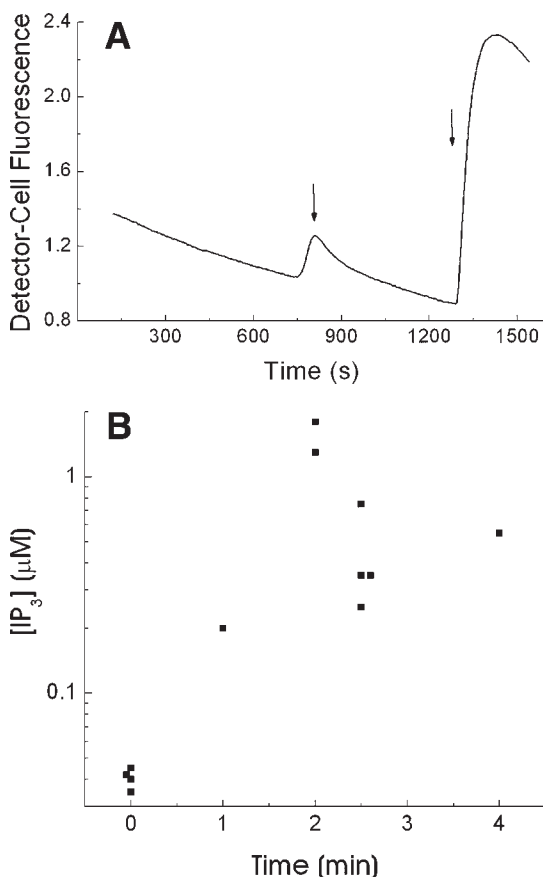


Fig. 4. Measurement of IP_3 in *Xenopus* oocytes. (A) Electrophoretic trace of a cytoplasmic sample obtained from an oocyte after application of LPA. After 2-min exposure to LPA ($10 \mu\text{M}$), cytoplasm (10 nL) was loaded into a capillary and electrophoresed onto a BHK-21 detector cell. The elution time of the peak was identical to the migration time of an IP_3 standard (first arrow). At the time identified by the second arrow, electrophoresis was terminated, and the detector cell was calibrated by the addition of IP_3 ($5 \mu\text{M}$) to the cell chamber. In this example, the measured IP_3 was $1.3 \mu\text{M}$ as determined by comparison to the calibration curve. (B) Measurement of IP_3 at varying times after the addition of LPA ($10 \mu\text{M}$). Each point represents the calibrated IP_3 concentration measured in individual oocytes as described in Fig. 4A.

4. Notes

1. For the IP_3 measurements described, the free calcium concentrations in the buffers are critical. Typically, buffers with no added calcium contain micromolar concentrations of free calcium derived from glassware or plasticware and other sources of low-level contamination. Accurate free-calcium concentrations in these buffers must be achieved using an EGTA buffer system as previously described (11,12).

2. If desired, a small amount of low-melting-temperature agarose (1.5%) can be poured around the edges of the oocyte to hold it in position.
3. Healthy oocytes can leak or extrude small amounts of the microinjected reagents into the surrounding media. These buffer contaminants can enter the capillary prior to insertion of the capillary into the oocyte, confounding subsequent measurements. To eliminate this possibility, the buffer surrounding the oocytes should be replaced with fresh buffer just prior to cytoplasmic sampling.
4. We have found that an upward flow of fluid from the buffer reservoir housing the detector cell into the capillary positioned above the cell is detrimental to the cell's response to IP₃ (6). For this reason, the fluid surface of the reservoir in which the oocyte is placed is positioned at a height 4 cm above that of the fluid surface of the detector cell reservoir. This positioning maintains a slight gravity-driven flow of fluid in a downward direction relative to the detector cell and improves detector cell responsiveness (6).
5. The cell utilized as the IP₃ detector (*see Subheading 3.3.*) becomes less responsive as the exposure time to the electrophoretic voltage increases; therefore, each cell is used for a single measurement (6). For this same reason, the outlet of the capillary is placed 2 to 3 mm above the detector cell and is lowered to a position 200 μm above the cell 1 to 2 min before the measured analyte is expected to electrophorese from the capillary outlet (*see Subheading 3.3.2.*).
6. Permeabilization of the detector cell's plasma membrane must be carefully performed. Incubation of the cells in the digitonin solution for excess times will lead to permeabilization of internal membranes and poor response to IP₃. We have found that different lots of digitonin vary significantly in their activity, and digitonin, even when stored at 4°C in powdered form, may lose potency over 3 to 6 mo. Typical shelf life for the digitonin solution used in permeabilizing the detector cells is 2 wk at 4°C. When a new solution of digitonin is prepared, proper digitonin concentration is determined by incubating cells for 1 to 2 min while following permeabilization. Typically, the concentration of digitonin used should lead to permeabilization of the plasma membranes of most cells after 1- to 2-min incubation at room temperature. Permeabilization is judged by the loss of cytoplasmic fluorescence (loss of Mag-fura-2) from the cytoplasm with retention in the endoplasmic reticulum.

Acknowledgment

This work was supported by an NIH grant (GM57015) to N. L. A.

References

1. Watzig, H. and Gunter, S. (2003) Capillary electrophoresis—a high performance analytical separation technique. *Clin. Chem. Lab. Med.* **41**, 724–738.
2. Shen, Y. and Smith, R. D. (2002) Proteomics based on high-efficiency capillary separations. *Electrophoresis* **23**, 3106–3124.
3. Shear, J. B., Fishman, H. A., Allbritton, N. L., Garigan, D., Zare, R. N., and Scheller, R. H. (1995) Single cells as biosensors for chemical separations. *Science* **267**, 74–77.
4. Fishman, H. A., Orwar, O., Allbritton, N. L., et al. (1996) Cell-to-cell scanning in capillary electrophoresis. *Anal. Chem.* **68**, 1181–1187.
5. Luzzi, V., Sims, C. E., Soughayer, J. S., and Allbritton, N. L. (1998) The physiologic concentration of inositol 1,4,5-trisphosphate in the oocytes of *Xenopus laevis*. *J. Biol. Chem.* **273**, 28,657–28,662.

6. Luzzi, V., Murtazina, D., and Allbritton, N. L. (2000) Characterization of a biological detector cell for quantitation of inositol 1,4,5-trisphosphate. *Anal. Biochem.* **277**, 221–227.
7. Wu, H., Smyth, J., Luzzi, V., et al. (2001) Sperm factor induces intracellular free calcium oscillations by stimulating the phosphoinositide pathway. *Biol. Reprod.* **64**, 1338–1349
8. Wagner, J., Fall, C. P., Hong, F., et al. (2003) A wave of IP₃ production accompanies the fertilization Ca²⁺ wave in the egg of the frog, *Xenopus laevis*: theoretical and experimental support. *Cell Calcium* **35**, 433–447.
9. Luzzi, V., Lee, C. L., and Allbritton, N. L. (1997) Localized sampling of cytoplasm from *Xenopus* oocytes for capillary electrophoresis. *Anal. Chem.* **69**, 4761–4767.
10. Lee, C. L., Linton, J., Souhayer, J. S., Sims, C. E., and Allbritton, N. L. (1999) Localized measurement of kinase activation in oocytes of *Xenopus laevis*. *Nature Biotech.* **17**, 759–762.
11. Tsien, R. and Pozzan, T. (1989) Measurement of cytosolic free Ca²⁺ with quin2. *Methods Enzymol.* **172**, 230–262.
12. Sims, C. E. and Allbritton, N. L. (1998) Metabolism of inositol 1,4,5-trisphosphate and inositol 1,3,4,5-tetrakisphosphate by the oocytes of *Xenopus laevis*. *J. Biol. Chem.* **273**, 4052–4058.
13. Allbritton, N. L., Meyer, T., and Stryer, L. (1992) Range of messenger action of calcium ion and inositol 1,4,5-trisphosphate. *Science* **258**, 1812–1815.
14. Hausen, P. and Riebesell, M. (1991) *The Early Development of Xenopus Laevis*, Springer-Verlag, Berlin.
15. Horvath, J. and Dolnick, V. (2001) Polymer wall coatings for capillary electrophoresis. *Electrophoresis* **22**, 644–655.
16. Weinberger, R. (2000) *Practical Capillary Electrophoresis*, Academic Press, San Diego, CA.
17. Hofer, A. M., Schlue, W. R., Curci, S., and Machen, T. E. (1995) Spatial distribution and quantitation of free luminal [Ca] within the InsP₃-sensitive internal store of individual BHK-21 cells: ion dependence of InsP₃-induced Ca release and reloading. *FASEB J.* **9**, 788–798.
18. Clapham, D. E. (1995) Calcium signaling. *Cell* **80**, 259–268.

Monitoring Protein Kinase A Activities Using Expressed Substrate in Live Cells

Jing Wang and X. Johné Liu

Summary

Protein kinase A (PKA) activity is regulated by intracellular cyclic adenosine monophosphate. Conventional protein kinase assays after cell lysis are hence not suitable for analyzing PKA activities. In this chapter, we describe a new method for monitoring PKA activity in live cells. A tripartite substrate for PKA (Myr-HA- β_2 AR-C) is constructed that contains an N-terminal myristylation sequence followed by an antigenic hemagglutinin epitope tag and a substrate motif (the C-terminal tail of human β_2 adrenergic receptor). The PKA phosphorylation status of the substrate in frog oocytes is determined either by two-dimensional electrophoresis followed by HA epitope immunoblotting or by direct SDS-PAGE followed by immunoblotting using anti-P- β_2 adrenergic receptor antibodies specifically recognizing the PKA-phosphorylated C-terminus. We also describe the application of this strategy in mammalian somatic cells through DNA transfection. Myr-HA- β_2 AR-C should be widely adaptable as an *in vivo* PKA activity indicator.

Key Words: Antibodies; cAMP; expressed substrate; PKA activity indicator; protein kinase A; 2D gel electrophoresis.

1. Introduction

Protein kinase A (PKA), also known as cyclic adenosine monophosphate (cAMP)-dependent protein kinase, is a tetrameric complex consisting of two regulatory subunits (PKAr) and two catalytic subunits (PKAc). In the absence of cAMP, the holoenzyme exists in its tetrameric form and is inactive. Upon the binding of cAMP to the regulatory subunits, the two catalytic subunits are released from the holoenzyme and become active (*1*). Because PKA activity is regulated by intracellular cAMP concentrations, any *in vitro* protein kinase assays after cell lysis would not accurately represent intracellular PKA activity.

To resolve this problem, several groups have developed protein substrates as PKA activity indicators in live cells. Nagai et al. (*2*) constructed a fluorescence-based expressed substrate to measure PKA activity in live cells. The substrate contains two

green fluorescence protein (GFP) variants of different excitation/emission spectra, linked by a PKA substrate motif. In the absence of PKA phosphorylation (or activation of PKA), the two GFP variants are in close contact and hence produce a phenomenon called fluorescence resonance energy transfer (FRET), which can be measured optically by sophisticated microscopy. When PKA is activated, the substrate motif becomes phosphorylated and assumes a more relaxed conformation; therefore, the two GFP variants become further apart, hence reducing FRET. The major drawback of this strategy is the very modest FRET change because of the intrinsic background FRET (in the absence of PKA activation) and the overlapping fluorescence spectra of the two GFP variants. This will seriously limit its application in the whole animal.

A similar FRET-based substrate (AKAR for A-kinase activity reporter) by Zhang et al. (3) improves the activation/background ratio. However, neither withdrawing dibutylryl (db)-cAMP from the culture medium nor the inclusion of PKA inhibitor (H-89) reverses the FRET change induced by db-cAMP, raising the possibility that the substrate motif within A-kinase activity reporter may be phosphorylated by other protein kinases in addition to PKA in live cells.

A third PKA indicator has been developed by Zarrine-Afsar and Krylov (4), who employed capillary electrophoresis and an expressed PKA substrate to monitor intracellular activation of protein kinase A. However, based on the evidence presented in their article, their substrate lacks the specificity and therefore is unlikely to be an acceptable indicator.

To circumvent these problems, we developed a novel assay to monitor endogenous PKA activity in live cells (5). The rationale of this assay is to introduce a specific PKA substrate into live cells with a PKA phosphorylation status that can be analyzed following cell lysis. We constructed a triparti substrate for PKA, Myr-HA- β_2 AR-C, with an N-terminal myristylation sequence derived from the c-Src protein (6), followed by a hemagglutinin (HA) epitope and the PKA substrate motif. We chose the C-terminal tail of human β_2 -adrenergic receptor (β_2 AR) as the PKA substrate (7). This construct, Myr-HA- β_2 AR-C, was transcribed in vitro, and the resulting messenger RNA (mRNA) was injected into frog oocytes. The phosphorylation status of Myr-HA- β_2 AR-C protein, and hence the intracellular PKA activity, was determined by two-dimensional (2D) gel electrophoresis followed by anti-HA immunoblotting. Alternatively, the PKA phosphorylation of the substrate can be determined by direct immunoblotting with antibodies recognizing the PKA-phosphorylated C-terminus of β_2 AR. In this chapter, we describe the application of this strategy for analyzing PKA activities in both frog oocytes and mammalian somatic cells.

2. Materials

1. Myr-HA- β_2 AR-C complementary DNA (cDNA) construct: the construction of this expression plasmid has been described in detail (5).
2. mMessageMachine kit with Sp6 polymerase (Ambion, Texas).
3. OR2: first prepare and autoclave Ca²⁺-free OR2: 83 mM NaCl, 2.5 mM KCl, 1 mM MgCl₂, 1 mM Na₂HPO₄, 5 mM HEPES at pH 7.8. To Ca²⁺-free OR2, add CaCl₂ to 1 mM and gentamicin to 100 µg/mL. All solutions are stored at room temperature. Ca²⁺-free OR2 is good for weeks, whereas OR2 is prepared within the week.

4. Extraction buffer: 20 mM HEPES, pH 7.2, 50 mM glycerophosphate, 2.5 mM MgCl₂, 0.25 M sucrose, 0.1 M NaCl, 1% Triton X-100; store at 4°C. Before use, the following protease/phosphatase/kinase inhibitors are added:
 - a. Phenylmethylsulfonyl fluoride, dissolved in dimethyl sulfoxide (DMSO; 200 mM) and frozen in 20-μL aliquots; 1/1000 dilution in ice-cold extraction buffer.
 - b. Leupeptin, dissolved in water (10 mg/mL) and frozen in 20-μL aliquots; 1/1000 dilution.
 - c. Sodium orthovanadate, dissolved in water (1 mM) and frozen in 20-μL aliquots; 1/1000.
 - d. H89 (Calbiochem), dissolved in DMSO (10 mM) and frozen in 20-μL aliquots; 1/1000 dilution.
 - e. Okadaic acid (Sigma), dissolved in DMSO (100 μM) and frozen in 20-μL aliquots; 1/100 dilution.
5. Mini-protein II Tube Module for first-dimension gel electrophoresis (Bio-Rad).
6. 2X First-dimension sample buffer: 8 M urea, 2% Triton X-100, 5% β-mercaptoethanol, 1.6% 5/7 ampholyte, and 0.4% 3/10 ampholyte (Bio-Rad). This buffer is mixed with an equal volume of extracts before loading on the tube gels.
7. First-dimension overlay buffer: 4 M urea, 0.8% Bio-Lyte 5/7 ampholyte, 0.2% Bio-Lyte 3/10 ampholyte, and 0.0025% bromophenol blue.
8. 2X SDS sample buffer: 125mM Tris-HCl, pH 6.8, 20% glycerol, 4.1% SDS, 0.005% bromophenol blue, 10% β-mercaptoethanol.
9. Anti-p-β₂AR (S345, S346) antibody (Santa Cruz).
10. Complete Dulbecco's modified Eagle's medium (DMEM): DMEM (Invitrogen) containing fetal bovine serum (FBS; 10%), penicillin, and streptomycin (50 U/mL) and fungizone (0.05 μg/mL).
11. Serum-free DMEM: complete DMEM minus FBS.
12. LipofectAMINE 2000 (Invitrogen).
13. Opti-MEM (Invitrogen).
14. db-cAMP (Sigma) dissolved in water (150 mM) and frozen in 50-μL aliquots; 1/100 dilution in serum-free DMEM for activation of PKA in live cells.
15. Phosphate-buffered saline, 10 mM phosphate buffer, pH 7.5, 150 mM NaCl; autoclave and store at room temperature.

3. Methods

The methods described next outline: (1) expression of Myr-HA-β₂AR-C in frog oocytes by mRNA injection and analyses of PKA phosphorylation by 2D electrophoresis; (2) expression of Myr-HA-β₂AR-C in a mammalian somatic cell line (COS7) and analyses of PKA phosphorylation; (3) sample preparation for direct immunoblotting using anti-p-β₂AR (S345, S346).

3.1. Analyzing PKA Activities in Frog Oocytes

We isolate plasmid DNA using Qiagen's Midi DNA columns. In vitro transcription (total volume 20 μL) is carried out using Ambion's mMessageMachine kit, with 2 to 3 μg of linearized DNA per reaction. Final mRNA preparation is dissolved in 20 μL water and stored at -70°C in 3- to 5-μL aliquots (*see Note 1*). We inject 10 to 20 nL mRNA into the cytoplasm of each stage VI oocyte (manually defolliculated; *see Chapter 3*, this volume). Injected oocytes are incubated for at least overnight at 18 to 20°C

in OR2 before subjecting to any drug treatment. The following describes sample preparation and 2D analyses.

1. Place 10 to 20 oocytes in an Eppendorf tube and remove excess OR2.
2. Pipet the desired amount (2 μL /oocyte) of ice-cold extraction buffer; lyse oocytes by forcing them through a yellow pipet tip (a few times are sufficient) in the extraction buffer (**Subheading 2., item 4**, with all the supplements).
3. Centrifuge extracts for 15 min at 13,500 cpm (in a refrigerated Eppendorf centrifuge), transfer the supernatant to a clean tube.
4. Mix the clarified supernatant with an equal volume of 2X first-dimension sample buffer.
5. Incubate the mixture at room temperature for 10 to 15 min before loading 22 μL of each sample onto individual minitube gels (*see Note 2*).
6. Carefully place 30 μL of first-dimension overlay buffer on top of the sample. This buffer provides a cushion between the sample and the electrolyte (100 mM NaOH).
7. After filling the lower tank with 10 mM H_3PO_4 , the tube gel adaptor is placed into the tank. Fill the chamber of the tube adaptor with 100 mM NaOH. Remove bubbles from the lower end of the tube gels with a bent needle attached to a syringe.
8. Carry out first-dimension electrophoresis at 750 V for 3.5 h.
9. Extrude the tube gel with the gel ejector and load the tube gel onto a mini-SDS (15%) polyacrylamide gel made with a “toothless” comb (*see Note 3*).
10. Overlay the tube gel with 1X SDS sample buffer (2X SDS sample buffer diluted 1/1 with water) sufficient to submerge the tube gel. Wait for 10 min before filling with SDS-PAGE running buffer and proceed to 2D run.
11. SDS-PAGE, transfer, and immunoblotting with antibodies against HA are carried out according to standard procedures (*see Note 4*).

Under these conditions, Myr-HA- $\beta_2\text{AR-C}$ appears as a single spot designated as spot 2 (**Fig. 1A**). Following 1-h incubation with progesterone, spot 2 diminishes, and correspondingly, a new spot (spot 1) becomes the predominant form (**Fig. 1B**). Spot 1 and spot 2 differ only in their isoelectrical points, with spot 2 more acidic and hence more phosphorylated. An unknown endogenous protein (indicated by an asterisk) that is recognized by anti-HA antibodies and that does not undergo progesterone-induced changes in its migration pattern serves as a convenient internal marker. To confirm that spot 2 represents the PKA-phosphorylated form of the substrate, we carry out similar analyses that indicate that Myr-HA- $\beta_2\text{AR-C/PKA- (7)}$, which lacks PKA phosphorylation sites, always appears as a single spot, spot 1 (**Fig. 1C,D**).

3.2. Analyzing PKA Activities in COS7 Cells

1. Cell culture is carried out using standard procedures.
2. Transfection is carried out in 6-cm plates when cells are 90 to 95% confluent.
3. Dilute 8 μg DNA in 500- μL Opti-MEM. Mix gently.
4. Dilute 20 μL of LipofectAMINE 2000 reagent in 500- μL Opti-MEM. Mix gently and incubate for 5 min at room temperature.
5. After 5-min incubation, combine the diluted DNA with the diluted LipofectAMINE 2000. Mix gently and incubate for 20 min at room temperature to allow the DNA-LipofectAMINE 2000 complexes to form.
6. Add the 1000- μL DNA-LipofectAMINE 2000 complexes to each 6-cm plate containing cells and medium. Swirl gently to make sure the cells are covered with the solution.

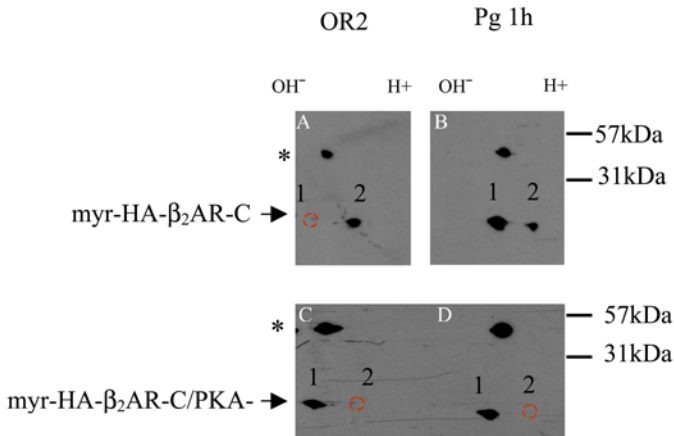


Fig. 1. Two-dimensional analyses of Myr-HA- β_2 AR-C phosphorylation in frog oocytes. Oocytes are injected with mRNAs for wild-type Myr-HA- β_2 AR-C (A,B) or Myr-HA- β_2 AR-C/PKA- (C,D). After 24-h incubation, oocytes in (B,D) are treated with 1 μ M progesterone for 1 h. Then, the oocytes from all groups are lysed and analyzed by 2D gel electrophoresis followed by HA immunoblotting. The asterisk indicates the nonspecific oocyte protein (*see text*) that serves as an internal marker for the positions of spot 1 and spot 2.

7. Incubate cells at 37°C incubator for 6 h, replace with 5 mL complete DMEM.
8. After 24 h, rinse cells with phosphate-buffered saline; follow with the addition of serum-free DMEM and further incubation for 24 h (*see Note 5*).
9. Add db-cAMP (1.5 mM final) to the serum-free medium and return to incubator for an extra 40 min.
10. Aspirate medium, lyse cells by scraping in 1X first-dimension sample buffer (containing 200 μ M phenylmethylsulfonyl fluoride, 10 μ g/mL leupeptin; 50 μ L) on ice.
11. Clarify cell extracts and analyze PKA phosphorylation exactly as described (**Subheading 3.1., steps 5–9**).

The results shown in **Fig. 2A** indicate that, after serum deprivation for 24 h, Myr-HA- β_2 AR-C appears as two spots of more or less equal intensity (**Fig. 2A**), corresponding to spot 1 and spot 2, respectively, in frog oocytes (**Fig. 1**). Brief incubation of these cells with db-cAMP resulted in disappearance of spot 1 such that Myr-HA- β_2 AR-C migrated as a single spot (spot 2). In contrast, Myr-HA- β_2 AR-C/PKA- migrated as a single spot 1 under any conditions (**Fig. 2B**).

3.3. Analyzing PKA Phosphorylation by Immunoblotting With Phosphor-Specific Antibodies

Myr-HA- β_2 AR-C contains multiple phosphorylation sites catalyzed by G protein-coupled receptor kinases, in addition to the known PKA phosphorylation site (RRSS³⁴⁶) (7,8). Phosphorylation of Myr-HA- β_2 AR-C by G protein-coupled receptor kinases or other protein kinases will complicate 2D gel analyses, as is the case in frog oocytes that have undergone maturation (5).

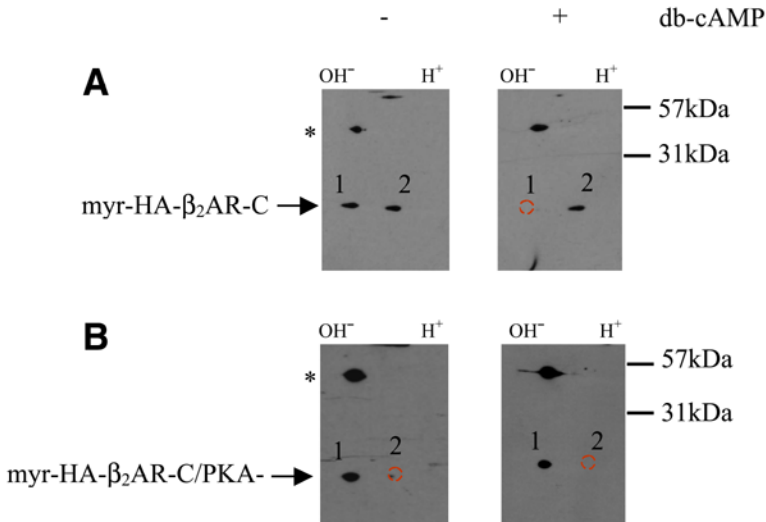


Fig. 2. Two-dimensional analyses of Myr-HA- β_2 AR-C phosphorylation in COS7 cells. COS7 cells are transfected with (A) Myr-HA- β_2 AR-C or (B) Myr-HA- β_2 AR-C/PKA-. The transfected cells are starved for 24 h in serum-free DMEM, followed by treatment with 1.5 mM db-cAMP for 40 min. Cells are then directly lysed into first-dimension sample buffer and are analyzed as in Fig. 1.

To circumvent this problem, we have sought to develop phosphor-specific antibodies against the PKA-phosphorylated β_2 AR C-terminus. Fortunately, Santa Cruz has recently made available PKA phosphorylation site-specific antibody (anti-p- β_2 AR; S345, S346). Although our mutagenesis studies have indicated that Myr-HA- β_2 AR-C is mostly likely phosphorylated by PKA on a single serine residue (S³⁴⁶) (5), the Santa Cruz antibodies clearly and specifically recognized PKA-phosphorylated Myr-HA- β_2 AR-C from both frog oocytes and COS7 cells. The following describe procedures for sample preparation for direct immunoblotting with anti-p- β_2 AR (S345, S346).

To prepare oocyte samples:

1. Follow **Subheading 3.1., steps 1 to 3** (see **Note 6**).
2. Mix clarified supernatant with an equal volume of 2X SDS sample buffer.
3. Heat the samples for 5 min at 85–100°C.
4. Load 10 μ L sample on a well in a 15% SDS polyacrylamide gel (see **Note 7**).
5. We normally run duplicate gels, each blotted with anti-HA (as expression/loading controls) and anti-p- β_2 AR (S345, S346).

To prepare COS7 cell samples:

1. Aspirate serum-free DMEM from the plate.
2. Add 100 μ L SDS sample buffer (2X is fine) directly to a 6-cm plate and lyse the cells by scraping.

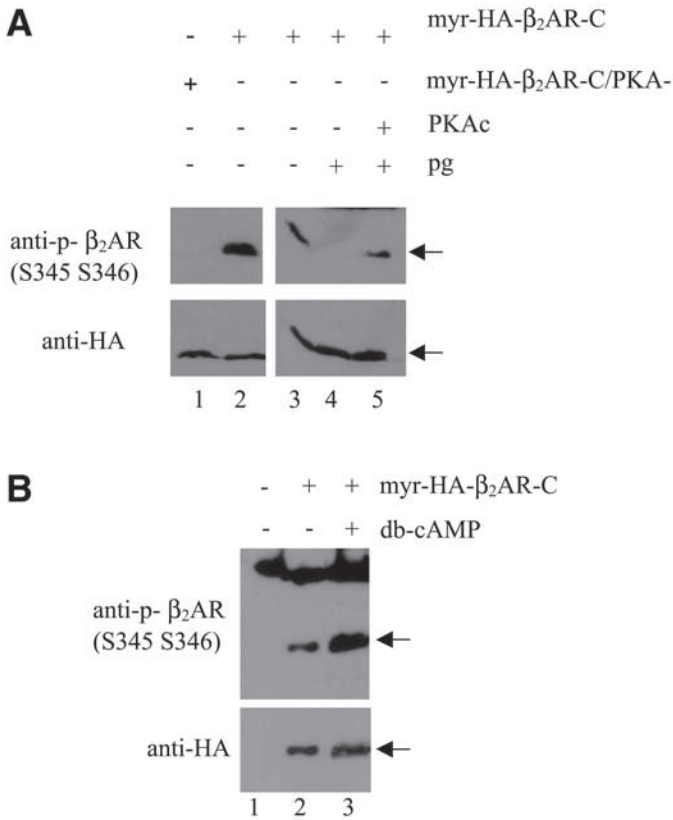


Fig. 3. Analyzing Myr-HA- β_2 AR-C phosphorylation by anti-p- β_2 AR (S345, S346). (A) Oocytes are injected with mRNA for Myr-HA- β_2 AR-C (lanes 2–5) or Myr-HA- β_2 AR-C/PKA- (lane 1). After 24 h incubation, oocytes are treated with 1 μ M progesterone for 1 h (lane 4). Oocytes in lane 5 have received a second injection of PKAc (0.8 U per oocyte) immediately before the addition of progesterone. All groups of oocytes were lysed and analyzed by SDS-PAGE, followed by immunoblotting using anti-HA and anti-p- β_2 AR (S345, S346). (B) COS7 cells are transfected with Myr-HA- β_2 AR-C and treated with or without db-cAMP (as described in Fig. 2). COS7 cell extracts are analyzed by SDS-PAGE, followed by immunoblotting using anti-HA and anti-p- β_2 AR (S345, S346).

3. Transfer the lysate to Eppendorf tubes. To reduce viscosity (caused by the presence of chromosomal DNA), pass the lysates through a 27-gage needle attached to a 1-mL syringe. Be careful not to “overdraw” the plunger or you will have difficulties recovering the samples.
4. Heat the samples for 5 to 10 min at 85 to 100°C.
5. Load 25 to 30 μ L of samples onto each well.

Figure 3A (lanes 2,3) shows that Myr-HA- β_2 AR-C expressed in G2 oocytes is prominently recognized by anti-p- β_2 AR (S345, S346), indicating that these oocytes

contain activated PKA. Extracts derived from progesterone-treated oocytes have lost this band (*lane 4*) despite the presence of Myr-HA- β_2 AR-C protein, as indicated by HA immunoblotting. A prior injection of catalytic PKA (PKAc) prevents the loss of anti-p- β_2 AR (S345, S346) recognition (*lane 5*). In contrast, a mutant form of Myr-HA- β_2 AR-C that lacks the PKA phosphorylation site (PKA-) is never recognized by anti-p- β_2 AR (S345, S346) (*lane 1* and data not shown). These results clearly indicate that Myr-HA- β_2 AR-C serves as a specific indicator of PKA activities in frog oocytes. Similarly, in COS7 cells, Myr-HA- β_2 AR-C can also function as an *in vivo* indicator of PKA activities (**Fig. 3B**).

4. Notes

1. We normally analyze 0.5 μ L of the mRNA sample on a 1% agarose gel to determine the quality of the mRNA (single band). Occasionally, we estimate mRNA quantities by comparing to mRNA standards of known concentrations. The 20- μ L transcription reaction usually produces approx 20 μ g of mRNA.
2. The tube gels (8.5-cm tube length with 1.3-mm inner diameter) can be prepared according to the Bio-Rad protocol provided with the Mini-Protein II Tube Gel Module a day earlier or on the same day (minimum polymerization time 30-min).
3. We often place two tube gels, both trimmed to reduce the length, head to tail on the same SDS-PAGE gel. This trick cuts the number of SDS-PAGE gels in half (an example is shown in **Fig. 1C,D**).
4. We use Amersham's ECLTM Western blotting detection reagents to develop immunoblots. We often need to expose the X-ray film for a few hours to see significant signals.
5. It is essential that cells are serum starved for at least 24 h. Cells that are continuously cultured in serum-containing medium contain only the PKA-phosphorylated form of the substrate, presumably because serum contains PKA-activating agents (such as growth factors).
6. It is not advisable to lyse oocytes directly in SDS sample buffer because the presence of large amounts of yolk proteins will adversely affect resolution of cellular proteins. In fact, we advise not to use any buffers that contain Tris base; in our experience, Tris base alone will extract yolk proteins and make it difficult to run "good" gels. The extraction buffer (**Subheading 2., item 4** with all the supplements, 5 μ L/oocyte) was used to prepare sample for direct SDS-PAGE.
7. Myr-HA- β_2 AR-C migrates on SDS-PAGE as less than 20 K relative molecular mass, so be careful not to run the protein off the gels. We normally run the gels until the dye front is 5 mm from the bottom of the gels.

Acknowledgments

We thank Robert J. Lefkowitz for providing the full-length cDNA constructs containing wild-type human β_2 AR and its mutant lacking PKA phosphorylation sites (S345AS346A). We also thank Veronique Montplaisir for performing experiments depicted in **Fig. 3B**. Work in the lab of X. J. L. is supported by operating grants from Canadian Institute of Health Research (CIHR) and Natural Sciences and Engineering Research Council (NSERC). J. W. is the recipient of a CIHR doctoral research award, and X. J. L. is the recipient of a Premier's Research Excellence Award.

References

1. Francis, S. H. and Corbin, J. D. (1994) Structure and function of cyclic nucleotide-dependent protein kinases. *Annu. Rev. Physiol.* **56**, 237–272.
2. Nagai, Y., Miyazaki, M., Aiju, R., Zama, T., Inouye, S., Hirose, K., Lino, M., and Hagiwara, M. (2000) A fluorescent indicator for visualizing cAMP-induced phosphorylation in vivo. *Nat. Biotechnol.* **18**, 313–316.
3. Zhang, J., Ma, Y., Taylor, S. S., and Tsien, R. Y. (2001) Genetically encoded reporters of protein kinase A activity reveal impact of substrate tethering. *Proc. Natl. Acad. Sci. U. S. A.* **98**, 14,997–15,002.
4. Zarrine-Afsar, A. and Krylov, S. N. (2003) Use of capillary electrophoresis and endogenous fluorescent substrate to monitor intracellular activation of protein kinase A. *Anal. Chem.* **75**, 3720–3724.
5. Wang, J. and Liu, X. J. (2004) Progesterone inhibits protein kinase A (PKA) in *Xenopus* oocytes: demonstration of endogenous oocyte PKA activities using expressed substrate. *J. Cell Sci.* **117**(Pt. 21), 5107–5116.
6. Aronheim, A., Zandi, E., Hennemann, H., Elledge, S. J., and Karin, M. (1997) Isolation of an AP-1 repressor by a novel method for detecting protein–protein interactions. *Mol. Cell. Biol.* **17**, 3092–3102.
7. Zamah, A. M., Delahunty, M., Luttrell, L. M., and Lefkowitz, R. J. (2002) Protein kinase A-mediated phosphorylation of the β 2-adrenergic receptor regulates its coupling to Gs and Gi. Demonstration in a reconstituted system. *J. Biol. Chem.* **277**, 31,249–31,256.

Using *Xenopus* Oocyte Extracts to Study Signal Transduction

Richard F. Crane and Joan V. Ruderman

Summary

Xenopus oocytes are naturally arrested at G2/M in prophase I of meiosis. Stimulation with progesterone initiates a nontranscriptional signaling pathway that culminates in the activation of Cdc2/cyclin B and reentry into meiosis. This pathway presents a paradigm for nongenomic signaling by steroid hormones and for the G2/M cell cycle transition. It has been extensively studied using intact oocytes, which are amenable to microinjection and biochemical analyses described elsewhere in this book. However, there are several experimental advantages in using in vitro systems consisting of cytosolic fractions of prophase-arrested oocytes. Because of their homogeneous nature, extracts avoid the difficulties of signaling asynchrony between individual oocytes. They are also amenable to biochemical manipulations such as protein immunodepletions, and proteins and pharmacological agents can be added easily. Despite these features, oocyte extracts have yet to achieve the widespread utility of *Xenopus* egg extracts, which can proceed through rounds of deoxyribonucleic acid (DNA) replication and mitosis in vitro. Here, we review the historical development of oocyte extracts and discuss the factors most crucial to success in reproducing the signaling pathway and the G2/M transition in vitro.

Key Words: Cdc2; extract; meiosis; nongenomic; oocyte; PKA; progesterone; signaling; *Xenopus*.

1. Introduction

1.1. Oocyte Maturation

Full-grown, “immature” *Xenopus laevis* oocytes are naturally arrested in prophase I of meiosis. Stimulation with progesterone, their presumed natural mitogen, initiates a nontranscriptional signaling pathway, culminating in the activation of the kinase Cdc2/cyclin B. This incompletely understood pathway is illustrated in **Fig. 1** and well reviewed (**1**).

The identity of the hormone receptor is still controversial (**2**), but current evidence favors the conventional progesterone receptor (PR), a dual-function receptor that can regulate both transcriptional and cytoplasmic signaling (**3–5**). A candidate membrane-

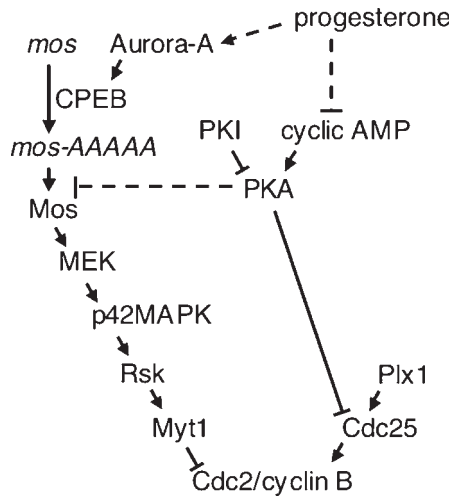


Fig. 1. Simplified diagram of signaling during oocyte maturation. Through a receptor yet-to-be-unambiguously identified (2), progesterone leads to a transient decrease in cAMP levels and protein kinase A (PKA) activity. PKA directly inhibits the phosphatase Cdc25 and thus helps suppress Cdc2 activation (20). PKA also inhibits several other signaling events through unknown mechanisms (shown as dotted lines). The kinase Aurora-A phosphorylates CPEB (cytoplasmic polyadenylation element-binding protein) and thus promotes the polyadenylation and translational activation of maternal mRNA encoding the kinase Mos (21,22). This in turn triggers a kinase cascade through MAPK, Rsk, and ultimately Cdc2 (23). For more details, see ref. 1. PKI, the heat-stable inhibitor subunit of PKA, can be used to stimulate signaling in oocyte extracts (10).

associated receptor, mPR, has been identified in fish and frog oocytes (6). Once activated, Cdc2/cyclin B triggers cell cycle reentry, meiotic progression, and differentiation into a “mature” fertilizable egg. Thus, *Xenopus* oocyte maturation has become an important paradigm for the G2/meiosis I cell cycle transition, and it is also an important system to study nongenomic mechanisms of steroid hormone effects.

1.2. Advantages of Studying Signaling in Oocyte Extracts

Historically, oocyte maturation has been studied using intact oocytes; ovary fragments are surgically isolated, and individual oocytes are released after defolliculation by collagenase. Signaling events can be followed by biochemical analysis of oocytes taken at different times following progesterone stimulation; entry to meiosis is conveniently marked by a white spot that appears at the animal pole following breakdown of the nuclear (germinal vesicle) envelope. Intact oocytes can be manipulated by microinjection of messenger ribonucleic acid (mRNA), protein, or chemical inhibitors.

However, synchrony among different oocytes is often poor, even within a batch from the same frog. It can be difficult to achieve sufficient loss of proteins through antisense or RNAi approaches because oocytes contain large stockpiles of maternally

supplied proteins. It is also difficult to gauge the cytosolic concentration of injected molecules because of variable leakage during injection and absorption by the yolk. Oocyte extracts are therefore attractive because they potentially offer synchronous signaling, immunodepletion of specific maternal proteins, and addition of precisely known concentrations of proteins or chemical inhibitors.

1.3. Difficulties Encountered With Oocyte Extracts

Extracts of *Xenopus* eggs can reliably complete one or more full cell division cycle in the test tube (7–9). For this reason, egg extracts have been developed to investigate many aspects of cell cycle regulation, including deoxyribonucleic acid (DNA) replication, replication licensing, spindle formation, mitotic entry, DNA damage and replication checkpoints, chromosome segregation, and proteolysis during mitotic exit.

By contrast, oocyte extracts have yet to achieve such widespread utility. Efforts to develop oocyte extracts that reproduce all events of the G2/meiosis I transition in vitro have met with two major obstacles. First, oocyte extracts tend to activate signaling spontaneously, probably because of transient decreases in cyclic adenosine monophosphate (cAMP) and protein kinase A (PKA) activity (see Fig. 1) or removal of inhibitors during extract preparation. Spontaneous activation can be suppressed by addition of the cAMP analog 8-[4-chlorophenylthio]-cAMP (10).

Second, it has not been possible so far to reproduce the complete signaling pathway from progesterone to Cdc2 activation. We have found that oocyte extracts can occasionally induce p42MAPK (p42 mitogen-activated protein kinase) activation in response to progesterone or testosterone, but only if the dose of 8-[4-chlorophenylthio]-cAMP is reduced to a level that risks spontaneous activation (R. C. and J. V. R., unpublished data, 2003). The separation of cytosolic and lipid fractions during extract preparation may also tend to disrupt membrane-associated signaling components. Consistent with this notion, mPR and a small but significant fraction of the other presumed *Xenopus* progesterone receptor (XPR), are membrane associated (5,6).

1.4. Examples of the Use of Oocyte Extracts

Despite the difficulties in reproducing progesterone-stimulated signaling, oocyte extracts have nevertheless proven to be a powerful system to investigate signaling events further downstream. Shibuya and colleagues developed oocyte extracts that can activate both p42MAPK and Cdc2 in response to specific stimuli (11). These stimuli include okadaic acid (a phosphatase inhibitor) and indestructible cyclin mutants used to demonstrate the existence of a positive-feedback loop from Cdc2 to p42MAPK. It was subsequently found that addition of purified Mos kinase to oocyte extracts can activate p42MAPK and Rsk (12,13) and even Cdc2 if the extracts are supplied with additional p42MAPK (14). Addition of the heat-stable inhibitor subunit of protein kinase A, PKI (protein kinase A inhibitor), was found to activate numerous signaling events known to occur in progesterone-stimulated intact oocytes, including the synthesis of Mos kinase and activation of p42MAPK, Plx1, and Cdc25 (15).

Signaling in oocyte extracts can be easily manipulated by the addition of purified proteins that antagonize the function of particular signaling molecules. For example, the addition of purified MAPK phosphatase inhibits p42MAPK in extracts (14), and puri-

fied p21(Cip1) inhibits Cdc2 (10). The suspected involvement of the kinase Raf in signaling from Mos to p42MAPK was ruled out using a dominant negative Raf protein (16).

Given appropriate antibodies, endogenous signaling proteins can be quantitatively removed from extracts by immunodepletion. For example, removal of Plx1 blocks PKI-stimulated activation of Cdc2 (10). Other reagents that fail to cross cell membranes can be added directly to extracts, thus widening the range of experimental opportunities. Finally, oocyte extracts have afforded an opportunity to study signaling proteins not normally involved in oocyte maturation. Examples include the oncogenic mammalian proteins H-Ras (V12) (12,17), and v-Src (18).

2. Materials

1. Materials for surgical removal of *Xenopus* oocytes (as described in Chapter 3): forceps, scissors, absorbent pads, anesthetic (MS-222, Sigma A5040, St. Louis, MO), stitches.
2. Dissecting microscope.
3. OR2 buffer: 5 mM HEPES/NaOH at pH 7.6 and 18°C, 82.5 mM NaCl, 2.5 mM KCl, 1 mM MgCl₂. A 10X stock can be prepared in advance and stored at 4°C for several weeks. Filter sterilize the 1X buffer before use and warm to 18°C.
4. Materials to defolliculate oocytes: 10-cm glass Petri dishes extensively washed to remove soap residue, 50-mL polypropylene tubes (e.g., Falcon), collagenase type 1A (Sigma C9891), trypsin inhibitors (type 1-S, Sigma T9003), bovine serum albumin (Sigma A4503).
5. ND96 buffer: 5 mM HEPES/NaOH at pH 7.6 and 18°C, 96 mM NaCl, 2 mM KCl, 1 mM MgCl₂, 1.8 mM CaCl₂. A 10X stock can be prepared in advance and stored at 4°C for several weeks. Before use, filter sterilize the 1X buffer, add penicillin/streptomycin (Invitrogen/Gibco 15140-148, Carlsbad, CA) and warm to 18°C.
6. Refrigerate or keep at 18°C.
7. Extract buffer: 250 mM sucrose, 100 mM NaCl, 2.5 mM MgCl₂, 20 mM HEPES/NaOH at pH 7.2.
8. Centrifugation equipment: tabletop clinical centrifuge, refrigerated ultracentrifuge with a swinging bucket rotor capable of 15,000g (e.g., Sorvall HB6 rotor, Asheville, NC), 13 × 51 mm ultracentrifuge tubes (Nalgene 3410-1351, Rochester, NY), and Versilube F-50 (a silicone oil; General Electric Corp., Westview, NY).
9. A mix of 10 mg/mL each of leupeptin (Sigma L2023), chymostatin (Sigma C7268), and pepstatin A (Sigma P4265) in dimethyl sulfoxide (DMSO); store at -20°C.
10. 20 mg/mL Stock of cytochalasin B (Sigma 6762) in DMSO; store at -20°C.
11. 2 mg/mL Stock of creatinine phosphate (Sigma C6507) in water; store at -70°C.
12. 100 mM EGTA [ethylene glycol bis(b-aminoethyl ether)-N,N,N',N'-tetraacetic acid; Sigma E4378], pH 5.2.
13. 1 mg/mL Ac-DEVD-CHO (caspase inhibitor; Biomol, Plymouth Meeting, PA) in DMSO; store at -20°C.
14. 25 mg/mL stock of 8-[4-chlorophenylthio]-cAMP (a cAMP analog; Sigma C3912) in DMSO; store at -20°C.
15. Dilution buffer: extract buffer (see above) with 1 mM sodium orthovanadate, 10 mM sodium fluoride, 5 mM EGTA at pH 5.2, 40 mM β-glycerophosphate. This solution should be filter sterilized and stored at 4°C. Immediately before use, add a protease inhibitor cocktail (e.g., Complete EDTA-free, Roche, Indianapolis, IN) and 10 μg/mL phenylmethylsulfonyl fluoride (Sigma P7626).
16. Signaling stimulus as necessary, for example: heat-stable inhibitor of protein kinase A (PKI; Sigma P0300), progesterone (Sigma P0130), or recombinant Mos protein (15).

3. Methods

The methods outline (1) harvest of oocytes, (2) the preparation of cytosolic extracts, and (3) use of the extracts to study signaling.

3.1. Harvesting *Xenopus* Oocytes

To obtain a final extract volume of 500 μL , between 3000 and 5000 oocytes should be harvested. It is inadvisable to combine oocytes from more than one frog because poor-quality oocytes from one frog are prone to lyse prematurely and may trigger apoptosis in the entire extract. The procedure for harvesting oocytes is described in detail in Chapter 3, but for completeness is briefly summarized here.

1. Anesthetize a female frog, make a lateral incision, and observe a small ovary fragment under the dissecting microscope. Oocytes with a pale or speckled animal pole generally give poor-quality extract, so the incision should be repaired and the frog allowed to recover. If the oocytes are good quality, surgically remove as much of the ovaries as possible into OR2 buffer.
2. Cut apart the ovary lobes and wash four or five times with 50 mL OR2 buffer to remove as much blood and tissue debris as possible.
3. Defolliculate the oocytes by gentle swirling in two or three 10-cm glass Petri dishes (rinsed free of soap residue), each containing 10 mL OR2 buffer with 5 mg/mL collagenase, 1 mg/mL trypsin inhibitors, and 1 mg/mL bovine serum albumin. Incubate for 90 min or until about half the oocytes are detached from the ovary (do not exceed 2 h). Using a 50-mL polypropylene tube, wash the oocytes several times in 50 mL OR2 buffer and then several times in 50 mL ND96 buffer. Be careful not to agitate the oocytes. See **Note 1** for alternative methods.
4. Select stage VI oocytes (the largest) using a sizing mesh or by manual transfer to a fresh 10-cm glass dish containing 10 mL ND96 buffer. For transferring oocytes, use a sawed glass pipet that has been blunted in a flame to give a smooth aperture larger than an oocyte. Remove any lysed or apoptotic oocytes (which have a marbled appearance) and wash further in ND96 buffer.
5. Allow the oocytes to recover for at least 8 h (or overnight) at 18°C.

3.2. Preparation of Cytosolic Oocyte Extracts

It is important to keep the oocytes at 18°C and the extract at 4°C from the time of centrifugation, so make sure all the buffers, tubes, and centrifuges are appropriately cooled in advance.

1. Using a sawed, blunted glass pipet, remove any lysed or apoptotic oocytes and wash twice in ND96 buffer (18°C) by gentle inversions in a 50-mL polypropylene tube.
2. Wash oocytes twice in extract buffer (18°C) and then twice in extract buffer containing 5 $\mu\text{g}/\text{mL}$ each of leupeptin, pepstatin, and chymostatin. Continue to remove lysed oocytes and take care not to agitate the tube. See **Note 2** for an alternative buffer.
3. Fill as many ultracentrifuge tubes (13 \times 51 mm) as necessary with oocytes, remove excess extract buffer, and add 200 μL Versilube F-50. Place the tubes inside 15-mL glass Corex tubes (to act as adaptors) and spin in a tabletop clinical centrifuge at 150g for 1 min, then 600g for 30 s. Versilube F-50 is a silicone oil that displaces the buffer surrounding the oocytes, resulting in tighter packing. See **Note 2** for an alternative centrifugation procedure.

4. Remove the Versilube F-50 and transfer tubes to an ultracentrifuge swinging bucket rotor chilled to 2°C. Spin at 15,000g for 15 min. The oocyte lysate will separate into an upper yellow lipid layer, a central straw-colored cytosolic layer, and a lower black yolk protein layer.
5. Place the tubes in an ice-cooled water bath. One by one, remove the cytosolic layer by piercing the side of tube with a 20-gage needle connected to a 1-mL syringe. Take care to aspirate slowly (it should take at least 20 s to remove the entire layer) but do not be concerned by minor contamination of the lipid or yolk layers. Before expelling the extract from the syringe, remove the needle to reduce shearing. Pool the cytosolic layers into a single ultracentrifuge tube and place in an ice-cooled bath.
6. Per 1 mL of the pooled cytosolic layer, quickly add the following: 1 μL 1 M MgCl_2 , 2.5 μL 10 mg/mL leupeptin/chymostatin/pepstatin mix, 0.5 μL 20 mg/mL cytochalasin B, 1 μL 2 mg/mL creatinine phosphate, 1 μL 100 mM EGTA at pH 5.2, 0.6 μL 1 mg/mL Ac-DEVD-CHO, and 2 μL 25 mg/mL 8-[4-chlorophenylthio]-cAMP. Mix gently using a sawed pipet tip. For a discussion of the necessity for each of these reagents, see **Note 3**.
7. Spin again at 15,000g for 15 min at 2°C. The extract will again separate into lipid, cytosolic, and yolk layers.
8. Slowly remove the cytosolic layer with a 20-gage needle (see **step 5**), again removing the needle before expelling extract from the syringe. Aliquot the extract into 1.5-mL tubes, either for immediate use or for freezing on liquid nitrogen for storage at -70°C (see **Note 4**).

3.3. Using Oocyte Extracts to Study Signaling

The 50- μL extract aliquots can be stimulated and manipulated in a variety of ways, some of which are listed next. At time-points following stimulus, typically hourly from 0 to 6 h, take 5- μL aliquots of the extract into 45- μL dilution buffer. For analysis by polyacrylamide gel electrophoresis, these diluted samples can be immediately mixed with sodium dodecyl sulfate sample buffer and boiled. For immunoblotting, loading the equivalent of 0.5 μL undiluted oocyte extract per lane will be appropriate for most antibodies.

Diluted samples can also be used for enzyme activity assays, for example, histone H1 kinase assays to monitor Cdc2 activity. To maintain phosphorylation and activity of certain kinases in the diluted samples (including Aurora-A but not p42MAPK), it is necessary to include the phosphatase inhibitor okadaic acid in the dilution buffer (final concentration 0.5 μM).

In published experiments using PKI-stimulated oocyte extracts, synthesis of Mos protein and the activation of p42MAPK, Plx1, Cdc25, and Cdc2/cyclin B all occur around 3 to 4 h (**10**); actual timing may vary according to temperature and extract quality.

The following list includes the more common manipulations of oocyte extracts. When designing an experiment, it is extremely important to minimize the dilution of extract by making stock reagents as concentrated as possible. It is also important to include controls for the potential effect of adding solvents to the extracts.

3.3.1. Stimuli

PKI (Sigma P0300): 400 nM (**15**).

Progesterone (Sigma P0130): we have initiated p42MAPK phosphorylation in oocyte extracts using a range of doses from 0.01 to 10 mg/mL (~ 0.03 – 30 mM) (R. C. and J. V. R., unpublished). A 10-mg/mL stock in anhydrous ethanol does not lose potency for

at least 3 mo at -20°C . Progesterone is also available in a cyclodextrin-encapsulated water-soluble form (Sigma P7556), but we have not thoroughly investigated its ability to stimulate oocyte extracts. Take great care to avoid contaminating laboratory equipment with progesterone because it strongly adheres to plastics.

Mos protein: 100 mg/mL (15). Bacterially expressed Mos protein is inactive but is activated on incubation with oocyte extract.

Rat p42MAPK (ERK2) to establish more robust signaling between Mos and Cdc2 (14): 44 mg/mL. This compares to the endogenous *Xenopus* p42MAPK concentration of 25 mg/mL. Avoid any commercial ERK2 preparations that are coexpressed in bacteria with constitutively active mitogen-activating protein kinase kinase (MEK).

3.3.2. Pharmacological Agents

Cycloheximide (protein synthesis inhibitor; Sigma C6255): 100 mg/mL (10). A 10-mg/mL stock solution in water can be stored indefinitely at -20°C .

Roscovitine (Cdc2 and Cdk2 inhibitor; Sigma R7772): 50 mM (19). Avoid using higher doses, which may cause nonspecific inhibition of a broader range of kinases.

UO126 (MEK inhibitor; Promega V1121, Madison, WI): 50 mM (10). A 20-mM stock solution in dimethyl sulfoxide is stable at -20°C for approx 2 wk.

3.3.3. Immune Depletions

For immune depletions from oocyte extracts, incubate 50 μL extract with 5 μL antibody-coupled beads for 1 h at 4°C (10).

4. Notes

1. Qian and coworkers (10) used calcium-free Barth's solution in place of OR2. They defolliculated oocytes by a 2-h treatment with 0.5 mg/mL dispase and then added collagenase for an additional hour. In place of ND96, they used 0.65X Dulbecco's modified Eagle's medium with 25 mM HEPES at pH 7.5 and penicillin/streptomycin. Previous studies from the same lab obtained oocytes by manual defolliculation (15,18). This method avoids the need for oocyte recovery after collagenase treatment but requires dexterity and yields fewer oocytes.
2. VanRenterghem and coworkers (15,18) were able to achieve p42MAPK activation in response to PKI, v-Src, or cyclin A using a cruder extract preparation. Oocytes were homogenized in 6 volumes of a buffer containing 20 mM Tris-HCl at pH 7.2, 15 mM MgCl_2 , 80 mM *b*-glycerophosphate, 20 mM EGTA, 1 mM phenylmethylsulfonyl fluoride, and 3 $\mu\text{g}/\text{mL}$ leupeptin and then centrifuged at 12,000g for 5 min. The supernatant was diluted twofold in 20 mM Tris-HCl at pH 7.2, 1 mM dithiothreitol prior to stimulation.
3. When extracts are incubated in the absence of stimulus, signaling pathways will often be activated spontaneously. On such occasions, p42MAPK threonine phosphorylation is typically observed after 2 h (R. C. and J. V. R., unpublished observations, 2003). Several factors may influence such "spontaneous activation." It is certainly important to observe strictly the required temperatures during extract preparation and to perform the extract procedure as rapidly as possible. Any apoptotic oocytes still present at the time of centrifugation will lyse and trigger apoptotic signaling; it is therefore essential to include Ac-DEVD-CHO in the extract. Finally, any transient decrease in the activity of cAMP-dependent PKA may be sufficient to trigger the oocyte maturation signaling pathway. To avoid this, the cAMP analog 8-[4-chlorophenylthio]-cAMP is included at 50 $\mu\text{g}/\text{mL}$

(100 μ M) in the extracts to maintain high PKA activity. While attempting to reproduce hormone-induced signaling, we have found it necessary to reduce the concentration of 8-[4-chlorophenylthio]-cAMP to 0.5 μ g/mL or lower (R. C. and J. V. R., unpublished observations, 2003).

4. Although frozen extract is capable of reproducing some aspects of signaling (**II**), it is advisable to use fresh extract whenever possible. Freezing destroys the extract's capacity to synthesize proteins, and *de novo* synthesis of Mos and perhaps other signaling proteins is necessary for oocyte maturation in intact oocytes.

References

1. Schmitt, A. and Nebreda, A. R. (2002) Signalling pathways in oocyte meiotic maturation. *J. Cell Sci.* **115**, 2457–2459.
2. Maller, J. L. (2001) The elusive progesterone receptor in *Xenopus* oocytes. *Proc. Natl. Acad. Sci. USA* **98**, 8–10.
3. Tian, J., Kim, S., Heilig, E., and Ruderman, J. V. (2000) Identification of XPR-1, a progesterone receptor required for *Xenopus* oocyte activation. *Proc. Natl. Acad. Sci. USA* **97**, 14,358–14,363.
4. Bayaa, M., Booth, R. A., Sheng, Y., and Liu, X. J. (2000) The classical progesterone receptor mediates *Xenopus* oocyte maturation through a nongenomic mechanism. *Proc. Natl. Acad. Sci. USA* **97**, 12,607–12,612.
5. Bagowski, C. P., Myers, J. W., and Ferrell, J. E., Jr. (2001) The classical progesterone receptor associates with p42 MAPK and is involved in phosphatidylinositol 3-kinase signaling in *Xenopus* oocytes. *J. Biol. Chem.* **276**, 37,708–37,714.
6. Zhu, Y., Bond, J., and Thomas, P. (2003) Identification, classification, and partial characterization of genes in humans and other vertebrates homologous to a fish membrane progesterone receptor. *Proc. Natl. Acad. Sci. USA* **100**, 2237–2242.
7. Lohka, M. J. and Maller, J. L. (1985) Induction of nuclear envelope breakdown, chromosome condensation, and spindle formation in cell-free extracts. *J. Cell Biol.* **101**, 518–523.
8. Murray, A. W. (1991) Cell cycle extracts. *Methods Cell Biol.* **36**, 581–605.
9. Desai, A., Murray, A., Mitchison, T. J., and Walczak, C. E. (1999) The use of *Xenopus* egg extracts to study mitotic spindle assembly and function in vitro. *Methods Cell Biol.* **61**, 385–412.
10. Qian, Y. W., Erikson, E., Taieb, F. E., and Maller, J. L. (2001) The polo-like kinase Plx1 is required for activation of the phosphatase Cdc25C and cyclin B-Cdc2 in *Xenopus* oocytes. *Mol. Biol. Cell* **12**, 1791–1799.
11. Shibuya, E. K., Polverino, A. J., Chang, E., Wigler, M., and Ruderman, J. V. (1992) Oncogenic ras triggers the activation of 42-kDa mitogen-activated protein kinase in extracts of quiescent *Xenopus* oocytes. *Proc. Natl. Acad. Sci. USA* **89**, 9831–9835.
12. Shibuya, E. K. and Ruderman, J. V. (1993) Mos induces the in vitro activation of mitogen-activated protein kinases in lysates of frog oocytes and mammalian somatic cells. *Mol. Biol. Cell* **4**, 781–790.
13. Nebreda, A. R. and Hunt, T. (1993) The c-mos proto-oncogene protein kinase turns on and maintains the activity of MAP kinase, but not MPF, in cell-free extracts of *Xenopus* oocytes and eggs. *EMBO J.* **12**, 1979–1986.
14. Huang, C. Y. and Ferrell, J. E., Jr. (1996) Dependence of Mos-induced Cdc2 activation on MAP kinase function in a cell-free system. *EMBO J.* **15**, 2169–2173.
15. VanRenterghem, B., Browning, M. D., and Maller, J. L. (1994) Regulation of mitogen-activated protein kinase activation by protein kinases A and C in a cell-free system. *J. Biol. Chem.* **269**, 24,666–24,672.

16. Shibuya, E. K., Morris, J., Rapp, U. R., and Ruderman, J. V. (1996) Activation of the *Xenopus* oocyte mitogen-activated protein kinase pathway by Mos is independent of Raf. *Cell Growth Differ.* **7**, 235–241.
17. Hattori, S., Fukuda, M., Yamashita, T., Nakamura, S., Gotoh, Y., and Nishida, E. (1992) Activation of mitogen-activated protein kinase and its activator by ras in intact cells and in a cell-free system. *J. Biol. Chem.* **267**, 20,346–20,351.
18. VanRenterghem, B., Gibbs, J. B., and Maller, J. L. (1993) Reconstitution of p21ras-dependent and -independent mitogen-activated protein kinase activation in a cell-free system. *J. Biol. Chem.* **268**, 19,935–19,938.
19. Yang, J., Winkler, K., Yoshida, M., and Kornbluth, S. (1999) Maintenance of G2 arrest in the *Xenopus* oocyte: a role for 14-3-3-mediated inhibition of Cdc25 nuclear import. *EMBO J.* **18**, 2174–2183.
20. Duckworth, B. C., Weaver, J. S., and Ruderman, J. V. (2002) G2 arrest in *Xenopus* oocytes depends on phosphorylation of cdc25 by protein kinase A. *Proc. Natl. Acad. Sci. USA* **99**, 16,794–16,799.
21. Mendez, R., Hake, L. E., Andresson, T., Littlepage, L. E., Ruderman, J. V., and Richter, J. D. (2000) Phosphorylation of CPE binding factor by Eg2 regulates translation of c-mos mRNA. *Nature* **404**, 302–307.
22. Mendez, R., Murthy, K. G., Ryan, K., Manley, J. L., and Richter, J. D. (2000) Phosphorylation of CPEB by Eg2 mediates the recruitment of CPSF into an active cytoplasmic polyadenylation complex. *Mol. Cell* **6**, 1253–1259.
23. Palmer, A., Gavin, A. C., and Nebreda, A. R. (1998) A link between MAP kinase and p34(cdc2)/cyclin B during oocyte maturation: p90(rsk) phosphorylates and inactivates the p34(cdc2) inhibitory kinase Myt1. *EMBO J.* **17**, 5037–5047.

Oocyte Extracts for the Study of Meiotic M–M Transition

Keita Ohsumi, Tomomi M. Yamamoto, and Mari Iwabuchi

Summary

In meiotic cell cycles, meiosis I (MI) is followed by meiosis II (MII) without an intervening S phase, whereas in mitotic cell cycles, an S phase necessarily alternates with an M phase. For the study of mitotic cell cycles, extracts prepared from unfertilized and parthenogenetically activated *Xenopus* eggs have been very useful as they can perform the progression of mitotic cycles in vitro. To establish a cell-free system to study the regulatory mechanisms of meiotic transition from MI to MII, extracts have been prepared from maturing *Xenopus* oocytes isolated from ovaries, stimulated with progesterone to induce the resumption of meiosis, and arrested at meiotic metaphase I by cold treatment. In oocyte extracts, the activity of cyclin B-Cdc2 complexes, the M phase inducer, fluctuates in the same manner as it does in maturing oocytes during the MI to MII transition period. By the use of oocyte extracts, it has been found that incomplete inactivation of Cdc2 at the end of MI is required for meiotic M-M transition. The meiotic extract should provide a useful tool to elucidate molecular mechanisms of meiotic M to M transition, including a role of Mos/mitogen-activated protein kinase cascade in the suppression of S phase entry after MI exit. In this chapter, we describe methods for the preparation and the uses of meiotic extracts. As a comparison, we also include a protocol for the preparation of mitotic extracts.

Key Words: Cell cycle regulation; cell-free system; cytoplasmic extract; egg; meiotic cycle; mitotic cycle; oocyte; oocyte maturation; sperm; *Xenopus laevis*.

1. Introduction

Since the success in the hormonal induction of meiotic resumption in vitro, the fully grown oocytes of *Xenopus laevis* have been widely used as a convenient tool for studying the regulatory mechanisms for cell cycle events during meiosis I (MI) and II (MII) or, more precisely, the period from prophase of MI (prophase I) to metaphase of MII (metaphase II) (1,2). This meiotic period is also called oocyte maturation because during this period oocytes incapable of starting embryonic development become eggs that, if fertilized, are able to carry out entire embryonic development. In contrast to mitotic cell cycles, meiotic cell cycles during oocyte maturation have many unique

From: *Methods in Molecular Biology*, vol. 322: *Xenopus Protocols: Cell Biology and Signal Transduction*
Edited by: X. J. Liu © Humana Press Inc., Totowa, NJ

regulatory mechanisms, such as prophase arrest in MI, hormonal induction of maturation-promoting factor and the subsequent prophase-to-metaphase transition, M phase-to-M phase transition between MI and MII, metaphase arrest in MII by the action of cytostatic factor, and finally the release from the metaphase arrest on fertilization (1,3–6). Among these, the transition from MI to MII without an intervening S phase is particularly intriguing as it is unique to the meiotic cycle and essential for the formation of gamete cells with the haploid genome.

The other interesting feature during this period is the separation of homologous chromosomes, which is unique in MI. In addition, during the maturation period, oocytes acquire the competence for remodeling a fertilizing sperm nucleus into a pronucleus, in which the male genome deoxyribonucleic acid (DNA) is replicated (7–12). In relation to this, oocytes during the MI to MII transition period also appear to possess higher cytoplasmic activity than mature eggs to reprogram nuclei of differentiated cells to restore the totipotency that supports the entire embryonic development (13).

Xenopus oocytes, like those of most mammals, undergo their entire growth in the ovary while arresting at prophase I. Although the chromosomes are arrested in diplotene stage, the nucleus and the cell undergo dramatic enlargement. Fully grown oocytes reach 1.2-mm diameter. A sexually matured *Xenopus* female maintained in laboratories contains tens of thousands of oocytes at all stages of oocyte growth (14). Thus, although only the fully grown oocytes are able to resume meiotic cycles by hormonal stimulation, thousands of such oocytes are available from a single female.

In addition, the resumption of meiosis is easily recognized by the appearance of a white spot at the animal pole region, which indicates the break down of the large oocyte nucleus, termed germinal vesicle breakdown (GVBD). However, it has long been known that meiotic progression in *Xenopus* oocytes is not as synchronous as mitotic progression in fertilized eggs; the time period from hormonal stimulation to the occurrence of GVBD is variable from oocyte to oocyte, even from the same female retrieved at the same time. Thus, it often occurs in a batch of oocytes hormonally stimulated at the same time that although some oocytes have reached metaphase II, others have not undergone GVBD.

The low degree of synchrony of meiotic progression has hampered the biochemical study of meiotic regulations in *Xenopus* oocytes, especially for MI to MII transition, which takes place within a short time period. It has been found, however, that in maturing *Xenopus* oocytes, the meiotic progression during the post-GVBD period is highly synchronous (15), and maturing oocytes can be reversibly arrested at metaphase I (16).

Based on these findings, we have developed the cell-free extract from metaphase I-arrested oocytes, which reproduces many of the cell cycle events during the MI to MII transition (16). In the oocyte extract, the activity of Cdc2 fluctuates just as it does in maturing oocytes. The oocyte extract does not support the formation of meiotic spindles from demembranated sperm nuclei but nevertheless can successfully induce the separation of sister chromosomes of mitotic spindles (i.e., the transition from metaphase to anaphase). Thus, the extract from metaphase I oocytes reproduces the meiotic cycle of maturing oocytes.

Like the mitotic cycling extract from eggs (17,18), the meiotic cycling extract from oocytes can be a powerful tool for biochemical and molecular analyses of various biological phenomena and their regulatory mechanisms in oocytes during the MI to MII transition period (16,19). In this chapter, we describe the method for preparing the cytoplasmic extract from metaphase I oocytes that performs in vitro the meiotic progression from metaphase I to metaphase II.

2. Materials

1. 0.2% Ethyl 3-aminobenzoate methanesulfonate (MS-222) solution: dissolve MS-222 at 2 g/L in tap water.
2. Marc's modified Ringer's (MMR): 100 mM NaCl, 2 mM KCl, 2 mM CaCl₂, 0.1 mM ethylenediaminetetraacetic acid, 1 mM MgCl₂, 5 mM HEPES-KOH at pH 7.8 (20).
3. 0.2% Collagenase solution: dissolve collagenase (type S-1, Nitta Gelatin Co., Osaka, Japan, or type I, Sigma-Aldrich Co., St. Louis, MO) at 2.0 mg/mL in MMR and store at -20°C (stable for several months).
4. Leibovitz's L-15 medium (Gibco): dilute Leibovitz's L-15 medium to 70%, sterilize by filtration, add 50 U penicillin and 50 µg/mL streptomycin, and store at 4°C.
5. Progesterone solution: dissolve progesterone at 10 mg/mL in ethanol (stock solution) and store at 4°C. Add the stock solution to MMR at 1/1000 and immediately mix well.
6. Extraction buffer (EB): 100 mM KCl, 5 mM MgCl₂, 20 mM HEPES-KOH at pH 7.5.
7. Cytochalasin B: dissolve at 10 mg/mL in dimethyl sulfoxide, and store at -20°C.
8. Energy mixture: 500 mM creatine phosphate, 50 mM MgCl₂, 50 mM adenosine triphosphate (ATP)-NaOH at pH 7.0 (18).
9. 5.0-µm Filter unit (UFC30SV00, Millipore Co., Bedford, MA).
10. Eppendorf Safe-Lock tube (1.5 mL) and its micropestle.
11. Sucrose-magnesium-hepes solution (SMH): 250 mM sucrose, 2 mM MgCl₂, 20 mM HEPES-KOH at pH 7.5.
12. 5 mg/mL Lysolecithin in SMH, made fresh.
13. 3% and 0.4% (w/v) Bovine serum albumin (BSA; fraction V; Sigma-Aldrich) in SMH.
14. DNA staining solution: 10 µg/mL Hoechst 33342, 3.4% formaldehyde, 30% (v/v) glycerol in EB (store at -20°C).
15. Kinase buffer: 80 mM β-glycerophosphate, 20 mM ethylene glycol bis(b-aminoethyl ether)-N,N,N',N'-tetraacetic acid, 5 mM MgCl₂, 20 mM HEPES-KOH at pH7.5.
16. Reaction buffer for histone H1 kinase assay: 80 mM β-glycerophosphate at pH7.4, 20 mM MgCl₂, 0.6 mM ATP, 30 µg/ mL leupeptin, 30 µg/mL aprotinin, 0.6 mg/mL histone H1 (Roche Diagnostics Co.), 1 µCi [γ -³²P]ATP.
17. 4X SDS sample buffer: 0.25 M Tris-HCl at pH 6.8, 40% (v/v) glycerol, 8% (w/v) SDS, 20% (v/v) β-mercaptoethanol, 0.01% (w/v) bromophenol blue.
18. Pregnant mare serum gonadotrophin: dissolve in MMR at 100 U/mL and store at -20°C.
19. Human chorionic gonadotrophin (hCG): dissolve in MMR at 1000 U/mL and store at -20°C.
20. 2.5% (v/v) Thioglycolic acid: titrate to pH 8.2 with NaOH.
21. 50 nM Calcium Ionophore A23187: dissolve Calcium Ionophore A23187 at 1.0 mM in dimethyl sulfoxide (stock solution) and store at -20°C. Add the stock solution to MMR at 1/2000 and immediately mix well.

3. Methods

The methods for the meiotic cycling extract from oocytes described next include: (1) synchronization of oocyte meiosis in metaphase I, (2) preparation of oocyte

extracts, and (3) monitoring of cell cycle transition in oocyte extracts. In addition, for comparison between meiotic and mitotic characters of cell cycle regulations, a preparation method for the mitotic cycling extract from activated eggs is described.

3.1. Meiotic Cycling Extracts From Metaphase I Oocytes

The method of preparing meiotic cycling extract from metaphase I oocytes is based on those for mitotic cycling extract from activated eggs. To prepare egg extracts that perform the cell cycle progression, it is recommended to use eggs of high quality and to minimize dilution of the cytoplasm with buffer on extraction (18). The same recommendations also apply to the preparation of meiotic extracts from oocytes. In addition, it is crucial to synchronize the oocytes at metaphase I because, as mentioned in **Subheading 1.**, the occurrence of GVBD (indicating the transition from prophase to metaphase in MI) is not highly synchronous in *Xenopus* oocytes induced to mature in vitro.

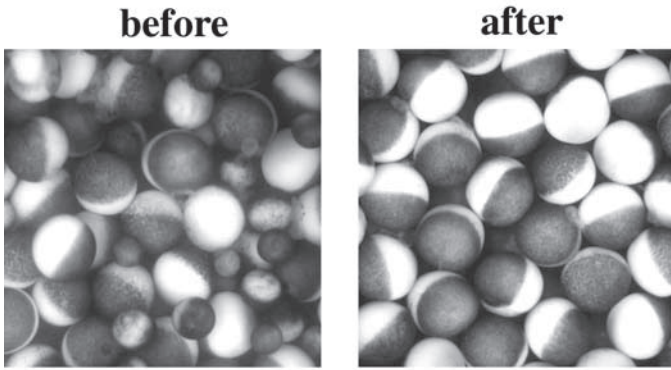
We have found, however, that in maturing *Xenopus* oocytes, the meiotic progression during the post-GVBD period is highly synchronous and can be arrested at metaphase I by cold treatment (16). Furthermore, the metaphase I arrest by cold treatment is reversible when restricted within 2 h; if the incubation temperature is shifted back to room temperature within 2 h of the onset of cold treatment, the oocytes resume meiosis and reach metaphase II according to the normal time schedule. These findings allow us to obtain large numbers of metaphase I oocytes sufficient for the preparation of cytoplasmic extracts.

3.1.1. Isolation of Oocytes From the Ovary

The quality and quantity of fully grown oocytes contained in a pair of ovaries are considerably variable from female to female. Unfortunately, it is very difficult, if not impossible, to know the state of ovarian oocytes in advance of ovary dissection. We recommend sacrificing females that have laid good eggs 2 to 3 mo before and have been maintained at room temperature. Ovaries of such females are most likely to contain fully grown oocytes of healthy appearance; that is, pigmentation is uniform in the animal hemisphere, and the boundary between pigmented and unpigmented areas is clear (see **Fig. 1A**). Fully grown oocytes of such appearance are generally high quality.

1. Anesthetize a female frog by immersion in 0.2% MS-222 in tap water for 30 to 40 min and then pith it.
2. Place the frog on its back in a tray covered with a paper towel and cut away the abdominal skin using a pair of fine surgical scissors.
3. Make lateral cuts in the muscle of the body wall at both sides of the abdominal midline using scissors. Care should be exercised to avoid cutting through the major vein running along the abdominal midline (see **Note 1**).
4. Remove both ovaries using scissors and place them in a Petri dish filled with MMR. Remove clotted blood and any remaining fat body from the ovaries with scissors and forceps.
5. Transfer ovaries into a 50-mL plastic tube with a screw cap and fill the tube with 0.2% collagenase in MMR (see **Note 2**). Incubate the ovaries on a rotator at room temperature for 2 to 2.5 h until more than three-fourths of the oocytes are freed from the ovarian tissues (see **Note 3**).

A Fully-grown oocyte selection



B GVBD oocyte selection

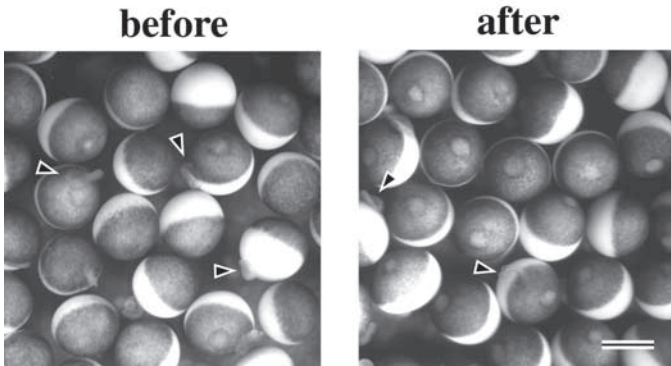


Fig. 1. Oocyte selection for meiotic extract preparation. (A) All stages of growing oocytes freed from ovarian tissue by collagenase treatment (before) and selected stage VI (14), fully grown oocytes (after). (B) Fully grown oocytes at 2.5 h after progesterone treatment (before) and selected GVBD oocytes on which a white spot, indicative of the occurrence GVBD, has appeared (after). Arrowheads indicate shrunk thecal layers. Bar indicates 1.0 mm.

6. Stand the tube for a few minutes to sediment oocytes, then pour off the collagenase solution by decantation.
7. Pour MMR into the tube and transfer oocytes into a 100-mL conical beaker filled with MMR. Gently wash oocytes several times in MMR and once in 70% Leibovitz's L-15 medium.
8. Using a pipet with an opening 5 to 10 mm in diameter, transfer oocytes to a 15-cm dish filled with 70% Leibovitz's L-15 medium supplemented with 50 U/mL penicillin and 50 μ g/mL streptomycin.
9. Incubate oocytes at 15°C for 8 to 12 h before progesterone treatment to induce meiotic resumption (*see Note 4*).

3.1.2. Synchronization of Oocyte Meiosis at Metaphase I

A large number of oocytes synchronized in metaphase I are obtained by selecting oocytes on which a white spot has just appeared, referred to as GVBD oocytes, followed by arresting their meiosis in metaphase I by cold treatment. The selection of GVBD oocytes is the crucial step in the preparation of oocyte extracts that must be quick, accurate, and skillful.

1. Wash oocytes in MMR and transfer to a Petri dish filled with MMR.
2. Using a truncated fire-polished Pasteur pipet with a 1.5- to 2.0-mm diameter opening, remove only fully grown oocytes (>1.1-mm diameter) to a new dish filled with MMR (see **Note 5**).
3. Transfer collected fully grown oocytes into a 50-mL beaker and remove the excess MMR. Add 10 to 20 mL 10 µg/mL progesterone in MMR and incubate for 10 min with occasional swirling.
4. Divide stimulated oocytes into several 5-cm dishes filled with MMR and incubate them at 22°C.
5. Observe oocytes under a dissecting microscope at 30-min intervals. When GVBD oocytes are found (**Fig. 1B**), remove them to a new dish filled with MMR using the truncated Pasteur pipet (see **Note 6**). Continue collecting GVBD oocytes for 30 min.
6. Incubate GVBD oocytes collected during the 30-min period for 30 min at 22°C or for 60 min at 18°C, followed by an additional incubation for 15 min at 22°C. During the incubation, oocyte meiosis attains to metaphase I. Transfer metaphase I oocytes to a dish filled with cold MMR and store on ice.
7. Repeat the oocyte selection and incubation at 30-min intervals until sufficient numbers of metaphase I oocytes are obtained (see **Note 7**).

3.1.3. Preparation of Cytoplasmic Extracts From Oocytes

To make the cytoplasmic extract as concentrated as possible, it is necessary to remove the maximum amount of buffer from oocytes. To achieve this, we pack oocytes tightly in a plastic tube by brief spins (**16**) instead of substituting buffer with a silicon oil as recommended (**18**). The oocyte packing by spins is easy to do and as effective as the buffer substitution.

1. Transfer metaphase I oocytes to a 50-mL beaker filled with ice-cold EB using a pipet with a 5- to 10-mm diameter opening and wash three times with ice-cold EB.
2. Prepare a 1.5- or 2.0-mL plastic tube containing 0.5 mL EB added with 50 µg cytochalasin B and transfer metaphase I oocytes to the tube with as little buffer as possible. Spin the tube for 10 s at 500g at 2°C to pack oocytes tightly and remove excess EB. Spin again for 10 s at 1000g at 2°C and remove EB together with the top layer of oocytes, which are loosely packed (about 5% of the total), and crush oocytes by centrifugation for 10 min at 15,000g at 2°C (see **Note 8**).
3. Remove the cytoplasmic fraction (between the lipid cap and the precipitated yolk pellet) to a new tube using a Pasteur pipet. Add the energy mixture to 2% of the extract and mix by gentle pipeting.
4. Centrifuge again at 15,000g for 15 min at 2°C and remove the cytoplasmic fraction into a new tube, making an effort to avoid drawing lipids at the top and turbid precipitates at the bottom. When extract is contaminated with shrunk thecal layers (see **Note 9**), remove them by filtration of the extract through a 5-µm pore membrane using the centrifugal filtration unit. Store extracts on ice until use (see **Note 10**).

3.2. Monitoring Cell Cycle Progression in Meiotic Extracts

3.2.1. Preparation of Membrane-Permeabilized Sperm Nuclei

Cell cycle progression of extracts can be examined by various methods, but one of the best is to examine the morphological change in sperm chromatin incubated in extracts (18). To obtain sensitive responses of sperm chromatin to the changes in the cell cycle phase in extracts, the plasma and nuclear membranes of sperm need to be permeabilized (21,22). The following method to prepare membrane-permeabilized sperm is adapted for small-scale preparation.

1. Inject a male frog with 50 U hCG a day before sperm preparation.
2. Anesthetize the frog by immersion in 0.2% MS-222 in tap water for 30 min and then pith it.
3. Place the frog on its back in a tray covered with a paper towel. Cut away the abdominal skin and make lateral cuts in the muscle of the body wall on each side of the midline.
4. Using a pair of scissors, remove the two testes attached to the bottom of the fat bodies and place them in a Petri dish filled with cold MMR.
5. Remove clotted blood and fat bodies attached to the testes as much as possible using a pair of fine forceps under a dissecting microscope.
6. Rinse the testes in cold MMR and transfer them to a 1.5-mL Eppendorf Safe-Lock tube containing 0.5 mL cold MMR; homogenize the testes by two strokes with the micropestle.
7. Spin down the debris at 100g for 10 s, remove the supernatant containing mature sperm to a 1.5-mL plastic tube, and spin the sperm down at 1500g for 10 min.
8. Resuspend sperm in 1 mL SMH, then spin down at 2000g for 10 min.
9. Resuspend sperm in 900 μ L SMH, transfer the sperm suspension to a 15-ml tube, then add 100 μ L of 5 mg/mL lyssolecithin; mix and incubate for 5 min at room temperature.
10. Add 5 mL cold SMH containing 3% BSA, mix gently, and spin down for 10 min at 2000g.
11. Wash the precipitated sperm twice in 5 mL SMH containing 0.4% BSA and once in SMH; suspend in SMH. Count the sperm concentration using a hemocytometer, adjust to a final concentration of 2.5×10^7 sperm nuclei/mL, and freeze 20- μ L aliquots in liquid nitrogen and store at -80°C (see Note 11).

3.2.2. Monitoring Cell Cycle Progression by Fluorescent Microscopy

1. Incubate extracts stored on ice at 22°C for 5 min.
2. Add sperm nuclei to extracts to a final concentration at 500 sperm/ μ L and mix well by pipeting and continue incubation at 22°C with periodical stirring by gentle pipeting (once every 5 to 10 min).
3. Take 1 to 2 μ L of extract to a glass slide and deposit 2 μ L DNA staining solution to the extract at regular intervals (5–15 min). After lowering a cover slip onto the mixture of extract and staining solution, observe the morphology of sperm nuclei with an epifluorescence microscope using a filter set for Hoechst fluorescence (see Note 12) (Fig. 2).

3.2.3. Histone H1 Kinase Assay

Distinct from the dynamic changes in sperm chromatin in mitotic cycling extracts, those in meiotic cycling extracts are less conspicuous owing to the lack of nuclear formation. Examination of the change in histone H1 kinase activity is strongly recommended to confirm progression of meiotic cycles in oocyte extracts.

1. Take 2 μ L of extract to a plastic tube at regular intervals (5–15 min), freeze quickly in liquid nitrogen, and store at -80°C .

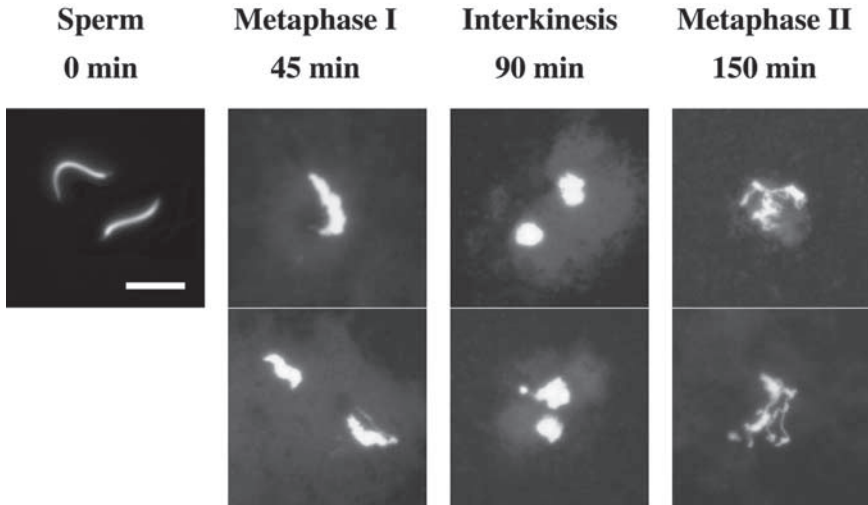


Fig. 2. Morphological changes in sperm nuclei in meiotic cycling extracts. Membrane-permeabilized sperm were added to oocyte extract and stained with Hoechst 33342, a DNA-specific fluorescent dye, at the indicated time after incubation. When incubated in meiotic cycling extracts, sperm nuclei with a ropelike structure (sperm) were decondensed with chromatin fibers disentangled at the periphery (metaphase I), transformed once to spherical structures with smooth contours (interkinesis) and then to disentangled chromatin fibers again (metaphase II). Two different pictures are shown for each of metaphase I, interkinesis, and metaphase II. Bar, 10 μ m.

2. Thaw the extracts by adding 18 μ L ice-cold kinase buffer; mix immediately by vortexing and store on ice.
3. Remove 10 μ L of diluted extract to a tube, mix with 20 μ L reaction buffer by brief vortexing and incubate for 30 min at 25°C.
4. Stop the reaction by adding 10 μ L of 4X SDS sample buffer and boiling for 2 min.
5. Separate histone H1 by electrophoresis on 12.5% SDS-polyacrylamide gels.
6. Measure 32 P incorporation by autoradiography. Alternatively, stain the gels in Coomassie solution (0.25% Coomassie brilliant blue/25% methanol/7% acetic acid) for 20 min and visualize protein bands by washing in destaining solution (25% methanol/7% acetic acid). Cut out histone H1 bands from the gel and quantify 32 P incorporation by the Cerenkov methods (Fig. 3).

3.3. Mitotic Cycling Extracts From Activated Eggs

One of the advantages of the *Xenopus* oocyte extract for the study of meiotic regulation is that it can be directly compared with the egg extract, for which extensive information on the regulatory mechanisms for mitotic cycles has been accumulated. Furthermore, the meiotic MI to MII transition without an intervening S phase in oocyte extracts can be converted into a mitotic M–S–M transition under certain conditions (see Note 13 and Fig. 4) (16). To make comparisons between meiotic and mitotic

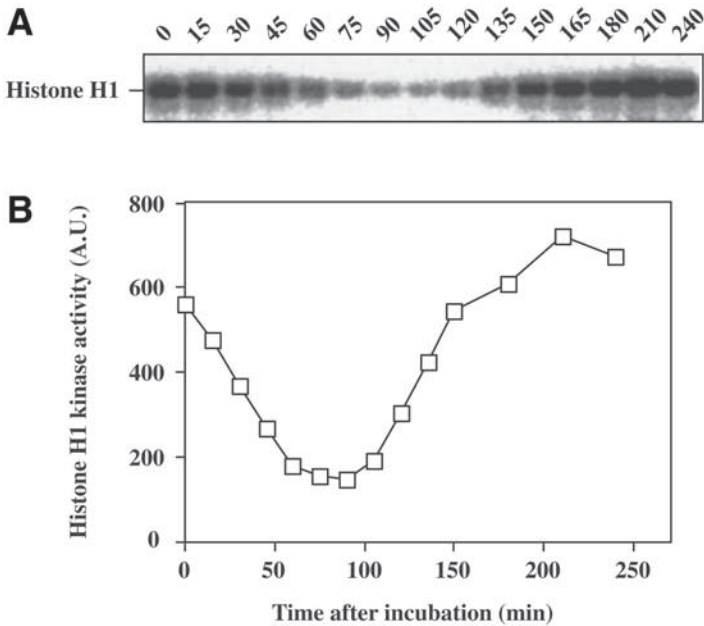


Fig. 3. The change in Cdc2 activity in meiotic cycling extracts. **(A)** Cdc2 activity of oocyte extracts at the indicated time after incubation was measured using histone H1 as a substrate. After incubation of histone H1 with extracts in the presence of [γ - 32 P] ATP, histone H1 was separated by SDS polyacrylamide gel electrophoresis and autoradiographed. **(B)** The extent of 32 P incorporation into histone H1 is quantitated and presented as a function of time. Note that the fluctuation of Cdc2 activity, consisting of three phases (i.e., gradual decline, swift increase, and persistence at a high level), is essentially the same as that in maturing oocytes during the meiotic period from metaphase I to metaphase II (15).

characters of cell cycle regulations, a modified version of Murray's preparation method for the mitotic cycling extract is described next.

1. Prime female frogs with 50 U pregnant mare serum gonadotrophin 3 to 4 d before egg collection and then with 500 U hCG the night before egg collection. Place each hCG-injected frog in a container filled with 0.8 to 1.0% common salt in tap water at 20 to 22°C and allow them to lay eggs for 12 to 16 h. Remove frogs from the containers and collect laid eggs to a beaker filled with MMR. If the amount of eggs is not sufficient, allow frogs to lay eggs for further 2 to 4 h; store collected eggs at 15°C until sufficient amounts of eggs are obtained.
2. Remove as much MMR as possible from the eggs and add 2.5% thioglycolic acid solution (pH 8.2), about a fourfold volume of eggs. Gently swirl the eggs at intervals until the eggs pack tightly without any visible separation by their jelly coats. Pour off the dejelling solution and wash eggs three times with MMR (see **Note 14**).
3. Transfer dejellied eggs to MMR containing 50 nM Calcium Ionophore A23187 and incubate for 3 min. Wash eggs five times with MMR and incubate for 12 min; during this incubation, remove as many damaged or lysed eggs as possible (see **Note 15**).

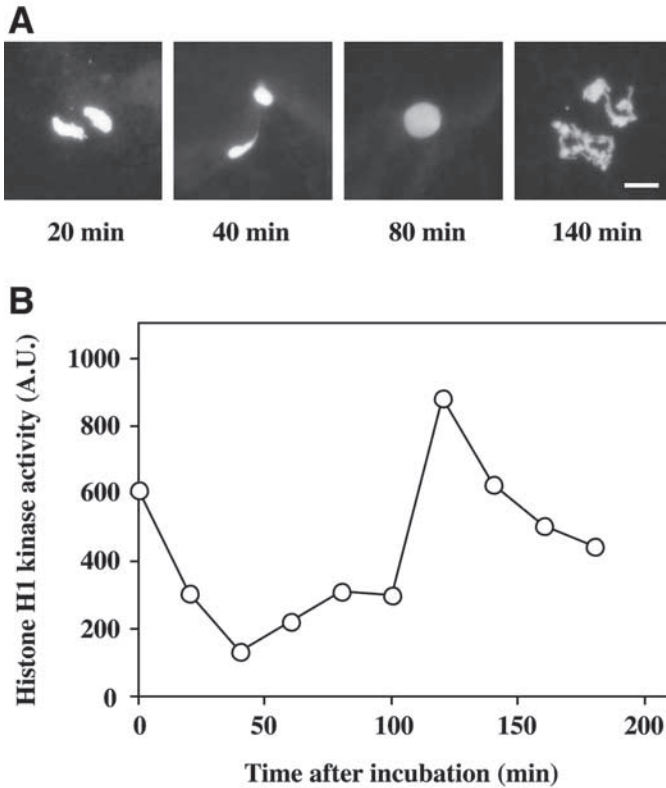


Fig. 4. Conversion of the M–M transition in meiotic cycling extract to an M–S–M transition by extract dilution. (A) In meiotic cycling extracts that had been diluted 1.3-fold with extraction buffer, nuclear formation of sperm chromatin was induced between the two successive M phases (80 min). It has been confirmed that nuclear formation in diluted extracts accompanies DNA replication (K. Ohsumi, unpublished data, 2000). Bar, 10 μ m. (B) The change in Cdc2 activity in diluted meiotic cycling extracts. The Cdc2 activity measured by histone H1 kinase activity is represented as a function of time. Note that in diluted extracts, Cdc2 activity drops rapidly; stays at low levels for a while, during which nuclei are formed; then increases abruptly. This fluctuation of Cdc2 activity closely resembles that in mitotic cycling extracts (*see* Fig. 5).

4. Wash eggs three times with EB; after a 10-min incubation (25 min after the commencement of A23187 treatment), transfer to ice-cold EB and incubate for 5 min on ice.
5. Prepare a 1.5-mL plastic tube containing 0.5 mL EB with 50 μ g cytochalasin B and transfer the chilled eggs to the tube with as little buffer as possible. By the same method for preparing oocyte extracts (**Subheading 3.1.3.**), pack eggs by brief spins, remove excess EB, crush eggs by centrifugation, and remove the cytoplasmic fraction. Store egg extracts on ice until use (*see* **Note 16**).
6. Incubate egg extracts at 22°C and monitor cell cycle progression in the extracts by the same method for oocyte extracts as described in **Subheadings 3.2.2., 3.2.3.** (**Fig. 5**).

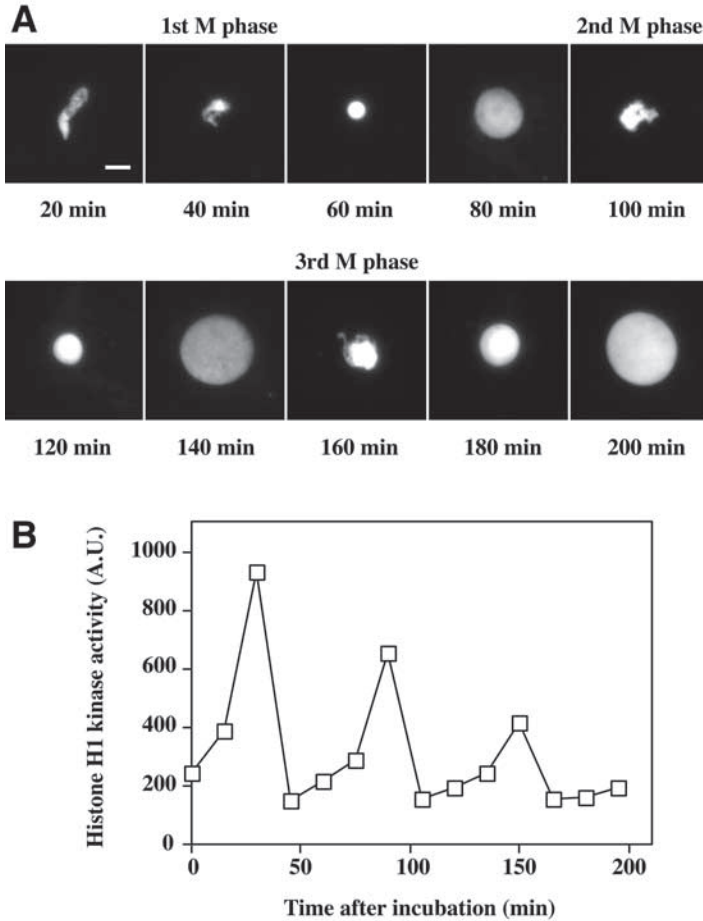


Fig. 5. Cell cycle progression in mitotic cycling extracts prepared according to the present method. (A) Morphological changes in sperm nuclei in mitotic cycling extracts. Membrane-permeabilized sperm were added to egg extract and stained with Hoechst 33342 at the indicated time after incubation. When incubated in mitotic cycling extracts, sperm nuclei were decondensed (20 min) and transformed into entangled chromosomes (40 min: M phase) then into nuclei (60 min), which grew with time (80 min). The cyclic change in sperm nuclear morphology was repeated at least three times at 60-min intervals. Note that the size of fully grown nuclei increased with the cycle round, presumably owing to chromosome replication in S phase without their segregation in M phase in extracts. Bar, 10 μ m. (B) The change in Cdc2 activity in mitotic cycling extracts. The Cdc2 activity measured by histone H1 kinase activity is represented as a function of time. In good concert with the occurrence of chromosome condensation, Cdc2 was periodically activated at 60-min intervals.

4. Notes

1. When the major vein is cut by mistake and the frog bleeds profusely, pour MMR on the injury and wipe away clotted blood with a paper towel.
2. Restrict the volume of ovary to 25 mL per single tube. Ovary fragments can be stored at 4°C for 2 d in the 70% Leibovitz's L-15 medium containing antibiotics.
3. Collagenase treatment longer than 3 h should be avoided as it sometimes causes the treated oocytes to resume meiosis spontaneously without hormonal stimulation during the subsequent incubation in the 70% Leibovitz's L-15 medium. Collagenase solution can be stored at -20°C for several months and reused several times after removing debris by centrifugation at 1500g for 10 min after use.
4. The half-day incubation before hormonal stimulation is strongly recommended as it accelerates the meiotic resumption in stimulated oocytes, shortening the period of time from hormonal stimulation to the occurrence of GVBD, presumably because of the restoration of protein synthetic activity (23).
5. In the oocyte selection at this stage, contamination of smaller oocytes does not matter, but as many oocytes as possible (more than 2000) should be collected.
6. The oocyte selection at this stage must be quick and accurate, and at the end of the 30-min selection, as few GVBD oocytes as possible should be left. To avoid missing GVBD oocytes, oocytes should be occasionally shuffled by swirling during the selection.
7. Approximately 250 μ L of extract is obtained from 1000 oocytes. A single layer of oocytes filling a 5-cm Petri dish contain roughly 500.
8. Oocytes to be crushed for extract preparation should be packed as tightly as possible. We recommend that spins for oocyte packing should be strengthened in a stepwise manner until oocytes at the bottom of the tube are slightly broken. The extent of extract concentration is measured by the protein concentration of extracts, which is determined by using Coomassie Protein Assay Reagent with BSA as a standard, and should be higher than 65 mg/mL.
9. In ovary, each oocyte is enclosed by follicle cells and a thin muscular layer (theca). This layer is not usually removed by collagenase treatment within 3 h but is spontaneously ruptured and detached from a maturing oocyte after hormonal stimulation, as it is during ovulation. Because the theca is contractile, it shrinks or contracts after detachment from oocytes, taking a beretlike shape. You can see a small semitransparent beret on some maturing oocytes (arrowheads in Fig. 1B). Contracted thecae are often transferred to tubes together with oocytes and, after centrifugation, are mostly localized in the separated cytoplasm. As many follicle cells attach to the thecae, contamination of extracts with the thecae can cause difficulty in the observation of sperm nuclei.
10. Oocyte extracts should be used within 2 h of preparation.
11. Sperm preparation according to the method generally yields 1×10^8 sperm with less than 5% contamination by other cells.
12. During the incubation of oocyte extracts at 22°C, fibrous aggregates are sometimes formed in the extract; these involve mostly sperm nuclei.
13. The meiotic MI to MII transition in oocyte extracts has been shown to depend on the dominance of Cdc2 activity over Wee1 activity at the end of MI; therefore, when the balance between the two protein kinase activities is upset by, for example, adding Wee1 to the extract, the cell cycle enters S phase after MI exit, failing to progress to M phase (16). Similarly, we have found that dilution of oocyte extracts with EB by 1.2- to 1.3-fold induces an S phase between the two successive M phases, probably because of acceleration of Cdc2 inactivation at the end of MI (Fig. 4). Thus, the meiotic M-M transition in

oocyte extracts can be easily converted to an M–S–M transition seen in the early embryonic mitotic cycle.

14. In contrast to cystein solution, thioglycolic acid solution can be stored at 4°C for several weeks. During storage, however, its pH sometimes lowers, accompanying a decrease in reducing activity. The pH of thioglycolic acid solution, which can be monitored by adding phenol red, should be kept at 8.0 to 8.4 by adding NaOH.
15. With respect to inducing the activation of unfertilized eggs, calcium ionophore treatment used in the present method is as effective as electric shock used in the original Murray's method.
16. Egg extracts should be used within 2 h of preparation

Acknowledgments

We thank W. Sawada for his contribution to establishing the meiotic cycling extract. We also appreciate T. Kishimoto for critical reading of the manuscript and K. Tachibana and E. Okumura for discussion.

References

1. Masui, Y. and Clarke, H. J. (1979) Oocyte maturation. *Int. Rev. Cytol.* **57**, 185–282.
2. Smith, L. D., (1989) The induction of oocyte maturation: transmembrane signaling events and regulation of the cell cycle. *Development* **107**, 685–699.
3. Ferrell, J. E., Jr. (1999) *Xenopus* oocyte maturation: new lessons from a good egg. *Bioessays* **21**, 833–842.
4. Nebreda, A. R. and Ferby, I. (2000) Regulation of the meiotic cell cycle in oocytes. *Curr. Opin. Cell Biol.* **12**, 666–675.
5. Maller, M. J., Schwab, M. S., Gross, S. D., Taieb, G. F., Roberts, B. T., and Tunquist, B. J. (2000) The mechanism of CSF arrest in vertebrate oocytes. *Mol. Cell. Endocrinol.* **187**, 173–178.
6. Bodart, J. F., Flament, S., and Vilain, J. P. (2002) Metaphase arrest in amphibian oocytes: interaction between CSF and MPF sets the equilibrium. *Mol. Reprod. Dev.* **61**, 570–574.
7. Gurdon, J. B. (1967) On the origin and persistence of a cytoplasmic state inducing nuclear DNA synthesis in frog eggs. *Proc. Natl. Acad. Sci. USA* **58**, 545–552.
8. Ohsumi, K., Katagiri, C., and Yanagimachi, R. (1986) Development of pronuclei from human spermatozoa injected microsurgically into frog (*Xenopus*) eggs. *J. Exp. Zool.* **237**, 319–325.
9. Cox, L. S. and Leno, G. H. (1990) Extracts from eggs and oocytes of *Xenopus laevis* differ in their capacities for nuclear assembly and DNA replication. *J. Cell Sci.* **97**, 177–184.
10. Zhao, J. and Benbow, R. M. (1994) Inhibition of DNA replication in cell-free extracts of *Xenopus laevis* eggs by extracts of *Xenopus laevis* oocytes. *Dev. Biol.* **164**, 52–62.
11. Lemaître, J. M., Bocquet, S., and Méchali, M. (2002) Competence to replicate in the unfertilized egg is conferred by Cdc6 during meiotic maturation. *Nature* **419**, 718–722.
12. Whitmire, E., Khan, B., and Coué, M. (2002) Cdc6 synthesis regulates replication competence in *Xenopus* oocytes. *Nature* **419**, 722–725.
13. DiBerardino, M. A. and Hoffner, N. J. (1982) Gene reactivation in erythrocytes: nuclear transplantation in oocytes and eggs of *Rana*. *Science* **219**, 862–864.
14. Dumont, J. N. (1972) Oogenesis in *Xenopus laevis* (Daudin). I. Stages of oocyte development in laboratory maintained animals. *J. Morphol.* **136**, 153–180.
15. Ohsumi, K., Sawada, W., and Kishimoto, T. (1984) Meiosis-specific regulation in maturing *Xenopus* oocytes. *J. Cell Sci.* **107**, 3005–3013.

16. Iwabuchi M., Ohsumi, K., Yamamoto, T. M., Sawada, W., and Kishimoto, T. (2000) Residual Cdc2 activity remaining at meiosis I exit is essential for meiotic M-M transition in *Xenopus* oocyte extracts. *EMBO J.* **19**, 4513–4523.
17. Murray, A. W. and Kirschner, M. W. (1989) Cyclin synthesis drives the early embryonic cell cycle. *Nature* **339**, 275–280.
18. Murray, A. W. (1991) Cell cycle extracts. *Methods Cell Biol.* **36**, 581–605.
19. Yamamoto, T. M., Iwabuchi, M., Ohsumi, K., and Kishimoto T. (2005) APC/C-Cdc20-mediated degradation of cyclin B participates in CSF arrest in unfertilized *Xenopus* eggs. *Dev. Biol.* **279**, 345–355.
20. Newport, J. and Kirschner, M. (1982) A major developmental transition in early *Xenopus* embryos. I. Characterization and timing of cellular changes at the midblastula stage. *Cell* **30**, 675–686.
21. Gurdon, J. B. (1976) Injected nuclei in frog oocytes: fate, enlargement, and chromatin dispersal. *J. Embryol. Exp. Morphol.* **36**, 523–540.
22. Lohka, M. J. and Masui, Y. (1983) Formation in vitro of sperm pronuclei and mitotic chromosomes induced by amphibian ooplasmic components. *Science* **220**, 719–721.
23. Smith, L. D., Xu, W., and Varnold, R. L. (1991) Oogenesis and oocyte isolation. *Methods Cell Biol.* **36**, 45–60.

Methods for Studying Spindle Assembly and Chromosome Condensation in *Xenopus* Egg Extracts

Thomas J. Maresca and Rebecca Heald

Summary

Methods are presented for preparing cytoplasmic extracts from *Xenopus laevis* eggs and their utilization to reconstitute and monitor events of the cell cycle in vitro. Addition of sperm nuclei to crude extracts and “cycling” of the reaction through interphase and back into metaphase promotes formation of bipolar spindles capable of segregating their duplicated chromosomes. Reactions can be “spun down” onto cover slips for immunofluorescence analysis. High-speed extracts support mitotic chromosome condensation, which can be observed live by fluorescence time-lapse video microscopy. Because of the biochemically accessible nature of the egg extract system, a wide array of biochemical techniques can be combined with spindle and chromosome assembly reactions to evaluate the roles of specific proteins in these processes.

Key Words: Anaphase; chromosome condensation; cytoplasmic extract; microtubule; spindle assembly; time-lapse fluorescence microscopy; *Xenopus laevis* egg.

1. Introduction

Cytoplasmic extracts prepared from the eggs of *Xenopus laevis* have proven extremely useful for studying events of the cell cycle in vitro. Like the eggs, extracts are synchronized in the cell cycle yet are open to biochemical manipulation and high-resolution observation by fluorescence microscopy. Laid eggs are arrested in metaphase of meiosis II with high cyclin B/Cdk1 kinase levels by cytostatic factor (CSF), a calcium-sensitive activity (1).

This chapter describes how to prepare cytoplasmic extracts from the eggs, termed CSF extracts, that maintain the metaphase arrest. Protocols are presented for using crude CSF extracts to reconstitute spindle assembly and chromosome segregation in vitro. These reactions require the addition of *Xenopus* sperm nuclei, the preparation of which is described elsewhere (2), as well as fluorescently labeled tubulin, which incorporates into the microtubule-based spindle (3). Sperm nuclei added directly to the CSF extract will induce the formation of half spindles as the basal body associated

with each demembrated sperm head matures into a centrosome that nucleates a polarized microtubule array orienting toward condensing chromatids (4).

In a more physiological reaction, crude CSF extracts can be induced to enter interphase by the addition of calcium, which causes degradation of CSF and mitotic cyclins, leading to nuclear envelope assembly around each sperm nucleus. Following DNA and centrosome replication, the addition of fresh CSF extract causes the system to reenter a metaphase-arrested state, forming bipolar spindles around duplicated chromosomes. Remarkably, calcium addition will induce the spindles to enter anaphase and segregate their chromosomes *in vitro* (5,6).

Two methods for visualizing these cell cycle events are presented. Simply mixing a small amount of the reaction with fixative and a DNA dye allows quick evaluation of chromosomes and microtubules by fluorescence microscopy. Reactions can also be “spun down” onto cover slips and fixed for immunofluorescence analysis.

In addition to studying spindle assembly and function, *Xenopus* egg extracts are also well suited to examine specific mitotic events in more detail. Protocols are presented for analyzing the process of chromosome condensation. Crude CSF extracts centrifuged at high speed still maintain their metaphase arrest. These high-speed extracts (HSEs) have better optical properties and can be used to assay the resolution and condensation of individual sperm chromatids by fluorescence time-lapse microscopy. However, the HSE does not support DNA replication or spindle assembly. To visualize duplicated mitotic chromosomes and kinetochores, a modified spin-down protocol is presented that maintains chromosome morphology.

The protocols in this chapter detail basic assays for studying mitotic processes *in vitro*. Functional evaluation of the role of individual factors in these processes is also possible through immunodepletion or other specific perturbations of the extract. Briefly introduced here, these procedures are described in more detail elsewhere (7).

2. Materials

2.1. Preparation of *Xenopus* Egg Extracts

1. Female *Xenopus laevis*.
2. Pregnant mare serum gonadotropin (PMSG; Calbiochem): 200 U/mL in sterile water. Store at 4°C.
3. Human chorionic gonadotropin (Sigma): 1000 U/mL in sterile water. Store at 4°C.
4. 1-mL Disposable syringes with 18- and 27-gage needles.
5. 4-L Plastic frog containers with tight-fitting lids, punctured with holes for air exchange.
6. 20X Marc's modified Ringer's (MMR): 100 mM HEPES (free acid), 2 mM ethylenediaminetetraacetic acid (EDTA), 2M NaCl, 40 mM KCl, 20 mM MgCl₂, 40 mM CaCl₂, adjust to pH 7.8 with NaOH. Autoclave and store at room temperature.
7. 16°C Room or large incubator.
8. Cutoff plastic disposable pipets and cutoff and fire-polished glass Pasteur pipets.
9. 20X Extract buffer (XB) salts: 2M KCl, 20 mM MgCl₂, 2 mM CaCl₂; autoclave and store at 4°C.
10. XB: 1X XB salts, 10 mM HEPES, pH 7.7, 50 mM sucrose; adjust to pH 7.7 with KOH. Prepare 500 mL fresh.
11. CSF-XB: add final concentrations of 2 mM MgCl₂ and 5 mM ethylene glycol *bis*(*b*-aminoethyl ether)-*N,N,N',N'*-tetraacetic acid (EGTA) to 200 mL XB. Prepare fresh.

12. Leupeptin, pepstatin, chymostatin (LPC): 10 mg/mL each of leupeptin, pepstatin, chymostatin in dimethyl sulfoxide (DMSO). Store in aliquots (~60 μ L) at -20°C ; can be thawed and refrozen.
13. CSF-XB+: add 50 μ L 10 mg/mL LPC stock to 50 mL CSF-XB. Prepare just before collecting eggs.
14. Cytochalasin D: 10 mg/mL in DMSO. Store in aliquots (~50 μ L) at -20°C ; can be thawed and refrozen.
15. Dejellinging solution: 1X XB salts, 2% L-cysteine (free base); adjust to pH 7.8 with NaOH. Prepare 250 mL fresh.
16. SW-55 Ultra-Clear centrifuge tubes (Beckman 344057).
17. 13-mL Plastic tubes (Sarstedt 55.518).
18. Clinical centrifuge.
19. High-speed centrifuge with Sorvall HB-4 or HB-6 rotor with rubber adaptors.
20. Tabletop ultracentrifuge (Beckman TL-100) with TLS-55 swinging bucket rotor, Ultra-Clear thin-walled tubes (Beckman 347356), and TLS-55 polycarbonate thick-walled tubes (Beckman 343778).
21. Energy mix: 150 mM creatine phosphate, 20 mM adenosine triphosphate, 2 mM EGTA, 20 mM MgCl_2 . Store in aliquots (~200 μ L) at -20°C ; can be thawed and refrozen.

2.2. *In Vitro Sperm Spindle Assembly Reactions*

1. 20°C Water bath equipped with rack to hold 1.5-mL reaction tubes.
2. Rhodamine-labeled tubulin stock (15–25 mg/mL) (3). Store in aliquots (~1 μ L) at -80°C .
3. Sperm nuclei stock (~100,000 nuclei/ μ L) (2). Store in aliquots (~3 μ L) at -80°C .
4. 10X Calcium solution: 4 mM CaCl_2 , 100 mM KCl, 1 mM MgCl_2 . Store in aliquots (~200 μ L) at -20°C ; can be thawed and refrozen.
5. Hoechst DNA dye: 10 mg/mL Hoechst dye no. 33342 (Sigma) in water. Store at 4°C in the dark.
6. Spindle fixative: 1X MMR, 48% glycerol, 11% formaldehyde, 5 μ g/mL Hoechst. Prepare fresh every 3 to 5 d.
7. 25 \times 75 mm Microscope slides.
8. 18, 18-mm no. 1 cover slips.
9. 12-mm Circular no. 1 cover slips.
10. Fluorescence microscope setup equipped with rhodamine, 4',6-diamidino-2-phenylindole (DAPI), and FITC excitation/emission filters and 20 \times , 40 \times , 60 \times , and 100 \times objectives.
11. Watchmaker's forceps.
12. Modified 15-mL glass Corex[®] tubes with plastic spin-down adaptors (made to order by Aladin Enterprises, San Francisco, CA).
13. High-speed centrifuge with Sorvall HB-4, HB-6, or HS-4 rotor with rubber adaptors.
14. Metal hook or bent microspatula for removing spin-down adaptors.
15. -20°C MeOH bath with ceramic slide holder for 12-mm circular cover slips.
16. Cover slip processing tray (e.g., a 15-cm round plastic Petri dish) with parafilm cut to fit.
17. 5X BRB80: 400 mM PIPES, 5 mM MgCl_2 , 5 mM EGTA; adjust to pH 6.8 with KOH. Filter sterilize and store at 4°C .
18. Spindle dilution buffer: 1X BRB80, 30% glycerol, 0.5% Triton X-100. Filter sterilize and store at room temperature.
19. Spindle cushion: 1X BRB80, 40% glycerol. Filter sterilize and store at 4°C .
20. Phosphate-buffered saline (PBS)-NP40: 1X PBS, 0.1% Nonidet P-40 (Sigma Igepal CA-630).

21. PBS-BSA (bovine serum albumin): 1X PBS, 3% BSA (w/v). Store in 1-mL aliquots at -20°C ; can be thawed and refrozen.
22. Vectashield[®] mounting medium without DAPI (Vector Laboratories, Inc.).

2.3. Visualizing In Vitro Chromosome Condensation

1. EB buffer: 80 mM β -glycerophosphate, 15 mM MgCl_2 , 20 mM EGTA, pH 7.3. Aliquot (200 μL) and store at -20°C ; can be thawed and refrozen.
2. Sytox Green nucleic acid stain: 5 mM in DMSO (Molecular Probes). Aliquot (5 μL) and store at -20°C ; can be thawed and refrozen.
3. Three-component oxygen scavenging system: 10 mg/mL glucose oxidase in 30% glycerol, 10 mg/mL catalase in 30% glycerol, 1M glucose. Prepare small aliquots (10–20 μL) of each component separately and store at -20°C ; can be thawed and refrozen.
4. 5X XBE2: 50 mM HEPES, 500 mM KCl, 10 mM MgCl_2 , 0.5 mM CaCl_2 , 25 mM EGTA, 250 mM sucrose; adjust to pH 7.7 with KOH. Filter sterilize and store at 4°C .
5. Chromosome dilution buffer: 1X XBE2, 2% formaldehyde, 0.25% Triton X-100. Prepare fresh.
6. Chromosome cushion: 1X XBE2, 30% glycerol. Filter sterilize and store at 4°C .

3. Methods

Outlined next are several fundamental procedures of *Xenopus* egg extractology (Fig. 1). The methods describe (1) preparation of two types of commonly utilized egg extracts, called crude and HSE; (2) procedures for assembling spindles and reconstituting chromosome segregation in crude extracts, including a protocol for fixing spindles onto cover slips for analysis by immunofluorescence; (3) protocols for visualizing chromosome condensation in this system; and (4) an introduction to techniques commonly used to examine the functional contribution of specific proteins to spindle assembly and chromosome condensation.

3.1. Preparation of *Xenopus* Egg Extracts

The steps described in Subheadings 3.1.1. and 3.1.2. outline the preparation of crude and high-speed egg extracts, respectively. Only freshly prepared crude extracts support spindle assembly and chromosome segregation; HSEs can be stored frozen and are optimal for observation of sperm chromatid condensation. In general, a well-rested frog will lay enough eggs to yield 1 to 2 mL of crude extract (see Note 1), from which 0.4 to 1 mL HSE can be recovered. High-quality eggs from multiple frogs can be pooled to prepare the extract.

3.1.1. Crude CSF Extract Preparation

Crude extracts prepared from *Xenopus* eggs in a manner that preserves their CSF metaphase arrest are commonly referred to as CSF extracts. Eggs dejellied by treatment with cysteine are washed and incubated in the presence of EGTA, which helps prevent calcium-induced degradation of CSF and mitotic cyclins. Eggs are packed by low-speed centrifugation to minimize dilution of the cytoplasm, followed by a higher speed spin that crushes the eggs. The concentrated cytoplasmic layer is then collected and stored on ice.

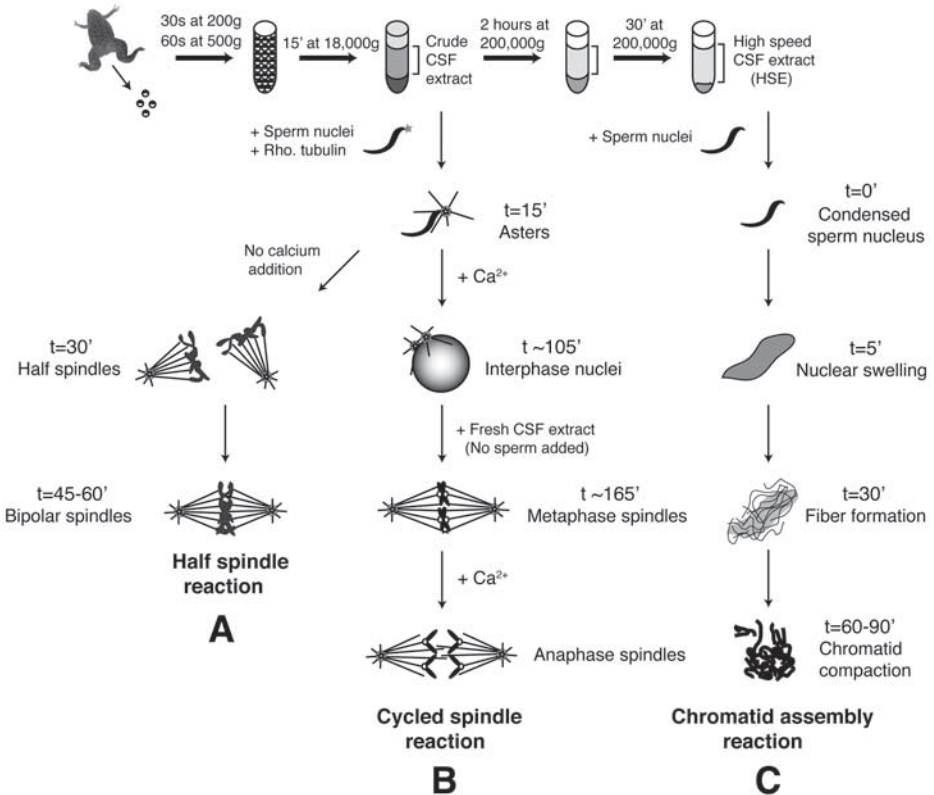


Fig. 1. Schematic diagram of crude and CSF high-speed extract (HSE) preparations and the various reaction conditions described in this chapter: (A) half-spindle reactions; (B) cycled spindle/anaphase reactions; and (C) chromatid assembly reactions. The star on each demembrated sperm nucleus represents the basal body, which matures into an active microtubule nucleating centrosome following addition to crude extract. Note the presence of paired sister chromatids and kinetochores (white circles) in the metaphase/anaphase spindles in (B).

1. At 3 to 4 d before a planned extract preparation, inject an appropriate number of frogs subcutaneously with 0.5 mL (100 U) PMSG using a 27-gage needle and 1-mL syringe. These "primed" frogs should be used within 2 wk of the PMSG injection, and the quantity of frogs to be primed depends on the number of extract preparations planned for that 2-wk period (*see Note 2*).
2. At 16 to 18 h before the extract is to be prepared, inject each frog subcutaneously with 0.5 mL (500 U) of human chorionic gonadotropin. Place each injected frog into its own container with 2 L 1X MMR prepared in deionized water and store the frogs overnight in a dark 16°C environment (*see Note 3*).
3. The next day, prepare 500 mL 1X MMR, 250 mL dejelling solution, and 500 mL XB. Use the XB to prepare 200 mL CSF-XB and subsequently 50 mL CSF-XB+ just prior to harvesting the eggs. All extract buffers should be prepared from deionized, Milli-Q-filtered water kept at between 16°C and room temperature.

4. Transfer frogs to a bucket of deionized water and inspect the eggs. Quality eggs have clearly defined animal (dark) and vegetal (light) poles and are not mottled in appearance. Remove lysed (white and puffy) or stringy eggs with a cutoff plastic pipet. If greater than 5% of the eggs are lysed or in strings, the entire batch is likely to be bad and should be discarded (*see Note 4*). Pour the eggs into a prerinsed 400-mL glass beaker for dejelling and washing. During the following wash steps, buffers should be carefully poured down the side of the beaker, and the eggs should be swirled gently to reduce lysing. Pour off as much buffer as possible between multiple washes without exposing the eggs to air. Remove additional lysed eggs throughout the procedure.
5. Wash the eggs three times with 100 to 150 mL MMR to remove detritus.
6. Pour off the MMR and add approx 80 mL of dejelling solution. When laid, eggs are enveloped in a jelly coat and do not pack tightly. Swirl the beaker and change the dejelling solution two or three times over 5 min. Once the eggs are dejellied, they occupy a much smaller volume and are now more fragile and will lyse if exposed to air or treated roughly. Wash the eggs soon after the eggs have packed. Additional MMR washes may be performed at this point if the buffer appears dirty.
7. Wash the eggs three times with approx 100 mL XB.
8. Wash the eggs three times with approx 50 mL CSF-XB.
9. Prior to the final CSF-XB wash, prepare sufficient SW-55 thin-wall tubes (extract tubes) by filling with 1 mL CSF-XB+ supplemented with 10 μ L cytocholasin D. One tube holds about 5 mL eggs and will yield 1 to 1.5 mL extract.
10. Pour off the final CSF-XB wash and add approx 50 mL CSF-XB+ to the eggs.
11. Transfer the dejellied washed eggs to the prepared extract tubes using a cutoff fire-polished Pasteur pipet. Avoid exposing the eggs to air by drawing some buffer into the pipet first and make sure the tip of the pipet is submerged in buffer before expelling the eggs. After filling, transfer each extract tube to a 13-mL Sarstedt adapter tube containing 0.5 mL water to prevent collapse of the tubes during centrifugation.
12. To pack the eggs, transfer the tubes to a clinical centrifuge and spin at 200g for 1 min before increasing the speed to 500g for 30 s. After spinning, aspirate excess buffer from the top of the eggs to minimize dilution of the cytoplasm.
13. To crush the eggs, transfer the tubes of packed eggs to an HB-4 or HB-6 rotor equipped with rubber adaptors and centrifuge at 10,500 rpm (~18,000g) for 15 min at 16°C.
14. After crushing the eggs, remove the extract tubes from the Sarstedt tube adaptors and put them on ice. The crushed eggs will have separated into three distinct layers: a top lipid layer (opaque yellow), a middle cytoplasmic layer (golden), and a bottom yolk particle/pigment layer (dark). Puncture the side of the tube at the bottom of the cytoplasmic layer using an 18-gage needle and a 1-mL syringe, orient the needle opening upward, and carefully remove the cytoplasmic layer, taking care to avoid contamination with the lipid (yellow) layer (*see Note 5*). Remove the needle before expelling the extract into an Eppendorf tube and keep on ice.
15. Supplement the extract with LPC (10-mg/mL stock) at a 1/1000 dilution, cytocholasin D (10 mg/mL stock) at a 1/500 dilution, and energy mix at a 1/40 dilution and mix by inverting the tube. The extract is now ready for use and should be used within 6 to 8 h as extract quality declines over time.

3.1.2. High-Speed CSF Extract Preparation

As the name implies, CSF HSEs are simply prepared by spinning crude extract at high speed in an ultracentrifuge. These clarified extracts are depleted of vesicles and

are much less viscous than crude extract. They do not support spindle assembly, DNA replication, or chromosome segregation but have been used to successfully visualize and characterize chromosome condensation (*see Note 6*).

1. Transfer 1.6 to 2 mL crude CSF extract to TLS-55 thin-wall tubes on ice.
2. Transfer tubes to a chilled TLS-55 rotor and centrifuge in a tabletop ultracentrifuge at 55,000 rpm (~200,000g) for 2 h at 4°C.
3. After centrifugation, the extract will generally separate into three layers: a top layer of residual lipids (small, white, and fluffy), a middle layer of extract, and a bottom layer of heavy membranes and glycogen. Carefully aspirate off the top lipid layer and then retrieve the middle extract layer with an 18-gage needle and 1-mL syringe as described in **Subheading 3.1.1, step 14**. Sometimes, a layer of membranes is present within the middle layer; remove it along with the extract.
4. Transfer the extract to a thick-wall TLS-55 tube and centrifuge in a TLS-55 rotor at 200,000g for 30 min at 4°C to pellet residual membranes.
5. Following centrifugation, remove the supernatant, taking care to avoid the membrane pellet, and transfer the clarified extract (HSE) to an Eppendorf tube on ice.
6. Prepare small aliquots (12.5–25 μ L) of HSE and flash freeze in liquid nitrogen. When stored at –80°C, a good HSE preparation is stable for a year or more.

3.2. In Vitro Sperm Spindle Assembly Reactions

Extract preparations do not contain endogenous chromosomes or microtubule organizing centers because the female meiotic spindle pellets during centrifugation, and the eggs lack centrosomes. However, addition of an exogenous chromatin source to crude CSF extracts is sufficient to drive spindle assembly. Demembranated *X. laevis* sperm nuclei are a convenient source of chromosomes to use in extract reactions (2). Because a flagellar basal body (or sperm centrosome) is associated with each sperm nucleus, a centrosome-mediated spindle assembly pathway can be reconstituted around sperm nuclei in crude extracts. **Subheadings 3.2.1** and **3.2.2** describe steps for setting up two different kinds of sperm spindle reactions in extract (**Fig. 1**), and **Subheading 3.2.3** describes a protocol for isolating structures onto glass cover slips for immunofluorescence and visualization by fluorescence microscopy.

3.2.1. CSF Half-Spindle Assembly Reactions

The CSF half-spindle assembly reaction is often used to test the functional activity of crude CSF extracts (*see Note 7*). It is referred to as a half-spindle reaction because each sperm nucleus brings in a single sperm centrosome, thereby generating monopolar structures around each nucleus. However, over time and depending on the quality of the extract, bipolar structures will also assemble through fusion of half-spindles and microtubule self-organization (4,8,9). In addition to sperm nuclei, all reactions are supplemented with fluorescently labeled tubulin to visualize spindle microtubules.

1. Add a final concentration of approx 50- μ g/mL rhodamine-labeled tubulin (1/500 dilution of a 25-mg/mL stock) to the crude CSF extract. Prepare a sufficient amount (usually 200–500 μ L) of extract plus rhodamine-labeled tubulin for a day of experiments. Keep on ice.
2. For each spindle assembly reaction, aliquot 20 to 50 μ L of extract plus rhodamine-labeled tubulin into 1.5-mL Eppendorf tubes. On ice, add sperm nuclei to a final concentration of

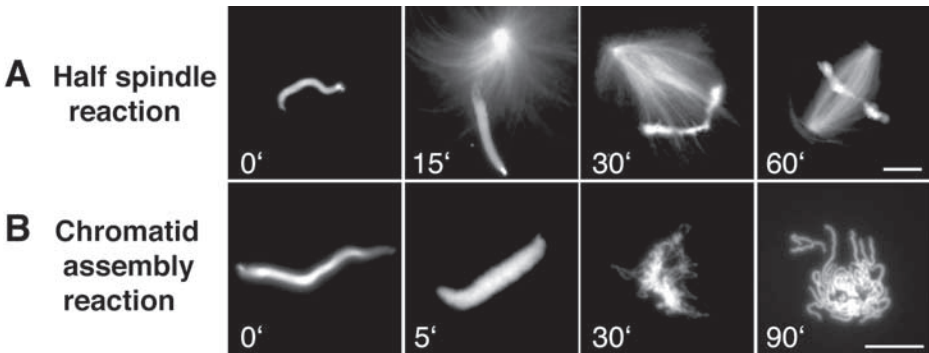


Fig. 2. (A) Fixed “squashes” of a half-spindle reaction in crude CSF extract acquired at 40 \times magnification at the indicated time points. Note that bipolar spindles are observed at 60 min. (B) Progression of a chromatid assembly reaction in CSF high-speed extract (HSE). The images are from a live squash reaction supplemented with Hoechst DNA dye and visualized at 60 \times magnification at the indicated times. Bars, 10 μ m.

250 to 500 nuclei/ μ L to each reaction (*see Note 8*). Do not exceed 50 μ L per reaction as this inhibits gas exchange and can lead to defective spindle assembly.

3. Incubate the reactions in a 20 $^{\circ}$ C water bath to begin spindle assembly.
4. Take fixed samples or “squashes” of the reactions at 0, 15, 30, 45, and 60 min by pipeting 1.5 μ L of the reaction onto a slide, overlaying 5 μ L of spindle fixative and gently covering with an 18 \times 18 mm cover slip before viewing by fluorescence microscopy.
5. The typical progression of an active CSF reaction is shown in [Fig. 2A](#). At the start of the reaction, only highly condensed sperm nuclei are observed, and microtubules have not yet polymerized. By 15 min, dense microtubule asters emanating from sperm centrosomes become apparent. At 30 min, the asters separate from the nuclei and organize into half-spindles with their microtubules oriented toward the sperm chromatin. By 45 to 60 min, both half-spindles and bipolar structures may be observed (*see Note 9*).

3.2.2. Cycled Spindle Reactions and Anaphase

The CSF arrest that supports half-spindle assembly in crude extracts can be released by the addition of calcium, causing entry into interphase and permitting a “cycled spindle” reaction ([Fig. 3](#)). During interphase, functional nuclei form, and sperm centrosomes and chromosomes replicate. Highly functional extract preparations will cycle back into a metaphase state at 60 to 120 min after calcium addition as the cyclin B protein is resynthesized ([10](#)).

However, a more reproducible technique to drive interphase extracts back into metaphase is by the addition of fresh CSF extract to the reactions. The bipolar structures assembled in these cycled reactions are true metaphase spindles with replicated and paired sister chromatids aligned on a metaphase plate between two spindle poles. Furthermore, these metaphase spindles can be induced to enter anaphase (chromosome segregation) by another round of calcium addition to the extract. As with the half-spindle reactions, cycling reactions should be kept at 20 $^{\circ}$ C throughout the procedure.

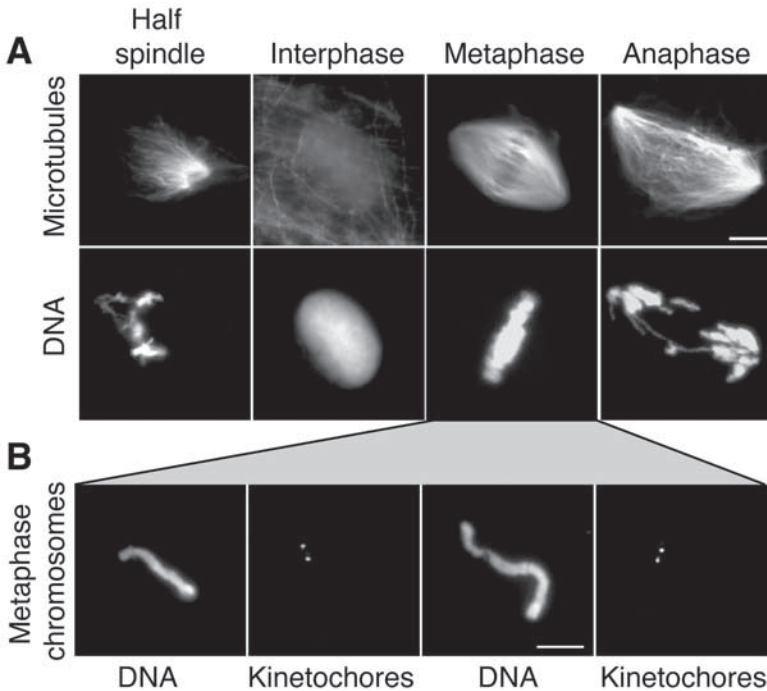


Fig. 3. (A) Progression of cycled spindle reactions and anaphase observed by fluorescence microscopy following spin-downs onto cover slips. The top panels show rhodamine-labeled tubulin, and the bottom panels show Hoechst dye-stained DNA. The images were acquired at 40 \times magnification following spin-down of reactions at the indicated stages. (B) Two metaphase chromosomes visualized at 100 \times magnification following the modified chromosome spin-down procedure described in **Subheading 3.3.2**. In this example, fixed chromosomes were stained with an antibody against a kinetochores marker, which is shown in the panels to the right of each chromosome image. Bars, 10 μ m.

1. Prepare half-spindle reactions (do not exceed 25 μ L/tube) on ice as described previously using extracts supplemented with rhodamine-labeled tubulin and sperm nuclei.
2. Add 1/10 volume 10X calcium solution to each reaction (e.g., 2.5 μ L to a 25- μ L reaction) and gently but thoroughly mix by flicking the tube.
3. Place reactions in the 20 $^{\circ}$ C water bath.
4. At 80 min after calcium addition, prepare a squash of each sample to determine if the extract has entered interphase as determined by the morphology of sperm nuclei. The interphase nuclei are large, round structures characterized by decondensed and diffuse Hoechst-stained DNA.
5. At 90 min after calcium addition, add an equal volume (e.g., 25 μ L) of fresh CSF extract plus rhodamine-labeled tubulin (*no additional sperm*) and mix.
6. Monitor spindle assembly by preparing squashes every 15 min. Bipolar structures should begin forming around 30 min after the addition of fresh extract.

7. Once robust bipolar spindles have formed (usually 45–60 min after adding fresh extract), they can be induced to undergo anaphase by a second addition of 1/10 volume 10X calcium solution to the reaction.
8. Monitor anaphase progression by preparing squashes every 5 min after the second calcium addition as segregation is generally complete within 25 to 35 min. Metaphase reactions can be split into smaller aliquots (10–15 μL) before the addition of calcium if you wish to do multiple anaphase reactions or maintain some reactions in metaphase.

3.2.3. Processing Spindle Reactions for Immunofluorescence: “Spin-Downs”

Although squashes are ideal for monitoring the progress of ongoing reactions, they have a number of limitations: (1) There is a high background of unpolymerized labeled tubulin fluorescence; (2) the slides cannot be stored for long periods (weeks to months); (3) there is a relatively small number of structures per fixed sample, making thorough quantification difficult; and (4) they cannot be processed for immunolocalization studies. The “spin-down” procedure outlined here for isolating and fixing spindle structures onto glass cover slips is an easy way to overcome these limitations.

1. Once spindles have been assembled, dilute the reactions 40-fold with spindle dilution buffer and mix by inverting the tube several times (*see Note 10*). Generally, 15 to 25 μL of a spindle reaction is used per spin-down.
2. Gently overlay each reaction mixture onto 5 mL “spindle cushion” in a 15-mL Corex spin-down tube previously prepared with cushion, plastic adaptors, and a 12-mm circular cover slip.
3. Centrifuge the spin-down tubes at approx 6000g for 20 min at 16°C (5500 rpm in an HS-4 rotor or 6000 rpm in an HB-6 rotor) using the proper rubber adaptors.
4. After the spin, aspirate off the cushion, remove the adaptors with a bent microspatula or metal hook (bent paperclips can also work), and transfer the cover slips with forceps to a cover slip holder in a -20°C methanol bath. Fix the submerged cover slips for 5 min at -20°C .
5. Transfer the cover slips, *reaction side up*, to a parafilm-covered processing tray and wash them five times with PBS-NP40 over a 5- to 10-min period to rehydrate the sample (*see Note 11*). If immunolocalizations will not be performed, go to **step 8**.
6. To process the cover slips for immunofluorescence, block the cover slips in PBS-BSA for 30 to 60 min before incubating with an appropriate dilution of the primary antibody in PBS-BSA for an additional 30 to 60 min.
7. Wash cover slips five times with PBS-NP40 before incubating them in an appropriate dilution of a fluorophore-labeled secondary antibody in PBS-BSA for 30 to 45 min.
8. Wash cover slips five times with PBS-NP40. Incubate cover slips in 5 $\mu\text{g}/\text{mL}$ Hoechst in PBS-NP40 for 1 to 2 min.
9. Wash cover slips five times with PBS-NP40 and mount them face down on a slide in approx 2 μL mounting media. Seal the cover slips with nail polish and store at 4°C.

3.3. Visualizing In Vitro Chromosome Condensation

Xenopus egg extracts also support chromosome condensation. However, chromosome morphology is often difficult to observe clearly by either squash or the spin-down protocols outlined. This subheading focuses on two techniques for more clearly visualizing condensation. Outlined in **Subheading 3.3.1.** is a protocol for examining

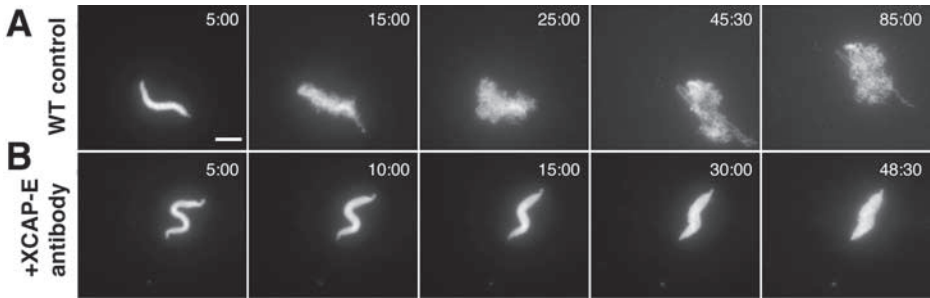


Fig. 4. (A) Frames from time-lapse fluorescence microscopy of a chromatid assembly reaction in HSE containing Sytox Green DNA dye to label the DNA. (B) Frames showing that a similar reaction in the presence of an antibody against the condensin complex component XCAP-E (at 0.1 mg/mL) fails to progress as the nucleus swells, but chromatids do not resolve. Bar, 10 μ m.

chromatid assembly in HSE by live microscopy (Figs. 2B and 4). Subheading 3.3.2. describes a modification of the spindle fixation procedure to isolate duplicated metaphase chromosomes from cycled crude extracts (Fig. 3B).

3.3.1. Time-Lapse Fluorescence Microscopy of Chromatid Assembly in HSE

The CSF HSE preparation has historically been used to visualize and characterize condensation of the 18 chromatids contained in each hypercondensed sperm nucleus (11). On addition to HSE, nuclei undergo dramatic morphological reorganization (Fig. 2B). In the first 5 to 10 min, nuclei swell as proteins from the extract (e.g., histones H2A and H2B) are loaded onto the sperm chromatin. Next, a meshwork of tangled chromatin fibers begin to appear. Finally, these fibers further compact and resolve into individual chromatids. This entire process can be visualized by time-lapse fluorescence microscopy in HSE reactions supplemented with a fluorescent DNA dye and oxygen-scavenging system to reduce photodamage (Fig. 4).

1. Thaw an aliquot of HSE and add an equal volume of EB buffer (see Note 12). Add energy mix at 1/20 to the reaction mixture and keep on ice (see Note 13).
2. Prepare a fresh 1- μ M solution of Sytox Green DNA dye in DMSO. Add the dye to the reaction mixture at 1/100 for a final concentration of 10 nM dye (see Note 14).
3. Prepare the oxygen-scavenging system by mixing an equal volume (~2 μ l of each) of the three components (glucose, glucose oxidase, catalase). The oxygen-scavenging mix should be prepared fresh and added at a 1/33 dilution shortly before starting the reaction. Mix well by pipeting.
4. Add sperm nuclei at a final concentration of approx 500 to 1000 nuclei/ μ L to the reaction mixture. Keep the tube on ice.
5. Pipette 5 μ L of the reaction to a clean slide and squash under a clean 18 \times 18 mm no. 1 cover slip.
6. After several minutes, transfer the slide to a fluorescence microscope setup and scan the sample in the FITC channel with a 60 \times oil immersion objective (1.40 numerical aperture) for stationary nuclei that appear to be swelling. Try to find nuclei near the center of the

cover slip as the edges tend to dry out over time (see **Note 15**). At this point, nuclei should be bright and require a short exposure time (50 ms) for visualization. If this is not the case, prepare a new reaction using more dye.

7. Once a suitable nucleus has been found, acquire an image every 30 to 60 s (generally, 50- to 200-ms exposures) for 60 to 90 min using commercially available image acquisition and analysis software such as *Metamorph*.
8. Reactions can also be incubated in their tubes at 20°C and monitored by preparing fixed squashes, as previously described, at various time points for up to 3 h.
9. Because chromosome morphology is sometimes not clearly visible in fixed squashes, 5- μ L live squashes (no spindle fixative) of the chromatid assembly reaction can be incubated at room temperature and periodically imaged (every 15 to 30 min) by fluorescence microscopy (**Fig. 2B**). The live squash technique yields beautifully resolved chromatids; however, they must be imaged immediately as the reactions will degrade after approx 3 to 4 h.

3.3.2. Processing Cycled Chromosomes for Immunofluorescence

The unreplicated chromatids assembled in HSE are unpaired and generally do not assemble functional kinetochores, the specialized sites assembled at centromeres where microtubules interact dynamically with mitotic chromosomes. To better visualize cycled chromosomes consisting of replicated and paired chromatids with kinetochores, crude extract reactions can be cycled and the metaphase structures subjected to a modified spin-down protocol using a dilution buffer and cushion that better preserves chromosome morphology (**Fig. 3B** and **refs. 12, 13**). This spin-down protocol does not stabilize microtubules; thus, spindles will not be present on the cover slips.

1. Set up cycling sperm spindle reactions as described in **Subheading 3.2.2**.
2. Once cycled metaphase structures have assembled, dilute the reactions 40-fold with chromosome dilution buffer and mix by inverting the tube several times.
3. Fix reactions at room temperature for 20 min.
4. After fixation, gently overlay each reaction mixture onto 5 mL chromosome cushion in a 15-mL Corex spin-down tube previously prepared with cushion, plastic adaptors, and a 12-mm circular cover slip.
5. Spin down the reactions and process as described in **Subheading 3.2.3., steps 3 to 9**.

3.4. Functional Studies in *Xenopus* Egg Extracts

Although the *X. laevis* extract system is biochemically and cytologically accessible, it is not practical for genetic analyses of cell cycle events. In contrast, extracts may be biochemically manipulated through a number of techniques that mimic some powerful tools available in genetic model systems. As *Xenopus* genome databases expand to facilitate proteomic analyses, the extract system is also developing as a tool to identify novel factors through biochemical and functional assays.

“Null mutantlike” extracts can be generated by immunodepletion of a factor. Antibodies that recognize a specific protein can be coupled to protein A or G beads, incubated in extracts, and then removed, thereby immunodepleting the factor (**7,13–15**). Reactions performed in the depleted extract are then compared to mock-depleted controls. If a phenotype is observed following the depletion, specificity can be demonstrated by complementing (rescuing) the phenotype by adding back the purified component to the depleted extract.

In some cases, selective inhibition of a specific protein in the extract can also be achieved by adding relatively high levels (0.1–1 mg/mL) of a specific affinity-purified antibody to the reactions (Fig. 4B). Complementation experiments utilizing depleted *Xenopus* egg extracts and homologous or mutant factors from other species could allow one to address evolutionary conservation of protein function and merge the strengths of a genetically accessible system like *Saccharomyces cerevisiae* with the functional and cytological assays available in the extract system.

Another general cell biology approach to address protein function is to overexpress or express dominant negative versions. These types of experiments are easily mimicked in the extract system by adding purified wild-type or mutant proteins to the reactions and assessing phenotypes (see Note 16). Furthermore, the localization of green fluorescence protein- or epitope-tagged proteins can be assessed by fluorescence microscopy.

Chemical genetics has emerged as a novel tool to imitate forward-genetic screens using *Xenopus* egg extracts (16,17). In this approach, individual compounds from large chemical libraries are added to extract reactions. If a phenotype is observed following the addition of a given compound, the compound can be coupled to a matrix and used to affinity-purify proteins that physically interact, allowing identification of potential targets by mass spectrometry (16). Applying this type of screen in extracts, especially devised in a high-throughput and automated fashion, has the potential to identify many new chemical inhibitors of critical cellular processes as well as novel spindle, chromosome, and cell cycle regulators.

4. Notes

1. One of the most challenging aspects of working with the *Xenopus* egg extract system is preparing quality and functional extracts in a reproducible fashion. Yield and quality of eggs and extracts is largely determined by the health of the frog. Taking good care of the frogs and allowing them to rest for at least 3 mo between usages is important because overworked frogs generally yield fewer eggs of lesser quality.
2. Injecting two frogs per every 1 to 2 mL of extract needed is generally a good idea in case one frog does not lay or gives low-quality eggs.
3. Never store the frogs in tap water or buffer prepared with tap water, which often contains chloramines or other chemicals that can kill them.
4. The highest-quality eggs can be obtained by gently squeezing the frog. However, if not performed properly, this can hurt the frog.
5. Just below the golden cytoplasmic layer and above the black layer is a grayish layer that contains mitochondria and other vesicles. This material is good to have in the extract and should be drawn out along with the cytoplasm, taking care to avoid the black material. It helps to rotate the syringe so that the needle opening can be directed. In contrast, the vesicles close to the yellow lipid layer should be avoided.
6. Clarified extracts can also be a good starting point for biochemical purifications of soluble cytoplasmic proteins. Both HSE and crude extracts can be flash frozen in aliquots of up to 200 μ L and stockpiled.
7. A small test reaction (20 μ L) run for 15 to 30 min at 20°C will monitor whether the extract is functional and CSF arrested, as judged by the presence of condensing chromatids and microtubule asters or half-spindles in a squashed sample by fluorescence

microscopy. This test is useful before embarking on a big experiment to ensure that reagents and time are not wasted on a nonfunctional extract.

8. If it is difficult to measure the appropriate amount of sperm or rhodamine-labeled tubulin because of a small reaction volume, a larger reaction can be prepared and aliquoted to individual reaction tubes. Alternatively, these reagents can first be diluted into extract on ice and then dispensed to the reactions at the appropriate final dilution.
9. Two major things can go wrong with an extract. If the CSF arrest was not maintained during extract preparation, the extract will be “interphasic,” which is indicated by the presence of many long microtubules and the formation of interphase nuclei. Another potential problem is if the extract becomes apoptotic, which most often occurs after long incubations. Despite the fact that the extract is a cell-free system, it is still capable of undergoing programmed cell death. Apoptotic extract is characterized by the absence of microtubules and the presence of small and dense Hoechst-stained balls of DNA. Extract problems are more likely if the reactions are diluted too much; in general, avoid adding more than 1/10 volume of buffer to the extract.
10. Addition of 0.1% glutaraldehyde to the spindle dilution buffer better preserves microtubule structures; addition of 2% formaldehyde is better to maintain chromosome morphology. A 10- to 20-min fixation step at room temperature should be performed if either fixative is added to the dilution buffer. If glutaraldehyde is used, the cover slips must be quenched with multiple changes of 0.1% NaBH₄ (w/v) in 1X PBS over a 10-min period after the methanol fixation step. Be aware of fixation artifacts with immunofluorescence as different localization patterns have been observed for some proteins under different fixation conditions.
11. If NP-40 (Igepal CA-360) is not available, PBS plus 0.1% Triton X-100 can be used for processing cover slips.
12. In addition to EB buffer, HSE can also be diluted in an equal volume of 1X XBE5 (same as 1X XBE2 with 5 mM MgCl₂ rather than 2 mM) for chromatid assembly reactions (14,18).
13. Addition of energy mix to HSE chromatid assembly reactions is an absolute necessity. If energy mix is not added to HSE reactions, nuclei will only progress as far as the swelling stage before the reaction stops. If chromatid reactions fail to progress even in the presence of energy mix, then either the HSE preparation did not work or the extract has been stored for too long and should be discarded.
14. We found that DNA dyes with ultraviolet excitation wavelengths (Hoechst and DAPI) did not work well for imaging chromatid assembly by time-lapse fluorescence microscopy as repeated exposures to ultraviolet light caused the chromatids to disintegrate. Use of DNA dyes with excitation/emission properties similar to FITC (like Sytox Green) or rhodamine generally bypassed this problem. However, we recommend adding low levels of Hoechst (1–2 µg/mL) rather than Sytox Green to live squash reactions and leaving out the oxygen scavenging system that will not be subject to a time lapse but rather monitored periodically by eye or by acquiring single images at longer intervals (e.g., every 30 min).
15. When searching for a nucleus to image by time lapse, look for nuclei that are stationary and have already started to swell. If chromatin fiber formation is not apparent within 15 to 20 min of visualizing a nucleus, search for a new nucleus or prepare another live squash.
16. When adding purified proteins to the extract, Tris-based buffers should be avoided. In general the extract can handle proteins dialyzed into PBS and XB-like buffers. Also avoid diluting the CSF extract with more than 1/10 volume of the protein solution (1/20 to 1/50 volumes are recommended).

Acknowledgments

We wish to acknowledge our colleagues who have pioneered use of the *Xenopus* egg extract system and shared their expertise, including Andrew Murray, Arshad Desai, Tatsuya Hirano, Claire Walczak, and Tim Mitchison. We would also like to thank Jon Soderholm for critical reading of the manuscript. This work was supported by National Institutes of Health grant GM57839.

References

1. Tunquist, B. J. and Maller, J. L. (2003) Under arrest: cytosstatic factor (CSF)-mediated metaphase arrest in vertebrate eggs. *Genes Dev.* **17**, 683–710.
2. Murray, A. W. (1991) Cell cycle extracts. *Methods Cell Biol.* **36**, 581–605.
3. Hyman, A. A., Dreschel, D., Kellogg, D., et al. (1991) Preparation of modified tubulins, in *Methods in Enzymology* (Vallee, R. B., ed.), Academic Press, San Diego, CA, pp. 478–485.
4. Sawin, K. E. and Mitchison, T. J. (1991) Mitotic spindle assembly by two different pathways in vitro. *J. Cell Biol.* **112**, 925–940.
5. Shamu, C. E. and Murray, A. W. (1992) Sister chromatid separation in frog egg extracts requires DNA topoisomerase II activity during anaphase. *J. Cell Biol.* **117**, 921–934.
6. Murray, A. W., Desai, A. B., and Salmon, E. D. (1996) Real time observation of anaphase in vitro. *Proc. Nat. Acad. Sci. USA* **93**, 12,327–12,332.
7. Wignall, S. M. and Heald, R. (2001) Methods for the study of centrosome-independent spindle assembly in *Xenopus* extracts. *Methods Cell Biol.* **67**, 241–256.
8. Heald, R., Tournebize, R., Habermann, A., Karsenti, E., and Hyman, A. (1997) Spindle assembly in *Xenopus* egg extracts: respective roles of centrosomes and microtubule self-organization. *J. Cell Biol.* **138**, 615–628.
9. Mitchison, T. J., Maddox, P., Groen, A., et al. (2004) Bipolarization and poleward flux correlate during *Xenopus* extract spindle assembly. *Mol. Biol. Cell.* **15**, 5603–5615.
10. Murray, A. W. and Kirschner, M. W. (1989) Cyclin synthesis drives the early embryonic cell cycle. *Nature* **339**, 275–280.
11. Hirano, T. and Mitchison, T. J. (1993) Topoisomerase II does not play a scaffolding role in the organization of mitotic chromosomes assembled in *Xenopus* egg extracts. *J. Cell Biol.* **120**, 601–612.
12. Losada, A., Yokochi, T., Kobayashi, R., and Hirano, T. (2000) Identification and characterization of SA/Sec3p subunits in the *Xenopus* and human cohesin complexes. *J. Cell Biol.* **150**, 405–16.
13. Wignall, S. M., Deehan, R., Maresca, T. J., and Heald, R. (2003) The condensin complex is required for proper spindle assembly and chromosome segregation in *Xenopus* egg extracts. *J. Cell Biol.* **161**, 1041–1051.
14. Hirano, T., Kobayashi, R., and Hirano M. (1997) Condensins, chromosome condensation protein complexes containing XCAP-C, XCAP-E and a *Xenopus* homolog of the *Drosophila* Barren protein. *Cell* **89**, 511–521.
15. Funabiki, H. and Murray, A. W. (2000) The chromokinesin Xkid is essential for metaphase chromosome alignment and must be degraded to allow anaphase chromosome movement in *Xenopus* egg extracts. *Cell* **102**, 411–424.
16. Wignall, S. M., Gray, N. S., Chang, Y. T., et al. (2004) Identification of a novel protein regulating microtubule stability through a chemical approach. *Chem. Biol.* **11**, 135–146.

17. Peterson, J. R., Lokey, R. S., Mitchison, T. J., and Kirschner, M. W. (2001) A chemical inhibitor of N-WASP reveals a new mechanism for targeting protein interactions. *Proc. Natl. Acad. Sci. USA* **98**, 10,624–10,629.
18. Ono, T., Losada, A., Hirano, M., Myers, M. P., Neuwald, A. F., and Hirano, T. (2003) Differential contributions of condensin I and condensin II to mitotic chromosome architecture in vertebrate cells. *Cell* **115**, 109–121.

Index

- Actin, *see* Confocal immunofluorescence microscopy, cytoskeleton
- AFM, *see* Atomic force microscopy
- Anaphase-promoting complex, *see* Ubiquitination
- Apoptosis, egg extract studies,
 advantages of system, 379, 380
 caspase activation assay, 388, 392
 cytochrome *c* release assay, 387, 388, 392
 egg collection, 383
 immunodepletion and protein addition studies, 391–393
 interphase egg extracts,
 fractionation,
 cytosolic, light membrane, heavy membrane, and glycogen fractions, 389, 390, 392, 393
 mitochondria isolation, 390
 preparation, 385, 386, 392
 materials, 380–383
 nuclear morphology assay, 388
 reconstitution assay,
 cytochrome *c*-induced apoptosis, 390, 391, 393
 cytosolic and heavy membrane fractions, 390, 393
 sperm chromatin demembranation for nuclear formation, 384, 385
 spontaneous apoptosis induction, 379, 385, 386, 392
- Atomic force microscopy (AFM),
 nuclear pore complex, calcium-mediated changes, 285
 materials, 275
 native complex imaging, 284, 285, 287
 nuclei isolation from oocytes, 276, 285, 287
 supports, 284, 287
 temperature-dependent plugging and unplugging, 285
- Borohydride, reduction of glutaraldehyde-fixed samples, 76
- Calcium flux, oocytes,
 advantages of study, 103
 confocal laser scanning microscopy, advantages, 110
 framescan versus linescan imaging, 110, 112
 instrumentation, 110
 setup, 113, 118
 dyes, 108, 109
 fertilization release assay, 402, 403
 flash photolysis of caged inositol 1,4,5-trisphosphate, 113, 114, 119
 materials for analysis, 104, 105, 115, 117, 118
 multiphoton laser scanning microscopy, calcium wave imaging after inositol 1,4,5-trisphosphate induction, 94–96
 oocyte preparation,
 defolliculation, 106
 epithelial layer removal, 105
 microinjection of caged inositol 1,4,5-trisphosphate, 106, 108, 117, 118
 surgery, 105

- principles of epifluorescence
 - microscopy and imaging, 109, 110
- total internal fluorescence
 - microscopy imaging, advantages, 114
 - image acquisition, 115
 - instrumentation, 114, 115
 - materials, 104, 105
 - principles, 114
 - vitelline membrane stripping, 108
- Capillary electrophoresis (CE),
 - advantages in biological separations, 413
 - protein kinase A live cell assay, 426
 - spatial resolution, 414
 - subcellular sampling of oocytes,
 - calibration curve preparation for inositol 1,4,5-trisphosphate, 421
 - capillary outlet positioning, 420
 - capillary preparation, 419
 - data analysis, 421
 - detector biosensor preparation and imaging, 420, 423
 - electrophoresis conditions, 419, 423
 - inositol 1,4,5-trisphosphate standards, 419, 420
 - materials, 414, 415, 422
 - oocyte preparation, 415, 423
 - sampling apparatus construction, 415, 417, 423
 - sampling volume determination, 418, 419
- Caspase, activation assay, 388, 392
- Cdc2, oocyte signaling studies, 438
- cDNA, *see* Complementary DNA
- CE, *see* Capillary electrophoresis
- Cell cycle,
 - fertilization studies, 403
 - meiotic MI–MII transition studies in oocyte extracts,
 - cell cycle progression monitoring, fluorescence microscopy, 451, 456
 - histone H1 kinase assay, 451, 452
 - membrane-permeabilized sperm nuclei preparation, 451, 456
 - cycling extract preparation from metaphase I oocytes,
 - extract preparation, 450, 456
 - oocyte isolation, 448, 449, 456
 - synchronization at metaphase I, 450, 456
 - materials, 447
 - mitotic cycling extracts from activated eggs, 452–454, 456, 457
 - overview, 445–447
 - regulator proteolysis studies,
 - metaphase-to-anaphase transition, immunodepletion and rescue assays, 229–231, 233
 - protein degradation assay, 228, 229, 232, 233
 - protein ubiquitination assay, 229, 233
 - mitosis exit and G1, 231, 232
- Cell-free chromosomal DNA
 - replication,
 - demembrated sperm chromatin preparation,
 - ethanization, 125
 - sperm concentration
 - determination and storage, 127, 136

- sperm extraction and purification, 125, 126, 136
- testes extraction, 15
- high-speed interphase extract
 - preparation, 129
- immunodepletion studies, 134–137
- low-speed interphase extract
 - preparation, 128, 129, 136
- materials, 123–125
- nuclear assembly extract assay
 - limitations, 121–123
- nucleoplasmic extract preparation,
 - nuclear assembly and growth monitoring, 130, 133
 - nuclear assembly reactions, 129, 130
 - nuclei harvesting, 131, 136
 - nucleoplasm isolation, 131
- oocyte maturation, ovulation, and collection,
 - egg harvesting and dejellying, 128
 - egg laying induction with human chorionic gonadotropin, 127, 128
 - ovulation induction with pregnant mare serum gonadotropin, 127
- origin unwinding studies, 133, 134
- overview of egg extract system, 122, 123
- replication assay in nucleoplasmic extract, 131, 132, 136
- replication factor loading, 134
- Chaperones, *see* Heat shock proteins
- ChIP, *see* Chromatin immunoprecipitation
- Chromatin assembly assays,
 - materials, 142, 143, 145
 - micrococcal nuclease digestion assay, 144–146
 - oocyte preparation and single-stranded DNA microinjection, 143–145
- overview, 139–142
- supercoiling assay, 144, 145
- Chromatin immunoprecipitation (ChIP),
 - materials, 168–170
 - oocytes,
 - microinjection, 172, 173, 178
 - preparation, 170, 171
 - thyroid hormone receptor transcriptional regulation analysis, 173, 174, 178
 - principles, 166, 167
 - tadpole development studies,
 - chromatin preparation, 177, 179
 - immunoprecipitation, 177, 179
 - nuclei preparation,
 - intestine and liver samples, 175, 177
 - tail samples, 175, 178
 - overview, 174, 175
 - tissue preparation, 175
 - triiodothyronine treatment, 175
 - thyroid hormone receptor coactivator and corepressor analysis
 - overview, 167, 168
- Chromosomal DNA replication, *see* Cell-free chromosomal DNA replication
- Chromosome condensation, egg extract studies,
 - biochemical manipulation for functional studies, 470–472
 - cycled chromosome processing for immunofluorescence, 470
 - cytostatic factor extracts,
 - features, 459, 460
 - preparation,
 - crude extract, 462–464, 471

- high-speed extract, 464, 465, 71
 - materials, 460–462
 - overview, 459, 460
 - time-lapse fluorescence microscopy, 469, 470, 472
- CLSM, *see* Confocal laser scanning microscopy
- Complementary DNA (cDNA),
 - full-insert sequences, 8, 10
 - library resources, 3
- Confocal immunofluorescence
 - microscopy, cytoskeleton, antibodies,
 - secondary antibody selection, 77
 - storage, 77, 83, 84
 - types, 70, 71
 - bleaching, 76, 83
 - borohydride reduction of glutaraldehyde-fixed samples, 76
 - clearing and mounting, 78–80
 - dyes, 72, 77
 - fixation,
 - keratin filaments, 74
 - methanol fixation, 74
 - microtubules, 73, 74, 80, 83
 - hemisection for antibody penetration, 74–76
 - image acquisition, 82–84
 - instrumentation, 82
 - materials, 70, 83
 - oocyte/egg imaging advantages, 69
 - phalloidin staining of microtubules, 80, 81, 84
 - processing of samples, 77, 78, 83, 84
- Confocal laser scanning microscopy (CLSM),
 - calcium flux imaging in oocytes, advantages, 110
 - framescan versus linescan imaging, 110, 112
 - instrumentation, 110
 - setup, 113, 118
- immunofluorescence, *see* Confocal immunofluorescence
 - microscopy, cytoskeleton
 - nucleocytoplasmic transport assay in oocytes,
 - kinetic recordings, 263, 269
 - microchamber preparation and nucleus deposition, 263
 - nuclei isolation, 261–263, 267, 269
 - transport solution addition, 263
- CSF extract, *see* Cytostatic factor extract
- Cytochrome *c*, release assay for
 - apoptosis detection, 387, 388, 392
- Cytoskeleton imaging, *see* Confocal immunofluorescence microscopy, cytoskeleton
- Cytostatic factor (CSF) extract, *see* Chromosome condensation; Fertilization; Spindle assembly; Ubiquitination
- Defolliculation,
 - calcium flux studies, 106
 - collagenase treatment, 33, 34
 - overview, 31, 32
 - sandpaper stripping, 34–36
 - voltage clamp studies, 336, 342
 - Xenopus tropicalis* oocytes, 47, 48
- DNA microarray, Affymetrix chip
 - resources, 13
- DNA replication, *see* Cell-free chromosomal DNA replication
- Drug assay, *see* Patch-clamp, oocytes; Voltage clamp, oocytes

- Egg,
apoptosis studies in extracts, *see*
Apoptosis, egg extract
studies
chromosome condensation studies,
see Chromosome
condensation
cytoskeleton imaging, *see* Confocal
immunofluorescence
microscopy, cytoskeleton
DNA replication in extracts, *see*
Cell-free chromosomal
DNA replication
fertilization studies in extracts, *see*
Fertilization
Golgi apparatus disassembly
reconstitution, *see* Golgi
apparatus disassembly
nuclear assembly assay, *see* Nuclear
assembly assay
nucleocytoplasmic transport assay,
see Nucleocytoplasmic
transport
proprotein convertase studies, *see*
Proprotein convertases
protein degradation studies, *see*
Ubiquitination
spindle assembly studies, *see* Spindle
assembly
Electron microscopy (EM),
nuclear pore complex,
colloidal gold immunolabeling,
282–284, 287
cytoplasmic face of nuclear
envelope, 276, 287
embedding and thin sectioning,
282, 287
materials, 274, 275, 285, 287
negative staining, 277, 278, 287
nuclei isolation from oocytes,
276, 285, 287
nucleoplasmic face of nuclear
envelope, 276, 287
quick freezing/freeze-drying/
rotary metal shadowing,
278, 287
nucleocytoplasmic transport in
oocytes,
colloidal gold preparation, 306,
307, 311
gold conjugation of proteins, 307,
308, 312
gold conjugation of RNA, 308
materials, 305, 306
microinjection of colloidal gold
conjugates, 309, 312
oocyte preparation, 308, 309,
312
overview and advantages, 301–
303, 305
sample preparation, 309–312
Electrophysiology, *see* Patch-clamp,
oocyte; Voltage clamp,
oocytes
EM, *see* Electron microscopy
Endoplasmic reticulum, multiphoton
laser scanning microscopy
imaging, 99
EST, *see* Expressed sequence tag
Expressed sequence tag (EST),
databases, 3
Fertilization,
cell-free extract and raft studies,
cytostatic factor extract
preparation, 400
egg preparation, 399
fertilization, 399, 400, 409
mass spectrometry of raft-
associated proteins,
digestion and extraction of gel
bands, 405, 406

- expressed sequence tag
 - database, 408, 409
 - identification of proteins, 405–409
 - peptide mass fingerprinting, 407
 - product ion mass fingerprinting, 407
 - materials, 397, 398
 - raft preparation, 400, 409
 - signaling assays,
 - calcium release assay, 402, 403
 - cell cycle transition, 403
 - mitogen-activated protein kinase phosphorylation, 402, 409, 410
 - phospholipase C γ immunodepletion, 403
 - phospholipase C γ phosphorylation, 402, 409, 410
 - protein tyrosine kinases in raft fractions, 402
 - Src overexpression effects on raft fractions, 403, 410
 - Src phosphorylation, 402, 409, 410
 - sperm preparation,
 - demembrated sperm, 399
 - living sperm, 399
 - frog system advantages, 395, 396
 - Src activation, 396
- Genetic map, resources, 10, 11
- Genome physical map, resources, 11, 12
- Genome sequencing,
 - resources, 14–16
 - Xenopus tropicalis*, 12, 13
- Genomic libraries, resources, 11
- Germinal vesicle breakdown (GVBD),
 - assay, 49, 51
 - features, 446
- Golgi apparatus disassembly,
 - reconstitution from egg extracts and semi-intact Mardin-Darby canine kidney cells,
- biochemical analysis,
 - immunodepletion, 362, 363
 - kinase inhibitors, 362
- egg extract preparation, 359, 364
- galactosyltransferase-green fluorescent protein reporter,
 - cloning, 359
 - stable transfection, 359
- incubation conditions, 360, 364
- materials, 358, 359
- morphometric analysis, 360
- overview, 357, 358
- semi-intact cell preparation, 360, 364
- GVBD, *see* Germinal vesicle breakdown
- Heat shock proteins (Hsps),
 - classification, 213
 - protein refolding assays,
 - luciferase activity assay after microinjection,
 - heat-denatured protein, 218, 220
 - heat-denatured protein with Hsp30C, 219, 220
 - luminometer settings, 217
 - nondenatured protein, 217, 218, 220
 - sample preparation, 217
 - materials, 214, 215
 - oocyte isolation and protein microinjection, 217, 220

- overview, 214
- recombinant Hsp30C preparation,
 - bacteria expression and induction, 215, 220
 - purification, 215, 216, 220
- Hsps, *see* Heat shock proteins
- Immunoblot, *see* Western blot
- Immunodepletion,
 - apoptosis studies in egg extract, 391–393
 - cell cycle regulator proteolysis and rescue assays in egg extracts, 229–231, 233
 - cell-free chromosomal DNA replication studies, 134–137
 - Golgi apparatus disassembly studies, 362, 363
 - nuclear import studies in reconstituted nuclei, 298, 299
 - oocyte signaling studies, 441
 - phospholipase C γ studies in fertilization, 403
- Immunofluorescence microscopy, *see* Confocal immunofluorescence microscopy, cytoskeleton
- Inositol 1,4,5-trisphosphate (IP $_3$),
 - caged compound studies, *see* Calcium flux, oocytes
 - subcellular sampling and analysis of oocytes, *see* Capillary electrophoresis
- Intermediate filament, *see* Confocal immunofluorescence microscopy, cytoskeleton
- IP $_3$, *see* Inositol 1,4,5-trisphosphate
- Karyopherins, nucleocytoplasmic transport mediation, 243–246
- Keratin filament, *see* Confocal immunofluorescence microscopy, cytoskeleton
- Lipid rafts, *see* Fertilization
- MAPK, *see* Mitogen-activated protein kinase
- Mardin-Darby canine kidney cell, *see* Golgi apparatus disassembly
- Mass spectrometry (MS), raft-associated proteins,
 - digestion and extraction of gel bands, 405, 406
 - expressed sequence tag database, 408, 409
 - identification of proteins, 405–409
 - peptide mass fingerprinting, 407
 - product ion mass fingerprinting, 407
- Mechanosensitive channels, *see* Patch-clamp, oocytes
- Membrane transplantation, oocytes,
 - cytoplasmic injection of membranes, 354
 - materials, 348, 349, 353
 - membrane preparation for transplantation,
 - cell lines, 350, 352, 343
 - mammalian brain tissue, 349, 350, 353
 - oocyte preparation, 349
 - rationale, 347, 348, 353
 - voltage clamp recordings, 353, 354
- Messenger RNA polyadenylation,
 - cytoplasmic polyadenylation element, 184
 - oocyte assays,
 - materials, 185, 186
 - RNA polyadenylation changes, DNA template generation, 194

- gel electrophoresis and autoradiography, 195
- overview, 192–194, 196
- radiolabeled RNA probe generation, 194, 196
- RNA extraction, 194, 195
- 3'-untranslated region
 - translational effects, DNA template generation for in vitro transcription, 189, 195
- dual-luciferase reporter assay, 192
- overview, 186, 188, 189, 195
- RNA microinjection, 190–192, 196
- runoff assay and messenger RNA quantification, 189, 190, 195, 196
- overview, 183, 184
- translational control, 184, 185
- Messenger RNA splicing, *see* Pre-messenger RNA splicing
- Micrococcal nuclease, *see* Chromatin assembly assays
- Microinjection,
 - caged inositol 1,4,5-trisphosphate into oocytes, 106, 108, 117, 118
 - colloidal gold conjugates into oocytes, 309, 312
 - DNA into oocytes for chromatin immunoprecipitation assay, 172, 173, 178
 - membrane transplantation, 352–354
 - pre-messenger RNA splicing studies, antisense U2 DNA, 156, 161, 162
 - needle preparation, 156
 - radiolabeled pre-messenger RNA, 157, 158, 162
 - rescuing U2 small nuclear RNA, 157, 162
 - proteins into oocytes, 217, 220
 - receptor and channel constructs into oocytes, 337, 338, 342, 343
 - RNA into oocytes, 190–192, 196
 - single-stranded DNA into oocytes, 143–145
 - viral RNA into oocytes, 370, 371, 377
- Microtubule, *see* Confocal immunofluorescence microscopy, cytoskeleton
- Mitochondria,
 - isolation from eggs, 390
 - multiphoton laser scanning microscopy imaging, 96, 98
- Mitogen-activated protein kinase (MAPK),
 - oocyte signaling studies, 437, 438
 - phosphorylation assay in fertilization, 402, 409, 410
- Molecular chaperones, *see* Heat shock proteins
- MPLSM, *see* Multiphoton laser scanning microscopy
- MS, *see* Mass spectrometry
- Multiphoton laser scanning microscopy (MPLSM),
 - advantages in oocyte imaging, 87, 88
 - calcium wave imaging after inositol 1,4,5-trisphosphate induction, 94–96
 - endoplasmic reticulum imaging, 99
 - image acquisition, 93, 94
 - instrumentation, 88, 90, 91
 - limitations in oocyte imaging, 99
 - materials, 92
 - mitochondria imaging, 96, 98

- pigmented versus albino oocyte studies, 92, 93
- principles, 90–92
- Mutagenesis, resources, 13, 14
- Neurotransmitter receptors, *see* Voltage clamp, oocytes
- Nuclear assembly assay, egg extract assays, demembrated sperm chromatin preparation, 294, 295 fractionation of extracts, 292, 293, 295 frog priming and egg-laying induction, 291, 292, 299 materials, 290, 291 nuclei reconstitution, 295, 296, 299 overview, 289, 290 limitations, 121–123
- Nuclear envelope, *see* Nucleocytoplasmic transport
- Nuclear pore complex, *see* Nucleocytoplasmic transport
- Nucleocytoplasmic transport, diffusion control, 236, 237 egg extract assays, demembrated sperm chromatin preparation, 294, 295 fractionation of extracts, 292, 293, 295 frog priming and egg-laying induction, 291, 292, 299 import assays, immunodepletion studies, 298, 299 reconstituted nuclei, 297, 298 substrate preparation, 297 materials, 290, 291 nuclei reconstitution, 295, 296, 299 overview, 289, 290 history of study, 235, 236, 260 karyopherin-mediated transport, 243–246 nuclear envelope structure, 236, 237 nuclear localization signals, 243–246 nuclear pore complex, atomic force microscopy, calcium-mediated structural changes, 285 materials, 275 native complex imaging, 284, 285, 287 nuclei isolation from oocytes, 276, 285, 287 supports, 284, 287 temperature-dependent plugging and unplugging, 285 electron microscopy, colloidal gold immunolabeling, 282–284, 287 cytoplasmic face of nuclear envelope, 276, 287 embedding and thin sectioning, 282, 287 materials, 274, 275, 285, 287 negative staining, 277, 278, 287 nuclei isolation from oocytes, 276, 285, 287 nucleoplasmic face of nuclear envelope, 276, 287 quick freezing/freeze-drying/rotary metal shadowing, 278, 287 inert molecule permeability, 242, 243, 252 nucleoporin types and structures, 240–242

- structure, 238, 240, 242, 273, 274
- translocation mechanism models,
 - affinity gradient model, 250
 - oily spaghetti model, 250
 - reduction-of-dimensionality model, 252
 - selective-phase model, 250, 252
 - Stewart model, 250
 - virtual gating model, 250
- NXF-mediated export of
 - ribonucleoproteins, 246–248
- oocyte assays,
 - confocal laser scanning microscopy,
 - kinetic recordings, 263, 269
 - microchamber preparation and nucleus deposition, 263
 - nuclei isolation, 261–263, 267, 269
 - transport solution addition, 263
- electron microscopy,
 - colloidal gold preparation, 306, 307, 311
 - gold conjugation of proteins, 307, 308, 312
 - gold conjugation of RNA, 308
 - materials, 305, 306
 - microinjection of colloidal
 - gold conjugates, 309, 312
 - oocyte preparation, 308, 309, 312
 - overview and advantages, 301–303, 305
 - sample preparation, 309–312
- materials, 260, 261
- optical single transport recording,
 - chamber preparation, 265
 - data evaluation, 267, 270, 271
 - kinetic recordings, 266, 267, 269
 - nuclear envelope preparation, 265, 270
 - nuclei attachment to test compartments, 265, 270
 - nuclei isolation, 265
 - principles, 260, 269, 270
 - overview, 260
- NXF proteins, ribonucleoprotein export mediation, 246–248
- Oocyte,
 - anatomy of developed oocyte, 19, 20
 - calcium flux imaging, *see* Calcium flux, oocytes
 - cell cycle studies, *see* Cell cycle
 - chromatin assembly, *see* Chromatin assembly assays
 - chromatin immunoprecipitation, *see* Chromatin immunoprecipitation
 - electrophysiology, *see* Patch-clamp, oocytes; Voltage clamp, oocytes
 - isolation and enucleation,
 - defolliculation,
 - collagenase treatment, 33, 34
 - overview, 31, 32
 - sandpaper stripping, 34–36
 - enucleation,
 - functional studies, 37, 39, 40
 - Western blot analysis, 37, 39, 40
 - materials, 32, 33
 - ovarian tissue isolation, 33, 39
- maturation and ovulation, 26, 27, 435, 436
- membrane transplantation, *see* Membrane transplantation, oocytes
- messenger RNA polyadenylation assay, *see* Messenger RNA polyadenylation

- microinjection, *see* Microinjection
- multiphoton laser scanning microscopy, *see* Multiphoton laser scanning microscopy
- nucleocytoplasmic transport studies, *see* Nucleocytoplasmic transport
- oogenesis,
 - overview, 20, 21
 - stage I, 22
 - stage II, 22
 - stage III, 22, 23
 - stage IV, 23
 - stage V, 23
 - stage VI, 24
- ovary, *see* Ovary
- protein expression, *see also* T7 RNA polymerase expression system,
 - advantages, 55
 - applications, 55, 56
 - approaches, 56
 - receptors and channels, *see* Voltage clamp, oocytes
- protein kinase A assay, *see* Protein kinase A
- protein refolding assay, *see* Heat shock proteins
- RNA splicing, *see* Pre-messenger RNA splicing
- RNA virus replication, *see* RNA virus replication, oocytes
- signaling studies,
 - advantages, 436, 437
 - difficulties, 437
 - examples, 437, 438
 - extract preparation, 439–442
 - immunodepletion, 441
 - materials, 438
 - oocyte harvesting, 439, 441
 - pharmacological agents, 441
 - stimuli, 440, 441
 - subcellular sampling, *see* Capillary electrophoresis
 - vitellogenesis, 24, 25
 - Xenopus tropicalis* oocytes, *see* *Xenopus tropicalis*
- Optical single transport recording (OSTR), nucleocytoplasmic transport assay in oocytes,
 - chamber preparation, 265
 - data evaluation, 267, 270, 271
 - kinetic recordings, 266, 267, 269
 - nuclear envelope preparation, 265, 270
 - nuclei attachment to test compartments, 265, 270
 - nuclei isolation, 265
 - principles, 260, 269, 270
- OSTR, *see* Optical single transport recording
- Ovary,
 - anatomy, 17–19
 - oocyte maturation and ovulation, 26, 27
 - oogenesis, *see* Oocyte
 - steroidogenesis, 25, 26
- Patch-clamp, oocytes,
 - drug assays,
 - automation, 332
 - defolliculation, 336, 342
 - expression of channels and receptors, incubation, 338
 - microinjection, 337, 338, 342, 343
 - materials, 332–335
 - recording, 339, 341, 344
 - voltage-gated channel mechanosensitivity, channel expression density, 316, 317

- dose-response studies, 323, 326
- endogenous currents,
 - gadolinium carbonate artifacts, 325
 - overview, 323, 324
 - stretch-activated cation
 - nonselective current, 323, 325, 326
- materials, 316
- mechanostimulator, 321
- micromanipulator adjustments
 - and oocyte flattening, 319
- microscopy, 317, 319
- oocyte advantages versus mammalian cells, 316
- overview, 315, 316
- patch history, 319, 320
- recording pipets, 320
- series resistance effect, 326
- single-channel measurements, 323
- solutions, 320, 321
- stretch/clamp techniques, 321, 322
- Peptide mass fingerprinting, *see* Mass spectrometry
- Pesticide assay, *see* Patch-clamp, oocytes; Voltage clamp, oocytes
- Phospholipase C γ ,
 - immunodepletion studies in fertilization, 403
 - phosphorylation assay in fertilization, 402, 409, 410
- PKA, *see* Protein kinase A
- Poliovirus, *see* RNA virus replication, oocytes
- Pre-messenger RNA splicing,
 - machinery, 149
 - model systems, 150
- oocyte studies,
 - advantages, 150, 161
 - materials, 150–153
 - microinjection,
 - antisense U2 DNA, 156, 161, 162
 - needle preparation, 156
 - radiolabeled pre-messenger RNA, 157, 158, 162
 - rescuing U2 small nuclear RNA, 157, 162
 - nuclear isolation, 158, 159, 162
 - oocyte preparation,
 - anesthesia, 155, 161
 - separation and isolation, 155, 156, 161
 - surgery, 155, 161
 - overview, 150
 - RNA synthesis,
 - pre-messenger RNA, 154
 - U2 small nuclear RNA, 153, 154, 161
 - splicing assay, 159, 160
- Protein convertases,
 - classification, 199
- egg extract translation system
 - studies,
 - autocatalytic processing, 204, 210
 - complementary RNA preparation, 201, 209
 - endogenous activity, 204–206
 - glycosylation inhibition, 202–204
 - materials, 200, 201
 - overview, 200
 - pH-dependent aggregation, 206, 207
 - translation, 202, 209, 210
 - transmembrane domain
 - identification in protease protection, 207–209

- structure, 199, 200
- 7B2 as substrate, 205, 206
- Proteases, *see* Proprotein convertases
- Protein degradation, *see* Ubiquitination
- Protein kinase A (PKA),
 - live cell assays,
 - capillary electrophoresis assay, 426
 - fluorescence resonance energy transfer-based substrates, 425–426
 - Myr-HA- β 2AR-C as substrate, COS7 cell assay, 428, 429, 432
 - materials, 426, 427
 - oocyte assay, 427, 428, 432
 - overview, 426
 - phosphorylation analysis with Western blot, 429–432
 - subunits, 425
- Protein refolding assay, *see* Heat shock proteins
- Rafts, *see* Fertilization
- RanGTP, nucleocytoplasmic transport role, 243–246, 252
- RNA splicing, *see* Pre-messenger RNA splicing
- RNA virus replication, oocytes,
 - infectious viral particle production, 374, 375, 378
 - internal ribosome entry site-dependent translation requirements, 375, 376, 378
 - materials, 368, 369
 - overview, 367, 368
 - RNA replication assays,
 - all newly-synthesized RNA, 372, 377
 - negative-strand RNA synthesis, 372–374, 377
 - translation of genomic RNA, microinjection of viral RNA, 370, 371, 377
 - poliovirus RNA purification from virions, 369, 370
- Semi-intact cell, *see* Golgi apparatus disassembly
- Small nuclear RNA, *see* Pre-messenger RNA splicing
- Spindle assembly, egg extract studies,
 - biochemical manipulation for functional studies, 470–472
 - cycled spindle reactions and anaphase, 466–468
 - cytostatic factor extracts, features, 459, 460
 - preparation,
 - crude extract, 462–464, 471
 - high-speed extract, 464, 465, 71
 - half-spindle assembly reactions, 465, 466, 471, 472
 - materials, 460–462
 - overview, 459, 460
 - spin-down processing for immunofluorescence, 468, 472
 - Xenopus tropicalis*, 49, 50
- Src,
 - fertilization activation, 396
 - phosphorylation assay in fertilization, 402, 409, 410
 - overexpression effects on raft fractions in fertilization, 403, 410
- Stretch, *see* Patch-clamp, oocytes
- Subcellular sampling, *see* Capillary electrophoresis

- T7 RNA polymerase expression system,
 advantages, 56
 cytoskeleton imaging, *see* Confocal
 immunofluorescence
 microscopy, cytoskeleton
 expression plasmids,
 cDNA constructs, 58
 vector, 58
 ion channel expression, 57, 65
 materials, 57, 58
 metabolic labeling, 64, 65
 oocyte,
 injection with RNA polymerase/
 cDNA mixture, 64
 maintenance, 61, 64
 preparation, 61
 RNA polymerase preparation,
 activity assay, 61
 bacterial transformation and
 induction, 58, 59
 cell disruption, 59, 60
 dialysis, 60
 gel electrophoresis, 60
 purification, 60
 storage, 61
 yield, 61
 validation, 65, 66
 Tadpole, *see* Chromatin
 immunoprecipitation
 Thyroid hormone receptor, *see*
 Chromatin
 immunoprecipitation
 TIRFM, *see* Total internal fluorescence
 microscopy
 Total internal fluorescence microscopy
 (TIRFM), calcium flux
 imaging in oocytes,
 advantages, 114
 image acquisition, 115
 instrumentation, 114, 115
 materials, 104, 105
 principles, 114
 vitelline membrane stripping, 108
 Translation assay, *see* Messenger RNA
 polyadenylation
 Two-dimensional gel electrophoresis,
 protein kinase A assay in
 live cells,
 COS7 cell assay, 428, 429, 432
 materials, 426, 427
 oocyte assay, 427, 428, 432
 overview, 426
 Two-electrode voltage clamp, *see*
 Voltage clamp, oocytes
 Ubiquitination,
 anaphase-promoting complex,
 cell cycle regulators proteolyzed
 in mitosis exit and G1, 231,
 232
 ubiquitin ligase activity, 224
 egg extract studies,
 cell cycle regulators proteolyzed
 in metaphase-to-anaphase
 transition,
 immunodepletion and rescue
 assays, 229–231, 233
 protein degradation assay, 228,
 229, 232, 233
 protein ubiquitination assay,
 229, 233
 cytostatic factor extract
 preparation, 226, 228
 interphase extract preparation,
 226–228, 232
 materials, 224–226
 enzymes, 224
 UniGene clusters, resources, 8, 14
 Vitellogenesis, process, 24, 25

- Voltage clamp, oocytes,
 drug assays,
 automation, 332
 defolliculation, 336, 342
 expression, channels and receptors,
 incubation, 338
 microinjection, 337, 338, 342,
 343
 materials, 332–335
 neurotransmitter receptor ligands,
 agonists, 341, 344
 antagonists, 341, 342
 two-electrode voltage clamp,
 electrode preparation, 339, 343
 recording, 339, 343, 344
 rig wiring, 338
 overview, 331, 332
 transplanted membrane recordings,
 353, 354
- Western blot,
 cytochrome *c* release assays, 387,
 388, 392
 mitogen-activated protein kinase
 phosphorylation in
 fertilization, 402, 409, 410
 oocyte enucleation for analysis, 37,
 39, 40
 phospholipase C γ phosphorylation
 in fertilization, 402, 409,
 410
- protein kinase A assays in live cells,
 Myr-HA- β 2AR-C as substrate,
 COS7 cell assay, 428, 429,
 432
 materials, 426, 427
 oocyte assay, 427, 428, 432
 overview, 426
 phosphorylation analysis, 429–
 432
- Src phosphorylation in fertilization,
 402, 409, 410
- Xenopus tropicalis* oocyte lysate
 preparation, 50
- Xenopus tropicalis*,
 advantages in developmental studies,
 43, 44
 genetic resources, 1–16
 genome sequence, 12, 13
 oocyte studies,
 defolliculation, 47, 48
 germinal vesicle breakdown
 assay, 49, 51
 isolation, 46, 47
 lysate preparation,
 histone H1 kinase assay, 51
 Western blot, 50
 materials, 44, 45, 51
 maturation induction, 45, 46, 48
 spindle formation assays, 49, 50
 popularity of use, 2, 3, 13

Xenopus Protocols

Cell Biology and Signal Transduction

Edited by

X. Johné Liu

Ottawa Health Research Institute, Ottawa Hospital, Ottawa, Ontario, Canada

Although *Xenopus* oocytes are very hardy and robust in terms of experimentation and offer unusually simple and inexpensive opportunities for the delivery of mRNA to the cytoplasm and DNA to the nucleus, they are underutilized as an experimental model. In *Xenopus Protocols: Cell Biology and Signal Transduction*, hands-on researchers describe standard and cutting-edge techniques for using *Xenopus* oocytes and oocyte/egg extracts to reconstitute biological and cellular processes. These readily reproducible methods take advantage of the oocyte's impressive protein abundance (for example, 50–70 ng catalytic subunit of PKA per oocyte), its striking protein translation capacity (200–400 ng protein/oocyte per day), and its breathtaking possibilities for the assembly of infectious viral particles by single-cell injection of multiple RNAs. The authors focus on the versatility of frog oocytes and egg extracts in cell biology and signal transduction and cover all the major uses of oocytes/extracts as experimental models. The protocols follow the successful *Methods in Molecular Biology*™ series format, each offering step-by-step laboratory instructions, an introduction outlining the principles behind the technique, lists of the necessary equipment and reagents, and tips on troubleshooting and avoiding known pitfalls.

Comprehensive and highly practical, *Xenopus Protocols: Cell Biology and Signal Transduction* serves perfectly to instruct novices in the use of *Xenopus* oocytes/extracts, as well as seasoned investigators interested in developing novel models and uses.

FEATURES

- Readily reproducible methods for using *Xenopus* oocytes and oocyte/egg extracts
- Coverage of all the major uses of oocytes/extracts as experimental models
- Focus on the versatility of frog oocytes and egg extracts in cell biology and signal transduction
- Step-by-step instructions to ensure successful results
- Tricks of the trade and notes on troubleshooting and avoiding known pitfalls

ISBN 1-58829-362-9

